



RMUTCON

E - PROCEEDINGS
11th RMUTIC

**The 11th Rajamangala University of Technology
International Conference**

Collaboration with

**The Materials Research Society of Thailand
Prachachuen Research Network**

18 - 20 May, 2022

Royal Cliff Grand Hotel, Pattaya, Thailand



The 11th Rajamangala University of Technology International Conference

***“RMUT Driving toward Innovation, Economy and
Green Technology for Sustainable Development”***

Preface

Rajamangala University of Technology Thanyaburi has been appointed to host the 12th Rajamangala University of Technology National Conference (12th RMUTNC), the 11th Rajamangala University of Technology International Conference (11th RMUTIC), and 4th RMUT Innovation Awards 2022 in collaboration with The Materials Research Society of Thailand and Prachachuen Research Network. The conference held on May 18-20, 2022 at Royal Cliff Grand Hotel, Pattaya, Banglamung district, Chonburi province. It is an academic conference that will promote and support the exchange of knowledge of academic works in a various fields including social sciences and humanities, research in science and technology, research to improve teaching and learning, and master’s and doctoral students’ thesis. This academic conference is an important forum for exchanging knowledge between researchers, academics, faculty members and students both inside and outside the university, which will bring benefits in building academic cooperation and network that will lead to sustainable use of research.

This academic conference has exhibited works from researchers and academics from various fields, both domestically and internationally. It includes lecture section and poster section. There are 300 national research presentations, 129 international research presentations, and 87 inventions and innovations and creative projects contest with 6 guest speakers and panelists, 8 national guest speakers, and 28 international guest speakers.

In this regard, the university sincerely hopes that this academic conference will be beneficial to the participants and will contribute to continuous development as well as cooperation between faculty members, educational personnel and students which will promote the development of higher education of the nation in the future.



The 11th Rajamangala University of Technology International Conference
“RMUT Driving toward Innovation, Economy and Green Technology for Sustainable Development”

Message from the Chairman

Rajamangala University of Technology Thanyaburi together with other 8 Rajamangala Universities of Technology, The Materials Research Society of Thailand and Prachachuen Research Network to host the 12th Rajamangala University of Technology National Conference (12th RMUTNC), the 11th Rajamangala University of Technology International Conference (11th RMUTIC), and 4th RMUT Innovation Awards 2022. The conference was held on May 18-20, 2022 at Royal Cliff Grand Hotel, Pattaya, Banglamung district, Chonburi province. Its purpose is to disseminate research, innovation, and creativity of the faculties, academics, students, and people to the public both domestically and internationally. This is an important mechanism for building knowledge base from research, innovation and creativity, exchanging knowledge and experiences, and building network of academic cooperation in order to drive the knowledge-based economy on research and innovation. To create a better quality of life for the society and economy of the country, the 12th Rajamangala University of Technology National Conference (12th RMUTNC), the 11th Rajamangala University of Technology International Conference (11th RMUTIC), and 4th RMUT Innovation Awards 2022 will, therefore, be held under the concept of “RMUT Driving toward Innovation, Economy and Green Technology for Sustainable Development”.

On behalf of 9 RMUT, I would like to thank the related organizations for being co-host and both Thai and foreign guest speakers, qualified both inside and outside the university, researchers, the meeting attendees who will present researches, the action committee involving in organizing meetings. Most importantly, I would like to thank Professor Supachai Pathumnakul, M.D., Ph.D., A Deputy Permanent Secretary of Ministry of Higher Education, Science, Research and Innovation for giving a special lecture and presiding the conference.

(Assoc. Prof. Dr. Sommai Pivsa-Art)

Chairman

Rajamangala University of Technology Thanyaburi



The 11th Rajamangala University of Technology International Conference
“RMUT Driving toward Innovation, Economy and Green Technology for Sustainable Development”

Conference Committee

Advisory Chair:

Assoc. Prof. Dr. Sommai PIVSA-ART President of Rajamangala University of Technology Thanyaburi, Thailand

Secretary:

Asst. Prof. Dr. Warunee ARIYAWIRIYANAN Director of Research and Development Institute, Rajamangala University of Technology Thanyaburi, Thailand

International Advisory Committee:

Prof. Dr. Marcello M.	BONSANGUE	Leiden Institute of Advanced Computer Science, Leiden University, The Netherlands
Prof. Dr. Ian	THOMPSON	University of Oxford, England
Prof. Dr. Hidemitsu	FURUKAWA	Yamagata University, Japan
Prof. Dr. Young Lee	HEE	Yeungnam University, Republic of Korea
Prof. Dr. Seiichi	KAWAHARA	Nagaoka University of Technology, Japan
Prof. Dr. Hongbin	LIU	Institute of Automation (CASIA), Hong Kong Institute of Science & Innovation, Chinese Academy of Sciences, China
Assoc. Prof. Dr. Takahashi	KATSUYUKI	Iwate University, Japan
Prof. Dr. Yuji	ASO	Kyoto Institute of Technology, Japan
Prof. Dr. Kiyoshi	YOSHIKAWA	Kyoto University, Japan
Prof. Hirohiko	KANEKO	Tokyo Institute of Technology, Japan
Prof. Dr. Katsunori	OKAJIMA	Yokohama National University, Japan
Prof. Dr. Yoko	MIZOKAMI	Chiba University, Japan
Prof. Dr. Arunachala Mada	KANNAN	Arizona State University, USA
Assoc. Prof. Dr. Lav R.	KHOT	Precision Agriculture Washington State University's Centre for Precision and Automated Agricultural Systems and Department of Biological Systems Engineering, USA
Assoc. Prof. Dr. Hemantha	JAYASURIYA	Sultan Qaboos University, Oman
Prof. Dr. Witoon	PRINYAWIWATKUL	School of Nutrition and Food Sciences Louisiana State University, USA
Assoc. Prof. Dr. John Yew Huat	TANG	Universiti Sultan Zainal Abidin, Malasia



The 11th Rajamangala University of Technology International Conference
“RMUT Driving toward Innovation, Economy and Green Technology for Sustainable Development”

National Advisory Committee:

Assoc. Prof. Dr. Krischonme	BHUMKITTIPICH	Vice President for Academic and Research, Rajamangala University of Technology Thanyaburi, Thailand
Dr. Apitep	SAEKOW	Stamford International University, Thailand President of Prachachuen Research Network, Thailand
Prof. Dr. Santi	MAENSIRI	President of The Materials Research Society of Thailand, Thailand
Assoc. Prof. Dr. Chutiporn	ANUTARIYA	Asian Institute of Technology (AIT), Thailand
Dr. Manzul	HAZARIKA	Asian Institute of Technology (AIT), Thailand
Dr. David	MAKARAPONG	Chief Innovation Officer Senovate AI Co., Ltd., Thailand
Assoc. Prof. Dr. Jinpitcha	MAMOM	Thammasat University, Thailand
Assoc. Prof. Dr. Wisanu	PECHARAPA	King Mongkut's Institute of Technology Ladkrabang, Thailand
Prof. Dr. Therdchai	CHOIBAMROONG	National Institute of Development Administration NIDA, Thailand
Dr. Warayuth	SAJOMSANG	National Nanotechnology Center (NANOTEC), Thailand
Assoc. Prof. Dr. Pakorn	OPAPRAKASIT	Thammasat University, Thailand
Assoc. Prof. Dr. Daniel	CRESPY	Vidyasirimedhi Institute of Science and Technology (VISTEC), Thailand
Assoc. Prof. Dr. Nathdanai	HARNKARNSUJARIT	Kasetsart University, Thailand
Assoc. Prof. Dr. Pichai	JANMANEE	Rajamangala University of Technology Krungthep, Thailand
Assoc. Prof. Dr. Rerkchai	FOOPRATEEPSIRI	Rajamangala University of Technology Tawan-ok, Thailand
Dr. Natworapol	RACHSIRIWATCHARABUL	Rajamangala University of Technology Phra Nakhon, Thailand
Assoc. Prof. Dr. Udomvit	CHAIKAKUNKERD	Rajamangala University of Technology Rattanakosin, Thailand
Asst. Prof. Dr. Jutturit	THONGPORN	Rajamangala University of Technology Lanna, Thailand
Prof. Dr. Suwat	TANYAROS	Rajamangala University of Technology Srivijaya, Thailand
Assoc. Prof. Pramuk	UNAHALEKHAKA	Rajamangala University of Technology Suvarnabhumi, Thailand
Assoc. Prof. Dr. Kosit	SREEPUTHORN	Rajamangala University of Technology Isan, Thailand
Asst. Prof. Dr. Saichol	CHUDJUARJEEN	Rajamangala University of Technology Krungthep, Thailand



The 11th Rajamangala University of Technology International Conference
“RMUT Driving toward Innovation, Economy and Green Technology for
Sustainable Development”

Dr. Anan	PONGTORNKULPANICH	Rajamangala University of Technology Tawan-ok, Thailand
Dr. Chalakorn	UDOMRAKSASAKUL	Rajamangala University of Technology Phra Nakhon, Thailand
Dr. Santi	THAIYUENWONG	Rajamangala University of Technology Rattanakosin, Thailand
Asst. Prof. Nopporn	PATCHARAPRAKITI	Rajamangala University of Technology Lanna, Thailand
Asst. Prof. Praphasri	SRICHAI	Rajamangala University of Technology Srivijaya, Thailand
Assoc. Prof. Napat	WATJANATEPIN	Rajamangala University of Technology Suvarnabhumi, Thailand
Dr. Aniwat	HASOOK	Rajamangala University of Technology Isan, Thailand
Dr. Kitipoom	VIPAHASNA	Faculty of Industrial Education, Rajamangala University of Technology Thanyaburi, Thailand
Asst. Prof. Dr. Jakree	SRINONCHAT	Faculty of Engineering, Rajamangala University of Technology Thanyaburi, Thailand
Dr. Siriphatr	CHAMUTPONG	Faculty of Integrative Medicine, Rajamangala University of Technology Thanyaburi, Thailand
Asst. Prof. Dr. Chatchai	WEERANITISAKUL	Faculty of Engineering, Rajamangala University of Technology Thanyaburi, Thailand
Asst. Prof. Dr. Santikorn	PAMORNPATHOMKUL	Faculty of Business Administration, Rajamangala University of Technology Thanyaburi, Thailand
Dr. Pimpika	THONGROM	Faculty of Liberal Arts, Rajamangala University of Technology Thanyaburi, Thailand
Prof. Dr. Mitsuo	IKEDA	Mass Communication Technology, Rajamangala University of Technology Thanyaburi, Thailand
Assoc. Prof. Dr. Janprapa	POUNGSUWAN	Mass Communication Technology, Rajamangala University of Technology Thanyaburi, Thailand
Assoc. Prof. Dr. Amorn	CHAIYASAT	Faculty of Science and Technology, Rajamangala University of Technology Thanyaburi, Thailand
Asst. Prof. Dr. Nipat	JONGSAWAT	Faculty of Science and Technology, Rajamangala University of Technology Thanyaburi, Thailand
Asst. Prof. Dr. Arranee	CHOTIKO	Faculty of Science and Technology, Rajamangala University of Technology Thanyaburi, Thailand

Contents

	Page
Preface	C
Message from the Chairman	D
Conference Committee	E
Contents	H
 Invited and Instrument Presentation	
IV-iDTBI-001 Digital Technology and AI-Enabled Education Transformation <i>Chutiporn Anutariya*</i>	2
IV-iDTBI-002 Geospatial Data and Technologies – RECENT Advances and Applications <i>Manzul Kumar HAZARIKA*</i>	3
IV-iDTBI-003 Role of Innovation to Drive Business Performance and Improve Industry Standard Success Case: Innovation for Tropical Small and Medium Dairy Farms <i>David Makarapong*</i>	4
IV-iDTBI-004 Digital Technology in Detecting Poor Software Design Decision <i>Marcello M. Bonsangue*</i>	5
IV-iTIE-001 Sustainable Treatment of Industrial Wastewaters <i>Ian P Thompson*</i>	6
IV-iTIE-003 Nanostructured Materials and Composites for Energy Storage Applications <i>S. Maensiri*, S. Chaisit, U. Wongpratrat, S. Sonsupab, J. Khajonrit, T. Sichumsaeng, O. Kalawa, W. Senanon, P. Kidkhunthod, and N. Chanlek</i>	7
IV-iTIE-004 Transparent Conducting Oxides and Their Applications in Modern Display Devices <i>Hee Young Lee*</i>	8
IV-iMSH-001 “New Technologies in Healthcare”: Concept, Experience, Innovation Potentials and Development <i>Jinpitcha Mamom Sathiyamas*</i>	9
IV-iMSH-002 Robotic Haptic Sensing and Interaction for Surgery <i>Hongbin Liu*</i>	10
IV-iNAM-001 Agricultural and Environmental Applications of Plasma Discharges over Water Surface Generated by Pulsed Power Generator <i>Katsuyuki Takahashi* and Koichi Takaki</i>	11
IV-iNAM-002 Bioproduction of Renewable Feedstocks from Biomass Using Engineered Microbes <i>Yuji Aso*</i>	12



	Page	
IV-iNAM-003	Fine Bubble Technology and It’s Applications <i>Kiyoshi YOSHIKAWA*</i>	13
IV-iNAM-004	Optically Functional Nanomaterials Synthesized by One-Step Nanochemical Process for Optical Energy Harvesting Applications <i>Wisanu Pecharapa*</i>	14
IV-iTCC-001	Humanizing Technologies for High Value Tourism: Unlock Thailand Capability to Sustainability <i>Therdchai Choibamroong*</i>	15
IV-iVI-001	Information Input Interface Based on Eye Fluctuations <i>Hirohiko Kaneko*</i>	16
IV-iVI-002	Object Appearance Beyond Color Perception <i>Katsunori Okajima*</i>	17
IV-iVI-003	Color And Material Appearance Influenced by Lighting Conditions <i>Yoko Mizokami*</i>	18
IV-iCOM-001	Ionic Metal Ions and Its Chelation from Lab to Commercial Products <i>Warayuth Sajomsang*, Nuttaporn Pimpha, Sudkaneung Singto, Chalita Ratanatawanate, Sineenat Thaiboonrod, Pattarapond Gonil</i>	19
IV-iCOM-002	Nano Composite Material Based Gas Diffusion Layer for Proton Exchange Membrane Fuel Cell <i>A.M. Kannan*</i>	20
IV-iCOM-003	Functional Materials Based on Degradable Polylactide Copolymers and their Chemical-Recycling Products <i>Pakorn Opaprakasit*</i>	21
IV-iCOM-004	New Coatings for Anticorrosion <i>Daniel Crespy*</i>	22
IV-iFIS-005	Agriculture 4.0: Technology Landscape to realize the Farms of the Future <i>Lav R. Khot*</i>	23
IV-iFIS-006	Technology Adoption Needs in Farming and Processing for Food Security in 21 st Century <i>Hemantha Jayasuriya*</i>	24
IV-iFIS-001	Developing Sodium-Reduced Products Using Sensory Science Approaches <i>Witoon Prinyawiwatkul*</i>	25
IV-iFIS-002	New and Emerging Food Safety Issues <i>John Yew Huat Tang*</i>	26
IV-iFIS-004	Food Packaging and Sustainable Developments in BCG Economy <i>Nathdanai Harnkarnsujarit*</i>	27

	Page
Session 1: Digital Technology and Business Innovation	
iDTBI-002	29
Detection of Nutrients in Fertilizer with Image Processing based Chemical Reaction <i>Pichate Kunakornvong* and Dhiya Mahdi Asriny</i>	
iDTBI-003	40
Air Dust Level Detection Real-Time Online Monitoring <i>Prasert Nonthakarn*</i>	
iDTBI-004	48
The Impact of Mobile Applications on Improving an Organizational Personnel Performance <i>Chanchai Choksamai and Benjaporn Meeprom*</i>	
iDTBI-008	58
An Empirical Study of the Cross-Cultural Consumer Experience of a Pharmaceutical Shop During the Pandemic in the Retailing Setting <i>Gumporn Supasettaysa*, Phiraya Chetupong, Araya Buranakul, Viranpatch Asampinpongs, Piyapan Suwannawach, Tikumporn Kaewcheaknang and Parichat Chuanrakthum</i>	
iDTBI-P001	65
The Configuration of 3D Model Suitable for Creating World Scale Augmented Reality (AR) <i>Teerasan Lailang*</i>	
iDTBI-P002	72
The Design of English Flash Cards with Augmented Reality Technology about Food & Drink <i>Kamonthip Torsabsinchai*, Bennapa Patanapipat and Nattha Thammo</i>	
Session 2: Technology and Innovation for Engineering	
IV-iTIE-005	82
Discovery of Nanomatrix Structure of Natural Rubber and Its Application <i>Seiichi Kawahara*</i>	
iTIE-002	86
Effect of Fluid Velocity in Piping System Physical Properties for Shrimp Harvesting <i>Songphon Thoetrattanakiat and Kiattisak Sangpradit*</i>	
iTIE-005	97
A Comparative Study on Criteria for Sustainable Supplier Selection <i>Surasak Choobthaisong and Rapee Kanchana*</i>	
iTIE-008	106
The Site Survey and Study of 8 kW Hybrid Wind Solar PV Air-Compress System for Water Treatment Process (Case Study at CPF Saraburi Province) <i>Sirisak Pangvuthivanich, Wirachai Roynarin* and Nima Azhari and Suthep Simala</i>	
iTIE-009	116
An Assessment of Environmental Impact of Gas Flaring in Thailand: A Case Studies of Petrochemical Industry <i>Parnuwat Usapein* and Orathai Chavalparit</i>	

		Page
iTIE-010	The Analysis and Comparisons of 200 kW PV Rooftop Between Energy to Grid with Energy Storage at Wongsakorn Green Market in Thailand <i>Suthep Simala, Wirachai Roynarin*, Wongsakorn Wisatesajja and Nima Azhari</i>	123
iTIE-013	The Simulation of Water Quality Monitoring System for Shrimp Farming Pond <i>Weena Janrachakool*, Nongluk Promthong, Nutchapol Saivawe, Shareef Rodmanee and Suvil Chomchaiya</i>	131
iTIE-014	Real Time Security System with Face Recognition <i>Nongluk Promthong*, Weena Janrachakool, Komsun Chettreerith, Khongthep Boonmee and Burasakorn Yoosooka</i>	138
iTIE-015	Railway Area Detection Using Deep Segmentation Networks <i>Saifun Khruetakhrui, Jakkree Srinonchat* and Seán Danaher</i>	147
iTIE-P001	Drying Kinetics Models of Mini Heat Pump Dryer for Sliced Bananas <i>Phairoach Chunkaew*, Aphirak Khadwilard and Chakkraphan Thawongamyingsakul</i>	151
iTIE-P008	Analysis of a Concave Bulletproof Plate for Refracting the Bullet Impact Direction with Finite Element Method <i>Nuttapong Meesanu, Prasert Wirotcheewan, Duongruitai Nicomrat and Prakorb Chartpuk*</i>	161
iTIE-P009	The Parameter Analysis of the Tungsten Carbide and SUS304 Armor Plate with a Finite Element Method <i>Maitree Thawornsin, Songwut Mongkonlerdmanee, Duongruitai Nicomrat and Prakorb Chartpuk*</i>	169
 Session 3: Medical Science and Herb		
iMSH-P008	Total Phenolic Content, Antioxidant and Anticancer Activity of <i>Calophyllum inophyllum</i> <i>Luksamee Vittaya*, Chakhriya Chalad, Juntra Ui-eng and Sittichoke Janyong</i>	181
iMSH-002	Use of Herbs and Traditional Medicine Among Asian Youths in the Digital Age: Cosmetics, Beauty, and Anti-Aging <i>Lavanchawee Sujarittanonta*, Lin fan and Rajendra Khimesra</i>	187
 Session 4: Nanotechnology and Applied Materials		
iNAM-005	Effects of Modified Palm Oil and Surface Treatment on the Properties and Biodegradability of the Thermoplastic Starch <i>Piyawan Polpanich, Kullawadee Sungsanit* and Somkiat Thitipoomdecha</i>	202

		Page
iNAM-P010	Preparation of Flat Sheet Polysulfone Membrane Coated with PDMS for Carbon Dioxide/Methane Gas Separation at Low Pressure <i>Arisa Jaiyu*</i> , <i>Julaluk Phunnoi</i> , <i>Passakorn Sueprasit</i> , <i>Nattaporn Chutichairattanaphum</i> , and <i>Borwon Narupai</i>	212
iNAM-P014	Preparation and Characterization of Typha Natural Fiber Reinforced Poly(lactic acid) Biocomposite <i>Rattikarn Khankrua*</i> , <i>Bawornkit Nekhamanurak</i> and <i>Supakij Suttiruengwong</i>	220
iNAM-P018	Investigation of Dielectric and Ferroelectric of Niobium and Lithium Co-Doped Bismuth Sodium Potassium Titanate Ceramics <i>Thanaporn Boonchoo</i> , <i>Chatchai Kruea-In</i> , <i>Phatraya Srabua</i> and <i>Wilaiwan Leenakul*</i>	228
iNAM-P019	Copper(II) Oxide/Reduced Graphene Composite Electrodes for Supercapacitors Performance <i>Santi Rattanaveeranon*</i> , <i>Knavoot Jiamwattanapong</i> , <i>Eugene Kilayco</i> and <i>Rungsan Ruamnikhom</i>	233
 Session 5: Tourism Cultural and Creative technology		
iTCC-002	The Creation of Rong Ngeng Rhythms on Drum Set <i>Sittichok Kabilapat*</i>	241
iTCC-003	The Creation of the Song Power of Love: Orchestral Arrangements <i>Suttirak Iadpum*</i> and <i>Atipon Anukool</i>	250
iTCC-004	The Creation of Power of Love: A Cappella Arrangements <i>Suttirak Iadpum*</i> and <i>Sahaphat Aksornteang</i>	258
iTCC-005	Disney Song Concert: The Creation Brass Ensemble Concert for Undergraduate Bachelor of Music <i>Weerasak Aksornteang</i> and <i>Theerawut Kaeomak</i>	269
iTCC-006	The Creative Song for Piano "Lagu Kayoh Sampan" a Urak-Lawoi's Song <i>Sanya Phaophuechphandhu</i>	276
iTCC-010	Thailand's Case: The Destination Country's Influence on Tourist Satisfaction <i>Thanaphon Ratchatakulpat</i> , <i>Walisara Yongyingpraser</i> , <i>Gumporn Supasettaysa</i> , <i>Holger Kieckbusch</i> , <i>Varunya kaewchueaknang</i> and <i>Lalida Joomsoda</i>	283
iTCC-011	Arrangement of Lenang Songs for Violin Solo <i>Wichai Mesri*</i>	290

		Page
Session 6: Visual Information Processing and Color Vision		
iVI-002	Color Constancy Assessed by the Elementary Color Naming under RGB-LEDs <i>Phubet Chitapanya, Chanprapha Phuangsuwan, and Mitsuo Ikeda</i>	297
iVI-003	Simultaneous Color Contrast on an Electronic Display with or without a Tissue Paper under Various Room Illuminances <i>Janejira Mepean*, Mitsuo Ikeda and Chanprapha Phuangsuwan</i>	302
iVI-004	Individual Identify Face Detection by Principal Component Analysis (PCA) <i>Supannika Yongsue*, Kamron Yongsue, Onsucha Upakit, Yuvayong Anumanrajadhon and Chirapong Yanuchit</i>	307
iVI-005	Colors for Designing Advertisement Facebook Post Image of Food and Beverage Products on Facebook Fanpage <i>Natchaphak Meeusah*, Sirawadee Kramsuk and Juthamas Podoy</i>	315
iVI-006	Features of Visually Impaired Persons’ Evacuation Behaviors Indoors During Earthquakes <i>Mariko Wayaku*, Eisuke Ikuta1, Daiki Imai2, Yukari Murakawa and Hitoshi Watanabe</i>	324
iVI-007	Color Naming of Red-Green Color Deficiencies <i>Miyoshi Ayama*, Minoru Ohkoba and Tomoharu Ishikawa</i>	333
iVI-008	Dessert Appetite Aroused by A Direction of Lighting Setup <i>Chatchai Nuangcharoenporn*, Uravis Tangkijivivat and Waiyawut Wuthiastarn</i>	343
iVI-010	Color Name and Aroma of Thai Flowers <i>Chanida Saksirikosol, Akaradet Tongawang, Chanprapha Phuangsuwan And Kitirochna Rattanakasamsuk*</i>	349
iVI-014	The Effectiveness of Augmented Reality Data Access through a Smartphone <i>Kanok Chinda, Chanida Saksirikosol* and Ploy Srisuro</i>	354
iVI-015	The Comparison of the Weather Forecast Program with Thai Sign Language and Captioning between Hearing Impaired, Deaf and Hearing <i>Waiyawut Wuthiastarn</i>	358
Session 8: Food Innovation and Smart Farm		
iFIS-P002	Effect of Temperature on Ascorbic Acid and Lycopene in Mixed Tomato Juice and Mandarin Juice <i>Wattana Wirivutthikorn* and KMS Jodie Lazuardi Haickal</i>	364
iFIS-003	Study of Relative of UAV Imagery and NDVI for Maize Yield Estimation <i>Phoomchai Traidalanon and Kiattisak Sangpradit*</i>	374



		Page
iFIS-004	A Smart Trap Device for Detection of Corn Armyworm in Maize Harvest <i>Jérôme Planchais and Kiattisak Sangpradit*</i>	383
iFIS-P012	The Study of Melon Pulp Color on Physicochemical Properties and Antioxidant Activity of Melon Juices and Melon Powders <i>Siriluck Surin, Pimpan Pimonlat, Nantipak Chantadirokporn, Sudarat Bunbanterng and Peerapong Ngamnikom *</i>	391
iFIS-P003	Effect of Solvent Types and Concentrations on the Bioactive Compound from Lime Peel by Low Power Ultrasound Assisted Extraction <i>Suriyaporn Nipornram* and Riantong Singanusong</i>	402
iFIS-002	Parameter Study for Scratch Detection in The Poultry Industry <i>Jullachak Chunluan, Nattida Juewong and Kiattisak Sangpradit*</i>	410
iFIS-P011	Influence of Germination Time on Some Properties of Soybean and Black Sesame <i>Naruemon Mongkontanawat* and Witit Lertnimitmongkol</i>	418
iFIS-007	A Comparative Study of the Quality of Dietary Fiber from Defatted Rice Bran Extracted using Different Methods <i>Piyatida Deeam and Pilairuk Intipunya*</i>	426
iFIS-008	Physicochemical Quality of Gotu Kola Juice Treated by Non-Thermal Plasma <i>Nunnapus Bumrunghanichthaworn and Pilairuk Intipunya*</i>	438
	List of 11th RMUTIC 2020 Reviews	450



RMUTCON

Invited Presentations

Digital Technology and AI-Enabled Education Transformation

Chutiporn Anutariya *

*Department of Information and Communication Technologies, School of Engineering and
Technology, Asian Institute of Technology, Klong Luang, Pathumthani 12120, Thailand*

**Corresponding email: chutiporn@ait.ac.th*

Abstract

During the past few decades, the digital technology advancement, and applications of artificial intelligence (AI) are a key factor that has caused transformation and disruption in diverse industries. The transformative impact of these technologies in the education industry across the world has been inevitable and become clear, especially with the pandemic acceleration. This has given a new perspective for students, teachers, education experts and institutes as well as policy makers to adapt, and to plan their directions and actions accordingly. This talk highlights the roles of digital technology and AI in education, their impacts as well as opportunities and challenges in several dimensions including the teaching, the learning, the academic management, and the administrative management dimensions.

Keywords: Education Transformation, AI in Education, Personalized Learning, Data Analytics in Education, Education Trend

Geospatial Data and Technologies – RECENT Advances and Applications

Manzul Kumar HAZARIKA*

*Director, Geoinformatics Center, Asian Institute of Technology,
Klong Luang, Pathumthani 12120, Thailand
Corresponding email: manzul@ait.asia

Abstract

Geospatial data and technologies, such as Geographic Information Systems (GIS), Remote Sensing, and Global Positioning System (GPS), have the capabilities to capture and process location-specific data and information for visualizing, understanding problems and issues, and providing solutions through spatial analysis and modeling in areas such as in disaster management, agricultural crop monitoring, environment management etc.

Satellites can map a vast area at a regular interval, while drones can map a small area at a very high resolution on demand at a very low cost. While data coming from the satellites or drones provide a bird-eye view, but data coming from the ground through IoT sensors or mobile phones (crowdsourcing) can provide actual status in real-time.

This eventually contributes to the “big data” where pertinent data/information are gathered from a large number of sources, and “data analytics” subsequently helps in converting it into significant information for decision making and tackling issues at scale and speed. Machine Learning and Artificial Intelligence (AI) algorithm have made it easy to handle and process the enormous volume of this wide range of data.

A few innovative applications of the geospatial data and technologies in disaster management, agricultural crop monitoring, and environment management will be covered. These include applications of geospatial data and technology in (1) Post-disaster disaster response & reconstruction, (2) Multi-hazard Risk Assessment for risk mitigation, (3) Agro-Ecological Zoning for crop suitability assessment, (4) Weather Index Insurance product development, and (5) Plastic litter monitoring at city scale.

Keywords: Geospatial data, Geographic Information Systems (GIS), Remote Sensing, Global Positioning System (GPS), Internet of Things, Machine Learning, and Artificial Intelligence (AI)

Role of Innovation to Drive Business Performance and Improve Industry Standard Success Case: Innovation for Tropical Small and Medium Dairy Farms

David Makarapong*

Director of Senovate AI Co., Ltd., Bueng Kum, Bangkok 10240, Thailand

**Corresponding email: David.ishd@gmail.com*

Abstract

As a technology entrepreneur in technology and innovation management from Chulalongkorn university. I have learnt how to create new value by using academic knowledge and industry knowledge to create new business in Thailand. I 'd transformed my company and trained my staff to achieve the new goals to develop something new that can solve social and industry problem. My invention named Pre-Aseptic-Sterilization System plus (PASS+), thin-film design increases the liquids' exposure to UV-C, enabling greater efficacy and consistency in pre-treatment. The Laminar flow of the liquid over the lamps inside thin film chamber ensures an inactivation and the multiple-lamp system guarantees added food-safety by extending shelf life of the liquids. Our technology delivers trustful, countable UV-C efficiency.

PASS+ for improving quality of raw milk from small and medium size dairy farm in Tropical countries. The mechanism of this invention, the microorganism inactivation system uses short wave light to improve the quality of raw milk for small and medium dairy farms. The 254-nanometer wavelength is used to reduce the number of microorganisms in raw milk without affecting the quality. This is a new alternative in controlling the number of microorganisms in raw milk during the transport from farms to milk collection centers. It is the innovation that provides farmers in small and medium dairy farms with access to novel food technology at affordable cost. As a result, these dairy farmers will be able to generate higher income, have better quality of life and preserve their royal granted career, leading to sustainable development of the country.

The efficacy of this innovation had been approved by National Institute of metrology (Thailand) under by Ministry of science and technology. They validated our innovation's efficacy by using the spectroradiometric method using the CAS 140CT-154 Spectrometer to compare with USFDA part 179.39. The resulted was higher than normal standard and declared the scientific evidence that this innovation can “reduce of pathogenic microorganisms in raw milk to add the value for the farmers”.

This solution better than using cooling system because PASS+ can reduce and control while cooling system only can offer for control in controlled temperature. The initiate investment PASS+ cheaper 50% than cooling system and offer higher margin to dairy farmers and break even point will be on 2-3 years.

Keywords: Dairy technology, Dairy innovation, Nonthermal technology, Tropical Dairy Farms Technology, Inhibition microorganism

Digital Technology in Detecting Poor Software Design Decision

Marcello M. Bonsangue*

*Leiden Institute of Advanced Computer Science, Leiden University
Niels Bohrweg , 2333 CA Leiden, The Netherlands*

**Corresponding email: m.m.bonsangue@liacs.leidenuniv.nl*

Abstract

Software systems are increasingly pervasive in today world, influencing all activities and processes in which businesses operate. The development of large software systems is a complicated process involving many design and implementation decisions, which if poorly done increases fault proneness and code complexity and reduces software system maintainability. Code smells are properties of software that may indicate the presence of such flaws in its design or some poor implementation choices. Differently from a bug, code smells do not necessarily affect the technical correctness of a program, but rather they may be interpreted as symptoms of the bad quality of a software system.

Due to the subjectivity of their definition, detection of code smells, and the associated code refactoring to eliminate them, are non-trivial tasks. The manual detection process requires tremendous efforts and is infeasible for large-scale software. In this talk, we will present how different digital technologies and AI based techniques can help in automatically detecting of code smells to overcome some of the challenges software developers are facing in the design of correct software. The talk is based on joint work with Chitsutha Soomlek (Khon Kaen University) and Jan N. van Rijn (Leiden University).

Keywords: Code smells, Machine learning, Software engineering

Sustainable Treatment of Industrial Wastewaters

Ian P Thompson*

*University of Oxford, Department of Engineering Science, Parks Road, Oxford OX1 3PJ, UK.
Corresponding email: ian.thompson@eng.ox.ac.uk

Abstract

Many industrial wastewaters are challenging to treat since they are recalcitrant, toxic, with high organic loads. Furthermore most conventional treatment methods require expensive specialist equipment that are costly to run and very energy demanding. The overall objective of this study was to explore the potential of biological treatment of metal working fluids (MWF) wastewaters which was selected as representative of the challenge sustainable treatment of problematic wastewaters. MWF are extensively employed in industry, are difficult to treat biologically since they are formulated specifically to resist biodegradation and contain high concentration of biocides. Despite the inhospitable nature of MWF they are eventually colonised by microbial communities.

Thus the specific objective of this study was to undertake an extensive investigation of the temporal and spatial diversity of MWF in samples collected temporally and spatially, globally. This revealed that overall the diversity of MWF bacterial communities was very low, but some common species were ubiquitously distributed in geographically separated samples. The subsequent objective was to enrich and isolate bacteria from the characterised MWF bacterial community and assemble consortia that were effective at degrading the chemical constituents of the waste. In total 6 consortia were tested in terms chemical oxygen demand load, used as the measure of treatment effectiveness.

The third objective was to scale-up from laboratory flask to 5000 litre bioreactors and test the performance of the best bacterial consortia for treating waste MWF when grown as a biofilm grown on holding matrices. This demonstrated that the fixed biofilm could reduce MWF carbon loads of 80,000 mg/L to around 5000 within 48hrs. Subsequent performance at full commercial scale was found to be equally impressive. In more recent studies application of nano-scale iron oxide and MWF pretreatment with an electronic beam stimulated biotreatment even further.

Keywords: Wastewater, biotreatment, metal working fluids, bioreactors, bacterial community

Nanostructured Materials and Composites for Energy Storage Applications

S. Maensiri^{1,2,3,*}, S. Chaisit^{1,2,3}, U. Wongpratad^{1,2,3}, S. Sonsupab^{1,2,3}, J. Khajonrit^{1,2,3}, T. Sichumsaeng^{1,2,3}, O. Kalawa^{1,2,3}, W. Senanon^{1,2,3}, P. Kidkhunthod⁴, and N. Chanlek⁴

¹ School of Physics, Institute of Science, Suranaree University of Technology, Nakhon Ratchasima 30000, Thailand

² SUT Center of Excellence on Advanced Functional Materials, Suranaree University of Technology, Nakhon Ratchasima, 30000 Thailand

³ SUT-NANOTECH RNN on Nanomaterials and Advanced Characterizations, Suranaree University of Technology, Nakhon Ratchasima, 30000, Thailand

⁴ Synchrotron light Research Institute, Nakhon Ratchasima, 30000, Thailand

*Corresponding email: santimaensiri@g.sut.ac.th, santimaensiri@gmail.com

Abstract

With the rapid increase in energy demand, energy storage devices with high power and energy densities, long cycle life, and environmentally friendly have emerged as potential candidates for current and next-generation technologies. In supercapacitors, the energy storage performance is largely determined by the structural and electrochemical properties of electrode materials. Consequently, numerous studies have focused on the developing electrode materials for achieving high-performance supercapacitors. In this work, we report the development of electrode materials consisting of biomass-derived porous carbon materials, nanostructured oxides and composites, and glass-based ceramic materials. The nanostructured materials and composites are prepared through various synthetic methods including sol-gel, hydrothermal, electrospinning, and so on. The physical characteristics of the materials are deliberated and discussed in detail using basic and synchrotron-based characterization techniques. The electrochemical performances of the materials are evaluated in aqueous-based electrolytes via electrochemical techniques consisting of cyclic voltammetry (CV), galvanostatic charge/discharge (GCD), and electrochemical impedance spectroscopy (EIS). Lastly, a simple fabrication of energy storage devices using the developed electrode materials as cathode/anode is demonstrated for energy storage applications.

Keywords: Electrode materials, Nanomaterials, Electrochemical properties, Energy storage, Supercapacitor

Transparent Conducting Oxides and Their Applications in Modern Display Devices

Hee Young Lee

School of Materials Science and Engineering, Yeungnam University, Gyeongsan, 38541, Korea

Abstract

Transparent conducting oxides have long played important roles in the development and evolution of modern electronic devices and components, including chemical gas sensors, touch panel screens, front top electrodes for a variety of display devices, solar cells, etc. Among many successful candidate materials, a ternary oxide system In-Zn-Sn-O has proven its competency to be used as a transparent electrode as well as a transparent semiconductor for thin film field effect semiconductor applications. In this presentation, our research activities on this important class of materials will be reviewed in some detail.

“New Technologies in Healthcare”: Concept, Experience, Innovation Potentials and Development

Jinpitcha Mamom Sathiyamas*

Department of Adult Nursing and the Aged, Faculty of Nursing, and Center of Excellence in Creative Engineering Design and Development, Faculty of Engineering, Thammasat University, Khlong Luang, Pathum Thani 12121, Thailand

**Corresponding email: jinpitcha@nurse.tu.ac.th*

Abstract

Innovative technology played an important role in developing healthcare of global nursing today. Healthcare technology needs high-intensive nursing and accurate of diagnostic for treating patients. It is important to note that innovative healthcare can enhance assistive technology, medical device, and clinical service. Healthcare professionals are effective patient-centered care, medical technology, information system, and supportive service. Technology adoption of innovative provides a flexible care, patient-centered, virtual medication, and technical innovations that enhance the quality of life. A new paradigm shift in innovative healthcare, responsibility of disease prevention, and health management. Taken together, developing innovative healthcare will open up new approaches to prevention, therapeutic, diagnostic system, device, and technology. Mainly these innovations are geared to optimize the patient comforts and concedes more freedom mobility. New healthcare to bring innovative nursing will facilitate appropriate health service to patient needs. Technology provides clinicians with information and tools, such as clinical decision support that can improve the quality of care, which reduces potential medical errors. Medical device technology is shifted from personal digital assistance (PDAs), decreasing cost, developing new products, furthering research and development, and providing better cares.

Keywords: Innovative healthcare, Innovative technology, Medical technology

Robotic Haptic Sensing and Interaction for Surgery

Hongbin Liu

Institute of Automation (CASIA), Hong Kong Institute of Science & Innovation, Chinese Academy of Sciences, China

Abstract

Haptic capability, both sensing and interaction, is essential for a robot working in unstructured environments, yet robotic haptic technology today is still very primitive compared to even the simplest biological creatures. Haptic interaction is a cornerstone of many medical interventions/practices to ensure safety and efficacy. Our lab designs robots with advanced haptic perception and interaction capabilities to address unmet needs in medicine, enabling safer and more effective diagnosis and treatment. We commit our work to benefit both patients and the medical profession while advancing the frontier of haptic robotics research. In this lecture, I will share our experience of how to create augmented haptic sensing for medical instruments, and how we achieve effective haptic interaction during diagnosis and robotic endoscopy.

Agricultural and Environmental Applications of Plasma Discharges over Water Surface Generated by Pulsed Power Generator

Katsuyuki Takahashi^{1,2*} and Koichi Takaki^{1,2}

¹Faculty of Science and Engineering, Iwate University, 4-3-5 Ueda, Morioka Iwate 020-8551, Japan

²Agri-Innovation Center, Iwate University, 3-18-8 Ueda, Morioka Iwate 020-8550, Japan

*Corresponding email: ktaka@iwate-u.ac.jp

Abstract

Electrical pulsed discharge plasma produces various powerful oxidizing agents, such as hydroxyl radicals and ozone, which have high oxidation potential. These species play an important role in the decomposition of persistent organic compounds in wastewater. Because highly concentrated oxidants are directly produced inside plasma, plasma realizes high speed wastewater treatment without pretreatment of samples such as pH adjustment. The pulsed discharge plasma generated over water surface and inside bubbles is highlighted as a highly efficient method for plasma generation and radical supply into wastewater. In this paper, the physical and chemical properties of the discharge plasma generated over a water surface are described. The decomposition of persistent organic compounds dissolved in wastewater, such as 1,4-dioxane, formic acid and dichloromethane, by plasma discharge is demonstrated, and their mechanisms are discussed. These persistent compounds, which have strong toxicity and stability, can be efficiently decomposed and removed quickly from solutions by plasma treatment. Furthermore, the treatment of nutrient solutions used in hydroponic systems for plant cultivation is also introduced as a novel application of plasma, and the effects of bacterial inactivation, decomposition of allelochemicals and improvement in plant growth by plasma are demonstrated.

Keywords: Plasma, Wastewater, Nutrient solution, Advanced oxidation process, Hydroxyl radical

Bioproduction of Renewable Feedstocks from Biomass Using Engineered Microbes

Yuji Aso*

Department of Biobased Materials Science, Kyoto Institute of Technology, 1 Hashigami-cho,
Matsugasaki, Kyoto 606-8585, Japan

*Corresponding email: aso@kit.ac.jp

Abstract

Among diols, 1,2-propanediol (1,2-PDO) is one of the most versatile chemicals with two optical isomers, *R*-1,2-PDO and *S*-1,2-PDO. These compounds can be produced from glucose by engineered microbes possessing 1,2-PDO synthetic genes *pct*, *pduP*, and *yahK*, which encode propionate CoA-transferase, aldehyde dehydrogenase, and alcohol dehydrogenase, respectively. 1,2-PDO can be produced in engineered microbes via a pathway in which glucose is first converted to D- and L-lactate, followed by the synthesis of *R*- and *S*-1,2-PDO from D- and L-lactate, respectively, in which cofactors such as acetyl-CoA, NADH, and NADPH are required. This suggests that microbes producing the 1,2-PDO precursor lactate at a high titer are suitable as production hosts for 1,2-PDO production, and that *R*- and *S*-1,2-PDO can be separately produced in D- and L-lactic acid producers, respectively. Therefore, the present study demonstrated the production of *R*- and *S*-1,2-PDO using engineered *Lactococcus lactis* NZ9000 and AH1, respectively, through an exogenous 1,2-PDO production pathway, according to a previously reported demonstration using engineered *E. coli*. The L- and D-lactic acid-producing *L. lactis* strains NZ9000 and AH1 were transformed with the plasmid pNZ8048-ppy harboring *pct*, *pduP*, and *yahK* genes for 1,2-PDO biosynthesis, resulting in *L. lactis* LL1 and LL2, respectively. These engineered *L. lactis* produced *S*- and *R*-1,2-PDO at concentrations of 0.69 g/L and 0.50 g/L with 94.4% *ee* and 78.0% *ee* optical purities, respectively, from 1% glucose after 72 h of cultivation. Both 1% mannitol and 1% gluconate were added instead of glucose to the culture of *L. lactis* LL1 to supply NADH and NADPH to the 1,2-PDO production pathway, resulting in 75% enhancement of *S*-1,2-PDO production. Production of *S*-1,2-PDO from 5% mannitol and 5% gluconate was demonstrated using *L. lactis* LL1 with a pH-stat approach. This resulted in *S*-1,2-PDO production at a concentration of 1.88 g/L after 96 h of cultivation.

Keywords: 1,2-propanediol, *Lactococcus lactis*, fermentation, engineered microbes

Fine Bubble Technology and It's Applications

Kiyoshi YOSHIKAWA*

*Counselor, Rajamangala University of Technology, Thanyaburi. Pathumtani, Thailand
Professor Emeritus, Institute of Advanced Energy, Kyoto University, Uji, Kyoto, Japan*

**Corresponding email: yoshikawa.kiyoshi.58u@st.kyoto-u.ac.jp*

Abstract

The Fine-bubble(FB) technology is an emerging technology developed aggressively in Japan, and its origin can date back to The 2005 World Exposition, Aichi, Japan, where both fresh water and sea water fishes were shown swimming in the same aquarium filled with fine bubble water(youtube with English narrations at <https://www.youtube.com/watch?v=mvBiHcWT1B8>)

After many experiments of various kinds, it is found now that the FB has very unique functions and applicable to versatile fields as shown below. Although still, some basic features are not clearly verified, but nevertheless, application fields have made great progress. In this talk, some of the important and interesting fields appropriate to Thailand will be introduced.

Environments: • Factory wastewater treatment, •Sludge volume reduction, •Water purification (control of algae, etc.), •Improvement of water quality (measures against hypoxia, etc) by *Microbial activation, Highly efficient reaction of gas, Reaction promotion, Highly efficient dissolution of oxygen.*

Agriculture: •Growth promotion, •Increased yield, •Quality improvement by *Bioactive effect.*

Food: •Keeping freshness, •Antioxidant, •Reduction of drug usage by *Deoxidizing effect (gas replacement), Effective use of gas by improving reactivity.*

Fisheries: •Growth promotion, •Decrease of mortality rate, •Keeping fish fresh by *Highly efficient dissolution of oxygen, Bacterial suppression, Immunity improvement, Deoxidizing effect (gas replacement).*

Cleaning: •Toilet cleaning, •Washing clothes, •Cleaning metal parts, •Food cleaning by *Improved permeability, Peeling effect, Physisorption, Peeling effect, Floating separation, Sterilization using gas.*

Industry: •Precision peeling, •Silicon wafer thin film separation by *Improved permeability.*

Beauty: •Hot spring (bubble bath), •Face wash / scalp wash, •Shower head, •Nanotech cosmetics by *Hot bath effect, Oil removal (permeability), Improved permeability.*

Others: •Medical and medical equipment, • Ships, • Energy by *Sterilization by using gas, Improved propulsion (decreased resistance), Improved combustion efficiency.*

Keywords: Fine bubbles, Application to versatile fields, Sterilization, Accelerated growth of plants, Reactive oxygen species (ROS)

Optically Functional Nanomaterials Synthesized by One-Step Nanochemical Process for Optical Energy Harvesting Applications

Wisanu Pecharapa *

*College of Materials Innovation and Technology,
King Mongkut's Institute of Technology Ladkrabang, Bangkok, 10520, Thailand
Corresponding email: Wisanu.pe@kmitl.ac.th

Abstract

Sonochemical synthesis process is one of effective method for preparing various optically functional nanomaterials without further post treatment process. Uniform F/Sb-codoped SnO₂ conductive nanoparticles were synthesized by single-step sonochemical process without further heat treatment. With good infrared absorption due to surface plasmon resonance property, these conductive nanoparticles could be proposed as potential materials for infrared and thermal shielding applications. This facile technique was proposed for synthesizing various types of ultraviolet- and visible-driven photocatalysts including Zn-, Mn-, Co-doped TiO₂, ZnTiO₃ and Mn-, Yb-, Er-doped BiVO₄ nanoparticles with enhanced photocatalytic performance. Ultrasound-assisted process could be also an alternatively cost-effective process for synthesizing cellulose nanostructures from sugarcane bagasse that can be applied as ultraviolet shielding material.

Keywords: Optical material, Sonochemical process, Optical energy harvesting

Humanizing Technologies for High Value Tourism: Unlock Thailand Capability to Sustainability

Therdchai Choibamroong

PhD. Program Director, Graduate School of Tourism Management, National Institute of Development Administration (NIDA), Thailand

Abstract

As evident nowadays, the world is being tremendously disrupted by many powerful factors, making most global development drivers “VUCA”. Besides the pandemic Covid 19, as a sheer pressure, technological advancement has also been playing an important role in shaping the global development path. The tourism industry, composed of many supply chains, has no exception to avoid the unpredictable changes. Due to the special characteristics, sensitive and people-oriented, the industry has employed technological tools to cater the changing demand of new specie tourists who call for better service quality in the nowness manner and sustainability under the concept of “give and take”. In Thailand, the Ministry of Tourism and Sports, the Royal Thai Government, has recently announced the 3rd National Tourism Development Masterplan, highlighting “the Philosophy of Innovating Thailand High Value Tourism for Sustainability”. Under the aforementioned concept, the country is likely to regard technology innovations as a vital engine to move the tourism industry forward. It seems contradictory, while the technological tools are considered the hardware, the goal of the Thailand tourism is aimed at increasing the value as a soft power, both financial and spiritual values. Above all, all tourism actions need to pay high attention to environmental sustainability. This has led to many questions remaining unanswered on how to manage technologies to go along well with the tourism industry where the core product is “human hospitality” as well as how to employ them not to harm the environment. The keynote presentation will address many issues and provide answers regarding technology management to effectively deliver the human touch and finally leads to environmental sustainability. The case studies both national and international will be critically analyzed and presented.

Keywords: Humanizing Technologies, High Value Tourism, Thailand Capability, Sustainability

Information Input Interface Based on Eye Fluctuations

Hirohiko Kaneko*

Tokyo Institute of Technology, 4259-G2-3 Nagatsuta, Midori-ku, Yokohama, 226-8502, Japan

**Corresponding email: kaneko.h.ab@m.titech.ac.jp*

Abstract

Eye positions and attentional locations are not always the same, though they are closely related. It would be very useful if there was a tracking system of attention, not eyes. However, no such a system has been developed. The purpose of this study is to propose an attention tracking system.

In our series of studies, we found that there are relationships between the characteristics of eye fluctuations and stimulus properties at attentional location. When there are objects with different luminance or different spatial frequency and one pays attention to one of them while staring at another point, the pupillary response occurs depending on the luminance or spatial frequency of the stimulus (Kaneko and Tanaka 2011, Hu et al 2019). In addition, when two areas with different directions of motion arranged on the left and right areas, the gain and frequency of OKN (optokinetic nystagmus) corresponding to the attended motion were enhanced (Kanari et. al 2017). The magnitudes of pupillary response and OKN when paying attention to an object is smaller than when directing the eyes to the object, but the response characteristics of eye movements are qualitatively similar both when paying attention and when directing eyes. We can use the relationship to estimate the attentional location using the distribution of visual information, such as luminance, spatial frequency and motion in the scene, and the eye responses.

The proposed method using eye fluctuations to estimate attention location can be used as a means of information input system for the ALS (Amyotrophic Lateral Sclerosis) patients with locked-in state, who cannot move their eyes. In addition, the proposed method of estimating attention location using eye fluctuation has advantages over the existing methods using EEG and eye tracking in that it does not require quantitative calibration and that the estimation is valid.

Keywords: Attention, Pupil response, Eye movements, Interface

Object Appearance Beyond Color Perception

Katsunori Okajima *

Yokohama National University, Japan
**Corresponding email: okajima@ynu.ac.jp*

Abstract

In general, color can be described three-dimensionally, such as when using XYZ, LMS and HSV values. However, real objects have a variety of visual textures (gloss, roughness, softness etc.) in addition to colors and shapes, and visual texture can be defined as a two-dimensional distribution of chromatic values. For example, we can visually estimate the aging of artificial materials without using any comparative control stimulus of the new materials. These abilities suggest that there is a mechanism for perceiving the aging of materials in our visual system. I introduce an image processing method that simulate the aging by sunlight for dyes and pigments according to human perception and physical change (discoloration and corrosion etc.) of aging materials and an image processing method for renewing old objects. In addition, we validated the approach by conducting a psychophysical experiment and clarified the cues for perceiving such oldness and newness. Our methods can arbitrarily control the oldness and newness in the appearance of object images, so it must be useful as a visual effect in pictures, movies and arts. In addition, our method may be a tool for generating visual stimuli for human material perception research.

On the other hand, we can visually estimate the freshness of vegetables without touch. We showed that luminance distribution information is a critical cue for estimating visual freshness of vegetables, such as strawberries and cabbages and that visual freshness estimation does not depend on the color of the vegetable surface. These results indicate that we can perceive and estimate freshness of natural materials without comparative control stimulus of the fresh materials, suggesting that there are mechanisms for perceiving freshness of foods in our visual system. I introduce that chimpanzee have the same ability as human-beings.

In my lab, we developed some image processing techniques to modify the food's appearance naturally. The first method is Visual Texture Exchange (VTE). VTE enables us to change the visual texture of food from the original surface to another actual one, e.g., from Tuna to Salmon, and from Black Coffee to Café Latte in real time. The second method is Luminance Distribution Manipulation (LDM). We found that LDM can modify the moistness and softness of foods in appearance. The third method is Gloss/Shade Filter Operation (GSFO) which can create any Oily/Dried and Burned/Raw foods from an original food image in appearance. By applying such image processing methods and Augmented Reality technology, we are investigating cross modal effects of food appearance to the taste while keeping the ingredients intact, indicating that we can artificially control the taste by modifying food appearance with image processing.

Keywords: Object appearance, Color perception, Visual Texture Exchange

Color And Material Appearance Influenced by Lighting Conditions

Yoko Mizokami

Chiba University, 1-33, Yayoi-cho, Inage-ku, Chiba-shi, Chiba, 263-8522, Japan

Abstract

The appearance of an object is influenced by its color, material, shape, and lighting conditions. More variety of lighting environments is possible because of the development of solid-state lamps with flexible spectral power distribution and light distribution. Here, we introduce our research on color and material appearance influenced by lighting conditions.

First, we demonstrate the colorfulness adaptation effect that a scene or objects appear desaturated after adapting to the high color-gamut lighting or vice versa. Objects were viewed in a light booth equipped with a spectrally tunable light. The illuminant was varied in steps from a blackbody spectrum to a wide-gamut spectrum while keeping the illuminant color constant. Observers chose the illuminant so that the object color appeared most natural after adapting to either the blackbody or the wide-gamut illuminant. The result showed that the objects appeared more natural under the test illumination shifted toward the adapting illuminant, suggesting that color perception can rapidly adapt to changes in the color gamut produced by artificial lighting.

We also show that lighting diffuseness influences the appearance of objects. We examined if lighting with moderate diffuseness was suitable for reproducing a surface appearance of an object as seen in a natural environment. Observers first memorized the appearance of various objects in daily environments and then evaluated the object appearance under different diffuseness conditions. The result shows that the moderate diffuseness condition best reproduced the objects' faithful and ideal appearance. This indicates that a very low or high diffuseness, which is unfamiliar, is not suitable for reproducing an object's surface appearance faithfully and ideally.

These studies suggest that it is important to consider both lighting and object properties to evaluate an object's appearance. Also, it would be possible to control a suitable lighting condition for reproducing object appearances.

Keywords: Color, Colorfulness, Adaptation, Material appearance, Lighting diffuseness

Ionic Metal Ions and Its Chelation From Lab to Commercial Products

Warayuth Sajomsang^{*}, Nuttaporn Pimpha, Sudkaneung Singto, Chalita Ratanatawanate, Sineenat Thaiboonrod, Pattarapond Gonil

National Nanotechnology Center (NANOTEC), National Science and Technology Development Agency (NSTDA), Thailand Science Park, Pathum Thani 12120, Thailand

^{}Corresponding email: warayuth@nanotec.or.th*

Abstract

Even though metal ions are an integral and important part of many structural and functional components in human, animal, and plant, the applications of metal ions to commercial products are limited due to stability, toxicity, and absorption. The chelation technology can meet the needs and suit to solve this problem. However, it is not easy to be successful research by moving technology from lab to market. The concept of chelation in this work is replacement of water molecule around the metal ions by using a chelating agents such as amino acid, fatty acid, protein, surfactant, oligomer or polymer to make a stable metal complex or metal chelate via forming a chemical bond, and prevent anion from organic compound in an environment. In this talk, the chelation of various metal ions such as zinc ions, copper ions, manganese ions, iron ions, chromium ions, and silver ions and its applications will be presented. Chelated zinc ions are selected to develop in disinfectant formulation because they have low toxicity and are generally considered to be safe compared to mercury ions, silver ions and copper ions. The cation of chelated zinc ions at nanometer scale is highly stable, can be dispersed in a film coating on the surface which provide long-lasting stabilization performance. Moreover, how to create innovation and commercial disinfectant products, technology readiness level, industrial process scale-up and so on will be discussed in this talk.

Keywords: Metal ions, Chelation, Disinfectant, Zinc ions, Innovation

Nano Composite Material Based Gas Diffusion Layer for Proton Exchange Membrane Fuel Cell

A.M. Kannan

School of Manufacturing Systems and Networks, Ira A. Fulton Schools of Engineering, Arizona State University, Mesa, AZ 85212, USA

Abstract

Gas diffusion layers (GDLs) were fabricated using commercially available carbon paper as macro-porous layer substrate. Functionally graded nano-porous layers were designed by combining carbon nano-fibers with nano-chain type Pureblack carbon (75:25–0:100 wt.%) in the z-direction towards the catalyst layer and Teflon content (say 15–30 wt.%) to obtain variation in pore diameter and also hydrophobicity. On the top of the nanoporous layer, a thin layer of hydrophilic inorganic oxide (fumed silica) was also deposited to retain moisture content to maintain the electrolyte wet, especially when the fuel cell is working at lower relative humidity (RH) conditions, which is typical for automotive applications. The surface morphology, contact angle, bulk characteristics and pore size distribution of the layered GDLs were examined using FESEM, Goniometer, Interferometer and Hg Porosimeter, respectively. The GDLs assembled into MEAs were evaluated in single cell PEMFC under various operating conditions (temperature and RH) using H₂/O₂ and H₂/air as reactants. It was observed that the functionally graded nano-porous GDLs with hydrophilic layer showed an excellent fuel cell performance with a peak power density of about 0.46 W/cm² at 85 °C using H₂ and air at 50% RH.

Prompted by our earlier study that fumed silica on gas diffusion layer favored a performance improvement of the single fuel cell at lower RH conditions, the present study has been carried out with inorganic oxides in the nanoscale such as TiO₂, Al₂O₃, commercially available mixed oxides, hydrophilic silica and aerosil silica. The structure of each of the oxide coating on the GDL surface has resulted in refinement with graded pore dimension as seen from the Hg porosimetry data. The fuel cell evaluation at various RH conditions (50–100%) revealed that the performance of all the inorganic oxides loaded GDL is very high compared to that of pristine GDL. The results confirm our earlier observation that inorganic oxides on GDL bring about structural refinement favorable for the transport of gases, and their water retaining capacity enable a high performance of the fuel cell even at low RH conditions.

Keywords: Gas diffusion layers, Functionally graded, Pureblack® carbon, Carbon nano-fibers, Surface morphology, Pore size distribution

Functional Materials Based on Degradable Polylactide Copolymers and their Chemical-Recycling Products

Pakorn Opaprakasit*

*School of Bio-Chemical Engineering and Technology, Sirindhorn International Institute of
Technology (SIIT), Thammasat University, Pathum Thani, 12120 Thailand*

**Corresponding email: pakorn@siit.tu.ac.th*

Abstract

Poly lactide (PLA) is widely used in both the industrial and research community owing to its unique biocompatibility and degradability. In our laboratory, various functional materials have been developed based on PLA copolymers for a wide range of applications, especially in packaging, cosmetic, biomedical, agricultural, and environmental fields, by using specific fabrication processes. These PLA (co)polymers have been employed as additives for enhancing properties and providing functionality to commercial bioplastics. Micro- and nano-particles with tunable structures have been developed and applied in cosmetic and biomedical applications. The materials are also used to encapsulate various drugs and other active compounds. To align with the circularity concept, processes for chemical recycling of these degradable PLA products have been designed and developed to convert their disposable wastes into small-sized molecules for further use as value-added starting materials for specialty products. The resulting products are utilized to prepare lactide-based polyurethanes, suitable for use either as single-component materials, e.g., 3D-printing filaments and degradable adhesives, or as toughness-enhancing agents. PLA-based nanofibers with superhydrophobicity have been fabricated. The materials possess high oil absorption capacity and adsorption-desorption repeatabilities for oil/water separation.

Keywords: Polylactide, Copolymers, Functional materials, Chemical recycling

New Coatings for Anticorrosion

Daniel Crespy*

Vidyasirimedhi Institute of Science and Technology (VISTEC), Rayong, Thailand

**Corresponding email: daniel.crespy@vistec.ac.th*

Abstract

Corrosion of metals, *i.e.* the deterioration of metallic materials by reactions with their environment, is a huge financial plague, which typically accounts for economic losses evaluated to 3 to 5% of the gross national products of each country. Herein, we show various strategies for preparing anticorrosion coatings. A first approach consists in embedding functional nanomaterials to in a polymer matrix to create coatings with sensing, corrosion inhibition, or/and self-healing properties. A second strategy relies on the fabrication of functional coatings matrixes by conjugating a corrosion inhibitor to the side chain of polymers. The advantages and drawbacks of these two strategies and the perspectives in this research field will be also discussed.

Keywords: Anticorrosion, Coating, Controlled release, Nanosensor, Self-healing.

Agriculture 4.0: Technology Landscape to realize the Farms of the Future

Lav R. Khot

*Precision Agriculture and Interim Director of WSU's Agricultural Weather Network, Washington
State University, USA*

Abstract

Precision crop management involves use of technological resources to effectively ***monitor*** variability in soil, crop, and weather and then ***manage*** input resources for improved crop production and produce quality. In recent years, precision agriculture domain is being infused with futuristic technologies to realize concept capabilities of digital agriculture (Ag 4.0) for real-time monitoring, grower decision support, and smart management. This talk provides overview of these technologies and pertinent on-going research efforts in perennial specialty and field crops by WSU Precision-Ag Lab in collaboration with industry recognized researchers within the U.S. Discussed will also be the pertinent technology adoption/transfer challenges and path forward to realize farms/orchards of the future.

Keywords: Digital Agriculture; Crop stressors; Decision support; Smart Management

Bio: Dr. Lav R. Khot is Associate Professor of Precision Agriculture and Interim Director of WSU's Agricultural Weather Network at Washington State University. His research and extension program focus on “Sensing and automation technologies for precision management of production agriculture”. These efforts help ensure optimal use of resources, such as chemicals, water, energy, and labor, as well as improved produce quality. Dr. Khot is recipient of ‘Fruit + Vegetable 40 Under 40, Class of 2021’ from Fruit Growers News and ‘2018 New Innovator in Food and Agriculture Research’ Award from Foundation for Food and Agriculture Research. He has published 100+ peer-reviewed papers in this area and 350+ combined national and international conference talks, extension/outreach workshops and short courses. He currently serves as the Associate Editor for American Society of Agricultural and Biological Engineers (ASABE) Transactions. He also chairs the ‘Mechanization, Digitization, Sensing and Robotics Workgroup’ of ISHS-International Society of Horticultural Science.

Technology Adoption Needs in Farming and Processing for Food Security in 21st Century

Hemantha Jayasuriya

Department of Soils Water and Agricultural Engineering, Sultan Qaboos University, Oman

Abstract

Producing quality food for increasing population has become one of the greatest challenges for the humankind that happened in the 21st century. After passing several developmental and adoption eras such as industrialization era, mechanization era, nutrition and fertilizer era, information technology era, and scientists, researchers engaged in agricultural production sector are now laboring on more innovative developments targeting highly productive, goal oriented approaches to accomplish agricultural sustainability and food security. When compared to goals of few decades ago, now the scientists and researchers have to meet with additional goals such as minimizing food wastes through value-addition or processing, environmental friendliness such as minimum exploitation of soil and water, minimum emissions of compounds such as CO₂, NO_x, H₂S, CH₄ and other greenhouse gasses during the agricultural production activities. Therefore, the ultra-modern era came up with adopting high-tech agricultural production approaches that have been designated precision farming, controlled environment farming, hydroponics, aquaponics, and also food factory and vertical farming concepts. In precision farming concept, the main accomplishment was to optimize the use of resources including farm power, and to minimize the chemical applications. All these modern techniques encompass the environment friendly and organic farming guidelines with high productivity features. However, the increased energy demand for this technology adoption is yet to meet certain challenges; selection of energy options and reduced production costs, diverting to renewable energy sources such as wind and solar energy. There is no limit for innovative developments and accomplishing such tasks will be fallen on shoulders of new generations of scientists and researchers.

Keywords: Food security, Technology adoption, Controlled-environment agriculture, Precision farming, Smart farming

Developing Sodium-Reduced Products Using Sensory Science Approaches

Witoon Prinyawiwatkul

School of Nutrition and Food Sciences, Louisiana State University, Agricultural Center, Baton Rouge, Louisiana 70803-4200, USA

Abstract

Salt (NaCl) is essential for normal functioning in human, and the second most used food additive. More than 40 % of Na consumed is originated from 10 types of foods, of which the top five foods are breads and rolls, cold cuts and cured meats, pizza, fresh and processed poultry, and soups. Globally, correlation exists between excessive sodium consumption and high blood pressure which leads to possible coronary heart disease, stroke, heart and kidney failure. In the United States, high blood pressure alone affects over 75 million adults, which potentially leads to heart disease and stroke, the leading cause of death regardless of gender or age. It is estimated that 75% of the sodium is consumed through restaurants and processed foods, promoting overconsumption of sodium. In the United States, the average daily Na intake is more than 3,400 mg (equivalent to 8.5 g salt), which exceeds the current maximum recommended intake level (2,300 mg/d Na or 5.8 g/day salt). Awareness of potential negative effects of high Na consumptions is critical for public safety. However, reducing sodium and salt in foods is a challenge faced by the food industry as it may negatively affect sensory quality, product acceptance, human emotion, and purchase intent. In this presentation, the three recent major approaches used to reduce sodium in foods--chemical mechanisms, cognitive mechanisms, or modification of the food product structure-- will be demonstrated. Various sensory science approaches used as a tool to achieve salt reduction in foods will be briefly discussed.

Keywords: KCl, Salt, Salt substitutes, Sodium, Sodium-reduction

New and Emerging Food Safety Issues

John Yew Huat Tang*

Faculty of Bioresources and Food Industry, Universiti Sultan Zainal Abidin (Besut Campus),
22200 Besut, Terengganu, MALAYSIA.

*Corresponding email: jyhtang@unisza.edu.my

Abstract

It is the fundamental right for everyone to have sufficient, nutritious and safe food for consumption. However, foods are continuously exposed to the physical, chemical and microbiological hazards. Of these, microbiological hazard is more dynamic than other hazards due to microorganisms are continuously evolving and capable of growing under favorable conditions. Although technological advances have reduced microbiological risk to a minimum, foodborne pathogens continue to cause outbreaks, morbidity, and death. Globalization of food supply chain increases the risk and spreading of virulent pathogen strain from one country to another. New and emerging food pathogens pose a serious risk to human health especially the vulnerable groups such as the elderly, immunocompromised, pregnant woman and young children. Several factors such as new food types, consumer preferences, population growth, violations of food standards and climate change have been recognized to cause the emergence of new foodborne pathogens. In addition, food processing that aim to produce a stable and longer shelf life food products were thought to be responsible for pathogen selection, e.g. refrigeration has caused the emergence of *Listeria monocytogenes*. Pathogens with increased virulence capable of causing foodborne diseases even in small numbers and resistance towards multiple antibiotics may cause unsuccessful treatment. In order to control these pathogens, alternative method that utilizes bacteriophage has gained interest worldwide to combat pathogens particularly antibiotic resistant strain. Bacteriophage is widely available in the environment and its host specific characteristic make it a useful biocontrol agents in food. Lytic bacteriophages have shown promising efficacy against pathogens such as *Listeria monocytogenes*, *Campylobacter* spp. *Salmonella*, *Escherichia coli*, and *Staphylococcus aureus*.

Keywords: emerging food pathogens, antibiotic resistance, virulence, biocontrol, bacteriophage

Food Packaging and Sustainable Developments in BCG Economy

Nathdanai Harnkarnsujarit*

*Department of Packaging and Materials Technology, Faculty of Agro-Industry, Kasetsart
University, 50 Ngam Wong Wan Rd., Latyao, Chatuchak, Bangkok 10900, Thailand*

**Corresponding email: nathdanai.h@ku.ac.th*

Abstract

Food packaging has major impact on sustainability. Inappropriate handling and management of package waste produce pollutions and negative impact on the environments. Global concern on sustainable living drives food industry towards environmentally friendly manufacturing. Modern consumers and food manufacturers agree well with the concept of sustainable development goals (SDG), adopting by the United Nations. Bio-Circular-Green (BCG) economic model has been recently proposed by the government to facilitate sustainable economy. Thailand has high potential to apply BCG model into several industries including food and packaging industries. Numerous natural-derived raw materials e.g., starch, protein and other polysaccharides can be produced into bioplastic food packaging, serving the bio-based economy. Enhancing performance of bioplastic polymers for quality preservation of packaged foods are important research focus by global researchers and packaging manufacturers. Recycle of the plastic package closes the loop, facilitating circular economy. The performance of recycled materials and safety issue due to post-consumer contamination are major concern. Safety assessments are necessary to ensure the safe use of recycled plastic for food packaging. Green economy aims to decrease environmental risks and shortage of natural resource, while preserving ecology systems. The environmental impact of packaging should be monitored throughout the supply chain. Several attempts to reduce environmental impact of the packaging include reduce, reuse and recycle. However, packaging has direct impact on product shelf-life and reduction of packaging features may cause adverse effects on product quality. Sustainable developments of food packaging, therefore, require holistic views. Optimization between package performance, waste management and food quality would provide successful developments of packaging for food industry.

Keywords: Food Packaging, Packaging Technology, Sustainability, Innovation



RMUTCON

Session 1:

**Digital Technology and
Business Innovation**

Detection of Nutrients in Fertilizer with Image Processing based Chemical Reaction

Pichate Kunakornvong^{1*}, Dhiya Mahdi Asriny²

¹Rajamangala University of Technology Thanyaburi Pathumthani, Thailand

²Master of Information System Management, Binus University, Indonesia

* Corresponding email: pichate_k@rmutt.ac.th

Abstract

This research proposes the image processing technique with color comparison methods for Nutrient detection in the chemical fertilizer based on chemical reaction image. There are two methods of color comparison for nutrient detection of fertilizer sample as: the sampling and the histogram comparisons. The sampling method compared between the sampling areas form Region of Interest (ROI) of fertilizer solution and each color in the standard color plate. The histogram comparison method compared between the histogram ROI of fertilizer solution and each color in the standard color plate. The accuracy of classification based on laboratory test between human and proposed methods are 58.5 and 89 percent by the sampling and histogram comparison method, respectively.

Keywords: NPK, Nutrient detection, Image processing, Color comparison

Introduction

Nowadays, the cultivation in agriculture moving to organic farming without the chemical used. But the chemical fertilizer is still used a lot, which can be observed from the global market value nearly \$104.9 billion in 2018 and expected growing to \$121.3 billion in 2022 T. B. R. Company (2019). The high marker values are the cause of the counterfeit, debased in fertilizer, it makes the lack of standard fertilizer. To precise inspection the nutrient in fertilizer is costly because it needs the standard laboratory with standard techniques. This work focuses on creating the simple methods to eliminate the weaknesses of fertilizer inspection.

There are many techniques for nutrient checking such as Nitrogen checking with Kjeldahl method proposed by Dane Johan Kjeldahl since 1800 consist of 4 steps: sample digestion, ammonia distillation, titration to determine nitrogen content and, calculate the protein value from the nitrogen content in the test substrate. The molybdenum blue method for Phosphorus checking by reducing the yellow complexes of molybdophosphate, Mo(VI) with reducer such: ascorbic acid, tin(II) chloride to get the blue complex (Mo(V)), this method often used to detect the composition of phosphorus T. B. R. Company (2019). However, molybdenum blue method takes a long time because the batch spectrometry must wait for the reaction balancing. The flow injection analysis (FIA) and sequential injection analysis (SIA) are extended techniques based on the molybdenum blue method for checking phosphorus in solution, there were used in many research T. B. R. Company (2019), Phansi et al., (2020), Taylor et al., (2015), Nagul et al., (2015), Barros Azeredo et al., (2022). The major disadvantages of FIA are a chemical dumping during the sample injection and requires the specific injection equipment. Comparing with FIA, the SIA techniques used less chemical injection, but the equipment is very costly. The hydrodynamic sequential injection (HSI) which reduced the chemical usage by FIA techniques and the equipment is cheaper comparing with SIA techniques. The HSI be applied to analytic the phosphate and silicate in the wastewater Panyaying et al., (2017), In addition to phosphates, this method can analyze nitrite and nitrate in the water Khongpet et al., (2020). The potassium checking can be done by using atomic emission spectrometer with the wavelength 766.5 nm Somnam et al., (2014).

In addition, the nutrient can be detected with light detector. The light emitting diode, LEDs, are used as light source. The reflection from 3 LEDs light which passing through optical fiber are detecting by photodiode Kathong and Ruangviriyachai (2014), Gavade (2017), Masrie et al., (2018), Masrie et al., (2017). Some weakness of this technique is probe calibration issue, its need to calibrates with standard color table. The light from receiver probe is converted to electrical signal by Phototransistor. Then the electronic signal technique with Ion selective electrode (ISE) and Ion selective field effect transistor (ISFET) sensors were proposed Ramane et al., (2015), the ion from soil solution is absorbed into sensors.

The preliminary testing on the chemical fertilizer can be done by the KU5 test kit develop by the soil fertilizer environment academic development project department of Soil Science Faculty Agriculture Kasetsart University. This test kit used for detecting nitrogen in Urea form, ammonium nitrate, useful phosphorus, and soluble potassium, moreover, it is also possible to approximate the fertilizer formula. The chemical test results will interpret the color of the solution obtained from the test compared to the standard color sheet.

The color comparison of image is the useful method which applied in many kind of applications, such as agricultural application Wabali et al., (2017), food quality control Ji et al., (2016), person identification with skin segmentation and color comparison applied to a part of face skin detection Shaik et al., (2015), Yadav and Nain (2015).

This work proposed the application of image processing techniques in fertilizer formula inspection. The hypothesis of this work is based on the standard chemical rapid test set, KU5, can work correctly, the fertilizer formula validation will be correct. The preliminary result shows the color of chemical reaction interpreter and the comparison between interpreting results with the human eye and image processing techniques. The finally, color analyzing station was designed and used as field test equipment that used for analyzing the color of the chemical reaction solution from KU5 rapid test.

This paper is organized as follows; Section II, theory of nutrient analysis principle of color and image processing. Section III presents the methodology of this research. Then, result is shown in section IV. Finally, the conclusion will be drawn.

Theory

A. Nutrient analysis

There are various techniques for detecting the nutrient in fertilizer or soil. The simple techniques to detect the nitrogen in the chemical fertilizer is used the limewater, however the limewater is basically and limited used only nitrogen in the form of NH_4 , it cannot be used with nitrogen in the form of Urea and these techniques cannot quantify the nitrogen in fertilizer.

The standard nutrient analysis can be done in laboratory by many techniques which reported by Kimura Kimura (2018): the total nitrogen can be verify from one of the methods: Kjeldahl method, Combustion method, Davarda's alloy- Kjeldahl method, Reduce iron- Kjeldahl method or calculation with ammonia and nitrate nitrogen, the ammoniac nitrogen determine by Distillation or Formaldehyde method, the nitrate nitrogen can be verify by Devarda's alloy-distillation method or Reduceiron-distillation or Phenol sulfuric acid method. The Ammonium vanadomolybdate absorptiometric analysis and Quinoline gravimetric analysis can verify the total phosphoric acid, soluble phosphoric acid, Citrate-soluble phosphoric acid, Water-soluble phosphoric acid. Liquid mixed fertilizers containing phosphonic acid or phosphite can verify the Water-soluble phosphoric acid. Flame atomic absorption spectrometry or flame photometry and Sodium tetraphenylborate gravimetric analysis can verify total potassium, citrate soluble potassium, and water-soluble potassium. Sodium tetraphenylborate volumetric analysis can verify citrate soluble potassium, and water-soluble potassium.

B. Chemical tester kit

The chemical tester kit can be used to check the basic formula of the fertilizer by comparison the color of solute from chemical reaction of fertilize solution and the chemical tester and the chemical reaction standard color plate, which shown in figure 1.

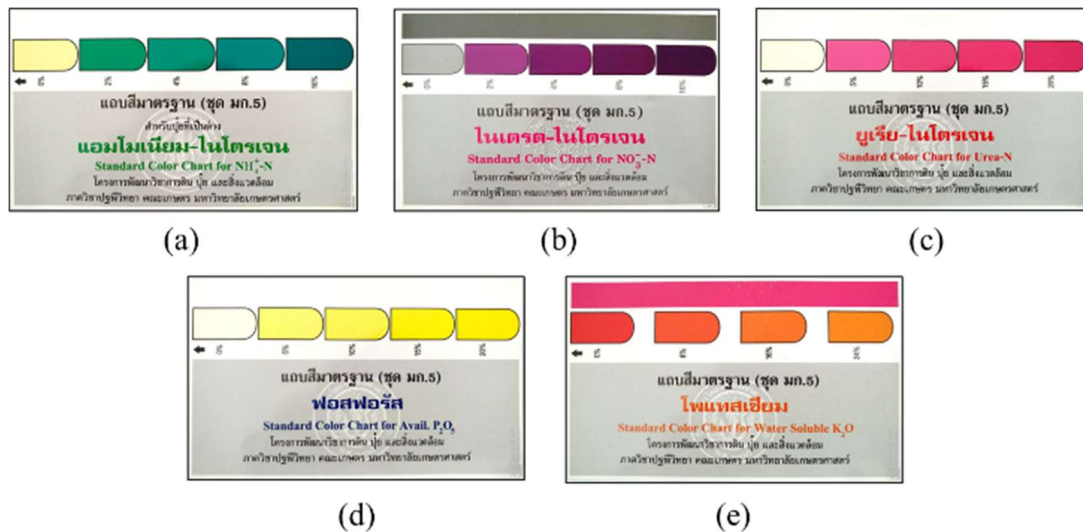


Figure 1 Chemical reaction standard color (a) $NH_4^+ - N$ (b) $NO_3^- - N$ (c) Urea-N (d) P_2O_5 (e) K_3O

C. Color principle

There are various color models which can be used in image processing and in the real world such: Gray, RGB, HSV or HSL, CMYK, etc. Gray color is the base model for explain another color models, it can be present 256 levels of color from black (0) to white (255) or dark (0) to bright (255) by using 8 bits per pixel. The RGB color model is widely used in various applications, it includes 3 elements; red, green, blue, be overlay and it can be display 16.7 million colors, real color, by its combination of 255 levels in each plane. This color model is useful for the monitor, computer graphic, etc. The concepts of HSV (Hue, Saturate, Value) model and HSL (Hue, Saturate, Lightness) model are from human eyes, the color depends on the degree and distance from central plane look like cone cell and the brightness or lightness depend on deep of the cone look like rod cells of human eyes. The different of HSL and HSV is the lightness format, in HSL model the L element is end with white color and in HSV model the V element is end with the highest brightness values of the color. The structure of HSL is called bicubic while HSV called cone which shown in figure 2 Wikipedia (2022). This model is useful in image processing because it can be extract and reduce the illumination effect from image by except the lightness or value channel.

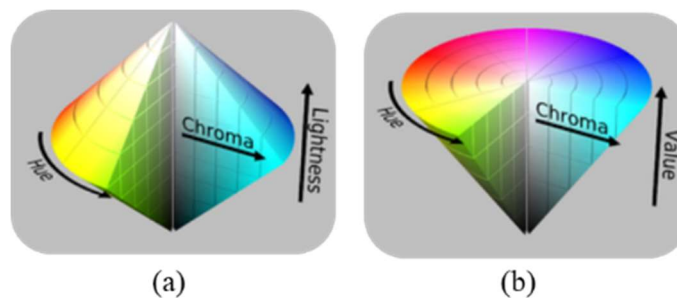


Figure 2 The structure of HSL (a) and HSV (b) color model

D. Classification

The well-known classification function is Euclidean distance. It is ordinary distance between two points in Euclidean space. The distance in Euclidean space is length of vector between two points. The distance between two points p and q , $d(p, q)$, can be define by equation (1).

$$d(p, q) = \sqrt{(x_q - x_p)^2 + (y_q - y_p)^2} \quad (1)$$

The Euclidean distance between train and test data can be classify the test data into the train classes.

Methodology

This research focus on applies image processing techniques to inspecting fertilizer formula. This research is interpreting result of chemical reaction from nutrient testing with image processing techniques comparison to interpret from human, and specify the formula of fertilizer with artificial intelligent which show the system overview in figure 3. The input image was captured by a small camera with optical size ¼ inch and supported video resolution at 1080p and the maximum still image resolution is 5 megapixels. The lighting used to capture the sample image is LED bar which installed in close environment.



Figure 3 System overview

A. Image processing

This research included two image processing techniques to interpret the chemical reaction between test kit and fertilizer such: direct comparison with sampling the color line and color histogram comparison. The sampling techniques is shown in figure 4. The techniques start from find the ROIs of the template color (standard color) and the sample (chemical substance). The sample color lines were selected from the ROIs then the average of color lines was calculated and finally with comparison the average with decision function.

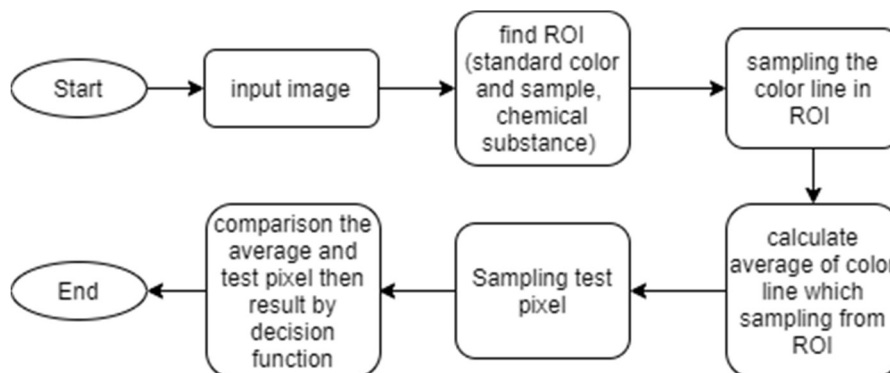


Figure 4 Flow diagram of sampling techniques

Histogram is the image property which can be represent the brightness of gray image or tone of color image. The numbers of histogram are the frequency of each pixel value. The research used the histogram properties to extract the color tone of the standard color and sample. The color histogram comparison techniques shown in figure 5, it begins with edge detection for ROI finding. Next the standard color areas and sample areas in ROI were selected. Then the histogram of selected

areas was calculated. The representative number of the histogram from each standard color area and sample area are defined from their histogram. Finally, the sample was compared to each standard color with decision function.

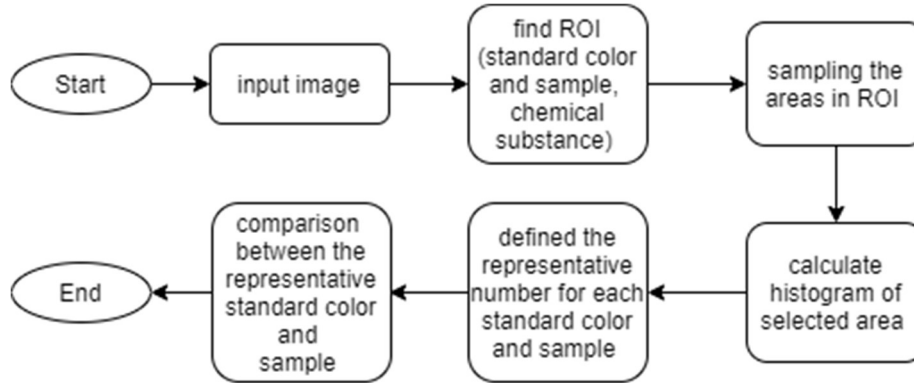


Figure 5 Flow diagram of color histogram comparison

B. Classification of each chemical reaction from sample

Three-dimensional Euclidean distance was used as the decision function for classification process in this work, which can be shown in equation (2).

$$dist_3 = \sqrt{(s_R - \bar{x}_R)^2 + (s_G - \bar{x}_G)^2 + (s_B - \bar{x}_B)^2} \quad (2)$$

where $dist_3$ is three-dimensional Euclidean distance, s_R, s_G, s_B are average of standard color in red, green and blue color plane respectively, $\bar{x}_R, \bar{x}_G, \bar{x}_B$ are average of sampling from chemical reaction of tested fertilizer in red, green and blue color plane, respectively.

Results and Discussion

This part shows the comparison result from the average specify of five persons as expertise, the hypothesis is the average specify by expertise be true. The performance test is the result comparing between average result from five expertises and proposed algorithms with 10 samples of fertilizer solution form chemical reaction in each fertilizer. The images used in experiment are capture by small camera, the capture size is set to 1600x1200 pixels or 2MP image.

A. Sampling method

This method was selected one column pixels from the part of standard color, such selected by center of that part. The selected column was defined as reference. The figure 6 (a) shows the part of standard color and, figure 6 (b) shows the plot of color from column 20 which separate into 3 bands, RGB. The sample of chemical reaction from mixed fertilizer is shown in figure 7. The sampling pixel was selected by selecting the pixel in center of ROI of the fertilizer solution. Figure 8 shows the plot of Euclidean distance between the sampling pixel from the sample of chemical reaction and the average of standard color plate, and the sample is closed to highest level of nutrient and match to human specify. Table 1 show the test result from 4 samples: urea fertilizer (46-0-0), mixed fertilizer (13-13-13, 16-16-16 and, 9-25-25). The result classification of sampling methods is compared to the average of expertise specify; column (a) – (e) are the result of the fertilizer chemical reaction for checked $NH_4^+ - N$, $NO_3^- - N$, Urea-N, P_2O_5 , K_3O , respectively. The fertilizer levels mapping is shown in Table 2.

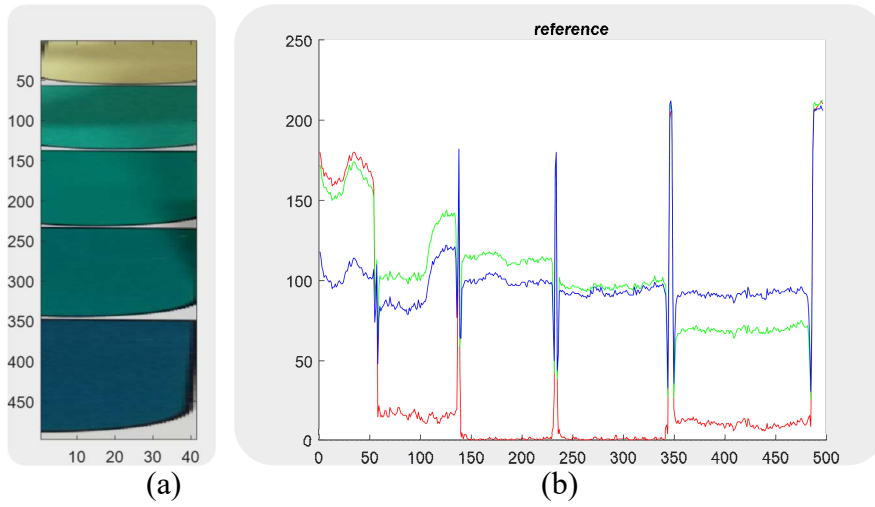


Figure 6 The standard color of amonium-nitrogen and the plot of color value from column 20; (a) the part of standard color and (b) the plot of color from column 20 which separate into 3 bands



Figure 7 Example of chemical reaction from mixed fertilizer (16-16-16)

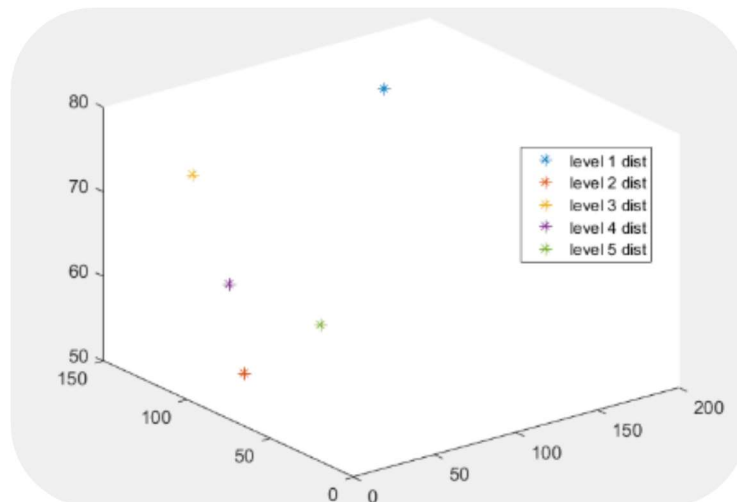


Figure 8 The plot of Euclidean distance between standard color $\text{NH}_4\text{-N}$ and sample from fertilizer formula 16-16-16

Table 1 Classification results comparison between human and the Sampling method

Sample No	Expertise					Sampling method				
	a	b	c	d	e	a	b	c	d	e
Urea fertilizer (46-0-0)										
1	1	1	2	2	3	1	1	3	2	3
2	1	1	2	2	3	1	1	3	3	2
3	1	1	2	2	2	1	1	2	2	3
4	1	1	2	2	3	1	1	2	2	2
5	1	1	2	3	3	1	1	3	2	4
6	1	1	2	2	2	1	1	2	2	2
7	1	1	2	2	2	1	1	3	3	3
8	1	1	2	2	3	1	1	4	4	4
9	1	1	2	2	3	1	1	3	3	3
10	1	1	2	2	3	1	1	3	3	3
Mixed fertilizer (13-13-13)										
1	5	3	1	4	4	4	3	1	3	4
2	5	3	1	4	4	4	4	1	3	4
3	4	3	1	4	4	4	3	1	3	4
4	4	4	1	5	4	4	4	1	4	3
5	5	3	1	4	4	4	4	1	4	4
6	4	3	1	4	3	3	4	1	4	3
7	5	3	1	4	3	4	4	1	4	3
8	5	3	1	5	3	4	3	1	4	4
9	4	3	1	4	3	3	3	1	3	4
10	4	3	1	4	4	3	4	1	3	4
Mixed fertilizer (16-16-16)										
1	5	4	1	5	4	4	4	1	4	4
2	5	4	1	5	4	4	3	1	4	3
3	5	5	1	4	4	4	3	1	3	4
4	5	5	1	4	3	4	4	1	3	3
5	4	4	1	5	4	3	3	1	3	4
6	5	4	1	5	4	4	4	1	4	3
7	4	5	1	5	3	4	4	1	4	4
8	5	4	1	5	4	3	4	1	3	4
9	4	5	1	5	3	4	3	1	4	3
10	4	5	1	4	4	4	3	1	4	3
Mixed fertilizer (9-25-25)										
1	5	1	1	5	4	4	1	1	4	4
2	5	1	1	4	3	3	1	1	4	3
3	5	1	1	5	3	4	1	1	4	3
4	5	1	1	4	3	4	1	1	4	3
5	4	1	1	4	3	3	1	1	4	3
6	4	1	1	4	3	3	1	1	3	3
7	4	1	1	4	4	4	1	1	3	4
8	5	1	1	4	4	4	1	1	3	4
9	4	1	1	5	4	4	1	1	4	4
10	5	1	1	5	4	4	1	1	4	4

Table 2 Fertilizer levels mapping

Level	(a) $NH_4^+ - N$,	(b) $NO_3^- - N$,	(c) Urea-N	(d) P_2O_5	(e) K_3O
1	0%	0%	0%	0%	0%
2	2%	2%	5%	5%	8%
3	4%	4%	10%	10%	16%
4	8%	8%	15%	15%	24%
5	16%	16%	20%	20%	-

B. Histogram comparison

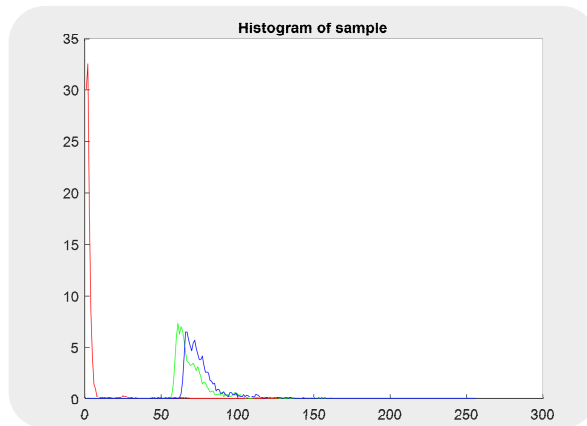


Figure 9 Histogram of sample chemical reaction image

In the histogram comparison method, the histogram of the fertilizer solution from chemical reaction and each standard color levels were calculated, figure 9 shows the histogram of fertilizer solution. The histogram of standard color amonium-nitrogen shown in figure 10. The average from three highest values of histogram are representative, the average was used to remove fluctuation of histogram. The distance vector between fertilizer solution and standard color levels are calculated which shown in figure 11. The shortest distance represents to nutrient levels of the sample fertilizer solution. In figure 11 the sample fertilizer solution has highest amonium-nitrogen nutrition. The comparison between human and proposed method are shown in table 3, there are different result scores. Finally, table 4 shows the performance comparison between the proposed methods: sampling and histogram comparison method, it shows that the histogram comparison method is better than sampling method.

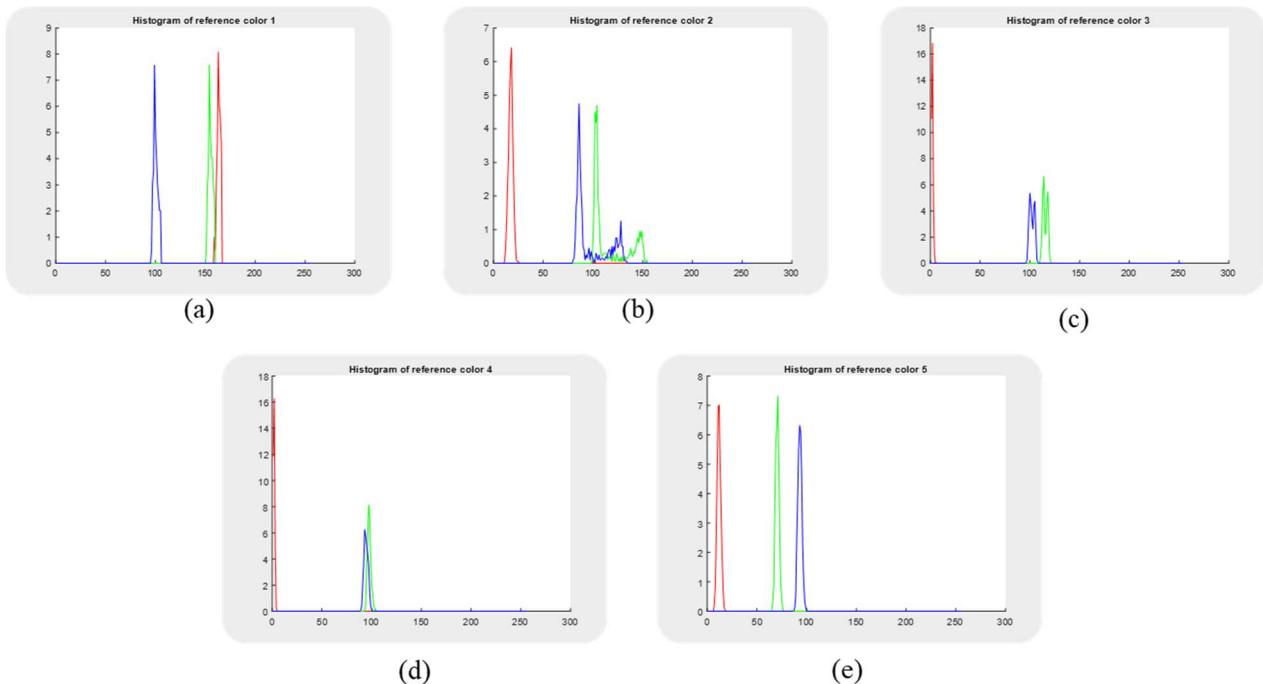


Figure 10 Histogram of standard color amonium-nitrogen (a. 0% b .2% c. 4% d .8% e. 16)

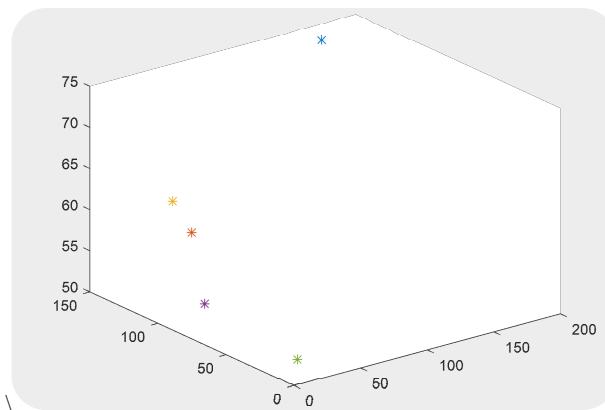


Figure 11 The plot of distance vector between the sample fertilizer solution and the standard color levels

Table 3 Classification results comparison between human and Histogram comparison method

Sample No	Expertise					Histogram comparison				
	a	b	c	d	e	a	b	c	d	e
Urea fertilizer (46-0-0)										
1	1	1	2	2	3	1	1	2	2	3
2	1	1	2	2	3	1	1	2	2	3
3	1	1	2	2	2	1	1	2	2	2
4	1	1	2	2	3	1	1	2	2	3
5	1	1	2	3	3	1	1	3	3	3
6	1	1	2	2	2	1	1	2	2	2
7	1	1	2	2	2	1	1	2	2	2
8	1	1	2	2	3	1	1	2	2	2
9	1	1	2	2	3	1	1	2	2	3
10	1	1	2	2	3	1	1	2	2	2
Mixed fertilizer (13-13-13)										
1	5	3	1	4	4	5	3	1	4	4
2	5	3	1	4	4	4	3	1	4	4
3	4	3	1	4	4	4	3	1	4	4
4	4	4	1	5	4	4	4	1	5	4
5	5	3	1	4	4	4	4	1	4	3
6	4	3	1	4	3	4	4	1	4	4
7	5	3	1	4	3	5	3	1	4	3
8	5	3	1	5	3	5	3	1	5	3
9	4	3	1	4	3	4	3	1	4	3
10	4	3	1	4	4	4	3	1	4	4
Mixed fertilizer (16-16-16)										
1	5	4	1	5	4	5	5	1	5	4
2	5	4	1	5	4	5	5	1	5	4
3	5	5	1	4	4	5	5	1	4	4
4	5	5	1	4	3	5	5	1	4	4
5	4	4	1	5	4	5	5	1	5	4
6	5	4	1	5	4	5	4	1	5	4
7	4	5	1	5	3	4	5	1	5	4
8	5	4	1	5	4	5	4	1	4	4
9	4	5	1	5	3	4	5	1	5	3
10	4	5	1	4	4	4	5	1	4	4
Mixed fertilizer (9-25-25)										
1	5	1	1	5	4	5	1	1	5	4
2	5	1	1	4	3	5	1	1	4	4
3	5	1	1	5	3	4	1	1	5	4

Sample No	Expertise					Histogram comparison				
	a	b	c	d	e	a	b	c	d	e
4	5	1	1	4	3	4	1	1	5	4
5	4	1	1	4	3	4	1	1	5	4
6	4	1	1	4	3	4	1	1	5	4
7	4	1	1	4	4	4	1	1	5	4
8	5	1	1	4	4	5	1	1	5	4
9	4	1	1	5	4	4	1	1	5	4
10	5	1	1	5	4	5	1	1	5	4

Table 4 The performance of proposed methods

Techniques	Accuracy			
	True		Error	
	N	%	N	%
Sampling	117	58.5	83	41.5
Histogram comparison	178	89	22	11

Conclusion

This research proposed the simple image processing method which apply to nutrient detection in the fertilizer from chemical reaction. The use of image processing techniques in the verification of fertilizer formulations is reliable and can be pre-tested at low cost before the laboratory and used a shorter time to verify. Additional, it is useful for checking the quality of fertilizers. Including the detection of counterfeit products. The use of histogram was found to be reliable and closer to human-eye results than the sampling technique when the sampling technique was facing more tolerance. The tool implemented in the research can be used as a model for further development.

Acknowledgment

This study was financially supported by the RMUTT research fund grant number NRF62D0603. Researcher would like to thank Faculty of Science and Technology, Rajamangala University of Technology Thanyaburi for providing the infrastructure and support.

References

- Barros Azeredo, N. F., Ferreira Santos, M. S., Sempionatto, J. R., Wang, J., & Angnes, L. (2022). Screen-Printed Technologies Combined with Flow Analysis Techniques: Moving from Benchtop to Everywhere. *Analytical Chemistry*, 94(1), 250-268.
- Gavade, L. C. (2017). Detection of N, P, K using Fiber Optic Sensor and PIC Controller. *International Journal of Engineering Science and Computing (IJESC)*, 7(7), 3.
- HSL and HSV. In *Wikipedia*. (n.d.). from https://en.wikipedia.org/wiki/HSL_and_HSV.
- Ji, B., Wang, J., & Liu, W. (2016). Color-based automatic quality control for roasting chicken. *Computers and Electronics in Agriculture*, 123, 49-56.
- Kathong, S., & Ruangviriyachai, C. (2014). Determination of Nitrogen, Phosphorus and Potassium in Liquid Organic Fertilizer. *KKU Research Journal*, 14(4), 12.
- Khongpet, W., Yanu, P., Pecharee, S., Puangpila, C., Hartwell, S. K., Lapanantnoppakhun, S., Yodthongdee, Y., Paukpol, A., & Jakmunee, J. (2020). A compact multi-parameter detection system based on hydrodynamic sequential injection for sensitive determination of phosphate, nitrite, and nitrate in water samples. *Analytical Methods*, 12(6), 10.
- Kimura, M. (2018). *Testing methods for Fertilizers*, Japan: Administrative Agency Food and Agricultural Materials Inspection Center.

- Masrie, M., Rosli, A. Z. M., Sam, R., Janin, Z., & Nordin, M. K. (2018). Integrated optical sensor for NPK Nutrient of Soil detection. 1-4.
- Masrie, M., Rosman, M. S. A., Sam, R., & Janin, Z. (2017). Detection of nitrogen, phosphorus, and potassium (NPK) nutrients of soil using optical transducer. 1-4.
- Nagul, E. A., Mckelvie, I. D. Worsfold, P., & Kolev, S. D. (2015). The molybdenum blue reaction for the determination of orthophosphate revisited: Opening the black box. *Analytica Chimica Acta*, 890, 60-82.
- Panyaying, C., Kanna, M., & Somnam, S. (2017). The Determination of Available Phosphorus in Soils Using an Economic Hydrodynamic Sequential Injection System. *Journal of Science and Technology*, 25(1), 124-136.
- Phansi, P., Koin, J., & Nacapricha, D. (2020). Determination of Phosphate in Surface Water of Lopburi Province Using a Simple Flow Injection Analytical System. *RMUPT Research Journal Science and Technology*, 14(2), 122-134.
- Ramane, D. V., Patil, S. S., & Shaligram, A. (2015). Detection of NPK nutrients of soil using Fiber Optic Sensor. *International Journal of Research in Advent Technology (no. Special Issue) National Conference “ACGT 2015”*.
- Somnam, S., Motomizu, S., Grudpan, K., & Jakmunee, J. (2014). Hydrodynamic sequential injection with stopped-flow procedure for consecutive determination of phosphate and silicate in wastewater. *Chiang Mai Journal of Science*, 41(3), 606-617.
- Shaik, K. B., Ganesan, P., Kalist, V., Sathish, B. S., & Jenitha, J. M. M. (2015) Comparative Study of Skin Color Detection and Segmentation in HSV and YCbCr Color Space. *Procedia Computer Science*, 57, 41-48.
- T. B. R. Company. (2019). *Chemical Fertilizers Market by Segments (Nitrogen Fertilizers, Phosphate Fertilizers, Potash Fertilizers), By Types, By Countries and By Key Players – Global Forecast to 2022*. Retrieved May 2020, from <https://www.thebusinessresearchcompany.com/report/chemical-fertilizers-market>.
- Taylor, E., Bonner, J., Nelson, R., Fuller, C., Kirkey, W., & Cappelli, S. (2015). Development of an in-situ total phosphorus analyzer. In MTS/IEEE Oceans '15, Washington, D.C.
- Wabali, V. C., Esiri, A., & Zitte, L. (2017). A sensory assessment of color and textural quality of refrigerated tomatoes preserved with different concentrations of potassium permanganate. *Food Science & Nutrition*, 5(3), 434-438.
- Yadav, S., & Nain, N. (2015). Fast Face Detection Based on Skin Segmentation and Facial Features. 663-668.

Air Dust Level Detection Real-Time Online Monitoring

Prasert Nonthakarn*

*Faculty of Science and Technology, Rajamangala University of Technology Srivijaya
Nakhon Si Thammarat, Thailand*

** Corresponding email: prasert.n@rmutsv.ac.th*

Abstract

This article presents the development of real-time online airborne dust level monitoring system to facilitate notification and reporting of pollution and airborne dust conditions, which are the main problems and are likely to be increasing in Thailand. The developed system works using a microcontroller for receiving and processing signals from sensors. The microcontroller then sends wi-fi data to the cloud to store and display data. The system can display data through multiple channels including Google sheet, LINE application, mobile dashboard, and PC dashboard. Besides that, the system can measure and alert dust levels for all three sizes of dust: PM1.0, PM2.5 and PM10. The system tested by installing a set of meters at 11 different points in Thung Song Municipality. The system's performance showed that it was able to accurately measure and transmit data accurately without errors.

Keywords: dust, monitoring, real-time, dust level monitoring, PM2.5

Introduction

Now a day economic development Social and environmental changes affect the environment and ecosystems. From the Environmental Pollution Situation Report in Thailand, it was found that air pollution is a major problem especially the problem of dust. The problem of pollution from smog in the North and the South, including Bangkok and the perimeter tends to occur more frequently and more widely. This problem causes impacts on the health of people in the area both in the short term and in the long term. International organizations and Thailand by the Ministry of Natural Resources and Environment and the Ministry of Public Health have given importance to Because there is clear academic evidence to support that small dust particles cause impact on public health including respiratory diseases; pneumonia chronic obstructive pulmonary disease Cardiovascular disease, cancer, and maternal and child health and the results from the WHO reported in March 2014. Each year, 7 million people die from air pollution worldwide (1 in 8 deaths worldwide).

In Thailand, the definition of dust is defined as Total Suspended Particulate (TSP), which is a large dust with a diameter of 100 or less. The fine dust (PM10) refers to dust with a diameter of 10 microns or less. Particulate matter was Bangkok's number one pollution problem in 1998. The World Bank funded a study on health impacts, with levels of severity similar to studies from cities across the country. The level of microscopic dust can cause 4,000 to 5,500 premature deaths in Bangkok every year. Hospitalizations were also found to be associated with small particulate matter and economic assessments. Shows that if the amount of PM10 in the atmosphere can be reduced by 10 microns, it will reduce the health impact amounting to 35,000 – 88 billion baht per year Kaosa-ard and Pednekar (1996). Therefore, relevant agencies must work together to solve the problem at the source of pollution as well as contaminating the environment and protecting public health from the hazards of air pollution by relying on environmental and health surveillance in operations to point out the situation of air pollution problems and health impacts. Lead to communication, warning and problem-solving management Querol et al., (2019), Okokpujie et al., (2018), Duangsuwan et al., (2018), Taştan and Gökozan (2019), Liu et al., (2011), Bhattacharya et al., (2012), Kumar and Jasuja (2017), Mansour et al., (2014), Arroyo et al., (2019), Benammar et al., (2018).

From the importance and problems mentioned above. The research team has the idea to create a dust level monitor in the air all the time. which will be displayed through the Internet In designing such a system, the researcher divided two main components is the part of the Real-Time system that displays current information and sensor control system This is a work in the form of an Internet of Things technology system that is a wireless data connection using various sensors to measure air quality such as a dust sensor when the sensor is measured, it sends the data to the cloud. and will be displayed in the Real-Time system through the application of the smartphone and display the results on the computer for speed and convenience for users can see the difference of the weather and dust through the Internet.

Methodology

There will be a total of 8 steps in conducting research, the details of which are as follows.

A. System design

Find information on the components required to measure dust levels and weather conditions as shown in Figure 1. These include topography, precipitation, and wind speed. including the suitability of measurements during different time periods and design tools suitable for the area. Including the installation point, the installation area ease of collection device security by designing various equipment to be suitable for the area. The design uses 1 set of sensors, including a dust sensor PM1.0 PM2.5 PM10. There is a set to collect and process various values and control the reporting system and alert when the value is overdue as shown in Figure 1.

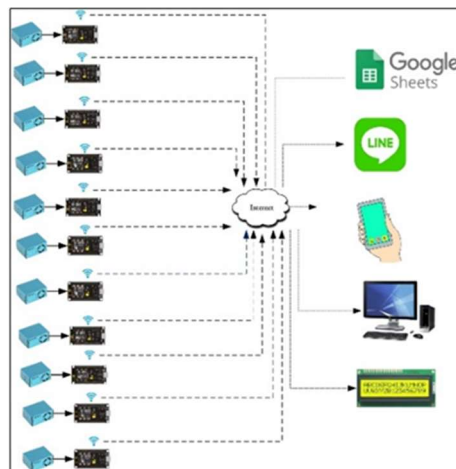


Figure 1 System components

B. Install system

Bring all the equipment to install in the area. The unit consists of a sensor, a data monitoring and data collection unit, a processing part, a display unit, as shown in Figure 2.



Figure 2 System unit

C. Generate code

Write system commands to receive values, display values, store data, and alert, as shown in the example program in Figure 3. The sensor transmits the dust amount data and sends the data to the processor. The processor sends the data to the air quality reporting and alerting suite to function as designed.



Figure 3 Example program

D. Trial

The experiment will use a real on-site experiment. As shown in Figure 4. The operation of the system to test and use it to find faults. To bring the problem to be ready for use. The trial period will be 1 week to observe the work for example, is the humidity correct and appropriate? Are the dust values sent directly, and correct? The data was calibrated with the DustBoy dust meter of Chiang Mai University.



Figure 4 System test

E. Improve

Solve problems to be ready for use using data from the experiment. After improvement, it will be tested for about 1 week to check the integrity of the entire system of the program and hardware system.

F. Operate the system

This step is a step to use the actual system. actual use by collecting information such as the resulting amount problem including the integrity of the display and notification

G. Summary of use

Summarize the collected data and compare.

Experimental Results

Installation in the work of the system will be installed at 11 points in Thung Song Municipality, Thung Song District, Nakhon Si Thammarat Province. The installation point is shown in Figure 5.



Figure 5 Installation location

A. LCD display

The values shown in the installation box are displayed by LCD by showing 4 values, namely temperature value, PM1.0 dust value, PM2.5 dust value and PM10 dust value as shown in Figure 6.



Figure 6 LCD Display

B. Units Google sheets display

The values are displayed and stored in Google sheets by showing 4 values, date and time, PM1.0 dust value, PM2.5 dust value and PM10 dust value, AQI value, daily average, temperature value and display graph. Shown as shown in Figure 7.

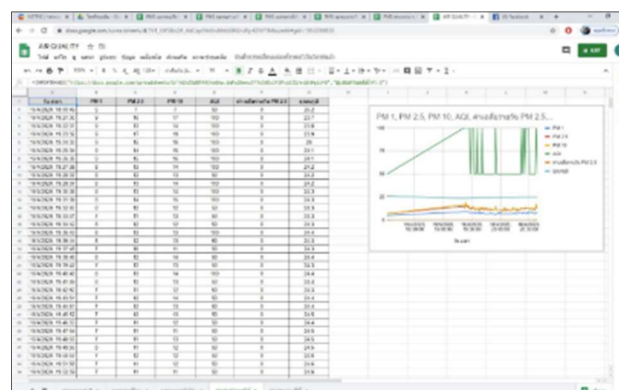


Figure 7 Google sheets displayed

C. Dashboard display

The values displayed on the computer dashboard display 4 values, date and time, PM1.0 dust value, PM2.5 dust value and PM10 dust value, AQI value, daily average, temperature value as shown in Figure 8.

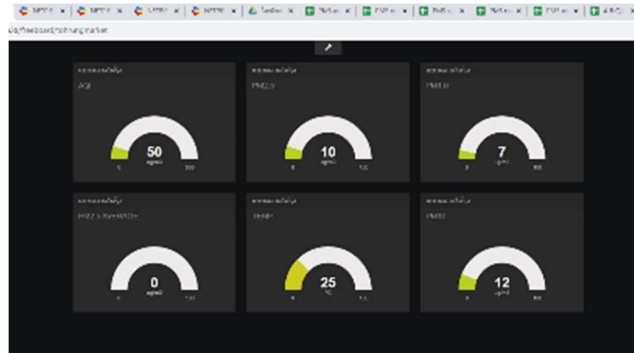


Figure 8 Dashboard display values

D. Mobile dashboard display

The values displayed on the smartphone dashboard display 4 values, date and time, PM1.0 dust value, PM2.5 dust value and PM10 dust value, AQI value, daily average, temperature value, shown in Figure 9.

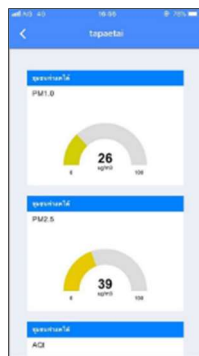


Figure 9 Dashboard smartphone display

E. LINE application warning

Values that display alerts in the LINE application via computers and smartphones. by showing a warning when the PM1.0 dust value, PM2.5 dust value and PM10 dust value, the temperature is too high, which is used by the Pollution Control Department that set the dust value not more than 50 PPM as shown in Figure 10.

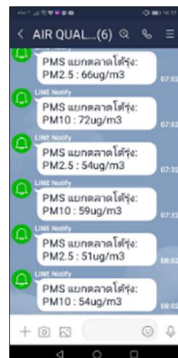
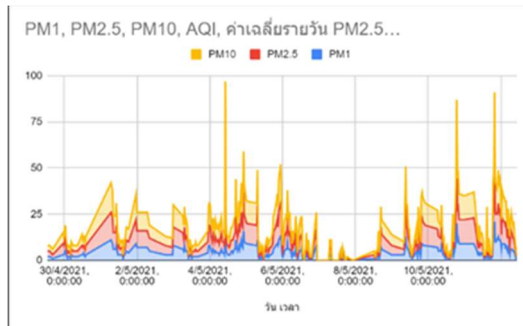


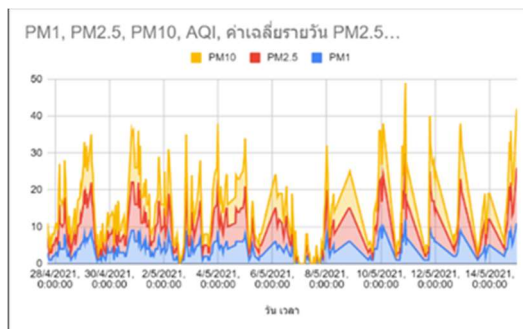
Figure 10 LINE application warning

Summarize the results and discuss

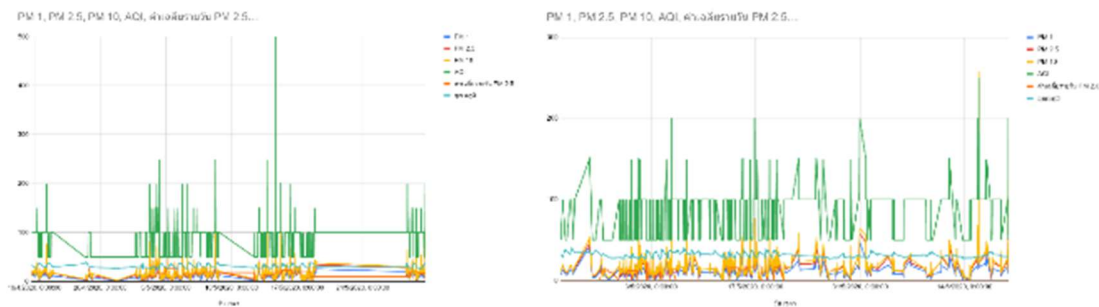
From the experimental results, the air quality numerical data were collected for a period of 1 month, then compared and the data collection quality was consistent. The values obtained from the system are functional, they are consistent with standard toolkits. Data transmission with data transmission at a preset time no data loss as shown in Figures 11-20.



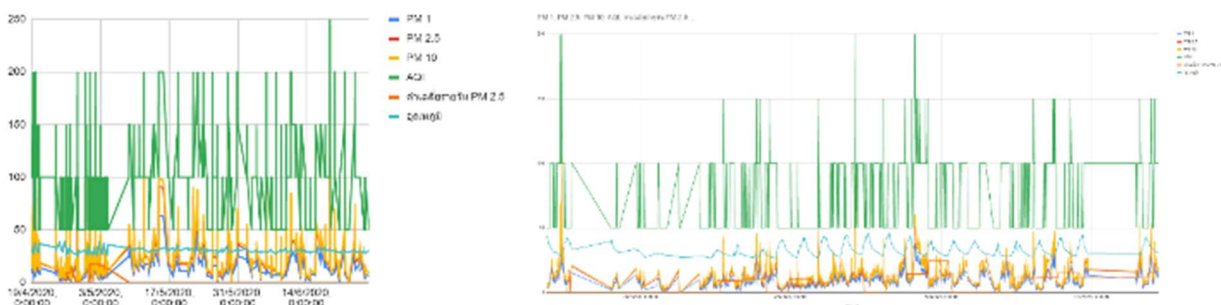
Figures 11 Strategic Community



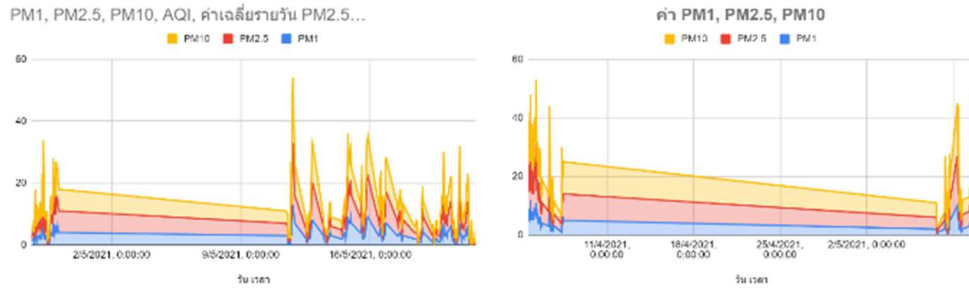
Figures 12 Chai Chumphon Intersection



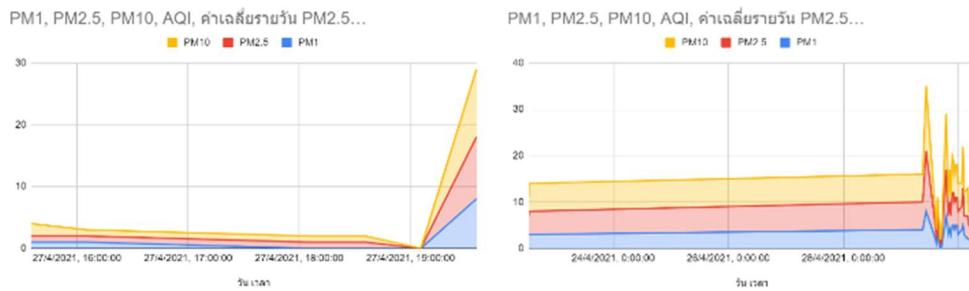
Figures 13 the data collection1



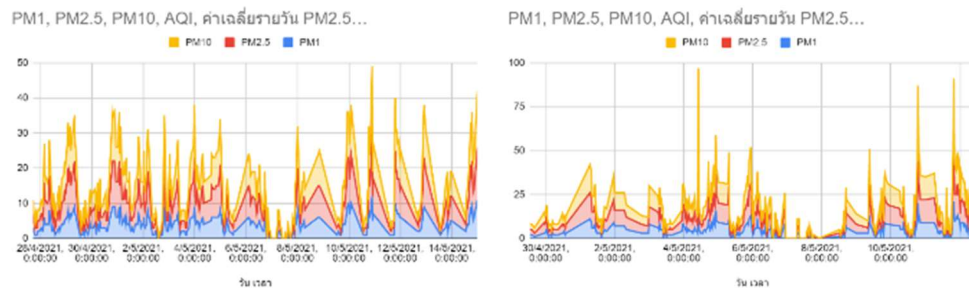
Figures 14 the data collection2



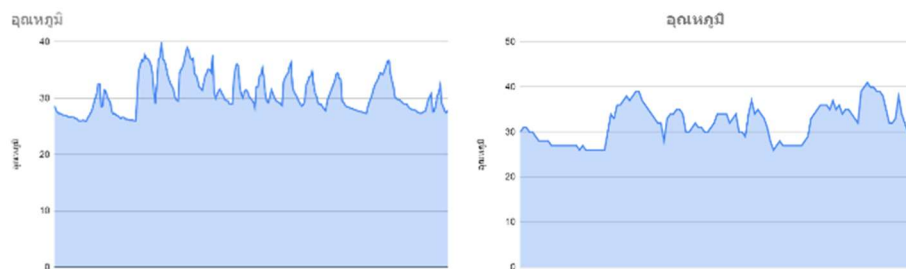
Figures 15 the data collection3



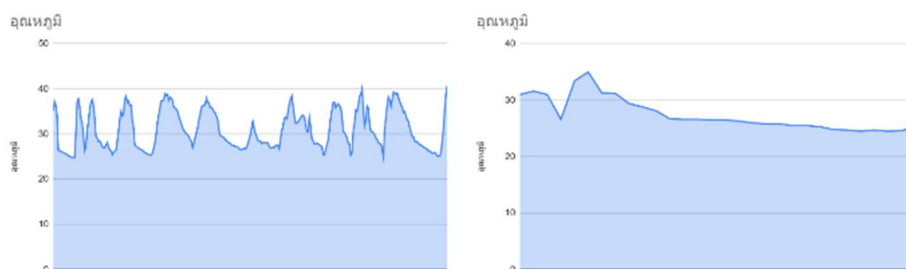
Figures 16 the data collection4



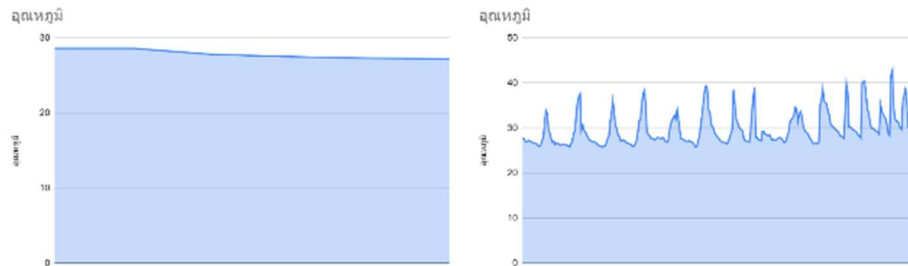
Figures 17 the data collection



Figures 18 the data collection5



Figures 19 the data collection6



Figures 20 the data collection7

Acknowledgment

Thank you to Thung Song Municipality for supporting the budget for all projects.

References

- Arroyo, P., Herrero, J. L., Suárez, J. I., Lozano, J. (2019). Wireless Sensor Network Combined with Cloud Computing for Air Quality Monitoring. *Sensors*, 19, 691.
- Benammar, M., Abdaoui, A., Ahmad, S. H. M., Touati, F., Kadri, A. (2018). A Modular IoT Platform for Real-Time Indoor Air Quality Monitoring. *Sensors*, 18, 581.
- Bhattacharya, S., Sridevi, S., & Pitchiah, R. (2012). *Indoor air quality monitoring using wireless sensor network*. 2012 Sixth International Conference on Sensing Technology (ICST). pp. 422-427.
- Duangsuwan, S., Takarn, A., Nujankaew R., & Jamjareegulgarn, P. (2018). *A Study of Air Pollution Smart Sensors LPWAN via NB-IoT for Thailand Smart Cities 4.0*. In 2018 10th International Conference on Knowledge and Smart Technology (KST), pp. 206-209.
- Kaosa-ard, M., & Pednekar, S. (1996). *Environmmental Stratgy for Thailand*. Natural Resources and Environment Program, Thailand Development Research Instute, Bangkok, Thailand.
- Kumar, S., & Jasuja, A. (2017). *Air quality monitoring system based on IoT using Raspberry Pi*. 2017 International Conference on Computing, Communication and Automation (ICCCA). pp. 1341-1346.
- Liu, J., et al. (2011). *Developed urban air quality monitoring system based on wireless sensor networks*. Fifth International Conference on Sensing Technology. pp. 549-554.
- Mansour, S., Nasser, N., Karim, L., & Ali, A. (2014). *Wireless Sensor Network-based air quality monitoring system*. 2014 International Conference on Computing, Networking and Communications (ICNC). pp. 545-550.
- Okokpujie, K. O., Noma-Osaghae, E., Odusami, M., John, S. N., & Oluga, O. (2018). A Smart Air Pollution Monitoring System. *International Journal of Civil Engineering and Technology (IJCIET)*, 9(9), 799-809.
- Querol, X., Tobías, A., Pérez, N., Karanasiou, A., Amato, F., Stafoggia, M., Pérez García-Pando, C., Ginoux, P., Forastiere, F., Gumy, S., Mudu, P., & Alastuey, A. (2019). Monitoring the impact of desert dust outbreaks for air quality for health studies. *Environment International*, 130, 104867.
- Taştan, M., & Gökozan, H. (2019). Real-Time Monitoring of Indoor Air Quality with Internet of Things-Based E-Nose. *Appl. Sci.*, 9, 3435.

The Impact of Mobile Applications on Improving an Organizational Personnel Performance

Chanchai Choksamai and Benjaporn Meeprom*

*Department of Western Languages, Faculty of Liberal Arts, Rajamangala University of Technology
Thanyaburi, Pathum Thani 12110, Thailand
* Corresponding email: benjaporn@rmutt.ac.th*

Abstract

This paper presents the impact of a customized mobile application on organizational personnel performance. Even though the performance review system is considered as one of the challenges for several firms regardless of size, many changes have been possible by the development of information and communication technology. Mobile applications become one of the most concerned and rapidly developing areas as it has harmonized as a basic essential for daily life, especially urban lifestyles. For these reasons, this study aimed at evaluating the impact of using mobile applications in optimizing personnel performance in the Thai local workplace where uses the English language as the communication medium. A questionnaire investigating the users' attitudes and experiences towards the mobile application was employed for the data collection, followed by a focus-group interview. The data was then analyzed using descriptive statistics and theme coding. The findings revealed that the targeted personnel group highly used the mobile application for work collaboration such as gathering clients' information, creating a project, and tracking a project as well as welfare supports such as applying for a leave request. Most employees informed the use of the mobile application more than four times a day, in different periods yet most frequently at night. The majority of the personnel agreed that overall features created better and clearer internal communication at a very high level. The application allowed ease of workflow while being flexible for task-related needs anywhere and anytime so that they accomplished the goals efficiently throughout the work-from-home protocol during the COVID-19 pandemic. The enhancements of its advantages as a corporate-supporting platform and as a data collection tool for practical utilization in a particular work setting in relation to certain challenges regarding time, location, technical support, and appropriate components are discussed.

Keywords: Mobile application, Personnel performance, English for specific purposes

Introduction

In the modern age of information and communication systems, personnel are habituated to use computers and computer applications. But mobile application use and development is a new and rapidly growing sector. There is a global positive impact of mobile applications. Using mobile applications are becoming facilitate for personnel or organization are upgrading themselves. By the way, contemporary information systems are based on database technology as a collection of logically related data and DBMS as a software system that allows users to define, create, maintain and control access to the database. The process of constructing such a kind of system is not so simple. It involves the mutual development of application programs and databases. The application program is actually the bridge between the users and the database, where the data is stored. Thus, the well-developed application program and database are very important for the reliability, flexibility and functionality of the system. These so-called systems differentiate from each other and their development comprises a great variety of tasks to be resolved and implemented.

Information system suggests a technology be used in order to provide information to users in an organization, as for the purposes of data transformation into useful information, computer hardware and software are designed and used. A particular case is the organizational process systems. This kind of system is responsible for storing data of the staff within the organization and generating reports upon request (Kancha, 2006). In the development of organizational process systems, the personnel performance in a company is needed to achieve personnel performance itself and also for the success of the company. Improving the performance of these employees is not only beneficial for the company, but also for the personnel themselves. Because with good performance, can theoretically achieve a better level of personnel career development (Sunandha, 2016).

Furthermore, according to (Studer, 2016), the personnel performance process is essential in the application of management specifically for planning, organizing, directing, and supervising personnel activities in order to achieve organizational goals. Nevertheless, numerous organizations have been trying to create a proper and systematic process in order to increase efficiency and productivity. It involves system plans by which all units are harmonized and consequently, effective communication in the organization is guaranteed. The organizational process is the means of strategy implementation for achieving desired goals and the necessity of flexibility for compatibility with the changing world is unavoidable (Englehardt and Simmons, 2002).

The Organizational Personnel Performance

Organizational personnel performance is defined as the generation, promotion and realization of new ideas in processes, which is different from the concept of creativity which only focuses on the generation of new and useful ideas (Janssen et al., 2004). The general presumption is that personnel improving the performance is always beneficial in order to do things better and are considered as an important source of an organization’s competitive advantage (Anderson et al., 2014). This is why most studies have focused on identifying factors that promote organizational personnel performance.

Janssen et al. (2004) gave an overall theoretical model of the positive sides (e.g., constructive conflict, performance improvement, positive job attitude, and well-being) and negative sides (e.g., destructive conflict, lowered performance, negative job attitude, and stress) of individual innovation, for example, Ariely and Gino (2012) found that a creative personality and a creative mindset could lead to an unethical performance by promoting an individuals’ ability to justify their performance.

Moreover, a meta-analysis from Harari et al. (2016) showed that improving the organizational personnel performance was positively related to task performance and organizational citizenship performance and negatively related to counterproductive work performance. The theoretical and empirical evidence in the literature shows that improving the organizational personnel performance is not always beneficial, sometimes gain profits, and other times pay the price, for engaging in innovative activities, they also have some hidden costs or damages. As mentioned by Anderson and Gasteiger (2008), innovation has a dysfunctional aspect, which is always less visible, but has surfaced repeatedly across empirical studies. If it is not correctly managed, then it can potentially be seriously harmful to individuals, work teams and even to the organization. The impact of the organizational personnel performance on personnel relationship conflict could have an influential effect on personnel themselves and on their in-role performance as evaluated by their supervisors. This is important for organizations in order to know how to efficiently manage personnel performance (Janssen et al., 2004).

Technological Advancement Overview

Technological advancement is the process of combining and reorganizing knowledge to generate new ideas. The development of technology has an impact on firm performance (Mumford, 2000). Technological advancement comes from internal advancement (Pavitt, 1990) and internal advancement comes from personnel capability. So, there is a close relationship between technological

advancement and personnel performance (Huselid, 1995). Technologies can only lead to increased productivity or improve performance when combined with other resources effectively and use technology productively and ethically (Akingbade and Dauda, 2011).

Technological advancement makes personnel more effective and firmer more efficient. Technological advancement can improve firm performance as well (Deng and Li, 1999). Personnel can more rapidly acquire new knowledge and further advancement competencies (Bassock et al., 1989). The motivation of the personnel has a direct influence on technological advancement (Amabile and Hennessey, 1998). The personnel performance is closely linked with technological advancement. Technological advancement can be managed effectively through personnel. Resource-based theory suggests that a firm’s resources are extremely important for the firm’s development and that human capital is a key resource of a firm. The function of this resource depends on the personnel’s ability and enthusiasm (Mumford, 2000).

Technological advancement has an enormous influence on personnel performance (Gulati and Nohria, 1996). Technological advancement is an important factor influencing the improvement of performance (Hitt et al., 1997). Most of the studies have repeatedly shown a positive relationship between a firm’s technological advancement, performance and concluded that technological advancement is important for personnel performance. Foster (1986) presented the comparison between non-technology instruments and digital-age instruments.

Non-Technology Instruments	Digital-Age Instruments
One-size-fit-all-instruments	Personalized optimizing and flexible resources for individuals’ needs
Advancement based primarily on time spent in workplace	Advancement based on the implementation and how personnel can improve the performance they have utilized
Fixed places and times for optimizing within workplace building	Anywhere and anytime optimizing both inside and outside workplace
Paper printed, static text, often out of date for the personnel performance resources	Digital content which provides interactive, flexible and also updated resources

Figure 1 Comparison of Non-Technology Instruments and Digital-age Instruments

Mobile Applications Overview

Mobile Applications is a very important role in mobile devices as they provide immense functionalities that will carry out useful purposes. Nowadays, mobile application development is becoming very competitive in the market because the creation of mobile applications has much of its roots in traditional software development. To make sure of the efficiency of your application in a certain complex scenario, an approach is needed to be followed to make a successful application development. Essentially mobile applications can be classified into two groups are native and web. A native mobile application is an application designed to run on a specific operating system of a mobile device.

In turn, a web mobile application consists of common Internet application that resides on a server and could be accessed via the Internet. Every time the application is executed, it is downloaded and processed locally. Moreover, it is an application designed to fit the screens of most mobile devices and written as web pages using languages supported by browsers, like HTML, CSS and JavaScript. For this reason, this kind of applications can be accessed from any device that has internet access and a compatible browser.

The major disadvantages of web applications compared to the native is related to the poorer user experience. Because access to physical resources of the device (e.g., buttons, GPS or camera) is limited, the performance, responsiveness and even the look and feel offered are lower than those offered by native applications. On the other hand, the greatest advantage of web applications is the lower cost of development, deployment and maintenance (Charland and LeRoux, 2011). These are system components of a web mobile application used in this study.

User Profile Management

With the structured representation of an individual user’s characteristics and personal preferences with respect to a software application or computing device, the variety and complexity of applications and mobile devices increase, there is a growing need and interest in personalization. This necessitates methods of managing user profile content such that it can be accessed, updated and potentially shared over communication networks (Daniel, Elhadi and Zhongxu, 2010).

Customer Relationship Management

The business approach integrates people, processes and technology to maximize relationships with customers (Goldenberg, 2008). Also, it is the core business strategy that integrates internal processes and functions and external networks. Moreover, it has been asserted that customer relationship management “characterizes a management philosophy that is a complete orientation of the company toward existing and potential customer relationships” (Ajami et al., 2008).

Management Information System

The system that converts data into information is communicated in an appropriate form to managers at levels of an organization. The information can contribute to effective decision making or planning to be carried out (Patterson, 2005). Also, basically involves the process of collecting, processing, storing, retrieving and communicating the relevant information for the purpose of efficient management operations and for business planning in any organization. Thus, the success of effective decision-making is considered as the heart of the administrative process, is highly dependent partly on available information and partly on the functions that are the components of the process (Badgujar and Nath, 2013).

Project Tracking System

The planning, organizing, directing and controlling of company resources for a relatively short-term objective that has been established to complete specific goals and objectives. Project tracking system is an application of knowledge, skills, tools and techniques to project activities to meet project requirements. A project tracking system is accomplished through the use of the processes such as: initiating, planning, executing, controlling and closing. The term project tracking system is sometimes used to describe an organizational approach to the management of ongoing operations also referred to as management by projects. In the same many aspects of ongoing operations are treated as projects so as to apply the project tracking system practices easily to them (Kerzner, 2003).

Content Management System

The application allows to publish, manage, edit, delete and modify content in a very effective and dynamic way. This system also organizes the content in a very easy way where end-users can access and operate very easily without prior knowledge of this system. Through this system, an editor has the ability to post articles or web pages using any desktop system and also by using small devices like mobile devices and tablets (Sunandha, 2016).

Note Taking System

The useful external memory device in today’s world. Utilized broadly across professional, academic and personal spheres, the note taking system has demonstrated its role as a systematic cue and aid for retention (Kiewra, 1989). As a practical way to capture information from a transient source, a note-taking system affords a medium to preserve semantic and episodic information, going beyond the limited information processing capacity of working memory alone (Miller, 1956).

Usability of Mobile Applications in Workplace

Nielsen (1993) defines the usability of a system to meet the needs of the users. He does not consider this to be part of usability but a separate attribute of a system. If a product fails to provide utility then it does not offer the features and functions required, the usability of the product becomes superfluous as it will not allow the users to achieve their goals. Likewise, the International Organization for Standardization (ISO) defined usability as the “extent to which a product can be used by specified users to achieve specified goals with effectiveness, efficiency and satisfaction in a specified context of use” (ISO/IEC, 1998). The usability of mobile applications impacts performance, culture and the structure of the company itself (Meeker et al., 2010). Some people believe that mobile applications improve communication, thus, will have a positive impact on their work. Others think that episodic devices used at the workplace will distract them from their jobs, which negatively influence their productivity.

Attributes of Usability	
Efficiency	Resources expended in relation to the accuracy and completeness with which users achieve goals
Satisfaction	Freedom from discomfort, and positive attitudes towards the use of the product
Learnability	The system should be easy to learn so that the users can rapidly start getting work done with the system
Memorability	The system should be easy to remember so that the casual users is able to return to the system after some period of not having used it without having to learn everything all over again
Errors	The system should have a low error rate, so that users make few errors during the use of the system and that if they do make errors they can easily recover from them. Further, catastrophic errors must not occur

Figure 2 Attributes of Usability

Results and Discussion

Behaviors

The personnel behaviors in using mobile applications for improving their organizational performance give an indication on various areas. Fig. 3 depicts the motivation in using the mobile applications. Results indicated that all of the them or 100% use the mobile application for creating and tracking a project, followed by applying a leave form at 89% at a very high level also compared to other functions as below 50%. On the other hand, some functions were inappropriate with their works as the lowest number such as uploading a file or reading an article, as shown in Fig. 4 has been used for predicting the frequency in using the mobile applications along with their motivation. Result obtained shows that the users at 67% responded that they use the mobile applications approximately three to four times a day, followed by more than five times a day at 22%. Whereas, the rest of the users at 11% use the application one or two times a day. In addition, it is noted from Fig. 5 that refer

their preferences between time and location as preferred active time at night (21.00-04.59) and regularly use mobile applications in their housing or lodging

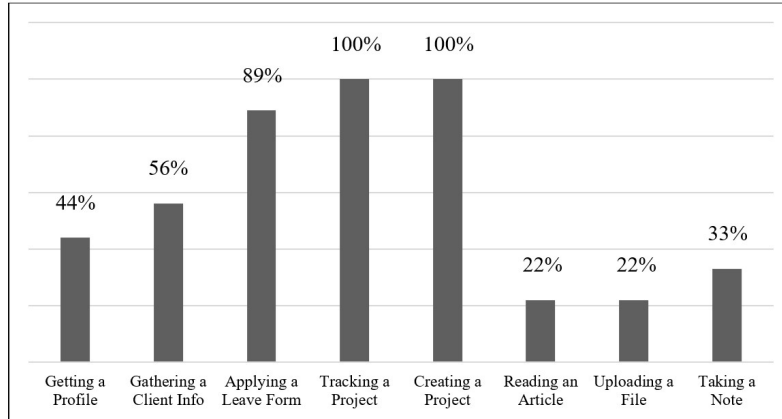


Figure 3 Motivation in Using the Mobile Applications

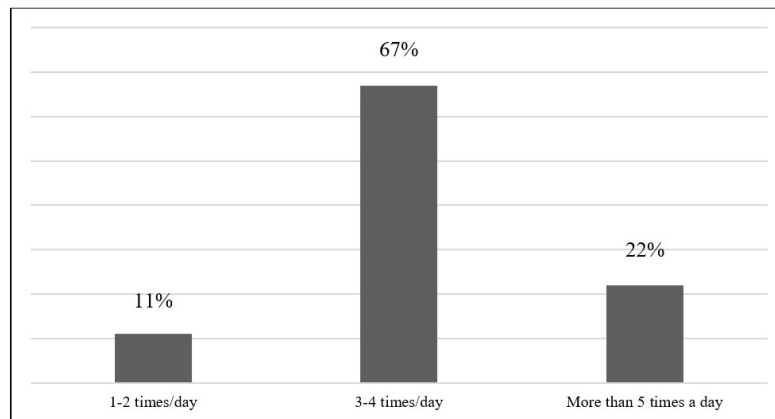


Figure 4 Frequency in Using the Mobile Applications

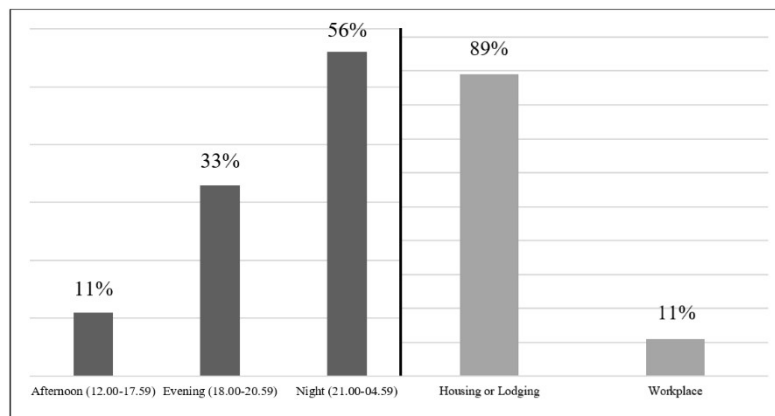


Figure 5 Time and Location Preferences

Mobile Applications’ Impact in the Personnel Perspective

Fig. 6 shows the impact of improving the organizational personnel performance. The analysis of personnel performance in this study is based on their attitudes and experiences, the majority of the

personnel agreed that overall features help them make a job easier with clear and understandable at a very high level.

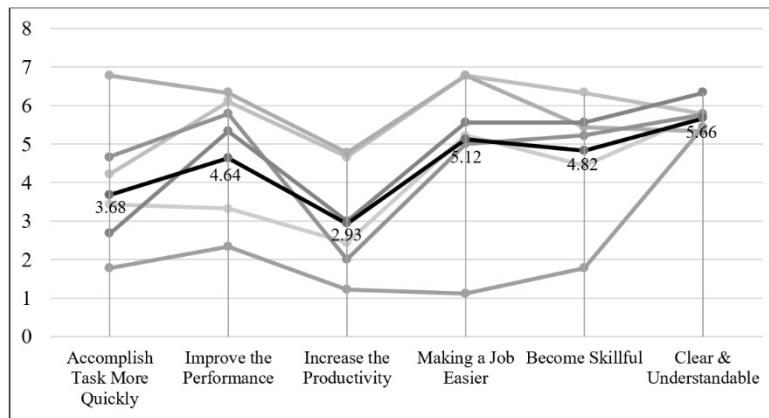


Figure 6 The Attitudes and Experiences in Using the Mobile Applications

Accomplish Task More Quickly

Technology spells progress for organizations. It speeds up antiquated systems, provides much-needed information, secures files, allows personnel to work from home or everywhere, saves your company time and encourages a positive community.

Improve the Performance

The performance processes are one of the most promising and relevant areas to support the mobile applications’ access in personnel to specify a viable performance solution for the in-charge administrator or senior consulting context.

Increase the Productivity

Mobile applications are providing opportunities to increase productivity, according to the findings of a study, revealed a direct correlation between personnel providing access to mobile applications and increased productivity. Also, believe that the company provides them with the technology needed to effectively perform in their role. The challenge of companies being able to afford advanced technologies and equipment is becoming less of an issue with the rise of Cloud computing and mobile devices, which eliminates capital costs and provides ready access to information and data. Providing personnel with the tools they need to succeed is a great first step in increasing productivity.

Making a Job Easier

The organization is not just storing their files securely but are using these solutions to organize, share, annotate, find, and retrieve them. In short, mobile applications automate the filing system. personnel can automate this task as well, indexing the items for easy search and retrieval later. Set up intelligent workflows, sending files through the motions so that the right people get their hands on them to approve, send back, make or modify the project easier.

Become Skillful

Technology is helpful to acquire relevant technical skills. There are many different tech skills that are applicable to technology-related works or jobs that use technology as mobile applications are important for tech management roles and positions where you work closely with others.

Fig. 7 presents that most users agreed that the Projects feature was the first thing that they use, followed by Leave Record features both of them were at a very high level. Also, the mobile

applications were beneficial for improving the organizational personnel performance in other ways. At the same time, some features such as Articles received less attention as they were considered less direct support to the personnel required performance even the articles were added by the executives to help enhance the employees’ new ideas that could apply to the ongoing work.

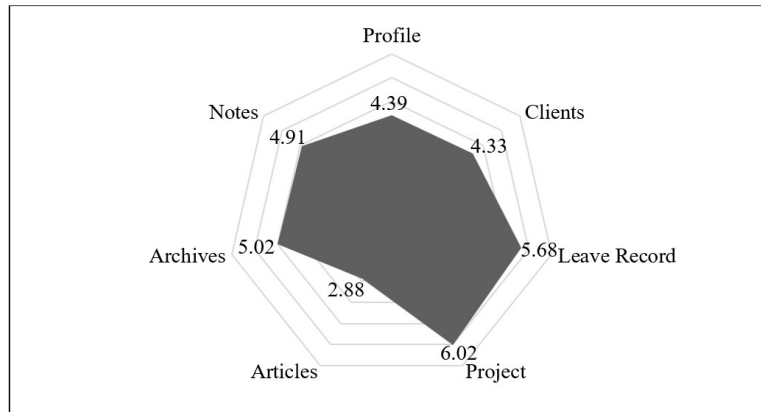


Figure 7 The Perspective in the Mobile Applications Features

Mobile Applications’ Impact in the Organization Perspective

Not only individuals or personnel, mobile applications also have a great impact on organization. The whole organization can be facilitated using the mobile applications. The efficiency of the mobile application is described below.

Save Time and Increase Productivity

In an organization, personnel can do their daily work like check a project, contact with business partner from any time in transportation, private car or walk. So, they leave no need to wait in a room or an office. By this way, the personnel can save time and increase time for work quality. The personnel’s productivity of society is increasing gradually.

Quick Communication

Some features like Notes which require small chatting platform and a comment system help the organization create a ubiquitous community that facilitates internal-organization communication and a practical collaboration. They can stay in touch where geographical distance is not a factor. So, the social relationship improves and make strong.

Improve IT Infrastructure and Job Vacancy

The uses of mobile applications improve the knowledge of people. Because they are accessing the Internet from everywhere. As a result, the IT infrastructure improves in the organization. As a matter of fact, the mobile applications development and mobile applications encourage a greater numbers of job vacancies in their organization or the society in a relevant IT field.

Sustainable Consumption and Production

When most of the personnel will use mobile applications for their daily simple work and getting facility from mobile applications, the computer uses will be less as well as the power consumption and the paper uses will be reducing the effect land pollution also consider the cost-saving.

There are so many other impact issues which all are ethically good for the organization. On the other hand, there are some bad impacts of mobile applications which are not ethically good for society. Those issues as beside the uses of mobile applications most of the people use mobile in

every place like transportation or office, somebody feels disturbed for them and frequently use of mobile is bad for health. Additionally, the organizations will also face different challenges (e.g., information overload, convincing personnel to use the mobile applications, security concerns) when adapting mobile applications into work routines. The adoption of mobile apps mainly depends on successful change management. Nevertheless, it is crucial to develop target-oriented mobile applications.

Limitation

The unavoidable limitations such as the limitation of time. There was also the limitation in selecting the users, the study was conducted only on a small number of users who attended personnel at a small-sized organization. To generalize the results, the study should involve more personnel from different organizations and include small-sized, medium-sized and large-sized organizations. Even though the application made a significant advance in improving the organizational personnel performance, the study found that the application use is still limited in the devices required only on mobile phones. Therefore, the various requirement for devices was very necessary in order to complete the study.

Conclusion

After all, the limitations of the organizational size and application devices requirement, the uses and popularity of mobile applications for improving the organizational personnel performance are increasing the personnel satisfaction and becoming a suitable tool for an efficient workflow. Most of the personnel are trying to use the mobile applications instead of desktops or illustrating the current shift away from paper-based for an easy task to new technology. The mobile applications are increasing the quality and functionality from previous work processes. So, the mobile applications are more capable and more usable for the personnel to continue using the mobile application. And the impacts of improving the organizational personnel performance on mobile applications are going high level.

References

- Ajami, A., Gargeya, V., Goddard, J., & Raab, G. (2008). Customer Relationship Management: A Global Perspective.
- Akingbade, A., & Dauda, Y. (2011). Technological Change and Employee Performance in Selected Manufacturing Industry in Lagos State of Nigeria: Australian Journal of Business and Management Research.
- Amabile, M., & Hennessey, A. (1998). Reward, Intrinsic Motivation and Creativity: American Psychologist (Vol. 53, pp. 674-5).
- Anderson, N., & Gasteiger, M. (2008). Helping Creativity and Innovation Thrive in Organizations: Functional and Dysfunctional Perspectives in Research Companion to the Dysfunctional Workplace: Management Challenges and Symptoms (pp. 422-440).
- Anderson, N., Potočnik, K., & Zhou, J. (2014). Innovation and Creativity in Organizations a State-of the Science Review, Prospective Commentary and Guiding Framework (Vol. 40, pp. 1297-1333).
- Ariely, D., & Gino, F. (2012). The Dark Side of Creativity: Original Thinkers Can be More Dishonest (Vol. 102, pp. 445-459).
- Badgular, M., & Nath, P. (2013). Use of Management Information System in an Organization for Decision Making. *ASM's International E Journal of Ongoing Research in Management And IT*, 2 (6), 160-171.
- Bassock, M., Chi, H., Glaser, R., Lewis, U., & Reitman, P. (1989). Self-Explanations: How Students' Study and Use Examples in Learning to Solve Problems (Vol. 13, pp. 145-82).

- Charland, A., & LeRoux, B. (2011). Mobile Application Development. *Web vs. Native*, 9(4), 20.
- Daniel, S., Elhadi, S., & Zhongxu, M. (2010). User Profile Management: Reference Model and Web Services Implementation (pp. 1-34)
- Deng, L., & Li, Y. (1999). A Methodology for Competitive Advantage Analysis and Strategy Formulation: An Example in a Transitional Economy, *European Journal of Operational Research* (Vol. 118, pp. 259-70).
- Englehardt, S., & Simmons, R. (2002). Organizational Flexibility for a Changing World. *Leadership & Organization Development Journal*, 23(3), 113-121.
- Foster, N. (1986). *Innovation: The Attacker's Advantage*, Summit Books, New York, The USA.
- Goldenberg, J. (2008). CRM in Real Time: Empowering Customer Relationships.
- Gulati, R., & Nohria, N. (1996). Is Slack Good or Bad for Innovation?: *Academy of Management Journal* (Vol. 39, pp. 245-64).
- Harari, B., Reaves, C., & Viswesvaran, C. (2016). Creative and Innovative Performance: A Meta-Analysis of Relationships with Task, Citizenship and Counterproductive Job Performance Dimensions (Vol. 25, pp 495-511).
- Hitt, A., Hoskisson, E., & Kim, H. (1997). International Diversification Effects on Innovation and Firm Performance in Product Diversified Firms: *Academy of Management Journal* (Vol. 40, pp. 767-98).
- Huselid, M. (1995). The Impact of Human Resource Management Practices on Turnover, Productivity and Corporate Financial Performance: *Academy of Management Journal* (Vol. 38, pp. 635-72).
- ISO 9241. (1998). Ergonomics Requirements for Office Work with Visual Display Terminals (VDTs) - Part 11: Guidance on Usability.
- Janssen, O., Van de Vliert, E., & West, M. (2004). The Bright and Dark Sides of Individual and Group Innovation: A Special Issue Introduction (Vol. 25, pp. 129-145).
- Kancho, K. (2006). *Employee Management System*. Växjö University, Småland, Sweden.
- Kerzner, H. (2003). *Project Management, A Systems Approach to Planning, Scheduling and Controlling*. John Wiley and Sons, New York, The USA.
- Kiewra, A. (1989). A Review of Note-Taking: The Encoding-Storage Paradigm and Beyond (Vol. 1, pp. 147-172).
- Meeker, M. (2010). Mobile Internet Will Soon Overtake Fixed Internet. Retrieved from. <https://gigaom.com/2010/04/12/mary-meeker-mobile-internet-will-soon-overtake-fixed-internet/>.
- Miller, A. (1956) The Magical Number Seven, Plus or Minus Two: Some Limits on Our Capacity for Processing Information (Vol.63, pp. 81-97).
- Mumford, M.D. (2000), *Managing Creative People: Strategies and Tactics for Innovation: Human Resource Management Review* (Vol. 10, No. 3, pp. 313-51).
- Nielsen, J. (1993). *Usability Engineering*. Academic press, California, The USA.
- Patterson, A. (2005). *Information Systems: Using Information. Learning and Teaching*.
- Pavitt, K. (1990). What We Know About Strategic Management of Technology: *California Management Review* (Vol. 33, pp. 17-126).
- Studer, S. (2016). Volunteer Management: Responding to the Uniqueness of Volunteers. *Nonprofit and Voluntary Sector Quarterly*, 45(4), 688-714.
- Sunandha, K. (2016). *Improving Data Efficiency Using Content Management System*. St. Cloud State University, Minnesota, The USA.

An Empirical Study of the Cross-Cultural Consumer Experience of a Pharmaceutical Shop During the Pandemic in the Retailing Setting

Gumporn Supasettaysa*, Phiraya Chetupong, Araya Buranakul, Viranpatch Asampinpongs, Piyapan Suwannawach, Tikumporn Kaewcheaknang and Parichat Chuanrakthum

Rajamangala University of Technology Phra Nakhon, 10300, Thailand

** Corresponding email: gumporn.s@rmutp.ac.th*

Abstract

The cross-cultural customer experience and the service environment were two of the most important aspects of retailing that should be prioritized, particularly in pharmacy shops. This research investigated the retail experience at the pharmacy store from the perspectives of people from a variety of diverse backgrounds and different geographical locations. The interview was planned and performed by the researcher using a semi-structured format. Participants were recruited from a variety of community-based pharmaceutical shop during the pandemic in the Bangkok areas. The researcher applied convenience sample with the assistance of the owner of the pharmaceutical shop. The analysis of the data were transcribed verbatim and analyzed for key themes via manual inductive coding and constant comparison. The research participants shared their personal experiences with purchasing drugs and associated items during the pandemic. They were also exposed to the store's atmosphere and sanitary environment. Misappropriation of retail space might be caused by dissatisfaction with the shopping experience. A variety of behavioral strategies that improved the retail experience, such as creating a dedicated section in the shop for relevant items or updating the in-store environment, may help improve the retail experience for customers. The authors provided suggestions for how retailers might use their newly acquired knowledge about consumer behavior. Each of these themes also offered the possibility of further investigation in the future.

Keyword: Customer experience, Cross-cultural examination Retailing, Pharmacy store, store's atmosphere

Introduction

Today it is increasingly changing business environment. Cultural concerns are widely acknowledged as critical components of a successful healthcare and pharmaceutical business. Recognize the importance of cultural competency in the profession of pharmacists. Pharmacists facilitate the ways how cultural divides helping pharmacists practice medicine so that the customer would have been delivered the proper response from the retail store. The pharmaceutical store's committed to providing healthcare to the communities they serve would be incomplete if they ignore considering the cultural aspects that influence the lives of patients or customers (Zweber, 2002). Bassett-Clarke et al. (2012) mentioned that the customers said that their healthcare experiences were highly variable and that the different local pharmacist did not meet their expectations in terms of health care. The communication styles of the pharmacists were found to impact severely on health, help-seeking, and medicines-taking behavior.

According to common thinking, customer experience refers to customers' internal and subjective reactions to every interaction with a company (Voss, 2010). Pine and Gilmore (1998) explain that experiences are inherently personal, existing only in the consciousness of an individual who has been involved on an emotional, physical, intellectual, or even spiritual level. Customers experience whenever they "contact" any component of a product, service, brand, or organization.

Customers have interactions across various channels and at a variety of points in time (Pantano and Milena, 2015). Touchpoints are interactions between businesses and consumers that occur multiple times along the customer's journey. These moments have a tremendous impact on both the consumer experience and the brand's impression. Businesses may take advantage of fair chances to enhance their client journey.

In today's economic context, cross-cultural marketing is essential to success. Cross-cultural marketing offers a new, more complicated, and sophisticated solution to the considerable challenges that traditional marketing strategies face during a pandemic and the company's ability to generate profits during the crisis and afterward. Clark (1990) and others suggest that different behavior characteristics are unique and consistent over time. They also find that these cross-cultural differences in strategy affect the negotiations' process and outcomes. These distinct behavior are a result of common cultural norms, beliefs, and acquired behaviors across geographic. Because of this, it is an essential resource for researchers that are investigating cross-cultural consumer differences. Its culture difference from the marketer uses the direct value inference approach, based on measuring the values of subjects in a sample to infer cultural characteristics. Thus, although Hofstede's classification of cultures provides (Soares et al., 2007). Due to regional differences, not all clients would have the same preferences and levels of satisfaction as one another (Kaynak, E., & Herbig, P., 2014)

The following is the article's structure, intended to respond to this research topic. A study of the literature is carried out, with particular emphasis placed on the topic's importance for retailing and customer experience. Research question: How do Customer's Culture and Geographical differences affect the pharmaceutical shop customer experience in the retailing setting during the pandemic?

Research methods

Understanding the distinctive elements of the various customer experience contact points is required while examining customer experience contact points. A qualitative research technique based on an in-depth knowledge of a scenario and the customer's diverse cultural background or geographical difference through an in-depth examination of recalled consumer experiences from informants while shopping at a pharmacy. The various stores were investigated. This technique permitted data collecting from different pharmaceutical shops, and it also enabled the display of a diverse range of customer experience information.

Informants were asked to reflect on a recent experience they had with a pharmaceutical store of their choosing at the starting of the interview. The informants were then asked to identify the retailer and provide a brief account of their pharmaceutical store's shopping experience. This was done to give the informants the comfort and flexibility to recount their experiences as accurately as possible (Arksey and Knight, 1999). Participants were asked what they hoped to accomplish during the experience (i.e., make a purchase, search for information, browse) and how much familiarity they had with the pharmaceutical store to provide additional context to the experience. Following, the informants were asked to recollect and describe any incidents they recalled. Experiences need not be tied to significant occurrences and might include any separate encounters that the client can reflect from their previous interactions. During the interview, the informants were questioned about the situations they had experienced at each stage of the consumer decision-making process to get further insights.

The researcher used purposive sampling for the one-month data collection before the government decided to increase COVID-19 restrictions. Data saturation often determines this sampling technique (Mack, 2005). The researcher applied convenience sample with the assistance of the owner of the pharmaceutical shop. The entire interview was by 20 customer experience narratives from different geographical areas. During the interview, several of the informants mentioned their

interactions with various merchants. The study method was discontinued after the 20th semi-structured interview since the information saturation resulted from the discussions done thus far (Guest et al.,2006).

The thematic analysis of the 20 customer experience tales highlighted recurrent themes, which further supported the information saturation decision when themes converged in one narrative (Eisenhardt, 1989). According to the across-case analysis of the repeating themes, no new topics emerged after the 11th interview. Nonetheless, it was decided to conduct more semi-structured interviews to confirm that no other themes were disclosed during the investigation. The interviews lasted an average of around 45 minutes each, on average. The following table depicts the demographic profile of the informants:

Table 1 Profile of the key informants

Participant	Sex	Age	Years of Customer Experience with pharmaceutical shop	Frequency of visiting the pharmaceutical shop during the pandemic	Geographical area
P1	M	30	7	2 times/week	North
P2	M	40	1	2 times/Month	Central
P3	F	45	5	3 times/Month	West
P4	M	27	3	4 times/week	West
P5	F	25	4	2 times/week	South
P6	F	26	3	3 times/Month	East
P7	F	28	15	1 time/week	South
P8	M	33	11	2 times/week	East
P9	F	19	5 months	1 time/Month	Central
P10	M	28	3	2 times/Month	Central
P11	F	20	6	2 times/week	West
P12	F	26	7	2 times/week	South
P13	F	50	3	2 times/Month	East
P14	M	46	16	3 times/Month	South
P15	M	53	7	1 time/week	East
P16	F	27	10	2 times/Month	South
P17	F	26	23	1 time/week	East
P18	M	34	15	3 times/week	North
P19	M	33	12	4 times/Month	Central
P20	M	46	12	3 times/Month	West

Data Analysis

Given that the purpose of this study was to identify the distinct elements of customer experience touchpoints through qualitative data, we used an inductive process to work from the words of each participant's responses to identify and code themes related to the specific elements of customer experience that were being investigated. The themes that developed were subjected to a cross-case analysis (Miles and Huberman, 1994) to determine the frequency with which themes were repeated across Informants.

The researchers recorded and transcribed the participants' responses. The participants' responses were characterized by iterative, reflexive, thematic processing of the data. After reading the customers' comments multiple times, the researcher recorded crucial topics, overall perceptions, and main findings. The two members of the researcher analyzed transcripts team for themes using manual inductive coding using constant comparison. The results were sorted into themes and sub-themes, utilizing constant comparison and reflection approaches. In reviewing the research process, themes, and sub-themes, the team of researchers came up with suggestions for how to better integrate them to facilitate the analysis and reporting process and assure the rigor and reliability of the findings.

Each of the themes has been refined and expanded in breadth because of this process, and definitions and titles for each topic have been developed to correlate to the themes. The titles of the identified themes were affected by the existing literature as well as the data gathered during the research process. This table contains a list of themes and their accompanying codes and examples of extracts from them.

Table 2 Result: Themes and codes from the thematic analysis

Theme	Code	Example
Payment	<ul style="list-style-type: none"> • Cash • Transfer 	<ul style="list-style-type: none"> • Our store accepted cash only. • Price was not the same • I was aware of markup cost increase • I did not have internet banking • You could buy the medicine. Please scan the QR code to transfer. • The method of payment was complicated during the covid situation • They did not accept credit card • I did not have a payment application. • I wanted to pay by cash • I did not think the transfer is the only way to pay.
Hygiene	<ul style="list-style-type: none"> • Sanitizer • Sign 	<ul style="list-style-type: none"> • Please use hand gel. • The store provided the clean environment • Keep distance, and No service was provided if you did not keep distance. • There was a sign to remind me of the social distancing • The store was cleaner than before • I saw the sign, but it seemed nobody paid attention. • The sign was too small, but it was more than three

Theme	Code	Example
Queue	<ul style="list-style-type: none"> • People • Waiting time • Waiting Line 	<ul style="list-style-type: none"> • There were so many people. I do not want to wait, but I needed to. • The waiting time was so long. • The waiting line was out of the store to the pathway. • People keep pushing to the line. • The waiting time was almost one hour • So many people was in front of the store • I did not see how I can get it to the store
Product Unavailable	<ul style="list-style-type: none"> • No more • Next week • Another brand 	<ul style="list-style-type: none"> • The seller said no more medicines. • I could buy only three packages. I could come back next week • It was the same quality, but it was a different brand • I was shocked when the seller told me that the medicine was not available again • It was challenging to buy the medication during the pandemic • I would come back again

Table 3 Result: Definitions of the touchpoint elements

Touchpoint elements	Definition
Payment	The act or practice of making a payment to someone or something, or of receiving a payment
Hygiene	A set of circumstances or activities that are favorable to preserving health and avoiding disease, mainly via cleanliness
Queue	A line or series of people in line or waiting to be attended to or moved forward inline
Product Unavailable	It is typical for a product that is always on your sale to be unavailable for a period when you are out of stock or awaiting the next delivery.

Discussion

Most of the research has focused on the customer experience, as all evaluations are based on a collection of experiences (Roseetal,2012). Such considerations will always limit our ability to comprehend the critical moments of truth between the customer and the store. Using a retail setting as an example, we looked at cross-culture individual backgrounds by identifying and characterizing the unique parts that make up customer experience in the retail store. The study's findings provide managers with a better knowledge of the many contact point aspects that occur during the customer journey and contribute to a positive customer experience overall. The insights gained from this research will allow managers to do "the importance of customer experience' to acquire a comprehensive picture of the customer experience from beginning to finish. As pharmacists frequently receive, patients express their dissatisfaction with their inability to comprehend what the customer would like to receive. Nevertheless, pharmacists often fall into the same mistake. Paying attention to the "language" we use while communicating with patients is an excellent place to start when overcoming communication difficulties

The mapping of critical customer experience and identifying the specific parts of a particular touchpoint that are important to other retail channels will provide pharmaceutical store managers with a more comprehensive understanding of the complete customer experience. The outcomes of this study demonstrate that retailing setting identification is essential. Customers' experiences at different touchpoints during pandemics are classified and defined for the first time in this study, which identifies, categorizes, and characterizes the diverse aspects that occur throughout these experiences. In-depth investigation of recalled reports of consumer experiences from informants helped the researcher better understand the situation.

Payment, hygiene, queueing, and product availability components were identified using a thematic analysis of the semi-structured in-depth interviews done as part of this study. These four different elements of cross-cultural customer experience contact points were identified through this study. The study's findings also indicate that other touchpoints contain various features depending on the retail environment. Furthermore, the research demonstrates that the same consumer experiences trigger not all aspects. It may include as few as one of the four touchpoint elements or as many as all four of them simultaneously.

Conclusion

This study contributes to the marketing literature. It provides the foundation for the construction of a theoretical model of customer experience that can be tested empirically from the perspective of a cross-cultural background. According to the study's findings, managers now have a better grasp of the many contact point aspects that occur along the customer journey and contribute to a positive customer experience. The results emphasize that touchpoint identification and measurement should be executed from the customer's perspective. This is in line with the claim of Payer.,L (1988), and the barrier to effective communication is the use of nonverbal communication techniques. According to behavioral scientists, nonverbal communication can account for 55, and 95 percent of a message conveyed (Spector, R.E.,1996; Tindall et al., 1994). The most frequently cited theme was pharmacists' solutions for overcoming language challenges with customers from different ethnic backgrounds. Modern, patient-centered professional practice has identified this as a significant challenge for all types of health care providers, regardless of specialty. The identified touch point elements and variety of diverse backgrounds and different geographical locations should be taken into consideration by managers to gain a more holistic and comprehensive understanding of the customer experience throughout the shopping and retailing experience.

References

- Arksey, Hilary, Knight, Peter T. (1999). *Interviewing for Social Scientists*. Sage Publications, London.
- B. Joseph Pine II, James H. Gilmore, B. Joseph Pine II, James H. Gilmore. *From the Magazine (July–August 1998)*.
- Bassett-Clarke, D., Krass, I., & Bajorek, B. (2012). *Ethnic differences of medicines-taking in older adults: a cross cultural study in New Zealand*. International Journal of Pharmacy Practice, 20(2), 90–98. <https://doi.org/10.1111/j.2042-7174.2011.00169.x>
- Clark, T. (1990). International Marketing and National Character: A Review and Proposal for an Integrative Theory. *Journal of Marketing*, 54(4). <https://doi.org/10.2307/1251760>
- Eisenhardt, KathleenM. (1989). *Building theories from case study research*. *Acad. Manag.* 14(4), 532–550.
- Guest, Greg, Bunce, Arwen, Johnson, Laura (2006). How many interviews are enough? An experiment with data saturation and variability. *Field Methods*, 18(1), 59–82.
- Kaynak, E., & Herbig, P.,(2014). *Handbook of cross-cultural marketing*. Routledge.

- Mack, N. (2005). *Qualitative research methods: A data collector's field guide*. Miles, Matthew B., Huberman, A. Michael, (1994). *Qualitative Data Analysis: An Expanded Sourcebook, Second Edition Sage Publications., Thousand Oaks, CA*.
- Pantano, Eleonora, Milena, Viassone, (2015). *Engaging consumers on new integrated multichannel retail settings: challenges for retailers. J. Retail. Consum. Serv., 25, 106–114*.
- Payer, L., *Medicine, and Culture*, Penguin, New York NY (1988) pp. 23-34
- Pine II, B. Joseph, Gilmore, James H. (1999). *The Experience Economy: Work Is Theatre and Every Business a Stage. Harvard Business School Press, Boston*.
- Rose, Susan, Clark, Moira, Samouel, Phillip, Hair, Neil, (2012). *Online customer experience in e-retailing: an empirical model of antecedents and outcomes. J. Retail. 88(2), 308–322*.
- Soares, A. M., Farhangmehr, M., & Shoham, A. (2007). Hofstede's dimensions of culture in international marketing studies. *Journal of Business Research, 60(3)*. <https://doi.org/10.1016/j.jbusres.2006.10.018>
- Spector, R.E., (1996), *Cultural Diversity in Health and Illness, 4th ed, Appleton & Lange, Stamford CT, p. 290*.
- Tindall, W.N., Beardsley, R.S. and Kimberlin, C.L. (1994). *Communication Skills in Pharmacy Practice, Lea & Febiger p. 38*
- Zweber, A. (2002). Cultural competence in pharmacy practice. *American Journal of Pharmaceutical Education, 66(2), 172-176*.
- Zomerdijk, Leonieke G., Voss, Christopher A. (2010). Service design for experience-centric services. *J. Serv. Res. 13(1), 67–82*.

The Configuration of 3D Model Suitable for Creating World Scale Augmented Reality (AR)

Teerasan Lailang*

*Department of Digital Media Technology, Faculty of Mass Communication Technology,
Rajamangala University of Technology Thanyaburi, Pathum Thani 12110, Thailand*

** Corresponding email: teerasan.la@rmutt.ac.th*

Abstract

The objective of the research study is to guide the application for developers and people who are interested in creating world-scale Augmented Reality (AR) by the configuration of a 3D model. The result of this paper would present the recommended model scale and configuration of AR cameras near and far. The researcher divides research methodology into three cases: 1) the size of a 3D model is the same as the physical area (3D Model size 617x481x764 cm. Physical area: 617x481x764 cm. 1:1), 2) the size of 3D model is smaller than the actual size or physical area (3D Model size 308.5x240.5x382 cm. Physical area: 617x481x764 cm. 1:2), and 3) the size of 3D model is bigger than the physical area (3D Model size 617x481x764 cm. Physical area 308.5x240.5x382 cm. 2:1). This study researcher creates world-scale AR by trial configuration 3D model and AR camera setup to define recommended value and define the relationship between 3D configuration and model scale. (1:1, 1:2, 2:1) The result reveals 1:1 ratio the model scale recommended value should be (0.00-0.01) camera near value should be (0.01-0.05) camera far value should be (3000-4000). The 1:2 ratio model scale value should be (0.001-0.002) camera near value should be (0.01-0.05) camera far value should be (2000-3000) and the 2:1 ratio model scale should be (0.50-1.00) camera near value should be (0.05-0.10) camera far value should be (4000-5000). This study researcher uses Samsung SM-G930FD to be AR camera device. It represents the mid-range mobile phone level that most people have. The experimental result is a device (AR camera)-specific and the result might be different if other devices are used. Indifference AR camera device also differences focal length camera cause optical effect to the perspective of viewer. However, there are several factors that this study did not cover such as, the different of limitations of the experimental area can affect to viewing area of user. The researcher will study further.

Keywords: Augmented Reality, World Scale AR, 3D Model

Introduction

According to Yuen, Steve Chi-Yin; Yaoyuneyong, Gallayanee; and Johnson, Erik (2011) Augmented Reality (AR) is emerging as one of the main drivers of the business technology economy. AR has been applied in many sectors such as medical training, real estate, repair & maintenance, design & modeling, business logistics, tourism industry, education training, field service, entertainment industry, public safety and more. AR was applied in businesses to enhance the consumer's interaction by interactive digital elements or computer generate image (CGI) over the surrounding real-world objects. According to Andrew Hong. (2021), there are two types of popular AR created and subsequently used today.

1. AR marker/Target image is AR which detects objects in target image or marker and overlay graphic CGI element on top real world and able to be interactive with user. AR marker can be anything from detection for example image, book, poster, picture on screen, physical objects also your face. The most popular AR we can see every day on social media as filter features. This AR uses facial recognition to detect and overlay graphic sticks on your face.

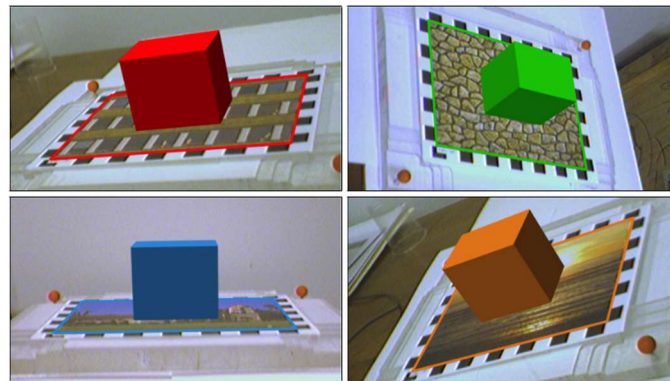


Figure 1 Target Image AR.

Retrieved from <https://www.vision.rwth-aachen.de/publication/00193/>

2. Real-scale AR Developers. ArcGIS (2021) reviews a type of AR in which scene content is overlaid on real-world physical position. This is also known in a variety of words such as world-scale AR, full-scale AR, real-world AR, and planet-scale AR. This paper defines meaning as world-scale AR.



Figure 2 World Scale AR

Retrieved from: <https://www.archdaily.com/913039/morpholio-unveils-ar-sketchwalk-an-augmented-reality-tool-to-immense-users-in-design>

World Scale AR is used to visualize a building 3D model using a mobile phone to scan on the surrounding area to see the environment simulate user into a virtual place. The problem with making world-scale AR is the size of the model is inappropriate size of the actual area. Configuration model can affect the display of the application there are contains numerical values that affect to model changes such as measure unit, model scale, near distance, far distance of AR camera as shown in figure 3.

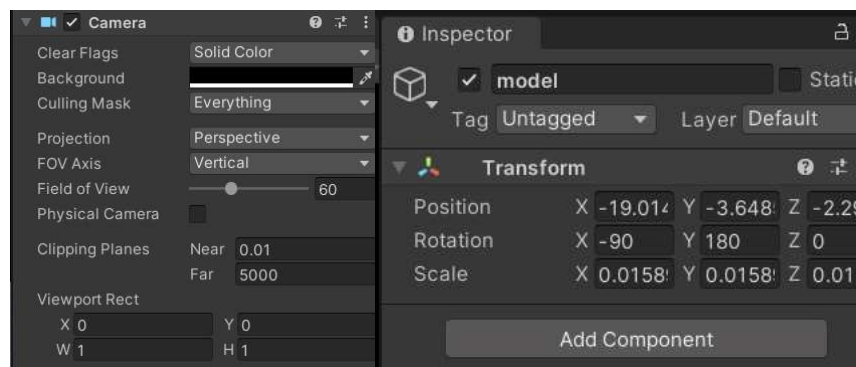


Figure 3 Configuration of 3D Model in Unity Software

Inappropriate model size settings cause problems with models larger or smaller than display area. Viewers need to walk away from the model to see whole model. Some cases may be limited by area because narrow areas or have obstructions. In some cases, viewers may not be able to see an overview of the model due to lost detect object because near and far configure inappropriately. In this paper, the researchers is interested in how to set up a model suitable for each area by defining the area into three cases.

1. The 3D model is the same scale as the physical area. 3D Model size 617x481x764 cm. Physical area size 617x481x764 cm. (1:1) This case represents some places are wide-area and unobstructed so that viewers can walk around to see the surrounding environment and be able to see from both internal and external areas.

2. The 3D model is smaller than the physical area. 3D Model size 1 308.5x240.5x382 cm. Physical area size 617x481x764 cm. (1:2). This case represents someplace where there are obstacles or limited spaces so viewers cannot view whole internal areas, may be able to see some part of the building.

3. The 3D model is larger than the physical area. 3D Model size 617x481x764 cm. Physical area 308.5x240.5x382 cm. (2:1). This case represents someplace cannot view outside areas they can only view inside areas. The illustration shown in figure 4

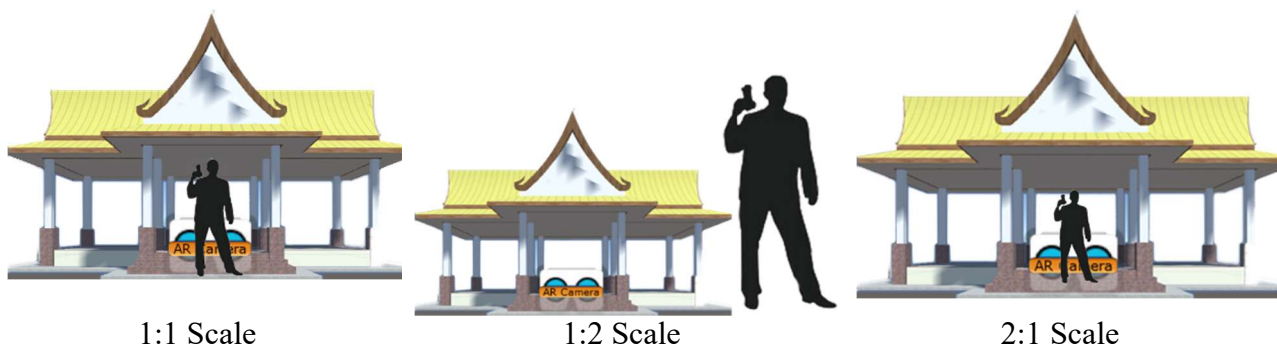


Figure 4 Illustration of experimental methodology

Materials

In this study, the researcher uses computer software to create world-scale AR by using Unity Software and model with the sample of a 3D temple model to simulate the place. In addition, this study requires a wide space to experiment, so the researcher use the stadium to be a trial field. A list of materials is shown, as follows.

- Computer
- Unity software
- 3D Model Temple (Large Scale)
- Tape measure surveying
- Wooden pegs
- Plastic rope
- SAMSUNG SM- G930FD (AR camera device)

Experiment

The experiment divided into three ratio 1:1, 1:2, 2:1.

Ratio 1:1 3D Model size XxYxZ 617x481x764 cm. physical area size: 617x481x764 cm.

Ratio 1:2 3D Model size XxYxZ 308.5x240.5x382 cm. physical area size: 617x481x764 cm.

Ratio 2:1 3D Model size XxYxZ 617x481x764 cm. physical area size: 308.5x240.5x382 cm.

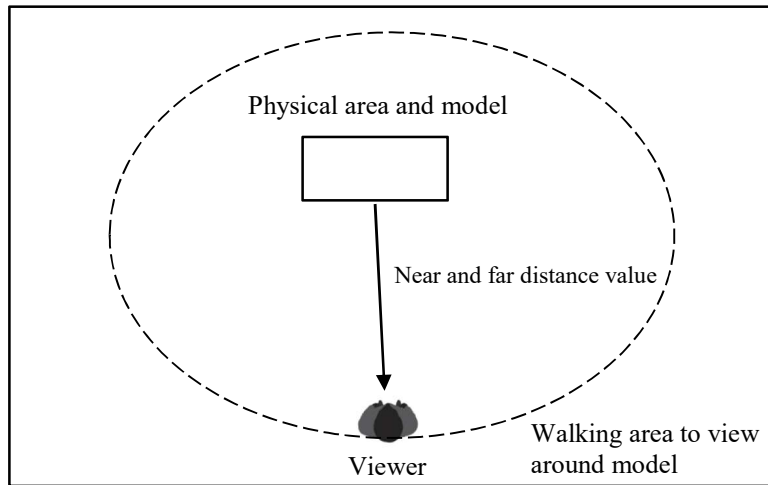


Figure 4 Experimental area plan

To record, the researcher creates an AR application and configuration model property to follow the experimental plan. Researcher trial view 3D model through mobile phone (SAMSUNG SM- G930FD AR camera device) to find out the most suitable value of the model.

Results

The results of trial configuration model in the difference ratio are recorded in the table.

Table 1 Results of 1:1 testing

Trial time	Model scale	AR Camera Near	AR Camera Far	Effect
1	0.00	0.01	1000	Detect lost when away
2	0.01	0.10	3000	Near and far do not effect
3	0.05	0.50	4000	Near and far do not affect and model almost large
4	0.10	1.00	5000	Detect lost when too close and model too large

According to the results, trial 1 Scale, Near, Far (S-N-F) value (0.00-0.01-1000) AR cameras lost detection when the viewer walk away from the model. When a viewer gets closer to the model detection is good. Trial 2 (S-N-F 0.01-0.10-3000) does not affect both near and far. Trial 3 (0.05-0.50-4000) does not affect both near and far and the model is almost too large. Trial 4 (0.10-1.00-5000) AR camera lost detect when the viewer is close to the model and the model is too large.

Table 2 Results of 1:2 testing

Trial time	Model scale	AR Camera Near	AR Camera Far	Effect
1	0.00	0.01	1000	Model too large
2	0.001	0.05	2000	Near and far do not effect
3	0.002	0.50	4000	Model almost small Detect lost when away
4	0.005	1.00	5000	Model too small and detect lost when away

According to the results trial 1 (S-N-F) value (0.00-0.01-1000). Model too large viewer have to away from the model. The viewer gets closer to the model detection is good. Trial 2 (S-N-F 0.001-0.05-2000) does not affect both near and far. Trial 3 (0.002-0.50-4000) model almost small and AR Camera lost detection when the viewer was far away. Trial 4 (0.005-1.00-5000) model too small AR camera lost detect when viewer away from the model.

Table 3 Results of 2:1 testing

Trial time	Model scale	AR Camera Near	AR Camera Far	Effect
1	0.00	0.01	1000	Model too small detect lost when far from a model
2	0.50	0.05	2000	Detect lost when far from a model
3	1.00	0.50	4000	Model almost large
4	2.00	1.00	5000	Model too large

According to the results trial, 1 (S-N-F) value (0.00-0.01-1000) model was too small and detection was lost when the viewer was far away from the model. Trial 2 (S-N-F 0.50-0.05-2000) model size appropriate with physical area and detection lost when viewer far away from the model. The trial 3 (1.00-0.50-4000) model is almost large and the AR camera do not affect. Trial 4 (2.00-1.00-5000) model is too large viewers need more space to walk around the model.

In the discussion, the researcher found the model’s different configuration ratio (1:1,1:2,2:1) affects the walking area of the viewer. In other words, if we setting model is large, the walking area is also wider because connected with AR camera far configuration. In the case of 1:2 ratio the model should be smaller than the actual area. The model is connected with AR camera near configuration. In the case of 1:1 ratio the configuration of both near and far should be relevant because the viewer is able to see the model from both internal side and external side.

Conclusion

According to the results, the researcher can summarize the relation between model size and AR camera. Configuration, as followed in figure 5.

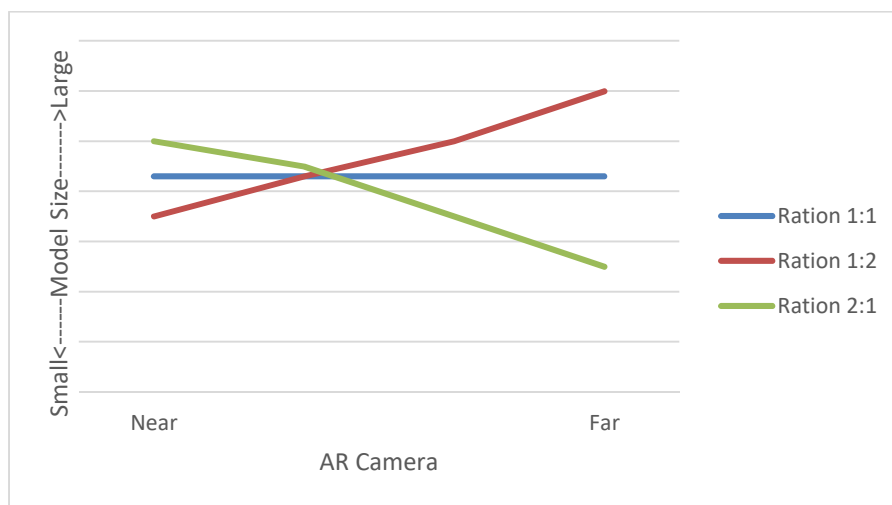


Figure 5 the relation between model size and AR camera setting

According to the results, the researcher was able to conclude the relation between model size and AR camera configuration, following the difference ratio 1:1, 1:2 and 2:1 as shown in the table

Table 4 Conclusion Results of 1:1 1:2 2:1 testing

Ratio	Recommended model scale	Recommended AR Camera Near	Recommended AR Camera Far
1:1	0.00-0.01	0.01-0.05	3000-4000
1:2	0.001-0.002	0.01-0.05	2000-3000
2:1	0.50-1.00	0.05-0.10	4000-5000

According to the table ratio 1:1, recommended model scale should be 0.00-0.01 because in practice it may be possible to correct the size of the model slightly to keep the model scale accurate with the actual area, e.g., archaeological site, exhibition room. It depends on the factor of physical location. Recommended AR camera near distance should be 0.01-0.05 due to in the real scale-AR viewer will be able to see the model from both internal and external model so AR camera near and far value should cover a range of user walking area.

The ratio 1:2 recommended model scale should be 0.01-0.02 to downsize the model to the proper physical area. Recommended camera near should be 0.01-0.05 because in this case, the model is smaller than the actual size so viewers would survey around the model from the outside only, e.g., pagoda, statue, pyramid. However, in practice may be adjusted model size according to a physical area.

The ratio 2:1 recommended model scale should be 0.5-1.0 nevertheless depending on model size and measure unit. This case model would be larger than the actual area so viewers be able to see the model only inside, e.g., an ancient tomb, pagoda, temple. In some case, if the developer need to viewer sees the model outside. They need to have a very large space to give viewers surveys around an example model of the great temple, the grand palace, historical park.

In conclusion, the result of this study researcher uses Samsung SM-G930FD to be an AR camera device because it represents the mid-range mobile phone level that most people have. The experimental result is a device (AR camera)-specific and the result might be different if other devices are used. Indifference AR camera device also differences focal length camera cause optically affect to perspective of the viewer. With the longer focal length, the angle of view is narrow, the shorter focal length, the angle of view is wider. However, there are several factors that this research did not cover such as, the different of limitations of the experimental area can affect to the viewing area of user. The researcher will study further.

References

- Hong A. (2021). *High Quality World-Scale Augmented Reality is Getting Closer-Partially because of Machine Learning*. Retrieved from website: <https://towardsdatascience.com/high-quality-world-scale-augmented-reality-is-getting-closer-partially-because-of-machine-975a68fa6fe5>
- Nuernberge, B., Ofek, E., Benko, H., & Wilson, A. D. (2016). *SnapToReality: Aligning Augmented Reality to the Real World*. (Proceedings). The 2016 CHI Conference on Human Factors in Computing Systems, May 2016 Pages 1233–1244.
- Developers.arcgis. (31.OCT.2021). *Real-scale AR*. Retrieved from website <https://developers.arcgis.com/documentation/glossary/real-scale/>
- Kato, H., Billinghurst, M., Poupyrev, I., Imamoto, K., & Tachibana, K. (2000) *Virtual object manipulation on a table-top AR environment*. Proceedings IEEE and ACM International Symposium on Augmented Reality (ISAR 2000) 1-2 DOI: 10.1109/ISAR.2000.880934
- Saidin, N. F., Halim, N. D. A., Yahaya, N. (2015, June). *A Review of Research on Augmented Reality in Education: Advantages and Applications*, 1-2.



Chi-Yin Yuen, S., Yaoyuneyong, G., & Johnson, E. (2011). *Augmented Reality: An Overview and Five Directions for AR in Education*. Retrieved from website: <https://aquila.usm.edu/jetde/vol4/iss1/11/>

The Design of English Flash Cards with Augmented Reality Technology about Food & Drink

Kamonthip Torsabsinchai*, Bennapa Patanapipat and Nattha Thammo

*Faculty of Mass Communication Technology, Rajamangala University of Technology Thanyaburi,
12110, Thailand*

**Corresponding Author E-mail: kamonthip_t@rmutt.ac.th*

Abstract

The purpose of this study is to design of English Flash Cards with Augmented Reality Technology about Food & Drink are: 1) To design English Flash Cards with Augmented Reality Technology about Food & Drink 2) To the comparison of learning achievement before and after use English Flashcards with Augmented Reality Technology about Food & Drink.

The process of this study is started by design English Flash Cards with Augmented Reality Technology about Food & Drink and conduct a media quality assessment by 6 experts. Then, put to test with a sample. A sample was selected from students grade 1 at Nongpromnor School in Nakhon Sawan for 30 people that acquired by Purposive Sampling. Finally, the results were summarized by finding mean, percentage, standard deviation, and efficiency.

The result of this study shown that: The media quality of English flashcards with augmented reality technology on food and beverages was deemed to be at the top level by specialists who assessed the quality of the media. It had an $\bar{X} = 4.67$. The total proficiency test score of the sample group had a mean total score after studying $\bar{X} = 52.30$ higher than before studying $\bar{X} = 29.77$ after learning English words through the use of English flashcards with technology. Augmented reality was statistically significant at the .05 level. due to the use of augmented reality technology with learning media make learning media It's new and interesting. Children experience exciting learning. As a result, children are more active in learning vocabulary and are not bored with the content they are learning.

Keywords: AR Flash Cards, English Flash Cards, Augmented Reality

Introduction

English is the lingua franca used by people all over the world to communicate with one another. ASEAN uses English as a medium of communication in which ASEAN countries. Thailand, like many other countries, has a national language other than Thai. However, English must be used in all aspects of international communication. As a result, it is critical for Thais to improve their English language skills. especially when dealing with children. (Iamsaard 2018, p. 34) Language learning results from cognitive abilities as children learn and adapt to their surroundings. It comes with reasoning ability in terms of children's language development. logic and decision-making as the brain grows rapidly, early childhood language development is critical for enhancing the child's future maturity. (Limpavaralai, Kinlumdrun, & Mahasaranon, 2019) which vocabulary is being learned This can be accomplished in a variety of ways. The most common way for children to learn in school is to learn to write the alphabet. Practice letter pronunciation, word combinations, spelling words, and reading aloud and remembering their meanings. This is a good way for children to learn. Learn quickly if your child has a good memory. Making the use flashcards or picture cards to increase the amount of vocabulary learned, they can be brought in to help teach alongside lessons. Because they are appropriate for the ages and interests of children aged 7-11 years, the flashcards and picture cards are appropriate for use as a medium to promote reading. That is, flashcards and picture cards are

organized learning materials created by teachers. Created to allow students to go over the material again. In the lesson, increase your knowledge and understanding. and assist in the development of additional thinking skills. (Noosong, Promkuntha & Papor, 2019)

Nowadays, technology is now playing an increasingly important role in teaching and learning media. The use of technology to stimulate memorization and learning skills in teaching and learning management. There is a demand for media that is diverse and interesting. to draw learners' attention to their interests, resulting in concentration in learning, in addition to teaching in front of the class alone (Sangsuthi, Musee & Silakhaw, 2015) as a result, incorporating augmented reality technology into teaching or integrating it with teaching materials such as flashcards will benefit students. Have a new virtual reality experience. Learners participate in a collaborative learning process. Teachers increase students' knowledge through demonstrations and conversations, as well as by encouraging students to understand what they want to learn. Learners gain valuable experience. With virtual 3D images, connect the learned content to places or objects. (Meesuwan, 2014). And, while there are currently many teaching or learning materials that use technology, these media are not widely available in all areas, such as schools in remote areas. or small schools with a small number of teachers It could just be the media. There has been no incorporation of technology into the media. As a result, students are unable to gain experience using learning materials in conjunction with augmented reality technology. because of the significance of such issues as a result, the students wanted to create flashcards in English using augmented reality technology about food and beverages. Wat Nong Phrom Nor School Nakhon Sawan Province, a small school, has English flashcards with augmented reality technology to help students in elementary school grade 1 and provide a one-of-a-kind learning experience for more English words

Literature review

Augmented Reality Technology

Augmented reality technology (AR) refers to the technology that creates augmented images in the real world. in the form of an overlay between the supplementary image and the real world viewed through a smartphone device that illuminates the designated area to be displayed.

AR technology can be divided into two types: Marker-Based and Location-Based

1) Marker-Based: The most common type is marker-based. The simplest AR Markers use 2D barcodes, while more complex types use colorful images. Scan to a pattern that resembles a coach bar using a smartphone and an AR app. or symbols captured with a camera The software recognizes and processes digital images, 3D digital images, and images that move across the screen. The working principle of marker-based augmented reality, also known as recognition-based augmented reality.

2) Location-Based: Location-Based When the camera on a smartphone with a Location-Based AR application illuminates the actual location, GPS software remembers the location. recorded The app will present the location's information overlaid with the actual scene seen by the camera based on the recorded location and the detectors recorded via sensors such as the accelerometer and gyroscope. The working principle of Location-Based can be illustrated in the diagram. (Smiththiritha, 2015).

Augmented Reality Working Process

1) Image Analysis is the process of looking for markers in images captured by a camera and then looking them up in a database that stores the size and pattern of the markers. Marker-Based AR in Work and Analysis Marker-Based AR in Work and Analysis

2) Calculating the 3D Pose Estimation of the Marker relative to the Camera

3) 3D rendering adds detail to an image. Obtaining a virtual image using computed 3D position values, such as when a learner in a video camera visualizes a virtual object on a monitor and displays any interactions, such as touching an object seen on the screen. The software receives this new

information and processes the learners' reactions, resulting in the interactive changes of the real objects being displayed on the monitor once more. (Songkhla, 2018)

Using augmented reality technology in education and learning

At present, augmented reality technology is being used to improve teaching and learning. From research studies on Chokklang, Chantayochon, & Bochakphan (2016). Examine the efficacy of English vocabulary-building resources. After using augmented reality technology in the first grade, it was discovered that pupils who learnt English vocabulary had better learning outcomes after school. statistically significant at the.05 level, which corresponds to the findings of Noosong, Promkuntha, & Papor (2019). A study of the progress of grade 2 children' basic word reading achievement using flashcards and image cards. The results revealed that at the.05 level, the basic word reading achievement of grade 2 pupils taught utilizing flashcards and image cards after school was much greater than previously. Moreover, the study of Limpinan, P. (2019). Using augmented reality technology, learn how to memorize English vocabulary. Vocabulary persistence of Kindergarten 3 kids was found to be greater than pre-test scores when taking pre- and immediate-after-study tests utilizing augmented reality technology, according to the findings of the study. There were no changes between the test scores immediately after school and the test scores after 14 days of study. The augmented reality design was found to teach English words with visual flashcards that matched the meaning of the words. Vocabulary is displayed using 3D models that move interactively with the learner when utilized through the AR application, and the sound of reading the words can help Kindergarten 3 kids recall English vocabulary.

The purpose of this study was to create English flashcards based on food and beverages using augmented reality technology. and compare the learning achievements of kids that use learning materials using English flashcards integrated with augmented reality technology before and after school.

Research Methodology

Participants

30 primary school students, academic year 2020, Nongpromnor School, Nakhon Sawan province, by purposive sampling.

Experimental Design

The main goal of the experimental design was to investigate the learning outcomes of students' English vocabulary by combining learning through English flashcards with augmented reality technology. Food and beverages will be made up of 60 words thanks to the use of augmented reality technology in the design of English flashcards. The researcher chose the words from the media. 60th years. Her Royal Highness Princess Maha Chakri Sirindhorn. which is used as a supplementary media for the English language course for Grade 1 students. The contents of the flashcards are divided into 3 parts as follows:

The first section, the front of the card, contains words and illustrations that can be used as display markers.

The second section on the back includes lowercase, uppercase, words, and definitions. The third section is a guide to using flashcards. Shown in Fig.1-4.

Students must test their knowledge before and after using English flashcards with augmented reality technology. The learning outcomes were then compared and further examination of the data.



Figure 1 Shows an example of the front and back of the English card design elements.



Figure 2 shows an example of an English flashcard design.

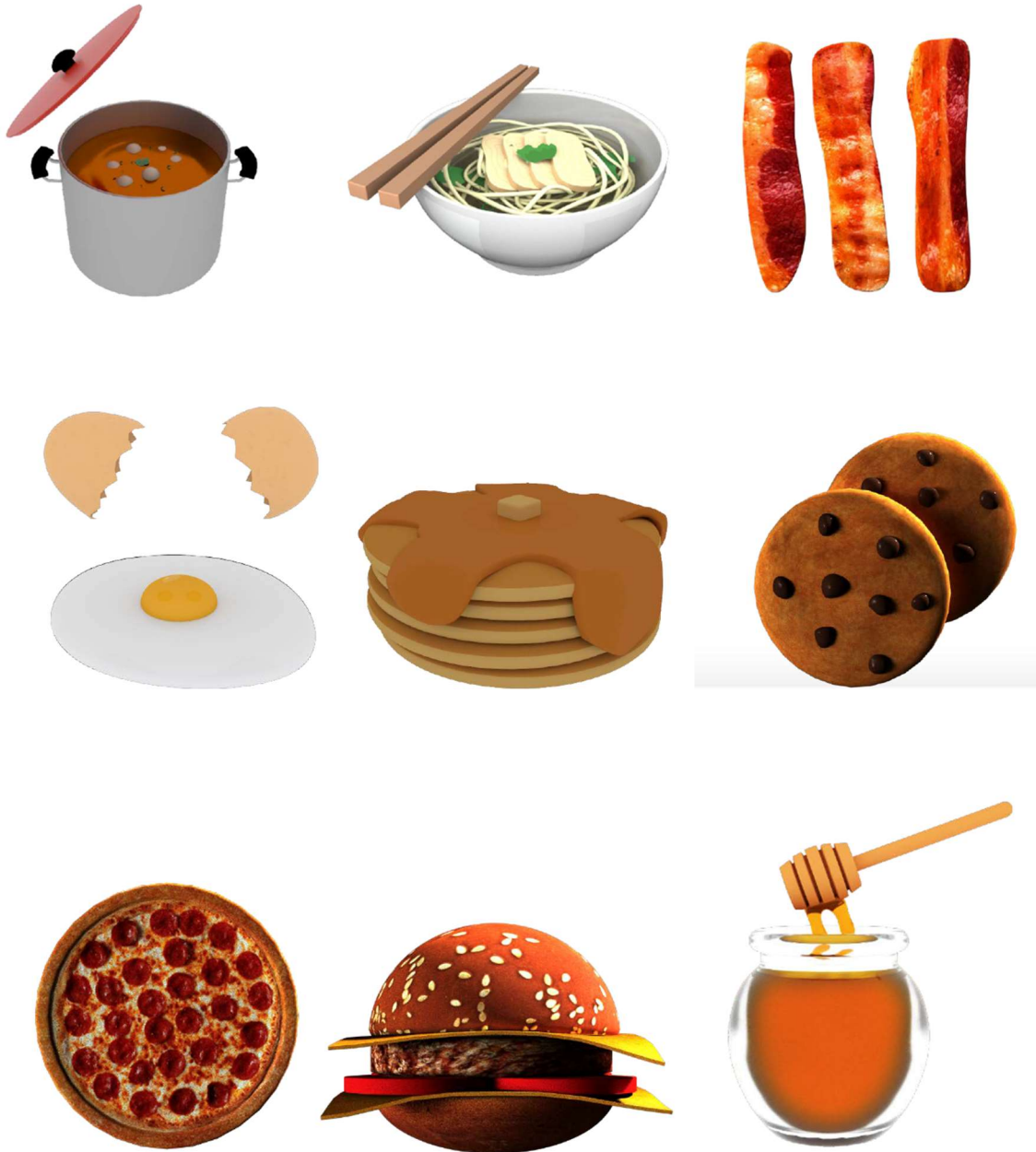


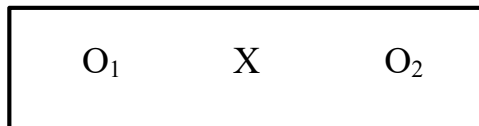
Figure 3 shows an example of a 3D food model that will be displayed when scanning a flashcard.



Figure 4 shows a guide for playing the flashcards.

Procedures

The researchers prepared the sample group with equipment, material, and cognitive assessments prior to the exam. The research team stated the study's goals. and advising on how to use the device in its most basic form The researcher performs the study by having the students complete learning activities in accordance with their learning styles. as follows: utilizing the One Group Pretest-Posttest Design study model:



Symbols that can be found on research forms

- O₁ The pre-learning knowledge test
- X English flashcards utilizing augmented reality technology
- O₂ The post-learning knowledge test

The participants in the study performed a 60-word English vocabulary pre-test. Following that, the sample group acquired 60 words of English vocabulary using English flashcards and augmented reality technology. test After using the media, the sample group took an English vocabulary knowledge test.

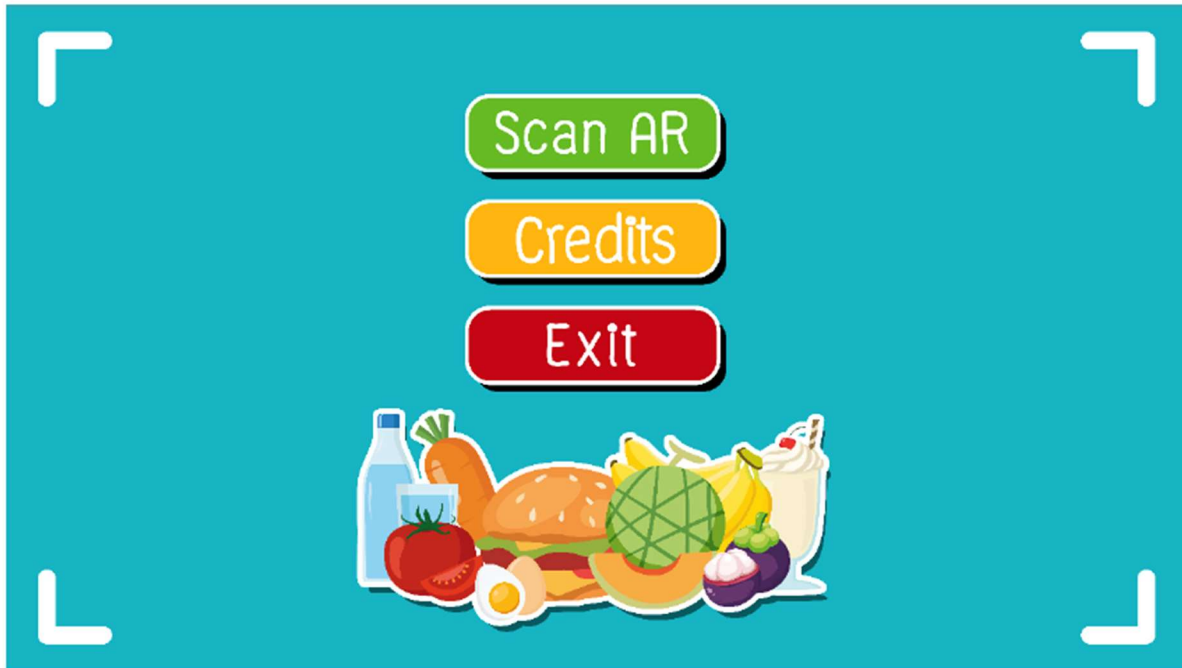


Figure 5 shows the image of the AR application page. and simulating the use of English flashcards

Data Collection

The purpose of the test was to collect knowledge scores before and after the sample group used English flashcards in conjunction with augmented reality technology. The study team gathers data and summarizes the experiment's findings. Using the T-test, compare knowledge before and after studying. Mean analysis and dependent analysis are two types of analysis. as well as standard deviation.

Results and Discussion

Table 1 Shows the results of the quality assessment of flash cards with augmented reality technology by experts.

Content	\bar{X}	S.D.	Quality Level
The overall of the flashcard content evaluations.	4.70	.40	the most quality
The overall of the flashcard design evaluations.	4.77	.41	the most quality
The overall of the AR technology design evaluations.	4.53	.59	the most quality
Total	4.67	.47	the most quality

The assessment of the quality of English flashcards in combination with augmented reality technology on food and beverages. Overall, it's at the highest level. which had a mean of 4.67 and a standard deviation of 0.47. When each aspect was considered, it was discovered that the average was highest in terms of English flashcard design ($\bar{X} = 4.77$, S.D. = .41), followed by the content aspect of the English flashcards ($\bar{X} = 4.70$, S.D. = .40), and the presentation of the English flashcards with AR technology ($\bar{X} = 4.53$, S.D. = .59) along with from other interviews Experts have stated that the text is simple to comprehend. When describing the content, be specific. and the information is correct, with vivid images and a suitable font style in terms of the 3D model's presentation, it was discovered that the model had the correct shape. and the model's image conveys the message of the words clearly Flashcards are also easier to understand when provided in AR style. as well as more enjoyment.

Table 2 shows the results of the comparison of pre-study and post-study knowledge of the sample group (n=30).

knowledge test score (full score 60 points)	\bar{X}	S.D.	T-test	P-value
Pre-test	29.77	4.065	-36.288	.000*
Post-test	52.30	4.292		

*p<.05

The comparison of knowledge test scores before and after Learn to use English flashcards with augmented reality technology is shown in Table 1. based on the mean analysis and the standard deviation The total proficiency test scores of the samples after studying with AR flashcards were found to be higher than ($\bar{X} = 52.30$) the pre-study test scores ($\bar{X} = 29.77$) at the .05 level, statistically significant. Because of the incorporation of augmented reality technology into learning media, learning media It's novel and intriguing. Children have fun while learning. As a result, children are more engaged with the content they are learning and are more active in learning vocabulary. It is not simply sitting and listening to the teachers' lectures. which is in accordance with the findings of

Limpinan, P. (2019) and Chalermdit, Wittayakhom & Jeerungsuwan (2018). It was discovered that learning English words through augmented reality technology makes it easier for students to remember them. This is due to the fact that the media kit includes flashcards that show the exact meaning of the phrases. when employing augmented reality 3D representations that interact with learners are used to display vocabulary. and the syllables' sound as a result, students will have an easier time comprehending and remembering English terms. as well as to entice students to become more enthusiastic about studying.

Conclusion

The research of the creation of English flashcards using augmented reality technology on food and beverages was summarized in this report. To provide students with new and exciting learning resources. By selecting a specific sample group, the results of the cognitive test from the sample of 30 pupils in grade 1 of the academic year 2020 at Wat Nong Phrom Nor School, Nakhon Sawan Province, were discovered. It was found that the total proficiency test score of the sample group had a mean total score after studying $\bar{X} = 52.30$ higher than before studying $\bar{X} = 29.77$ after learning English words through the use of English flashcards with technology. Augmented reality was statistically significant at the .05 level. due to the use of augmented reality technology with learning media make learning media It's new and interesting. Children experience exciting learning. As a result, children are more active in learning vocabulary and are not bored with the content they are learning.

References

- Chokklang, C., Chantayochon, W., & Bochakphan, S. (2016). The Development of English Vocabulary Learning of Pratomsuksa 1 Students by Using Virtual Reality Technology. *Journal of Project in Computer Science and Information Technology*, 2(1), 73-82.
- Chalermdit, J., Wittayakhom, N., & Jeerungsuwan, N. (2018). CHALLENGES ON AUGMENTED REALITY FOR EDUCATION 4.0. *Journal of Education Naresuan University*, 20(2), 266-279.
- Iamsaard, A. (2018). Teaching English for Primary Education. *Academic Journal of Buriram Rajabhat University*, 10(1), 31-45.
- Limpinan, P. (2019). Promoting Mahasarakham Tourism by using Augmented Reality. *Journal of Technology Management Rajabhat Maha Sarakham University*, 6(1), 8-16.
- Limpavaralai, M., Kinlumdrun, L., & Mahasaranon, W. (2019). The Factors Influencing Normal Expressive Language Development of Early Childhood In Sukhothai Province. *Journal of Nursing and Health Sciences*, 13(4), 78-90.
- Meesuwan, W. (2014). *Developing Augmented Reality media using Processing and OpenSpace3D*. Bangkok: Chulalongkorn University Printing House.
- Noosong, N., Promkuntha, P., & Papor, P. (2019). THE DEVELOPING IN BASIC WORD READING ACHIEVEMENT OF PRATHOMSUKSA 2 STUDENTS TAUGHT BY VOCABULARY CARDS AND PICTURE CARDS. *Journal of Panya*, 26(2), 1-9.
- Sangsuthi, N., Musee, T., & Silakhaw, Y. (2015). Development of Instruction Multimedia based on Behaviorism Theory, Topic: "Hello ASEAN". *Journal of Project in Computer Science and Information Technology*, 1(1), 69-74.
- Smiththiritha, W. (2015). Augmented Reality (AR)?. Bangkok, The Office of policy and academic journalism and television.
- Songkhla, JN. (2018). *Digital learning design*, Bangkok, Chulalongkorn University Printing House.



RMUTCON

Session 2:

**Technology and Innovation
for Engineering**

Discovery of Nanomatrix Structure of Natural Rubber and Its Application

Seiichi Kawahara*

Nagaoka University of Technology, Japan

* Corresponding email: kawahara@mst.nagaokaut.ac.jp

Introduction

Preparation of the synthetic rubber with outstanding mechanical properties, which is identical to natural rubber, is a long-standing, important subject to study since early 20th century. It is still significant subject to study and crucial target for many polymer chemists in 21st century. The reason why the synthetic rubbers are distinguished from natural rubber may be explained to be due in part to a lack of information of structure of natural rubber since many approaches have been made to prepare the synthetic rubbers, so far. It is, therefore, quite important to analyze the structure of natural rubber from a different perspective.

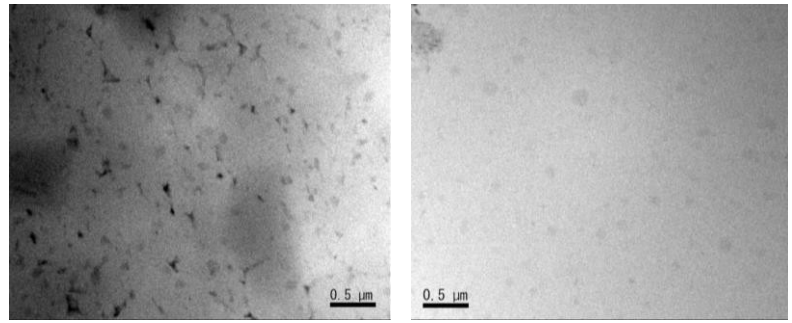
The study on the structure of natural rubber began with a determination of chemical composition. Faraday (1826) determined a ratio of carbon to hydrogen of natural rubber, i.e., 7.5, in 1826. From the result, C₅H₈ was proposed as a chemical composition of natural rubber. In 1860, Williams (1860) isolated isoprene from natural rubber by destructive distillation of the rubber. In 1884, Tilden (1884) proposed a correct structural formula of isoprene as CH₂=C(CH₃)-CH=CH₂. Staudinger (1925) discovered that natural rubber was a macromolecule consisting of isoprene units, in 1920. In 1925, Katz (1925) reported *cis*-1,4 configuration of isoprene units for natural rubber, based on analysis of crystalline form through X-ray diffraction technique. In 1994, Tanaka et al., (1994) found the existence of two *trans*-1,4-isoprene units at ω -terminal side and linked fatty acids at α -terminal side. Based on the history of the structural analysis, it is evident that the study on structure of natural rubber in 19th century and 20th century focused only on a primary structure of the rubber.

We discovered that natural rubber is a naturally occurring nanocomposite Kawahara et al., (2011), which consists of *cis*-1,4-polyisoprene as a major component and non-rubber components such as proteins and lipids as a minor component. The *cis*-1,4-polyisoprene is prepared from isopentenyl diphosphate by biosynthesis of plants, and the proteins and lipids contribute to the biosynthesis as enzyme and biological membrane, respectively. The biosynthesis is homogeneous in the initial stage since monomers and substrates are hydrophilic. However, the reaction undergoes homogeneous to heterogeneous during biosynthesis due to chain extension of natural rubber since *cis*-1,4-polyisoprene is hydrophobic. Thus, phase separation takes place during biosynthesis of *cis*-1,4-polyisoprene to form an oil in water emulsion, i.e., latex. The proteins and lipids exist on the surface of the natural rubber particles to stabilize the latex since they are amphipathic. The nanophase separated structure is, thus, inevitably formed in natural rubber when bulk natural rubber is prepared from the latex. It consists of the natural rubber particles with a diameter of about 1 μ m and matrix of the non-rubber components with a thickness of several ten-nanometer. We, thus, named this nanophase separated structure “nanomatrix structure” in 2011 Kawahara et al., (2011) since the thickness of the matrix was several ten-nanometer. In this presentation, we report the discovery of nanomatrix structure of natural rubber and structural design of its mimetic composites.

Discovery of the Nanomatrix Structure

Figure 1 shows TEM images for natural rubber and deproteinized natural rubber (DPNR), in which bright domains represent natural rubber and dark domains represent the proteins. In the TEM image for natural rubber, the rubber particles with an average diameter of 1 μ m were well dispersed

in the matrix of the non-rubber components such as the proteins and phospholipids with a thickness of several ten-nanometer. This nano phase separated structure was similar to the nanomatrix structure proposed in our previous study Kawahara et al., (2003), Kawahara et al., (2008). By contrast, for DPNR, no nanophase separated structure was observed in TEM image Chaikumpollert et al., (2012). In other words, the nanophase separated structure



Natural Rubber DPNR
Figure 1 TEM images of natural rubber and DPNR

of natural rubber disappeared after removal of proteins from the rubber Chaikumpollert et al., (2012)

Figure 1 shows TEM images for natural rubber and deproteinized natural rubber (DPNR), in which bright domains represent natural rubber and dark domains represent the proteins. In the TEM image for natural rubber, the rubber particles with an average diameter of 1 μm were well dispersed in the matrix of the non-rubber components such as the proteins and phospholipids with a thickness of several ten-nanometer. This nano phase separated structure was similar to the nanomatrix structure proposed in our previous study Kawahara et al., (2003). By contrast, for DPNR, no nanophase separated structure was observed in TEM image Chaikumpollert et al., (2012). In other words, the nanophase separated structure of natural rubber disappeared after removal of proteins from the rubber Chaikumpollert et al., (2012).

To prove the nanophase separated structure of natural rubber, we centrifuged natural rubber latex to prepare DPNR and serum rubbers Kosugi and Kawahara (2015). Table 1 shows dry rubber content (DRC) and nitrogen content (N%) of natural rubber, DPNR and serum rubbers, in which N% is converted to the protein content by multiplying 6.25. Values of the DRC and N% of natural rubber were 62.4 and 0.229 wt%, respectively, and they were reduced to 25.3 and 0.013 wt% after removal of the proteins. The values of the DRC and N% of the serum rubbers were dependent upon the rotational speed of the centrifuge; the larger the rotation speed, the lower the DRC and the higher the N%. The highest value of the N% was 2.285 wt%, which was about 10 times higher than that

of HANR. This demonstrates that natural rubber with a large amount of the proteins (high protein natural rubber) is prepared from HANR.

Table 1 DRC and N% of natural rubber, DPNR and serum rubber

Specimen	DRC (w/w%)	N% (w/w%)
DPNR	25.3	0.013
HANR	62.4	0.229
Serum 2K	25.3	0.482
Serum 5K	15.6	0.971
Serum 7K	11.9	1.305
Serumi 10K	7.0	2.285

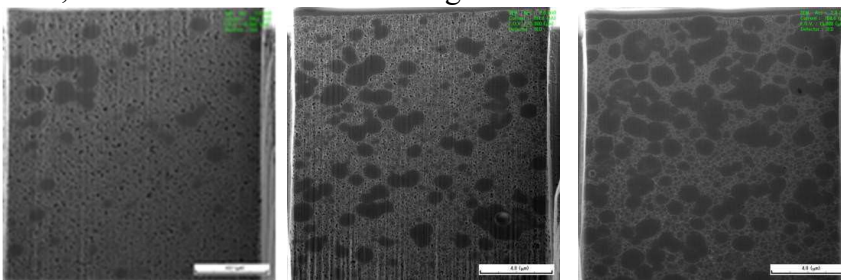


Figure 2 SEM images of the cross-section of the serum rubber.

Figure 2 shows SEM images of the cross section of the serum rubber after the rubber was stained with glutaraldehyde followed by OsO₄. Fewer voids were observed in SEM images of the cross sections, indicating that we could suppress formation of the voids by fixation of the proteins with glutaraldehyde

before staining the rubber with OsO₄. Furthermore, we investigated the effect of temperature in staining process on the morphology to determine the suitable staining condition. The effect of the temperature of OsO₄ on morphology is shown Figure 2 (a) and (b). It was found that staining with OsO₄ at 35 °C is more effective than 5 °C. In Figure 2 (b) and (c), effect of the temperature of glutaraldehyde on morphology is shown and no voids were observed for the sample stained with glutaraldehyde at 20 °C. Therefore, the suitable staining condition, where no voids were observed, was found to be at 20 °C for glutaraldehyde and 35 °C for OsO₄. Figure 2 shows SEM images of the etched surface of the serum rubber stained with 25 % glutaraldehyde aqueous solution for 12 h followed by 4 % OsO₄ aqueous solution for 48 h. Temperature for each process is as follows: (a) glutaraldehyde at 35 °C and OsO₄ at 5 °C, (b) glutaraldehyde at 35 °C and OsO₄ at 35 °C and (c) glutaraldehyde at 20 °C and OsO₄ at 35 °C. After we stained the serum rubber under the suitable condition, we performed three-dimensional observation by repeating etching with FIB and observing with FE-SEM alternately. Figure 3 shows three-dimensional reconstruction image of the serum rubber. The box size in the image is about X = 6 μm, Y = 4 μm, Z = 7 μm. Since non-rubber components are stained with OsO₄, bright domain represents non-rubber components and dark domain represents rubber particles. Because of no voids, we successfully reconstructed three-dimensional image of the nanomatrix structure for the serum rubber. It is found that natural rubber particles of about 200 nm in diameter are dispersed in the matrix of non-rubber components with a thickness of several ten-nanometer.

Preparation of Novel Synthetic Rubber

The nanomatrix structure is formed by covering rubber particles with nanoparticles followed by coagulation of the resulting nanoparticles-covered rubber particles. In this case, the rubber particles are required to chemically like to the nanoparticles to stabilize the nanomatrix structure in equilibrium state. Especially, for synthetic rubbers, the chemical linkages may be formed by graft-copolymerization of a monomer onto the rubber particles in latex stage, since the rubber particles in the latex are dispersed in water. Therefore, in the present study, the graft-copolymerization of styrene onto synthetic *cis*-1,4- polyisoprene (PI) particles was performed in latex stage WO2019/138449.

Figure 4 shows the TEM image (5000x) of PI-graft-PS.

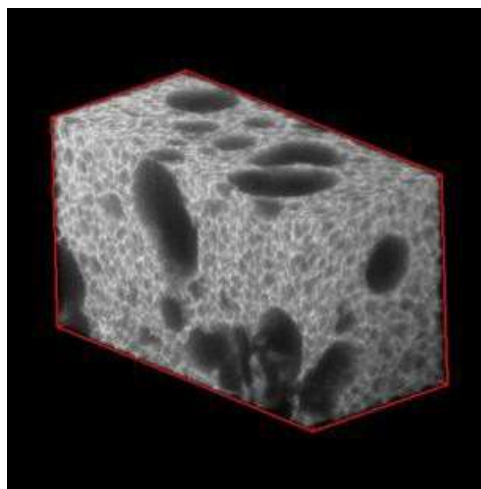


Figure 3 3D SEM image for the serum rubber

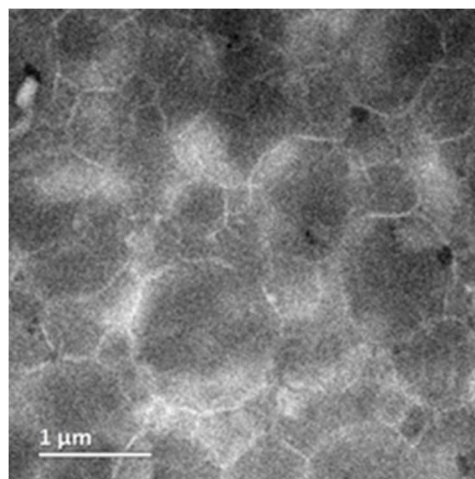


Figure 4 TEM image of the nanomatrix structure formed with isoprene rubber and polystyrene.

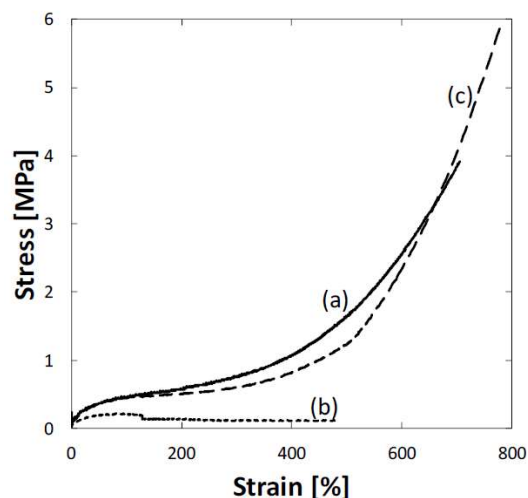


Figure 5 Stress-Strain curves. a:PI-graft-PS90, b:PI, c: natural rubber

The dark domains represent the PI particles and the bright domains represent polystyrene (PS) nanoparticles. The TEM image for PI-graft-PS, the PI particles with an average diameter of 1 μm as a dispersoid were well dispersed in the nanomatrix of polystyrene with a thickness of several ten-nanometer. It is, thus, found that the nanomatrix structure is formed by graft-copolymerization of styrene onto the PI particles in latex stage.

Figure 5 shows stress-strain curves for PI-graft-PS, PI and natural rubber in the unvulcanized state. The stress-strain curve for PI-graft-PS was almost identical to that of natural rubber, whereas it was distinguished from the stress-strain curve for PI. This may be explained to be due to the formation of the nanomatrix structure in PI. Consequently, it is proved that the nanomatrix structure is the origin of outstanding mechanical properties intrinsic to natural rubber.

References

- Chaikumpollert, O., Yamamoto, Y., Suchiva, K., Kawahara, S. (2012). *Colloid. Polym. Sci.*, 290, 331.
- Chaikumpollert, O., Yamamoto, Y., Suchiva, K., Nghia, P. T., Kawahara, S. (2012). *Polym. Adv. Technol.*, 23, 825.
- Eng, A. H., Ejiri, S., Kawahara, S. and Tanaka, Y. (1994). *J. Appl. Polym. Sci., Appl. Polym. Symp.*, 53, 5.
- Eng, A. H., Kawahara, S. and Tanaka, Y. (1994). *Rubber Chem. Technol.*, 67, 159.
- Faraday, M. (1826). *Q. J. Sci.*, 21, 19
- Katz, J. R. (1925). *Naturwissenschaften*, 19, 410.
- Kawahara, S., Chaikumpollert, O., Akabori, K., Yamamoto, Y. (2011). *Polym. Adv. Technol.*, 22, 2665.
- Kawahara, S., Kawazura, T., Sawada, T., Isono, Y. (2003). *Polymer*, 44, 4527.
- Kawahara, S., Yamamoto, Y., Fujii, S., Isono, Y., Niihara, K., Jinnai, H., Nishioka, H., Takaoka, A. (2008). *Macromolecules*, 41, 4510.
- Kosugi, K., Kawahara, S. (2015). *Colloid Polym. Sci.*, 293, 135.
- Staudinger, H. (1920). *Ber. Dtsch. Chem. Ges.*, 53, 1073.
- Tilden, W. A. (1884). *J. Chem. Soc.*, 47, 411.
- Williams, C. G. (1860). *Proc. Roy. Soc. London, Ser. A*, 10, 516.
- WO2019/138449

Effect of Fluid Velocity in Piping System Physical Properties for Shrimp Harvesting

Songphon Thoetrattanakiat¹ and Kiattisak Sangpradit^{2*}

¹*Engineering Field of Study, Faculty of Engineering, Rajamangala University of Technology Thanyaburi, Pathum Thani 12110, Thailand*

²*Department of Engineer, Faculty of Engineering, Rajamangala University of Technology Thanyaburi, Pathum Thani 12110, Thailand*

* *Corresponding email: k.sangpradit@rmutt.ac.th*

Abstract

The objective of this research has studied the harvesting pattern of white shrimp (*Litopenaeus vannamei*) for Thailand agriculture. The closed ponds and partial harvesting method is provided the information on the design of white shrimp centrifugal pump catching machines which is studied the effect of force acting on white shrimp in terms of force acting on white shrimp.

In this work 4,040 kg of white shrimps were harvested in the closed pond with a number of 20 white shrimps/kg. The total number of 85,502 shrimp were harvested. A biomechanics study of samples were conducted to determine where the point of samples body were vulnerable and damaged when using a shrimp catching machine for transportation. The biological mechanics of white shrimp is pulled out of 38 samples and sending white shrimps by using PVC pipe. The diameter of 10 inches, distance 360 meters, water flow rate 400 m³/hr. is conducted in the experiment for sending 300 kg of white shrimp by designing PVC pipe. It has a point for adding white shrimp to connect a water pump with diameter of 10 inches of the outlet size. 10 horsepower is used to supply water into the pipe system.

The results was found that, the biomechanics of white shrimps were able to withstand average tensile strength of 1.79 kg-force, a maximum of 2.3 kg-force, and a minimum of 1.18 kg-force with 400 cubic meter/hour of flowing rate . White shrimp can be delivered within 5 minutes. The dissolved oxygen at the inlet point is 6.11 parts per million (PPM) and outlet point is 5.2 PPM which is not less than 5 parts per million (PPM). 46 people of workers were able to harvest 1,000 kg/hour of white shrimp. The 4,040 kilograms of white shrimp in the rate of 20 pieces/kg was found. The 79.68 kilograms of injurious shrimp was found in this harvesting and representing of 1.972%.

Keywords: Vannamei white shrimp, closed pond harvesting, partial harvesting, white shrimp biomechanics, fluid harvesting

Introduction

White shrimp farming industry in Thailand and Southeast Asia accounted for 35% of the world's total shrimp production in 2018 (W Miao & W Wang, 2020). Specifically, Thailand used to have the highest white shrimp production in 2011 amounted to 600,000 tons/year and decreased sequentially because of the EMS epidemic (Early Mortality Syndrome) and reached lowest point in 2014 at a capacity of 250,000 tons/year (Suthida & Somthawin, 2018). The aforementioned problems, government agencies have developed a process for raising white shrimp called “Good Aquaculture Practices or GAP for Marine Shrimp Farms (Ts.7401-2019) under the Agricultural Standards Act B.E. 2008 (Thailand National Bureau of Agricultural Commodity and Food Standards Ministry of Agriculture and Cooperatives, 2018).

The system combines the steps in raising white shrimp. Such as preparing water and killing various diseases, area management and other important topics. However, in harvesting white shrimp,

comprising closed pond harvesting and partial harvesting. There has been no development or standardization of standards for white shrimp. The management of small-scale agriculture also uses water in and out of ponds based on natural tide and aquaculture that is medium and large shrimp farms. The method of harvesting white shrimp is still the traditional method of harvest. By harvesting using nets for general shrimp farms, it is a method that employs large numbers of workers and has a constant flow of labor that risks the spread of white shrimp disease by tracking workers while harvesting white shrimp in siege nets. There are also process and method for work and transporting that cause damage to white shrimp as well.

In the past, efforts have been made to improve the harvesting shrimp process by reducing the labor force in the harvest process by experimenting with using a fishing machine for harvesting white shrimp with satisfactory results. (L. Ohs, Scott W. Grabe, & R. LeRoy Creswell, 2018). However, in the experiment, there is also a lack of details regarding the size of the standard market edible size of 18-80 shrimp/kg in the specific experiment and the harvest quantity of 400,000 small white shrimp, which cannot be proven. It can be used in large industries such as countries in Asia, China, India, especially countries in the Southeast Asia region such as Thailand, Vietnam. Because of the aforementioned problem of harvesting large white shrimp, size 18-80 pieces/kg, an attempt was made to design a shrimp harvest specifically to prevent white shrimp from passing through the impeller area of the harvest by developing a shrimp suction system. With the experimental vacuum, it turns out that the suction power cannot overcome the escape force of the white shrimp, preventing the apparatus from harvesting the shrimp, which is in the next development stage (Rizki & Sam, 2013).

This research is studied the variables that affect the white shrimp while harvesting, which is caused damage to the white shrimp, such as the tensile strength of the white shrimp is caused the white shrimp to be damaged. The experiment of transporting white shrimps by pipes with variables were the water velocity and the flow of water suitable for the shrimp transportation by the pipe system. The distance of the pipeline, as well as the DO (Dissolve Oxygen) and the ratio of biomass with water suitable for the transportation of white shrimp that keep the white shrimp alive and still of good quality experimental research Overview in this document it comprises a study on one study and two main of experimental research.

1. Study of the general harvesting of white shrimp in medium to large shrimp farms by netting method. The objectives to provide standard reference data for the development of white shrimp harvesting, such as labor rate, time, harvest quantity, risk point, damage rate of white shrimp.

2. Experiment on transferring white shrimp with a 360 meter pipe. The aim is studied the effects of various factors caused by transferring white shrimp in the pipeline system, such as water velocity, water volume, temperature change, value decreased dissolved oxygen, the quality of white shrimp after tubular transportation, and the ratio of white shrimp biomass per water content.

3. Experiment on biomechanics of white shrimp the tensile force of the white shrimp will be studied to determine the tensile force that can damage the white shrimp. The aim is found a suitable linear equation to be used as a data for determining the force acting on the white shrimp that would not damage the white shrimp from the harvest process.

Experiment

1. Study of the general harvesting of white shrimp in medium to large shrimp farms by netting method. Common methods of harvesting shrimp on the farm shrimp harvesting in a large shrimp farm that is an industrial system of harvesting white shrimp is divided into 2 methods: First the closed pond type is a white shrimp harvesting when the white shrimp has reached the desired size and the white shrimp is harvested until the pond is empty and the pond is cleaned to prepare the water for the next generation of shrimp. Second partial harvest during aquaculture to reduce the density of white shrimp in shrimp pond normally, in shrimp aquaculture, the biomass of white shrimp in the pond is

controlled by 2-2.25 kg shrimp/cubic meter of water, difference in catching white shrimp in a closed pond and partially harvesting white shrimp. The method of harvest to close the pond and partial harvest will have 2 different decorations: the first closing the pond will reduce the water level in the pond to a depth of 50 centimeters so that workers can easily walk around the nets. During partial harvest, the water level will not be lowered as white shrimp will have to continue to be reared until the maturity date. Second the amount of white shrimp harvesting in closed ponds is caught until the whole pond harvested while the partial harvest will harvest 10-15% of the number of white shrimp in the pond before harvest. The rate of biomass was maintained at 2-2.25 kg shrimp/m³. In partial harvest, the number of harvesting is 2-3 times/rising age. It depends on the size of the white shrimp to be reared when the pond is closed. Harvesting white shrimp first of all reduce the water level in the shrimp pond from 2 to 1.5 meters to a depth of 0.5 meters. Workers prepare the equipment for catching white shrimp, comprising nets, shrimp carrying baskets, 1000 liter water tanks, ice, and mini trucks. 12 workers were worked in this experiment. 7 people will walk the nets along the edge of the shrimp pond to surround the nets to cover as much space as possible for walking. 5 workers waiting in the pond will help pull the nets to make the area smaller. To collect shrimp in a limited area, 7 workers inside the pond 5 workers will stand and hold the nets, and 2 workers will be outside the nets, 1 in 2 scoops the white shrimp into the basket and brought it to one worker to make a link at the basket for people standing on the edge of the well to pull up. 5 workers at the edge of the well will share their duties, 2 will pull the ropes up to the edge of the well, 2 will lift the drums to the edge of the mini truck, and the other 1 person will perform the duty of circulating the basket into the pond for the workers in the water who carry the shrimp to continue using. Mini trucks will have 2 staff members who will lift the shrimp seedlings and pour them into a 1000 liter water tank, inside which will contain ice. By allowing the water to reduce the water temperature not higher than 7 degrees which is order for reducing the damage from the shrimp bouncing around. It will take 30 minutes to harvest white shrimp 500 kg of harvest. In the tank, an air diffuser is placed and pure oxygen is delivered into the tank to prevent the lack of oxygen of the white shrimp during transport. Transport the white shrimp to the white shrimp sorting yard. There are 2 workers in the mini truck to go to the white shrimp sorting yard will take the white shrimp down to the shrimp sorting yard for the harvest white shrimp will continue until all the white shrimp are nothing in the pond. The workers will perform alternate duties according to items 1-6 until the white shrimp is exhausted from the pond.



Figure 1 Worker dragging a net around the pond



Figure 2 Surrounding and scooping white shrimp



Figure 3 The white shrimp scooped into mini truck



Figure 4 The condition of the shrimp soaked in cold water to knock the white shrimp to stun



Figure 5 A boat raising white shrimp from an agricultural vehicle to a white shrimp sorting yard

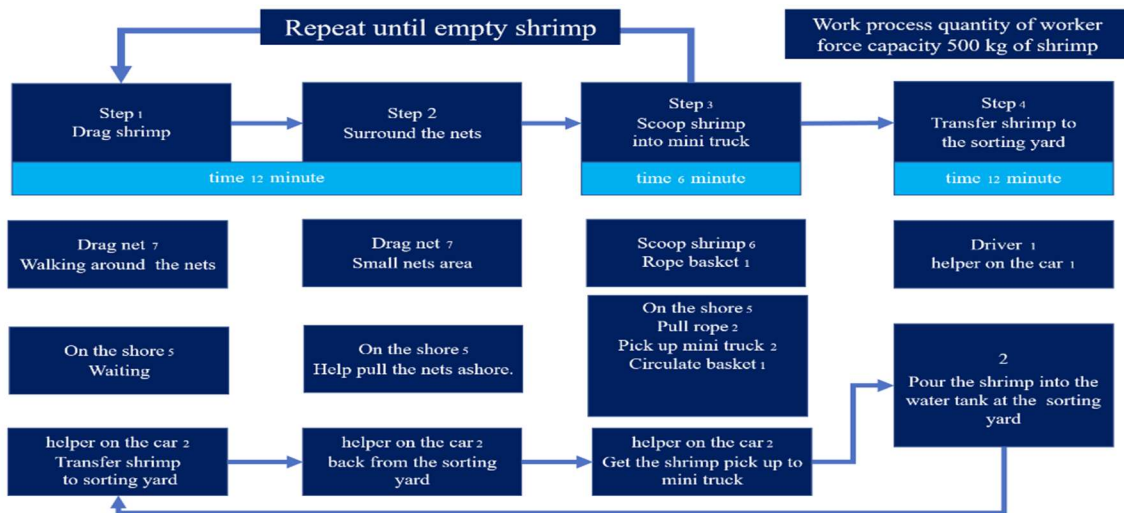


Figure 6 Shows the flowchart of the white shrimp harvesting process

2. Experimental research on transferring white shrimp with a 360 meter pipe

The important factor in the transportation of white shrimp is the quality of the white shrimp that is harvested and sent to the shrimp sorting yard. Conventional transport is carried out in 1000 liter tanks and packed with ice to a temperature of less than 7 degrees C and install the air diffuser head tank and oxygen to provide DO (Dissolved Oxygen) over 5 parts per million (Part Per Million,

ppm), which is the value that white shrimp can live well. The time of transportation of white shrimp in the pipeline system is variable between the ratios of white shrimp to the water flow-rate delivered

Was the ratio that influenced white shrimp? Because white shrimp oxygen consumes by 1 kg of white shrimp = 0.7 Kg O₂/hr./1 Kg. divided into 0.35 Kg O₂/hr./1 Kg white shrimp and small aquatic plants and small animals in water. About 0.35 Kg O₂/hr. /Kg white shrimp.

Experimental purpose, the maximum amount of white shrimp that can deliver white shrimp in a 10-inch pipe system. The rate of flowing water and the water velocity that can send white shrimp ,ratio of white shrimp / water quantity in the pipe, the amount of oxygen in the water DO (Dissolved Oxygen) decreased when the white shrimp traveled in the pipe. Time of delivery of white shrimp from origin to destination, the quality of white shrimp when delivered by pipe system such as mortality rate, white shrimp quality condition, white shrimp body color.

Equipment PVC pipe, size 10 inches, length 360 meters ,4 PVC joints of size 10, 3-way joints for 1 shrimp water separator 1 set ,Submersible water pump, submersible pump, outlet pipe size 10 inches, 10 power, 3 phase, HTC brand, model L250A. , Shrimp size 20 pieces/kg, amount 300 kg (6,000 pieces), Water oxygen meter, YSI brand, and model Pro 20, Water flow meter, IMARI brand, model CLM-700

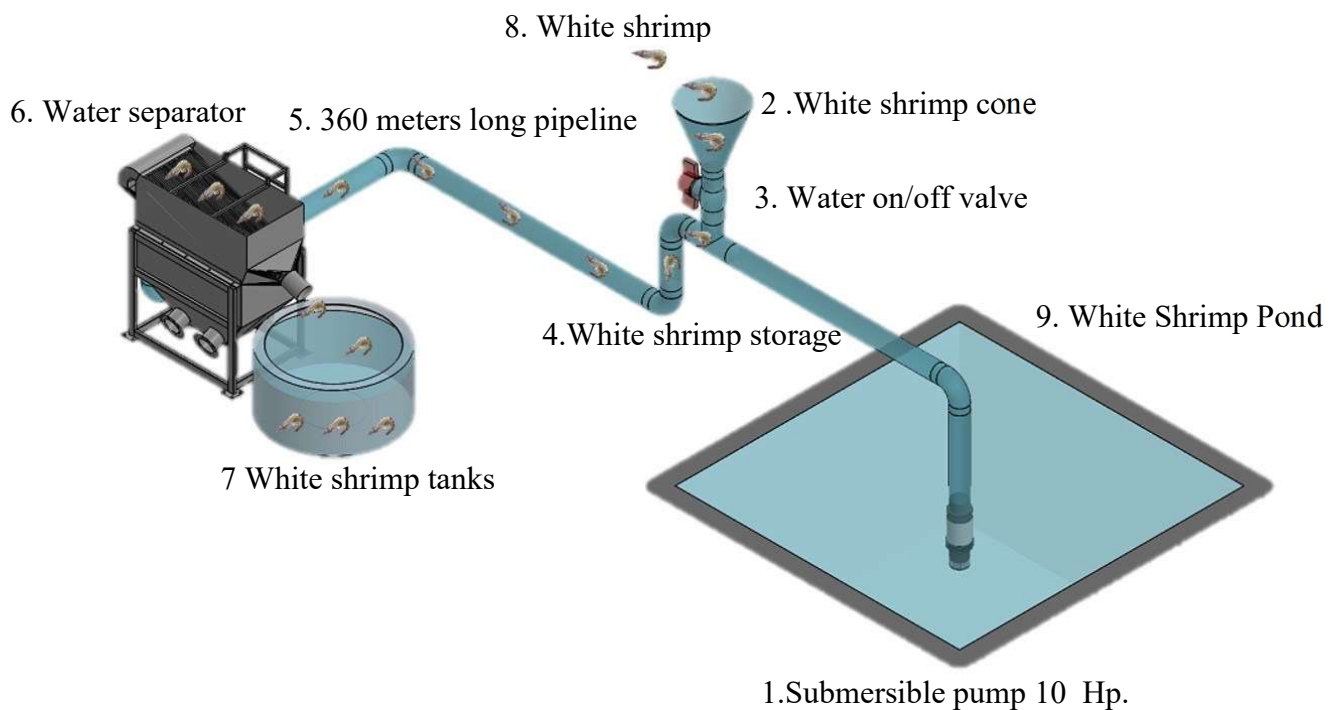


Figure 7 Pipeline layout and equipment for testing the transmission of white shrimp with a 360 meter pipe

Experimental procedure is connected a PVC pipe, diameter 10 inches, length 360 meters. The source is connected to a submersible pump. Dip into the white shrimp pond and connect a long pipe from the bottom of the pond and connect PVC 3 way joint. The starting point is opened the channel for packing the white shrimp into the white shrimp pipeline at the top of the PVC 3 Way joint and connect the pipe 360 meters long. At the end, there is a water separator unit in the white shrimp sorting yard.

Experiment following steps: first turn on the submersible pump to allow water to fill the pipe system. Adjust the inverter to control the water pump rpm. Cycle to achieve the desired amount of water and flow rate. Measure the oxygen in the water; fill the white shrimp in the tray to allow the white shrimp to enter the pipe. Gradually fill the white shrimp until 300 kg. During the fill of the

white shrimp, open the water from the submersible pump and gently send it into the pipe system to feed the system so that the white shrimp in the pipe system is sufficient. Oxygen in water, after filling the white shrimp, close the 1st water valve to prevent water back out through the shrimp fill point, turn on the water pump to send the shrimp. Start timer, the end point of pipe the water separator unit is to separate the white shrimp and the water from each other. Time the water arrives at the water separator unit; record the starting time for the first set of white shrimp, timers arrives at the water separator unit. Time for the last white shrimp to arrive at the water separator unit, measure the flow rate of water inside the pipe., checking the condition of the white shrimp for any spots and damage and the last record the data.



Figure 8 Shows a shrimp pond with a submersible pump installed



Figure 9 Shows a 10-inch pipe, 360 meters



Figure 10 Water separator



Figure 11 Inner the separation



Figure 12 Measures DO Dissolve Oxygen% oxygen saturation and temperature before and after

Table 1 Details of the experimental transfer of white shrimp with a pipe distance of 360 m

Experiment details		
Experimental site	Tart provincial Thailand	
Date of trial	20/09/2021	
<i>white shrimp</i>		
Shrimp Size	20	pieces/kg
weight	300	Kg.
Quantity	6000	pieces
<i>pipe and pump systems</i>		
Pipe length	360	Meters.
PVC pipe diameter	10	inch
Flow rate	400	Cubic meters/hour.
Submersible pump	HTC brand,	Model L-250 A
Power	10	HP

3. Experimental research biomechanics of white shrimp

In order to design white shrimp harvesting process and equipment or machine to improve shrimp harvest processes. It is necessary to know the weakest point of white shrimp and their tensile strength since the white shrimp harvesting process is a water pressure generation all process. Piping system physiological studies of white shrimp and questionnaires and surveys of shrimp workers showed that the most vulnerable point of shrimp damage was at the junction between the white shrimp head and the shrimp body. White shrimp had this point was the weakest point of the white shrimp under the physiology of the white shrimp. The biomechanics and the direct experience of the shrimp farmer, therefore in the study, the biomechanics of the white shrimp will study the tensile forces at the joints that are critical points of the white shrimp.

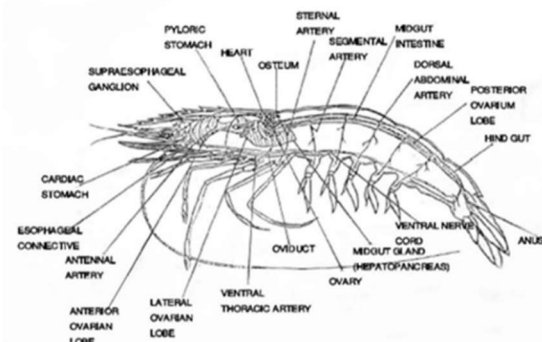


Figure 13 Physiology of white shrimp



Figure 14 Shows a white shrimp

Equipment and material

White shrimp, size 20 pieces/kg, 38 pieces, Digital Scales, String and fishing hook number 4, The tank contains water and ice. And video recorder

Experimental method

The live white shrimp with the weight of 20 kg are immersed in a bucket of ice water with a temperature not exceeding 7 degrees C to knock the white shrimp into an unconscious state. The hook at the tail of the 2nd crater from the tail and hook the white shrimp head at the center of the head

centered on the length and height of the white shrimp head. At the head of the fishing line about the shrimp head, one end is tied to a digital scale. Place the shrimp tendon and digital scales in the horizontal plane with the ground. Pull out the tail part by keeping the head tied to the digital eye fixed in place, Record images and videos of digital scales to record the maximum tensile point at the end record the data.



Figure 15 Biomechanical experiment tensile strength that the white shrimp



Figure 16 shows a cold water tank for keeping white shrimp quality

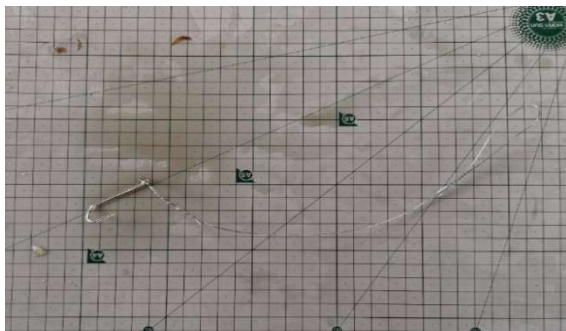


Figure 17 Hook No. 4 hooking the white shrimp to pull



Figure 18 Harvesting location of white shrimp around the tail and head



Figure 19 The moment the white shrimp is damaged by traction



Figure 20 Shows a sample of white shrimp studied

Results and Discussion

Experimental results from the study found that:

1. The results shows that, the general harvesting of white shrimp study of closed pond, the key step is to lower the water level so that workers can safely walk in and lay the nets. The number of workers in the workforce is 14 people, capable of harvesting 1,000 kg/hour of white shrimp. Each of them has different roles in harvesting white shrimp. From the study, it was found that the duties were

clearly divided and uninterrupted. Another important factor in the closed pond harvesting of white shrimp is the stunning of white shrimp by immersion in cold water less than 7 °C to reduce the movement of white shrimp due to shock and stress surrounding the net. During transportation to the shrimp to sorting yard, importance of the movement of shrimp is not reduced, the shrimp will be wounded during transportation, causing the quality of the white shrimp to deteriorate.

2. Results of the experimental research on transferring white shrimp with a 360 meter pipe and 300 kg of (6,000) white shrimp, no white shrimp were found dead. No wound damage was found, and the shrimp were in good health and bouncing well. There was no white necrosis of the white shrimp due to shock or stress. From the experiment, the DO (Dissolved oxygen) value in the source water was 6.11 PPM, the destination out of the water separator unit was at 5.2 PPM, which was the ideal value to allow the white shrimp to stay comfortably in the water without stress or damage from the lack of DO. In water, the delivery time for water and shrimp was 5 minutes with a water supply of 400 m³ / hour. From the above data, we found the ratio of white shrimp and water 9 kg/m³ water or white shrimp biomass 9 kg/ m³ water. It is an appropriate rate for the delivery of white shrimp through the pipeline system.



Figure 21 The condition of the white shrimp tested through the pipeline system

Table 2 Results of the experimental transport of white shrimp with a tube distance of 360 m.

The results of the experiment of transport white shrimp 360 m		
<i>White shrimp release point</i>		
Dissolved oxygen value	6.11	PPM
% saturation of oxygen in water	84.8	% saturation
Water temperature	29.6	degrees C
<i>The end point of the shrimp and water separator pipe</i>		
Dissolved oxygen value	5.2	PPM
% saturation of oxygen in water	74.2	% saturation
Water temperature	31.2	degrees C
<i>time</i>		
Water release time and white shrimp	9.28	o'clock
water and white shrimp to water separator	9.33	o'clock
The delivery time for white shrimp is	5	minus
<i>White shrimp quality</i>		
condition	vigorous and alive	
Die	non	
Damaged, broken neck, torn tail	non	
body marks	non	
White meat, from shock, none	non	

3. Results of the experimental research biomechanics of white shrimp from the testing were found that white shrimp had the least stressful area. The joint point between the body and the shrimp neck as expected. From the experiment with the size of 20 white shrimps/kg, the results were as shown in the table. The table shows the results of the white shrimp biomechanics experiment with the tensile strength of 20 white shrimp/kg.

Table 3 Shows the results of the biomechanical experiment of white shrimp with head extraction of white shrimp

No.	breaking load Kg-force	breaking point	Physical	No.	breaking load Kg-force	breaking point	Physical
1	1.27	Headless	normal	20	1.57	Headless	Small sized 30 pieces/kg.
2	1.18	Head lacerate	soft shell	21	2.06	Headless	normal
3	1.57	Headless	normal	22	2	Headless	normal
4	1.65	Headless	normal	23	1.75	Headless	normal
5	1.58	Headless	normal	24	1.72	Headless	normal
6	2.06	Headless	normal	25	1.45	torn tail	soft shell
7	2.13	Headless	normal	26	2.2	Head lacerate	soft shell
8	2	Headless	normal	27	1.55	torn tail	soft shell
9	1.84	Headless	normal	28	1.39	Headless	soft shell
10	1.92	Headless	normal	29	1.93	Headless	normal
11	2	Headless	normal	30	1.72	Headless	normal
12	1.89	Headless	normal	31	1.39	torn tail	soft shell
13	1.9	Headless	normal	32	1.43	torn tail	soft shell
14	1.98	Headless	normal	33	2.07	Headless	normal
15	2.32	Headless	normal	34	1.95	Headless	normal
16	1.89	Headless	normal	35	1.79	Headless	normal
17	1.97	Headless	normal	36	1.79	Headless	normal
18	2.1	Headless	normal	37	1.58	Headless	Small sized 30 pieces/kg.
19	2.07	Headless	normal	38	1.38	Headless	soft shell

From the experiment, it was found that the number of white shrimp in the experiment was 38 white shrimp, 20 shrimp/kg. Compared to the number of harvesting shrimp, it was found that white shrimp were soft shelled because of the recent molt. The shrimp molting process and shrimp that is smaller than standard size are mixed with several shrimp because white shrimp cannot grow to the same size throughout the pond. So white shrimp is harvested with a mixture of normal size, smaller shrimp and soft shell shrimp are also mixed because of the natural molting of the white shrimp aquaculture farmer cannot force the simultaneous molting throughout the pond. However, the ratio of split size shrimp and soft shell shrimp was the standard ratio of large shrimp farming.

From the experiment, we found white shrimp can be quantified from Linear regression where $R^2 = 0.9956$ $y = 0.0011x^6 - 0.0425x^5 + 0.6327x^4 - 4.5413x^3 + 16.556x^2 - 26.645x + 15.145$ $y =$ number of white shrimp $x =$ tensile force (kg-force) From the white shrimp harvest data; it is found that the ratio of soft shell shrimp is 1% and small shrimp is 12%. Therefore, in order for the data to be used in the design of a suitable white shrimp harvest, it must be able to be used with shrimp that

soft shell too Therefore, the design value should be 1.18 kg-force, which will be the most suitable value.

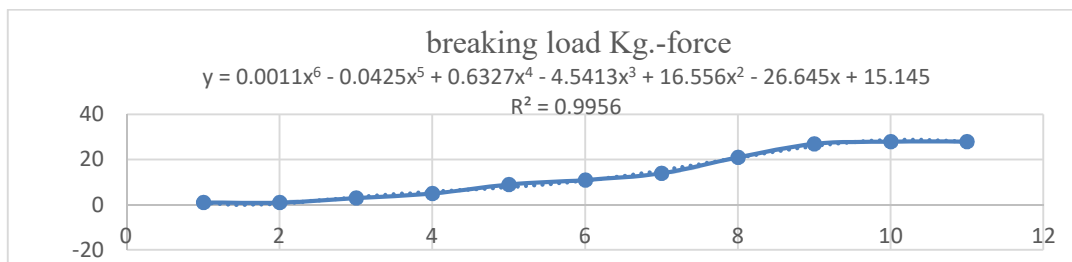


Figure 22 Shows the linear regression relationship $y = \text{number of white shrimp}$ $x = \text{Breaking load (Kg.-force)}$

Conclusion

Depends on the results of these 3 experiments: 1. Study of the general harvesting of white shrimp in medium to large shrimp farms by netting method. 2. The research experiment of transport white shrimp with a pipe distance of 360 meters. 3. White shrimp biomechanical research experiment.

In the past, the development of harvesting white shrimp has been a very controversial topic, as the feasibility of piping for white shrimp is because of the high DO consumption. There is also an impact on the quality of white shrimp. From these three studies and trials, we found it was possible to develop a process for harvesting white shrimp by pipe transport of 360 m or more. If it is possible for a white shrimp delivery rate of 3.6 tons/hour and be able to design a white shrimp harvest with a design that does not exert a force on the shrimp at 1.18 kg force. It must be capable of delivering water at a minimum of 400 m³/hour, white shrimp can be delivered in a biomass ratio of 9 kg/m³ of water. The oxygen in the delivery water (DO) must not be less than 5 ppm. The design must consider the capability of the shrimp. In order to swim away from the suction force, the shrimp harvest must be designed the power source must not injure the white shrimp. When referring to shrimp harvest data, white shrimp harvest must be capable of harvest over 1,000 kg/hour of white shrimp.

Reference

- Maulaya, R., Herodian, S., Design of A Vacum Type Shrimp Penaeus sp Harvester, *Indonesian Society of Agriculture Engineer JTEP pertania*, ISSN 2338-8439, 27(1), Apr.
- Miao, W., Wang, W. (2020), *Trends of Aquaculture Production and Trade: Carp, Tilapia, and Shrimp*, Published by the Asian Fisheries Society, 2020, 6-15.doi.org/10.33997/j.afs.2020.33.S1.001.
- Ministry of Agriculture and Cooperatives of the Kingdom of Thailand, Bureau of Agricultural Commodity and Food Standards Ministry of Agriculture and Cooperatives, (2561), *THAI AGRICULTURAL STANDARD TAS 7422-2018, GOOD AQUACULTURE PRACTICES FOR MARINE SHRIMP HATCHERY AND NURSERY*, Bangkok. (MOAC) Retrieved from http://www.ratchakitcha.soc.go.th/DATA/PDF/2562/E/298/T_0003.PDF
- Ohs, L., Grabe, S. W. and Creswell, R. L. (2018), *The Utilization of a Fish Pump for Harvesting Shrimp from Tanks and Ponds* Cortney, Fisheries and Aquatic Sciences, March 2018. Retrieved from <http://edis.ifas.ufl.edu>
- Panichpatanakit, S., Siriburananon, S. (2018) “The structure of the Thai shrimp industry and future challenges”, *Seminar on Economics in the Southern Region of 2018*, 12 June 2018, Bank of Thailand. Retrieved from https://www.bot.or.th/Thai/MonetaryPolicy/Southern/DocLib/shrimp_minisym.pdf

A Comparative Study on Criteria for Sustainable Supplier Selection

Surasak Choobthaisong and Rapee Kanchana*

*Department of Industrial Engineering, Faculty of Engineering, Rajamangala University of
Technology Thanyaburi, Pathum Thani 12110, Thailand*

** Corresponding email: rapee.k@en.rmutt.ac.th*

Abstract

Supplier selection and evaluation is as an important strategic decision-making process of an organization to increase its supply chain performance. Due to changing customer needs and increasing the degree of global sustainability, many organizations try to adjust their supplier selection and evaluation criteria in order to choose the most suitable supplier for their business. For this reason, this paper aims to analyze and comparative study on criteria used for supplier selection and evaluation emphasized on sustainability perspective. Moreover, a comparative study on supplier selection and evaluation criteria among selected industries is also presented.

The study initially relies on literature reviews ranging from 2015-2020 which mostly focused on the terms of sustainable supplier selection and sustainability manufacturing in order to identify the criteria used for supplier selection and evaluation. Then Pareto principle is used to analyze in order to identify the most popular criteria used for selecting the sustainable supplier. Three industry sections; automotive, electrical appliance & electronic and fashion & textile are selected for a comparative study in order to investigate the similarity or difference among criteria used for sustainable supplier selection and evaluation.

The results show that the criteria used for sustainable supplier selection and evaluation can be classified into three main dimensions; economic, environmental and social perspectives. By a comparative study among industries, it found that there have similarities on three main criteria used for sustainable supplier selection and evaluation. The results of this study will be beneficial for any industry to use them as a guideline to adjust its supplier selection and evaluation strategy in order to fit the organization's strategy sustainably.

Keywords: Supplier selection and evaluation, Sustainable supplier selection criteria

Introduction

According to the Sustainable Development Goals (SDGs) concept initiated by the United Nations organization with its 15-years framework (2015-2030), nowadays of global pressure from diverse stakeholder groups for sustainability, industries and companies are finding ways to meet this ever increasing demand to remain highly competitive so that many organizations have started to implement sustainable business practices (Khan *et al.*, 2018). Moreover, Chang *et al.*, (2021) mentioned that to minimize the impact on society, environment, resources and human life as much as possible, sustainable production is as a concept that takes into account environmental and social factors while maintaining profits to help the companies achieve a competitive advantage. In short, it can be said that companies nowadays face increasing pressure on sustainability manufacturing from governments, consumers and stakeholders as shown Figure 1. Due to the fact that, companies have to focus on how to manage the overall sustainability performance of organizations. Ahmadi *et al.*, (2020) and Taherdoost and Brard., (2019) said that supplier's performance is an important element for building an efficient sustainable innovative supply chains and enhancing organizational performance then evaluating and selecting the right supplier become a key importance strategic decision in doing business today. A good sustainable supplier selection model in a dynamic competitive and regulatory environment can help to reduce the environmental and legal risks and

increase the competitiveness of a firm (Girubha *et al.*, 2016). Therefore, to select the right supplier, various criteria should be considered and evaluated with respect to each supplier's attribute (Khan *et al.*, 2018).

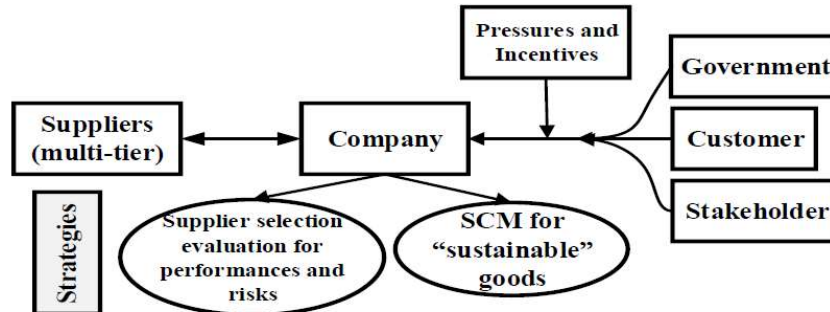


Figure 1 Drivers on sustainable supply chain management

Triple Bottom Line (TBL) was concept created by John Elkington in 1997 (see Figure 2), pointing out that a business can grow sustainably that must grow in balance in all three dimensions; economic environmental, and social dimensions. The TBL concept where all three dimensions of sustainability are considered needs to be incorporated into the supplier selection policies of the buyer company, if the buyer organization seeks to move toward sustainable manufacturing(SM) Ghadimi & Heavey, (2014) and Braccini and Margherita, (2019).

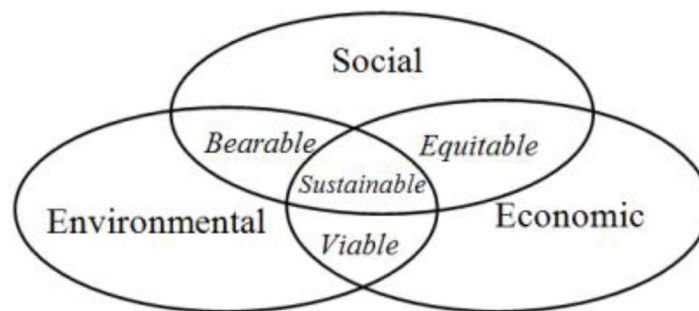


Figure 2 Three Pillars of Sustainability

The traditional supplier selection criteria mainly concentrate on economic benefit and cost optimization but at present there is increasingly not only focus on environmental performance to be green supplier but also need to consider their social responsibility (Taherdoost and Brard., 2019). Supplier selection criteria are typically divided into quantitative and qualitative attributes, and the selection of suitable criteria also depends on the purchasing situation (Zhou and Xu., 2018). The process of evaluating suppliers is choosing the right criteria. Girubha *et al.*, (2016) and Chang *et al.*, (2021) confirmed that for being sustainable supplier management it requires consideration of the economy, environment, and society. It means that the criteria for sustainable supplier selection (SSS) should be based on three dimension factors: economic, environmental and social. Establishing criteria for SSS to make an appropriate assessment Sustainability therefore, has become an integral part of today's business strategy (Zhou and Xu., 2018).

Therefore, this paper aims to analyze and comparative study on criteria used for supplier selection and evaluation emphasized on sustainability perspective. Moreover, a comparative study on supplier selection and evaluation criteria among selected industries is also presented.

Materials and methods

In order to achieve the above objectives, there are many tasks that have to be undertaken. The first task began with studying on literature reviews ranging from 2015- 2020 which mostly emphasized on the terms of supplier selection & evaluation and sustainability manufacturing. Key criteria for sustainable supplier selection were identified with the frequency of citations. The next task is to examine the literature with Pareto principle in order to identify the most popular criteria used for selecting the sustainable supplier. Three industry sections; automotive, electrical appliance & electronic and fashion & textile are selected for a comparative study in order to investigate the similarity or difference among criteria used for sustainable supplier selection and evaluation. The last major task is to provide a guideline on establishing a framework for developing the criteria used in the selection of sustainable suppliers in each industry. Figure 3 presents the overall of research methodology of this study.

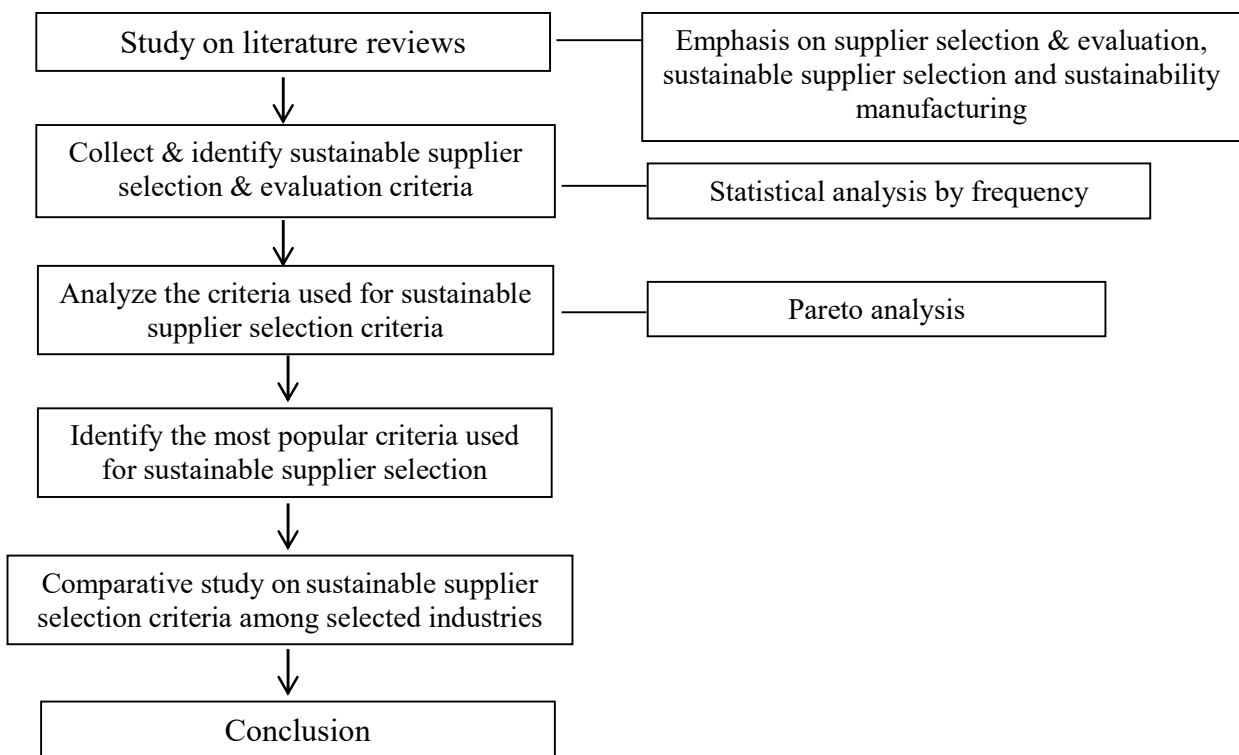


Figure 3 Research Methodology

Results and Discussion

Based on literature reviews, it found that prior to 2016 the supplier selection criteria trended to focus on the most popular used for supplier selection criteria were quality, cost, and delivery criteria and have been used as key criteria until now. For example, Phusavat *et al.*, (2007) stated seven major criteria that are regularly mentioned: quality, cost, delivery, technical service, management, responsiveness and environment/safety which consistent with K. Mukherjee (2014) and Hassanzadeh & Cheng., (2016). Sustainable manufacturing, defined by US Department of Commerce (2007) mean the creation of manufactured products that use processes that minimize negative environmental impacts, conserve energy and natural resources, are safe for employees, communities, and consumers and are economically sound. Therefore, a supplier selection as the most important process of an organization is an issue with many criteria of strategic importance for an organization and its supply chain, Aksoy *et al.*, (2014) and Rezaei & Behnamian, (2021). However, many organizations have started to implement sustainable business practices since 2016, (Khan *et al.*, 2018). Supplier selection

is a process by which the firms identify, evaluate, and select the suppliers of their required raw materials. In other words, the definition of sustainable manufacturing when combined with a sustainable supplier selection. It means integrating sustainability that encompasses social responsibility, environment and economy with production come together to create a product or service, Molamohamadi *et al.*, (2013). Then, supplier selection and evaluation criteria have been adjusted by increasing considerations based on the three main determinants of sustainable development namely, economic, environmental and social perspectives in order to ensure sustainability across the supply chain. The study initially relies on literature reviews ranging from 2015-2020 which mostly focused on the terms of sustainable supplier selection and sustainability manufacturing in order to identify the criteria used for supplier selection and evaluation. The results of this study, then describe the criteria used for supplier selection and evaluation emphasized on sustainability perspective with Economic, Environmental and social dimensions, see Table1, Table 2 and Table 3, respectively.

Table 1 Comparison of Sustainable supplier selection Economic Dimension Criteria

Dimension	20 Criteria	Authors														f							
		Jia et al., (2015)	Girubha et al., (2016)	Zimmer et al., (2016)	Amindoust & Saghafinia (2016)	Faisal et al., (2017)	Fallahpour et al., (2017)	Badri Ahmadi et al.,(2017)	Khan et al., (2018)	Senet et al., (2018)	Jain & Singh., (2018)	Rabiehal et al., (2019)	Rashidi & Cullinan., (2019)	Nugraha et al., (2019)	Ahmadi et al., (2020)		Chauhan et al., (2020)	Hendiani et al., (2020)	Okwu & Tartibu., (2020)	Aslami et al., (2021)	Chang et al., (2021)	Wu et al., (2021)	
Economic	QUL	●	●	●	●	●	●	●	●	●	●	●	●	●	●	●	●	●	●	●	●	●	19
	CST	●	●	●	●	●	●	●	●	●	●	●	●	●	●	●	●	●	●	●	●	●	20
	DLV	●	●	●	●	●	●	●	●	●	●	●	●	●	●	●	●	●	●	●	●	●	17
	FNS		●																				8
	FLX			●		●	●																10
	PFC				●					●	●	●		●									6
	EPS																					●	1
	MGO									●			●										2
	TNC		●	●							●	●	●			●	●	●		●	●		10
	RPT																			●			1
	RPS		●					●	●	●	●		●										6
	ATD		●																				1
	ISV															●							1
	PSP															●							1
	OPT											●											1
	SQC											●											1
	LTR			●								●											2
	LGC			●									●									●	3
	RLT																		●				1
	AVP																		●				1

Remark: QUL: Quality, CST: Cost, DLV: Delivery, FNS: Financial Status, FLX: Flexibility, PFC: Production facility and capacity, EPS: Enterprise size, MGO: Management and organization, TNC: Technical capacity, RPT: Reputation and references, RPS: Repair services, ATD: Attitude, ISV: Increased sustainability value, PSP: Producing sustainable products, OPT: Operational controls, SQC: Supply qualitative criteria, LTR: Long-term relationship, LGC: Logistical costs, RLT: Reliability, AVP: Availability of products.

Table 2 Comparison of Sustainable supplier selection Environment Dimension Criteria

Dimension	13 Criteria	Criteria													f								
		Jia et al., (2015)	Girubha et al., (2016)	Zimmer et al., (2016)	Amindoust & Saghafinia., (2017)	Faisal et al., (2017)	Fallahpour et al., (2017)	Badri Ahmadi et al.,(2017)	Khan et al., (2018)	Senet et al., (2018)	Jain & Singh., (2018)	Rabiehal et al., (2019)	Rashidi & Cullinane., (2019)	Nugraha et al., (2019)		Ahmadi et al., (2020)	Chauhan et al., (2020)	Hendiani et al., (2020)	Okwu & Tartibu., (2020)	Aslani et al., (2021)	Chang et al., (2021)	Wu et al., (2021)	
Environment	EMS	•	•	•	•	•	•	•	•	•	•	•	•	•	•	•	•	•	•	•	•	•	16
	POC	•	•	•	•	•	•	•	•	•	•	•	•	•	•	•	•	•	•	•	•	•	13
	GNT	•	•	•	•	•	•	•	•	•	•	•	•	•	•	•	•	•	•	•	•	•	13
	RSC	•	•	•	•	•	•	•	•	•	•	•	•	•	•	•	•	•	•	•	•	•	9
	REC	•	•	•	•	•	•	•	•	•	•	•	•	•	•	•	•	•	•	•	•	•	7
	GED	•	•	•	•	•	•	•	•	•	•	•	•	•	•	•	•	•	•	•	•	•	12
	WMS	•	•	•	•	•	•	•	•	•	•	•	•	•	•	•	•	•	•	•	•	•	8
	ENC	•	•	•	•	•	•	•	•	•	•	•	•	•	•	•	•	•	•	•	•	•	4
	RVL	•	•	•	•	•	•	•	•	•	•	•	•	•	•	•	•	•	•	•	•	•	1
	GNW	•	•	•	•	•	•	•	•	•	•	•	•	•	•	•	•	•	•	•	•	•	2
	GTP	•	•	•	•	•	•	•	•	•	•	•	•	•	•	•	•	•	•	•	•	•	3
	TCC	•	•	•	•	•	•	•	•	•	•	•	•	•	•	•	•	•	•	•	•	•	1
	HGM	•	•	•	•	•	•	•	•	•	•	•	•	•	•	•	•	•	•	•	•	•	1

Remark: EMS: Environmental Management System, POC: Pollution control, GNT: Green Technology, RSC: Resource consumption, REC: Recycling/Reuse, GED: Green products/Eco-design, WMS: Waste management system, ENC: Energy consumption, RVL: Reverse Logistics, GNW: Green warehousing, GTP: Green transportation, TCC: Toxic chemical usage control, HGM: Harmful gas missions

Table 3 Comparison of Sustainable supplier selection Social Dimension Criteria

Dimension	18 Criteria	Criteria																		f		
		Jia et al., (2015)	Girubha et al., (2016)	Zimmer et al., (2016)	Amindoust & Saghafinia., (2017)	Faisal et al., (2017)	Fallahpour et al., (2017)	Badri Ahmadi et al.,(2017)	Khan et al., (2018)	Senet et al., (2018)	Jain & Singh., (2018)	Rabiehal et al., (2019)	Rashidi & Cullinane., (2019)	Nugraha et al., (2019)	Ahmadi et al., (2020)	Chauhan et al., (2020)	Hendiani et al., (2020)	Okwu & Tartibu., (2020)	Aslani et al., (2021)		Chang et al., (2021)	Wu et al., (2021)
Social	ROE	•	•	•	•	•	•	•	•	•	•	•	•	•	•	•	•	•	•	•	•	11
	BSC	•	•	•	•	•	•	•	•	•	•	•	•	•	•	•	•	•	•	•	•	1
	EMP	•	•	•	•	•	•	•	•	•	•	•	•	•	•	•	•	•	•	•	•	9
	HSA	•	•	•	•	•	•	•	•	•	•	•	•	•	•	•	•	•	•	•	•	21
	INF	•	•	•	•	•	•	•	•	•	•	•	•	•	•	•	•	•	•	•	•	4
	SOC	•	•	•	•	•	•	•	•	•	•	•	•	•	•	•	•	•	•	•	•	16
	ROS	•	•	•	•	•	•	•	•	•	•	•	•	•	•	•	•	•	•	•	•	6
	LEO	•	•	•	•	•	•	•	•	•	•	•	•	•	•	•	•	•	•	•	•	1
	CHL	•	•	•	•	•	•	•	•	•	•	•	•	•	•	•	•	•	•	•	•	1
	STI	•	•	•	•	•	•	•	•	•	•	•	•	•	•	•	•	•	•	•	•	5
	ETH	•	•	•	•	•	•	•	•	•	•	•	•	•	•	•	•	•	•	•	•	1
	WOP	•	•	•	•	•	•	•	•	•	•	•	•	•	•	•	•	•	•	•	•	1
	SUA	•	•	•	•	•	•	•	•	•	•	•	•	•	•	•	•	•	•	•	•	3
	LCI	•	•	•	•	•	•	•	•	•	•	•	•	•	•	•	•	•	•	•	•	5
	DSP	•	•	•	•	•	•	•	•	•	•	•	•	•	•	•	•	•	•	•	•	1
	REL	•	•	•	•	•	•	•	•	•	•	•	•	•	•	•	•	•	•	•	•	1
	REH	•	•	•	•	•	•	•	•	•	•	•	•	•	•	•	•	•	•	•	•	1
	CUS	•	•	•	•	•	•	•	•	•	•	•	•	•	•	•	•	•	•	•	•	2

Remark: ROE: Rights of employee, BSC: Buyer supplier constraints, EMP: Employment Practice, HSA: Health and Safety, INF: Information disclosure, SOC: Social responsibility, ROS: Rights of stakeholders, LEO: Local employment opportunities, CHL: Child and force labor, STI: Stakeholder influence, ETH: Ethical behavior, WOP: Workplace diversity, SUA: Supportive activities, LCI: Local communities influence, DSP: Donations for sustainable projects, REL: Restriction on under age labor, REH: Restriction on long working hours, CUS: Customer’s satisfaction & Customer service

The Pareto principle (The 80/20 Rule) is then applied to identify the most popular criteria used for sustainable supplier selection (SSS) for each three dimension for overall industry perspective,

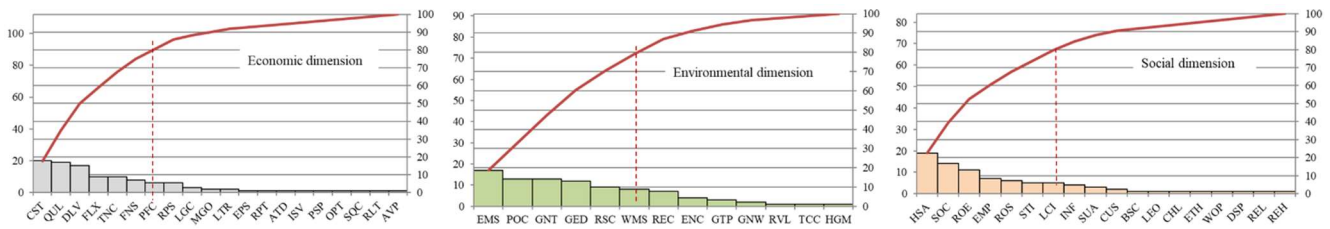


Figure 4 Identification of the most popular criteria used for SSS based on Pareto principle

The results as shown in Figure 4, illustrate that for economic dimension; the most popular criteria used for (SSS) emphasize on cost (CST), quality (QUL), delivery (DLV), flexibility (FLX), technical capacity (TNC), financial status (FNS) and Production facility and capacity (PFC) while environmental management system (EMS), pollution control (POC), green technology (GNT), green products/eco-design (GED), resource consumption (RSC) and waste management system (WMS) identify as key importance considerations for environmental dimension. On the other hand, there are seven key criteria concerns for social dimension namely; health and safety (HAS), social responsibility (SOC), rights of employee (ROE), employment practice (EMP), including rights of stakeholders (ROS), stakeholder influence (STI) and Local communities influence (LCI).

To investigate the similarity or difference criteria used for SSS among three industry sections; automotive, electrical appliance & electronic and fashion & textile, a comparative study is implemented. The results present as Table 4.

Economic dimension: The focus of Economic dimension is to ensure economic viability of the organization achieved through a sustainable method. Economic sustainability requires us to focus on the long-term sustainability of increasing revenue, market shares, and share prices rather than seeking short-term profit. Du *et al.*, (2020) stated economic benefits of an enterprise (gross output value/production cost) are an important part of measuring enterprise performance. Moreover, Okwu & Tartibu, (2020) noted that cost, advanced technology, on-time delivery, reliability, quality, and product availability are the factors that are identified as relating to the economic issues of the industry. The results of this study have confirmed that a set of key criteria on economic dimension consists with the literature reviews. The three key criteria become similarly importance used for SSS in three industries, namely cost (CST), quality (QUL) and delivery (DLV), while, flexibility (FLX), technical capacity (TNC) and financial status (FNS) have only more consideration for SSS in both automotive and electrical appliance & electronic industries.

Environmental dimension: since environmental sustainability defined as a meeting the resource and services needs of current and future generations without compromising the health of the ecosystems, Badri Ahmadi *et al.*, (2017). The results of this study show the similarity of a set of key criteria used for SSS for this dimension among three industries. The four similarity criteria include environmental management system (EMS), pollution control (POC), green technology (GNT) and green products/eco-design (GED) while, resource consumption area become importance criterion considered for automotive and fashion & textile industries.

Social dimension: This dimension focused on working place and employee' progresses with supportive activities including, local community influence as a key social factor of sustainability, (Okwu & Tartibu, 2020). Besides this, social responsibility also involves protection of consumer rights, social welfare, green safety, and other components (Du *et al.*, 2020). In short, this dimension focus on operating with social responsibility in business processes covering human rights issues legal labor rights fair business practices Creating a good working environment and ensuring the safety of

employees of the organization to the development of quality services for customers. The results of this study illustrate that health and safety (HAS), social responsibility (SOC) and rights of employee (ROE) have similarly importance consideration for SSS in all three industries, but, employment practice (EMP), stakeholder influence (STI) including local communities influence (LCI) have more concern only automotive and electrical appliance & electronic industries.

Table 4 Summary on comparative study criteria used for SSS among three industry sections

SSS Economic dimension Criteria				SSS Environment dimension Criteria				SSS Social dimension Criteria						
Abb./Industry	Overall	Elec&Elect Appliance	Automotive	Fashion.&Textile	Abb./Industry	Overall	Elec&Elect Appliance	Automotive	Fashion.&Textile	Abb./Industry	Overall	Elec&Elect Appliance	Automotive	Fashion.&Textile
CST	●	●	●	●	EMS	●	●	●	●	HSA	●	●	●	●
QUL	●	●	●	●	GED	●	●	●	●	SOC	●	●	●	●
DLV	●	●	●	●	POC	●	●	●	●	ROE	●	●	●	●
FLX	●	●	●	●	GNT	●	●	●	●	EMP	●	●	●	●
TNC	●	●	●	●	RSC	●	●	●	●	ROS	●	●	●	●
FNS	●	●	●	●	WMS	●	●	●	●	STI	●	●	●	●
PFC	●	●	●	●	REC	●	●	●	●	LCI	●	●	●	●
RPS	●	●	●	●	ENC	●	●	●	●	INF	●	●	●	●
MGO	●	●	●	●	GTP	●	●	●	●	SUA	●	●	●	●
OPT	●	●	●	●	GNW	●	●	●	●	BSC	●	●	●	●
LGC	●	●	●	●	TCC	●	●	●	●	LEO	●	●	●	●
LTR	●	●	●	●						ETH	●	●	●	●
										WOP	●	●	●	●
										REL				●
										REH				●

Conclusion

This paper provides a systematic literature review of articles published in 2015–2020 on supplier selection and evaluation criteria emphasized on sustainability perspective. Since sustainable manufacturing means integrating sustainability that encompasses social responsibility, environment and economy with production come together to create a product or service, then a supplier selection strategy need to be consistency with its organization’s strategy sustainably. The results of this study classified the sustainable supplier selection criteria into three dimensions based on sustainable manufacturing; economic, environmental and social aspects. The results of this paper illustrate that the three key criteria on economic dimension, namely cost (CST), quality (QUL) and delivery (DLV) become similarly importance used for SSS among three industries. As for environmental dimension, all three industries have similarity on a set of key SSS criteria include environmental management system (EMS), pollution control (POC), green technology (GNT) and green products/eco-design (GED), while, the health and safety (HAS), social responsibility (SOC) and rights of employee (ROE) have similarly importance consideration for SSS in all three industries. The last but not least, this study will be beneficial for any industry to use them as a guideline to adjust its supplier selection and evaluation strategy in order to fit the organization's strategy sustainably.

References

- Ahmadi, H. B., Lo, H.-W., Gupta, H., Kusi-Sarpong, S., & Liou, J. J. H. (2020). An integrated model for selecting suppliers on the basis of sustainability innovation. *Journal of Cleaner Production*, 277, 123261. doi:https://doi.org/10.1016/j.jclepro.2020.123261
- Aksoy, A., Sucky, E., & Öztürk, N. (2014). Dynamic Strategic Supplier Selection System with Fuzzy Logic. *Procedia - Social and Behavioral Sciences*, 109, 1059- 1063. doi:https://doi.org/10.1016/j.sbspro.2013.12.588
- Amindoust, A., & saghafinia, A. (2017). Textile supplier selection in sustainable supply chain using a modular fuzzy inference system model. *Journal of the Textile Institute*, 108, 1250-1258. doi:10.1080/00405000.2016.1238130
- Aslani, B., Rabiee, M., & Tavana, M. (2021). An integrated information fusion and grey multi-criteria decision-making framework for sustainable supplier selection. *International Journal of Systems Science: Operations & Logistics*, 8(4), 348-370. doi:10.1080/23302674.2020.1776414
- Badri Ahmadi, H., Hashemi Petrudi, S. H., & Wang, X. (2017). Integrating sustainability into supplier selection with analytical hierarchy process and improved grey relational analysis: A case of telecom industry. *International Journal of Advanced Manufacturing Technology*, 90. doi:10.1007/s00170-016-9518-z
- Braccini, A. M., & Margherita, E. G. (2019). Exploring Organizational Sustainability of Industry 4.0 under the Triple Bottom Line: The Case of a Manufacturing Company. *Sustainability*, 11(1). doi:10.3390/su11010036
- Chang, T. - W., Pai, C. -J., Lo, H. - W., & Hu, S. -K. (2021). A hybrid decision-making model for sustainable supplier evaluation in electronics manufacturing. *Computers & Industrial*
- Chauhan, A. S., Badhotiya, G. K., Soni, G., & Kumari, P. (2020). Investigating interdependencies of sustainable supplier selection criteria: an appraisal using ISM. *Journal of Global Operations and Strategic Sourcing*, 13(2), 195-210. doi:10.1108/JGOSS-02-2019-0017
- Du, Y., Zhang, D., & Zou, Y. (2020). Sustainable Supplier Evaluation and Selection of Fresh Agricultural Products Based on IFAHP- TODIM Model. *Mathematical Problems in Engineering*, 2020, 4792679. doi:10.1155/2020/4792679
- Fallahpour, A., Udony Olugu, E., Nurmaya Musa, S., Yew Wong, K., & Noori, S. (2017). A decision support model for sustainable supplier selection in sustainable supply chain management. *Computers & Industrial Engineering*, 105, 391- 410. doi:https://doi.org/10.1016/j.cie.2017.01.005
- Faisal, M. N., Al-Esmael, B., & Sharif, K. J. (2017). Supplier selection for a sustainable supply chain. *Benchmarking: An International Journal*, 24(7), 1956-1976. doi:10.1108/BIJ-03-2016-0042
- Fallahpour, A., Udony Olugu, E., Nurmaya Musa, S., Yew Wong, K., & Noori, S. (2017). A decision support model for sustainable supplier selection in sustainable supply chain management. *Computers & Industrial Engineering*, 105, 391- 410. doi:https://doi.org/10.1016/j.cie.2017.01.005
- Ghadimi, P., & Heavey, C. (2014). Sustainable Supplier Selection in Medical Device Industry: Toward Sustainable Manufacturing. *Procedia CIRP*, 15, 165– 170. doi:10.1016/j.procir.2014.06.096
- Girubha, J., Vinodh, S., & Vimal, K. E. K. (2016). Application of interpretative structural modelling integrated multi criteria decision making methods for sustainable supplier selection. *Journal of Modelling in Management*, 11, 358-388. doi:10.1108/JM2-02-2014-0012
- Hassanzadeh, S., & Cheng, K. (2016). Suppliers Selection in Manufacturing Industries and Associated Multi- Objective Decision Making Methods: Past, Present and The Future. *European Scientific Journal, ESJ*, 12, 93-93.
- Hendiani, S., Bagherpour, M., Tvaronavičienė, M., Banaitis, A., & Antucheviciene, J. (2020). Analyzing the Status of Sustainable Development in the Manufacturing Sector Using Multi-

- Expert Multi- Criteria Fuzzy Decision- Making and Integrated Triple Bottom Lines. *International Journal of Environmental Research and Public Health*, 17, 3800. doi:10.3390/ijerph17113800
- Jain, N., & Singh, A. R. (2020). Sustainable supplier selection criteria classification for Indian iron and steel industry: a fuzzy modified Kano model approach. *International Journal of Sustainable Engineering*, 13(1), 17-32. doi:10.1080/19397038.2019.1566413
- Jia, P., Govindan, K., Choi, T.-M., & Rajendran, S. (2015). Supplier Selection Problems in Fashion Business Operations with Sustainability Considerations. *Sustainability*, 7(2), 1603- 1619. Retrieved from <https://www.mdpi.com/2071-1050/7/2/1603>
- Khan, S. A., Kusi-Sarpong, S., Arhin, F. K., & Kusi-Sarpong, H. (2018). Supplier sustainability performance evaluation and selection: A framework and methodology. *Journal of Cleaner Production*, 205, 964-979. doi:<https://doi.org/10.1016/j.jclepro.2018.09.144>
- Molamohamadi, Z., Ismail, N., Leman, Z., & Zulkifli, N. (2013). Supplier Selection in a Sustainable Supply Chain. *Journal of Advanced Management Science*, 278- 281. doi:10.12720/joams.1.3.278-281
- Mukherjee, K. (2014). Supplier selection criteria and methods: past, present and future. *International Journal of Operational Research*, 27. doi:10.1504/IJOR.2016.10000076
- Nugraha, I., Hisjam, M., & Sutopo, W. (2019). Sustainable Criteria in Supplier Evaluation of the Food Industry. *IOP Conference Series: Materials Science and Engineering*, 598, 012006. doi:10.1088/1757-899X/598/1/012006
- Okwu, M. O., & Tartibu, L. K. (2020). Sustainable supplier selection in the retail industry: A TOPSIS- and ANFIS-based evaluating methodology. *International Journal of Engineering Business Management*, 12, 1847979019899542. doi:10.1177/1847979019899542
- Phusavat, K., Kanchana, R., & Helo, P. (2007). Supplier management: Past, present and anticipated future perspectives. *International Journal of Management and Enterprise Development*, 4, 502- 519. doi:10.1504/IJMED.2007.013455
- Rabieh, M., babaee, I., Rafsanjani, A., & Esmaeili, M. (2019). Sustainable Supplier Selection and Order Allocation: An Integrated Delphi Method, Fuzzy TOPSIS and Multi- Objective Programming Model. *Scientia Iranica*, 26, 2524-2540. doi:10.24200/sci.2018.5254.1176
- Rashidi, K., & Cullinane, K. (2019). A comparison of fuzzy DEA and fuzzy TOPSIS in sustainable supplier selection: Implications for sourcing strategy. *Expert Systems with Applications*, 121, 266-281. doi:<https://doi.org/10.1016/j.eswa.2018.12.02>
- Rezaei, S., & Behnamian, J. (2021). Strategic supplier selection based on modified sandcone theory and alignment principle. *Sustainable Production and Consumption*, 26, 256- 274. doi:<https://doi.org/10.1016/j.spc.2020.10.013>
- Sent, D. K., Datta, S., & Mahapatra, S. S. (2018). Sustainable supplier selection in intuitionistic fuzzy environment: a decision-making perspective. *Benchmarking: An International Journal*, 25(2), 545-574. doi:10.1108/BIJ-11-2016-0172
- Taherdoost, H., & Brard, A. (2019). Analyzing the Process of Supplier Selection Criteria and Methods. *Procedia Manufacturing*, 32, 1024- 1034. doi:<https://doi.org/10.1016/j.promfg.2019.02.317>
- Wu, C., Lin, Y., & Barnes, D. (2021). An integrated decision-making approach for sustainable supplier selection in the chemical industry. *Expert Systems with Applications*, 184, 115553. doi:<https://doi.org/10.1016/j.eswa.2021.115553>
- Zhou, X., & Xu, Z. (2018). An Integrated Sustainable Supplier Selection Approach Based on Hybrid Information Aggregation. *Sustainability*, 10, 2543. doi:10.3390/su10072543
- Zimmer, K., Fröhling, M., & Schultmann, F. (2016). Sustainable supplier management – a review of models supporting sustainable supplier selection, monitoring and development. *International Journal of Production Research*, 54(5), 1412-1442. doi:10.1080/00207543.2015.1079340

The Site Survey and Study of 8 kW Hybrid Wind Solar PV Air-Compress System for Water Treatment Process (Case Study at CPF Saraburi Province)

Sirisak Pangvuthivanich¹, Wirachai Roynarin^{2*}, Nima Azhari^{1,3} and Suthep Simala¹

¹ Doctor of Engineering Program in Energy and Materials Engineering Faculty of Engineering Rajamangala University of Technology Thanyaburi, Thanyaburi, Pathumthani, Thailand

² Energy Research and Service Center Faculty of Engineering Rajamangala University of Technology Thanyaburi, Thanyaburi, Pathumthani, Thailand

³ Bazme alley, Valasr st, Enghelab st, Tehran, Iran

* Corresponding email: wirachair.en@rmutt.ac.th

Abstract

In the present, the production of oxygen and purifying water in water treatment process use the electricity sources from fossil. The electricity from fossil generate Co₂ and P.M.2.5 dust to the air, therefore the water treatment made more pollution to the air for the traditional system. This research shows the new concepts of water treatment by net zero CO₂ using wind turbines and solar PV to generate the compressed air to water treatment pond. The system compound with 5kw air compress wind turbines with 3kw PV for generates electricity to air compressor. Both wind and PV produce the air to the water treatment pond. The fossil fuels, which is causing global warming and making the air and soil polluted therefore will not occurred in this design. From the analysis of wind speed at the CPF aeration pond, Kaeng Khoi, Saraburi province, from the research team showed the appropriated design that will install a 5 kw and 3kw PV in hybrid system. These can be displayed as shown in the result of the average wind speed, which is processed by the wind speed model analysis program. This system show the average wind speed in the area at the location of the CPF aeration pond. The analysis of the area obtained from the CPF Kaeng Khoi aeration pond survey revealed that the annual average wind speed was about 3.17 m/s at an altitude of 10 m from the ground and at a wind speed of 4.8 m/s at the altitude of 50 meters. However, the investigation result shown the average wind speed about 4.5m/s could be used to simulate the airflow form the wind machine about 600 liters of compressed air per minute, which is processed by the wind speed model analysis program compared to the wind machine specification. Additionally, for the solar radiation power density was simulated using the PVsyst software to analyst the direct normal irradiation to the focused area. The power density results shows 1,284 kwh/m² to estimate the air flow from the PV system per year. It was found that the power generation capacity of the system was approximately 4,482 electrical units per year. This will result in the use of clean energy for the environment. The hybrid wind solar system if applied to the site will replace electric bill to the investor or customers about 350,000 baht per year. The system is cost-effective and the payback time will be about 3.5 years, while the system has designed for the lifetime of more than 15 years.

Keywords: Air compressor wind turbines, Water treatment, Hybrid System

Introduction

Energy is an important factor in sustaining human life. We use energy to generate electricity for transportation, service goods, production in agriculture, manufacturing industries, living and other purposes. The majority of raw materials from which electricity is created are fossil fuels. Crude oil, natural gas, and coal, for example, are the primary suppliers to most power plant sectors. Since global warming is caused by these various factors, in order to reduce the amount of carbon dioxide in the

air, CPF (Thailand) Public Company Limited has realized the importance of solving such problems. The solution to the problem is sustainable and permanent. The goal is to offer clean renewable energy that can be featured as a landmark to the current system in the original areas. While solving problems that do not affect the existing power generation sector. In addition, the potential of setting up a learning center for renewable energy and expanding the results to various departments/types of the company across Thailand for example, the location of the water supply plant within the chicken processing plant. These types of plants have the potential to generate electricity with low wind speed turbines and combine them with one of the best solar cell locations in the country, as well as be able to create a model place for study tours on renewable energy.

PV–wind system a considerable amount of wind power is found to be generated during half of the year when average PV power production is comparatively less. The cost of electricity from the simulation model is found to be \$0.488/kWh while renewable fraction in the total electricity share is obtained to be 0.90. From the actual performance of the plant, maximum wind penetration is observed to be 32.75% (Subhadeep B. and A. Shantanu, 2015)

The demand for electricity is increasing day by day, which cannot be fulfilled by non-renewable energy sources alone. Renewable energy sources such as solar and wind are omnipresent and environmental friendly. The renewable energy sources are emerging options to fulfill the energy demand, but unreliable due to the stochastic nature of their occurrence. Hybrid renewable energy system (HRES) combines two or more renewable energy sources like wind turbine and solar system. (Vikas K., Savita N., and Prashant B., 2016)

The study to develop a new application for a wind turbine machine as a power source for shrimp farm aeration process. A Vertical Axis Wind Turbine (VAWT) machine was designed, constructed and applied to a selected shrimp farm in southern Thailand to replace two-stroke diesel engines commonly used in the aeration process. Two-stroke diesel engines produce noise and black-smoke pollution from their exhausts to surrounding farm areas. By using the wind machine these environmental problems fairly well solved. Approximately, every litre of diesel fuel used by a typical two-stroke diesel engine in this application produces about 2.36 kg of carbon dioxide to the atmosphere per year. (Roynarin, W., 2003).

Among all existing energies, along with solar energy wind is one of the most developed renewable energies across the world. Wind energy systems have been greatly developed since the original windmill principle was discovered by the Persians around 200 B.C. High power modern designs were achieved in the 20th and 21st centuries, as described by the timeline of M.R. Islam et al. (Islam, M.R.; Mekhilef, S.; Saidur, R.)

With this potential, the company can collaborate with the Energy Research and Service Center of Rajamangala University of Technology Thanyaburi, which has expertise in wind energy and sunlight. The university staff will use the data to help study the feasibility of exploring and analyzing the survey of the renewable energy prototype project in the combined compressed air systems. For the sustainable use of renewable energy consistent with the domestic business sector, many companies in the country have a policy of compelling their companies to set a scientifically greenhouse gas reduction goal (SBTi). The goal is to reduce greenhouse gas emissions to a level that does not raise global temperatures by more than 2 degrees Celsius. Moreover, to follow the resolutions of the Thai Leaders' COP 26 meeting in Glasgow earlier this month, is a way to make key commitments such as reducing carbon emissions to achieve net zero greenhouse gas emissions, or Net Zero.

For the best potential outcome, the Energy Research and Service Center Faculty of Engineering at Rajamangala University of Technology Thanyaburi has consulted the staff of CPF (Thailand) to survey the areas at the water supply plant within the chicken processing plant in Kaeng Khoi, Saraburi Province. The results of the survey are as follows:

Wind energy measurement results around the CPF aeration pond, Kaeng Khoi, Saraburi Province

From the analysis of wind speed at the CPF aeration pond, Kaeng Khoi, Saraburi province, by the Energy Research and Service Center. The Faculty of Engineering at Rajamangala University of Technology, Thanyaburi, will install a compressed air windshield with a capacity of 5 kilowatts. These can be displayed as shown in the result of the average wind speed, which is processed by the wind speed model analysis program. For the average wind speed in the area at the location of the CPF aeration pond.



Figure 1 The area of the wind speed and solar intensity measurement point

Figure 1 show the area of the wind speed and solar intensity measurement point. In this regard, the Energy Research and Services Center performed two computational models that are correlated in the analysis of wind speed data and wind power generation from wind turbines. The Wind Atlas Analysis and Application Program (WAsP) is developed by the Wind Atlas Analysis and Application Program (WAsP). Wind Energy Department under Risø DTU: National Laboratory for Sustainable Energy, Denmark. This is because wind resource assessment is an important step in the pre-operation phase of the wind turbine project. In order to minimize project risks, an accurate assessment of wind resources is required.

The research team has studied the potential of wind energy at CPF aeration pond(Show in Figure 1), which is around the aeration pond. It uses the wind power layer as a range of wind power values to show the potential of the wind power source in that area. By using wind power density measurements at 2 standard heights, which are 10 meters and 50 meters, the wind speed increases with the height above the ground. The analysis of the area obtained from the CPF Kaeng Khoi aeration pond survey revealed that the annual average wind speed was about 3.17 m/s at an altitude of 10 m from the ground and at a wind speed of 4.47 m/s at the altitude is 50 meters, as shown in Figures 2 and 3.

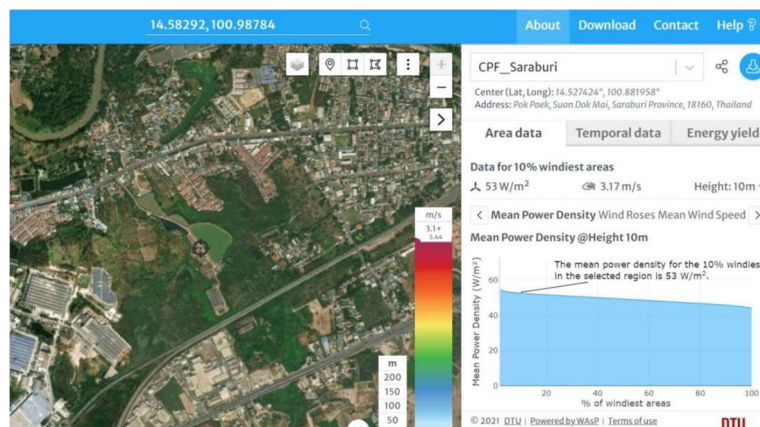


Figure 2 Average wind speed chart at the edge of the Kaeng Khoi CPF aeration pond with a wind speed model at an altitude of 10 m.



Figure 3 Average wind speed chart at the edge of the Kaeng Khoi CPF aeration pond with a wind speed model at an altitude of 10 m.

The results of the analysis of average wind speed revealed that At the CPF aeration pond, Kaeng Khoi, Saraburi. The wind turbines can be installed to generate 10 kilowatts of low-speed wind power because of the annual average wind speed of 10 meters above the ground in the vineyard area. This is approximately 3.17 meters per second for the low wind speed turbines that are present. It started generating electricity at a wind speed of 2.5 meters per second. The turbine column has a height of 18 meters, and the embankment around the aeration pond is raised by more than 2 meters. Therefore, the average wind speed can be higher than that analyzed.

Based on the data obtained from the World Bank model, these will be in the form of a GWC file, which the study team has made into a data file. The Wind Atlas Analysis and Application Program (WAsP) model was used for forecasting wind potential to examine the accuracy in detail and found that the WAsP model analyzed wind speeds in the same area as annual mean wind speeds. It's 3.41 meters per second and 4.77 meters per second. which is greater than the wind speed from the World Bank model as shown in Figure 4, which is the wind speed in the range of the low rated power generation matching low wind speed wind turbines. The system can start producing electricity at wind speeds of up to 2.5 meters per second as well.

Therefore, from the analysis with both models, it was found that the average wind speed in the measurement area for the installation of low wind speed wind turbines for aeration in the pond was installation can be performed.

The result of the model is a statistical analysis of wind data. On Figure 4, its shows the wind frequency (left-hand image) called Wind rose (divided into 12 sectors). Wind rose is a diagram showing the condition. speed quantity and the direction of the wind at any given time. At the measurement area, wind direction charting data requires average wind speed and wind direction data. The collected wind speed data is arranged in each wind direction and calculated as a percentage of the time the wind blows from a given direction. The data is displayed in a pie graph. The wind direction information will be arranged. It divides the circle into twelve arcs that support an angle equal to 30 degrees, and the radial length of each of the twelve segments. Shows the percentage of time the wind blows in that direction.

Another element for determining wind speed potential is the Weibull distribution (right-hand figure). It is a statistical method of frequency distribution of wind speed values. This shows the continuous probability distribution of any function. It also contains parameters that represent how the data is distributed. This is a popular distribution used to analyze wind statistical data. The parameters of the Weibull distribution consist of a shape parameter (K), a parameter that characterizes the

distribution of wind speed data. Low values indicate low wind speeds. Rest more often than high wind speeds. Along with the accompanying table above each figure.

The wind rose in Figure 4 shows that most of the winds blow south at 180 degrees and southwest at 210 degrees. The study shows that this is an open area and there are no buildings blocking the path of the wind.

For the Weibull distribution, the wind velocity values at different points are described. For example, from the results of simulated analysis on the edge of the aeration pond, it was found that The wind speed was 4.91 m/s. It represents 12.7% of the total wind speed that will occur in the area. The K value is the shape parameter equal to 1.74, which means the wind around the field and the ground wind, as shown in Figure 5.

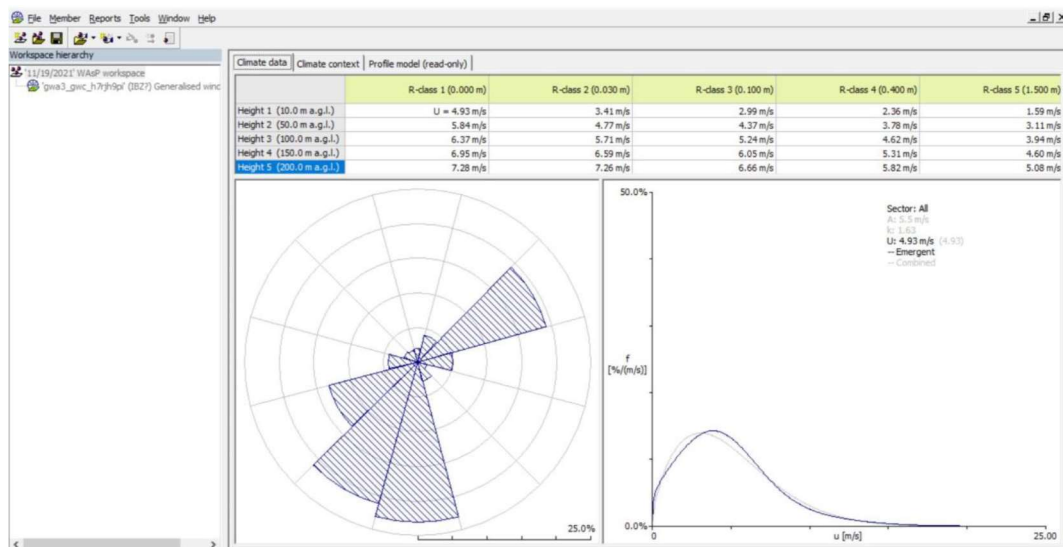


Figure 4 Wind velocity analysis results at Kaeng Khoi CPF aeration pond using WAsP model

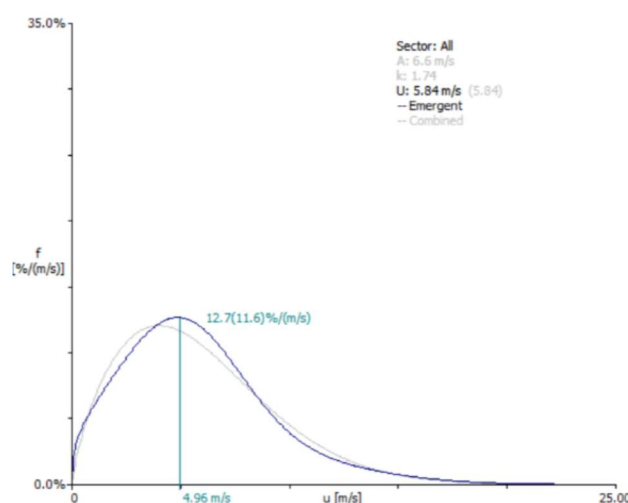


Figure 5 Weibull distribution

Installation of ground-mounted solar power generation systems

From surveying the area around the CPF Kaeng Khoi aeration pond, it was found that if installing a solar power generation system 3 kW capacity to maximize the benefits for pond aeration at all times. (During the day, the power from the solar power generation system can be used in

conjunction with the compressed air turbine. During nighttime with good wind, the system will only use energy from wind turbines)

From the simulation of the installation of solar power generation systems on the ground, capacity of 3 kilowatts, as assessed by the World Bank's energy generation model. It was found that the power generation capacity of the system was approximately 4,482 electrical units per year, as shown in Figure 6.

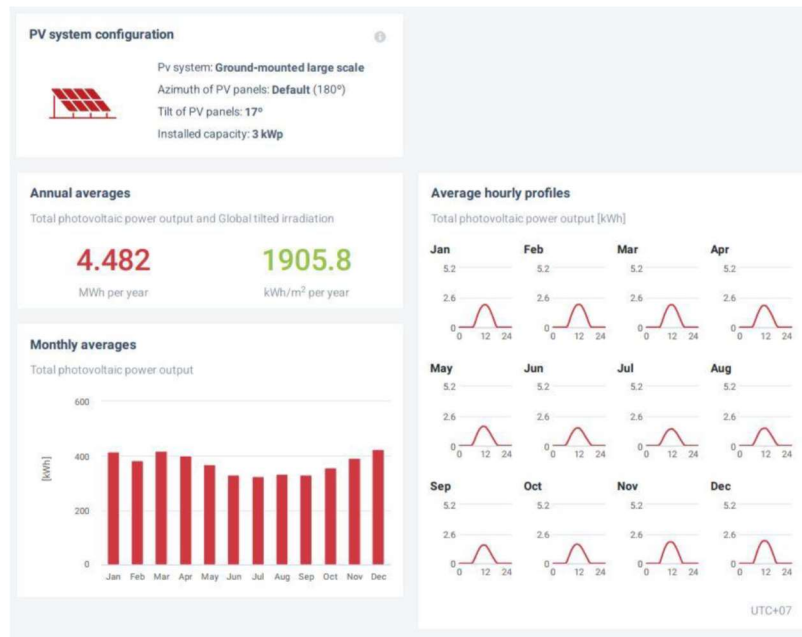


Figure 6 simulates the installation results of a ground-mounted solar power generation system. Capacity 3 kilowatts

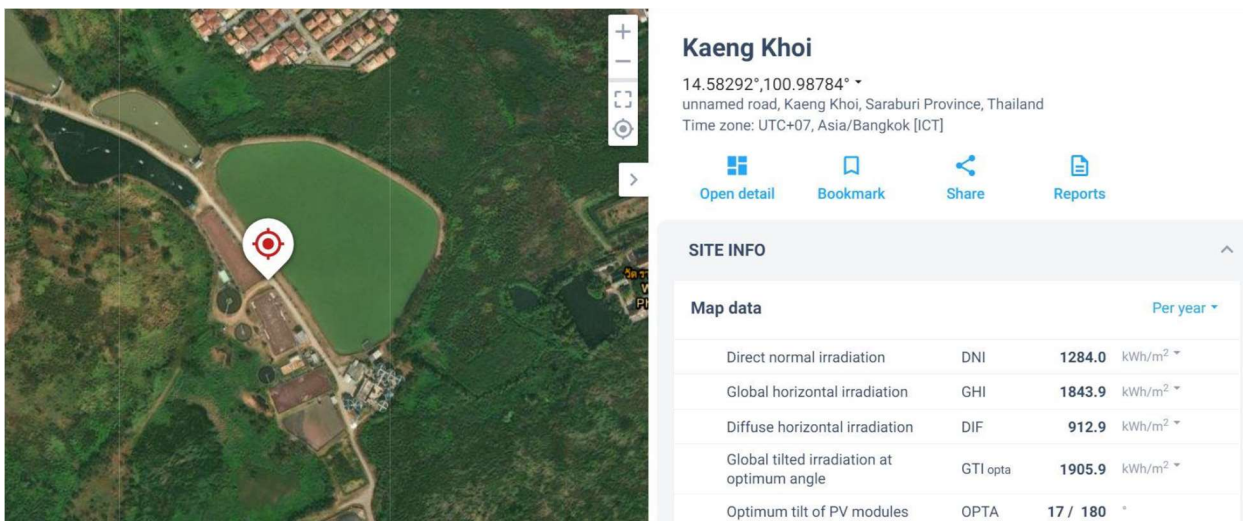


Figure 7 Ground-mounted solar power generation system installation area Capacity 3 kilowatts

Average hourly profiles

Total photovoltaic power output [kWh]

	Jan	Feb	Mar	Apr	May	Jun	Jul	Aug	Sep	Oct	Nov	Dec
0 - 1												
1 - 2												
2 - 3												
3 - 4												
4 - 5												
5 - 6												
6 - 7		0	0	0	0	0	0	0	0	0	0	0
7 - 8	0	0	0	0	0	0	0	0	0	0	1	0
8 - 9	1	1	1	1	1	1	1	1	1	1	1	1
9 - 10	1	1	1	1	1	1	1	1	1	1	2	1
10 - 11	2	2	2	2	2	2	1	2	2	2	2	2
11 - 12	2	2	2	2	2	2	1	2	2	2	2	2
12 - 13	2	2	2	2	2	2	1	2	2	2	2	2
13 - 14	2	2	2	2	1	1	1	1	1	1	2	2
14 - 15	2	2	2	1	1	1	1	1	1	1	1	2
15 - 16	1	1	1	1	1	1	1	1	1	1	1	1
16 - 17	1	1	1	1	1	0	1	0	0	0	0	1
17 - 18	0	0	0	0	0	0	0	0	0	0	0	0
18 - 19		0	0	0	0	0	0	0				
19 - 20												
20 - 21												
21 - 22												
22 - 23												
23 - 24												
Sum	13	14	14	13	12	11	11	11	11	12	13	14

Figure 8 Capacity (power unit) hourly per month Throughout the year of the solar power generation system From a 3 kW floor-standing PV power generation model

The results of the analysis of the hourly energy production of the system ground-mounted PV system with a capacity of 3 kilowatts. The results obtained from the model at the water supply plant within the chicken processing plant, Kaeng Khoi, Saraburi Province. It can be analyzed that the system will start generating power from 8:00 a.m. through 4:00 p.m. every day with moderate sun light. The system will produce peak energy during the period between 10:00 - 15:00 hrs. Solar panels will produce electricity with the highest efficiency, as shown in Figure 8.

Renewable Energy Prototype Project / Installation project plan and layout / Included a combination of compressed air system, a water supply plant, a chicken processing plant

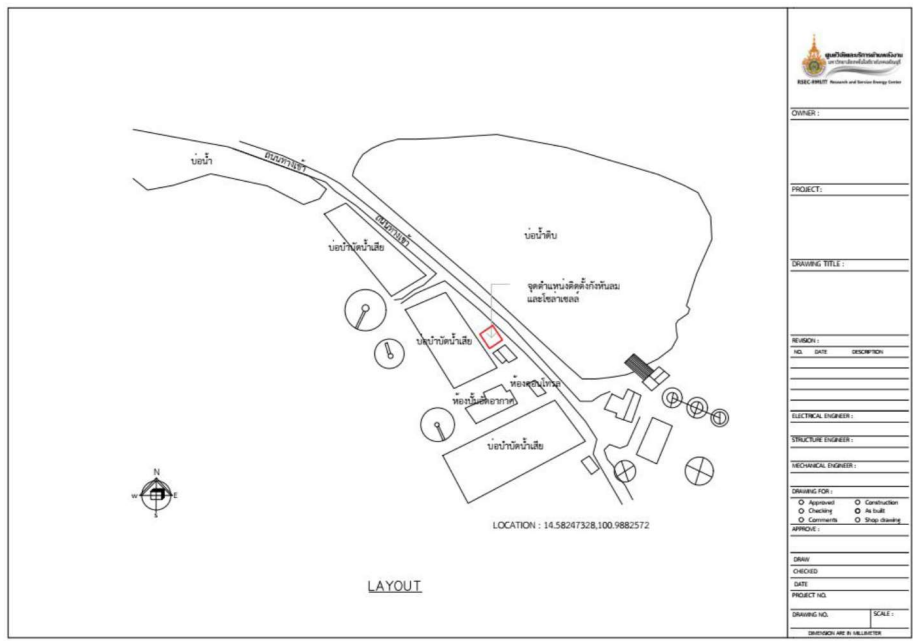


Figure 9 Layout of the aeration system at the water supply plant of the chicken processing plant, Kaeng Khoi, Saraburi Province

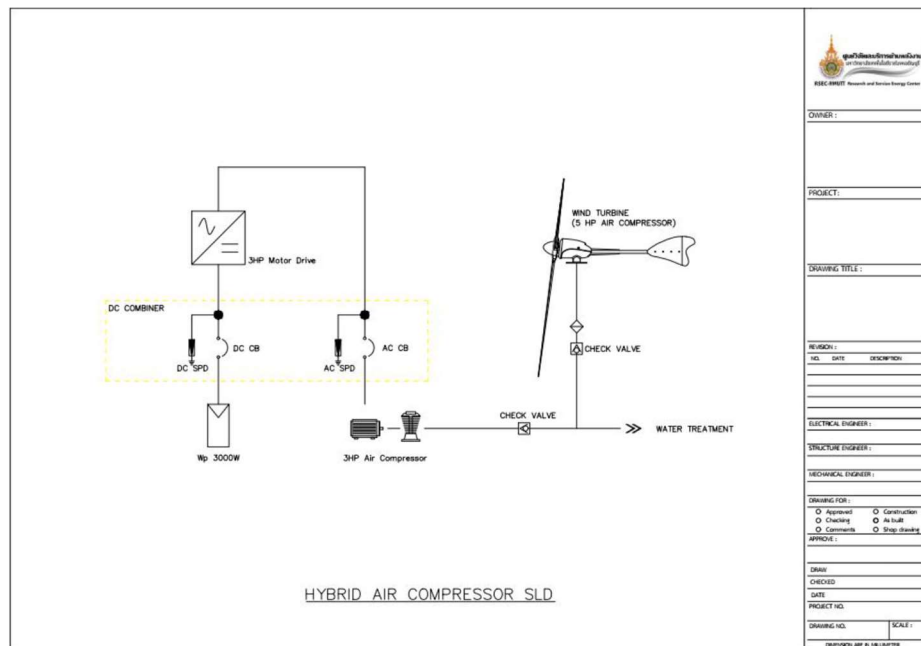


Figure 10 SLD model of aeration system at water supply plant, chicken processing plant, Kaeng Khoi, Saraburi province

Figure 9 show the layout of the aeration system at the water supply plant of the chicken processing plant, Kaeng Khoi, Saraburi Province, and Figure 10 show the single line diagram of aeration system at water supply plant.

Economic analysis

The Energy Research and Service Center finalized the design of hybrid power systems with renewable energy supplemental to the water supply plant at Kaeng Khoi Chicken Processing Plant, Saraburi Province. The results in an analysis of the cost-effectiveness of investing in the plant to install just one low-speed wind turbine power generation system of 5 kilowatts. (Case of Option 1). Also, a hybrid power generation system from terrestrial solar power of 3 kilowatts. With a power generation system combined with a low-speed wind turbine of 5 kilowatts, totaling a total of 8 kilowatts of renewable energy (Alternative Option 2). These will serve as suitable guidelines for the installation and development of energy consumption in the current location/project for the maximum benefit.

For these hybrid renewable energy systems, the investment objective is based on the simple payback period theory.

Calculation of payback period in the base case

It is a calculation of the period of return in the form of cash flows. Regardless of the value of the money over the relevant period. The payback period is calculated only by looking at cash flows and not the profit or loss of the business. At the point where the cumulative cash inflow is equal to the initial investment, and the payback period will only be obtained. Therefore, the analysis of the payback period is suitable for the analysis of investment projects that have a relatively long-term period.

In this regard, the survey team conducted a feasibility study in economics as an alternative multiple approaches as follows:

- Option 1 case consists of single low-speed wind turbine of 5 kilowatts.

- Option 2 case consists of a 3 kW stand-alone solar power system and a single 5 kW low-speed wind turbine. (Hybrid system)

Table 1 Investment expenses Alternative 1 case has a renewable energy system and mobile energy storage system with control room

Alternative case	Renewable Energy	production capacity (kW)	Total price (Baht)	Payback period (years)
1	low-speed wind turbine of 5 kilowatts	5	950,000	3.45
2	3 kilowatt solar power system and 1 5 kilowatt low wind turbine	8	1,200,000	3.38

The payback period of the two alternative cases can be described as follows:

Table 2 Technical table of 5KW air compressor wind turbine

Motor cycle (rpm)	Pressure (Bar)	Flow rate (liters per minute)	Air temperature (C°)	Electric power (watt)
100 rpm at wind 2.5 m/s	3.2	60	25.2	500
200 rpm at wind 4 m/s	4.1	150	25.2	1500
300 rpm at wind 5 m/s	4.5	550	26.4	3200
400 rpm at wind 6 m/s	5.1	650	27.1	3800
500 rpm at wind 7 m/s	6.2	780	29.2	4200
600 rpm at wind 8 m/s	7.4	1162	32.5	4800
700 rpm at wind 9 m/s	8	1654	38.4	5500

(safety release)

Alternative case 1

From Table 2 and the wind speed analysis results in Figure 5, from the model, the wind speed of 4.91 m/s is 12.7%, which is the highest wind speed range of the various wind speed levels. all that happened So at an average wind speed of 5 meters per second Compressed air pumps out approximately 550 liters per minute.

Technical details of compressed air turbine at an average wind speed of 5 meters per second Its daily average is an average working pressure of approximately 4.5 bar, with an average flow rate of 550 liters of air per minute in actual use. Approximately 0.19 electrical units. Therefore, if the actual measurement Will be charged for electricity at 5 baht per unit throughout the project will be saving $0.55 \text{ m}^3 \times 0.19 \text{ kWh} \times 60 \text{ min} \times 24 \text{ hr} \times 365 \text{ day} \times 5 \text{ baht} = 2.75$ hundred thousand baht per year

As in the case of Option 1, the payback period is approximately 3.45 years for the investment of one low-speed wind turbine of 5 kilowatts. Investment is about 9.5 hundred thousand baht. It is estimated to save about 2.75 hundred thousand baht per year in electricity from the use of compressed air turbines in actual use. as needed in water management Therefore, in the actual operation of the correct management, the wind turbine compressed air can save electricity costs. It helps to reduce emissions (CO₂) and extend the service life of the electric air pump.

Alternative case 2

It feature a Hybrid renewable energy system from a 3 kilowatt solar power system, equivalent to an average of 500 liters of compressed air per minute, with an average of about 2 kilowatts of electricity at an average light intensity of 1,900 watts per square meter at the installation site. Water Supply Plant, Chicken Processing Plant, Kaeng Khoi, Saraburi Province (Results from light intensity simulation, Fig. 6) Average working 7 hours per day of Chola cells. (Refer to the hourly power generation simulation results Figure 8) into the motor for compressed air. So you can say $0.5 \text{ m}^3 \times 0.19 \text{ kWh} \times 60 \text{ min} \times 7 \text{ hr} \times 365 \text{ day} \times 5 \text{ baht} = 72,800 \text{ baht per year}$ when combined with a 5 kilowatt wind turbine system will make the time for the payback equal to $120000 / (275,000 + 72,800) = 3.38 \text{ years}$.

Conclusion

The Hybrid renewable compressed air option/system is best for the water supply plant in the chicken processing plant CPF (Thailand) Public Company Limited, Kaeng Khoi, Saraburi Province. The hybrid system will have a faster payback period compared to the installation of just a low-speed wind turbine system of 5 kW.

From the Energy Research and Service Center, our suggestion and recommendation to the water supply plant, chicken processing plant, and CPF (Thailand) Public Company Limited at Kaeng Khoi, Saraburi Province is the following. The best alternative energy system is the hybrid compressed air system with comparison to the wind turbine with a compressed air standalone system. The benefit of solar energy is that it can be used in the daytime together with wind energy, as long as there is no wind condition during the day. The hybrid system can still operate independently from solar energy. In addition, the payback period is less than in the case of installing a wind turbine with compressed air alone. Importantly, it also responds to the preparation for aligning with the current company green policy. An organization that improved emissions carbon until we can emit a net zero greenhouse gas or Net Zero and potentially extend the success story to other chicken factories of CPF (Thailand) Public Company Limited, nationwide as well.

References

- Islam, M.R., Mekhilef, S., Saidur, R., Progress and recent trends of wind energy technology. *Renew. Sustain. Energy, Rev.* 2013, 21, 456–468
- Roynarin, W. (2003). Using wind turbine machine to reduce carbon dioxide emissions in shrimp farm aeration process
- Subhadeep B. and A. Shantanu. (2015). PV–wind hybrid power option for a low wind topography. *Energy Conversion and Management, 89*: 942-954.
- Vikas K., Savita N., and Prashant B. (2016). Solar–wind hybrid renewable energy system: A review. *Renewable and Sustainable Energy Reviews, 58*: 23-33.

An Assessment of Environmental Impact of Gas Flaring in Thailand: A Case Studies of Petrochemical Industry

Parnuwat Usapein^{1*} and Orathai Chavalparit²

¹*Rattanakosin College for Sustainable Energy and Environment, Rajamangala University of
Technology Rattanakosin, Nakhon Pathom, 73170, Thailand*

²*Department of Environmental Engineering, Faculty of Engineering, Chulalongkorn University,
Bangkok, 10330, Thailand*

* Corresponding email: parnuwat.usa@rmutr.ac.th

Abstract

A gas flare is one of the operations that every petrochemical industry needs. This unit was operated for safety and operational reasons. However, without proper controls, doing so could result in energy losses and higher production costs as well as environmental impacts. Therefore, a systematic study and guideline for flare gas reduction technology are of paramount importance. This research aims to 1) evaluate the technology to reduce greenhouse gas emissions from gas flaring 2) assess the emission factor of gas flaring in the Thai petrochemical industry 3) assess the other environmental impacts such as acidification, photochemical effect, and health impacts, and 4) propose the recommendations and limitations for reducing GHG emission from gas flaring of Thai petrochemical industry. Life cycle assessment (LCA) was used as a tool to assess the environmental impact of the gas flaring. The goal is to identify the environmental impacts of gas flaring and propose options to reduce its impacts. The scope of this study was gate-to-gate. IMPACT 2002+ was applied for calculating environmental impact assessment. The results showed that the greenhouse gas emission factor of gas flaring from the petrochemical plants in this case study were in the range of 2.26E-05 – 2.12E-01 ton CO₂eq /scf and the average value was 3.03E-02 ton CO₂eq/scf. In addition, the result of the environmental impact assessment identified that the factory case study can emit the highest impact of respiratory inorganics, terrestrial acid/nutria, and aquatic acidification for 11,0870 kg PM_{2.5}eq, 4,780 kg SO₂eq, and 609,721 kg SO₂eq per year, respectively.

Keywords: Gas flaring, Greenhous gas emission, Life cycle assessment, Petrochemical industry

Introduction

Thailand was one of the countries that signed the United Nations Framework Convention on Climate Change (UNFCCC) at the COP21 conference in Paris, France. Many countries have jointly to set goals together for reducing greenhouse gas emissions. The Thai government also signed a commitment that Thailand will take part in reducing greenhouse gas emissions by 20-25 percent within in the year 2030 (Thailand Greenhouse Gas Management Organization, 2015). In addition, the Ministry of Energy, as an important part of the achievement of the greenhouse gas reduction plan, has formulated a 20-year energy conservation plan (2011-2030) with a goal of reducing energy intensity by 25 percent in 2030 compared to 2005 and reducing final energy use by 20 percent in 2030 (Ministry of Energy, 2011).

To achieve the target, it is necessary to clearly have the energy conservation plan which suitable for both investment and environmental friendliness. Petrochemical industry is high energy consumption and consists of a complex manufacturing process. Besides, the petrochemical industry has many sources of greenhouse gas emissions, for example, fuel combustion, gas flaring, hydrocarbon leakage and so on (Usapein & Chavalparit, 2017). Flare is a unit that every plant in the petrochemical industry needs due to safety reasons and the operation of the factory system

(Department of Industrial Works, 2013). However, if there is no proper flare control, such action will cause energy losses, increase production costs, and affect the environment. Flared gas is recognized as a major source of global warming and climate change (Giwa, S.O., et al. 2017).

Therefore, it is important to study and formulate a systematic approach to the reduction flare combustion technology. Zadakbar et al (2008) investigated the option of flare gas recovery in oil and gas refineries; they found that two case studies of installing flare gas recovery unit can reduce operating costs, air pollution emissions, and fuel gas consumption. Suitable conditions of air-and steam-assist on flaring operation was identified by Ahsan et al (2019); this resulted in high combustion efficiency and low pollutant emissions.

Unfortunately, the study of gas flaring reduction is very rare in Thailand. The objective of this study is to 1) evaluate the technology to reduce greenhouse gas emissions from gas flaring 2) assess the emission factor of gas flaring in the Thai petrochemical industry 3) assess the other environmental impacts such as acidification, respiratory inorganic, and terrestrial acid/nutrition, and 4) propose the recommendations and limitations for reducing GHG emission from gas flaring of Thai petrochemical industry.

Materials and Methods

Case study selection

Petrochemical plants were selected based on voluntary participation to site visit and data collection. Seven petrochemical plant case studies were selected: three factory case studies for propylene and polypropylene; two factory case studies for olefins products; and two factory case studies for aromatic products. All case studies were in Map Ta Phut Industrial Estate, Rayong province, Thailand.

Data collection

In this section, the data related on gas flaring system, for instance, type of flare, flare burner, were gathered from reliable documents. At site visit, the data were collected by interviews with plant managers or people involved in the flare system. The flow rate of gas flaring and flare gas composition were collected in this stage. Opportunities and obstacles for the reduction of gas flaring were identified. After that, the possible options were proposed and analyzed to represent the potential option of gas flaring reduction.

Environmental impact estimation

LCA was used as a tool to determine environmental impact from gas flaring. The goal was to calculate the greenhouse gas (GHG) emission factor of gas flaring in Thailand. In addition, the other impact, i.e., respiratory inorganics, terrestrial acid/nutria, and aquatic acidification, were also estimated in this study. The scope of this study was gate-to-gate. Only direct emission was considered in this study. All emission calculated in this study were based on gas flaring in a one year as a functional unit. Data related to the amount of gas flaring were gathered from petrochemical plant case studies in one year. IMPACT 2002+ was applied for calculating environmental impact assessment (Jolliet et al., 2003).

Results and Discussion

Flare composition

Gas flaring composition was collected from the petrochemical plant case study. The result showed that the gas flaring composition in each plant was different. However, the sample collection is quite dangerous, and the cost of sampling is high. Therefore, some case study plants use a method of hypothesizing gas flaring composition based on the main activities, as shown in Table 1.

The gas flaring composition of each plant case study has a different composition depending on the production process and the duration of the activity. Factory B has a main process for producing propylene; the main composition of gas flaring consists of hydrogen (85.69%). The case study plants (Factory D and E) has a cracking process as the main process to produce olefin products, gas flaring composition mainly consisting of low molecular weight hydrocarbon, such as methane, ethane, and propane. When considering aromatic plants (Factory F and G), the main activities is fractional distillation which resulted in producing useful aromatic hydrocarbon products. It was found that the main flare composition consisted of hydrogen (51-63%), followed by methane (14-22%), ethane (11-13%), and propane (6-8%).

Table 1 Gas flaring composition

Factory	Gas Composition (%mol)											MW	Sources
	CH ₄	C ₂ H ₄	C ₃ H ₆	C ₄ H ₈	C ₅ H ₁₀	C ₆ H ₁₂	CO	CO ₂	H ₂	N ₂	NH ₃		
Factory A	n/a	2.59	97.17	0.24	n/a	n/a	n/a	n/a	n/a	n/a	n/a	41.67	• Based on main activities
Factory B	12.52	0.47	0.86	0.22	0.12	n/a	0.00	0.11	85.69	0.00	n/a	4.50	• Lab sample
Factory C	90.08	2.51	0.74	0.33	0.12	n/a	0.00	4.48	0.00	1.75	n/a	18.27	• Based on main activities
Factory D	n/a	80.19	19.81	n/a	n/a	n/a	n/a	n/a	n/a	n/a	n/a	30.77	• Based on main activities
Factory E	61.45	0.20	0.00	0.00	0.00	n/a	0.06	0.97	37.30	0.00	0.00	11.09	• Based on main activities
Factory F	22.14	13.09	8.11	2.47	1.01	0.00	0.00	1.16	51.35	0.66	0.00	14.23	• Lab sample
Factory G	14.66	11.45	6.52	1.64	0.99	0.00	0.76	0.00	63.13	0.78	0.00	11.74	• Lab sample

GHG emissions

Emission factors calculated in this study were calculated based on gate-to-gate boundary. GHG emission from gas flaring combustion and other activities related in factory were considered. The results of estimation are shown in Figure 1.

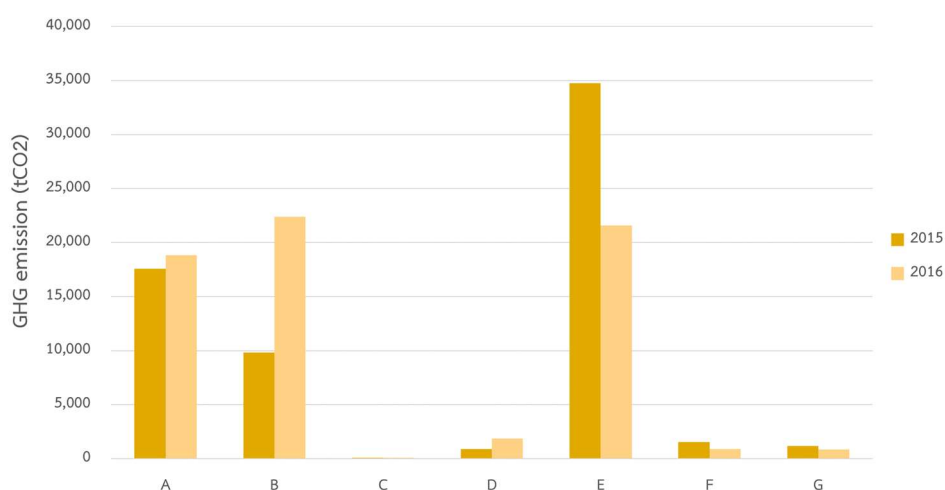


Figure 1 The amount of GHG emissions of gas flaring from petrochemical plant case studies (year 2015 – 2016)

The result indicates that each factory case study had different GHG emissions from its activity. Factory E showed the highest of GHG emissions from gas flaring by the average value of 28,179 tCO₂ per year. The lowest of GHG emissions was Factory C, with the average value of 77.74 tCO₂ per year. When considering the GHG emission factors, the result was shown in Table 1.

Table 1 GHG emissions factor of petrochemical plant case studies

Factory	A	B	C	D	E	F	G	Unit
GHG emission factor	2.12E-01	2.26E-05	3.04E-05	1.26E-04	1.19E-04	3.65E-05	5.20E-05	tCO ₂ /scf

GHG emissions factor from gas flaring combustion has different values from each plant case study. This is because the composition of gas flaring is different. Gas flaring composition mainly consisted of hydrogen gas have low GHG emission factors, while gas flaring with high hydrocarbon content has high value of GHG emission factors.

Respiratory inorganic

In this section, due to the nitrogen content was not occurred in Factory A, B, D, and E, the impact of respiratory inorganic was not determined for those factories. The effect of respiratory inorganic is shown in Figure 2. The gas flaring combustion in Factory F showed the highest impact with 11,0870 kg PM_{2.5}eq per year, followed by Factory C (85,013 kg PM_{2.5}eq), and Factory G (51,460 kg PM_{2.5}eq), respectively. Main factors of this impact depend on the nitrogen content in gas flaring composition. Nitrogen content was converted to nitrogen oxide from combustion process.

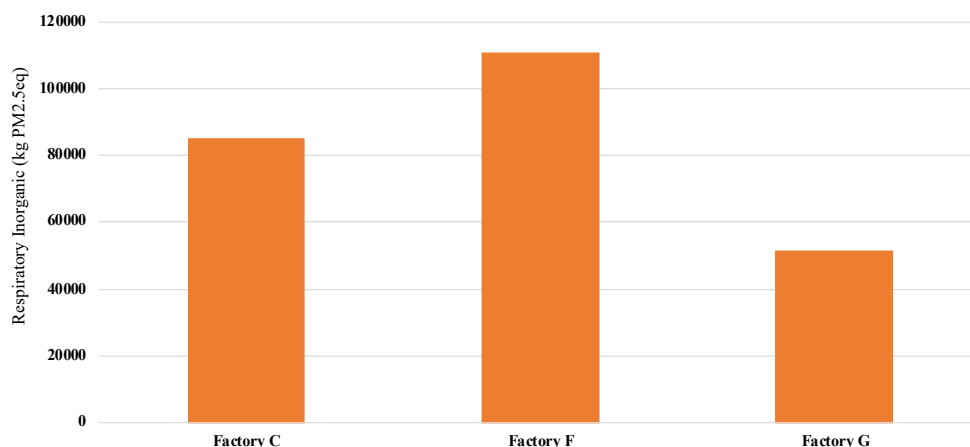


Figure 2 Respiratory inorganic of gas flaring from petrochemical plant case studies

Terrestrial acid/nitrification

The impact of terrestrial acid/nitrification is shown in Figure 3. This impact was calculated in the unit of kg SO₂eq into air. Factory C dominate of emitted this impact due to its high amount of gas flaring combustion. The highest emission of terrestrial acid/nitrification generated from Factory F by 4,780-ton SO₂eq per year.

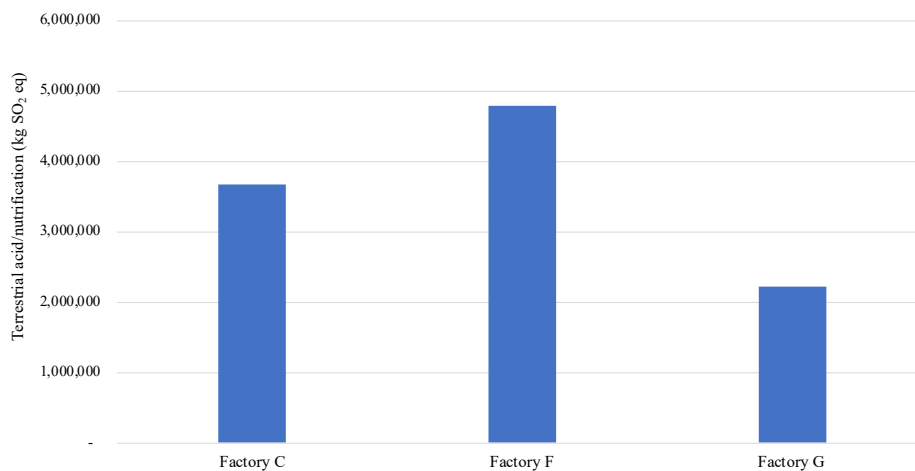


Figure 3 Terrestrial acid/nutrication of gas flaring from petrochemical plant case studies

Aquatic acidification

Main pollutants to generate the impact of aquatic acidification come from ammonia (NH₃), nitrogen oxides (NO_x) and sulphur oxides (SO_x). Therefore, if the flare composition contains this element at high level, the result of acidification impact will be high also. As shown in Figure 4, Factory F has the highest of aquatic acidification impact by 609,721 kg SO₂eq per year.

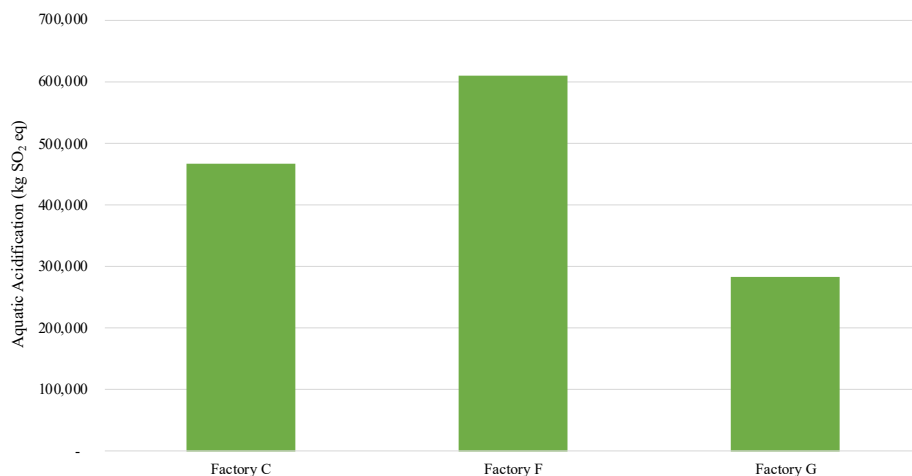


Figure 4 Aquatic acidification of gas flaring from petrochemical plant case studies

Proposed flare reduction measures

The measure was received from petrochemical plant case studies and literature review from previous studies. The potential measures were selected and recommended as follows:

- Controlling Net Heating Value (NHV) of the flare gas: the combustion zone of flare gas should be $NHV \geq 270$ btu/scf. If the NHV below 270 btu/scf, operator must add fuel gas such as propane or natural gas, then the steam may be required to the flare to burn in an environmentally-sound manner.
- Installing flare gas recovery unit (FGRU): FGRU is a technology for recovering flare gas back into the production process inside the factory. The installation of a FGRU can reduce flare gas combustion by up to 98%, thereby reducing both CO₂ emissions and other adverse effects. However,

this system requires investment due to the need to install additional equipment, whose payback time depends on the specifics of the plant.

Conclusion

This study investigated the GHG emission factor of gas flaring from petrochemical industry in Thailand. The potential of gas flaring reduction was proposed. Seven petrochemical plant case studies were selected. All case studies located in Map Ta Phut, Rayong province.

The evaluation of GHG emission factor can be summarized that GHG emission factors of petrochemical plant case studies are in the range of 2.26E-05 – 2.12E-01 tonCO₂eq /scf. The average value is 3.03E-02 tonCO₂eq/scf. In addition, three environmental impacts were conducted: respiratory inorganic, terrestrial acid/nitrification, and aquatic acidification. The results of the assessment were concluded that the petrochemical plant case studies emitted the highest level of three impacts approximately 11,0870 kg PM_{2.5}eq, 4,780 kg SO₂eq, and 609,721 kg SO₂eq per year, respectively. If the measures are applied or installing FGRU technology, it can significantly reduce these effects.

From the above research results, it can summarize recommendations and limitations to reduce the environmental impact of flare gas combustion in petrochemical industry as follows: (1) FGRU technology is a technology that has the potential to reduce greenhouse gas emissions and can utilize some of the energy from gas flaring to the production process. Therefore, it is recommended that factories in the upstream petrochemical industry should be considered first; (2) in case of survey and design found that it cannot be carried out, for example, long payback period, low heating value, alternative approaches should be used instead; (3) an approach to controlling heating value of flare gas is a useful and cost-effective approach, in addition, reducing the smell of hydrogen sulfide in case of incomplete combustion.

Acknowledgments

This work was supported by National Research Council of Thailand (2019). In addition, the authors would like to thank the Rattanakosin College for Sustainable Energy and Environment (RCSEE) at Rajamangala University of Technology Rattanakosin for supporting this research.

References

- Ahsan, A., Ahsan, H., Olfert, J. S., & Kostiuk, L. W. (2019). Quantifying the carbon conversion efficiency and emission indices of a lab-scale natural gas flare with internal coflows of air or steam. *Experimental Thermal and Fluid Science*, 103, 133-142.
- Department of Industrial Works. (2013). *Guideline to Good Practice for Industrial Flare Use*. Retrieved from <http://php.diw.go.th/env/wp-content/uploads/2016/04/flare.pdf>
- Giwa, S. O., Nwaokocha, C. N., Kuye, S. I., & Adama, K. O. (2019). Gas flaring attendant impacts of criteria and particulate pollutants: A case of Niger Delta region of Nigeria. *Journal of King Saud University-Engineering Sciences*, 31(3), 209-217.
- Jolliet, O., Margni, M., Charles, R., Humbert, S., Payet, J., Rebitzer, G., & Rosenbaum, R. (2003). IMPACT 2002+: a new life cycle impact assessment methodology. *The International Journal of Life Cycle Assessment*, 8(6), 324.
- Ministry of Energy. (2011). *Energy Efficiency Plan; EEP 2015*. Retrieved from <http://www.eppo.go.th/images/POLICY/PDF/EEP2015.pdf>
- Thailand Greenhouse Gas Management Organization. (2015). *Renewable energy, the path to the reduction goal Greenhouse Gas in Thailand*. Retrieved from <http://www.tgo.or.th/2020/index.php/th/post/>

- Usapein, P., & Chavalparit, O. (2017). A start-up MRV system for an emission trading scheme in Thailand: A case study in the petrochemical industry. *Journal of Cleaner Production*, 142, 3396-3408.
- Zadakbar, O., Vatani, A., & Karimpour, K. (2008). Flare gas recovery in oil and gas refineries. *Oil & Gas Science and Technology-Revue de l'IFP*, 63(6), 705-711.

The Analysis and Comparisons of 200 kW PV Rooftop Between Energy to Grid with Energy Storage at Wongsakorn Green Market in Thailand

Suthep Simala¹, Wirachai Roynarin^{1*}, Wongsakorn Wisatesajja¹, Nima Azhari²

¹*Energy Research and Service Center, Faculty of Engineering Rajamangala University of Technology, Thanyaburi, Thanyaburi, Pathumthani, THAILAND*

²*Bazme alley, Valasr st, Enghelab st, Tehran, Iran*

* *Corresponding email: wirachai_r@rmutt.ac.th*

Abstract

This article presents the analysis and comparisons of 200 kW PV rooftop between energy to grid with energy storage at Wongsakorn Green Market in Thailand to compare the electrical energy. The systems are included a 200-kW solar rooftop, a 150-kW hybrid inverter and 100 kWh lithium battery. The results from monitoring system in november are the average power of the 200 kW solar rooftop was 556.58 kWh and the 100 kWh battery storage average power was 224.64 kWh. Also, the result of average electrical power from PVsyst program in november was 17,610 kWh. The measured values are enough to meet the demands of the Wongsakorn Market loads. The results of this hybrid system test can be used as data for comparative analysis.

Keywords: Energy Storage, Hybrid Systems, Photovoltaic Rooftop

Introduction

Currently, the installed capacity of photovoltaic (PV) (Junhui et al., 2019), (Miswar A. Syed, Muhammad Khalid, 2021) is increasing every year. Photovoltaic power generation technology is developing rapidly. Traditional energy sources contribute greatly to global warming, because they use fossil fuels to produce energy. Which leads to widespread production of carbon dioxide around the world, efforts are being made to accelerate the use of renewable energy resources. as a safe future renewable energy source with very low operating costs. The demand for photovoltaic (PV) production continues to increase at a faster rate due to low maintenance and higher reliability however, the higher installation costs and greater installation requirements of PV systems have inspired consumers to opt for roof top systems to reduce retrofit costs and higher initial costs (Satpathy et al., 2021). The falling cost of solar PV systems has led to the rapid uptake of 600 GW of installed capacity worldwide in 2019, including a significant increase in (distributed) solar rooftops. Important the same is true for utility-scale terrestrial solar power in recent years. The IEA's 2019 Renewable Energy Forecast indicates that by 2024 solar PV will grow globally by 1,200 GW, including 500–600 GW in distributed PV, with bigger long-term growth potential. A single country has more than 1 potential, 1,000 GW according to NREL—the estimated size of the country's total current electrical system. Important factors that greatly influence the selection of solar roofs (Emon Chatterji, Morgan D. Bazilian, 2020). (included with battery storage) from the customer's point of view is the savings on the electricity bills that are provided. There is an important analysis on this topic including several websites such as Google Sunroof that provide estimates of roof panel sizes. Other common tools such as Aurora, PV Watts, etc. Typically, renewable energy (Ammar Atif, Muhammad Khalid, 2020) sources, solar photovoltaic panels are weather dependent and produce unsynchronized power with load requirements, Typical standalone PV-battery energy system as show in Figure 1.

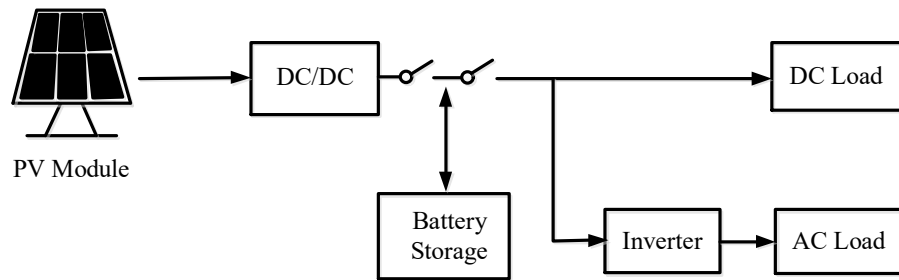


Figure 1 Typical Standalone PV-Battery Energy System.

Photovoltaic Rooftop

Solar photovoltaic (PV) power generation uses renewable energy that is natural, safe and sustainable. A hybrid renewable energy system with solar rooftop and battery storage as well as power supply to the load. PV systems used for many hybrid photovoltaic and battery storage system everywhere, hybrid system is technology development in future. A schematic diagram of solar photovoltaic (PV) system as show in Figure 2 (Ngamprasert et al., 2020).

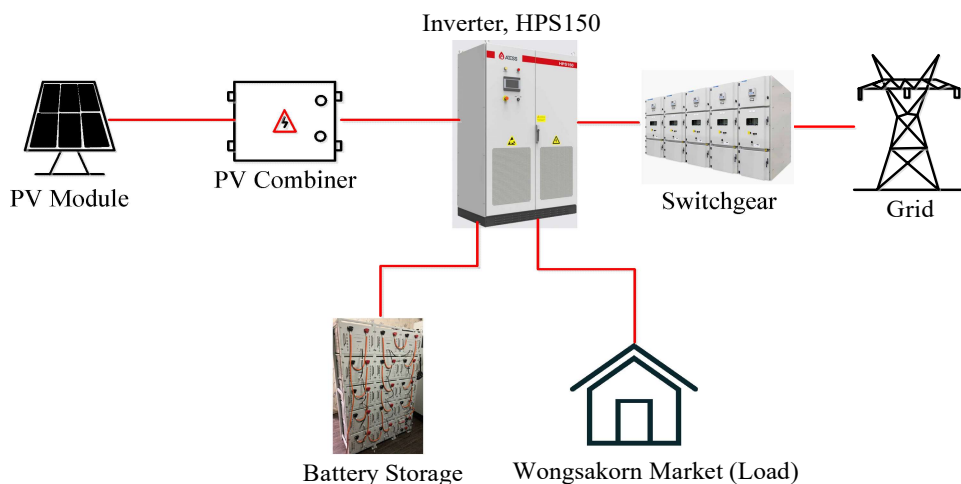


Figure 2 Schematic Diagram of a PV System

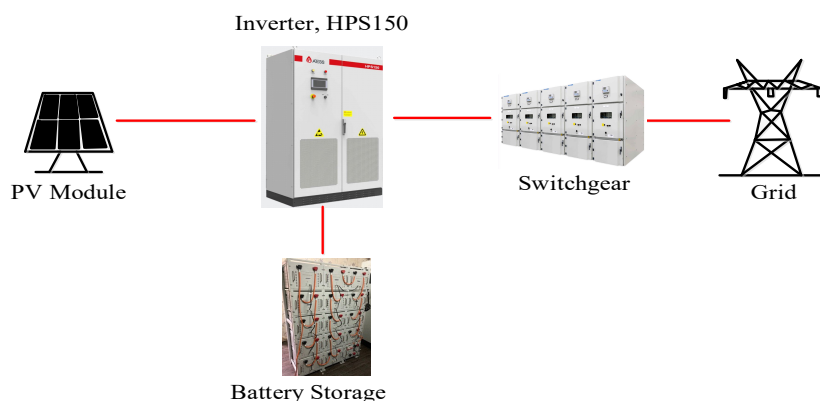


Figure 3 Hybrid System

Hybrid systems include PV array system which consists of two or more solar panel that converts sun light into electricity. Photovoltaic system is a non-conventional source of energy like wind turbine etc. It is used with dynamic voltage recover (DVR) system for energy storage. This system will provide energy to dc source which is used by inverter system to convert DC energy into AC energy

for further applications of DVR system. The equivalent circuit model of hybrid systems is shown in Figure 3 (Ngamprasert et al., 2020), (Ngamprasert et al., 2019).

The solar energy generated by solar panels is the result of multiplying several factors panel area (m^2), solar panel yield or efficiency (%), average solar radiation over a certain period (kWh/m^2), and ratio. Efficiency based on the data from the values of the efficiency ratio depending on site conditions. type of technology and this parameter system size specifies the loss coefficient for many factors such as inverter loss. Temperature loss DC power cable losses AC line losses, shading, dust and weak radiation by efficiency ratio (PR) range from 0.5 to 0.9, with the most typical of 0.75. The most exact of all the parameters in the calculation (Rosyad et al., 2020). The electrical characteristics of a solar cell can be shown using the I-V curve, which is used to determine the maximum output power of the solar cell, where I represents the current, represented by a vertical curve, and V refers to the voltage, which is represented by a horizontal curve. I-V curve can be created by measuring the open circuit voltage to obtain the voltage A, then the solar cell to supply the load to the maximum current. In short circuit current, which is the current value at point B, I-V Curve as shown in Figure 4.

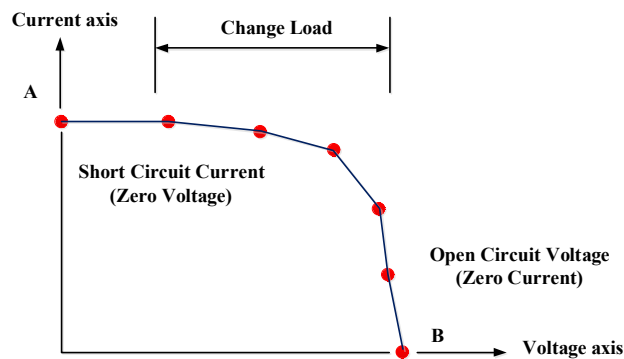


Figure 4 I-V Curve

Energy Storage

An ideal energy storage device in a standalone PV power system should be able to supply high power and high-power demands to meet situations such as sudden changes in solar radiation and electrical loads requiring high starting currents. such as electrical appliances such as air conditioners, refrigerators and electric machines requires a high starting current which may be 7 to 10 times the normal operating current. Energy storage in the form of static electricity has a higher energy density than lead-acid battery, which allows them to absorb or discharge a lot of energy in a very short time. Characteristics of typical lead-acid battery and super capacitor battery are listed and compared in Table 1 (Jing et al., (2017).

Table 1 Characteristics of typical lead-acid battery and SC

Characteristics	Lead-Acid Battery (LA)	Super capacitor (SC)
Specific Power Density	10 - 100 Wh/kg	1 – 10 Wh/kg
Specific Energy Density	< 1,000 W/kg	< 10,000 W/kg
Life Cycle	1,000	< 500,000
Charge/Discharge Efficiency	70 – 85 %	85 - 98 %
Typical Charge Time	1 – 5 h	0.3 – 30 s
Discharge Time	0.3 – 3 h	0.3 – 30 s

The generated power from the solar panels is influenced by the amount of subjected irradiation. The following equation has been used to calculate the solar-generated power

$$P_{pv}(t) = \varepsilon * S_{pv} * \eta_{cell} \quad (1)$$

where ε (w/m^2) is the global horizontal radiation of the photovoltaic panels whereas the surface of the panels is denoted with S_{pv} . The efficiency of solar conversion is cell give by and 10% is assumed for the solar conversion [5].

Case Study

In this study, a hybrid system with PVsyst was compared and measured values for a 200 kW Solar rooftop versus 100 kW Battery storage are shown in Table 2.

Table 2 Case study of Solar Rooftop 200 kW and Battery storage 100 kW.

Case	Test	Size (kW)
1	Solar rooftop	200
2	Battery storage	100

From Table 2, the average power of a 200 kW solar roof and 100 kW average battery storage power can be tested in a hybrid model shown in Figure 5 and datasheet shown in Table 3.

Figure 5 Hybrid Model

Table 3 Datasheet Inverter HPS 150

AC (Grid Connected)	ATESS HPS 150	AC (Off-Grid)	ATESS HPS 150	DC (Battery and PV)	ATESS HPS 150
Apparent Power	165 kVA	Apparent Power	165 kVA	MAX PV Open-Circuit Voltage	1000 V DC
Rated Power	150 kW	Rated Power	150 kW	MAX PV Power	225 kWp
Rated Voltage	400 V	Rated Voltage	400 V	PV MPPT Voltage Range	480 V-800 V DC
Rated Current	217 A	Rated Current	217 A	Battery Voltage Range at Max.Charge Power	500 V-600 V
Voltage Range	360 V-440 V	THDU	≤2% Linear	Battery Voltage Range	352-600 V
Rated Frequency	50/60 Hz	Rated Frequency	50/60 Hz	Max.charge Power	225 kW
Frequency Range	45~55/55~65 Hz	Overload Capability	110%-10 mins 120 %-1 min	Max.Discharge Power	165 kW
THDI	<3%			Max.charge Current	450 A
PF	0.8 lag – 0.8 lead			Max.Discharge Current	467A
AC Connection	3/N/PE				
AC Input	250 kVA				

Results

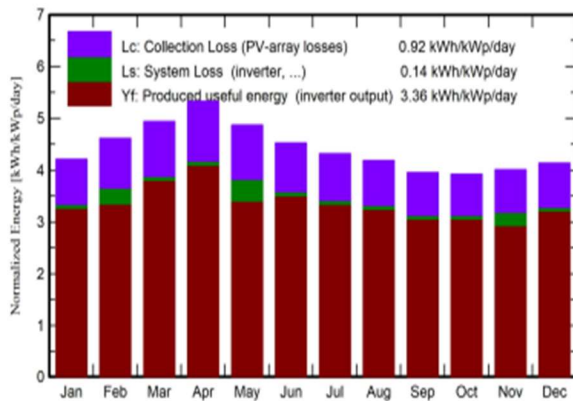
As a result of hybrid system testing using PVsyst program and energy values measured from mathematical experiments with PVsyst program, 17.61 MWh of energy was obtained for November. As shown in Figure 6.

Main results

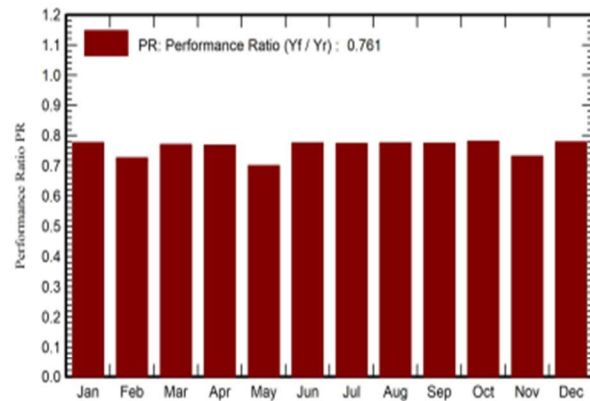
System Production

Produced Energy 245.1 MWh/year Specific production 1226 kWh/kWp/year
 Performance Ratio PR 76.06 %

Normalized productions (per installed kWp)



Performance Ratio PR



Balances and main results

	GlobHor	DiffHor	T_Amb	GlobInc	GlobEff	EArray	E_Grid	PR
	kWh/m ²	kWh/m ²	°C	kWh/m ²	kWh/m ²	MWh	MWh	ratio
January	135,4	63,28	27,07	130,6	122,0	20,72	20,28	0,776
February	133,9	77,33	28,59	129,1	121,1	20,48	18,75	0,726
March	159,1	85,77	29,83	153,1	144,1	24,09	23,60	0,771
April	166,0	89,62	30,27	159,9	150,8	25,09	24,57	0,769
May	157,0	84,10	30,17	151,0	142,2	23,72	21,14	0,700
June	141,2	79,77	29,26	135,7	127,7	21,52	21,05	0,776
July	139,3	77,36	29,35	133,9	126,1	21,19	20,71	0,773
August	135,1	80,89	29,19	129,8	122,3	20,60	20,14	0,776
September	123,6	66,10	28,25	118,6	111,4	18,78	18,35	0,774
October	126,4	81,04	28,58	121,5	114,0	19,40	18,97	0,781
November	124,8	67,40	27,93	120,3	112,3	19,15	17,61	0,732
December	132,9	66,81	27,24	128,1	119,6	20,39	19,96	0,779
Year	1674,7	919,47	28,81	1611,6	1513,5	255,13	245,13	0,761

Legends

GlobHor Global horizontal irradiation
 DiffHor Horizontal diffuse irradiation
 T_Amb Ambient Temperature
 GlobInc Global incident in coll. plane
 GlobEff Effective Global, corr. for IAM and shadings
 EArray Effective energy at the output of the array
 E_Grid Energy injected into grid
 PR Performance Ratio

Figure 6 PVsystem Results

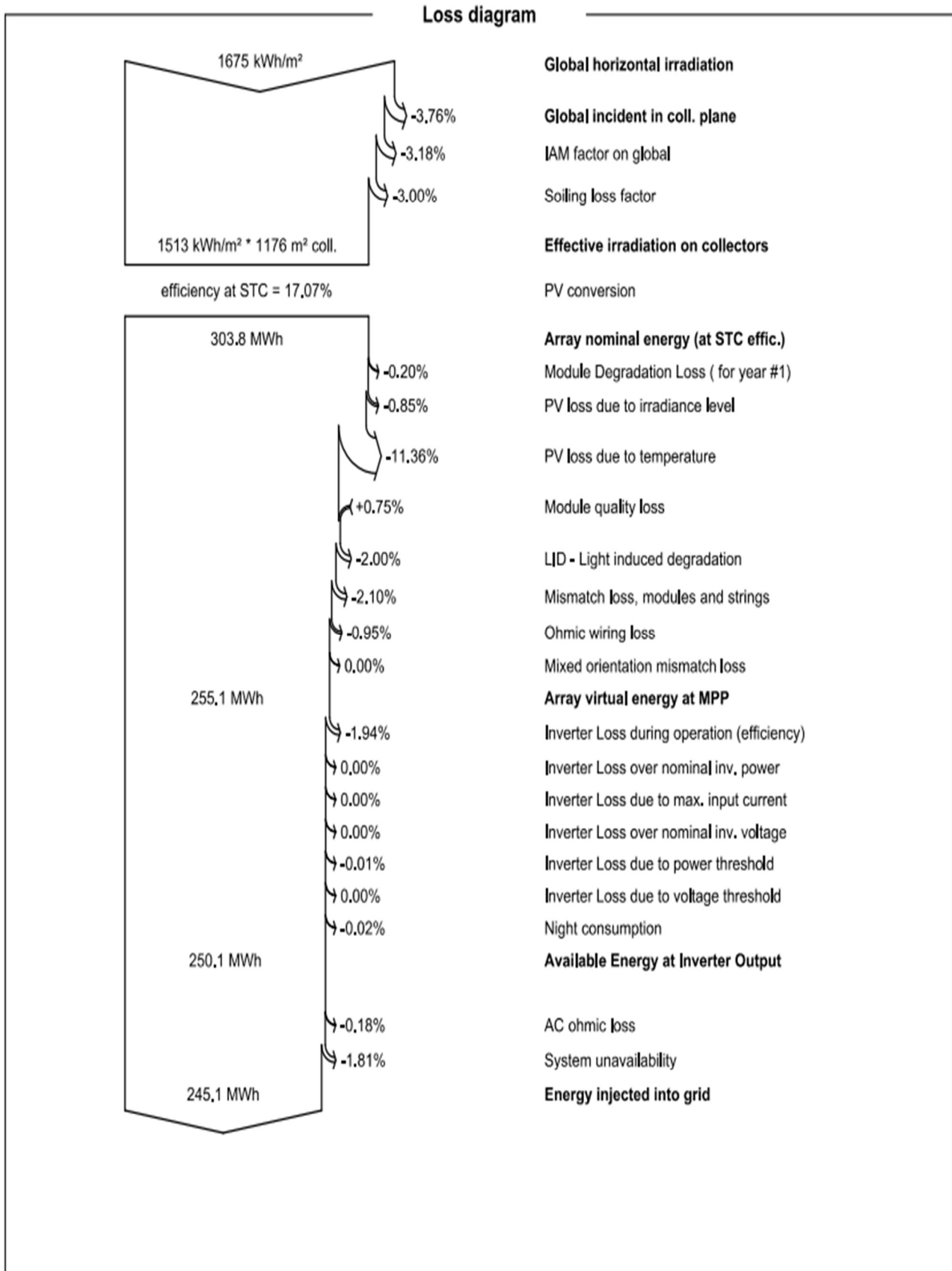


Figure 7 Loss Diagram

From the test from the measured values will be average power of the 200 kW solar rooftop was 556.58 kWh and the 100 kW battery storage average power was 224.64 kWh for november, as shown in Figure 8.

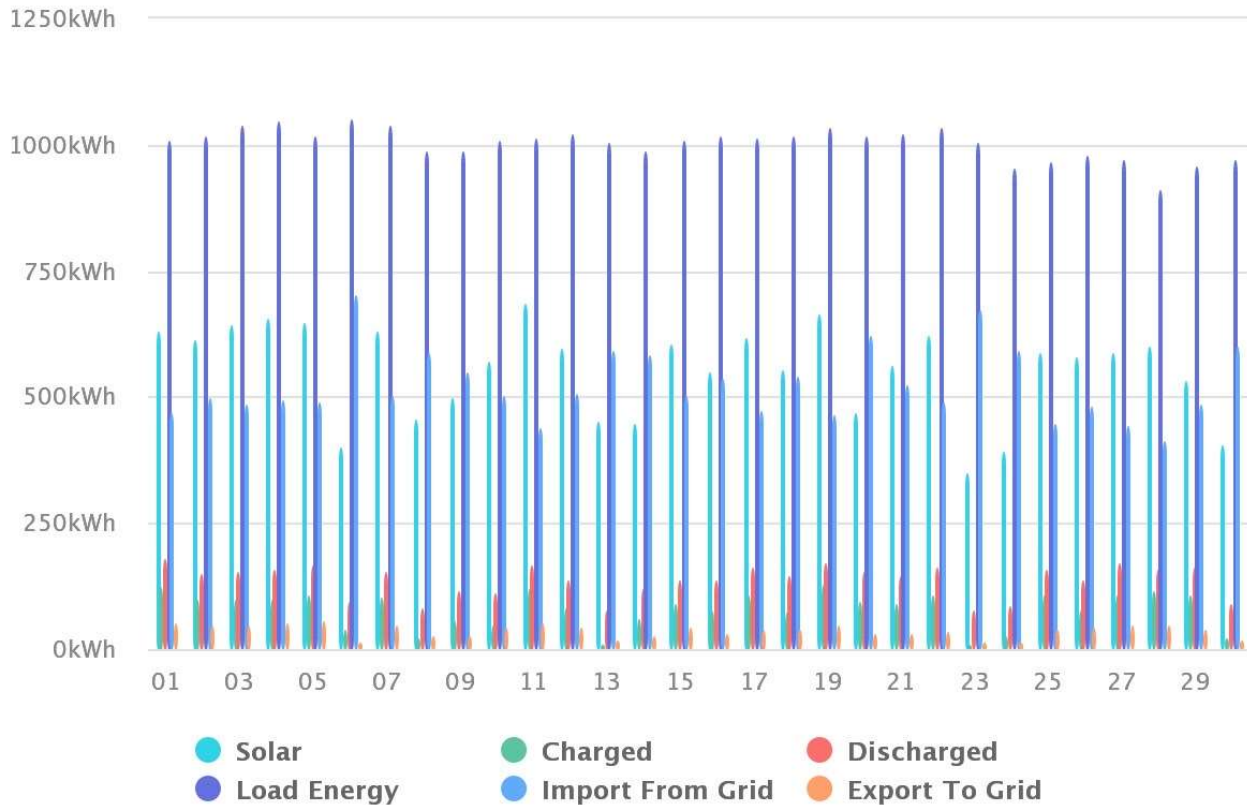


Figure 8 Energy Values Measured in November

Conclusion

Installation results after doing the analysis and comparisons of 200 kW PV Rooftop between energy to grid with energy storage at Wongsakorn Green Market in Thailand for 1 month, it was found that the hybrid power generation system from the solar roof works on average 4.5-5 hours per day, charge 556.58 kWh per day, electricity per month 16.69 MWh, and throughout the year have a total electric power of 200.28 MWh. Battery storage, charge per day 312 kWh, monthly electricity 6.73MWh and throughout the year, the total electricity cost is 80.76 MWh and is suitable for economic investment. to save energy reduce global warming and make the best use of renewable energy from the sun.

Acknowledgments

The research team would like to thank Wongsakorn Green Market in Thailand, Rajamangala University of Technology Thanyaburi and all working groups for supporting the researcher to study this project.

References

- Ammar, A., Muhammad, K. (2020). “Savitzky–Golay Filtering for Solar Power Smoothing and Ramp Rate Reduction Based on Controlled Battery Energy Storage”, *IEEE Access*, 8, 33806 – 33817.
- Chatterji, E., Bazilian, M. D. (2020). “Smart Meter Data to Optimize Combined Roof-Top Solar and Battery Systems Using a Stochastic Mixed Integer Programming Model”, *IEEE Access*, 8, 133843 – 133853.
- Jing, W., Ling, D. K. X., Hung Lai, C., Wong, W. S.H., Wong, M. L. D. (2017). “Hybrid energy storage retrofit for standalone photovoltaic-battery residential energy system”, *2017 IEEE Innovative Smart Grid Technologies - Asia (ISGT-Asia)*, Dec. 2017.
- Junhui, L., Hongfei, Y., Jun, Q., Ming, K., Shining, Z., Hongguang, Z. (2019). “Stratified Optimization Strategy Used for Restoration with Photovoltaic-Battery Energy Storage Systems as Black-Start Resources”, *IEEE Access*, 7, 127339 – 127352.
- Ngamprasert, P., Wannakarn, P., Rugthaicharoencheep, N. (2020). “Enhance Power Loss in Distribution System Synergy Photovoltaic Power Plant”, *2020 International Conference on Power, Energy and Innovations (ICPEI)*.
- Ngamprasert, P., Rugthaicharoencheep, N., Woothipatanapan, S. (2019). “Application Improvement of Voltage Profile by Photovoltaic Farm on Distribution System”, *2019 International Conference on Power, Energy and Innovations (ICPEI)*, Oct. 2019.
- Ngamprasert, P., Woothipatanapan, S., Wannakarn, P., Rugthaicharoencheep, N. (2020). “Improvement for Voltage Sag with Photovoltaic Performance on Distribution System”, *IEET - International Electrical Engineering Transactions*, 6(1), (10), 28-33.
- Rosyad, A. Y., Wahyudi, C. A.D., Noakes, C. J. (2020). “Profitability assessment of PV rooftop implementation for prosumer under net metering scheme in Indonesia”, *CIREN 2020 Berlin Workshop (CIREN 2020)*, Sept. 2020.
- Satpathy, P. R., Sudhakar Babu, T., Shanmugam, S. K., Popavath, L. N., Alhelou, H. H. (2021). “Impact of Uneven Shading by Neighboring Buildings and Clouds on the Conventional and Hybrid Configurations of Roof-Top PV Arrays”, *IEEE Access*, 9, 139059 – 139073.
- Syed, M. A., Khalid, M. (2021). “Moving Regression Filtering with Battery State of Charge Feedback Control for Solar PV Firming and Ramp Rate Curtailment”, *IEEE Access*, 9, 13198 – 13211.

The Simulation of Water Quality Monitoring System for Shrimp Farming Pond

Weena Janrachakool^{1*}, Nongluk Promthong¹, Nutchapol Saivawe¹,
Shareef Rodmanee¹ and Suvil Chomchaiya²

¹ Rajamangala University of Technology Thanyaburi, Pathumthani 10110, Thailand

² King Mongkut's University of Technology Thonburi, Bangkok 10140, Thailand

* Corresponding email: weena_j@rmutt.ac.th

Abstract

The objective of this project is to develop the method for inspection the water quality in shrimp farming pond with the application of sensor technologies. This developed method is about the measurement of dissolved oxygen level and water quality data logging via mobile communication which will wirelessly alarm farmer when the water quality is tending to be out of control.

The simulation of such developed warning system, in which oxygen level, temperature and acidity were being monitored, yield the deserved accuracy where the warning was in form of mobile alarming. Any out-of-range water quality data is properly logged and recorded into the storage media pertaining to the pre-set time interval. This enables shrimp farmers to diagnose the water quality situation base on the mobile delivered data.

Keywords: wireless communication, dissolved oxygen, water quality inspection

Introduction

Marine shrimp products are both socially and economically important for Thailand as source of food and national revenue from exporting respectively. The shrimp farming business is operated in an industrial format with more than one million people involved in various production chain, upstreaming from breeder raising cultivation and nursery, rearing and final processing for preprocessing as various instant products. Therefore, the proper farming is required because those processes are important to the growth and yield of shrimp. The use of proper aerators and air pumps to fill oxygen into the sea or fresh water is sufficient to meet the life needs of the shrimp and aquatic and sedimentary organisms. Therefore, the rearing management is important to maintain the ecological balance in the shrimp farming pond to keep shrimps to be healthy, stress-free and to reduce production costs in terms of power energy consumption as well as reducing the amount of carbon dioxide emissions from marine shrimp farming. These variables are important factors in the competitiveness of Thai shrimp exports markets.

Shrimp farming in Thailand is still the traditional method, either along the coast or along the river in brackish water. It relies on the personal experience and knowledge to assess situations such as observing the color of the water and the behavior of the shrimp. This is caused by the changes in the pH and the amount of oxygen in the water. There may be data discrepancies problems caused by factors in the current environment, for example, the intensity of sunlight may affect the human eye's reading of the color of the white shrimp pond water. Moreover, there are also uncontrollable natural factors such as extreme temperatures at certain times or sudden heavy rains and so far. These factors can affect the water quality that for raising shrimp.

Therefore, the organizers have adopted the Internet of things (IoT) to assist farmers in managing the environment of shrimp ponds. All three types of sensors were installed at the shrimp ponds to collect the environment data. The values collected from the sensor will be displayed to the farmers in

real time and alert if any water quality abnormality is detected. This will enable farmers to entirely manage the environment inside the shrimp pond.

Literature review

Internet of thing: IoT

The Internet of Things concept was invented by Kevin Ashton in 1999, starting with the "Auto-ID Center" project at Massachusetts Institute of Technology (MIT). Beginning from the Radio Frequency Identification (RFID) technology. It is a system that uses radio waves to wirelessly communicate data between two devices. In the post-2000 era, various technologies have developed and evolved rapidly. A large number of electronic devices began to exponentially emerged and extensively available with affordable prices with widely use of prefix “smart”, such as smart grid, smart home, smart device, smart network, etc, which means that these electronic devices can be connected to the Internet world. This allows such devices to communicate and exchange information using the sensor to communicate with each other. Kevin Ashton initially defined the term “Internet-like” which is later the term “Things” replaced electronic devices.

Internet of Things means everything is connected to the Internet world. This allows humans to control the use of various devices via the Internet, such as turning on-off electrical appliances, cars, mobile phones, communication tool Agricultural tools, buildings, houses, various daily appliances via the Internet network, etc. Internet of Things (IoT) technology is useful in many ways. However it comes with risks because if the security of the device and the Internet network is insufficient which may introduce malicious actions such as the information stealing or privacy violation. Therefore, the development of the Internet of Things (IoT) requires the development of measures and IT security systems in parallel.

Environmental monitoring system with wireless sensor network for lemon growing areas

The system design uses an Arduino microcontroller, which make easy for those who desire to develop further. As a result of testing, the sensor node can transmit data values that consist of relative humidity air temperature brightness of light soil temperature and moisture, and the remaining battery power level. Data can be sent to the base node by single-hop method, and individual base nodes can communicate using multi-hop method. The data from each base node is transmitted to the station node. To save data into the database to analyze the environment of the lemon farm. These data can be displayed in tables and graphs. The disadvantage is that the environment is not alerted. at the point of danger.

Development of a water quality measurement system in white shrimp ponds

In this article, a method for measuring water quality in white shrimp ponds has been developed. By applying the necessary water quality sensors together with wireless data communication to record the various water quality values that need to be controlled and alerted to white shrimp farmers. If the controlled value exceeds the preset value, the performance of water quality measurement system can work properly. It can alert the pond keeper with visual and audible signals. Shrimp farming can know if the water quality value is lower or higher than the set value. Data transmission, date-time recording and water quality value on the recording media can be complete within the set time interval. Farmers can read the water quality value or bring can be analyzed further Disadvantages Notifications are siren and sound alerts. Thus, users cannot be recognized if they are not on the farm.

Materials and methods

Development steps

Model development of oxygen alarm system, temperature, acid-base, and oxygen content control in shrimp ponds Internet of things (IoT) technology has been applied in research and has

implemented the Software Development Life Cycle (SDLC) based on the adapted waterfall model as follows:

- 1) To study the technology that can be used in the development of agriculture.
- 2) Gather information used to develop technology. Internet of things (IoT) in order to manipulate sensor connectivity and determine the pros and cons.
- 3) System analysis and design from research studies that have applied technology Internet of things (IoT) is used in agriculture in many ways, including crops, vegetables, water management. Researchers have studied the application of Internet of things (IoT) technology act as a facilitator for agriculture as shown in figure 1.

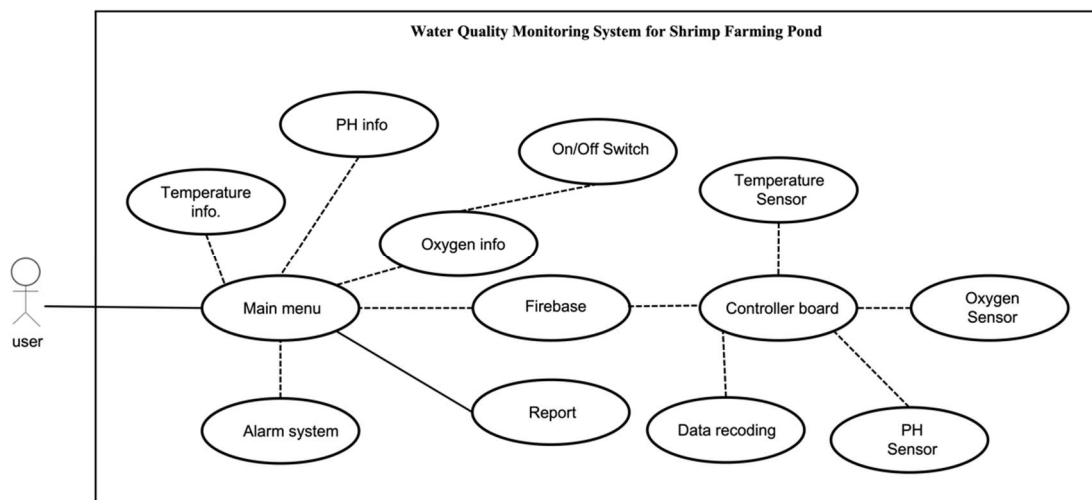


Figure 1 System analysis and design using IoT technology in shrimp farming pond

- 4) Designing screens and buttons to users
- 5) Check and correct the correctness of the system.
- 6) Test the performance of the system
- 7) Verify and correct the correctness.

Development tools

- 1) Computer equipment for the development of control systems such as portable computers Intel core i7-5500 CPU 2.4GHz, spare memory 4.00 GB
- 2) Temperature sensor model DS18B20 is a sensor used to measure temperature in degrees Celsius in the range of -55 to +125 degrees Celsius.
- 3) Dissolved Oxygen Kit is a device used to detect the concentration of oxygen in water that there is only very little quantity The sensor will measure the value and have a processor. Users can store the measured values and process them by interface with the module through the serial port. Just send a command to the module to get the information as needed.
- 4) pH Sensor Kit (PH Sensor Kit) is a sensor kit that is used to detect acid - alkalinity through a control module that serves to detect the analog signal measured from the sensor. Processing and sending data to users via Serial Port
- 5) The microcontroller board (Node MCU ESP8266) is a device used to control the operation of each sensor. It is also able to connect to the Internet in order to store that data in Firebase and store the data in the database for further use.

- 6) The relay is an electronic device that acts as a switch-to-circuit. By using electromagnets and to make them work, the required power is required by using the microcontroller board to control
- 7) Power supply is a device used to supply power to sensors and control boards.

Results and Discussions

Operations from the design and development of a model of the oxygen alarm system, temperature, acid-base, and oxygen content control in shrimp ponds. The function details are as the follows.

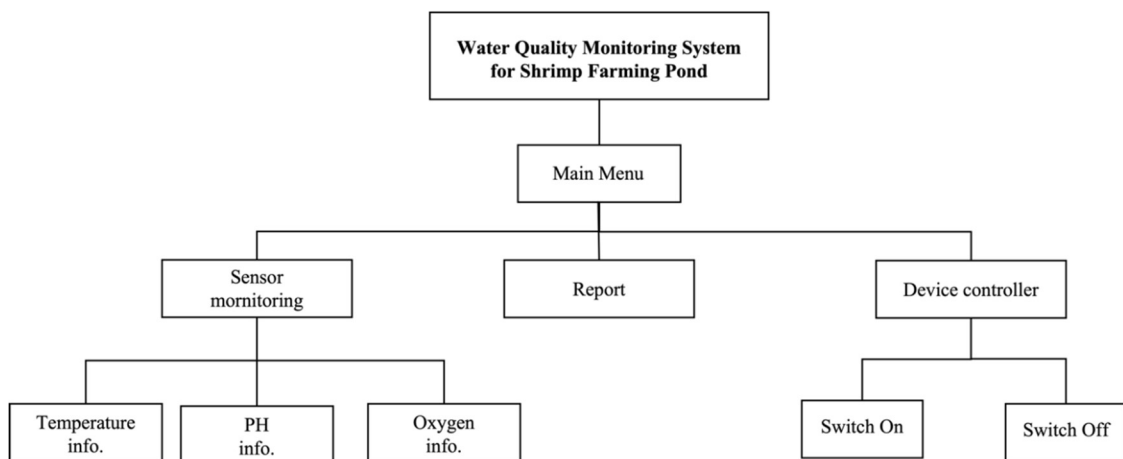


Figure 2 The function details of the controlling system for the shrimp farming pond.

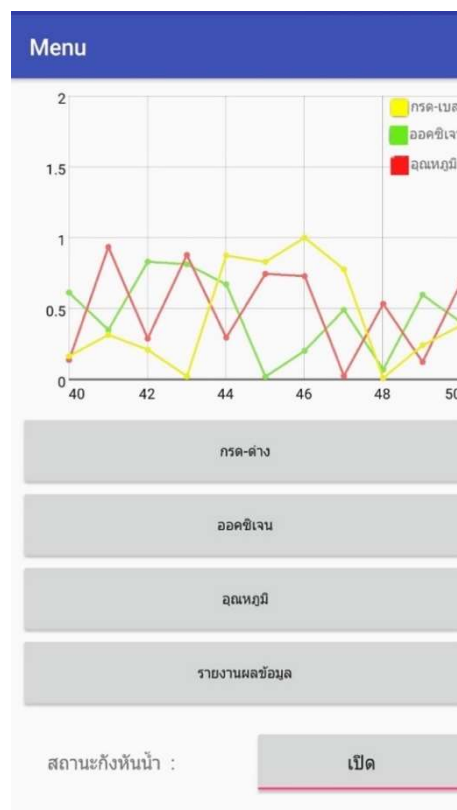


Figure 3 User interface of the controlling system for the shrimp pond

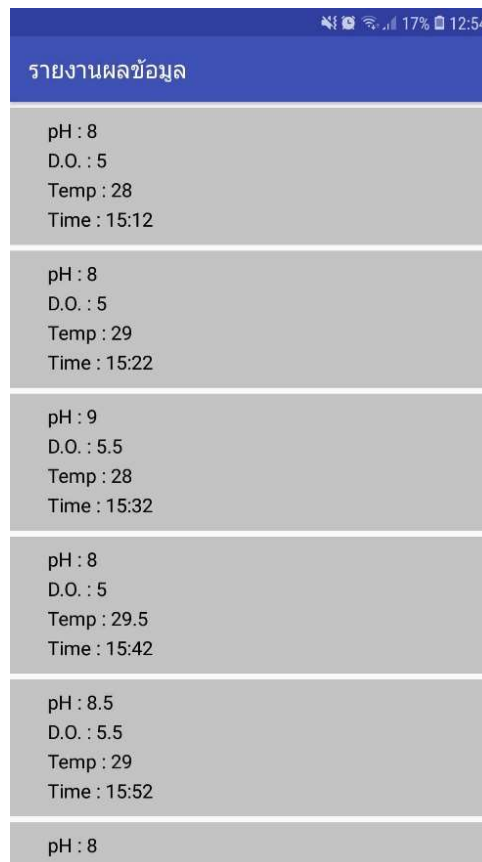


Figure 4 User interface of the sensors’ data report for the shrimp pond

Testing results

The effective testing of the controlling system for the shrimp farming pond had been conducted to evaluate the correctness and accurateness of temperature sensor, acid-alkali sensor and water oxygen sensor by comparing between real value and value from the sensors. The results of temperature sensor, acid-alkali sensor and water oxygen sensor have been showing in table 1 to table 3 respectively.

Table 1 Testing results of Temperature from sensor at 31 degrees Celsius

No.	Temperature Sensor (Celsius)
1	31
2	30
3	31
4	31
5	31

Table 2 The acid-base value from PH sensor

No.	Acid-base value	Acid-base sensor
1	8	8.5
2	4	4.5
3	10	10.5
4	8	7.8
5	4	3.7

Table 3 The comparison between oxygen in water and oxygen from sensor

No.	Normal water oxygen	Oxygen sensor
1	8	9.32
2	8	9.32
3	8	9.32
4	8	9.32
5	8	9.32

The correctness and accurateness of the set of sensors, as results shown in table 1 – 3, were entirely inexact value because these sensors were for general and education purpose, not for industry use. However, the system can facilitate farmers for water quality monitoring task in practical.

Conclusion

Research on the model of the oxygen alarm system, temperature, acid-base and oxygen content control in shrimp ponds. Developed for facilitating shrimp farmers, the functions that work are: Retrieving data from the temperature sensor, retrieving data from acid-base sensors, retrieving data from water oxygen sensors turn on/off the device.

From the performance test of the model of the oxygen alarm system, temperature, acid-base and oxygen content control in shrimp ponds. As for the hardware tests, it was concluded that the sensors were able to transmit similar but not entirely accurate values because the sensors were for general purpose, not for industry use. So, the values obtained are not entirely accurate. It was shown that the oxygen alert system model, temperature, acid-base and oxygen content control in shrimp ponds were proof that it can facilitate farmers for water quality monitoring task in practical.

Based on the development of a model for the alarm system for oxygen, temperature, acid-base and oxygen content control in shrimp ponds, there are suggestions as a guideline for further development as follows:

- 1) Use sensors suitable for the shrimp industry in order to make that value come out as accurate as possible.
- 2) Optimize the application for general users make it easy to understand.
- 3) Analyze the collected data and use it to make forecasts for farmers.

References

- Akyildiz, I.F., Weilian, S., Sankarasubramaniam, Y., and Cayirci, E. (2002). A survey on sensor networks, *IEEE Communications Magazine*, 40(8), pp. 102-114.
- Arunruek, J., Chantharat, S., Yamwajee, W. (2015). Development of a water quality measurement system in white shrimp ponds. *7th National Conference on Information Technology: NCIT*, 2015, pp. 177-181.
- BoonLiam, W., Boonthong, P., Yuyen, A. (2017). Development control acidity-alkalinity automatomivaly shrimp industry. RMUTR. Retrieve form: <https://repository.rmutr.ac.th/bitstream/handle/123456789/1216/fulltext.pdf?sequence=1&isAllowed=y>.
- Chee-Yee, C., and Kumar, S.P. (2003). Sensor networks : evolution, opportunities and challenges, *Proceedings of the IEEE*, 91(8), pp. 1247-1256.
- López, M., Gómez, J.M., Sabater, J. A. (2010). *IEEE 802.15.4 based Wireless monitoring of pH and temperature in a fish farm*. In: MELECON 2010-2010 15th IEEE Mediterranean electrotechnical conference. IEEE, pp 575-580.
- Mahgoub, M.I.a.I., and Networks, H.o.S. (2005). *Compact Wireless and Wired Sensing Systems*, Compact Wireless and Wired Sensing Systems, Washington, D.C.: CRC Press.

- Meadthaisong, S., Meathaisong, T., Chaosaku, S. (2013). *The Environmental monitoring system with wireless sensor network for lemon farm area*. 5th ECTI-CARD 2013.
- MCU: *What is the Internet of Things (IoT)?*. MCU (Thailand) Co., Ltd., Retrieved from <http://www.mcuthailand.com/articles/iot/IOT.html>.
- Passabut, T., Sripadungtham, P. (2009). *Automatic dissolved oxygen enhancement system for pond powered by solar cells*. © ECTI-CARD 2009, pp. 25-30.
- Supittayapornpong, S., *Wireless Sensor Network*, Asian Institute of Technology, Retrieved from http://www.thaitelecomkm.org/TTE/topic/attach/Wireless_Sensor_Network/index.
- Thongluam, T., Chuenta, W., Dinsakul, H., Charoenphan, B. (2014). *Automated Water Quality Measurement System for Pomegranate Cage*. ECTI-CARD Proceedings 2014, Chiang Mai, Thailand.
- USA: ‘The Zigbee Alliance’, *ZigBee Specification*, Retrieved from <http://www.zigbee.org/>
- USA: ‘The Bluetooth Special Interest Group (SIG)’, *Wibree Datasheet*, Retrieved from <http://www.wibree.com/>
- USA: ‘Internet Society’, *6LoWPAN: Overview, Assumptions, Problem Statement and Goals*, Retrieved from <http://www.ietf.org/>
- VEEDVIL. *Internet of Thing (IOT) Trends*. VEEDVIL Tech News & Info., Retrieved from <http://www.veedvil.com/news/internet-of-things-iot>

Real Time Security System with Face Recognition

Nongluk Promthong^{1*}, Weena Janratchakool¹, Komsun Chettrreerith¹,
Khongthep Boonmee¹ and Burasakorn Yoosooka²

¹Field of Computer Science, Faculty of Science and Technology, Rajamangala University of Technology Thanyaburi, Thanyaburi, Pathumthani, Thailand

²Field of Computer Engineering, Faculty of Engineering, Rajamangala University of Technology Phra Nakhon, Bangsue, Bangkok, Thailand

* Corresponding email: nongluk_p@rmutt.ac.th

Abstract

This research project is to develop the real-time surveillance system with real-time facial recognition technique. The operational process of this developed system, with C# as the major development tool, is to compare the real-time images from the camera to the images stored in the database, with the application of Harr-like algorithm. Such algorithm will depict facial images of whoever passing within the camera viewing radius and consequently store them. Any facial images with sufficient quality for further processing will consequently applied with Eigen facial recognition technique and Open CV libraries to enhance the image validities and operational performance. The developed system has been performance tested with 20 volunteers with the use of images and lux for facial recognition benchmarking. The testing results indicated the performance regarding the facial recognition comparing in “good” level. However, the correctness of recognition can be enhanced with the more images and the proper light intensity. In conclusion, the developed system yielded the “good” level of overall personal identification.

Keywords: surveillance system, facial recognition, real-time

Introduction

Image processing technology has played an increasingly important role in human daily life. Sharp images are essential in image processing. In order to be able to use such images to analyze quantitative data such as size, shape and direction of movement of objects in the image to analyze correctly. Currently, image processing technologies are classified into several categories, one of which is security system with face recognition via webcam. by recognizing faces that have undergone a face recognition process that the camera captures with the faces in the stored person's face data file to know who it is and to be able to protect and stay safe.

Nowadays, security systems generally come in many forms. Each of these formats has its weaknesses in fast detection. They cannot work to cover home security that results in theft in which scammers may use the disadvantages of the security system. It is the point of entry for theft that can cause damage. Looking at the statistics of burglaries in 2013, it was found that 43,060 cases were reported, and 18,710 arrests were made (Ministry of Social Development and Human Security, 2013: online). From the importance of such problems, the researchers therefore developed a real-time facial recognition security system to reduce theft. This is because a typical security camera system will have to take the footage from the CCTV to find the intruder later. But the real-time facial recognition security system will immediately alert the security guards, when there are unauthorized people entering the area. It makes possible to increase the safety of life and property in a timely manner.

Research Objectives

To develop a security system with real-time facial recognition and has alerted officers by sound. The system facilitates the use, up speed in the investigation of unauthorized persons, enhancing the security system and reducing crime.

Research and Related Theories

Intruder Warning System, this project is designed and develop a program for alerting strangers within residential buildings. By applying digital image processing techniques to process, check and receive images in real time by using webcams or cameras that can be found in general. And it is inexpensive to receive images and process them. This project must continue to develop in the program after receiving the image and then decide to send the alarm to the security under the risk conditions we have set. We hope that the program will act to replace the defects caused by human or help security personnel. It provides better protection and security of residents or property loss. (Krakrit Direksoontorn and Sasinan Khomduen, 2011: online)

Development of Face Recognition System by Kritika Sripongsuk, Nattha Panyaphuntrakul and Thanawut Chotichanapiban, Department of Computer Science Faculty of Science Srinakharinwirot University is a project that has been prepared for use in facial recognition of a person working on a personal computer with a webcam attached. The recognition technique used in this system is the Eigen facial technique. The operation of the system can be divided into two parts: the learning process. This will take a picture of the face of the person you want to recognize and analyze the key components. and a recognition process that analyzes a person's test face images to determine if they match any of the facial images stored in the learning process. (Kritika Sripongsuk, Nattha Panyapoontrakul and Tha Nawut Chotichanapiban, 2011: online)

Face Recognition system considered to be one of the systems used for biometric authentication, the face recognition system works by comparing faces from digital photographs or a video camera image of an interested person with an existing database of faces. When the comparison is complete, the results will be displayed in the database with the same faces as the images that were compared. Facial recognition systems are constantly being developed. At present, facial recognition systems have evolved greatly. Make the facial recognition system more reliable. Until the face recognition system has been widely used. In many foreign countries, facial recognition systems have been installed in airports to prevent criminals escaping into the country. There is a facial recognition system for identity verification in various cases too. (Banha Rajainthong, 2011: Online)

In general, a facial recognition system consists of two main steps: Face detection and face recognition.

- 1) Face Detection is the process of finding a person's face from an image or video after that, the resulting face image will be processed for the next step to make the detected face image easy to recognize. One of the methods used to detect faces is capable of fast processing and has a high detection accuracy rate. It was invented by Paul Viola and Michael J. Jones called the Viola-Jones method. A method for representing images is presented called the integral image, which can calculate characteristics faster and the learning algorithm has been improved. It is based on AdaBoost which selects only the critical feature. The most efficient grouping style which also describes the inclusion of a cascade classifier, which allows the background of the image to be rejected faster and focusing the calculations on the area that resembles the object of interest more. The underlying principle of Viola-Jones' algorithm is a snippet scan to detect faces from an input image. Conventional image processing uses a different scaling of the incoming image to various sizes and uses a fixed size detector to find objects. Viola-Jones has proposed a new way by resizing the detector instead of scaling the incoming image and use the detector to find the object several times (each cycle uses a different size). The detector is built using the Hair-like process image separation characteristics. The principle of Viola-Jones' page search algorithm is that the detector scans the image multiple times

over the same image with different sizes even if there is more than one face. Many sub-window outputs are still negative non-faces. Reject non-faces instead of face search because deciding which area is not that face it's faster than finding faces. A cascaded classifier was created, which is a grouping of several sequentially. When a sub-window is categorized as Non-Face, it will be rejected immediately. But on the other hand, if a sub-search is classified as May-Face, it will be passed on to the next cluster in order. The higher group layer will be the higher chance that the sub-windows will be faces.

2) Face Recognition is a process in which the detected and processed image of faces from the face detection procedure is compared with a database of faces to indicate that the detected faces correspond to a particular person. One face recognition algorithm, Principal Component Analysis is a mixing technique. Features in the import vector to create a new vector in the subspace that has less dimensions than the original vector. The combination used is a linear combination that is a feature is multiplied by a certain constant. Then add them together using principal component analysis and facial recognition systems. It can be done by converting a two-dimensional image of a person's face to a one-dimensional vector and stored in the database when wanting to compare the faces of interested persons. It will convert the image of the face into a one-dimensional vector. The vectors are then compared with the images in the database to find the results.

Human face recognition uses the Eigenface for Face Recognition technique. Eigenface is an algorithm used for face recognition and identification. It is based on the principle of principal component analysis. The faces are represented by linear equations of vectors that are perpendicular to each other by finding the Eigen vector of the covariance matrix from the images database. Then taking each image in the database, collecting vector data and then finding the average vector of the images. The faces must be modeled in Gray Level. Because it uses less memory to store data than gray images. It can save memory compared to the storage of gray images, grayscale images take faster processing time than color images. Therefore, the image used must be converted to a gray format image. (Banacha Rajainthong, 2011: online)

Scope of Research

1. The system can process facial images and compare the person's identity from the data file.
2. The system can send an audible alarm to the authorities when it detects unauthorized persons.
3. The system can capture images at a distance of up to 5 meters.
4. The system must store at least one portrait of the person in order to compare the face of the person in the image file.
5. The system cannot compare a person when part of their face is covered.
6. The system can compare faces of no more than 2 people at a time.
7. Real-time face comparison system
8. The system can record images when a person enters the designated area and can browse image from data files.
9. The system can detect only in the specified area.
10. The system can only capture straight faces.

Experiment

The algorithm conducts research of security systems with real-time face recognition as the most important thing. The system will detect motion to detect faces using Eigen's principle that there are 3 main working steps as follows.

1. Preparing Eigen's face for use in recognition.

1.1 Collect a training set of face images and convert them into a single row matrix and merge them into a set ($S = \{\Gamma_1, \Gamma_2, \Gamma_3, \dots, \Gamma_M\}$)

1.2 The mean image Ψ is calculated from the set of images converted to matrix as shown in Equation 1.

$$\Psi = \frac{1}{M} \sum_{n=1}^M \Gamma_n \quad (1)$$

1.3 Find the difference between the image mean and the newly obtained image as shown in Equation 2.

$$\Phi_i = \Gamma_i - \Psi \quad (2)$$

1.4 Find Orthonormal vectors (u_n) equal to the number of input images that best describe the distribution of the data, where the k (u_k) vector is chosen with the following equation 3.

$$\lambda = \frac{1}{M} \sum_{n=1}^M \left(u_k^T \Phi_n \right)^2 \quad (3)$$

1.5 Then find the covariance matrix according to the procedure as shown in Equation 4 as follows:

$$\begin{aligned} C &= \frac{1}{M} \sum_{n=1}^M \Phi_n \Phi_n^T \\ &= AA^T \end{aligned} \quad (4)$$

1.6 Then we get the Eigen vector v_1, v_2 as shown in equation 5.

$$A = \{ \Phi_1, \Phi_2, \Phi_3, \dots, \Phi_n \} \quad (5)$$

2. Recognition consists of the following steps:

2.1 Take the image that you want to test recognition and convert it into Eigen's face. After that, the image was compared with the average image to find the difference of the input figure and the mean. Then multiply the difference with the Eigen vector of each figure that is in the set of images used in training which will get the weight (Weight) and then store it in the vector Ω as in Equation 6 and 7.

$$\omega_k = u_k^T (\Gamma - \Psi) \quad (6)$$

$$\Omega^T = [\omega_1, \omega_2, \dots, \omega_M] \quad (7)$$

2.2 Find out which image in the set of training images is closest to the input image by finding the Euclidean Distance as shown in Equation 8.

$$\varepsilon_k = \|\Omega - \Omega_k\|^2 \quad (8)$$

2.3 It knows whether the input is a face of a person or not by assigning the lowest input threshold to it after comparing it with the smallest input value. Then you can know whether the imported image is a face or not. Then we have to find out whether the face is a face of a known person or not. By assigning another minimum input value, it compares whether the input image is close enough to one of the images in the training image set (the smaller the distance value, the more the closeness).

3. In face comparison, if the face does not match the recorded image, the system will record the faces found in the intruder's file and send an audible alarm.

The steps of system development: the visual studio program and the MguCV OpenCV library were applied to develop facial recognition security systems. The structure of the entire system for user interface function page was designed. As well as the use of security systems with real-time face recognition, all can be diagrammed and designed as follows.



Figure 1 Real-time face recognition security system flowchart

Use Case Diagram shows how the security system works with real-time face recognition. There are various functions of the system which show the relationship in the form of use cases as shown in Figure 2.

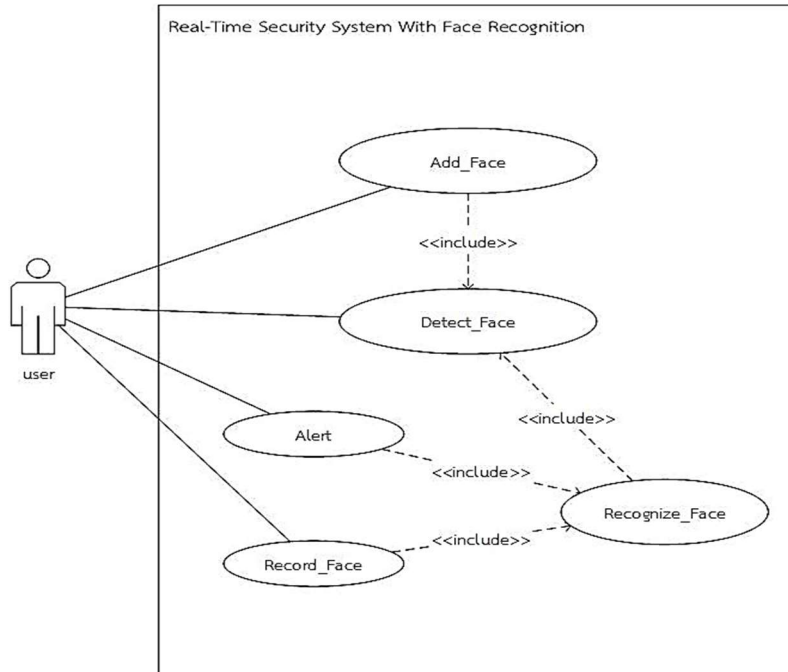


Figure 2 Real-time facial recognition security use case diagram

A real-time face recognition security system consists of classes and their relationship between classes as shown in Figure 3.

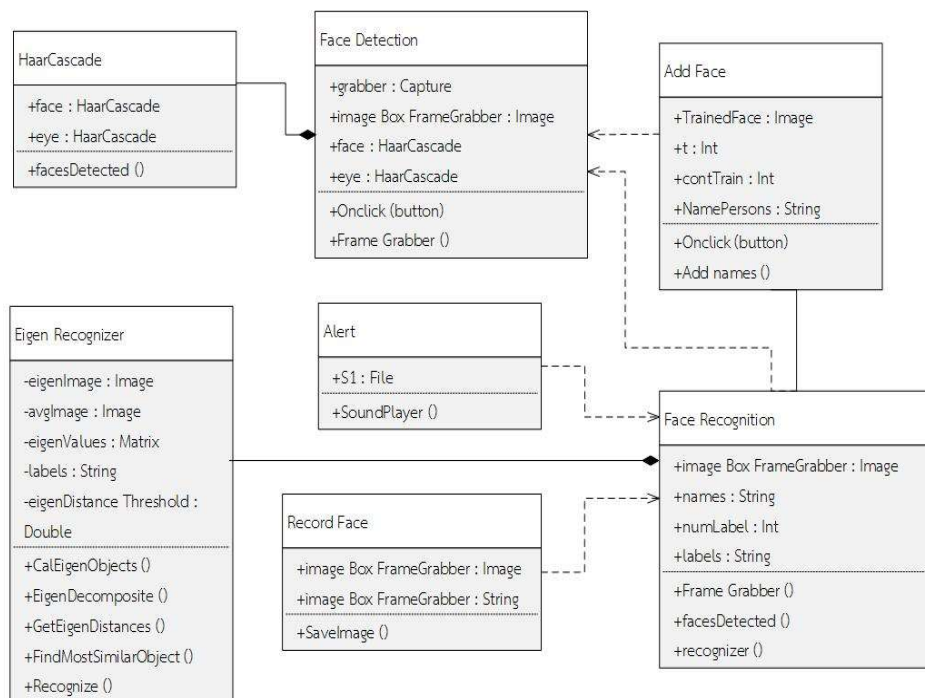


Figure 3 A class diagram of a real-time face recognition security system

Results and Discussion

Once the development of a real-time facial recognition security system is completed. It have tested the work in front of the laboratory SCI 807 room, Faculty of Science and Technology, Rajamangala University of Technology Thanyaburi. It was found that it could perform all the functions as defined in the above planned scope in all ten areas. The research team has recorded the details of the system's operation in different parts as follows:

1. Start from the home screen of the real-time facial recognition security program, start it by pressing the start button. Then the program will open the camera and save the face and list of people in the organization to save to the database.

2. The system captures incoming faces and saves images to a file. Then they was compared with the images in the database. If they match, it will show that person's name but if it doesn't match, it will save the image to the intruder's file and sound an alarm as shown in Figure 4.

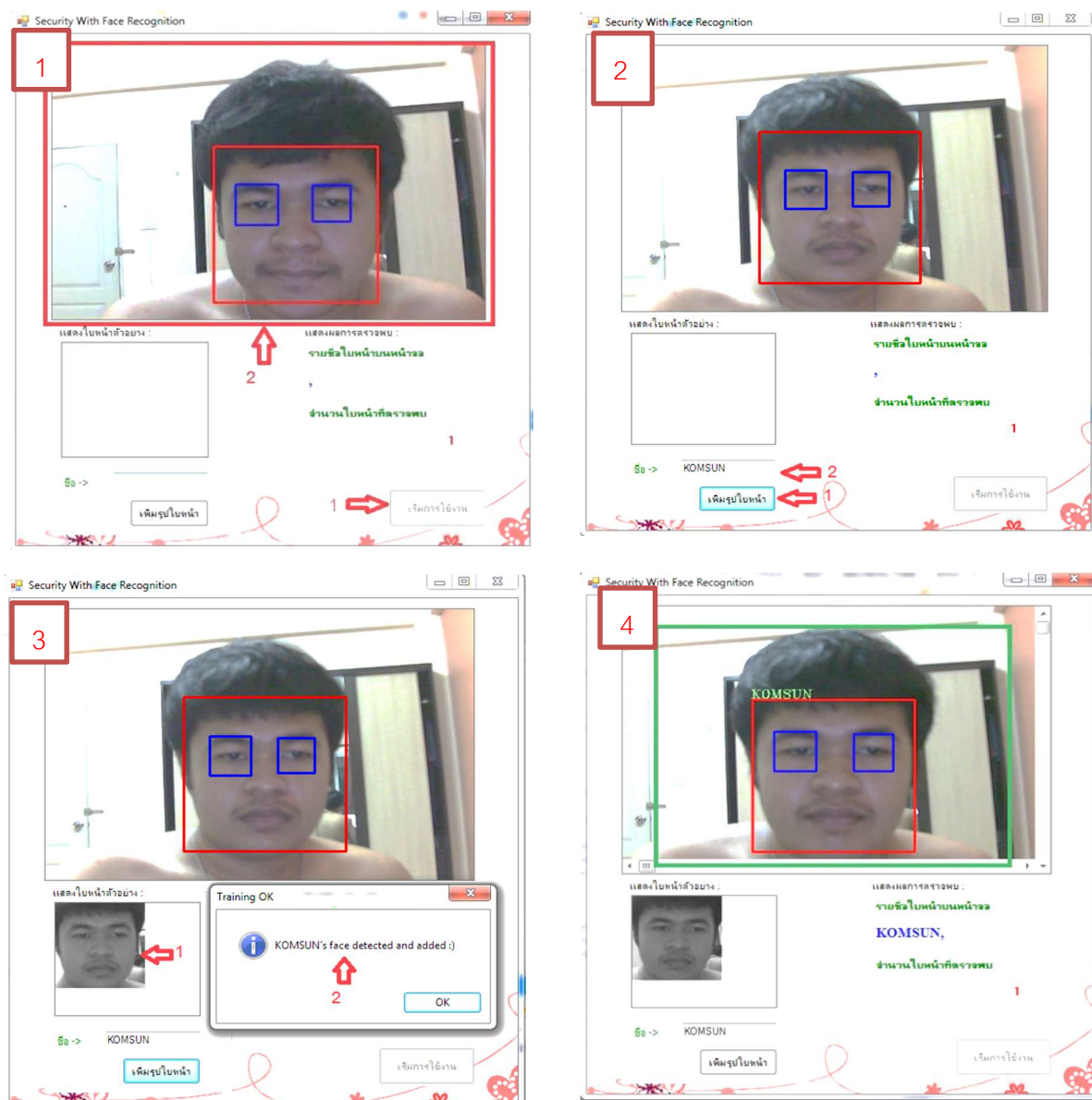


Figure 4 System operation steps

From the data collection experiment, the number of faces in the database were used for comparison, 1 image, 5 images and 10 images, and use the light value 160-190 lux and 20-50 lux, tested 20 human faces, the results are shown in Table 1 and Table 2 as follows:

Table 1 Summarizes the results of the accuracy test at an exposure level of 160-190 lux

Light value 160-190 lux		
number of people	number of faces in the data file	Precision
20	1	10%
	5	60%
	10	80%

Table 2 Summarizes the results of the accuracy test at an exposure level of 20-50 lux

Light value 20-50 lux		
number of people	number of faces in the data file	Precision
20	1	20%
	5	60%
	10	90%

Based on the results of real-time facial recognition security system analysis results, the results were presented in a tabular form. Several factors were used in the test used to compare the images, namely the number of images contained in the data file of 1, 5, and 10 images, and used two illumination ranges, 160-190 lux and 20-50 lux, the result of which came out that:

- 1) If the number of faces in the data file is 1, the accuracy is in the range of 10-20%.
- 2) If the number of faces in the data file is 5, the accuracy is in the range of 60%.
- 3) If the number of faces in the data file is 10, the accuracy is in the range of 80-90%.
- 4) If there is no number of faces in the data file will have accuracy in the range of 80-90%.

From the test results, the light has little effect on accuracy. But the more faces to compare in the file, the more accurate the system will be. The best result of the test when the number of faces in the data file is 10. The accuracy of the system depends on the detection distance and degree of face detected.

Conclusion

A real-time facial recognition security system has applied a number of techniques. Human face recognition using the Eigen facial technique that was introduced into the system. The system must collect a picture of that person's face to be used as a proof of identification. The working process of the system starts with the user saving a person's face to a file. With the working principle of the Harr-like algorithm, lets the camera capture faces using the Eigen facial technique and the OpenCV library. It helps to identify the next display which the operation of all the above mentioned systems has been developed from the C# language.

Based on the results of the evaluation of the system's performance test with 20 testers using the number of images and exposure, they were compared with facial recognition for use in testing. The test results are pretty good compared to facial recognition. If the number of images is greater and the light level is between 20-50 lux, it will make facial recognition accuracy up to 90 percent. Suggestions for installing a camera in use should select a good quality and high resolution webcam.

References

- AUTOMATIC_VEHICLE_MODEL_DETECTION_SYSTEM. (2013). [Retrieved March 20, 2015].
- Chansod, E., Ratanatai, S. and Rojanawas, P. Haar-like feature, [online]. Accessed from: http://202.44.34.144/nccitedoc/admin/nccit_files/NCCIT-20143010153601.pdf, 2013. . [Retrieved March 25, 2016].
- Direksunthorn, K. and Khomduen, S. (2011) Intruder Alert System, [online]. Retrieved from: www.research.eng.ku.ac.th, [Retrieved March 20, 2015].
- Human face recognition using the Eigen face technique, [online]. Accessed from: <http://www.bantronix.com/2011/10/eigenface-for-face-recognition.html>, 2011. [Retrieved on April 8, 2015].
- Ibookengineering. Open CV, [Online]. Retrieved from: <http://ibookengineering.blogspot.com/2013/08/opencv-21-windows-microsoft-visual.html>, 2556. [Retrieved 19 March 2016].
- Ingkasantatikul, P. (2007). Development of Face Recognition System. Master's Thesis. Applied Physics Chiang Mai University, [Retrieved January 10, 2016].
- IT Encyclopedia. What is XML, [online]. Accessed from: [http://www.mindphp.com/What is XML.html](http://www.mindphp.com/What%20is%20XML.html), 2012. [Retrieved March 21, 2016].
- K John Peter, G. Gimini Sahaya Glory, Dr. S. Arguman, G. Nagarajan, Sanjana Devi. V. V and Dr. K. Sentamarai Kannan. Improving ATM Security Via Face Recognition, [Online]. Available: http://ieeexplore.ieee.org/xpl/login.jsp?tp=&arnumber=5942118&url=http%3A%2F%2Fieeexplore.ieee.org%2Fxppls%2Fabs_all.jsp%3Farnumber%3D5942118, 2011. [Retrieved 20 March 2015]
- Lakshmiprabha, N.S., Bhattacharya, J. and Majumder, S. Face Recognition using Multimodal Biometric Features. [Online]. Available: http://ieeexplore.ieee.org/xpl/login.jsp?tp=&arnumber=6108945&url=http%3A%2F%2Fieeexplore.ieee.org%2Fxppls%2Fabs_all.jsp%3Farnumber%3D6108945, 2011. [Retrieved 20 March 2015].
- Ministry of Social Development and Human Security. (2014) Theft incident, [online]. Accessed from: <http://www.m-society.go.th>, [Retrieved April 19, 2015].
- Nation TV, police open 1 year Thai crime statistics [online]. Access from: <https://www.nationtv.tv/news/378837414> [Retrieved February 7, 2016].
- Phakkratok, W. (2014). Functionality of Emgu CV, [online]. Accessed from: <http://visual-studio-express-project.blogspot.com/2014/01/emgucvcvinvoke-invoke-opencv-function.html>, [Retrieved on March 18, 2016]
- Rajainthong, B. (2011). Face Recognition, [online]. Retrieved from: <http://www.bantronix.com/2011/10/face-recognition.html>, [Retrieved 9 April 2015].
- Sripongsuk, K., Panyapoontrakul, N. and Chotichanapiban, T. (2011) Development of Face Recognition System. Thesis. Computer Science Srinakharinwirot University, [Retrieved January 10, 2016].
- Wanpraphan, M. and Indy, E. Gray Scale Image, [online]. Accessed from: <http://www.research-system.siam.edu/images/thesistee/>

Railway Area Detection Using Deep Segmentation Networks

Saifun Khruetakhrui¹, Jakkree Srinonchat^{1*} and Seán Danaher²

¹Signal Processing Research Laboratory Department of Electronics and Telecommunications
Engineering Faculty of Engineering, Rajamangala University of Technology Thanyaburi
39 Moo 1, Rangsit-Nakhon Nayok, Pathum Thani 12110, Thailand

²Northumbria University, Newcastle, UK

* Corresponding email: jakkree_s@rmutt.ac.th

Abstract

Detecting obstacles or suspicious objects in the railway area is essential for rail transport, especially high-speed trains. However, the detection system is developed using image processing by adjusting parameters and features, but there are limitations in the system's performance and accuracy when used in a complex environment. This paper, therefore, presents an exploring deep segmentation network for railway area detection at the pixel level. The system was designed based on the SegNet technique combined with a pre-trained convolutional neural network VGG-16. The 1,000 input dataset was collected from the captured video frames from the front rail vision divided into 80% and 20% training and testing sets, respectively. The parameter value of the number of training sessions is 100 cycles. In testing, brightness and darkness were improved by the gamma correction technique to analyze the endurance performance of the system.

Keywords: deep segmentation network, convolution neural networks, rail area detection

Introduction

The railway system is recently essential to transport goods and humans. However, accidents have always occurred on the railway track due to object obstacles. Therefore, railway obstacle detection systems with cameras in front of trains for rail obstacle detection have been developed, such as railway obstacle detection (Ruder et al., 2003), (Maire, Bigdeli, A. (2010). Rail surface inspection (Shang et al.), (Chen, X. Zhang, H.) and rail obstacle detection (Deqiang et al.). It can be noticed that the railway area detection techniques are focused on inspecting obstacles using the front view of the train. However, it is still challenging due to complex background processing and ambient lighting changes that may result in errors.

Nowadays, the advancement of artificial intelligence technology has been applied in the transportation system, such as the driver assistance system (Hsieh et al.), (Lin et al.). It aims to develop a safety system using image data processing. Therefore, this research presents a system designed for railway area detection using deep segmentation networks.

This research presents the application of a deep segmentation network for railway area detection to determine the location and recognize objects or pedestrians entering the railway track. The proposed method uses the SegNet technique (Badrinarayanan et al., 2017) consisting of two main encoder steps. The first step is to use a neural network to achieve the pixel-level classification of the railway environment image. The second step of this method is to optimize the geometry of the separated railway areas by using the polygon modulation method.

Methodology

Depth Image Segmentation

The SegNet is an internally structured architecture consisting of an encoder and a decoder network. The encoder network consists of the convolutional thirteen layers similar to VGG-16, eliminating the connection of the total number of layers to make the network smaller and easier to

train. The decoder network is an essential component of SegNet. It consists of a hierarchical decoder in each encoder layer, using the max-pooling derived from the encoding layer to upsample the input match [8]

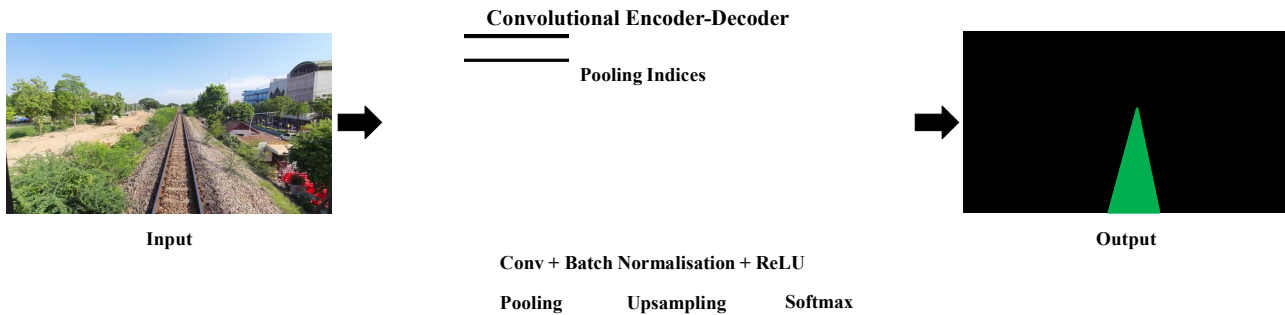


Figure 1 SegNet architecture

In the experiment, the input to estimate the effectiveness of the proposed model is the five video data of the intercity rail route, which takes from the front view of the train commander. It has a 1,280 x 720 pixels resolution and 24 frames per second for a frame rate. There are a variety of lighting conditions and different ambient conditions, as shown in Figure 2. The video input is converted to be each image frame in every second which these images are selected and classified to be suited for training the proposed model. Then the pixel label technique is then applied to describe the image detail, divided into two classes: rail track and background environment. These images are separated into training and testing data as 80% and 20%, respectively, as shown in Table 1.



Figure 2 Sample frames from a video dataset

Table 1 The input images

Items	Training (80%)	Testing (20%)	Total
Video 1	240	60	300
Video 2	27	7	34
Video 3	241	60	301
Video 4	86	21	107
Video 5	206	52	258
Total	800	200	1,000

Experiment and Results

The experiment was processed with an Intel i7-4790K 4.00GHz CPU. The accuracy of the proposed method is measured by the means Intersection-over-Union (MIoU) metrics and the means Average pixel (mAP). The formulas are shown in equations (1) and (2).

$$mAP = \frac{1}{k} \sum_{j=1}^k \frac{n_{jj}}{t_j} \quad (1)$$

$$mIoU = \frac{1}{k} \sum_{j=1}^k \frac{n_{jj}}{n_{ij} + n_{ji} + n_{jj}} \quad (2)$$

Table 2 accuracy of the proposed method

Testing data	mPA	mIoU
$\gamma = 1/2$	81.76%	69.85%
$\gamma = 1$ (Original)	86.92%	73.62%
$\gamma = 1.5$	74.53%	61.23%

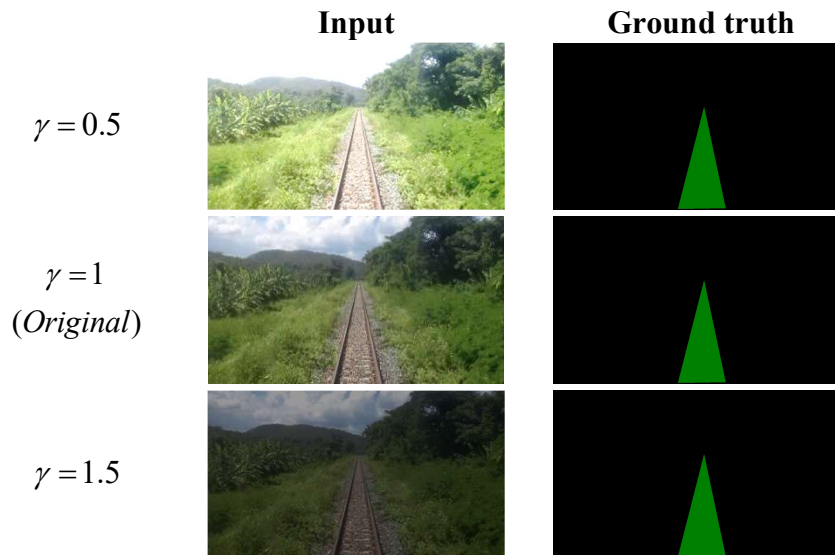


Figure 3 Examples of rail area detection

Conclusion

This research presents the deep learning technique for railway area detection. The results show that the accuracy of performance measurements can be improved when the images are applied with two levels of grammar adjustment. It can be seen that the original image can detect the railway area more effectively than the image with the light adjustment.

References

- Badrinarayanan, V. Kendall, A. and Cipolla, R. (2017). "SegNet: A deep convolutional encoder decoder architecture for image segmentation", *IEEE Trans. Pattern Anal. Mach. Intell.*, 39(12), pp. 2481-2495.
- Chen, X. Zhang, H. Rail Surface Defects Detection Based on Faster R-CNN.
- Deqiang He, Yefeng Qiu, Jian Miao, Zhiheng Zou, Kai Li, Chonghui Ren, Guoqiang Shen bImproved Mask R-CNN for obstacle detection of rail transit.
- Hsieh ,C.-H. Lin, D.-C. Wang , C.-J. Chen, Z.-T. and Liaw ,J.-J. Real-Time Car Detection and Driving Safety Alarm System With Google Tensorflow Object Detection API.

- Lin, C.-C. Lin, C.-W. Huang, D.-C. and Chen, Y.-H. (2008). "Design a Support Vector Machine-based Intelligent System for Vehicle Driving Safety Warning", *IEEE Conference on Intelligent Transportation Systems*, pp. 938-943.
- Maire. Bigdeli, A. (2010). " Obstacle- free range determination for rail track maintenance vehicles", *Proc. ICARCV*, pp. 2172-.
- Ruder, M. Mohler, N. and Ahmed, F. (2003). " An obstacle detection system for automated trains", *Proc. IEEE IV*, pp. 180-185.
- Shang, L. Yang, Q. Wang, J. Lei, W. Detection of rail surface defects based on CNN image recognition and classification

Drying Kinetics Models of Mini Heat Pump Dryer for Sliced Bananas

Phairoach Chunkaew*, Aphirak Khadwilard and Chakkraphan
Thawonngamyingsakul

*Department of Mechanical Engineering, Faculty of Engineering, Rajamangala University of
Technology Lanna Tak, Muang, Tak 63000, Thailand*

Abstract

The objective of this research is to model a mini heat pump dryer from sliced bananas. Six models of Newton, Henderson and Pabis, Logarithmic, Two-term, Modified Henderson and Pabis, and Diffusion approach from the literature are selected and adapted for prediction of the drying kinetics of sliced bananas from the mini heat pump dryer. The experiments are carried out at a drying temperature of 60 °C, with air flow rates of 0.117, 0.128, and 0.140 m³ s⁻¹ and evaporator bypass air at 60%. To test, an air system with a closed loop and a heat pump's working fluid R134a are used. Sliced bananas have an initial moisture content of 244 - 281% dry basis and are dried until their final moisture content is lower than 6.24 ± 0.007% dry basis. Their constants in the models of selected models are fitted with experimental data by non-linear regression analysis. The criteria for evaluating the models are the values of the coefficient of determination (R^2), the root mean square error (RMSE), and the reduced chi-square (χ^2). It was found that among the models tested, the diffusion approach model of this study could be considered the most appropriate.

Keywords: sliced banana, drying kinetics, models, heat pump dryer

Introduction

A drying kinetics model is an important equation for the system simulation and is necessary to be capable of predicting the water removal rate. It is considered important for the optimization of the drying process. In the literature, the mathematical models of drying kinetics are classified into three types: theoretical, semi-theoretical, and empirical models for drying simulation. The theoretical model has been described by Fick's second law (Crank, 1975) and the diffusion model. In addition, more semi-theoretical and empirical models have been discovered in the literature, including the Newton model, Henderson and Pabis model, Logarithmic model, Two-term model, Modified Henderson and Pabis model, and Diffusion Approach Model. Semi-theoretical and empirical models are easy to apply for prediction, in which the predicted results and the experimental data show good agreement. These models are investigated by considering the coefficient of determination (R^2), the root mean square error (RMSE), and the reduced chi-square (χ^2) as criteria for determining the suitability of the different drying kinetics models. The semi-theoretical and empirical models had a coefficient of determination (R^2) greater than the theoretical model (Chunkaew, 2014).

Heat pump dryer technology has high efficiency because there is heat recovery from removing relative humidity in the air by an evaporator. The dried material had good product color and quality (Chunkaew, 2005). The high temperature and the high velocity are affected by the heating load at the condenser. Then the drying rate is high and the drying time is short. Then, the coefficient of performance (COP_h) and the specific moisture extraction rate (SMER) are high too (Chunkaew & Kosalanun, 2018). According to the literature, no more than 60 °C is achieved by a single heat pump cycle (Chunkaew *et al.*, 2017). Moreover, the other conditions such as bypass air at the evaporator, the type of working fluid, and the type of controlling drying temperature are affected by the performance of the heat pump dryer.

The equipment in a heat pump dryer (Aktas *et al.*, 2016) is mostly adapted from air conditioner or refrigerator equipment. The system of air conditioning has four main parts: a compressor, a condenser, an expansion valve, and an evaporator. The compressor has three types: an open-type compressor, a semi-hermetic compressor, and a hermetic compressor. The condenser has 3 types of an air-cooled condenser, a water-cooled condenser and an evaporative condenser. The expansion valve has six types: a hand expansion valve, an automatic expansion valve, a thermostatic expansion valve, a capillary tube, a low-side float valve, and a high-side float valve. The evaporator has 2 types of finned-tube evaporation: a shell and a tube evaporator. Then, accessory equipment for safety in the heat pump cycle has more to choose from, such as a filter drier, a solenoid valve, a low pressure switch, and a high pressure switch. Finally, the refrigerant types have been divided into 3 groups: chlorofluorocarbon (CFC), hydrochlorofluorocarbon (HCFC) and hydrofluorocarbon (HFC). The CFC refrigerants are R-11, R-12, R-13, R-500, R-502, R-503, R-113, R-114, and R-115. The HCFC refrigerants are R-22, R-123, R-124, R-401A, R-401B, R-402A, R-402B, R-403B, R-406A, R-408A, R-409A, and R-69L. The HFC refrigerants are R-134a, R-143a, R-404A, R-407A, R-407C, R-410A, R-125, R-507, R-32, and R-23 (Tor Siriwatthana, 2003). In the Thai market, we can buy the refrigerant in groups of HCFC and HFC only because the HCFC refrigerant has a low ozone depletion potential (ODP) and the HFC refrigerant does not have an ozone depletion potential. Nowadays, HFC refrigerants such as R-134a and R-32 are currently used in refrigeration and air conditioning systems.

Banana flour can be modified for food applications. Banana flour production has a drying step in the process. From the literature, when the thickness of sliced bananas increased as the drying rate decreased. Rahmam *et al.*, (2018) reported that a thickness of the sample of 4 mm and a moisture ratio of 0.7 to use a drying time of 2 hours. The sample's thickness was then increased to 6 mm, with a drying time of 3.1 hours. Finally, the thickness of the sample was 8 mm, which had a drying time of 4.9 hours. Moreover, the drying rate of sliced bananas increased with the increase in the drying temperature and the drying velocity.

The process in the simulation for studying the other side of the heat pump dryer, such as the performance, the condition effects, and the optimization, of decreasing the moisture content of sliced banana for banana flour needs a mathematical model for prediction of the moisture content of sliced banana at all time in period drying. The objective of this research is to develop an appropriate drying kinetics model for the sliced bananas from the mini heat pump dryer by fitting the experimental data to several models from the literature.

Materials and methods

Materials

A raw banana was used as a drying material in the process. It was to be sliced, which had a thickness of about 2 mm. Their moisture content was determined by experiment. Samples were dried in a hot air oven at 130 °C for 3 hours to obtain the dry bone mass. The moisture content was 244 - 281 on a % dry basis. Figure 1 shows the process of processing banana flour.



Figure 1 Raw banana slices for testing and banana flour (Chunkaew, 2021)

Drying apparatus

A mini heat pump dryer is shown in Figure 2. It consists of a blower, a bypass valve of air, a condenser, a drying chamber, an evaporator, an expansion valve, a solenoid valve, and a condenser. The hermetic compressor of Kultorn AE1360Y size 497 W, which uses a voltage of 220 volts, is selected for the mini heat pump dryer. The condenser dimension was 330x440x30 mm³ and it can transfer heat up to 1,800 W. The evaporator dimension was 140x403x130 mm³. The expansion valve of a capillary tube was used in this study. The accessory equipment of the solenoid valve was to be used with the temperature controller to reduce the use of electrical energy in the dryer by increasing the stop period time of the compressor. In the refrigerant cycle, when the compressor was to stop, the refrigerant at high pressure was pumped to low pressure by flowing through the expansion valve to the evaporator. With this behavior, the air temperature at the condenser fell quickly. The refrigerant R134a was selected as the working fluid. The blower, which was part of the air conditioning system, was selected in this study. It was driven by a motor of 74.6 W at high speed and had a function of three speeds. The temperature controller of TOHO TTM-004 was used to control the compressor and the solenoid valve. The function of the temperature controller was set to stop at 60 °C and continue to operate at 58 °C. Figure 3 shows the schematic diagram of the air cycle system and the heat pump cycle system.

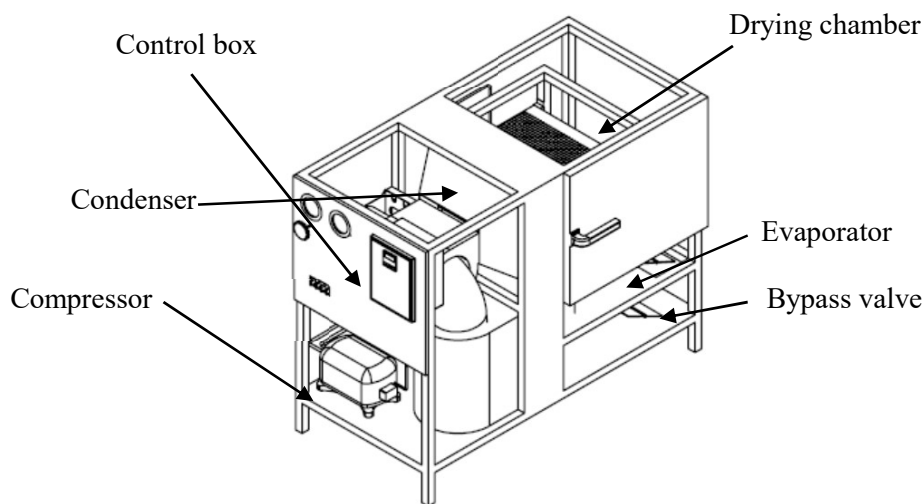


Figure 2 The experimental apparatus of mini heat pump dryer (Chunkaew, 2021)

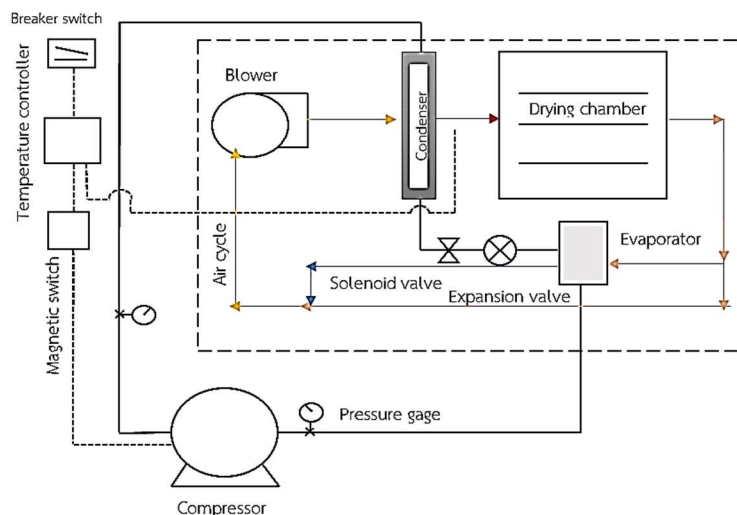


Figure 3 The schematic diagram of mini heat pump dryer (Chunkaew, 2021)

Drying experiments

Experiments were carried out at three different air flow rates (0.117, 0.128, and 0.140 m³/s⁻¹) with one maintaining a constant air temperature of 60 °C and the other bypassing air at evaporator 60% with a close loop air system (Chunkaew, 2021). In each experiment, the samples were withdrawn from the dryer and their mass was measured by a digital balance (± 0.1 g) and the mass of sliced bananas was measured every 15 min. Samples were dried until lower than the moisture content (6.35% dry basis). All experiments were carried out in triplicate.

Table 1 Some physical attributes of the sliced banana and experimental conditions covered in the present study.

Name of material	Sliced bananas
Shape of sliced banana	Thick circle
Average diameter (mm)	30
Thickness (mm)	2
Air flow rates (m ³ s ⁻¹)	0.117, 0.128, 0.140
Drying air temperature (°C)	60
Mass of sliced banana (g)	400-500
Air cycle system	Closed loop
Bypass air at evaporator (%)	60
Initial moisture content, M_{in} (%dry basis)	244-281
Final moisture content (%dry basis)	Lower than 6.35

Theoretical considerations

- Mathematical modeling of drying curves

The moisture ratio (MR), a dimensionless measure of moisture content, was calculated using the following equation:

$$MR = \frac{M_t - M_{eq}}{M_{in} - M_{eq}} \quad (1)$$

Where M_t , M_{eq} , and M_{in} are at time t , equilibrium, and initial moisture content, respectively. The value of M_{eq} normally approaches zero for drying in the mini heat pump dryer because the humidity ratio in the air cycle system is removed into the environment at the evaporator. From previous research of drying sliced bananas with a hot air dryer, at conditions of a temperature of 60 °C, an air velocity of 2.4 m s⁻¹ and relative humidity of 15%, there was equilibrium moisture content of 0.019% on a dry basis (Doymaz, 2010).

Mostly, the experimental result of decreasing moisture content is presented in the form of a drying rate, as shown in the equation.

$$DR = \frac{m_{t+dt} - m_t}{DT} \quad (2)$$

Where DR is the drying rate, DT is the drying time, m_t and m_{t+dt} are the masses of sliced bananas at t and the mass of sliced bananas at $t + dt$, respectively.

In this research, the lists of semi-theoretical and empirical models in Table 2 were used to describe the drying kinetics of sliced bananas by the mini heat pump dryer. Six models available from the literature were adapted to experimental drying data at different air flow rates. Non-linear regression was utilized to determine constants in the model of six models.

- The effectiveness of model fit

A coefficient of determination (R^2), a root mean square error (RMSE), and a reduced chi-square (χ^2) were evaluated to determine the effectiveness of model fit. These parameters can be calculated as shown below.

$$R^2 = \frac{\sum_{i=1}^N (MR_{pre,i} - \overline{MR}_{ex})^2}{\sum_{i=1}^N (MR_{ex,i} - \overline{MR}_{ex})^2} \quad (3)$$

$$RSME = \left[\frac{1}{N} \sum_{i=1}^N (MR_{pre,i} - MR_{ex,i})^2 \right]^{0.5} \quad (4)$$

$$\chi^2 = \frac{\sum_{i=1}^N (MR_{ex,i} - MR_{pre,i})^2}{N - z} \quad (5)$$

Where \overline{MR}_{ex} is the average experimental moisture ratio, $MR_{ex,i}$, and $MR_{pre,i}$ are the experimental and predicted moisture ratios, respectively. N is the number of observations and z is the number constants.

Non-linear regression was performed to fit the experimental data using six models from the literature.

Table 2 Semi-theoretical and empirical models applied to drying curves.

No.	Model names	Model	Reference
1	Newton or Lewis	$MR = \exp(-kt)$	(Lewis, 1921), (Panchariya <i>et al.</i> , 2012), (Srinivasakannan & Balasubramanian, 2009)
2	Henderson and Pabis	$MR = a \exp(-kt)$	(Henderson & Pabis, 1961), (Madhiyanon <i>et al.</i> , 2009), (Koua <i>et al.</i> , 2009), (Promvonge <i>et al.</i> , 2011)
3	Logarithmic	$MR = a \exp(-kt) + b$	(Doymaz, 2004), (Akgun & Doymaz, 2005), (Sacilik & Elicin, 2006), (Wang <i>et al.</i> , 2007)
4	Two term	$MR = a \exp(-kt) + b \exp(-kt)$	(Togrul & Pehlivan, (2004)
5	Modified Henderson and Pabis	$MR = a \exp(-kt) + b \exp(-gt) + c \exp(-ht)$	(Vega-Gálvez <i>et al.</i> , 2011)
6	Diffusion approach	$MR = a \exp(-kt) + (1 - a) \exp(-kbt)$	(Perea-Flores <i>et al.</i> , 2012)

Results and discussion

Behavior of drying kinetics by the drying rate

Sliced bananas were dried from 244–281 % on a dry basis to about 6.35 % on a dry basis at the air flow rates of 0.117, 0.128, and 0.140 m³ s⁻¹, which had a drying time of 180 min, and the reduction of moisture content at the air flow rate of 0.140 m³ s⁻¹ was a little more than 0.117 and 0.128 m³ s⁻¹. Figure 4 shows the drying rate for the first period, at 15 min, which is higher than the other periods. The drying rate of air flow rate of 0.140 m³ s⁻¹ is the highest. Then, the drying rate is decreased after the drying time of 30 min.

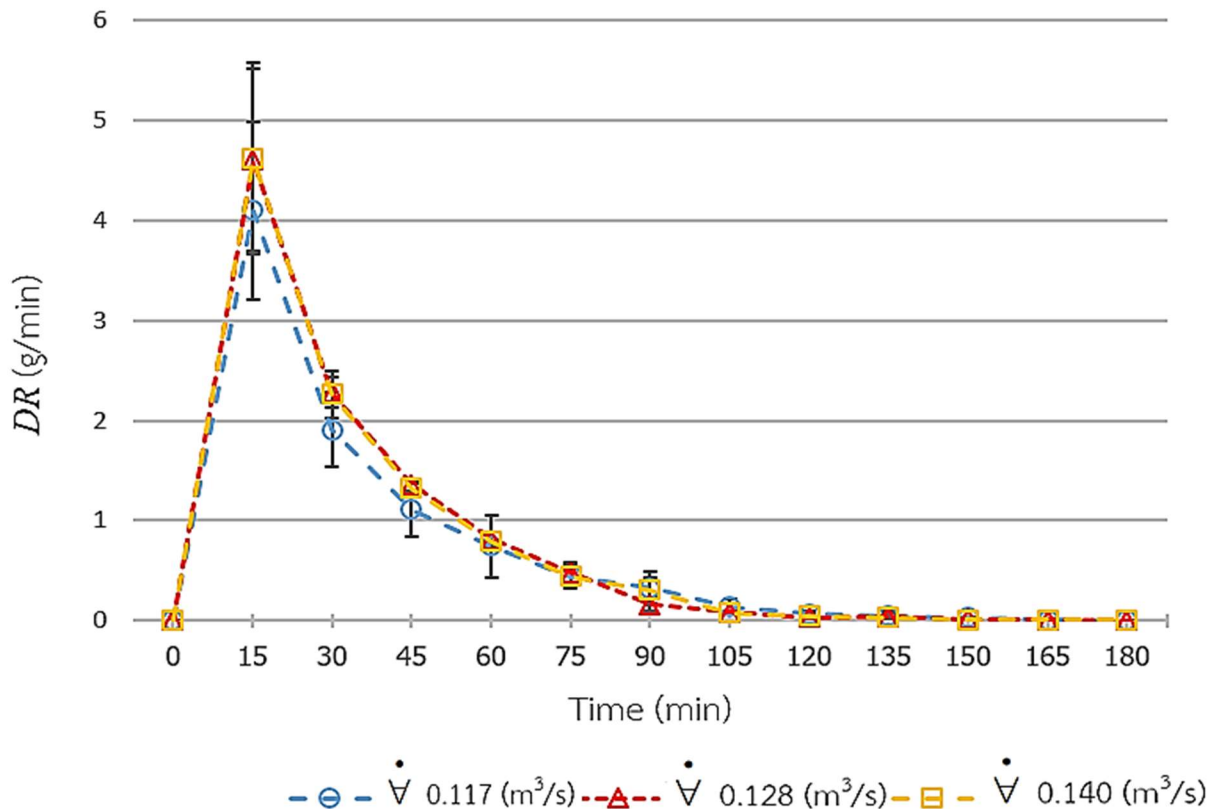


Figure 4 Drying rate at different air flow rates for the sliced bananas by mini heat pump dryer

Constants in model and statistical results of mathematical models

Moisture content data obtained at various drying air velocities with a constant air temperature of 60 °C were converted into the *MR* and fitted to determine the constants in the model of the six models listed in Table 3. The moisture content results of predictions from six models were calculated by the finite differences method and converted into the *MR*. Then, the *MR* from experimental data and the prediction result from the model were calculated to determine the effectiveness of the model fit. The statistical results, values of R^2 , $RMSE$, and χ^2 for different air flow rates were presented in Table 3. It was found that six models had $R^2 = 0.83807-0.98858$, $RMSE = 0.01092-0.04236$, and $\chi^2 = 0.00012-0.00184$. Among the models tested, the diffusion approach model ($R^2 = 0.98233-0.98858$, $RMSE = 0.1092-0.03235$, $\chi^2 = 0.00012-0.00107$) could be considered the most appropriate because the results had the highest values of R^2 and the lowest values of $RMSE$ and χ^2 .

Table 3 Constants in model and effectiveness results of the model fit from six models for different air flow rates

No.	Model names	Air flow rates, m ³ s ⁻¹	Constants in model	R ²	RMSE	χ ²
1	Newton	0.117	k=0.021238	0.83807	0.03394	0.00118
		0.128	k=0.021238	0.86145	0.02024	0.00041
		0.140	k=0.021238	0.83969	0.01852	0.00035
2	Henderson and Pabis	0.117	a=1.048942, k=0.018	0.94272	0.02887	0.00085
		0.128	a=1.048942, k=0.018	0.96903	0.01955	0.00039
		0.140	a=1.048942, k=0.018	0.94455	0.01769	0.00032
3	Logarithmic	0.117	a=1.078418, k=0.014539, b=-0.028481	0.97602	0.04236	0.00184
		0.128	a=1.078418, k=0.014539, b=-0.028481	0.98455	0.03633	0.00134
		0.140	a=1.078418, k=0.014539, b=-0.028481	0.97792	0.03190	0.00103
4	Two term	0.117	a=6.65636, k=0.01599, b=-5.60742	0.93283	0.03648	0.00136
		0.128	a=6.65636, k=0.01599, b=-5.60742	0.95886	0.03116	0.00098
		0.140	a=6.65636, k=0.01599, b=-5.60742	0.93464	0.02776	0.00078
5	Modified Henderson and Pabis	0.117	a=0.320426, k=0.329524, b=0.320426, g=0.644962, c=0.644962, h=0.015	0.92183	0.03122	0.00100
		0.128	a=0.320426, k=0.329524, b=0.320426, g=0.644962, c=0.644962, h=0.015	0.94755	0.02545	0.00065
		0.140	a=0.320426, k=0.329524, b=0.320426, g=0.644962, c=0.644962, h=0.015	0.92362	0.02303	0.00053
6	Diffusion approach	0.117	a=-0.740595, k=0.060465, b=0.509348	0.98233	0.03235	0.00107
		0.128	a=-0.740595, k=0.060465, b=0.509348	0.98858	0.01451	0.00021
		0.140	a=-0.740595, k=0.060465, b=0.509348	0.98342	0.01092	0.00012

Figure 5 to Figure 7 show the comparison prediction results of six models (Newton, Henderson and Pabis, Logarithmic, two-term, modified Henderson and Pabis, and diffusion approach at air flow rates of 0.117, 0.128, and 0.140 m³ s⁻¹, respectively). The diffusion approach models of three air flow rates were very close to their experimental values.

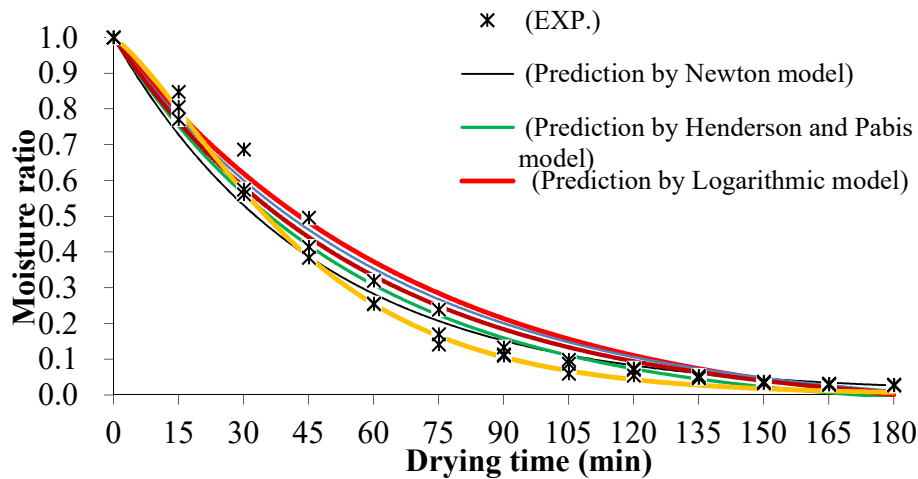


Figure 5 Experimental and predicted moisture ratio at 60 °C at 0.117 m³ s⁻¹ by different models for

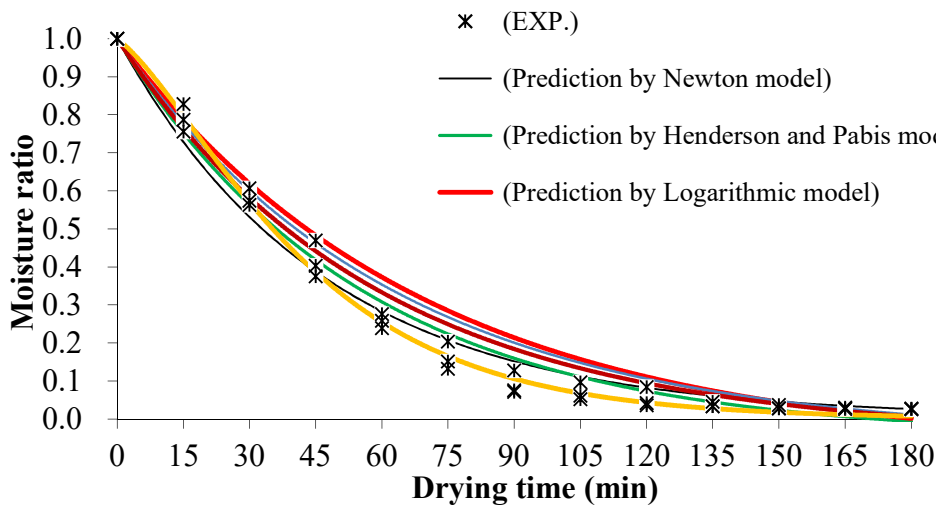


Figure 6 Experimental and predicted moisture ratio at 60 °C at 0.128 m³ s⁻¹ by different models for sliced bananas

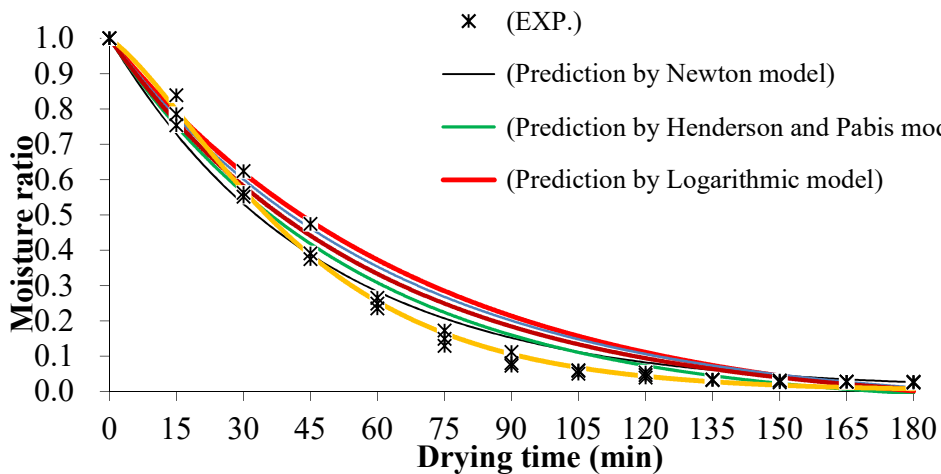


Figure 7 Experimental and predicted moisture ratio at 60 °C at 0.140 m³ s⁻¹ by different models for sliced bananas

Conclusions

Sliced bananas were dried from 244–281 % dry basis to approximately 6.35 % dry basis at an air temperature of 60 °C and air flow rates of 0.117, 0.128, and 0.140 m³ s⁻¹, respectively. All three air flow rates used the drying time of 180 min. The maximum air flow rate of 0.140 m³ s⁻¹ had a high drying rate during a period of high moisture content in the sliced bananas because the heat rate in the air that could be transferred to the sliced bananas was higher than the air flow rates of 0.117 and 0.128 m³ s⁻¹. The reduction of moisture content in all three air flow rates had a slight difference because the blower produced fewer different air flow rates. The fitting of the experimental data of non-linear regression by six models from the literature was selected for the prediction of the drying kinetics of sliced bananas by the mini heat pump dryer. The accuracies of the models were measured using R^2 , $RMSE$, and χ^2 . It was found that the six models had $R^2 = 0.83807$ - 0.98858 , $RMSE = 0.01092$ - 0.04236 , and $\chi^2 = 0.00012$ - 0.00184 . Among the models tested, the diffusion approach model ($R^2 = 0.98233$ - 0.98858 , $RMSE = 0.1092$ - 0.03235 , $\chi^2 = 0.00012$ - 0.00107) could be considered the most appropriate.

Acknowledgements

The authors express their sincere appreciation to the Faculty of Engineering, Rajamangala University of Technology Lanna Tak (Thailand) for supporting this study.

References

- Akgun, N.A. & Doymaz, I. (2005). Modelling of olive cake thin-layer drying process. *Journal of Food Engineering*, 68, 455–461.
- Aktas, M., Sevik, S. & Aktekeli, B. (2016). Development of heat pump and infrared-convective dryer and performance analysis for stale bread drying. *Energy Conversion and Management*, 113, 82-94.
- Crank, J. (1975). *The mathematics of diffusion*. Second ed., Clarendon Press, Oxford.
- Chunkaew, P. (2005). *Design of longan flesh heat pump dryer*. Master of Engineering (Mechanical Engineering), Chiang Mai University.
- Chunkaew, P. (2014). *Effect of air distributor types and distribution techniques on fluidized bed drying of sunflower seeds*. Doctor of Philosophy (Mechanical Engineering), Chiang Mai University.
- Chunkaew, P., Kosalanun, S. & Phathana-im, N. (2017). Testing and analysis of heat pump dryer performance by using two evaporators with one condenser. in *Proceeding of 4th CRCI & 2nd ISHPMNB 2017 “Innovation for social engagement environment and enterprise:3E”*. 26-27 July 2017, at Chiangmai Grandview Hotel & Convention Center, Chiang mai, Thailand, 538-544.
- Chunkaew, P. & Kosalanun, S. (2018). Heat pump dryer driven by single piston engine used LPG gas fuel. in *Proceeding of 5th CRCI Conference on research and creative innovations*, 6-8 December 2018, at Rajamangala University of Technology Lanna Tak, Muang, Tak, Thailand, 1362-1368.
- Chunkaew, Ch. (2021). Development and evaluation of mini heat pump dryer for slice banana. *RMUTP Research Journal*, 15(1), 179-192.
- Doymaz, I. (2004). Drying kinetics of white mulberry. *Journal of Food Engineering*, 61, 341–346.
- Doymaz, I. (2010). Evaluation of mathematical models for prediction of thin-layer drying of Banana Slices. *International Journal of Food Properties*, 13, 486-497.
- Henderson, S.M. & Pabis, S. (1961). Grain drying theory I temperature effect on drying coefficient. *Journal of Agriculture Engineering Research*, 6(3), 169-174.
- Koua, K.B., Fassinou, W.F., Gbaha, P. & Toure, S. (2009). Mathematical modelling of the thin layer solar drying of banana, mango and cassava. *Energy*, 34, 1594–1602.

- Lewis, W.K. (1921). The rate of drying of solids materials. *Journal of Industrial and Engineering Chemistry*, 13(5), 427-432.
- Madhiyanon, T., Phila, A. & Soponronnarit, S. (2009). Models of fluidized bed drying for thin-layer chopped coconut. *Applied Thermal Engineering*, 29, 2849-2854.
- Panchariya, P.C., Popovic, D. & Sharma, A.L. (2002). Thin-layer modelling of black tea drying process. *Journal of Food Engineering*, 52, 349–357.
- Perea-Flores, M.J., Garibay-Febles, V.J., Chanona-Pérez, J., Calderón-Domínguez, G., Méndez-Méndez, J.V., Palacios-González, E. & Gutiérrez-López, G.F. (2012). Mathematical modelling of castor oil seeds (*Ricinus communis*) drying kinetics in fluidized bed at high temperatures. *Industrial Crops and Products*, 38, 64– 71.
- Promvongse, P., Boonloi, A., Pimsarn, M. & Thianpong, C. (2011). Drying characteristics of peppercorns in a rectangular fluidized-bed with triangular wavy walls. *International Communications in Heat and Mass Transfer*, 38, 1239–1246.
- Rahmam, M.H., Ahmed M.W. & Islam, M.N. (2018). Drying kinetics and sorption behavior of two varieties banana (Sagor and Sabri) of Bangladesh. *SAARC J.Agric*, 16(2), 181-193.
- Srinivasakannan, C. & Balasubramanian, N. (2009). Estimation of diffusion parameters in fluidized bed drying. *Advanced Powder Technology*, 20, 390–394.
- Sacilik, K. & Elicin, A.K. (2006). The thin layer drying characteristics of organic apple slices. *Journal of Food Engineering*, 73, 281–289.
- Togrul, I.T. & Pehlivan, D. (2004). Modeling of thin layer drying of some fruits under open-air sun drying process. *Journal of Food Engineering*, 65, 413–425.
- Tor Siriwatthana, Ch. (2003). *Refrigeration and air conditioning*. Bangkok: Technology Promotion Association (Thailand-Japan), 416.
- Vega-Gálvez, A., Miranda, M., Díaz, L.P., Lopez, L., Rodriguez, K. & Scala, K.D. (2110). Effective moisture diffusivity determination and mathematical modeling of the drying curves of the olive-waste cake. *Bioresource Technology*, 101, 7265–7270.
- Wang, Z., Sun, J., Liao, X., Chen, F., Zhao, G., Wu, J. & Hu, X. (2007). Mathematical modeling on hot air drying of thin layer apple pomace. *Food Research International*, 40, 39–46.

Analysis of a Concave Bulletproof Plate for Refracting the Bullet Impact Direction with Finite Element Method

Nuttapong Meesanu¹, Prasert Wirotcheewan¹, Duongruitai Nicomrat²
and Prakorb Chartpuk^{1*}

¹*Department of Mechanical Engineering, Faculty of Engineering, Rajamangala University of Technology Phra Nakhon, Bangkok, Thailand*

²*Division of Environmental Sciences and Natural Resources, Faculty of Science and Technology, Rajamangala University of Technology Phra Nakhon, Bangkok, Thailand*

* *Corresponding email: prakorb.c@rmutp.ac.th*

Abstract

This research has designed a concave shape of bulletproof plate with SKD11 material which leads to the bullet changing direction when the bullet impacts on a bulletproof plate at the speed 880 m/s, according to the National Institute of Justice (NIJ), Level 4. The bullet was made of tungsten carbide referred from the theory of damage simulation of Johnson-Holmquist (JH-2) with finite element simulation using the Ansys/Explicit dynamics program. The bullet was shot at the middle of the bulletproof plate at 5-, 6-, 7-, and 8-mm depths of concave area. It showed that the plate could not resist the penetration from the bullet and there was no reflection when the bullet impacted the middle of the plate. The hooting position which aimed from the center with a radius of 7.5 mm could change the bullet direction when it hit the bulletproof plate. It penetrated in the middle of the plate and scattered into small metal pieces. The result of these 2 simulation models indicated that the bulletproof plates could not resist bullet penetration. This parameter analysis can be used to analyze the direction of the bullet's refraction to reduce the damage from 7.62 mm bullet destruction. The significant parameters were concentrated on the material type used for making the bulletproof plate and the thickness of the bulletproof plate.

Keywords: Concave bulletproof plate, Bullet impact, NIJ 4

Introduction

Development and design for a quality bulletproof plate from the reference theory which was molded from SKD11. The plate was designed to have a concave hole in the middle of the plate which was supposed to change the bullet direction (referring to finite element theory). The theory was split into 2 tests. G. Tiwari et al. (2018) evaluated the resistant competency of the plate made from 1100-H12 Aluminum grade with 1 mm thickness. The simulation of finite elements was made by ABAQUS/Explicit finite element stimulation program. The plate designed for the test was in a round shape with the following magnitudes of 68, 100, 150, 200, 255, 350, 450, 550, 650 or 750 mm. At the back of the plate, the width is magnified at 150 mm. The result indicated that 2 layered bulletproof plates were damaged by a 19 mm magnitude bullet if the frontal plate's magnitude was set at 68, 100, 150, 200 or 255 mm with the width of 4.5 mm. The result from the real test was similar of E. A. Flores-Johnson et al. (2011) using the pressure gun. Their research described the damage simulation for plate layers 1, 2 and 3. In their study, 2 types of materials were used for the 2-layer plates; the frontal, first layer plate was made of Weldox 700E metal grade and 7075-T651 aluminum grade, which had better bullet-resistance than the single layer, and the plate layer 2 and 3 were made of SKD11 with the concave shape at the middle in order to help change the bullet direction and to help better resistant to the bullet penetration.

Materials and Experimental Procedures

Parameters of Bullet and Armor plate

The bullet material used for shooting in the simulation was made of tungsten carbide which use the same bullet core for the test to observe the impact result.

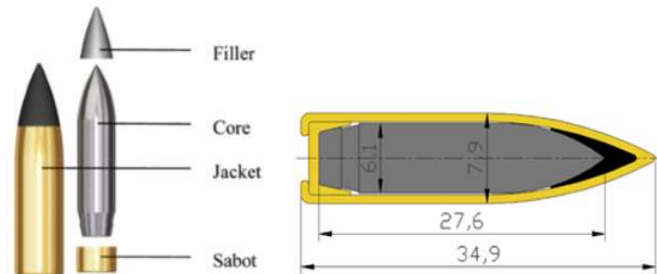


Figure 1 The characteristic of bullet core and all bullet sizes (mm) (T. Børvik et al., 2011)

The finite element simulation for the research was determined by the Johnson-Holmquist failure model (JH-2) model. It indicated the damage to fragile material, ceramic under enormous pressure and other stimulators (Ballistic stimulation).

If Y is Yield Stress, equitation as follows:

$$Y = [A(p^* + T^*)^n(1 - D) + B(p^*)^m D][1 + C \ln(\dot{\epsilon}_p^*)] \quad (1)$$

$$p^* = \frac{p}{p_{HEL}} \quad T^* = \frac{T}{p_{HEL}} \quad (2)$$

Where p_{HEL} is the pressure of the Hugoniot Elastic Limit (HEL), T is the maximum hydrodynamic tensile strength and A, B, C, n, mis material parameter, the HEL value is yield limit of uniaxial strain in a single direction .There are 2 quotations for calculating yield stress if $D = 1$ or $D < 1$ referred from the Johnson-Holmquist. The Yield stress value is the value of D continuous damage value. Damage simulation model “active” for the case of $D = 0$ (no damaged) and $D = 1$ (damaged), Yield stress regression value from following equitation (F. M. John et al., 2010)

$$Y = A(p^* + T^*)^n[1 + C \ln(\dot{\epsilon}_p^*)] \quad (\text{Intact}, D=0) \quad (3)$$

$$Y = B(p^*)^m[1 + C \ln(\dot{\epsilon}_p^*)] \quad (\text{Fragmented}, D=1) \quad (4)$$

The property value and parameter value of tungsten carbide for the test were shown in Table 1.

SKD11 material displayed a hardening value of 60-62 HRC (Rockwell scale C) (G. Zhang et al., 2014) with 30×30 mm size and has a concave depth radius of 20mm, depth at 5 mm and all plate width at 11, 12 and 13 mm. The varied concave depths were observed as 6, 7 and 8 mm, shown in Figure 2.

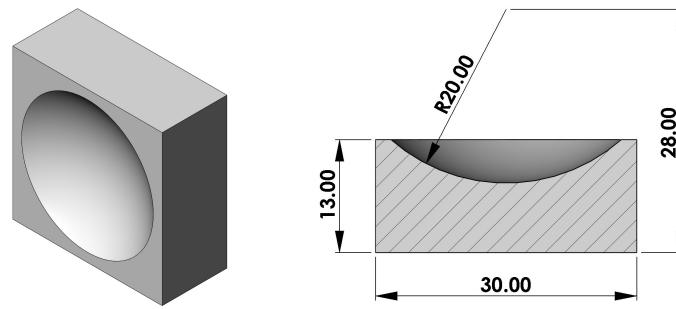


Figure 2 Concave depth size

Table 1 Properties and parameter JH of tungsten carbide (F. M. John et al., 2010)

Properties	Tungsten carbide
Density (ρ , g/cm^3)	14.56
Young's modulus (E, GPa)	539
Poisson ratio (ν)	0.23
Bulk modulus (GPa)	332
Shear modulus (GPa)	219
Tensile yield strength (GPa)	3.85
Compressive yield strength (GPa)	4.53
Johnson-Holmquist Strength (Continuous JH-2)	
Damage type	Gradual (JH2)
Hugoniot elastic limit (HEL, GPa)	656
Intact strength constant (A)	0.9899
Intact strength exponent (n)	0.0322
Strain rate constant (C)	0
Fracture strength constant (B)	0.67
Fracture strength exponent (m)	0.0322
Maximum fracture strength ratio	1000
Damage constant (D1)	1
Damage constant (D2)	0
Hydrodynamic tensile limit (GPa)	-4

The damage stimulation model of the Johnson-Cook Model (JC) was developed to explain the transformation of metal strain, stress, and temperature value. The JC Model revealed the damage function obtained from the strain of frozen transform, hardening, and hot melting value as shown in the following equation.

$$\sigma = [A+B(\epsilon_p)^n][1 + C \ln(\dot{\epsilon}/\dot{\epsilon}_0)][1 - \{(T - T_0)/(T_m - T_0)\}^m] \quad (5)$$

At initial yield stress value, B is the hardening constants value, ϵ_p is equivalent plastic strain value, n is the hardening exponent value, $\dot{\epsilon}/\dot{\epsilon}_0$ is the reference strain-rate value and $\dot{\epsilon}$ is the plastic strain rate value, C is the strain rate constant value, m is temperature softening exponent value, $(T - T_0)/(T_m - T_0)$ is the absolute temperature if T, T_0 and T_m is the temperature value, room

temperature and melting temperature (J. L. Li et al., 2009). These properties and parameter were shown in Table 2.

Table 2 Properties and parameter obtained by the simulation with JC for SKD11 (62 HRC) material (J. L. Li et al., 2009).

Properties	SKD11
Density (ρ , kg/m ³)	8400
Modulus of elasticity (E, GPa)	208
Poisson ratio (ν)	0.3
Bulk modulus (GPa)	173
Shear modulus (GPa)	80
Thermal conductivity (W/m.K)	20.5 (350 °C)
Thermal expansion (m/m.K)	11
Specific heat (J/kg.°C)	461
Johnson-cook strength	
Initial yield stress (A, MPa)	1766
Hardening constant (B, MPa)	904
Hardening exponent (n)	0.39
Strain rate constant (C)	0.012
Thermal softening exponent	3.38
Melting temperature (K)	1733

Numerical method

An Ansys/Explicit dynamics program was used for analysis of a bulletproof plate simulator to 880 m/s speed, referred to NIJ 4 (N. Klangtup and P. Chartpuk, 2019), and compared with NIJ3 with 850 m/s (A. Saicharoen et al., 2022) speed to build shooting simulations into 2 models. Model 1: Shooting the bullet at the middle of the plate was operated to observe the bullet’s impact. Model 2: The position of the bullet’s impact was aimed at the area from the middle of the plate with a 7.5 mm radius (W. Liu et al., 2016) as shown in Figure 3.

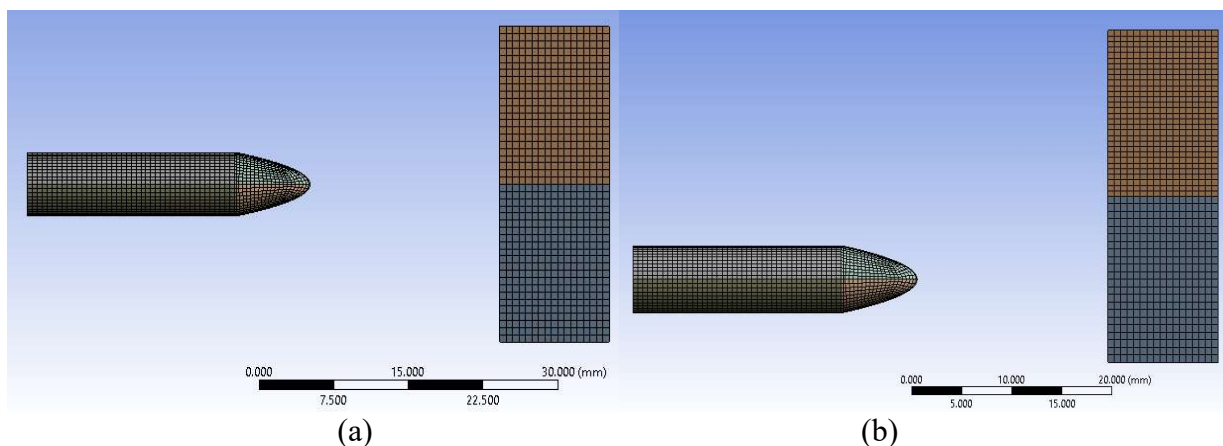


Figure 3 Shooting simulation models (a) Simulation no. 1: aim the bullet to the middle of the plate and (b) Simulation no. 2: aim the bullet out of the middle by 7.5 mm radius

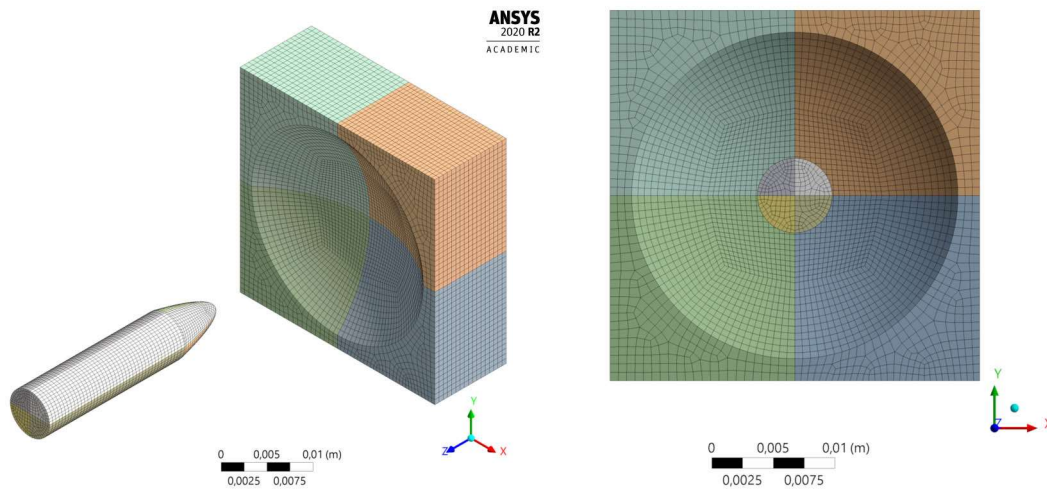


Figure 4 Finite element mesh refinement

The bullet has 0.5 mm mesh size and 1 mm plate mesh width. The mesh shape is hexahedral and it is composed of 61,200 nodes and 65,340 elements as shown in Figure 4. This type of mesh takes less time and is less fallacious than tetrahedral mesh type (ANSYS Inc., 2019). The gripping part was fixed to support at 4 plate corners, after the shooting simulation test within NIJ level 3 and 4 standards.

Results and discussion

The first simulation model test indicated that when the bullet impacted the plate at 11, 12, and 13 mm thickness and 6, 7 and 8 mm width of the concave area. The plate cannot resist the 7.62 mm bullet's penetration but the bullet head was broken and dispersed, broken into tiny metal pieces, and buried in the plate (Figure 5).

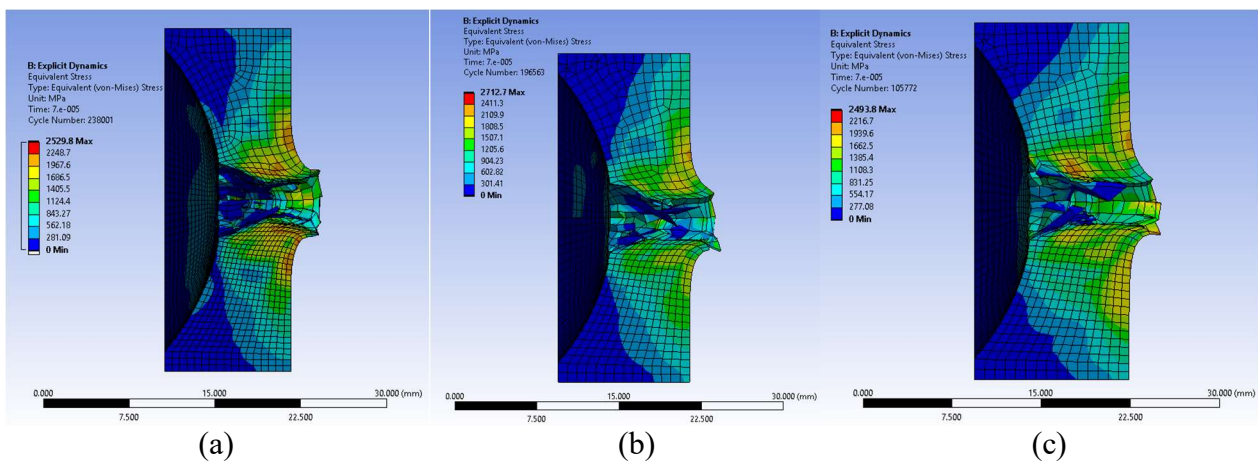


Figure 5 The bullet perforation mark of the concave plate at Time step of 0.07 ms and the plate width thick at (a) 11 mm (b) 12 mm and (c) 13 mm.

The penetration mark is made on the 11 mm plate. There are marks at the front and the back of the bulletproof plate at 12- and 13-mm thickness. The front of all 3 plate sizes had similar bullet impact magnitude marks but the back of the plate depends on the plate thickness. The second

simulation model was tested for the bullet impact on the area from the middle of the bulletproof plate by 7.5 mm. The results showed that the plate could not resist bullet penetration (Figure 6).

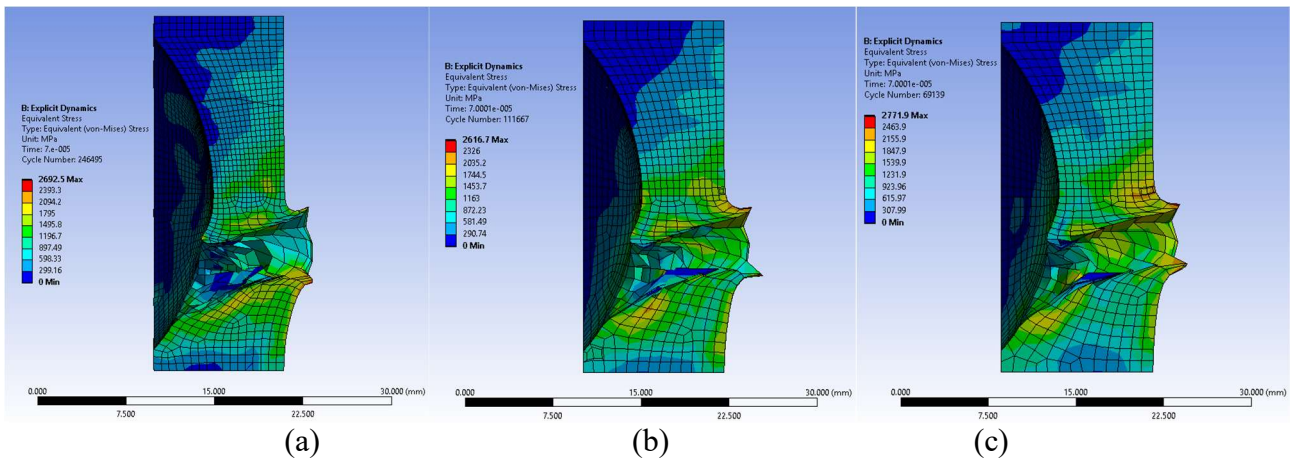


Figure 6 The bullet perforation mark of the concave plate at time step of 0.07 ms from the 2nd simulation model (a) 11 mm plate thickness (b) 12 mm plate thickness and (c) 13 mm plate thickness

The bullet impact position was situated in the concave area and deviated from the middle direction of the plate (concave areas) in Figure 7. The results of bullet penetration marking the magnitudes on all 3 sizes of plate samples are similar except those of the bullet marks on the back of the plate because of the varying plate thickness. The results were likewise corresponding to those obtained from the first stimulation test. However, the bullet refraction was determined only.

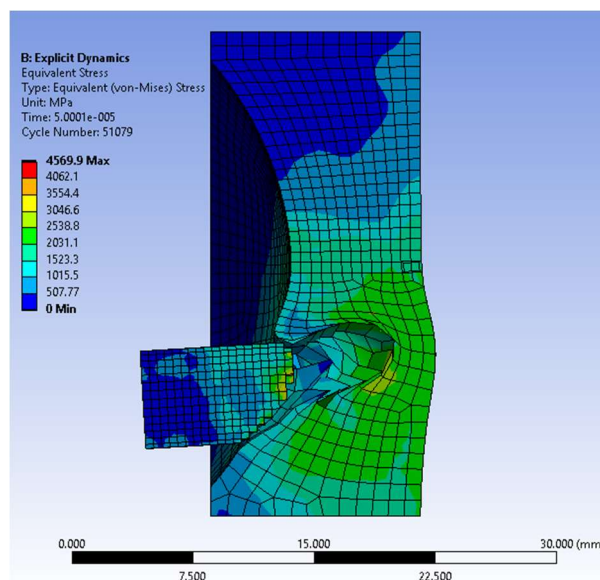


Figure 7 The bullet refraction when impacting to the concave area

The results obtained with the NIJ 3 model were different from those simulated with NIJ 4 because the speed determined by NIJ 3 is 30 m/s, which is less than that of NIJ 4. Additionally, there are insignificantly different penetration results from both 2 simulation tests since the bulletproof plates could not resist the penetration of a 7.62 mm bullet (Figure 8).

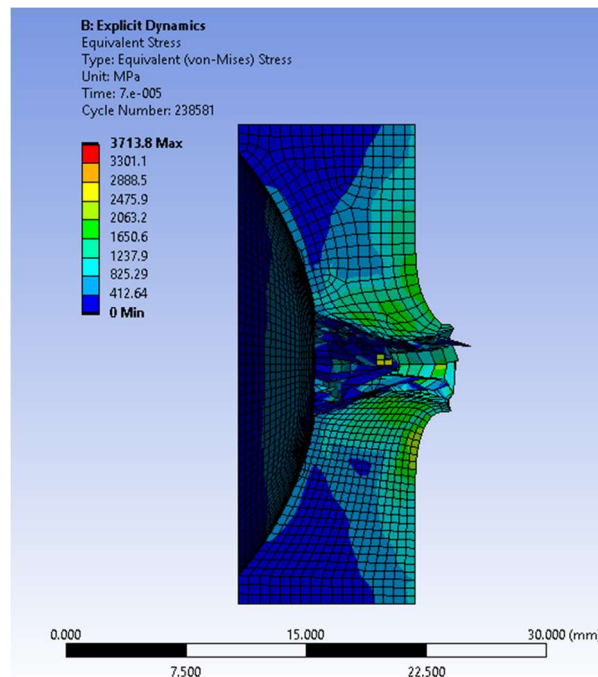


Figure 8 The penetration of the bullet under the standard NIJ3 test model

Both simulation models 1 and 2 bring the result that the bulletproof cannot resist the penetration of the bullet. The change in bullet direction into a concave area thus impacts on the aimed area. Moreover, models 1 and 2 using the standard NIJ 4 produce no different results as shown in Figure 9.

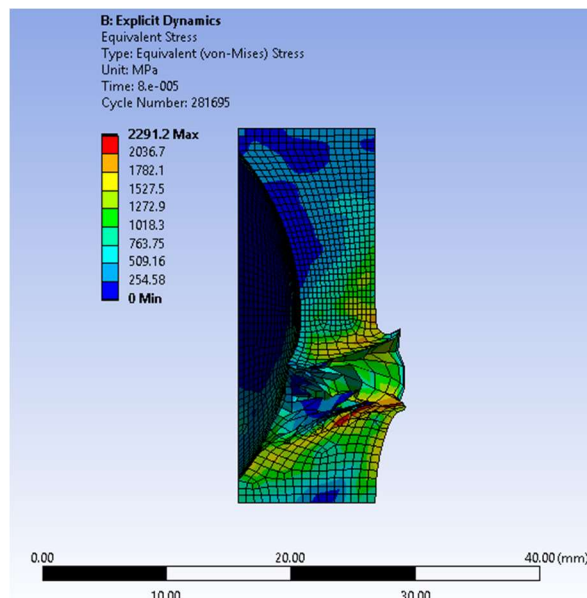


Figure 9 The penetration direction of the bullet as concave area under the NIJ4 standard

Conclusion

The shooting finite element with the 7.62 mm bullet speeding at 880 m/s was simulated. The bulletproof plate was molded into a curved shape with SKD11 material under the standard NIJ 4 model. The plates with a size of 30×30 mm and width at 20 mm varied in their thicknesses at 11, 12

and 13 mm. The penetration results as the concave area width of 6, 7 and 8 mm were determined by two simulation tests. The first simulation is the shooting of a bullet into the middle of the plate and the second simulation is that of a bullet with a 7.5 mm radius from the middle of the plate. The results of penetration observed by two simulation tests can predict that there is no resistance of the plates to the bullet's penetration, but the plates are destroyed by the bullet's head. No different penetration marks are found on the front plate but there are various marks on the back of the bulletproof plate. They are dependent on the thickness and width of the plate. The less penetration is shown on the plate, with more thickness and width but less bullet mark's magnitude. The bullet refraction is another additionally observed from the simulated result determined by model 2 set for the bullet speed simulated by NIJ3 than by NIJ4 at 30 m/s or 850 m/s. The observed simulation with the standard NIJ4 model displayed no different results for model 1 and 2.

Acknowledgement

The authors would like to express the appreciation to the National Research Council of Thailand (NRCT), National Research Policy and Strategy for the financial support according to the contract no. 47/2561 and Rajamangala University of Technology Phra Nakhon (RMUTP) for supportive facilities.

References

- ANSYS Inc., “Lecture 2: Introduction to Explicit Dynamics.” Document from CAD-IT Consultants (Asia), 07-Jun-2019.
- Børvik, T., Olovsson, L., Dey, S. and Langseth, M. “Normal and oblique impact of small arms bullets on AA6082-T4 aluminium protective plates,” *Int. J. Impact Eng.*, 38(7), pp. 577–589, Jul. 2011.
- Flores-Johnson, E. A., Saleh, M. and Edwards, L. “Ballistic performance of multi-layered metallic plates impacted by a 7.62-mm APM2 projectile,” *Int. J. Impact Eng.*, 38(12), pp. 1022–1032, Dec. 2011.
- John, F. M., Jan Arild, T., Stian, S., Svien Morten, B., Lasse, S.-E. and Haakon, F. “Development of material models for semi-brittle materials like tungsten carbide,” 09-Nov-2010.
- Klangtup, N. and Chartpuk, P. “Parameter analysis of SKD11 and SUS304 bulletproof plate that resistance penetration of bullet 7.62 mm according to standard NIJ 4 by finite element method,” *International Journal of Mechanical Engineer and Technology*, 10, 207–221, Sep. 2019.
- Li, J. L., Jing, L. L. and Chen, M. “An FEM study on residual stresses induced by high-speed end-milling of hardened steel SKD11,” *J. Mater. Process. Technol.*, 209(9), 4515–4520, May 2009.
- Liu, W., Chen, Z., Cheng, X., Wang, Y., Amankwa, A. R. and Xu, J. “Design and ballistic penetration of the ceramic composite armor,” *Compos. Part B Eng.*, 84, 33–40, Jan. 2016.
- Saicharoen, A., Tinprabath, P. and Chartpuk, P. “Parameter Analysis that Affects the Ability to Resistance Penetration of Ammunition on the Aluminum Armor Surface Using Finite Element Method,” *RMUTP Research Journal*, 16(1), 192-208, 2022.
- Tiwari, G., Iqbal, M. A. and Gupta, P. K. “Energy absorption characteristics of thin aluminium plate against hemispherical nosed projectile impact,” *Thin-Walled Struct.*, 126, 246–257, May 2018.
- Zhang, G., Zhang, Z., Ming, W., Guo, J., Huang, Y. and Shao, X. “The multi-objective optimization of medium-speed WEDM process parameters for machining SKD11 steel by the hybrid method of RSM and NSGA-II,” *Int. J. Adv. Manuf. Technol.*, 70, 2097–2109, 2014.

The Parameter Analysis of the Tungsten Carbide and SUS304 Armor Plate with a Finite Element Method

Maitree Thawornsin¹, Songwut Mongkonlerdmanee¹, Duongruitai Nicomrat²
and Prakorb Chartpuk^{1*}

¹*Department of Mechanical Engineering, Faculty of Engineering, Rajamangala University of Technology Phra Nakhon, Bangkok, Thailand*

²*Division of Environmental Sciences and Natural Resources, Faculty of Science and Technology, Rajamangala University of Technology Phra Nakhon, Bangkok, Thailand*

* *Corresponding email: prakorb.c@rmutp.ac.th*

Abstract

In the wake of the unrest of three southern provinces, riots and the use of powerful weapons for detriment, bulletproof armor plates have been developed and designed from materials with capability of destroying 7.62 mm bullets with speed of 878 ± 9.1 m/s in accordance with National Institute of Justice Level 4 (NIJ 4). The research using materials tungsten carbide (WC) with 6, 8, and 10-mm thickness and SUS304 with 5, 6, 8, and 10 mm thickness were performed according to the Johnson-Holmquist failure model damage theory (JH-2) and the Steinberg-Cochran-Guinan-Lund-model's theory of damage, respectively. Both plates of the material were stacked in two layers when the bullet head were slammed into plate 1, broken and caused the bullet penetrated through to the second plate, where it could embrace the bullet scrape. Each plate was thus simulated by the finite element method. For plate 1, a WC material at all thickness of 6, 8 and 10 mm could not withstand the penetration of the bullet and was damaged by the bullet whereas plate 2, SUS304 material at thicknesses of 5, 6, 8, and 10 mm could not withstand the penetration of the bullet, but at a thickness of 5 and 6 mm, the bullets were broken and damaged. These bullets changed to fuselage debris and penetrated through the plate at a thickness of 8 and 10 mm. These damaged and shattered bullet metals were clearly observed on the back of the plates. Therefore, with all thickness parameters for being a double stacking plate, the armor plates are not yet able to withstand the penetration of the 7.62 mm bullets because the increased thickness of the first WC plate had resulted in the damage to the bullet head but also caused the metal fragments penetrating the armor plate and showing broken plate pieces together with the metal fragments. As the thickness of plate 2 made of SUS304 increased, the weakening of the plate decreased. It would result in less bullet metal holding. In the details, it was observed that at the increased thickness, the metal fragments were less dispersed after penetrating the armor plate. The increases in the same thickness at 12, 14, 16 mm for both plates 1 made of WC, and plate 2 made of SUS304 confirmed that the armor plates at thicknesses of at least 16 mm began to withstand the penetration of a 7.62 mm bullet.

Keywords: 7.2 mm bullet, Armor plate, Finite element method

Introduction

Unrest occurring at the southern border includes various riots and powerful weapons action. These situations bring such development and design of bulletproof armor plates to effectively prevent destructive attacks by insurgents. The materials with capability of destroying 7.62 mm bullet-sized projectiles analyzed by simulating the fine elements were tungsten carbide (WC) and SUS304 materials. The front and the back plates were made of WC and SUS304, respectively. The simulation utilizing the Johnson-cook damage model was for aluminum 6061-T6.

In summary, mesh sizes varied for different mesh damage were displayed as expected in that the stress value could cause an increase in DOP value correctly when mesh sizes were created at very fine (0.5 x 0.5 x 0.5 mm), fine (1 x 1 x 1 mm), rough (1.5 x 1.5 x 1.5 mm), and very rough (2 x 2 x 2 mm) particles. The results simulated with the LS-Dyna program demonstrated whether the armored materials were damaged increasing or not it was depending on the change in temperature. As the temperature rises, the deep penetration of the bullet increases. If the temperature drops, the deep penetration decreases (T. Binar et al., 2018). Characteristics of aggregated debris formed by a round shaped aluminum ball could affect the collision of the materials Al-2024 and Ti-Al-nylon at a speed of 6.50 km/s. The backlight made of a laser measuring at a wavelength of 532 nm with a pulse width of 10 ns, displayed a visual view of the debris aggregated characteristics clearly. It demonstrated that the collision shape of the debris caused by the Ti-Al-nylon bumping was different from that of the Al-2024 plate. It showed that a cluster of debris, except for large parts, could penetrate through the plate with a translucent appearance and the collision of a ti-al-nylon plate had a darker color on the group of debris than that of the Al-2024 material, possibly because of dispersion of the materials. Due to the impact of high collision speeds and debris clusters used to calculate the speeds. The experimental results could suggest that the debris aggregates had the speed of hitting the plate. Ti-Al-nylon is equal to 6.71 km/s, which is higher than that of AL-2024 at 6.020 km/s. The radial speeds of the debris aggregates of Ti-Al-Nylon and Al-2024 were 2.30 km/s and 2.04 km/s, respectively (P. L. Zhang et al. 2019). Ceramic material belonging to a front plate made of 99.5% Alumina and a back-up assembled plate of Twaron fibers, shown in 2D models (2D), axi-symmetric, dynamic-explicit. The behaviors of the Johnson-Cook, the Johnson-Holmquist, and the Composite-damage materials used for being ceramic bullet materials and composite materials. Brittle fracture and ceramic dispersion, counted to be the damage criteria of fibrous or matrix fractures of mixed materials and erosion or adhesion of bullets during penetration, especially at remaining time and puncture time, were compared with the simulated results of existing analytical models. The results indicated that when ceramic parts were hit by a bullet, ceramic parts broke off from the plate, and the edge of the ceramic had a decrease in initial speed (S. Feli et al., 2011). thus simulated by the finite element method. It could analyze the resistance of armor plates made of WC and SUS304 materials to the penetration.

Material Model

In the finite element simulation, the bullet size of 7.62 mm and the first bulletproof armor plate made of WC with the size of 30 cm x 30 cm, thickness at 6, 8, and 10 mm were chosen. The bullet banged into the plate and then broke into fragments, expressing the mechanical properties using parameters according to the damage simulation of the Johnson-Holmquist failure model (JH-2), shown in Table 1. The damage equation was as follows:

When Y is Yield stress

$$Y = [A(p^* + T^*)^n(1 - D) + B(p^*)^m D][1 + C \ln(\dot{\epsilon}_p^*)] \quad (1)$$

$$p^* = \frac{p}{p_{HEL}}, \quad T^* = \frac{T}{p_{HEL}} \quad (2)$$

p_{HEL} is the pressure at Hugoniot Elastic Limit (HEL), T is the maximum hydrodynamic tensile strength, whereas A, B, C, n, and m are the parameters of the materials. HEL is the value of the yield limit at uniaxial strain when the material loads in the same direction. Therefore, there are 2 separate equations for the values of the yield stress, either $D = 1$ or $D < 1$, in the Johnson-Holmquist model. The Yield stress value is the function of the continuous damage of D, so the material model with this

property is called the "active" fracture model for special cases; $D = 0$ (no damage) and $D = 1$ (damaged). The Yield stress value is lower according to the equation (F. M. John et al. 2010).

$$Y = A (p^* + T^*)^n [1 + C \ln (\dot{\epsilon}_p^*)] \quad (\text{Intact, } D=0) \quad (3)$$

$$Y = B (p^*)^m [1 + C \ln (\dot{\epsilon}_p^*)] \quad (\text{fragmented, } D=1) \quad (4)$$

Table 1 Properties and parameter JH of tungsten carbide (F. M. John et al., 2010)

Properties	Tungsten Carbide	Johnson-Holmquist Strength (Continuous JH-2)	
Density (ρ , g/cm ³)	14.56	Damage type	Gradual (JH2)
Young's modulus (E, GPa)	539	Hugoniot Elastic Limit (HEL, GPa)	656
Poisson ratio (ν)	0.23	Intact strength constant (A)	0.9899
Bulk modulus (GPa)	332	Intact strength exponent (n)	0.0322
Shear modulus (GPa)	219	Strain rate constant (C)	0
Tensile yield strength (GPa)	3.85	Fracture strength constant (B)	0.67
Compressive yield strength (GPa)	4.53	Fracture strength exponent (m)	0.0322
		Maximum fracture strength ratio	1000
		Damage constant (D1)	1
		Damage constant (D2)	0
		Hydrodynamic tensile limit (GPa)	-4

Plate 2 is made of a SUS304 material used to hold the bullet fragments after slamming into plate 1 and then breaking through the plates with a size of 30 x 30 cm, giving a typical SUS304 thickness starting at 1-5 mm, then setting at 6, 8, and 10 mm, etc. The thicknesses used in the simulation were 5, 6, 8, and 10 mm according to the Steinberg-Guinan Strength model's damage theory as a semi-experiment developed by situations having high stress rates and extended to low stress rates. (B. Banerjee, 2005). The equation is expressed as follows:

$$G = G_0 \left\{ 1 + \left(\frac{\dot{G}_p}{G_0} \right) \frac{p}{\eta^{1/3}} + \left(\frac{\dot{G}_t}{G_0} \right) (T - 300) \right\} \quad \text{or} \quad (5)$$

$$Y = Y_0 \left\{ 1 + \left(\frac{\dot{Y}_p}{Y_0} \right) \frac{p}{\eta^{1/3}} + \left(\frac{\dot{Y}_t}{Y_0} \right) (T - 300) \right\} (1 + \beta \epsilon)^n \quad (6)$$

$$\text{at } Y_0 = [1 + \beta \epsilon]^n \leq Y_{max}$$

When ϵ = Effective plastic strain, T = temperature (degree K), η = compression, and the parameters used, the subscripts p and T are derivatives of the parameters regarding the pressure and temperature at the reference state (T = 300 K, p = 0, ϵ = 0), the zero subscript also refers to the values of G and Y at that state. If the temperature of the material is higher than the specified molten temperature, the modulus of Shear and Yield Strength are set to zero. (Steinberg-Guinan Strength). The properties and parameters of SUS304 according to Finite element simulation are available in Table 2.

Table 2. Properties and parameter of SUS304

Properties	SUS304	Steinberg guinan strength	
Density (ρ , kg/m ³)	7900	Initial yield stress (Y, MPa)	340
Specific heat (J/kg °C)	423	Max. yield stress (Ymax, GPa)	2.5
Shock EOS linear		Shear modulus (GPa)	80
Gruneisen coefficient	1.93	Hardening constant (B)	43
Parameter (C1, m/s)	4570	Hardening exponent (n)	0.35
Parameter (S1)	1.49	Derivative (dG/dP , G ³ P)	1.74
Parameter quadratic (S2)	0	Derivative (dG/dT , G ³ T, MPa/°C)	-35
		Derivative (dY/dP , Y ³ P)	0.007684
		Melting temperature (Tmelt, °C)	2106.9
		Shear modulus (GPa)	77

Finite element method

In the Finite element simulation, the Ansys/Explicit Dynamics program is applied in which the bullet had a size of 7.62 mm with a speed of 880 m/s, providing a constant speed according to NIJ level 4 (N. Klangtup and P. Chartpuk, 2019) and the pattern generating a mesh for the bullet is hexahedral shaped with a size of 0.5 mm, 35,857 nodes and 65,861 elements. The mesh size is fine to reduce the errors caused by the simulation. The simulated firing is done into two types; type 1 which is the simulation for one shooting at a time on plate 1, which was made of tungsten carbide. On plate 2, made of SUS304, the mesh had a hexahedral shape with a size of 4 mm. The mesh size was squeezed into the middle of the plate 2 to a 15-times smaller size. Type 2 was categorized because both plates were composed of the front and back plates, made of tungsten carbide and SUS304, respectively, stacked into 2 layers (D. Bürger et al., 2012). The numbers of nodes and elements at the thickness of each parameter were set according to Table 3. The holders for the bulletproof armor plate were 4 supporters fixed on all 4 sides, creating the mesh as a hexahedral shape to reduce the numbers of nodes and elements (A. Saicharoen et al., 2022). The tetrahedral shaped mesh, oppositely, provides a larger number of nodes and elements and makes the run-program take longer time (M. A. Iqbal et al., 2015).

Table 3 Number of node and element

Thickness of plate	Armor plate 1 plate		Thickness of plate	Armor plate 2 plate	
	node	element		node	element
T = 5 mm	12,168	5,929	T ₁ = 6 mm, T ₂ = 5 mm	22,826	11,113
T = 6 mm	12,168	5,929	T ₁ = 6 mm, T ₂ = 6 mm	22,826	11,113
T = 8 mm	18,252	11,858	T ₁ = 8 mm, T ₂ = 8 mm	35,580	23,108
T = 10 mm	18,252	11,858	T ₁ = 10 mm, T ₂ = 10 mm	35,580	23,108

*T₁ = Thickness of the front plate, plate 1, T₂ = Thickness of the back plate, plate 2.

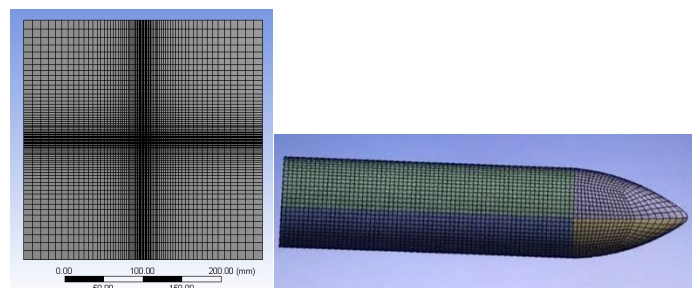
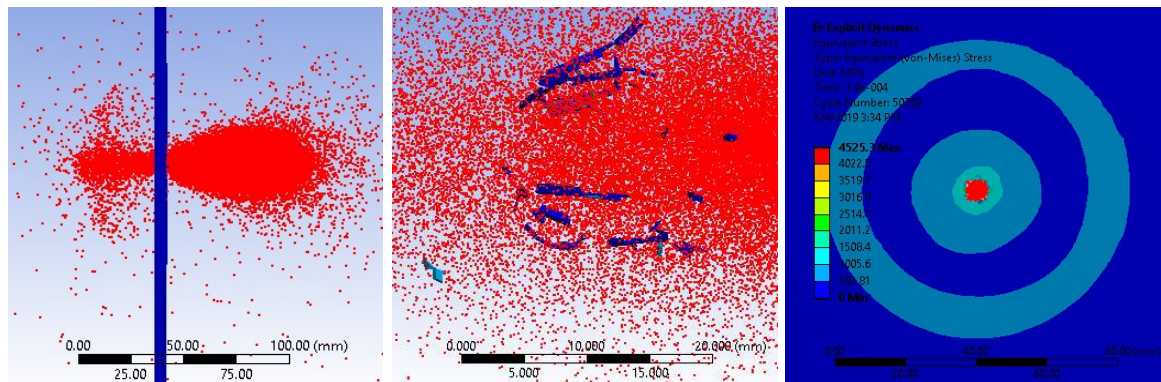


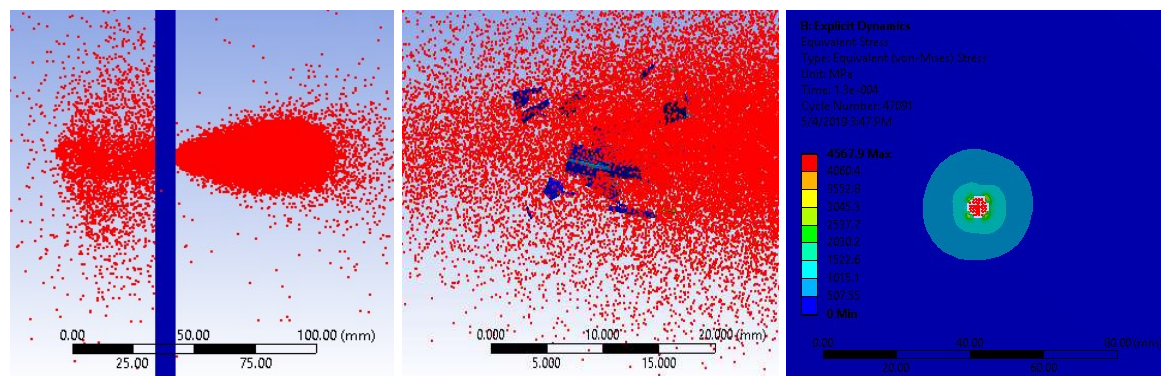
Figure 1 The pattern of mesh created on the armor plates and hexahedral shaped bullet

Result and discussion

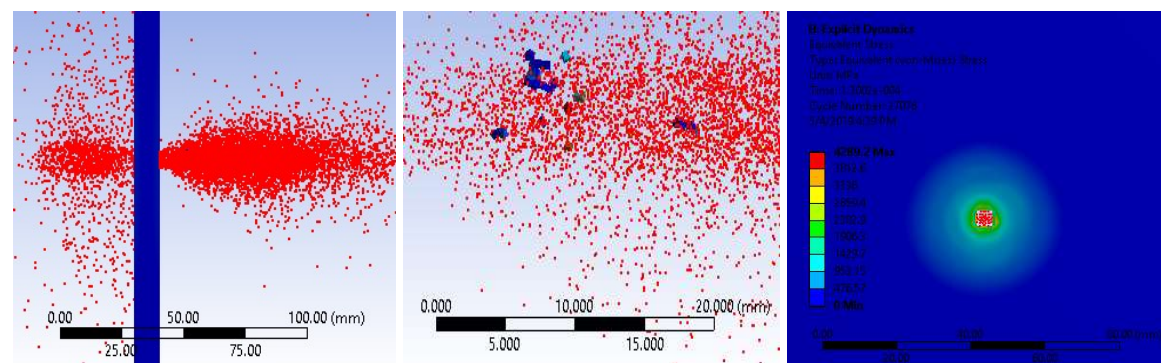
In the Finite element method, the simulation was done by firing a 7.62 mm bullet at a speed of 880 m/s on armor plate 1 made of tungsten carbide material at a thickness of 6, 8 and 10 mm. The armor plates could not withstand the penetration of the bullet in all these three thicknesses. However, at thicknesses of 6 and 8 mm, large pieces of bullets were scattered after hitting the plates, breaking apart, and penetrating through the plates. In the same way, the plate with 10 mm thickness had smaller metal fragments of the bullets, compared with those of 6 and 8 mm, as shown in Figure 2.



(A) The armor plate with thickness of 6 mm.



(B) The armor plate with thickness of 8 mm.



(C) The armor plate with thickness of 10 mm.

Figure 2 The illustrated simulation of the shooting of the bullets on the armor plate with various thickness (A, B, and C) at time step 13 ms.

Left: The puncture of the bullet after hitting on the armor plate.

Middle: The bullet fragments after a bullet penetrating through an armor plate.

Right: The dispersion of the Stress caused after a bullet penetrating through an armor plate.

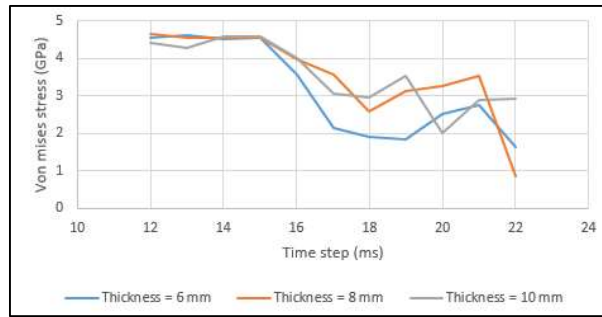


Figure 3 A graph of the Stress at time step of a WC plate with thickness of 6, 8 and 10 mm.

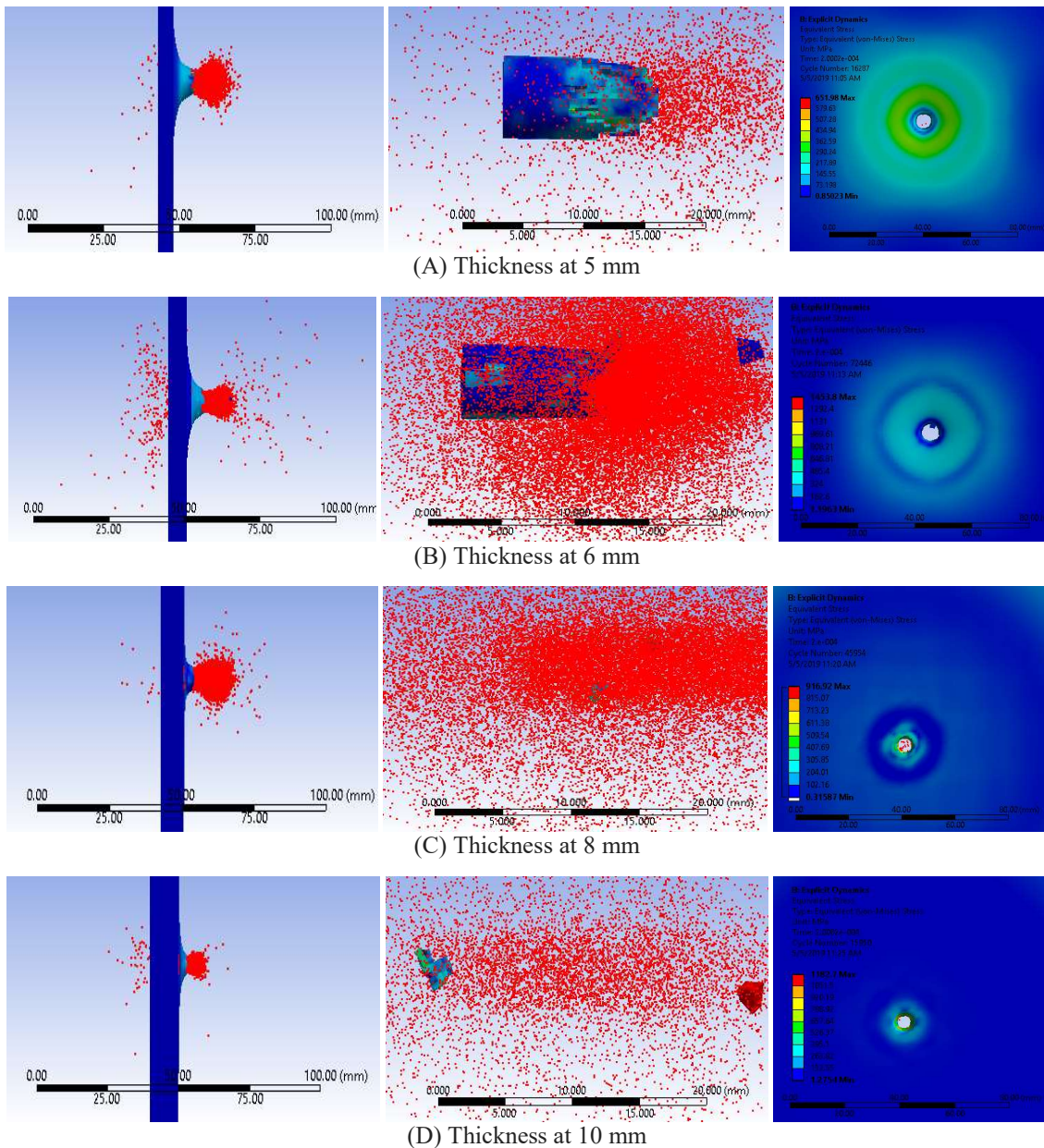


Figure 4 The illustrated simulation of the shooting of the bullets on the armor plate at various thickness (A, B, C, and D) at time step 20. Left: the puncture caused by the penetrating of the bullet after hitting the armor plate. Middle: the bullet fragments after penetrating through the armor plates. Right: the dispersion of the Stress caused after a bullet penetrating through an armor plate.

When comparing with the stress determined in Figure 3, among all three impacts, especially the shooting at 6 mm thick armor plates at the time step range of 16-20 ms could reduce and disperse the stress generated by penetration greater. This was because the armor plates with a 6 mm thickness were more deflated than those with 8- and 10-mm thickness. Moreover, at 8 and 10 mm thickness, the bullets could penetrate through the armor plate, resulting in stress distributed around the puncture mark less than that of 6 mm thickness. These results explained that the increased thickness causes the collapse of the armor plate to decrease.

In the second plate, it was a SUS304 material with a thickness of 5, 6, 8 and 10 mm. As a result, the armor plate could not withstand the penetration which was corresponding to those made of tungsten carbide material at thickness of 5 and 6 mm. The broken parts of bullets especially bullet body fragments, were detected after breaking and thus penetrating, but at a thickness of 8 and 10 mm, the bullets were found to have penetrated the armor plates in a cluster of bullet metal fragments as shown in Figure 4.

At 5 and 6 mm thickness, the armor plates collapsed more than those at 8 and 10 mm thickness, since the increase in thickness resulted in less collapsing of the plate. In contrast, at that increased thickness, when the bullet hit the armor plate, it caused the bullet head to break. The penetration characteristics on the back of the armor plate were demonstrated in Figure 5. At thicknesses of 5 and 6 mm, it was illustrated that the stress around the circumference of the perforated hole has a distribution greater than those at 8 and 10 mm.

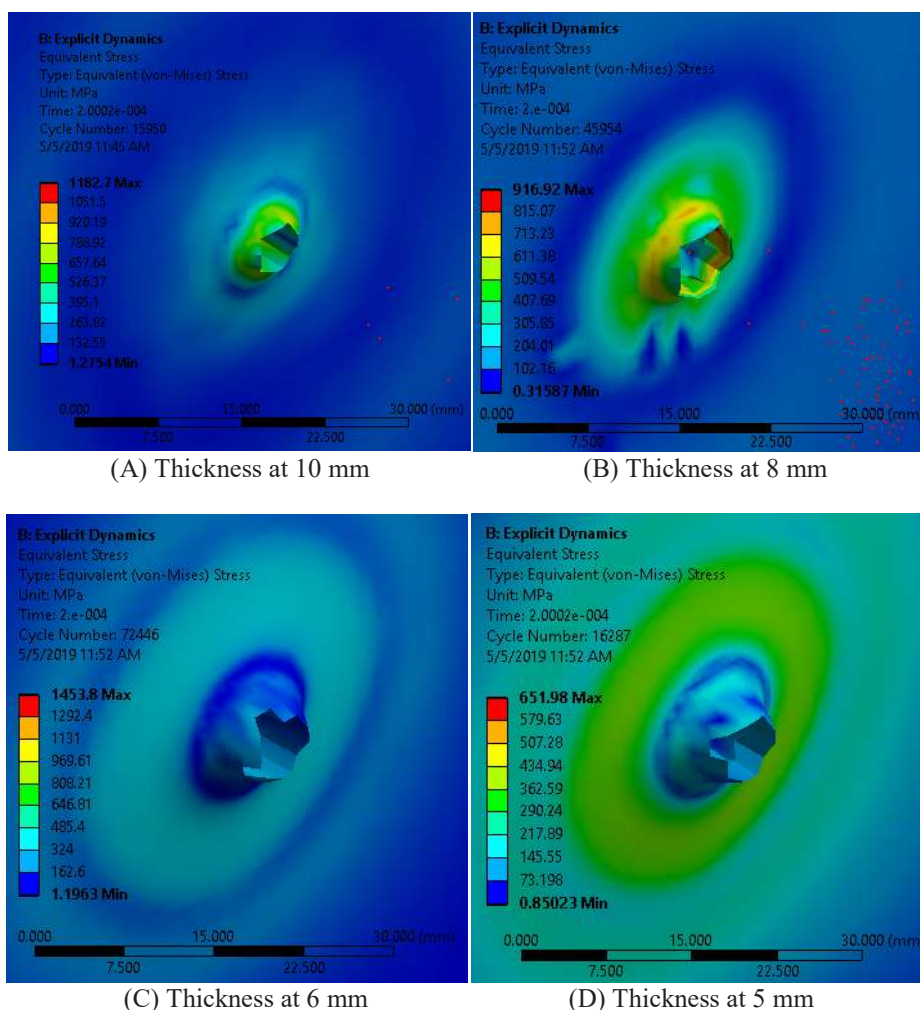
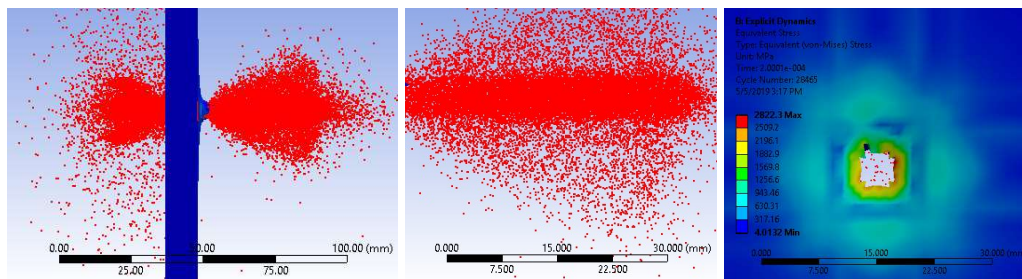
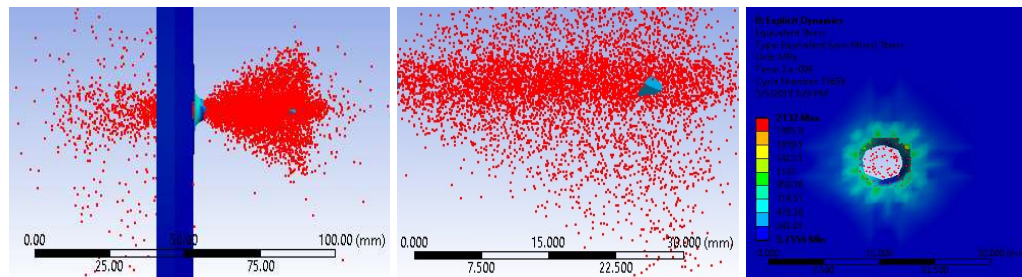


Figure 5 Penetration characteristics of the back armor plate at time step 20 ms.

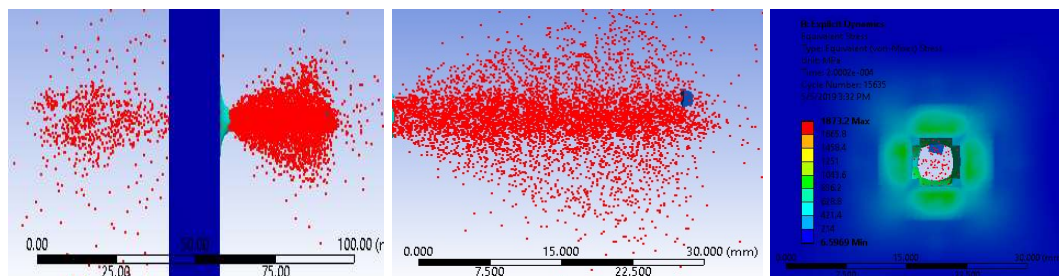
Therefore, the plates were stacked into 2 layers of plate 1 and 2, made of tungsten carbide and SUS304, respectively. The simulations were performed on 4 models; Model 1: plate 1 and 2 were set thicknesses at 6 and 5 mm, respectively. Model 2, 3, and 4: plate 1 and 2 had the same thickness sizes, set at 6, 8, and 10 mm. As a result of these four simulations, the armor plates were unable to resist the penetration of the 7.62 mm bullet, but the bullet was broken when it slammed into the armor plate and then changed to various clusters of scrap metals as shown in Figure 6.



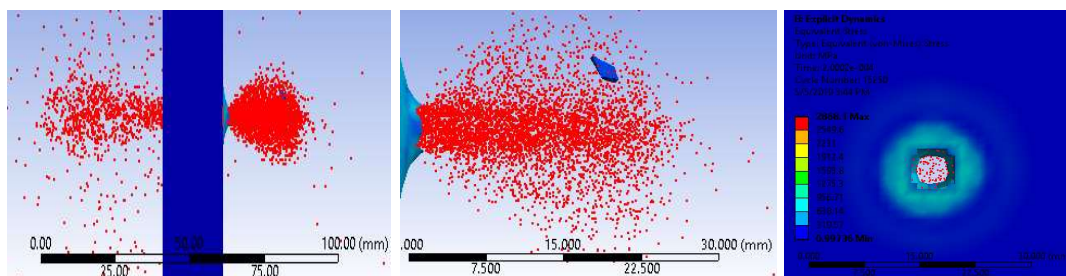
(A) Simulated Model I: T₁ = 6 mm. T₂ = 5 mm.



(B) Simulated Model 2: T₁ = 6 mm. T₂ = 6 mm.



(C) Simulated Model 3: T₁ = 8 mm. T₂ = 8 mm.



(D) Simulated Model 4: T₁ = 10 mm. T₂ = 10 mm.

Figure 6 Simulated Model 1-4 (A, B, C, and D).at time step 20 ms.

Left: Penetrating of the bullet after hitting the armor plate. Middle: The bullet fragments after penetrating through the armor plates. Right: Distribution of stress caused after bullet penetration through an armor plate.

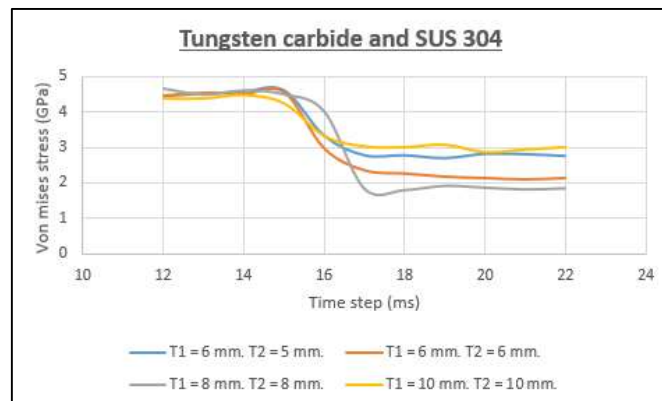


Figure 7 A graph of time step stress of WC and SUS 304 plates.

From the graphs in figure, at the time step 15 – 20 ms, in the simulated Model 3, plate 1 and 2 with thickness of 8 mm could reduce the stress generated by penetration of the bullet more than the armor plates in simulated Model 1, 2, and 4. In addition, the increased thickness of the plates causes smaller sizes of metal clusters after penetrating out. In this case, it was possible if given the thickness of both plates 1 and 2 was equally increased, both plates could withstand the penetration of 7.62 mm of the bullet.

Therefore, the thickness of the two materials stacked onto an armor plate was increased to the same size, starting at 12 mm or more onto the armor plates. It could withstand the penetration of 7.62 mm bullets (P. Tan, 2014). It was found that at thicknesses of 12 mm and 14 mm, the armor plates could not be able to endure the penetration of the bullets, but the perforated metal clusters were getting smaller with the increased thickness as shown in Figure 8.

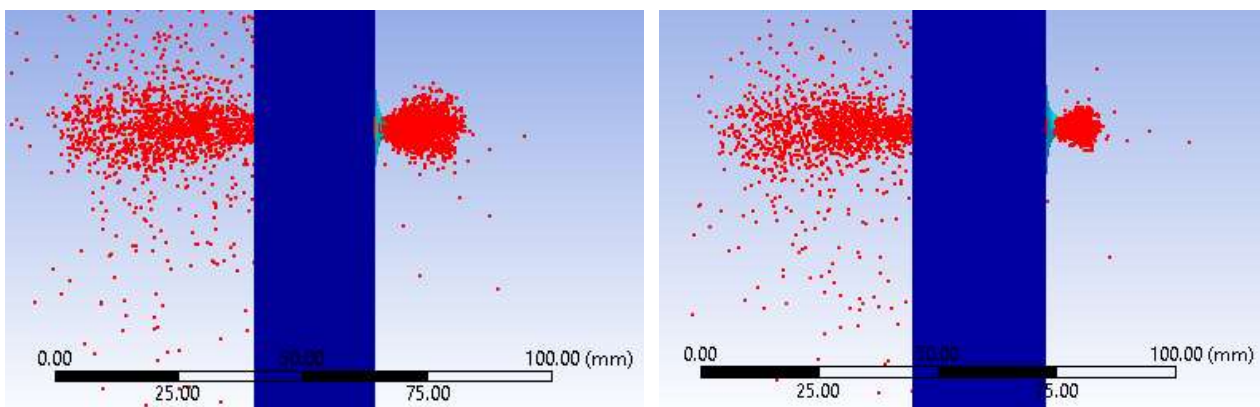


Figure 8 The thickness affected on an armor plate at time step 20 ms.

Left: Thickness $T_1 = 12$ mm and $T_2 = 12$ mm and Right: Thickness $T_1 = 14$ mm and $T_2 = 14$ mm.

Additionally, the thickness of plate 1 and 2 starting at 16 mm thick showed the beginning of resistance to the penetration, shown in Figure 9 and 10. The graph explained that the thickness of both sheets equal to 16 mm caused more stress on the armor plate than those of 12 and 14 mm, since the armor plate could resist the penetration of a 7.62 mm bullet though causing more the Strain accumulated on the armor plate.

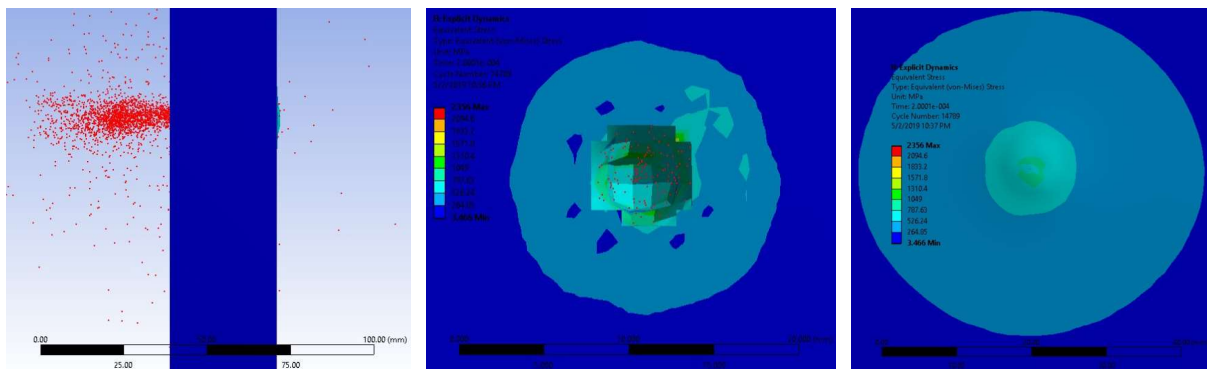


Figure 9 The resistance of armor plates at the thickness of 16 mm to the penetration at time step 20 ms.

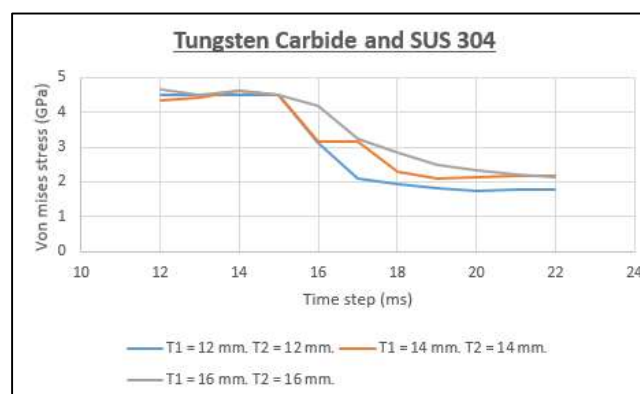


Figure 10 A graph of the compared stress at time step of WC and SUS 304 plates

Therefore, the armor plate at a thickness of 12 mm was compared to that of M.A. Iqbal (M. A. Iqbal et al. 2015). The penetration characteristics at the back of the armor plate had a smaller hole than that in the front plate, a fire element simulation that is close to the actual experiment as shown in Figure 10, so the studied simulation can be used to analyze the destructive situation occurring on the armor plates before developing a real armor plate.

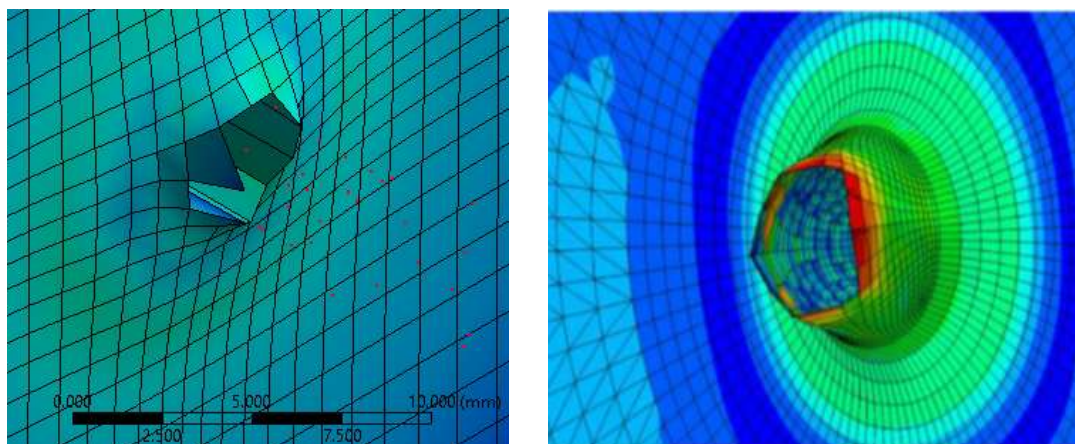


Figure 11 The resulted WC and SUS 304 armor plate 2 with thickness of 12 mm after penetration (Left) compared with simulated plates of mild steel with thickness of 12 mm determined by M.A. Iqbal (Right) (M. A. Iqbal et al. 2015).

Conclusion

Based on finite element simulation, 2 types of materials composed of tungsten carbide and SUS304 were employed as shielding plate material for a simulated firing with a 7.62 mm bullet at a speed of 880 m/s. For firing at each plate at a time, the plate could not withstand the penetration of the bullet. After two plates were stacked in two layers, with the front plate being tungsten carbide, and the back plate being SUS304, 4 simulated models were developed by the Finite element method. These simulations indicated the stacked plates could not withstand the penetration of the bullet. But when the bullet hit the first plate, the bullet was broken and its metal fragments accumulated with the armor plate metal could then penetrate the second plate, which was used to hold the scrap metal of the bullet. Since the metal fragments of the bullet were combined with the metal fragments of the first plate, these combined metal clusters induced the penetration of the second plate. The increase in the thickness of two stacked plates stacked into the armor plate to 16 mm could cause enduring penetration. It started to withstand the penetration of 7.62mm bullets, so at a thickness of more than 16mm or more, both plates were able to resist the penetration of a 7.62 mm bullet at a speed of 880 m/s.

Acknowledgement

The authors would like to express the appreciation to the National Research Council of Thailand (NRCT), National Research Policy and Strategy for the financial support according to the contract no. 47/2561 and Rajamangala University of Technology Phra Nakhon (RMUTP) for supportive facilities.

References

- Banerjee, B. “An evaluation of plastic flow stress models for the simulation of high-temperature and high-strain-rate deformation of metals,” p. 53, Dec. 2005.
- Binar, T., *et al.*, “The use of numerical simulation for the evaluation of special transparent glass resistance,” *Eng. Fail. Anal.*, 91, 433–448, Sep. 2018
- Bürger, D., Rocha de Faria, A., Almeida, S. F. M. de, Melo, F. C. L. de. and Donadon, M. V., “Ballistic impact simulation of an armour-piercing projectile on hybrid ceramic/fiber reinforced composite armours,” *Int. J. Impact Eng.*, 43, 63–77, May 2012.
- Feli, S. and Asgari, M. R. “Finite element simulation of ceramic/composite armor under ballistic impact,” *Compos. Part B Eng.*, 42(4), pp. 771–780, Jun. 2011.
- John, F. M., Jan Arild, T., Stian, S., Svien Morten, B., Lasse, S.-E. and Haakon, F. “Development of material models for semi-brittle materials like tungsten carbide,” *Norwegian Defence Research Establishment (EFI)*, 1–51, 09-Nov-2010.
- Klangtup, N. and Chartpuk, P. “Parameter analysis of SKD11 and SUS304 bulletproof plate that resistance penetration of bullet 7.62 mm according to standard NIJ 4 by finite element method,” *International Journal of Mechanical Engineer and Technology*, 10, 207–221, Sep. 2019.
- Tan, P. “Numerical simulation of the ballistic protection performance of a laminated armor system with pre-existing debonding/delamination,” *Compos. Part B Eng.*, 59, 50–59, Mar. 2014.
- Saicharoen, A., Tinrabath, P. and Chartpuk, P. “Parameter Analysis that Affects the Ability to Resistance Penetration of Ammunition on the Aluminum Armor Surface Using Finite Element Method,” *RMUTP Research Journal*, 16(1), 192-208, 2022.
- Zhang, P. L., *et al.*, “Study of the shielding performance of a Whipple shield enhanced by Ti-Al-nylon impedance-graded materials,” *Int. J. Impact Eng.*, 124, 23–30, Feb. 2019



RMUTCON

Session 3:

Medical Science and Herb

Total Phenolic Content, Antioxidant and Anticancer Activity of *Calophyllum inophyllum*

Luksamee Vittaya^{1*}, Chakhriya Chalad¹, Juntra Ui-eng¹ and Sittichoke Janyong²

¹ Department of General Education, Faculty of Science and Fisheries Technology, Rajamangala University of Technology Srivijaya, Trang 92150, Thailand

² Department of Marine Sciences and Environment, Faculty of Science and Fisheries Technology, Rajamangala University of Technology Srivijaya, Trang 92150, Thailand

Abstract

Calophyllum inophyllum is an important medicinal plant in the Calophyllaceae family. Various parts of the plant show different pharmacological properties including anti-inflammatory, antidiabetic, antioxidant, antibacterial and anticancer activities. The present study was performed to analyze the total phenolic content (TPC) of the flower, fruit, leaf, twig and bark of *C. inophyllum* extracted with hexane, ethyl acetate and methanol in order to polarity of solvents. Free radical scavenging activities were evaluated by two methods, 1,1-diphenyl-2-picrylhydrazyl radical scavenging activity (DPPH) and 2,2'-azinobis-3 ethylbenzothiazoline-6-sulfonic acid (ABTS). The anticancer activity was carried out from the cell growth inhibition determined using a resazurin microplate assay (REMA). Total phenolic contents were presented significantly in the ethyl acetate and methanol extracts higher than that of the hexane extracts. In addition, the ethyl acetate and methanol extracts of all parts showed a higher percentage of radical scavenging activity than the hexane extracts when measured by DPPH and ABTS. The positive correlation was established by the Pearson correlation test between two methods of free radical scavenging activity DPPH and ABTS ($r=0.945$). Interestingly, the free radical scavenging activity depends on structure-relationship of phenolic with positive correlation: $r=0.902, 0.872, 0.720$ for DPPH observed in flower, leaf and twig and $r=0.900, 0.758, 0.885, 0.752$ for ABTS observed in flower, fruit, leaf and twig, respectively. The anticancer activity was tested against the MCF7 human breast cancer cell line and the NCI-H187 human small cell lung cancer cell line. Leaf extracts were significantly active against NCI-H187 cancer cells.

Keywords: *Calophyllum inophyllum*, Phenolic content, Antioxidant, Anticancer

Introduction

Thailand has various kinds of medicinal plants which have been used to treat many diseases for a long time. Among these potential Thai plants, *Calophyllum inophyllum* is medicinal plants belonging to the Calophyllaceae family, which is widely used as Thai traditional medicine for therapy. It is generally growth in mangrove area which found dominant interface ecosystems between the land and the sea in the tropical forest. Almost parts of the plant can be used in traditional medicine for treatment of various ailments, for example, antibacterial (Malarvizhi and Ramakrishnan 2014; Sundaram et al. 1986) and anticancer activities (Ito et al. 2001). Bioactive compounds (alkaloid, flavonoid, steroid, terpenoid and saponin) were found in several parts of this plant (Santhi and Sengottuve 2016). Especially, phenolic substances (Periyasamy 2015) which are important secondary metabolites showing as bio-activities like antioxidant and antibacterial activities Mahmoudi et al (2016). Such substances help to stimulate the immune system and eliminate radicals reduced stress and prevent disease. Therefore, several research related to finding medicinal plants containing phenolic compounds has attracted. The main points of this work were to study the different total phenolic content (TPC) of flower, fruit, leaf, twig and bark from *C. inophyllum* and to investigate the

correlation between TPC and free radical scavenging activity by DPPH and ABTS methods and anticancer activities.

Materials and Methods

Plant material and extraction procedure

Fresh flower, fruit, leaf, twig and bark of *C. inophyllum* were collected from Rajamangala University of Technology Srivijaya, Trang Province which is located in the southern part of Thailand in September-October 2016. The dried powder of each part was extracted for a week with sequentially polar organic solvents hexane, ethyl acetate and methanol. The resulting extracts were evaporated to dry residue using a rotary evaporator at 45°C and refrigerated at 4°C until used. The yields of leaf, flower, fruit, twig and bark were recorded and the dried extracts were determined biological activities.

Standard and reagents

Folin-Ciocalteu reagent, gallic acid, butylhydroxytoluene (BHT), 2,2-diphenyl-1-picrylhydrazyl, 2,2'-azino-bis-(3-ethylbenzothiazoline-6-sulfonic acid diammonium salts) were used for the phenolic content, DPPH assay, and for the ABTS assay, respectively. Methanol and sodium carbonate were obtained from Merck and Fluka. All other chemicals and reagents of analytical grade were used.

Determination of total phenolic contents (TPC)

The TPC (mg/mL) of *C. inophyllum* extracts were determined as previously described using the Follin-ciocalteau method which is modified by Vittaya et al (2019). Total phenolic content was expressed as gallic acid equivalents (GAE) per milligram of dry crude extract (mg GAE/g crude extract) through the calibration curve of gallic acid. Its linearity range was from 20 – 100 mg/mL ($R^2 > 0.99$). For all extracts, the concentration of the samples was fixed using 1 mg/mL and 0.2 mL. Then, 2.5 mL of distilled water was added, followed by the Follin-Ciocalteu reagent 0.2 mL, respectively. The reaction mixture was vortexed and left to stand for a minute. After that, 2.0 mL of 7% sodium carbonate solution was added to the reaction mixture, which was then kept away from light for 60 minutes. The absorbance of all samples was collected at 765 nm using a UV-vis spectrophotometer.

Determination of free radical scavenging activity

DPPH assay

The free radical scavenging of flower, fruit, leaf, twig and bark extracts of *C. inophyllum* was measured using DPPH which was determined by slightly modifying the method of Vittaya et al (2019). Briefly, 0.5 mL of 0.15 mM methanolic DPPH solution was mixed with 0.5 mL of each sample (1 mg/mL) and BHT standard. The reaction mixture was shaken vigorously and allowed to stand at room temperature in darkness for 30 min. The control of DPPH was prepared without the addition of an extract samples. The absorbance of the solution was measured at 517 nm against the blank. The scavenging ability of each plant extract was calculated using the following equation as DPPH Scavenging activity (%) = $1 - (\text{Abs}_{\text{sample}} - \text{Abs}_{\text{sample blank}}) / \text{Abs}_{\text{control}}$ × 100, where $\text{Abs}_{\text{sample}}$ is the absorbance of the test sample with DPPH solution, $\text{Abs}_{\text{sample blank}}$ is the absorbance of the test sample only, and $\text{Abs}_{\text{control}}$ is the absorbance of DPPH solution. All measurements were performed in triplicate and expressed as average values.

ABTS assay

The 2,2'-azino-bis-3-ethylbenzothiazoline-6-sulphonate radical cation (ABTS⁺) decoloration assay was performed as described by Vittaya et al (2020). The ABTS radical cation (ABTS⁺) solution was prepared by mixing 5 mL of 7 mM ABTS with 880 µL of 140 mM K₂S₂O₈ (potassium persulfate). The mixture was allowed to stand in darkness for 16 h at room temperature and then diluted with

methanol to give an absorbance of 0.700 ± 0.025 units at 734 nm using the spectrophotometer. A sample extract of 0.1 mL was added to 0.9 mL of diluted ABTS⁺ solution. The reaction mixture was shaken and left to stand for 6 min in darkness. After incubation, absorbance was measured at 734 nm. The percentage of scavenging inhibition of ABTS⁺ was determined in triplicate and was calculated using the following equation as % inhibition = $[(Abs_{control} - Abs_{sample})/Abs_{control}] \times 100$, where $Abs_{control}$ is the absorbance of the extract without ABTS⁺ solution and Abs_{sample} is the absorbance of the extract with ABTS⁺ solution and carried out in triplicate time.

Anticancer activity screening

The anticancer activity of each extract was evaluated from the cell growth inhibition determined using a resazurin microplate assay (REMA) in a two human cell lines panel consisting of MCF7 breast cancer cells and NCI-178 small lung cancer cells. Results were compared with positive controls of Ellipticin, Doxorubicin and Tamoxifen. The extracts were tested at a single concentration (0.01 ppm) and the positive controls were dissolved in DMSO. The primary anticancer assay was performed at the National Center for Genetic Engineering and Biotechnology (BIOTEC) of the National Science and Technology Development Agency (NSTDA). Anticancer activity was determined by % cytotoxicity: < 50% was considered non-cytotoxic and > 50% was considered cytotoxic (IC₅₀ included) (Rattana 2016).

Statistical analysis

All data were expressed as means \pm standard deviation of triplicate measurements. Statistical analyses were conducted by one-way ANOVA followed by the Duncan's Multiple Range Test (DMRT) for phenolic content and the antioxidant activity (DPPH and ABTS) and the correlation between both values were carried out using Pearson Correlation (r) at the significant 0.01 level.

Results and Discussion

Phenolic content

The total phenolic content of all extracts was determined by the Folin-Ciocalteu method and the data are shown in Table 1. The total phenols of *C. inophyllum* extracts were calculated according to the equation $y = 0.004x - 0.0086$ ($r^2 = 0.998$) as gallic acid equivalent (GAE, mg/g crude extract). The total phenolic contents show values between 0.15 to 1.81 mg GAE/g crude extract in various extracts. With regard to the amounts of phenolic compounds in flower and fruit of *C. inophyllum* ethyl acetate extracts contained the highest content of phenolics (0.72-0.84 mg GAE/ g of crude extract), compared to hexane (0.18-0.19 mg GAE/ g of crude extract), and methanol extracts (0.20-0.57 mg GAE/ g of crude extract). In contrast to leaf, twig and bark of *C. inophyllum*, methanolic extracts contained the highest content of phenolics (1.81-0.77 mg GAE/ g of crude extract), compared to hexane (0.15-0.42 mg GAE/ g of crude extract), and ethyl acetate extracts (0.51-0.69 mg GAE/ g of crude extract). It has been hypothesized that the bioactive ingredients present in ethyl acetate and methanolic flower, fruit, leaf, twig and bark extracts of *C. inophyllum* may play an important role in the biological activity (Bazzaz 2011). Moreover, the variation in the antioxidant activity of all extracts presented may be attributed to differences in the total phenolic content as well.

Free radical scavenging activity

The antioxidant capacities were studied with 1,1-diphenyl-2-picrylhydrazyl (DPPH) and 2,2'-azino-bis-3-ethylbenzothiazoline-6-sulfonic acid diammonium salts (ABTS) methods. The results of these methods were shown in Table 1. Generally, the free radical scavenging activity was investigated from the reaction of DPPH with the crude extracts by following the changed color from purple to yellow of DPPH when DPPH accepts electrons or hydrogen free radicals. This ability of DPPH free radical to undertake a reduction by an antioxidant is measured in terms of decrease in its absorbance

at 517 nm (Kedare 2011). In this work, the scavenging activity of DPPH was observed ranging from 51% to 95% in flower, fruit, leaf, twig and bark. Interestingly, the free radical scavenging activity of ethyl acetate extract was similar to methanolic extracts. The DPPH antioxidant capacity of extracts was significantly correlated with phenolic contents, especially flower ($r = 0.902$; $p = 0.001$) and leaf ($r = 0.872$; $p = 0.002$), following by twig and bark which are shown in Table 2. Additionally, the ABTS⁺ method is a good tool to determine the antioxidant activity. The decolourization of ABTS⁺ radical indicates the capacity of an antioxidant species to give electrons or hydrogen atoms to inactivate the radical species (Santos-Sánchez 2019). In this work, the samples showed decrease in absorption with moderate scavenging activity, observed ranging from 19% to 99% in flower, fruit, leaf, twig and bark. This method has a result in the same way as DPPH, total phenolic content and ABTS of flower ($r = 0.900$; $p = 0.001$) and leaf ($r = 0.872$; $p = 0.002$), following by twig. Nevertheless, the total phenolic content in fruit and bark were no correlated with free radical scavenging activity. It is possible that other bioactive substances such as flavonoid, alkaloid, terpenoid or other primary metabolite as lipid, carbohydrate may be including in plant parts with different quantities. Additionally, DPPH and ABTS were significant correlated with $r = 0.954$; $p < 0.01$.

Table 1 Total phenolic contents and free radical scavenging activity of *C. inophyllum* extracts.

Part used	Solvents	Total phenolic Content (mg GAE/ g CE)	Free radical scavenging percentage (%)	
			DPPH assay	ABTS assay
Flower	Hexane	0.19 ± 0.02 ^{ij}	67.38 ± 1.34 ^e	36.84 ± 4.03 ^e
	Ethyl acetate	0.84 ± 0.07 ^c	95.49 ± 0.06 ^{abc}	99.47 ± 0.24 ^a
	Methanol	0.57 ± 0.05 ^{efg}	95.14 ± 0.12 ^{bc}	99.20 ± 0.30 ^a
Fruit	Hexane	0.18 ± 0.02 ^{ij}	51.39 ± 1.08 ^f	20.50 ± 3.52 ^f
	Ethyl acetate	0.72 ± 0.06 ^{cde}	95.18 ± 0.26 ^{bc}	99.15 ± 0.17 ^a
	Methanol	0.20 ± 0.02 ^{ij}	94.84 ± 0.20 ^{bc}	73.62 ± 4.20 ^c
Leaf	Hexane	0.15 ± 0.02 ⁱ	50.93 ± 1.42 ^f	19.85 ± 1.63 ^f
	Ethyl acetate	0.65 ± 0.28 ^{def}	95.10 ± 0.27 ^{bc}	96.51 ± 1.06 ^{ab}
	Methanol	0.77 ± 0.06 ^{cd}	94.71 ± 0.15 ^{bc}	98.51 ± 0.23 ^a
Twig	Hexane	0.33 ± 0.03 ^{hi}	82.93 ± 0.76 ^d	51.65 ± 1.53 ^d
	Ethyl acetate	0.69 ± 0.06 ^{cde}	94.76 ± 0.26 ^{bc}	97.71 ± 0.37 ^a
	Methanol	1.48 ± 0.13 ^b	94.58 ± 0.20 ^c	99.36 ± 0.15 ^a
Bark	Hexane	0.42 ± 0.02 ^{gh}	82.16 ± 0.69 ^d	53.69 ± 2.71 ^d
	Ethyl acetate	0.51 ± 0.03 ^{fg}	94.54 ± 0.20 ^c	93.42 ± 0.61 ^b
	Methanol	1.81 ± 0.14 ^a	95.83 ± 0.13 ^{ab}	99.37 ± 0.41 ^a
BHT	-	-	94.31 ± 0.26 ^c	98.94 ± 0.54 ^a

Note: Data were presented as means ± SD from analysis of three samples, in triplicate independent analyses. Different lower case letters (a-j) in each sample denote significantly different ($p < 0.05$). The concentration of the samples and standard were fixed using 1 mg/mL.

Table 2 Correlation coefficient (r) between variables of total phenolic contents followed by each of parts and free radical activity analyzed by two different methods.

Methods	TPC				
	Flower	Fruit	Leaf	Twig	Bark
DPPH	0.902 ($p = 0.001$)	0.521 ($p = 0.150$)	0.872 ($p = 0.002$)	0.720 ($p = 0.029$)	0.615 ($p = 0.078$)
ABTS	0.900 ($p = 0.001$)	0.758 ($p = 0.018$)	0.885 ($p = 0.002$)	0.752 ($p = 0.019$)	0.642 ($p = 0.062$)

Note: TPC = total phenolic content; DPPH = 1,1-diphenyl-2-picrylhydrazyl radical scavenging activity; ABTS = 2,2'-azino-bis(3-ethylbenzothiazoline-6-sulfonic acid)

Anticancer activity

Cancer is the abnormal growth of cells in our bodies that lead to the most serious diseases to affect humans. Plants are bioactive sources of drugs for the treatment of cancer and can help the development of novel anticancer agents. This research pointed to find a new anticancer agent from a natural product. In this work, almost part extracts of *C. inophyllum* showed the anticancer activity, presented in Table 3. The ethyl acetate of fruit, leaf, twig and bark extracts showed anticancer activity against the NCI-H187 small lung cancer cell, especially the leaf extract showed the highest anticancer with IC₅₀ values 10.09 ± 1.43 mg.mL⁻¹. In addition, hexane of leaf and bark extracts were shown anticancer activity against the NCI-H187 small lung cancer cell with similarly IC₅₀ values. From the results, it is concluded that the anticancer activity of these extracts could be not only attributed to the presence of phenolic substance but also other bioactive compounds. Previous studies showed that the fruit and seed oil extracts of *C. inophyllum* showed significant anticancer and cytotoxic to human colon cancer, non-small cell lung cancer (Oo 2018). The plant inhibits cell growth in human leukemia cell with isolated bioactive compounds (such as canophyllic acid, amentoflavone, oleanolic acid) from leaf (Oo 2018). Furthermore, a prenylated xanthone called caloxanthone O from twig is cytotoxic to human gastric cancer cell line with IC₅₀ less than 25 mg.mL⁻¹. Various xanthones from bark exhibited antiproliferative action on five cell lines (Oo 2018). None of the extracts inhibited the growth of MCF7 breast cancer cells. The results support the potential benefits of the reported use of this plant for the treatment of lung cancer in traditional medicine.

Table 3 IC₅₀ values of the *C. inophyllum* extracts against cancer cell lines.

Part used	Solvent	Cell lines IC ₅₀ (mg.mL ⁻¹)	
		MCF7	NCI-H187
Flower	Hexane	> 50	> 50
	Ethyl acetate	> 50	> 50
	Methanol	> 50	> 50
Fruit	Hexane	> 50	> 50
	Ethyl acetate	> 50	48.51 ± 0.28
	Methanol	> 50	> 50
Leaf	Hexane	> 50	17.45 ± 1.51
	Ethyl acetate	> 50	10.09 ± 1.43
	Methanol	> 50	> 50
Twig	Hexane	> 50	> 50
	Ethyl acetate	> 50	18.70 ± 0.27
	Methanol	> 50	> 50
Bark	Hexane	> 50	18.03 ± 0.09
	Ethyl acetate	> 50	19.80 ± 0.92
	Methanol	> 50	> 50
Ellipticine	-	-	2.02 ± 0.57
Doxorubicin	-	-	0.10 ± 0.03
Tamoxifen	-	7.92 ± 0.84	-

Note: The extracts with an IC₅₀ value > 50 mg/mL were considered inactive

Conclusion

The bioactive compounds of *C. inophyllum* showed good free radical scavenging activity which upon on the structure relationship of phenolic compounds in each extracts. In addition, ethyl acetate and methanol solvents were good organic solvents extracting bioactive compounds of

phenolic. The activities of hexane and ethyl acetate extracts of fruit, leaf, twig and bark against small cell lung cancer were comparable. The results of this study showed that extracts of *C. inophyllum* could be promising sources of antioxidants for pharmaceutical applications.

Acknowledgments

The authors acknowledge the Faculty of Science and Fisheries Technology, Rajamangala University of Technology Srivijaya, Trang Campus for providing laboratory facilities.

References

- Bazzaz BSF, Khayat MH, Emami SA, Asili J, Sahebkar A, Neishabory EJ. (2011). Antioxidant and antimicrobial activity of methanol, dichloromethane, and ethyl acetate extracts of *Scutellaria litwinowii*. *Sci Asia*, 37, 327-334.
- Ito C, Itoigawa M, Mishin Y, Tomiyasu H, Litaudon M, Cosson J-P, Mukainaka T, Tokuda, Nishino, H. Furukawa H. (2001). Cancer Chemopreventive Agents. New Depsidones from *Garcinia* Plants. *J Nat Prod*, 64(2),147–150.
- Kedare SB, Singh RP. (2011). Genesis and development of DPPH method of antioxidant assay. *J Food Sci Technol*, 48(4), 412–422.
- Malarvizhi P, Ramakrishnan N. (2014). Biogenic silver nano particles using *Calophyllum inophyllum* leaf extract: Synthesis, spectral analysis and antimicrobial studies. *World J Pharm Res*, 3, 2258-2269.
- Mahmoudi S, Khali M, Benkhaled A, Benamirouche K, Baiti I. (2016). Phenolic and flavonoid contents, antioxidant and antimicrobial activity of leaf extracts from ten Algerian *Ficus carica* L. varieties. *Asian Pac J Trop Biomed*, 6, 239–245.
- Oo, W.M. (2018). Pharmacological properties of *Calophyllum inophyllum*-update review. *International Journal of Photochemistry and Photobiology*, 2(1), 28-32.
- Periyasamy S, Jaikumar K, Mohamed MSN, Anand D. (2015). Phytochemical analysis of bioactive compounds from *Calophyllum inophyllum* L., leaf extract using GC-MS analysis. *Int J Pharmacogn Phytochem Res*, 7(5), 956-959.
- Rattana S, Cushnie B, Taepongsorat L, Phadungkit M. (2016). Chemical constituents and In vitro anticancer activity of *Tiliacora triandra* leaves. *Pharmacogn J*, 8(1), 1–3.
- Santos-Sánchez NF, Salas-Coronado R, Villanueva-Cañongo C, Hernández-Carlos B. (2019). *Antioxidant Compounds and Their Antioxidant Mechanism*. In (Ed.), *Antioxidants*. IntechOpen. DOI: 10.5772/intechopen.85270.
- Santhi K, Sengottuve R. (2016). Qualitative and quantitative phytochemical analysis of *Moringa concanensis* Nimmo. *Int J Curr Microbiol Appl Sci*, 5(1), 633-640.
- Sundaram BM, Gopalkrishnan C, Subramanian S. (1986). Antibacterial activity of xanthenes from *Calophyllum inophyllum* L. *Arogya. J Health Sci*, 12, 48-49.
- Vittaya L, Khongsai S, Ui-eng J, Chalad C, Leesakul N. 2019. Effect of total phenolic and flavonoid content of *Ampelocissus martini* on radical scavenging and antibacterial activities. *Agric Nat Resour*, 53, 154-160.
- Vittaya L, Aiamyang S, Ui-eng J, Knongsai S, Leesakul N. (2019). Effect of Solvent Extraction on Phytochemical Component and Antioxidant Activity of Vine and Rhizome *Ampelocissus martini*. *STA*, 24(3), 17–26.
- Vittaya L, Na Ranong S, Charoendat U, Junyong S, Leesakul N. (2020). Bio-Activity Investigations of Extracts of Different Parts of *Lumnitzera littorea* Voigt. *Trop J Nat Prod Res*, 4(8), 365–371.

Use of Herbs and Traditional Medicine Among Asian Youths in the Digital Age: Cosmetics, Beauty, and Anti-Aging

Lavanchawee Sujarittanonta^{1*}, Lin fan² and Rajendra Khimesra³

¹*Faculty of Science and Technology, Rajamangala University of Technology Phra Nakhon (RMUTP), Bangkok 10800, Thailand*

²*College of Management, National Sun Yat-sen University, Kaohsiung City 804, Taiwan*

³*Birla Institute of Management Technology (BIMTECH), Uttar Pradesh 201306, India*

* *Corresponding email: Lavanchawee.s@rmutp.ac.th*

Abstract

The new age of digital medicine has revolutionized treatments for health and beauty, including cosmetics and anti-aging. Various technological solutions and digital tools are now readily available and easily accessible to help people maintain not only their health but also improve their physical appearance. At the same time, there is also a strong “back to nature” and “sustainability” wave that avoids chemicals and scientific processing. This research explores the use of herbs and traditional medicine among Asian youths of the digital age because this is the age group that is most conscious about their physical appearance and is educated through social media to be more concerned about environmental pollution’s effect on health and aging. Therefore, open-ended questions were asked through social media to youths aged between 18-22 in Thailand, Taiwan, and India to find out their use of herbs and traditional medicine for health, beauty, and anti-aging purposes.

It was found that most of our Taiwanese and Thai youth informants found environmentally friendly ways of staying young and healthy through their use of herbal plants, some of which also can slow down the normal aging process. Similarly, Indian medicinal systems such as Ayurveda, Siddha, and Unani have a long history; and more and more Indian youths are following environment-friendly traditional Indian medicine-based products for vitality, beauty, cosmetics, and anti-aging. We also found that both LGBT lifestyles, plastic surgery, and the magic of digital solutions had an extremely positive influence on beauty ideals in Taiwan, where the cosmetic industry is booming; meanwhile, in Thailand, creative campaigns promote herbs used in Thai cooking for their medicinal properties in boosting immunity against COVID-19.

Keywords: herb, traditional medicine, cosmetics, beauty, anti-aging, digital age, Asian youths.

Introduction

This research explores the use of herbs and traditional medicine among Asian youths of the digital age. In particular, the focus is given to herbs in China, India, and Thailand because China and India both have a long history of traditional medicine and continuous use and development to the present day. Hence, Chinese and Indian cultures can be considered the world’s origin and roots of herbal treatments and remedies for the Asian region. Thailand has been strongly influenced by both Chinese and Indian cultures through trade, migration, and religious influences (e.g. Confucianism, Taoism, Buddhism, and Hinduism). It is also interesting to find out how Thailand evolved on its own in this field as well, as Thailand is increasingly known for medical tourism, as well as a world-renown destination for spirituality, wellbeing, and beauty, not only for Thai traditional massage and spa treatments, but also for cosmetics, and even cosmetic surgery and sex-change operations.

Youths of the digital age are the focus of this study as this is the age group that is more conscious about their physical appearance, and at the same time are educated through social media to be more concerned about environmental pollution’s effect on health and aging. While they find

beauty to be easily attainable through cosmetic surgery, they also have readily available access to both chemical and natural options in their choice of cosmetic products and beauty treatments. At the same time, amidst these high-tech treatments, there is also a strong “back to nature” and “sustainability” wave that avoids chemicals and scientific processing.

Inevitably, with better health, people live longer. Therefore, the anti-aging properties are also the additional benefits of herbs, not just only beauty and health benefits. With the aging society in several countries including Thailand, being beautiful through herbal cosmetics and skin care applications, and herb consumption can also mean living longer and remaining beautiful or even looking younger (reverse aging).

This research collected data on the usage of herbs among youths in Taiwan, India, and Thailand to find out which herbs are commonly used by the digital age population for purposes of enhancing beauty and anti-aging.

Literature Review

In the evolution of beauty and health throughout human civilization, the use of cosmetics and skincare had the aim of protecting oneself from the environment. For example, according to INB Medical (2019), in ancient Egypt, ancient Greek, and Medieval times, commonly found food, fruits, vegetables, and herbs were used to protect their skin from the elements, such as milk, honey, olive oil, animal fat, vinegar, berries, cucumber, oatmeal, sesame, aloe vera, rosemary, etc. The goal was not only to clean and moisturize the skin but also to protect it from damage from the sun and dry weather conditions.

In addition, even during ancient times, certain foods when applied to the skin were believed to help slow down aging as well, such as Greek yoghurt (INB Medical, 2019). In the 1780s and 1800, chemical non-food skincare and cosmetics were then developed with brands of their own that are still widely used today, such as baby powder, Vaseline, etc. Common iconic brands that we know of today such as Ponds, Clearasil, and Estée Lauder were developed in the 1900s (INB Medical, 2019; Life Pharmacy, 2021).

However, as technological, and biochemical developments in cosmetics and anti-aging skincare progressed, skincare products also turned to various chemical formulas for anti-aging creams and serums (e.g. La Sala, 2021; Sephora.com), digital innovation of facial hypnosis treatments (Pierre-Fabre.com), along with more intrusive treatments such as fillers and Botox injections were introduced (Life Pharmacy, 2021), which unfortunately sometimes produced unexpected results and side effects, if not carefully administered properly. Moreover, the new age of digital medicine has also revolutionized treatments for health and beauty, including cosmetics and anti-aging. Various technological solutions and digital tools are now readily available and easily accessible to help people maintain and improve their complexion, such as nanotechnology in skincare (e.g. Salbioni et al., 2021), facial re-contouring (e.g. Mu, 2010) for example. Also, medical innovations today are so highly advanced that it is even now possible for people to change their body shapes, whereby drastic procedures are now accepted as necessary in some societies, even for high-risk procedures with daunting names like mega liposuction, fat hypertrophy, full-body surgery, body reshaping, etc. (e.g., Perén, Gómez and Guerrero-Santos, 1999; Lambros, 2020; Saha et al., 2021; Mala, 2022).

At the same time, amidst these high-tech treatments, there is also a strong “back to nature” and “sustainability” wave that avoids chemicals and scientific processing. In particular, with consumers’ concerns over chemicals and the associated allergies and undesirable side effects that could happen in the longer-term future, there are those who now prefer to play safe and resort to using food, fruits, and vegetables for their beauty and anti-aging needs. This is well-founded, as studies show that there is anti-aging potential from food-derived bioactive compounds, which technological advancements also make it possible to produce effective nutricosmetic and cosmeceutical products from natural and common foods that we eat in our normal everyday lives (Hernandez et al.; 2021).

Therefore, the following subsections present reviews of Thai, Indian and Chinese herbs:

Thai Herbs for Beauty, Cosmetics, Health, Anti-Aging, and COVID-19

In Thailand, herbal cosmetic products are widely available in various forms for consumers to choose from, ranging from moisturizers, whitening lotions, creams, powder, toner, make-up cleansing, mask, cleansing oil, soap bar, anti-aging lotions, and creams (Thanisorn & Chanchai, 2012), and at present, there is a high market potential for local herbal cosmetics, beauty and anti-aging products (Harnvanich et al., 2020).

A well-known example of a Thai herb that is widely used to produce skincare products is the traditional folk medicinal root with the scientific name *Pueraria mirifica* (Thai common name White Kwao Krua) cultivated in the Northern region of Thailand (e.g. Chansakaow et al., 2000; Cherdshewasart & Sutjit, 2008). *P. mirifica* has been extensively researched in the laboratory for the benefits of its rich phytoestrogen content, which has been used to develop cosmetics to enhance skin conditions (e.g., Kim et al., 2004; Trisomboon et al., 2006).

Earlier on in 2018 before COVID-19, at the 15th National Herb Expo of Thailand held on 18-21 July 2018 at IMPACT Muang Thong Thani (Thailand Today, 2018), the Director of the Institute of Thai Traditional Medicine, Department for Development of Thai Traditional and Alternative Medicine gave an interview to Thailand Today television program. Back then, four Thai herbs were selected under the national master plan, namely Curcumin for aging symptoms and anti-cancer, Black Galingale, *Centella asiatica*, and *Zingiber montanum* which are used in Thai massage shops. These four so-called “product champion herbs” were strategically promoted to the general Thai population to be used as home-based remedies, and highlighted specific herbal preparations or formulas from these herbs. These four herbs have been studied extensively by scientists for their anti-aging properties and use in cosmetics to enhance beauty (e.g. Sivamaruthi et al., 2018; Rafiee et al., 2019; Puangpradab et al., 2020; Astuti et al., 2021; Scamoroscenco et al., 2021).

And now, ever since the COVID-19 pandemic has hit, two more Thai herbs have come to the forefront as having beneficial properties. Firstly, Galingale (also known as Kaempfer, Finger root, Chinese keys, Chinese ginger) which is a preventative herb that boosts immunity against contacting COVID-19, and secondly is Kariyat (*Andrographis paniculata*) which is believed to help patients who have contracted COVID-19 (Kittapoop, 2022). While these two herbs are not directly used in cosmetics for beauty or anti-aging purposes, they both have properties in promoting health, and hence have an impact on overall wellbeing, good-looking appearance, and longevity.

With the pandemic, Galingale was also used in drinks and dishes (beverages and foods), so that the average Thai person can conveniently consume the herb in everyday life. Additionally, other herbs that are commonly used in Thai dishes such as Tom Yum soup, curries, and salads, were also studied for their properties in boosting immunity against COVID-19 (Bangkok Business News, 2020). Naturally, other countries with herbal traditional medicine cultures also began to explore other candidate plants with medicinal properties to enhance immunity against Coronavirus, e.g. China (Ahmad et al., 2022) and India (Sharma et al., 2022).

Similarly, there are also new opportunities in the future to study the benefits of Cannabis which has just been legalized in Thailand for medicinal purposes (Assanangkornchai et al., 2022) There are already studies in other countries on cannabidiol CBD in cosmetic products thanks to its sebostatic and antioxidant activities as a new anti-aging ally (Schettino et al., 2021; Michailidis et al., 2021), CBD oil shampoo (Landman, 2018), and for anti-aging through full-spectrum CBD’s highly restorative, texture-refining properties (Cream, 2020). Even hemp seed oil (*Cannabis sativa*) is also studied for its application as a non-drug dermo-cosmetic agent mainly for skincare (Baral et al., 2020).

Indian Herbs for Beauty, Cosmetics, Health and Anti-Aging

Indian Ayurvedic, Siddha, and Unani medicine systems have herbal cosmetic solutions (Lal, 2002). Ayurveda and Siddha and Unani are alternative medicine systems with historical roots in India. Ayurveda word originates from Sanskrit which means “The Science of Life” and stems from the ancient Vedic culture. It encourages certain lifestyle interventions and natural herbal therapies. Siddha system is like Ayurveda written in Tamil - a South Indian language practiced in Tamil language-speaking parts of India. In addition to disease, it focuses on the patient’s age, and habits, and uses natural herbs for treatments. Unani system of medicine originated from Greece enriched by Arabs and was brought to India during the medieval period. However, the Unani system uses ingredients of animal and marine origin, in addition to natural herbs.

Herbal cosmetics are currently driving growth as more people prefer organic products over chemical ones. Because they want products designed specifically for Asian skin, Indian consumers are drawn to Ayurvedic products. For more than two millennia, Ayurvedic cosmetics have changed and evolved. In 2022, revenue in the Herbal Cosmetics segment in India is expected to be US \$853.9 million. The market is expected to grow at 2.90 percent annually from 2022 to 2026 (Statistica, 2022).

From findings of a study by Patkar, & Bole (1997) on herbal cosmetics in ancient India, Ayurvedic anti-aging herbal products are excellent for revitalizing the skin, defying aging, and maintaining youthfulness. Herbs deliver moisture and hydration while also repairing deeper layers of skin. These herbs add shine and luster to the skin by stimulating its natural metabolism. Indian herbal products are well-known for their ability to boost strength, vitality, and immunity. Chavayanprash – a superfood for all ages – is used by Indians of all ages, not just the young. Young Indian women use the Indian herb Henna as a super hair care solution. Shampoos and other modern hair care products contain chemicals that cause hair loss and premature greying in many people. Natural herbal henna is now a well-known hair treatment all over the world.

According to a report on Beauty and Wellness Industry in India (Deshpande, 2021), young Indians of the digital age today are concerned about wrinkles and overall well-being. However, experts are concerned about the overuse of chemical cosmetics and more invasive treatments. Today’s younger beauty consumers are better informed scientifically about skincare, while others express apprehension about premature aging and wrinkles. Herbal cosmetics are not a fad or trend, and they are going to stay. People are becoming more aware of the long-term consequences of putting harmful chemicals on their bodies and are looking for alternatives. Makeup can also boost a person's appearance and demonstrate a sense of self-care. The emphasis on visual content has shaped how Generation Z youth perceive themselves. Digitally -the savvy youth wish to project a youthful image while sharing photos on Instagram, Facebook, and other social media platforms. They believe that beauty and youth are intimately connected. Herbal cosmetics have enabled Indian women and youth to define their identities outside of traditional contexts, demonstrating confidence and empowerment. The expansion of the digital and manufacturing sectors has resulted in a significant increase in demand for cosmetic herbal products in India.

Chinese Herbs for Beauty, Cosmetics, Health and Anti-Aging

Traditional Chinese medicine is built on the idea that beauty comes from within. Nature provides a whole pharmacy of herbs and revitalizes life energy (qi). For example, dermatology is a recognized specialty in traditional Chinese medicine. Treatment for skin disorders (acne, rosacea, dermatitis, psoriasis, eczema, alopecia, dry skin, and hives) have been described as early as 1100–221 PCT in China. Traditional herbs strengthen the immune system, balance the internal organ systems, release toxins from the skin, and stabilize the yin and yang systems. One of the authors has been using herbs for a decade with visible rejuvenating effects. The application of sesame seeds to moisten dry skin on a daily basis had a lot to do with it. Indeed, sesame lubricates dryness, working as an emollient when applied to dry and cracked skin; it also relieves constipation. Sesame oil also

detoxifies. It destroys ringworm, scabies, and most fungal skin diseases. It is a superior massage oil for sore muscles and the pain of rheumatism/arthritis (Blakeway, cited in Jhin 2011: 86).

So many herbs promote beautiful skin, from sophora to gypsum, mother-of-pearl shell, rehmannia root, honeysuckle flower, and others. Chinese medicine relies on eight branches: acupuncture, nutrition, herbs, body treatments, moxibustion and cupping, exercise, spiritual activity and lifestyle. The various effects of plants and minerals have been documented on the human body. Chinese medicine uses about 400 different herbs (Rekanaty 2019).

Aging is a natural process for all living organisms. In China, people usually say that “if there is a sunrise, there must be a sunset”. You cannot cheat nature. The Chinese like most other cultures have long searched for an elixir for eternal youth, and while people live longer with modern procedures, nature wins in the end. You just cannot beat it, and it is far too strong. We all get old, despite scientific advances, surgery, pills, or gene-altering techniques. This thought is so depressing that it motivated us to write this paper and dig deeper into recorded hopes of a longer and fuller life, even if it cannot last forever. We only want to stay young: is it too much to ask? Anyway, every living organism on Earth has a given lifespan. The maximum human lifespan is around 125 years. Traditional Chinese medicine is called the lifespan Tian Nian, the Heaven age. Most of us will not reach it. Traditional Chinese medicine teaches that an anti-aging process should focus on the detection, prevention, and treatment of aging-related diseases. Spirituality also plays an important role in longevity and well-being. It is not just about the body. We should use our brains to think, daydream, and create beautiful art (Hu 2015: 40).

Now let us take a specific example. *Schisandra chinensis* is a plant with high potential for beneficial health effects because it protects human fibroblasts (cells that produce skin tissue) from UV radiation. Other compounds in this plant demonstrate anti-aging effects. Celebrities such as Gwyneth Paltrow praise it as nothing less than a “beautifying stamina booster” (Active Herb 2022). It tonifies qi as well as the kidneys. Indeed, the production of qi, blood, and other fluids tends to decline with age. This means from a Western perspective that the sebaceous oil glands are affected, in turn producing dry, aged-looking skin. Now the spleen is the primary organ for transforming nutrients from food into qi. When people have deficient qi, there isn’t enough blood to nourish their skin tissue. Blood stagnation and internal phlegm accumulate, and they get visibly old (ibid).

We could take hundreds of other examples. Our point is that the past yields even more solutions than the present. After all, as Xue (2021) points out, a Chinese empress may have had beautiful skin thousands of years before serums and foaming cleansers were invented. We want to urge our readers, therefore, to purchase these herbs. A quick trip to the Chinese pharmacy or a herbal clinic will make the three most often used herbs (bei qi, huang qi, and goji) available at a decent price. If you are still hesitant, ask yourself - how much would you price your own life? Isn’t health and beauty worth a little investment from time to time? You get the idea. Xue (2021) also reminds us of the necessity of learning which herbs are best for you, drinking the right tea, trying a jade roller, understanding the power of mung beans, and finally “DIY a turmeric mask”. Other common ingredients include ginseng, Solomon’s seal rhizome, wolfberry fruit, ginkgo leaves, dates, raspberries, Siberian ginseng, and pollen. All that stuff helps to maintain spotless skin. But again, if you are thinking of long-term consumption, better consult a physician for a customized prescription. Herbs will help the body repair itself; in other words, they will assist the body to function as if we were younger. Common foods recorded in ancient books for “beauty”, “anti-aging” and “rejuvenation” purposes are sesame, honey, mushrooms, dairy products, pumpkin seeds, lotus root, watermelon, cherries, wheat, and radish. So, if you get to hold them in your local grocery store or supermarket, don’t hesitate to go for them. You can’t be wrong there. And if you want to keep your skin healthy you can add white fungus, lily buds, red dates, bird’s nests, sea cucumbers, oysters, soft-shelled turtles, eels, pigskin, and animal bone marrow to your list. These ingredients nourish yin and promote blood production (Shen Nong 2022).

Finally, traditional Chinese medicine in cosmetics is based on the yin-yang principle of balance. These two opposite and interdependent aspects maintain a dynamic relationship. Once the balance is destroyed under certain conditions, the human body turns toward a pathological state, including beauty-damaging diseases. Traditional Chinese medicine treats these diseases using both internal and external therapies. Take the example of a dull complexion. Treatment regimens include the external application of Yun-Mu Cream, which improves blood circulation and defecation, but also rest a rational diet, and harmonized mental states. All of these factors influence skin appearance. So Eastern cosmetics have different connotations from their Western counterpart. They are rooted in thousands of years of Chinese pharmacological theories. Their guiding principle in the care of the qi, is not a focus on make-up or superficial decoration. If you want to retain youthful looks, try your best to stay in harmony with nature, and please, please don't move away from Tao (Li 2013).

Methodology

To collect data on herb usage for beauty and anti-aging, as well as herbs in cosmetics, open-ended questions were asked through social media and interviews (as appropriate) to Thai, Indian and Taiwanese youths aged between 18-22 to find out their use of herbs and traditional medicine for health, beauty, and anti-aging purposes. Given the pandemic that is still ongoing at the time of the research, there is also a question to help stimulate respondents' awareness of the potential of herbs to increase immunity against COVID-19.

Basically, the researchers were searching for the respondents' actual use of herbs, at the same time also hoping to find out if they know of other countries' herbs. The respective Thai, Indian, and Taiwan researchers were freely able to make judgments on the mode of social media, collecting data in the style that they considered most suitable in finding answers to these questions (approximately) as follows:

Please help share what you know about Indian, Thai, and Chinese herbs! Please share with your friends and family, especially youths! We also want to know if the digital age new generation of people still believes in traditional natural herbs.

Question 1: Do you know any herbs that are used for health and beauty care? (Can you share the names of the herbs and how you use them, e.g. eat/apply, etc.) We would like to know your awareness of Indian herbs, Thai herbs, Chinese herbs, and herbs from other countries. [Answer as far as you know]

Question 2: Personally, what herbs do you use for 1) taking care of your beauty/handsomeness 2) enhancing health 3) anti-aging 4) using it as a cosmetic 5) Can you give examples, tell me how to use it, and the product/brand (if you have)? (We would like to know which herbs/brands are well recognized.) [You might not be able to answer every question; it's OK]

Question 3: Do you know of any herbs that can help increase immunity and/or resist COVID-19, and what are the food dishes that contain these herbs? (We want to know more about your national food that can help fight Coronavirus.

In a casual friendly manner, the researchers encouraged the respondents to open up and share their knowledge and usage of herbs for cosmetics, beauty, and anti-aging, which for some might be a sensitive personal topic. It is also an opportunity for the researchers from 3 countries with different cultures (French researcher in Taiwan, Indian researcher, and Thai researcher) to learn more about popular herbal cosmetics brands in each country, to develop further in future research.

Findings and Analysis

It was found that most of our Taiwanese and Thai youth informants found environmentally friendly ways of staying young and healthy through their use of herbal plants, some of which also can slow down the normal aging process. Similarly, Indian medicinal systems such as Ayurveda, Siddha, and Unani have a long history; and more and more Indian youths are following environment-friendly traditional Indian medicine-based products for vitality, beauty, cosmetics, and anti-aging. We also found that both LGBT lifestyles, plastic surgery, and the magic of digital solutions had an extremely positive influence on beauty ideals in Taiwan, where the cosmetic industry is booming; meanwhile, in Thailand, creative campaigns promote herbs used in Thai cooking for their medicinal properties in boosting immunity against COVID-19.

Findings and Analysis from Thailand

The Thai data came from the highest number of respondents in this study, a total of 50 university students. The findings can be divided into 4 categories – Thai herbs, foreign herbs, herbs for combatting Coronavirus, and herbal brands.

For Thai herbs, the data collected included common vegetables as well as herbs. They are (in alphabetical order) *Acacia concinna* leaves, aloe vera, amla, basil, red basil, holy basil, black galingale or *Kaempferia parviflora* (KP), cannabis, cassia, *Centella asiatica*, chilli peppers, coconut oil, cucumber, galangal, garlic, ginger, lemongrass, liquorice, mint, lemon balm mint, *Mitragyna speciosa*, sesame seeds, tamarind, tomatoes, and turmeric.

Not surprising given Thai cultural linkage throughout history with China and India, the Thai youth respondents were familiar with Chinese herbs, namely Chinese Angelica or Dong quai, Chinese chrysanthemum tea, Chinese Fleeceflower Root, Chinese ginkgo, Chinese goji berry, and Chinese Lucid Ganoderma. For Indian herbs, the respondents specifically mentioned Indian cloves, Indian gooseberry, Indian Henna, and Indian turmeric. The respondents also mentioned other foreign herbs such as the neighboring ASEAN country's national herbs such as Myanmar Tanaka, Vietnamese turmeric, as well as the famous Korean ginseng, Italian oregano, and USA cranberries. One respondent mentioned *Madagascar centella* herb.

Not surprisingly, the herbs for combatting Coronavirus were overwhelmingly the nationally promoted galingale and Kariyat. But interestingly, other common herbs that were mentioned for combatting were amla, bael, lemongrass, turmeric, ginger, and one respondent offered an interesting herb, *Houttuynia cordata* Thunb.

The brands of herb products that were mentioned are not just Thai brands, but also international brands. The Thai brands were Bennett (a Thai soap brand), Kongka Herb (shampoo), Palmmade (skincare and oral care), Supaporn powdered turmeric. International brands were Carmex, Kiehl's, Nature Republic, Protex, Smooth E, Snail bright and Tropicana brand coconut oil. Several brands that youth respondents mentioned were all South Korean brands, namely CICA (a range of *C. asiatica* skincare products), Hanasol (aloe vera gel), JOJU and NAMI and SKIN1004; which is not surprising considering the success of K-Beauty, as South Korea's exports of cosmetic products continue to soar globally.

Apparently, Thai youths care a lot about their appearance and sought Thai herbs and foreign herbs in their natural form, both to eat and to prepare for use on their skin. Thai brands, as well as imported brands, were also familiar to Thai youths of the digital age. This could be because Thai culture is open to foreign influences and the Thai market is open to imports from overseas.

Findings and Analysis from India

The India survey form was responded to by 12 Indians. It was found that the most mentioned, and hence likely to be best known and most often used, were aloe vera and turmeric (haldi); followed by amla and neem; and the third most mentioned were ashwagandha, coriander seeds, giloy, mint,

parsley and Chyawanprash (mixed herb). Others that were mentioned one time each were ajwain, asofeditia, avocado, beetroot, Brahmi, cardamom, cilantro, cloves, cumin seeds, fennel seeds, fenugreek seeds, flaxseeds, gram flour, henna, lotus seeds, sandalwood (for acne), thyme and tulsi. Interestingly, marijuana and opium were also mentioned for medical use.

For combatting Coronavirus, findings suggest that it is not necessary to use unusual and rare herbs, as it is believed that commonly found herbs that are eaten in normal daily foods also help fight against COVID-19, namely adrak (ginger), amla (Indian gooseberry), basil, cinnamon, coriander, giloy, methi, neem, turmeric, and vati. Ganja or cannabis was also suggested that it might help to mitigate COVID-19.

From the findings above, as most of the respondents were using these herbal medicines and treatments, the Indian researcher of this study summarized the beauty-boosting and anti-aging properties of selected Indian herbs below:

- Turmeric or Haldi: This ingredient is undoubtedly indispensable in Indian culture for beauty and skin treatments. It is widely used for brides and grooms in Indian weddings to lighten and revitalize the skin for centuries. It can reduce pimples, and stretch marks, reduce wrinkles (anti-aging) and treat cracked heels. Hot milk with turmeric powder soothes the throat and prevents cough.
- Amla or Indian Gooseberry: It is widely used for hair treatment and nourishing hair.
- Neem: Neem is a popular wonder herb, and every part of its plant is very useful. It is used for the skin treatment of acne, which is common in Indian youth. Its treatment prevents dry skin. It is also used for controlling dandruff.
- Aswagandha: It can be called Indian ginseng for its usage by the young for energy, vitality, and immunity. Aswagandha supplements benefit male fertility and increase testosterone levels. It also treats to reduce stress and mental health issues that affect the overall well-being of youth.
- Chyawanprash: Chyawanprash herbal formulations improve vigor, and vitality, and delay the aging process due to their antioxidant properties. It also helps to remove toxins from the body and heart health by lowering cholesterol levels of youth increased by modern fast foods.
- Sandalwood: Sandalwood possesses antiseptic properties and even helps in blood circulation under the skin. It is used for a clear and glowing skin by youth widely and Indian film actresses as well.
- Henna: Also known as mehndi, henna is used for hair treatment in place of shampoos. It makes hair healthy and silky. It prevents premature hair fall also. Its antifungal and antimicrobial properties are beneficial for the hair and scalp, premature graying, and for reducing dandruff. Henna can cover gray hair and leave an auburn or reddish-orange tint on the strands.
- Brahmi: Brahmi or Bacopa monnieri is used by young people for boosting memory, and immunity, and reducing anxiety. Very popular among students during the examination period.
- Giloy: Giloy or Tinospora Cordifolia improves immunity and is used as an antiaging agent. It is full of antioxidants and helps to release toxins from the body. Giloy juice also detoxifies the skin. It is also used for liver diseases, urinary tract infections, and hard-related issues.

Indian brands of skincare that the respondents gave were: Himalaya, Patanjali, Vicco, and Young living. These brands are very well known and readily available throughout the Indian continent, and the brand Himalaya is now also available in Thailand at select convenience stores and pharmacies.

For those familiar with the LGBT Indian, scene, the ‘queer’ disposition is not a modern-age concept. Ancient mythologies display queer characters Shikhandi and Hindu deity Ardhanarishwar or the androgynous god – images now being realized by designers as a source of inspiration. In India, the Lakme Fashion Week was illuminated by celebrities like Prateik Babbar and Ranveer Singh reshaping the gender-based clothing norms by walking the runway in men’s skirts. As most fashion influencers comment, “it was so hot”. This is not surprising, as fashion experts realized that LGBT trends constitute “a silent but powerful kind of revolution, with new concepts breaking the conventional gender-based norms” (Apparel Resources 2021).

Findings and Analysis from Taiwan

By the same token, in Taiwan, the most powerful ideas about beauty and diet were found among LGBT students. We interviewed 78 students at three universities in Southern Taiwan (at Wenzao University, National Sun Yat-sen University, and National Kaohsiung University of Hospitality and Tourism). Among those, 34 were LGBT students who looked healthier and significantly younger than their straight counterparts. Pressed to find reasons why they told us that straight people had poor health management and limited taste in cosmetics. They also underuse dietary supplements and Chinese herbs. As Bobby (Wenzao University) clarifies,

“it’s just so visible, they don’t really care about their physical appearance. They assume it’s clear the other gender will have an interest in them. When we, LGBT members must fight to be recognized, that means we work harder on recognized looks. I mean, when I look at this guy over there [pointing], it’s clear he’s just bought his jeans from Zara and doesn’t clean his shoes. I bet he’s even bought these ugly trousers on the promotion rack [snarling], and don’t get me started on his face. He’s just not applying any cream anywhere, and he needs it!”

Jenny (National Sun Yat-sen University) concurs when she says that

“straight people usually don’t believe in traditional medicine. When my father explained how I could manage my yin and yang to look younger, I saw the point straight away. Look, it’s this simple equation, right? Younger = more attractive = more popularity = more potential girlfriends. Yes, I’ve studied accounting but I don’t need it to find that out, okay? It’s kinda of common sense. But you see [winking], lesbians love smart girls, whereas so many straight girls just want to be passive little dolls... they wait to be adopted and dominated by powerful males. I’ll never forget how the “Me Too” movement in Taiwan helped me realize that most men were dormant predators or, worse, rapists to be. It’s way safer to be a lesbian currently, like, I also get a stronger sense of solidarity from fellow LGBT people.”

Steven and Fiona, both from National Kaohsiung University of Hospitality and Tourism, use a combination of exercise, plastic surgery, and Instagram filters to rejuvenate their image. At 22 years old they have both undergone minor operations to get firmer, rounder, bigger breasts (Fiona) and a smaller nose and bigger eyes (Steven) for a decent price. As Steven reports,

“plastic surgery has been on the rise in Taiwan. There are many reasons behind this popularity: first, I’d say, it’s become much more affordable. You see, I spent only 32000NT for my nose job and I heard it was at least twice this price 15 years ago, for a more dubious result. How do you like my nose? [laughing] I know, my friends and family just love it. The surgeon is a star, my auntie got her new face from him and I was dying to see what he could do with my skin. The day after, I went to get this tattoo [he shows a muscled torso, with a tiger on it]. Yes, I know, it’s the year of the tiger, but that wasn’t the reason I did it [laughs]!”

Fiona explains the benefits of becoming an influencer on the right channels:

This was me 4 years ago [shows a photograph on her mobile phone]. Yes, I know, I looked terrible! And look at me now. I can't believe it myself. Do I need to tell you how terrible I paid for my boob job? No, okay, better that way [laughs]... I mean, I don't regret it at all. And let me tell you why. I'm an influencer on Instagram, I sing and play the piano, and I have around 850 followers now and growing. I need to look good. First, you need a good basis, a body that's watchable; then you add filters. You can choose among so many, and even when you don't have time to apply makeup a nice filter can do the trick, you know? So, don't underestimate the power of technology.

About 12 interviewees from these three universities mentioned traditional Chinese medicine without being prompted. When prompted, it became clear that LGBT students knew much more about the range of products and ways of applying or consuming them than straight students. We believe that this is because of a stronger focus on bodily and spiritual cultivation. As Steffy (National Sun Yat-sen University) confesses,

“My family didn't talk about herbs. I just found out that if I wanted to stay young and pretty, I'd have to care about my body. And what's better than the old-fashioned, natural stuff uh? So I went to fish for information on the internet. My uncle was like, “what's up, what are you doing browsing those strange pages?” And I said, “if you checked that kind of information before, you wouldn't look so old now!” [giggles]

So we conclude that traditional medicine and the cosmetic industry in Taiwan will keep growing to satisfy a dynamic and demanding youth.

Conclusion, Policy Implications, and Recommendations

The findings obtained from digital-age youths in Thailand, India, and Taiwan offer different perspectives of how digital-age youths respond to questions about herbs, and what they know about herbal properties on beauty, cosmetics, and anti-aging. To some, this topic might be considered sensitive, private, and personal. Nevertheless, the variety of responses from all three countries converge, and it can be concluded that digital age youths have considerable knowledge about herbs, despite the technological advancements in chemicals and surgical treatments for improving one's physical appearance.

Thai youths were not only familiar with Thai herbs, but also familiar with Chinese and Indian herbs, as well as herbs from other countries. However, this set of respondents did not mention specific Indian and Chinese brands, even though they have access to the Chinese and Indian herbs for the actual herbal content, rather than for the brands. A few Thai brands were mentioned, as well as international American brands. Instead, the Thai respondents mentioned mostly Korean brands that are being sold at convenience stores and pharmacies (e.g. 7-11, Watson's, Boots), which is evidently showing the successful efforts of K-Beauty campaign to Thailand.

Policy wise, Thai, Indian, Taiwanese and Chinese herbal brands can definitely learn from the success of Korea soft power which influences several aspects of a Thai youth's daily life, thanks to Korean actors in drama TV series, popular music and dance moves by K-Pop boy bands and girl bands, Korean food and snacks, and in particular, the novel features of Korean skin care and cosmetics which incorporates natural herbs with new technology (e.g. facial cream that turns into a clear easily absorbed liquid when massaged into the skin, etc.), and also skin care that is packaged very attractively that tempt youths to buy for the pretty containers.

It can be concluded from the Indian research findings that Indian herb-based cosmetics are widely used by Indian youths as well as Indian-origin youths. Although India is well known for

world-class IT talent, Indian youths of the digital age are fully aware of and trust the benefits of herbs used in Ayurvedic and other Indian medicine systems for skincare, haircare, health, vitality, immunity, etc. Long-term use of using chemical-based skincare and haircare products can result in early wrinkles, graying of hair, and hair fall. More and more Indian youths are using energy booster herbal supplements for vitality and immunity. Awareness about herbal treatments can be attributed mainly to family traditions, whereby an average Indian household would always have fresh and dried herbs readily available for daily cooking and conveniently around too alleviate minor discomfort, ailments and for external application on the skin.

The Indian researcher added that perhaps an explanation for why Thai respondents know about Indian herbs could be since herbal beauty and cosmetic products, in general, are available easily in Thailand at economical costs, adding to the fact that herbs are non-toxic, in comparison to chemical cosmetics and skincare products. The Indian researcher also recommends that Thai youth is educated about the advantages of herbal products in collaboration with Indian Ayurvedic institutions. Due to similar philosophies in Indian and Buddhist culture, there would be more synergy to promote herbal cultures in Thailand and other Asian countries.

The Taiwan findings comprised qualitative in-depth interview data from LGBT respondents, who are in general known for their emphasis on physical appearance. Thus, the data from the Taiwan research greatly helped to enrich the herbal information that was obtained by the Thai and Indian research, making the research well rounded and more complete, having a human side of emotion in relation to beauty and anti-aging concerns, rather than having just herb knowledge and herb usage information. Thai culture is also open to LGBT and can be considered to even celebrate sexual identity freedom. Thus, Taiwan data suggests that the LGBT aspect offers immense market opportunity since this group of digital youths not only are more particular about their beauty in real life but also give great attention to and are willing to put in more effort towards their online virtual image.

Correspondingly, the findings also suggest that there is a great opportunity for exporting herbs overseas, given the awareness and usage of herbs by youths in each country of this study. The youths could be introduced to another foreign country's herbs, perhaps through social media, possibly learning from the strategies of K-Beauty. For example, Indian youths could learn more about Chinese and Thai herbs, and Chinese youths could also be introduced to Indian and Thai herbs, etc. More recently, Bollywood movies have gained a sudden burst of popularity in Thailand, such as the top hit movie “Gangubai” on Netflix, which has caused a trend in Thailand among women from every echelon of Thai society to post themselves on social media posing and dancing while wearing all white saris and sporting a big red bindhi between their eyebrows, following the wardrobe of the main character Gangubai.

Since it was found that Thai respondents were the group that was most aware of Indian and Chinese herbs for enhancing the beauty and anti-aging, it could be suggested that the use of Indian and Chinese herbal solutions for skincare, haircare, immunity, and vitality has high potential in the Thai market, and will also likely increase in popularity among ASEAN youths, since countries like Myanmar, Cambodia, and Vietnam also recognizes Thai beauty brands. Moreover, as countries move to sustainability and BCG- bio circular & green economies, herbs have high appeal, especially among the youths of the digital age who grew up, with environmental protection concerns, and even experienced environmental pollution personally in real life, e.g., PM 2.5. With the forecast for increased consumption, it is important to bear in mind that herbs are agricultural produce, therefore their availability with growing demand may be a challenge.

As for herbs and COVID-19 prevention and cure, Thai and Indian respondents offered herbal remedies, which consisted of common herbs found in Indian and Thai cooking. This is not surprising in the case of Thailand, where the Thai government has been actively carrying out public campaigns to promote galingale and Kariyat. By nature of Thai food and Indian food which uses a lot of herbs

as an ingredient, in comparison to Chinese food which does not use many herbs, this study found that digital age youths in Thailand and India are also very aware of common herbs that are used in Thai and Indian food, how certain herbs can be used in daily foods, in regular daily cooking, for their medicinal properties in boosting immunity against COVID-19.

Acknowledgements

Authors gratefully acknowledge the help of Rajamangala University of Technology Phra Nakhon (RMUTP), National Sun Yat-sen University (NSYSU) and Birla Institute of Management Technology (BIMTECH) for supporting this research.

References

- Active Herb (2022) Feed Your Skin: How Chinese Medicine Enhances Your Beauty From The Inside Out, <https://www.activeherb.com/blog/feed-your-skin-anti-aging-effect.html> Last accessed February 09, 2022
- Ahmad, M. H., Afzal, M. F., Imran, M., Khan, M. K., & Ahmad, N. (2022). Nutrition: A Strategy for Curtailing the Impact of COVID-19 Through Immunity Booster Foods. In Handbook of Research on Pathophysiology and Strategies for the Management of COVID-19 (pp. 253-269). IGI Global.
- Alegría Perén, P., Barba Gómez, J., & Guerrero-Santos, J. (1999). Total corporal contouring with megaliposuction (120 consecutive cases). *Aesthetic plastic surgery*, 23(2), 93-100.
- Assanangkornchai, S., Thaikla, K., Talek, M., & Saingam, D. (2022). Medical cannabis use in Thailand after its legalization: a respondent-driven sample survey. *PeerJ*, 10, e12809.
- Astuti, I. Y., Yupitawati, A., & Nurulita, N. A. (2021). Anti-aging activity of tetrahydrocurcumin, *Centella asiatica* extract, and its mixture. *Advances in Traditional Medicine*, 21(1), 57-63.
- Bangkok Business News (2020). 7 อาหารไทยต้าน 'โควิด-19' เปิดสรรพคุณเด็ดที่ช่วยป้องกันไวรัส Seven Thai food against COVID-19. (18 March 2020). <https://www.bangkokbiznews.com/lifestyle/871359>
- Baral, P., Bagul, V., & Gajbhiye, S. (2020). Hemp Seed Oil for Skin Care (Non-Drug *Cannabis sativa* L.: A Review.
- Chansakaow, S., Ishikawa, T., Sekine, K., Okada, M., Higuchi, Y., Kudo, M., & Chaichantipyuth, C. (2000). Isoflavonoids from *Pueraria mirifica* and their estrogenic activity. *Planta medica*, 66(06), 572-575.
- Cherdshewasart, W., & Sutjit, W. (2008). Correlation of antioxidant activity and major isoflavonoid contents of the phytoestrogen-rich *Pueraria mirifica* and *Pueraria lobata* tubers. *Phytomedicine*, 15(1-2), 38-43.
- Cream, C. L. F. (2020). Where Nature & Science Meet Skincare, Haircare, Beauty & Wellness. Aging, 22.
- Deshpande, Rohan (2021). *Beauty and Wellness Industry in India Report 2020-2021*. Department of International Trade Promotion (DITP) Thailand. [https://www.crescendoworldwide.org/inner-common/report/BEAUTY%20AND%20WELLNESS%20INDUSTRY%20IN%20INDIA%20\(2\).pdf](https://www.crescendoworldwide.org/inner-common/report/BEAUTY%20AND%20WELLNESS%20INDUSTRY%20IN%20INDIA%20(2).pdf) Last accessed February 14, 2022
- Digital innovation: Taking care, living better. www.pierre-fabre.com/en/innovation-and-partnerships/360deg-innovation. Last accessed February 08, 2022
- Harnvanich, E. A., Wanichwecharungruang, S., Chandrachai, A., & Asawanonda, P. (2020). Market Potential Evaluation for Local Herbal Extracts Used in Skincare Through the New Product Development Process. *PSAKU International Journal of Interdisciplinary Research*, 9(2).
- Hernandez, D. F., Cervantes, E. L., Luna-Vital, D. A., & Mojica, L. (2021). Food-derived bioactive compounds with anti-aging potential for nutricosmetic and cosmeceutical products. *Critical Reviews in Food Science and Nutrition*, 61(22), 3740-3755.

- Hu, Helen H. (2015). Chinese Food Therapy Rx for Self Healing: Volume II, *Beauty and Longevity*, San Diego: Hu House Publishing International.
- INB Medical (2019). A brief history of skincare through the ages. www.inbmedical.com/the-evolving-role-of-skincare Last accessed February 08, 2022
- Jhin, Marie (2011). *Asian Beauty Secrets: Ancient and Modern Tips from the Far East*, San Francisco: Bush Street Press.
- Kim, B., Jung, S. W., Lee, J. D., Ryoo, H. C., & Cherdshewasart, W. (2004). Clinical Study of Cream Containing Pueraria mirifolia for Skin Elasticity. *Journal of the Society of Cosmetic Scientists of Korea*, 30(3), 385-388.
- Kittakoop, P. (2022). Folk Wisdom of Thai Traditional Medicine and Its Use as Products ภูมิปัญญาชาวบ้านของสมุนไพรไทยและการนำไปใช้เพื่อเป็นผลิตภัณฑ์. *The Journal of Chulabhorn Royal Academy*, 4(1), 15-23.
- La Sala, C. (2021). Dermatologists share the 18 best anti-aging skin care products of 2021. New York Post. <https://nypost.com/article/best-anti-aging-skin-care-products-per-dermatologists/>
- Lal, B. B. (2002). *The Sarasvatī flows on: the continuity of Indian culture*. Aryan Books International.
- Lambros, V. (2020). Commentary on: fat hypertrophy as a complication of fat transfer for hemifacial atrophy. *Aesthetic Surgery Journal*, 40(4), NP131-NP132.
- Landman, B. (2018). Your Annotated Awards Season Beauty Calendar: From CBD oil to extreme exerciser EmSculpt, anti-aging doctors and skin practitioners treating Lady Gaga and Rachel Weisz nail down what to do and when. *Hollywood Reporter*, 424(40), S74-S74.
- Li, Huiliang (2013) Traditional Chinese Medicine in Cosmetics. <https://www.cosmeticsandtoiletries.com/research/literature-data/article/21836138/traditional-chinese-medicine-in-cosmetics> Last accessed February 09, 2022
- Life Pharmacy (2021). A brief history of iconic skincare and must have brands you will love. www.lifepharmacy.co.nz/beauty-bible/brands-we-love/a-brief-history-of-iconic-skincare-and-must-have-brands-you-will-love/ Last accessed February 08, 2022
- Mala, A. J. (2022). Butt Reshaping/Gluteal Recontouring Surgeries in Aesthetic and Regenerative Gynecology. *Aesthetic and Regenerative Gynecology*. Springer, Singapore. 209-220.
- Michailidis, D., Angelis, A., Nikolaou, P. E., Mitakou, S., & Skaltsounis, A. L. (2021). Exploitation of *Vitis vinifera*, *Foeniculum vulgare*, *Cannabis sativa* and *Punica granatum* by-product seeds as dermo-cosmetic agents. *Molecules*, 26(3), 731.
- Mu, X. (2010). Experience in East Asian facial recontouring: reduction malarplasty and mandibular reshaping. *Archives of Facial Plastic Surgery*, 12(4), 222-229
- Patkar, K. B., & Bole, P. V. (1997). *Herbal cosmetics in ancient India with a treatise on planta cosmetic*. Bharatiya Vidya Bhavan.
- Puangpradab, R., Suksathan, R., Kantadoung, K., & Rachkeeree, A. (2020). Antioxidant and antityrosinase activities of rhizome extracts from six Zingiber species in Thailand. *Medicinal Plants-International Journal of Phytomedicines and Related Industries*, 12(1), 27-32.
- Rafiee, Z., Nejatian, M., Daeihamed, M., & Jafari, S. M. (2019). Application of curcumin-loaded nanocarriers for food, drug and cosmetic purposes. *Trends in Food Science & Technology*, 88, 445-458.
- Rekanaty, Helga (2019). *Beauty has its own Rules: Everything there is to Know on the New World of Beauty Treatments*, New York: Partridge.
- Saha, D., Thannimangalath, S., Budamakuntla, L., Loganathan, E., & Jamora, C. (2021). Hair Follicle Grafting Therapy Promotes Re-Emergence of Critical Skin Components in Chronic Nonhealing Wounds. *JID innovations*, 1(3), 100041.

- Salvioni, L., Morelli, L., Ochoa, E., Labra, M., Fiandra, L., Palugan, L., ... & Colombo, M. (2021). The emerging role of nanotechnology in skincare. *Advances in colloid and interface science*, 293, 102437.
- Schettino, L., Prieto, M., Benedé, J. L., Chisvert, A., & Salvador, A. (2021). A Rapid and Sensitive Method for the Determination of Cannabidiol in Cosmetic Products by Liquid Chromatography–Tandem Mass Spectrometry. *Cosmetics*, 8(2), 30.
- Scomoroscenco, C., Teodorescu, M., Raducan, A., Stan, M., Voicu, S. N., Trica, B., ... & Cinteza, L. O. (2021). Novel gel microemulsion as topical drug delivery system for curcumin in dermatocosmetics. *Pharmaceutics*, 13(4), 505.
- Sephora Anti-Aging Cream & Anti-Aging Products. www.sephora.com/shop/anti-aging-skin-care Last accessed February 08, 2022
- Sharma, A., Bhattacharyya, M., Bhatia, M., & Patni, B. (2022). Exploration of Some Candidate Plants with Medicinal Properties to Enhance Immunity against Coronavirus Pandemics: A Review.
- Shen Nong (2022) Keeping the Skin Young. http://www.shen-nong.com/eng/lifestyles/tcmrole_aging_skinyoung.html Last accessed February 09, 2022
- Sivamaruthi, B. S., Chaiyasut, C., & Kesika, P. (2018). Cosmeceutical importance of fermented plant extracts: A short review. *Int. J. Appl. Pharm*, 10, 31-34.
- Thailand Today (2018). Episode 195: The 15th national Herb expo (Thai herbal products & Thai local wisdom) Jul 17, 2018. https://youtu.be/TCreqhFM_iE Last accessed February 15, 2022
- Thanisorn, R., & Chanchai, B. (2012). Thai Consumers' Perception on Herbal Cosmetic Products: A Comparative Study of Thai and Imported Products. *Information Management and Business Review*, 4(1), 35-40.
- Trisomboon, H., Malaivijitnond, S., Cherdshewasart, W., Watanabe, G., & Taya, K. (2006). Effect of *Pueraria mirifica* on the sexual skin coloration of aged menopausal cynomolgus monkeys. *Journal of Reproduction and Development*, 0606220031-0606220031.
- Xue, Faith (2021) 5 Ancient Chinese Beauty Secrets for Better Skin. <https://www.byrdie.com/ancient-chinese-beauty-secrets> Last accessed February 09, 2022



RMUTCON

Session 4:

**Nanotechnology and
Applied Materials**

Effects of Modified Palm Oil and Surface Treatment on the Properties and Biodegradability of the Thermoplastic Starch

Piyawan polpanich, Kullawadee Sungsanit* and Somkiat Thitipoomdecha

Department of Materials and Metallurgical Engineering, Faculty of Engineering, Rajamangala University of Technology Thanyaburi, Pathumthani 12110, Thailand

** Corresponding email: Kullawadee.s@en.rmutt.ac.th*

Abstract

The application of thermoplastic starch with modified palm oil is to produce disposable food packaging with the properties of moisture resistance, dimension stability and heat resistance. These probably have effects on biodegradation. Therefore, this research aims to study the biodegradability and mechanism of thermoplastic starch packaging by using a co-digestion system with organic waste generated in the household. The thermoplastic starches specimens were prepared from the extrusion and compression process. Some of them were mixed with 5 phr. of modified palm oil that was prepared by ultraviolet irradiation. The results show that addition of modified palm oil into thermoplastic starch allows specimens to absorb less water and maintain their shape for more than 18 hours. Subsequent, the typical thermoplastic starch specimens with 5 phr. modified palm oil were treated with sodium hydroxide solution in concentration of 0.5 molar. The specimens were composed with organic waste in a specially designed fermentation tank. As the results, treated specimens caused in higher surface area that the microorganisms can fix with and causing faster degradation than without pretreatment and biodegradation occurs at a higher rate as well. The study also found that the typical specimens have been digested completely in 2 months whereas the specimens with modified palm oil can be digested in 3 months. Finally, the application of thermoplastic starch with modified palm oil can be composted completely via co-digestion with organic wastes using the low-cost fermentation tank model.

Keywords: Thermoplastic Starch, Biodegradation, Co-digestion, Organic Waste

Introduction

Nowadays, biodegradable plastics are increasingly being used instead of conventional plastics. Due to the problem of plastic waste that affects the environment including the high cost of general plastic waste disposal. Thailand is an agricultural country that is rich in agricultural raw materials such as rice, corn, sugarcane, cassava and beans, which can be used as raw materials for the production of bio-based plastics especially thermoplastic starches (TPS). However, the use of thermoplastic starches has a limitation, namely its sensitivity to moisture, toughness and low heat resistance. Therefore, the properties of thermoplastic starches have been improved to make them more versatile by mixing with other polymers such as polyethylene vinyl alcohol polylactic acid polybutylene succinate and polycaprolactone, etc. (Shin et al. 2011; K. Jarukumjorn et al. 2013; Huang et al. 2005; Da Roz et al. 2006; Rodriguez-Gonzalez et al. 2014). The researcher has the idea of using palm oil which is the main economic crop with excessive quantity (over 6 hundred thousand tons of the system) and resulted in lower prices. Especially, palm oil contains the same amount of saturated and unsaturated fatty acids that contains monoacids (oleic acid 38-44%) and polyunsaturated fatty acids (Linoleic acid 9-12%). There is the potential to be used to improve their chemical structure by ultraviolet irradiation as well as castor oil (Gironès et al. 2012; Vilaseca et al. 2007; Wattanaakornsiri et al. 2012; A. Polcharoen et al. 2015). These are the development of bio-based materials which are environmentally friendly and safe for product users to replace materials from petrochemicals that have problems with degradation. In addition, there is a way to dispose of organic

waste in the house together with the waste from biodegradable plastic by using co-digestion technique that can be applied in households or communities. Therefore, this research aims to study the biodegradability and mechanism of thermoplastic starch packaging via a co-digestion technique with organic waste to reduce the cost of waste management operations.

Materials and Methods

Materials

Cassava Starch Red Cat Brand of food grade, Glycerol and Sorbitol of food grade and Sodium Hydroxide Solution (NaOH Solution) from Bangkok Chemical Co., Ltd., Palm Oil Morakot Brand, Household Organic Waste (food waste and fresh vegetable scraps) , Photo Initiator Bis-Acylphosphine Oxide (BAPO) powder type, 1,6-Hexanediol diacrylate (HDDA) from Winson Screen Co., Ltd

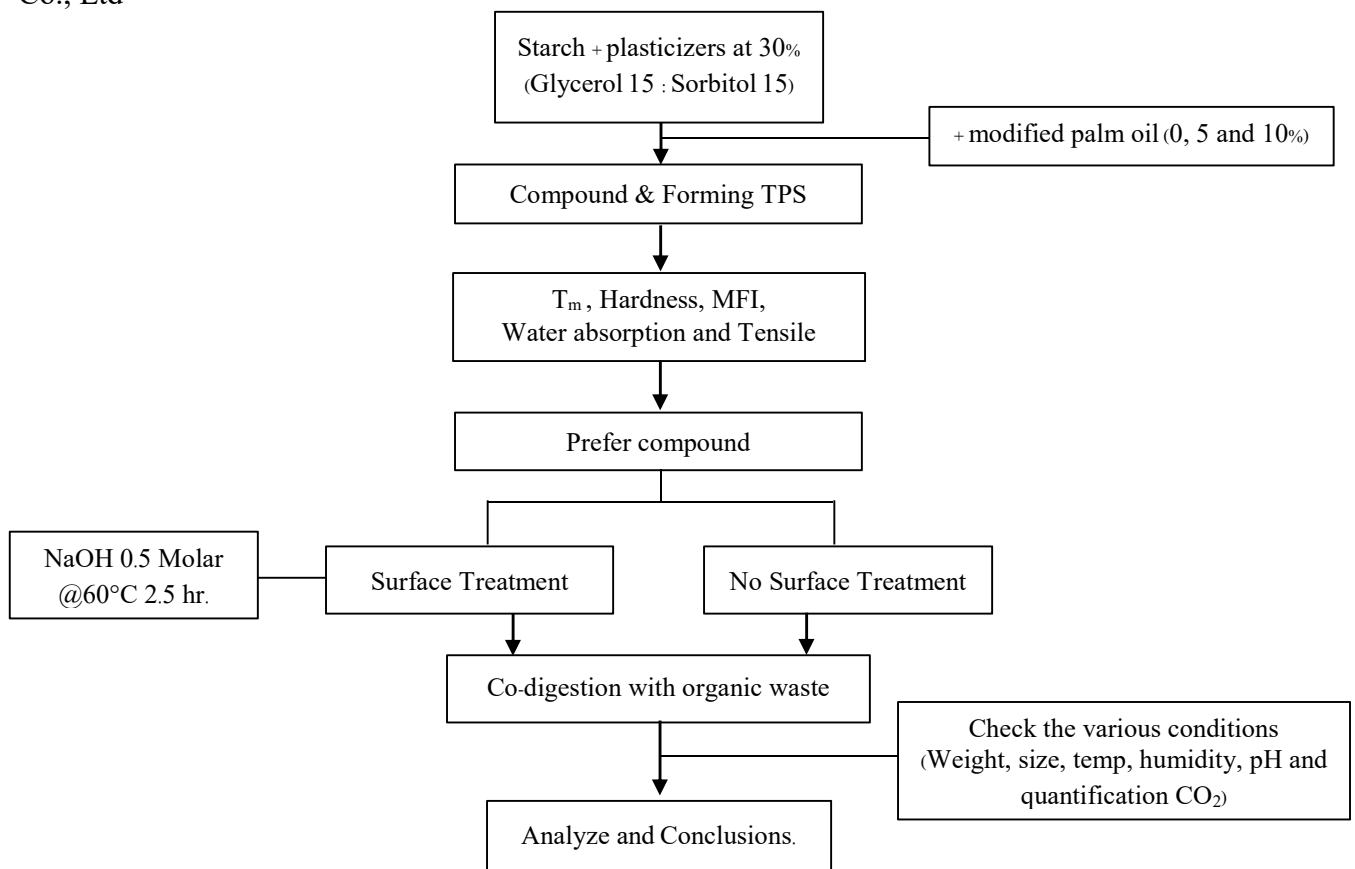


Figure 1 Methodology

Methods of operation in the compounding and forming process

Thermoplastic starch and modified palm oil at 0, 5 and 10% were compounded via twin screw extrusion at 160°C with 60 rpm. Of screw speed. Then the test specimens were prepared via compression molding at 150- 160°C to properties testing. Finally, the compound with proper properties has been taken to co-digestion with organic waste that the surface specimens were treated with 0.5 molar NaOH solution prior to the co-digestion process.

In this study, the specific details of the samples in this research are as follows:

- Thermoplastic Starch = TPS
- Thermoplastic Starch treated with NaOH = Treated TPS
- Thermoplastic starch mixed with modified palm oil 5 phr. = TPS/M-PO 5 phr.
- Thermoplastic starch mixed with modified palm oil 5 phr. and treated with NaOH = Treated

TPS/M-PO 5 phr.

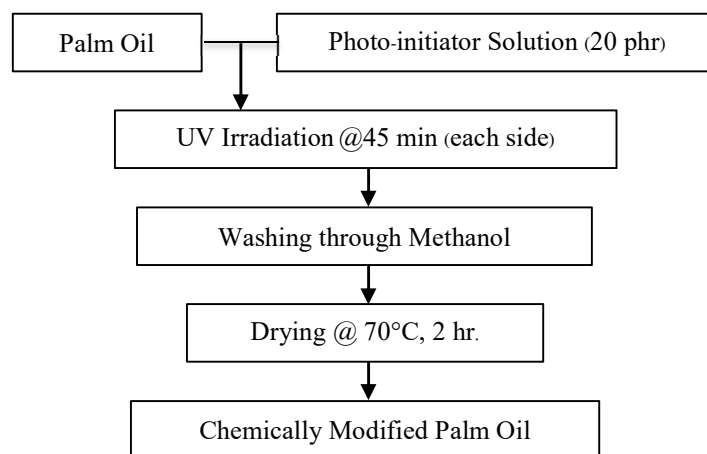


Figure 2 Process preparation of chemically modified palm oil

Method of modified palm oil preparation.

The 9 g. of photo-initiator (BAPO) was dissolved in 100 g. of diacrylate macromer (HDDA) by stirring for 1 h. The 20 phr. of photo-initiator solution was added to palm oil and mix for 5 min. Next, the mixture was brought to irradiation in the Ultraviolet cabinet with circa 390 nm. LED lamps for 45 min. (each side). Then, the irradiated palm oil has been washed in methanol for 3 times to eliminate the non-reactive oil. Lastly, the modified palm oil was dried in a hot air oven at 70°C for 2 h. and the rubber-like grains were obtained.

Characterizations

Water Absorption

The water absorption of TPS with/without modified palm oil was studied. The specimens were dried at 50°C for 24 h, allowed to cool in a desiccator, then weighed the sample before testing. The prepared specimen was immersed in distilled water for 24 hr. , then the specimen was wiped dry. and used to weigh the sample after immersion in distilled water. Calculate the percentage of weight gain or percentage of relative humidity from equation (1)

$$\% \text{ water absorption} = \frac{\text{weight after immersion} - \text{Weight before immersion}}{\text{weight before immersion}} \times 100\% \quad (1)$$

Flow Rate Test

Study the Melt Flow Index (MFI) of TPS was carried out according to ASTM D1238 at temperature 150°C, press weight 2.16 kg. Cut the plastic out of the die at a time of at least 5 example. Weigh the cut sample and calculate the flow index as in equation (2)

$$\text{MFI} = \frac{\text{weight (g)} \times 600}{\text{cutting time (sec)}} \text{ (g/10 min)} \quad (2)$$

Thermal Properties Test

The transition temperature of TPS with/without modified palm oil were annealed at temperature 60°C for 24 hr. before being subjected to Differential Scanning Calorimetry (DSC). The heating start from 25°C to 200°C with heating rate 10°C/min under nitrogen atmosphere.

Tensile Test

Study the tensile strength, % Elongation at break and Young's modulus was determined using a Universal Testing Machine. The specimens were cut into a dumbbell Type I shape according to the ASTM D638 standard, using the speed of test at 5 mm/min. The testing was performed at room temperature.

Morphology

Morphology of Thermoplastic starch prior and subsequent to digestion were studied by Scanning Electron Microscope (SEM). The voltage used at 10 KV with 500X magnification.

Co-digestion of TPS samples with organic waste.

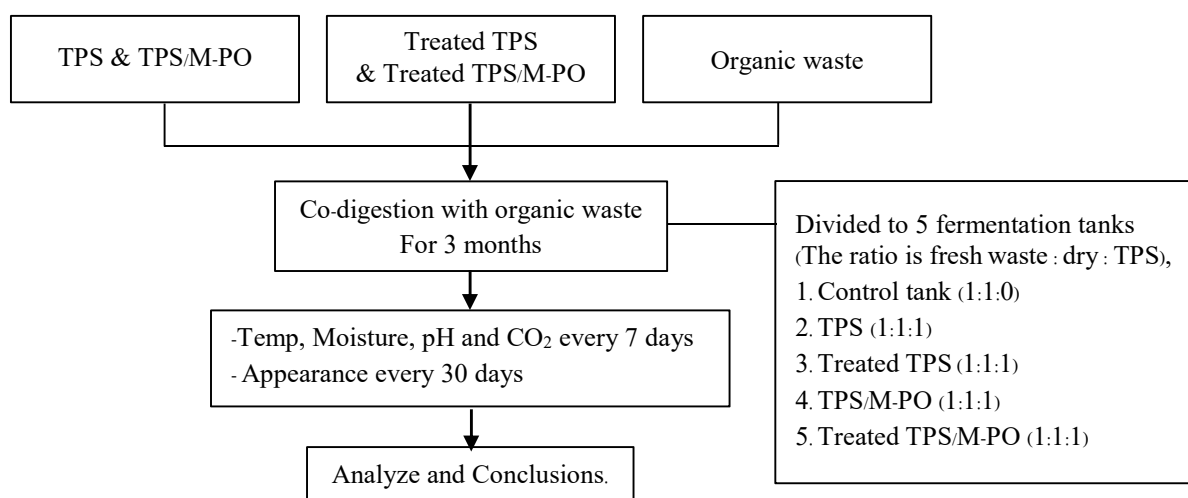


Figure 3 Co-digestion of TPS samples with organic waste

The surface treatment of TPS and TPS/ M- PO was prepared in NaOH solution at a concentration of 0.5 molar at temperature 60°C. The preparation of organic waste (food waste and fresh vegetable scraps) and agricultural waste (leaves, twigs and hay) must be crushed into small pieces prior to contain in fermentation tank and also the TPS and TPS/M-PO as well. The procedure of this examination was shown in Figure 3.

Results and Discussion

Table 1 Thermal and MFI Properties of TPS and TPS/M-PO by DSC

Sample	T _m (°C)	ΔH _m (mW/mg)	MFI (g/10 min)
TPS	172.8	0.70	0.03
TPS/M-PO 5 phr.	151.1	0.67	1.14
TPS/M-PO 10 phr.	158.5	0.76	2.47

From **Table 1**, it was found that the melting temperature decreased when modified palm oil was added. It shows that modified palm oil can penetrate between the polymer chains and generated more space between polymer chains resulting in easily slippage and also found that the M- PO enhanced the flow-ability of TPS as well. It was shown that addition of modified palm oil can penetrate between the chain gaps and act as an internal lubricant.

Table 2 Mechanical Properties of TPS and TPS/M-PO

Sample	Tensile strength (MPa)	Elongation at Break (%)	Modulus (MPa)
TPS	16.50±1.5	3.67±0.25	722.20±9.86
TPS/M-PO 5 phr.	7.15±0.58	2.89±0.64	565.40±3.58
TPS/M-PO 10 phr.	4.48±0.35	0.87±0.06	537.00±6.44

As the effect of adding M-PO into TPS acts as a chain lubricant so the results of tensile properties has shown in Table 2. The tensile strength and Modulus were decreased when modified palm oil was added to TPS. This impact has amended the stiffness of TPS specimens.

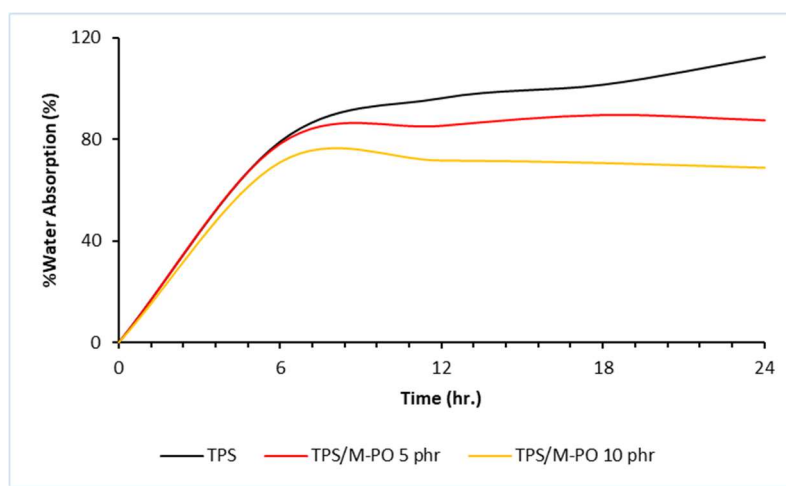


Figure 4 %Water Absorption of TPS and TPS/M-PO

Next, the water absorption of TPS and TPS/M-PO (5 and 10 phr.) were carried out (Figure 4). This was found that the first change (0-6 hr.) all specimens has expressed high water absorption rate. Then the rate tends to equilibrium at 80% after 8 hr. for both TPS/M-PO 5 and 10 phr. whereas TPS has increased steadily with specimen fragment. As TPS is more hydrophilic than TPS/M-PO because modified palm oil has compounded with starch led to water resistance. Subsequently, it is possible that the TPS/M-PO samples may take longer for digestion since the modified palm oil probably resist to moisture that delay the hydrolysis in microbial biodegradation.

In this study, the TPS and TPS/M-PO 5 phr. were chosen to be co-digested with organic waste to compare the degradation efficiency of 4 samples as shown in Figure 5.

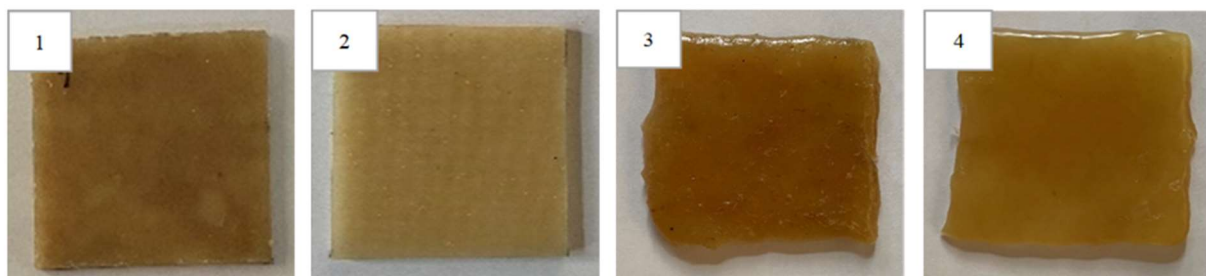


Figure 5 The appearance of specimens before co-digestion (1) TPS, (2) TPS/M-PO 5 phr., (3) Treated TPS and (4) Treated TPS/M-PO 5 phr.

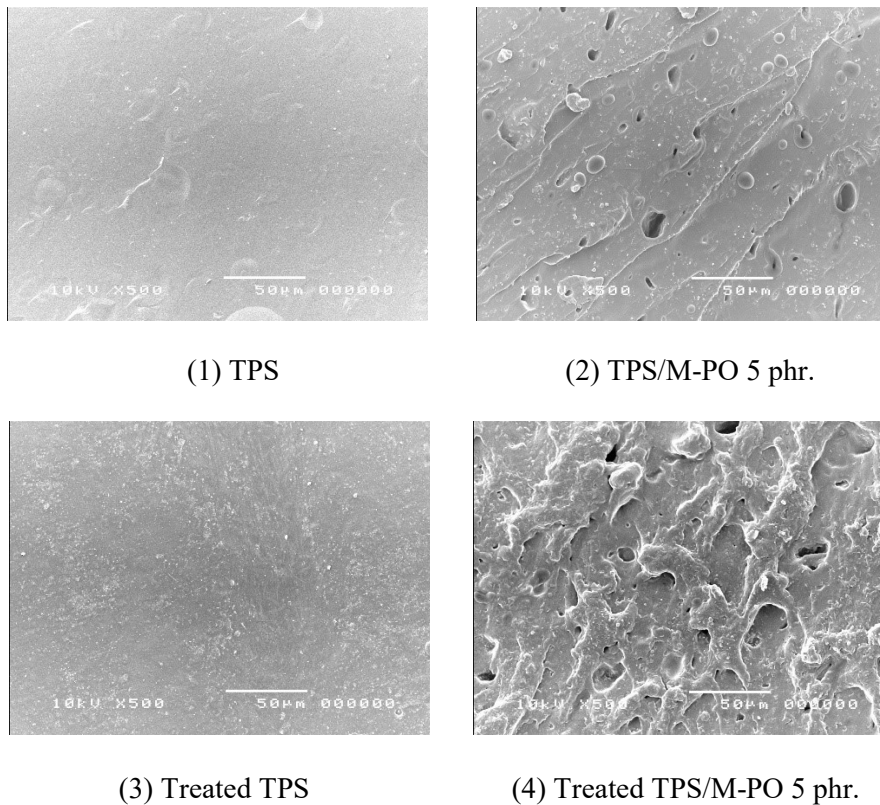


Figure 6 Morphology of TPS and TPS/M-PO (500X)

Biodegradation results by co-digestion with organic waste for 3 months

Biodegradation by co-digestion process with organic waste of various thermoplastic starches at 3 months has shown in Figure 7 and Table 3.

It was found that TPS and Treated TPS were biodegradable by co-digestion process with organic waste in fermentation tank completely within 2 months. Both of TPS and treated TPS specimen were damaged in small pieces after 7 days. As TPS is water absorbable, it results in rapid degradation. However, treated TPS specimens began to degrade and more fragmented than TPS in 7 days as specimens are subjected to corrosion from surface treatment resulting in a more roughness see Figure 6 (c). In case of TPS/M-PO 5 phr., after 3 days, the specimens retained their sheet form but had a softer surface due to the hygroscopicity of organic waste. Then the specimen began slightly fragment after 7 days. Conversely, treated TPS/M-PO 5 phr., were subjected to deformation and more fragment within 7 days. This was due to the treated specimens caused in higher surface area that the microorganisms can fix with and causing faster degradation than without pretreatment and biodegradation occurs at a higher rate as well.













3 Days	7 Days	2 Moths
		
(a) TPS		
		
(b) Treated TPS		
		
(c) TPS/M-PO 5 phr		
		
(d) Treated TPS/M-PO 5 phr		

Figure 7 Physical characteristics of organic waste co-composted thermoplastic starch samples

Table 3 Properties of compost in the fermentation tank before and after co-digestion for 3 months.

Measured values of Compost	Before	After	suitable value
pH	7.0-7.5	6.5-7.0	5.5-8.5
humidity	60-65%	35%	40-70%
temperature	30-45°C	27-31°C	20-45°C first period of decomposition 45-60°C The period of degradation throughout the pile lower 45°C period after decomposition
CO ₂	300 ppm	345-350 ppm	-

Table 3 shows the overall measured values of the composted pile of organic waste before and after co-digestion of the TPS/M-PO sample. It was found that the composted pile of organic waste decreased pH in the range of 6.5-7.0 from pH 7.0-7.5 which corresponds to the control tank. It also indicates that TPS/M-PO degradation could not impact to the acidity - alkalinity of the fermentation pile. This is commendable for the environment and suitable for use as compost. In case of humidity values, it seems to be too low than the suitable value. This was due to the fact that the winter weather during the co-digestion period is low relative humidity. Importantly, the increase of carbon dioxide content has confirmed that TPS/M-CO samples can be composted completely via co-digestion with organic wastes using the fermentation tank. For detailed information of various values recorded at each interval time in fermentation tanks of treated TPS/M-CO has shown in Figure 8.

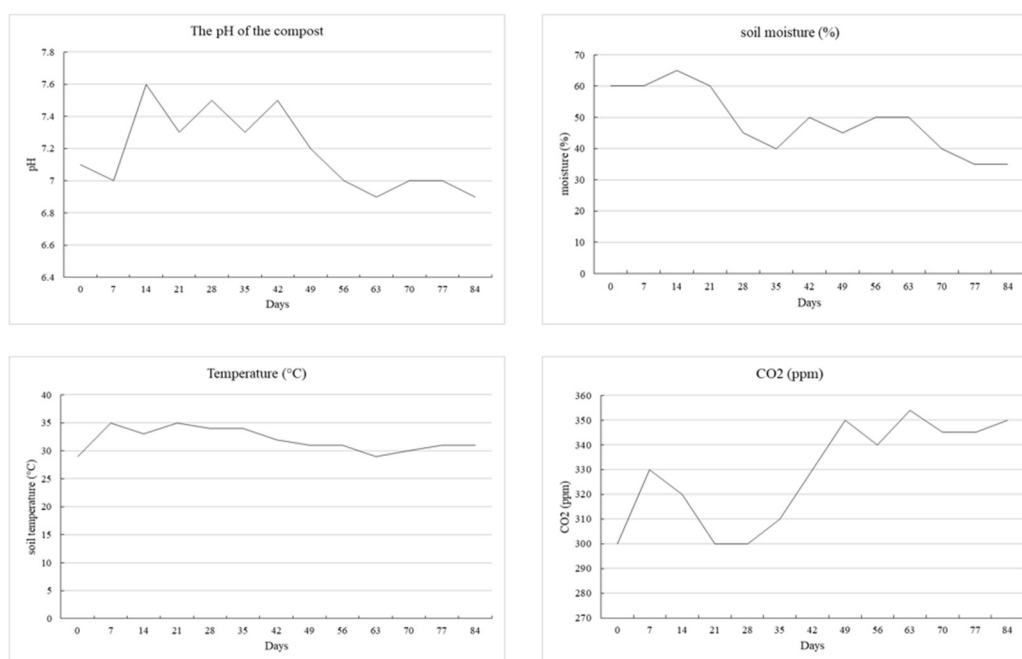


Figure 8 The measured valued of composted pile of organic wasted in fermentation tanks of treated TPS/M-CO.

From Figure 8 it was found that the pH level of the fermentation pile was maintained well. This means that microbial degradation is going well. Nonetheless, the humidity values of composted pile in the tank was very high about 60 -70 percent in the first week due to watering into fermentation

tank for helping the growth of microorganisms. It also accelerates the TPS and TPS/M-CO samples to be hydrolysed as well. So the carbon dioxide content was also observed in that period. It was concluded that the application of thermoplastic starch with modified palm oil can be composted completely via co-digestion with organic wastes during fermentation around the 3rd week and complete degradation occurs within 12 weeks or 3 months.

Conclusion

In this study it was found that the modified palm oil can penetrate between the polymer chains and generated more space between polymer chains resulting in easily slippage and also found that the M-PO enhanced the flow-ability of TPS as well. Both TPS/M-PO 5 and 10 phr. had the water absorption content equilibrium at 80% after 8 hr. The specimens were able to maintain their shape for more than 18 hours because modified palm oil has compounded with starch led to water resistance.

In terms of co-digestion investigation, TPS and TPS/M-PO 5 phr. were treated with sodium hydroxide solution in concentration of 0.5 molar. Most of the specimen began slightly fragment after 3 days. Importantly, treated TPS/M-PO 5 phr. specimens were subjected to deformation and more fragment within 7 days and the compostion was completed within 3 months. Whereas the TPS and treated TPS were composted entirely within 2 months. This was due to the treated specimens caused in higher surface area that the microorganisms can fix with and causing faster degradation than without pretreatment and biodegradation occurs at a higher rate as well. Finally, the increase of carbon dioxide content has confirmed that TPS/M-CO samples can be composted completely via co-digestion with organic wastes using the fermentation tank.

References

- Allen, N.S. (1996). Photoinitiators for UV and visible curing of coatings: mechanisms and properties. *J Photochem Photobiol A Chem*, 100, 101-107.
- Ashraf M. Salih et. al., (2015). Synthesis of Radiation Curable Palm Oil–Based Epoxy Acrylate: NMR and FTIR Spectroscopic Investigations. *Molecules*, 20, 14191-14211.
- Bozano, P., Nosiglia, V., and Vitali, G. (2012). CO-digestion of biowaste and commercial waste with agricultural residues-Experiences from Castelleone (Italy).
- Da Roz, A. L., Carvalho, A. J. F., Gandini, A., and Curvelo, A. A. S. (2006). The effect of plasticizers on thermoplastic starch compositions obtained by melt processing. *Carbohydr. Polym.* 63: 417-424.
- Deconinck, S. & De Wilde B. (2013). Benefits and challenges of bio- and oxo-degradable plastics. A comparative literature study.
- European bioplastics. Bioplastic materials. [online]. 2015. Available from: <http://www.european-bioplastics.org/bioplastics/materials> [27 June 2019]
- Fertier, L., et al. (2013). The use of renewable feedstock in UV-curable materials—a new age for polymers and green chemistry. *Prog. Polymer. Sci.*, 38, 932–962.
- F. Seniha Guner et al., (2006). Polymers from triglyceride oils. *Prog. Polym. Sci.*, 31, 633–670.
- Gan Seng Neon. (2018). Novel polymeric materials from palm oil derivatives. Available from: http://www.researchsea.com/html/article.php/aid/9605/cid/1/research/science/university_of_malaya/novel_polymeric_materials_from_palm_oil_derivatives.html [8 August 2018]
- Hansupalak, N., Srisuk, S., Wiroonpochit, P., & Chisti, Y. (2016). Sulfur-free preulcanization of natural rubber latex by ultraviolet irradiation *Ind. Eng. Chem. Res.*, 55, 3974
- Hebeish, A., and Guthrie, J. T. (1997). *The Chemistry and Technology of Cellulosic Copolymer*. New York: Springer-Verlag Inc., Berlin Heidelberg,
- Huang, M., Yu, J., & Ma, X. (2005). Ethanolamine as a novel plasticizer for thermoplastic starch. *Polym. Degrad. Stab.*, 90, 501-507.

- Jeffrey Gotro. (2018). “UV Curing of Thermosets Part 11: Using UV Rheology to Monitor Curing – 2”, Available from: <https://polymerinnovationblog.com/uv-curing-thermosets-part-11-using-uv-rheology-monitor-curing-2/> [10 August 2018]
- John, J. M. *Polymer Modification: Principles, Techniques and Applications*. New York: Marcel Dekker, 2000.
- Jarukumjorn, K., et al. (2013). *Compatibility and toughness improvement of thermoplastic/poly/(lactic acid) blends*. In research report. Faculty of Engineering Suranaree University of Technology Intellectual.
- Kim, H. M. et. al., (2010). Soybean Oil-Based Photo-Crosslinked Polymer Networks. *J Polymer Environ.*, 18(3), 291–297.
- Martin, O., and Averous, L. (2001). Poly(lactic acid): plasticization and properties of biodegradable multiphase systems. *Polymer*. 42, 6209-6219.
- Polcharoen, A. & Sungsanit, K. (2015). *Modification of Polystyrene by Compounding with Castor wax as an Additive*. IE Network Conference 2015: Academics- Industrial Research Collaborations in order to be Excellence in ASEAN (816-821). Bangkok: The Emerald Hotel.
- Qiao, X., Z. Tang, and K. Sun. (2011). Plasticization of corn starch by polyol mixtures. *Carbohydrate Polymers*, 83(2), 659-664.
- Rodriguez-Gonzalez, F. J., Ramsay, B.A, and Favis, B. D. (2004). Rheological and thermal properties of thermoplastic starch with high glycerol content. *Carbohyd. Polym.*, 58, 139-147.
- Salih, A., Yunus, W.M.Z.W., Dahlan, K.Z.M., Mahmood, M.H., Ahmad, M. (2012). UV-Curable Palm Oil Based-Urethane Acrylate/Clay Nanocomposites. *Pertanika J. Sci. Technol.*, 20, 435–444.
- Scientific Psychic. (2009). *Chemical Structure*. Accessed 22 October. Available from <http://www.scientificpsychic.com/fitness/carbohydrates1.html>.
- Shin, B. Y., Jang, S. H., and Kim, B. S., (2011). Thermal, morphological, and mechanical properties of biobased and biodegradable blends of poly(lactic acid) and chemically modified thermoplastic starch. *Polym. Eng. Sci.*, 51, 826-834.
- Tajau, R., Mahmood, M.H., Salleh, M.Z., Mohd Dahlan, K.Z., Che Ismail, R., Muhammad Faisal, S., Sheikh Abdul Rahman, S.M.Z. (2013). Production of UV-curable palm oil resins/oligomers using laboratory scale and pilot scale systems. *Sains Malays.*, 42, 459–467.
- Teixeira, E. M., Curvelo, A. A. S., Corrêa, A. C, Marconcini, J. M., Glenn, G. M, Mattoso, L. H. C. (2012). Properties of thermoplastic starch from cassava bagasse and cassava starch and their blends with poly(lactic acid). *Ind. Corp. Prod.* 37, 61-68.
- Tokiwa, Y., Calabia, B. P., Ugwu, C. U., and Aiba, S. (2009). Biodegradability of plastics. *International Journal of molecular sciences*, 10(9), 3722-3742.
- Vilaseca, F., et al.. (2007). Composite materials derived from biodegradable, starch polymer and jute strands. *Process Biochem*, 42, 329-334.
- Besse, V., et. al., (2016). Photopolymerization study and adhesive properties of self-etch adhesives containing bis(acyl)phosphine oxide initiator. *Dent Mater*, 32(4), 561-569.
- Wu, W. (2000). Anaerobic co-digestion of biomass for methane production: recent research achievements. Optimization. 1:1.
- Yagi, H., et. al., (2010). Bioplastic Biodegradation activity of anaerobic sludge prepared by preincubation at 55°C for new anaerobic biodegradation test. *Polymer Degradation and Stability*, 95(8), 1349-1355.
- Yu, L., and Christie, G., (2001). Measurement of starch thermal transitions using differential scanning calorimetry. *Carbohyd. Polym.*, 52, 101-110.
- Yu, L., Petinakis, E., Dean, K., Liu, H., and Yuan, Q. (2011). Enhancing compatibilizer function by controlled distribution in hydrophobic polylactic acid/hydrophilic starch blends. *J. Appl. Polym. Sci.*, 119, 2189-2195.
- Zamiri et al., “Fabrication of Silver Nanoparticles Dispersed in Palm Oil Using Laser Ablation,” *Int. J. Mol. Sci.* 2010, 11, 4764-4770.

Preparation of Flat Sheet Polysulfone Membrane Coated with PDMS for Carbon Dioxide/Methane Gas Separation at Low Pressure

Arisa Jaiyu*, Julaluk Phunnoi, Passakorn Sueprasit, Nattaporn Chutichairattanaphum, and Borwon Narupai

Expert Centre of Innovative Materials, Thailand Institute of Scientific and Technological Research, Khlong Luang, Pathumthani, 12120, Thailand

** Corresponding email: arisa@tistr.or.th*

Abstract

Biogas is a renewable energy that mainly consists of methane (CH₄) and carbon dioxide (CO₂). The CO₂ in the biogas reduces energy efficiency and can cause pipeline corrosion. So, it is necessary to remove CO₂ before using the gas in the system. In this study, flat sheet polysulfone membranes have been fabricated by a non-solvent induced phase separation method using water as a coagulant at room temperature. After drying the membrane via solvent exchange, the prepared polysulfone membrane was coated with a 3% Polydimethylsiloxane (PDMS) silicone elastomer solution in hexane with a contact time of 1 minute, and the membrane was cured at 100 °C for 2 hours. The pristine polysulfone membrane and polysulfone membrane coated with PDMS silicone elastomer were compared and characterized using EDS, FTIR, and SEM. The permeance of gas and the selectivity of CO₂/CH₄ at low pressure (1-2 bar) were determined using a single pure gas permeation experiment. The results showed that the flat sheet polysulfone membrane coated with PDMS had a dramatic increase in CO₂/CH₄ selectivity compared to the pristine polysulfone membrane.

Keywords: Biogas, Membrane, Polysulfone, PDMS, Gas Separation

Introduction

The treatment of agricultural wastewater, which leads to biogas production, is a significant source of renewable energy. Businesses and industries can use the energy they consume to help solve environmental issues and reduce wastewater treatment costs. This is considered an investment in the development of a system that will benefit both the economy and the environment. Biogas can be used as a burner fuel for boilers or hot oil boilers to replace fossil diesel, which can also be used as a fuel for gasoline engines to generate energy or power cars, as well as LPG gas and syngas (Teodorita et al. 2008). Biogas from industrial agro-industrial wastewater treatment typically contains 45–75% methane (CH₄), 15–50% carbon dioxide (CO₂), moisture, hydrogen sulfide gas, ammonia, nitrogen gas, and other 5–10% contaminants (Jin et al. 2017; Teodorita et al. 2008). CH₄ is the main component of biogas, which is utilized as a fuel. Another negative aspect of unpurified biogas is the presence of impurities. In particular, CO₂ accounts for a large portion of biogas but offers only a small amount of heat energy for burning, decreasing heat value. Unpurified biogas is difficult to ignite and burns slowly, causing the fuel in the combustion chamber to not completely burn. This results in significant heat loss from the hot exhaust flue temperatures (Nordic Energy Research 2010). Furthermore, when CO₂ interacts with water or moisture, it generates corrosive carbonic acid, which leads to all equipment exposed to biogas being readily destroyed and short-lived (Jin et al. 2017). This could result in sparks if there is a leak in the gas pumping system. It is important to improve the quality of biogas before it can be used by removing CO₂ to increase the purity of CH₄ contained in the biogas. (Jin et al. 2017; Sarker et al. 2018). Membrane technology is expected to drive the global as a means of enhancing the quality of biogas (Li et al. 2021; Powell et al 2006; Dai et al. 2019). Additionally, it saves space, has no moving parts, does not require chemical additives, has a long

service life of 10-15 years, and requires less energy to raise pressure (Zulhairun et al. 2014). As a result, a critical design consideration in the application of membrane technology for biogas enhancement is the development of CO₂-specific membrane materials. The purpose of this research is to develop polymer-based membrane materials capable of removing CO₂. A non-solvent induced phase separation method was used to prepare the flat sheet pristine polysulfone membrane. The polysulfone membrane was then coated with PDMS silicone elastomer using a conventional coating technique such as dipping. EDX, FTIR, and SEM were used to compare and characterize the pristine polysulfone membrane and the polysulfone membrane coated with PDMS silicone elastomer. At low pressures (1-2 bar), the permeance of gas and the selectivity of CO₂/CH₄ were determined using a single pure gas permeation experiment.

Materials and Methods

Reagents and Materials

Polysulfone (PSF) polymer was commercial grade and dried at 70°C for at least 12 hrs. PDMS base and PDMS hardener was also commercial grade and used as received. N-methyl-2-pyrrolidone (NMP), Methanol and hexane were purchased from RIC Labscan Limited.

Preparation of Polysulfone Membrane

The polymer solution was prepared by dissolving 15 wt% Polysulfone in 85% NMP at 50°C. The mixture was stirred for at least 3 hrs until the solution was formed and homogeneous. After that, the polymer solution was placed in an ultrasonic for 20 mins and left at room temperature to remove trapped bubbles. Then, the polymer solution was cast onto a glass substrate using a casting knife with a knife gap of 254 mm. Subsequently, the casting solution was smoothly immersed in a water coagulant bath until the membrane was completely solidified. The obtained membranes were left in the water for 24 hrs to completely remove the residual solvent used in membrane fabrication. Following this, the membranes were placed in the methanol for solvent exchange for 2 hrs. Subsequently, the membranes were dried in the ambient air for 2 days before further tests.

Preparation of PDMS-coated Polysulfone Membranes

3 vol% PDMS silicone elastomer solution was prepared by dissolving the PDMS base in hexane solution and stirring for 30 min. Then, the PDMS hardener was added to the mixture solution and stirred to form a homogeneous solution. Before the coating process, the polysulfone membranes were dipped in water for 1 min, and then the excess water was removed from the membrane surface using filter paper. Then, the polysulfone membranes were dipped in the PDMS solution for 1 min and placed in the oven at 100 °C for 2 hrs to completely cure the PDMS.

Membrane Characterization

A Scanning Electron Microscope (SEM; Thermoscientific model Prisma E) was used to characterize the surface and cross-section morphologies of polysulfone membrane and PDMS-coated polysulfone membrane. The SEM specimens to study the cross-section of the obtained membranes were prepared by fracturing the dried membrane samples in liquid nitrogen. The SEM specimens were covered with a thin layer of gold using a sputter coater. The presence of PDMS on the surface of polysulfone membranes was determined by energy-dispersive X-ray analysis (EDS; Bruker model X-Flash 6160) and attenuated total reflectance. Fourier transform infrared spectroscopy (ATR-FTIR; IRPrestige-21 Shimadzu)

Analysis of gas permeation and separation properties

The lab-scale gas permeation system (Fig. 1) was set up with a bubble soap flow meter to measure the membrane performance towards selected gases. The membranes were housed in a

chamber that consisted of two detachable parts. The membrane had an effective area of approximately 7 cm². The permeance of gas and selectivity of CO₂/CH₄ at low pressure (1-2 bar) at 25°C were determined using a single pure gas permeation experiment. The pressure-normalized flux or permeance, (Pi/l) was calculated by the equation:

$$\frac{P_i}{l} = \frac{Q_i}{A \Delta P} \frac{273.15 \times 10^6}{T} \quad (1)$$

where (Pi/l) is the gas permeance of a membrane in GPU (1 GPU = 1 x 10⁶ cm³ (STP)/cm² s cmHg); i represents the penetrating gas i, Qi is the volumetric flow rate of gas permeated through the membrane (cm³/s, STP); A is the effective membrane area (cm²); ΔP is the trans-membrane pressure (cmHg), and T is the temperature at which the permeation experiment is being performed (Pesk and Koros 1993; Zuhairun et al. 2015). The ideal selectivity of CO₂/CH₄ was simply determined as the pressure-normalized flux ratio of gas component CO₂ over CH₄ (Zuhairun et al. 2015):

$$\alpha \frac{CO_2}{CH_4} = \frac{(P_{CO_2}/l)}{(P_{CH_4}/l)} \quad (2)$$

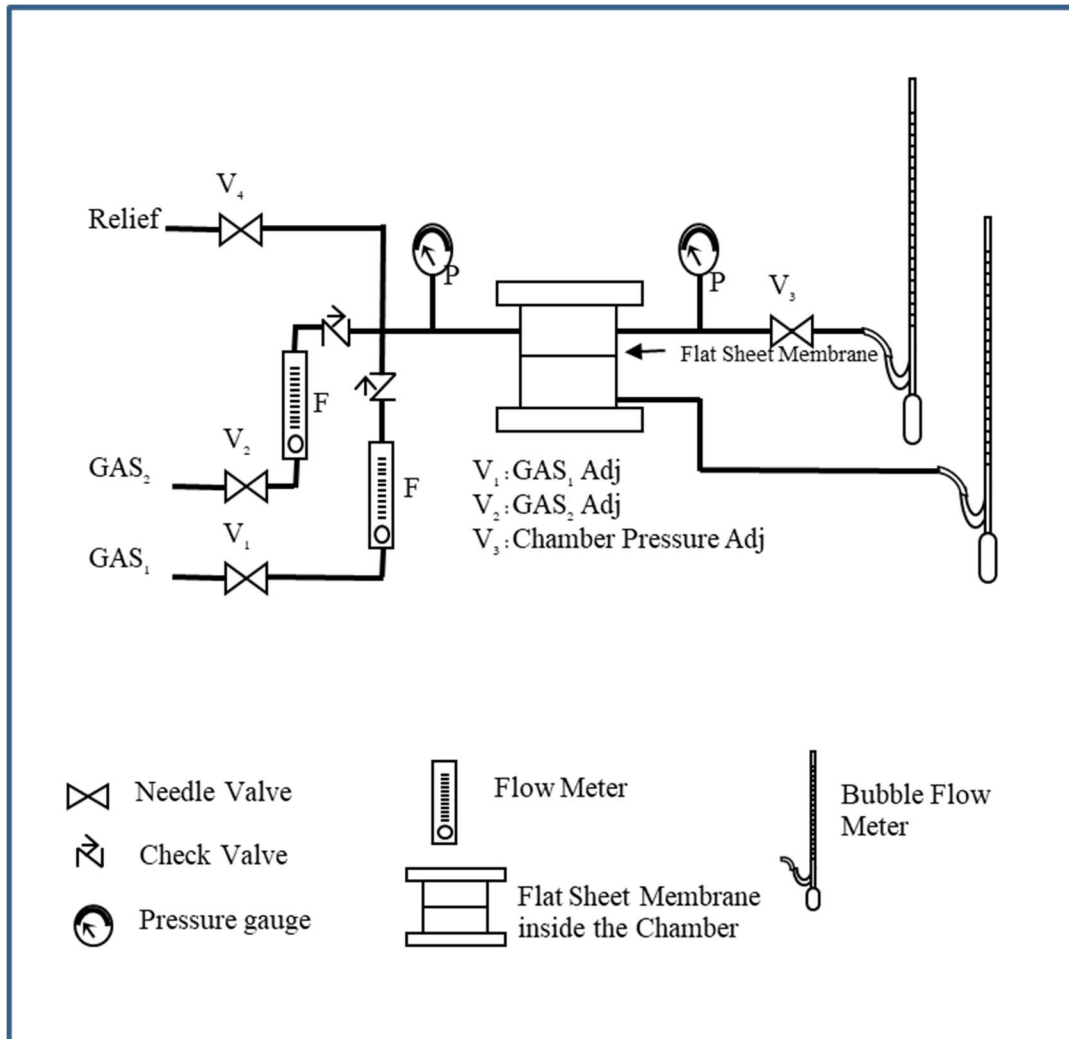


Figure 1 Schematic diagram of the lab-scale gas permeation system

Results and discussion

Membrane Structures and Morphologies

Membrane structures and morphologies of polysulfone membranes and PDMS-coated polysulfone membranes were characterized by EDS, FTIR, and SEM. The presence of Si in the PDMS-coated Polysulfone membrane surface was determined by EDS, which indicated the PDMS coating on the surface of the polysulfone membrane (Fig. 2). The Si was not detected in the pristine polysulfone membrane. The FTIR spectrum of the pristine polysulfone membrane and the PDMS-coated polysulfone membrane are compared in Fig 3. The FTIR spectrum of the pristine polysulfone membrane was different from the FTIR peak of the PDMS-coated polysulfone membrane. The PDMS-coated polysulfone membrane exhibited the IR peak of PDMS at $789\text{-}790\text{ cm}^{-1}$ (Si-CH₃), $1020\text{-}1074\text{ cm}^{-1}$ (Si-O-Si), $1260\text{-}1259\text{ cm}^{-1}$ (Si-CH₃), and $2950\text{-}2960\text{ cm}^{-1}$ (Si-CH₃) (Johnson et al 2013). The EDS and FTIR results confirmed the successful coating of PDMS on the polysulfone surface.

Fig. 4 shows the SEM image of a cross-section of a pristine polysulfone membrane and a PDMS-coated polysulfone membrane. The polysulfone membrane exhibited an asymmetric structure containing a thin selective top layer and an underlying porous structure. The porous layer of the membrane displayed a long finger-like structure with spongy-like cavities. An asymmetric structure is normally formed across the membrane via nonsolvent induced phase separation (Hamzah et al. 2014; Mohamad et al. 2016). The PDMS-coated polysulfone membrane revealed the dense PDMS layer on the surface of the polysulfone layer. From the SEM image, the thickness of the polysulfone and PDMS layers was approximately 160 ± 5 and 1 ± 0.15 mm, respectively. The SEM images of the outer surface of the polysulfone membrane and the PDMS-coated polysulfone membrane are shown in Fig 5. The defect in the polysulfone membrane can be detected by the SEM image, while no defect was revealed after coating the polysulfone with PDMS.

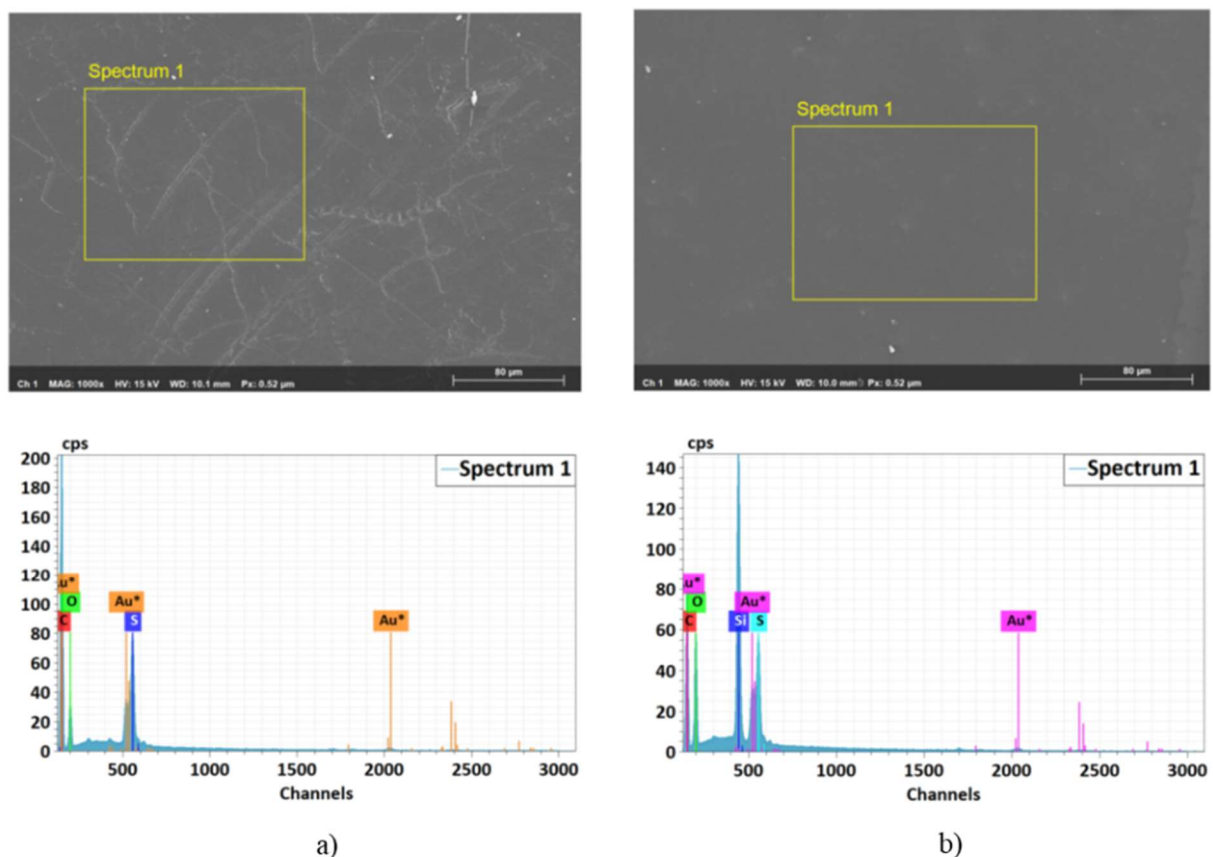


Figure 2 EDX spectrum of a) polysulfone membrane and b) PDMS-coated polysulfone membrane

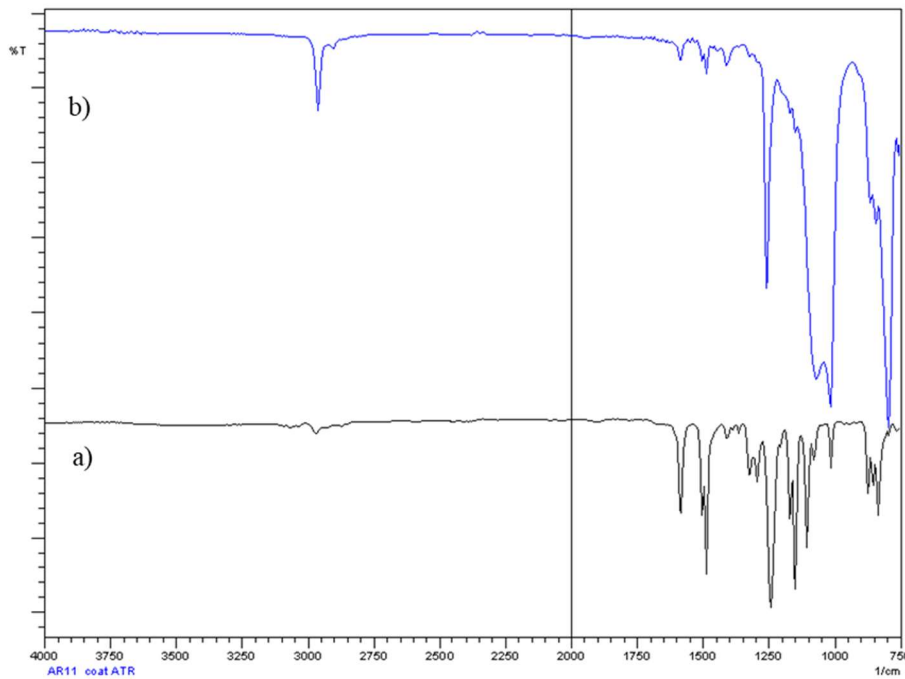


Figure 3 FTIR spectrum of a) Polysulfone Membrane and b) PDMS-coated Polysulfone membrane

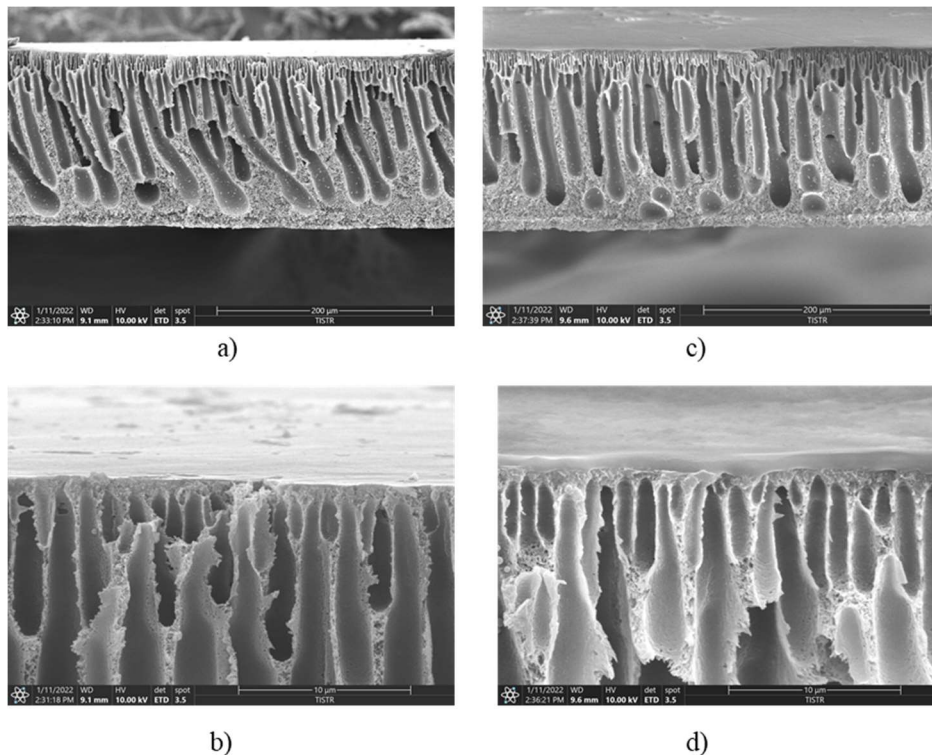


Figure 4 SEM images of the cross-section a) Polysulfone membrane at 500x magnification b) Polysulfone membrane at 8000x magnification c) PDMS-coated Polysulfone membrane at 500x magnification d) PDMS-coated Polysulfone membrane at 8000x magnification

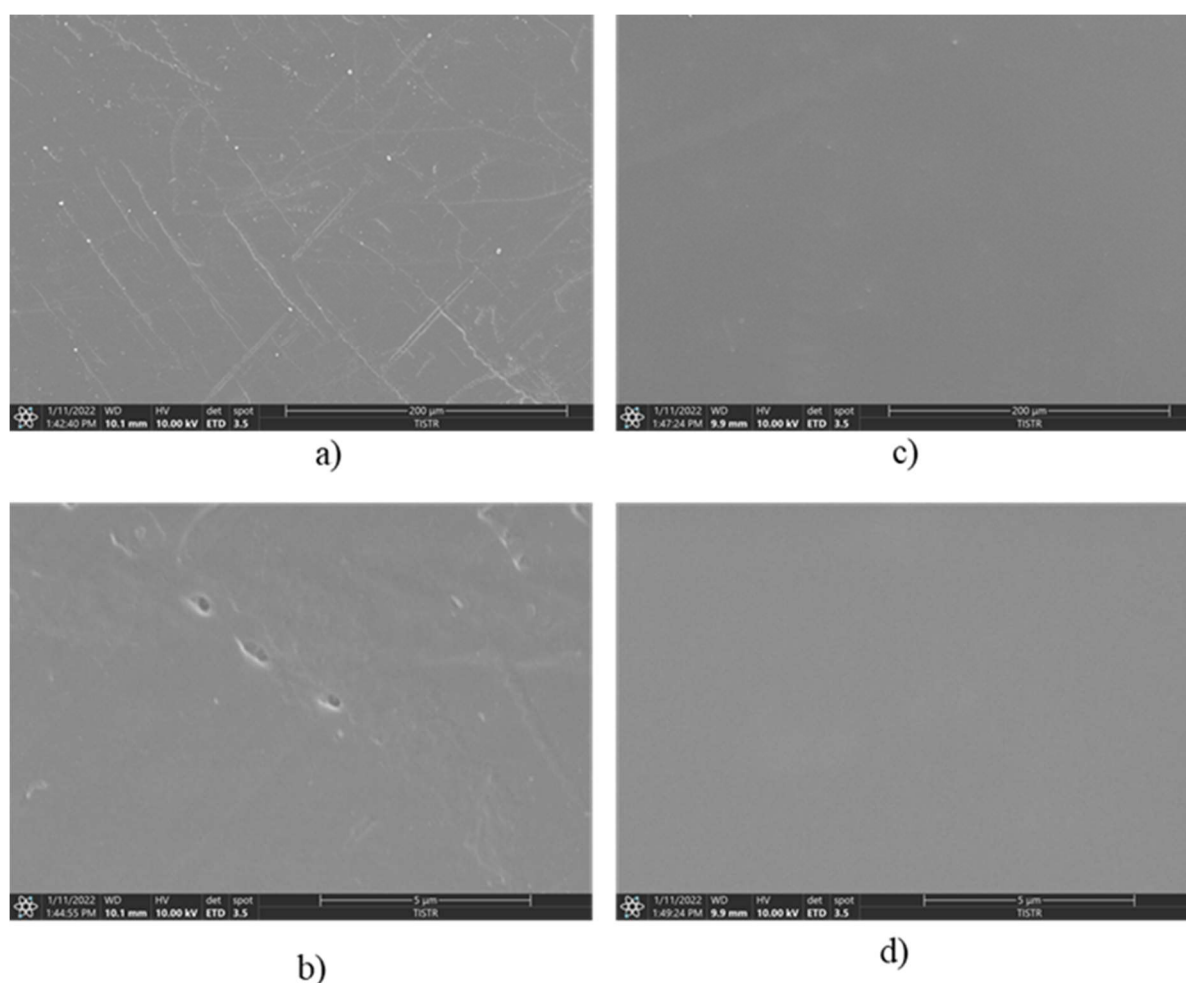


Figure 5 SEM images of the outer surface a) Polysulfone membrane at 500x magnification b) Polysulfone membrane at 8000x magnification c) PDMS-coated Polysulfone membrane at 500x magnification d) PDMS-coated Polysulfone membrane at 8000x magnification

Gas Permeability and Selectivity

The permeance of gas and the selectivity for CO₂/CH₄ of pristine polysulfone membrane and PDMS-coated polysulfone membrane at low pressure (1-2 bar) were determined using a single pure gas permeation measurement. The gas permeation and selectivity for CO₂/CH₄ results of both membranes are shown in Table 1. At 1 bar, the gas permeability of the pristine polysulfone membrane obtained in this study was 864 GPU for CO₂ and 1037 GPU for CH₄, with a CO₂/CH₄ selectivity of 0.83. There is no selectivity of CO₂/CH₄ of the pristine membrane at 1 bar, which may be due to the defect of the tested polysulfone membrane. Meanwhile, the gas permeability of permeance at 2 bar was 1295 GPU for CO₂ and 864 GPU for CH₄, with a CO₂/CH₄ selectivity of 1.5. The permeability of both CO₂ and CH₄ decreased when the surface of polysulfone was coated with PDMS. The CO₂ permeability of the PDMS-coated polysulfone membrane was 132 GPU at 1 bar and 145 GPU at 2 bar, while the CH₄ permeability was not observed because it was lower than the detection limit of the bubble flow meter used in this experiment. These results indicate that the PDMS-coated polysulfone membrane has very high CO₂/CH₄ selectivity at 1-2 bar gas permeability. The PDMS coated on the surface of the polysulfone membrane not only covers the defect of the polysulfone membrane, but the PDMS layer itself has a high affinity towards CO₂.

Table 1 Gas permeation properties for CO₂ and CH₄ measured at 1-2 and 25±3 °C

Membrane	Permeance (Pi/l), GPU				Selectivity (CO ₂ /CH ₄)	
	CO ₂		CH ₄		1 bar	2 bar
	1 bar	2 bar	1 bar	2 bar		
Polysulfone	864	1295	1037	864	0.83	1.5
PDMS-coated Polysulfone	132	145	ND	ND	Very High	Very High

ND = Not Detect (lower than detection limit)

Conclusion

In this study, the flat sheet polysulfone membrane and the PDMS-coated polysulfone membrane were fabricated via non-solvent induced phase separation using water as a coagulant. The success of the PDMS coating on the polysulfone surface was confirmed by EDS, FTIR, and SEM. The permeance of gas and the selectivity of CO₂/CH₄ at low pressure (1-2 bar) were determined using a single pure gas permeation experiment. The results showed that the flat sheet polysulfone membrane coated with PDMS had very high CO₂/CH₄ selectivity with a gas permeance of 132 GPU at 1 bar and 145 GPU at 2 bar. This indicated that the PDMS coating on the polysulfone membrane dramatically improved CO₂/CH₄ selectivity.

Acknowledgements

The authors gratefully acknowledge the Thailand Institute of Scientific and Technological Research (TISTR) and Thailand Science Research and Innovation (TSRI) for financial, material, and instruments support.

References

- Dai, Z., Deng, J., Ansaloni, L., Janakiram, S., & Deng, L. (2019, February). Thin-film-composite hollow fiber membranes containing amino acid salts as mobile carriers for CO₂ separation. *Membrane Science*, 578, 61-68.
- Hamzah, S.; Ali, N.; Ariffin, M. M.; Ali, A.; Mohammad, A. W. (2014) High performance of polysulfone ultrafiltration membrane: effect of polymer concentration *J. Eng. Appl. Sci. (Asian Res. Publ. Netw.)* 9(12), 2543-2550.
- Jin, P., Huang, C., Li, J., Shen, Y., & Wang, Liao. (2017, October). Surface modification of poly(vinylidene fluoride) hollow fibre membranes for biogas purification in a gas-liquid membrane contactor system. *Royal Society Open Science*, 4(11), 1-17.
- Johnson, L.M., Gao, L., Shields IV, C.W., Smith, M., Efimenko, K., Cushing, K., Genzer, J., & López, G.P. (2013, June). Elastomeric microparticles for acoustic mediated bioseparations. *Nanobiotechnology*, 11(1), 1-8.
- Li, G., Kujawski, W., Knozowska, K., & Kujawa, J. (2021, January). The Effects of PEI Hollow Fiber Substrate Characteristics on PDMS/PEI Hollow Fiber Membranes for CO₂/N₂ Separation. *Membranes*, 11(1), 56-79.
- Mohamad, M.B., Fong, Y.Y., & Shariff, A. (2016, December). Gas Separation of Carbon Dioxide from Methane using Polysulfone Membrane Incorporated with Zeolite-T. *Procedia Engineering*, 148, 621-629.
- Nordic Energy Research, 2010. Mapping Biogas in the Nordic Countries, *Report to Nordic Energy Research*
- Pesek, S.C., & Koros, W.J. (1993, January). Aqueous quenched asymmetric polysulfone membranes prepared by dry/wet phase separation. *Membrane Science*, 81, 71-88.

- Powell, C.E.; Qiao, G.G. (2006) Polymeric CO₂/N₂ gas separation membranes for the capture of carbon dioxide from power plant flue gases. *J. Membr. Sci.* 279, 1–49.
- Sarker S, Lamb JJ, Hjelme DR, Lien KM (2018). Overview of recent progress towards in-situ biogas upgradation techniques. *Fuel*, 226, 686–697.
- Teodorita Al Seadi DR, Prassl H, Köttner M, Finsterwalder T, Volk S, Janssen R (2008) Biogas handbook. University of Southern, Denmark, Esbjerg
- Zulhairun, A.K., Fachrurrazi, Z.G., Izwanne, M.N., & Ismail, A.F. (2015, March). Asymmetric hollow fiber membrane coated with polydimethylsiloxane-metal organic framework hybrid layer for gas separation. *Separation and Purification Technology*, 146, 85-93.
- Zulhairun, A.K., Ng, B.C., Ismail, A.F., Murali, R.S, & Abdullah, M.S. (2014, September). Production of mixed matrix hollow fiber membrane for CO₂/CH₄ separation. *Separation and Purification Technology*, 137, 1-12.

Preparation and Characterization of Typha Natural Fiber Reinforced Poly(lactic acid) Biocomposite

Rattikarn Khankruea^{1*}, Bawornkit Nekhamanurak¹ and Supakij Suttiruengwong²

¹ Department of Materials Engineering, Faculty of Engineering, Rajamangala University of Technology Rattanakosin, Salaya, Phutthamonthon, Nakhon Pathom 73170, Thailand

² Department of Materials Science and Engineering, Faculty of Engineering and Industrial Technology, Silpakorn University, Nakhon Pathom 73000, Thailand

* Corresponding email: rattikarn.kha@rmutr.ac.th

Abstract

This research aimed to study the mechanical properties, flow properties, morphology and sound absorption coefficient of poly(lactic acid) reinforced with cellulose fiber from Typha. The influences of fiber content between 10-40 phr on the biocomposites properties were investigated as well as the effect of compatibilizer. The biocomposites were prepared through twin screw extrusion process. The results showed that the impurities in fiber were removed after treatment by alkaline solution which confirmed by FTIR analysis. The morphology of the compatibilizer added composites exhibited the good adhesion between fiber and PLA matrix, however, agglomeration of fiber also could be observed. Flow properties showed that the MFI of composite decreased with fiber content increase. For the mechanical properties, the tensile strength, Young's modulus and impact strength of the biocomposites with compatibilizer addition were higher than those of the composites without compatibilizer. In addition, Young's modulus increased with fiber content whereas the elongation at break decreased. However, when fiber content increased to 40 phr, the elongation at break was closed to that of neat PLA. Sound Absorption test showed that the composites materials could not significantly absorb sound, but it could act as sound barrier materials instead due to its good reflection behavior.

Keywords: Poly(lactic acid), Typha, Natural fiber, Composite, Biopolymer

Introduction

Recently, poly(lactic acid) (PLA) has been well-known biopolymers because of its environmental advantages such as renewable resource-based origin, biodegradability and biocompatibility (Ikada & Tsuji, 2000). In addition, it possesses excellent mechanical strength and modulus, consequently, PLA has attracted significant attentions for several applications. However, PLA also exhibits some disadvantages such as low thermal stability, brittleness, and low impact resistance which obstruct its general purposes plastic application feasibility. In order to conquer such problems several studies have been investigated, for example, copolymerization, blending with other polymers, and composites. Composite materials are formed by combining two or more materials with different properties. They are composed of a continuous phase, so-called matrix phase, and the reinforce phase, which is a strong load-carrying material (Sanivada, Mármol, Brito, & Fanguero, 2020) such as ceramic powder and fiber. There have been many works of PLA reinforced with natural fiber, for instance, PLA/flax (Oksman, Skrifvars, & Selin, 2003), PLA/Jute (Sanivada et al., 2020) and PLA/Bleach Eucalyptus Kraft Pulps (Nanthananon, Seadan, Pivsa- Art, Hamada, & Suttiruengwong, 2018).

Typha is a genus of plants. It is available abundantly in nature with wetland habitats. It is renewable with low economic value. In addition, Typha possesses high cellulose fiber content that could be promising to be processed into fine powder and used as reinforcement part for polymer matrix

composites. However, there is also an important concern for composite systems which is the poor interaction between the polymer matrix and natural fibers. Hence, the reactive agents have been frequently used to improve bonding between the natural fiber and polymer matrix.

Therefore, this research aimed to study the mechanical properties, flow properties, morphology and sound absorption coefficient of poly(lactic acid) reinforced with cellulose fiber at various ratio. The influence of the natural fiber ratios and the reactive compatibilizer on all properties of composites were investigated.

Materials and Methods

1. Materials

Poly(lactic acid) (PLA) 2003D was purchased from NatureWork ® LLC, USA. Typha fiber were naturally acquired from Nakhon Pathom province, Thailand. An epoxy-based chain extender Joncryl® ADR-4368F as reactive compatibilizer (designed to CE), was obtained from BASF Chemical Co., Ltd., Bangkok, Thailand. Sodium Hydroxide (NaOH) was purchased from VRBIOSCIENCE Co.,Ltd, Bangkok, Thailand.

2. Preparation of cellulose fiber

Typha was washed and dried in oven at 70 °C for 24 hours and then grinded into fine powder. The fiber was sieved to obtain less than 0.5 mm in fiber size. Typha fiber was treated with alkaline solution (NaOH) at concentration of 0.5%wt for 24 hours. After that, fiber was washed with water for several times until pH of washed-water was neutral. Treated fiber was dried in oven at 70 °C for 24 hours.

3. Preparation of PLA/Typha fiber composites

PLA resin was first dried at 60°C for 12 hours prior further use to eliminate moisture. Then the PLA pellets were premixed with fiber before mixing in the twin screw extruder (ENMACH, ENT26/40). PLA/Typha composites were prepared with Typha fiber at the content of 0-40 phr. The reactive compatibilizer was fixed at 1 phr. The composites were prepared in the twin screw extruder under the temperature profile from feed zone to die set at 160 – 190 °C and the rotation speed was around 180 rpm. The extrudate was cooled in the water bath, then granulated and dried at 60 °C for 24 hours.

4. Characterization and testing

Treated fiber was characterized by Fourier-transform infrared spectroscopy (FTIR, Spectrum Two, Perkin Elmer) operated with the Spectrum software. The treated fiber was dispersed and mixed with the KBr powder and pressed into pellets for measurement by the KBr disk method. The sample was characterized at a resolution of 4 cm⁻¹ with background and sample 16 scans in the spectral range of 4,000 – 400 cm⁻¹.

The morphologies of all composites were analyzed by Scanning Electron Microscope (SEM, Hitachi TM3030) at an accelerating voltage of 15 kV. The extrudates from twin screw extrusion were cooled in the liquid nitrogen and then fractured. They were gold coated before analysis to avoid charging.

Melt flow index of all samples were performed on a melt flow indexer (Intro D7053, KAYENESS) operating at 190 °C with 2.16 kg load according to ASTM D1238.

Tensile properties of samples were tested by using Universal Testing Machine (Instron 5969, Instron) in accordance with ASTM D638 (Type V). The specimens were tested at a cross-head speed of 5 mm/min. Impact test was performed in accordance with ASTM D256 (Zwick B5102.202, Izod type). The specimens were prepared by compression molding, (CHAREON TUT CO., LTD., Thailand) at 190 °C.

The Normal incidence sound absorption coefficient was performed with WinZaxMTX (NOE Asia Pacific Co., Ltd., Thailand).

Results and discussion

1. Characterization of treated cellulose fiber

The FT-IR spectra of untreated and treated cellulose fiber were shown in the Figure 1.

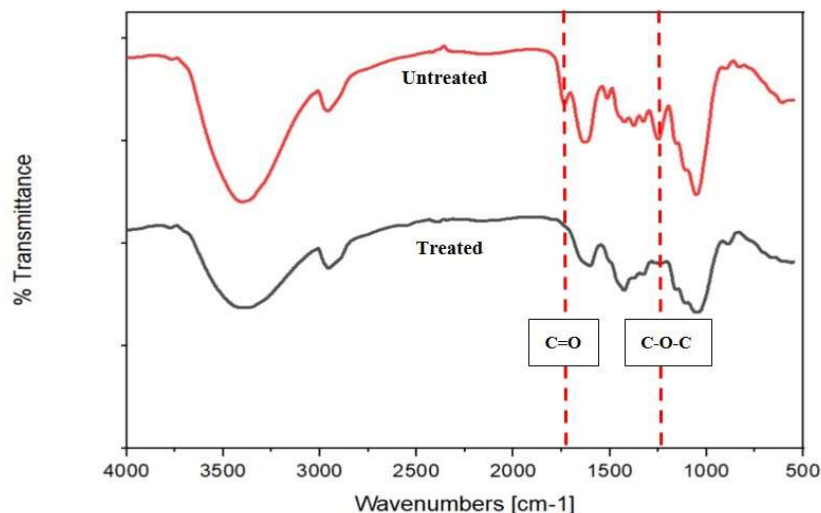


Figure 1 FT-IR spectra of untreated and treated cellulose fiber

The intensive peaks located at around 3500 cm^{-1} of both untreated and treated of cellulose fiber were referred to the hydroxyl group. The peak at 1736 cm^{-1} which was seen from untreated fiber corresponded to carbonyl group in hemicellulose. The peak (C-O-C) appeared at 1249 cm^{-1} belonged to the ester bond of lignin. After the treatment, the characteristic peaks of hemicellulose and lignin disappeared. The results clearly revealed that the treatment of fiber by alkaline solution could remove portion of hemicelluloses, lignin and contaminated matters from fiber. As a result, the fiber surface became cleaned (Kabir, Wang, Lau, & Cardona, 2012).

2. Morphology of composites

The morphology of PLA/Typha composite which added reactive compatibilizer (CE) and without compatibilizer were characterized by SEM as shown in the Figure 2 and Figure 3.

Figure 2 showed SEM micrograph of PLA/Typha at various fiber amount without reactive compatibilizer addition. It could be seen that fiber was well distributed into PLA matrix at lower fiber content, however, fibers agglomerated bundle were observed with increase of fiber content. Moreover, holes and large voids between PLA matrix and fiber were seen as well as some pull-outs of fiber (circle marks). The observations indicated the poor interfacial adhesion between PLA and fiber.

Considering the reactive compatibilizer added PLA/Typha composite as exhibited in Figure 3, it showed that fiber was embed into PLA matrix and the broken fiber was seen without voids between the fiber and PLA matrix (see arrows in Figure 3(c) and 3(d)). The results indicated a good adhesion between PLA matrix and fiber which corresponded to the excellent interfacial adhesion between the PLA matrix and fiber. This is because of the reactive compatibilizer.

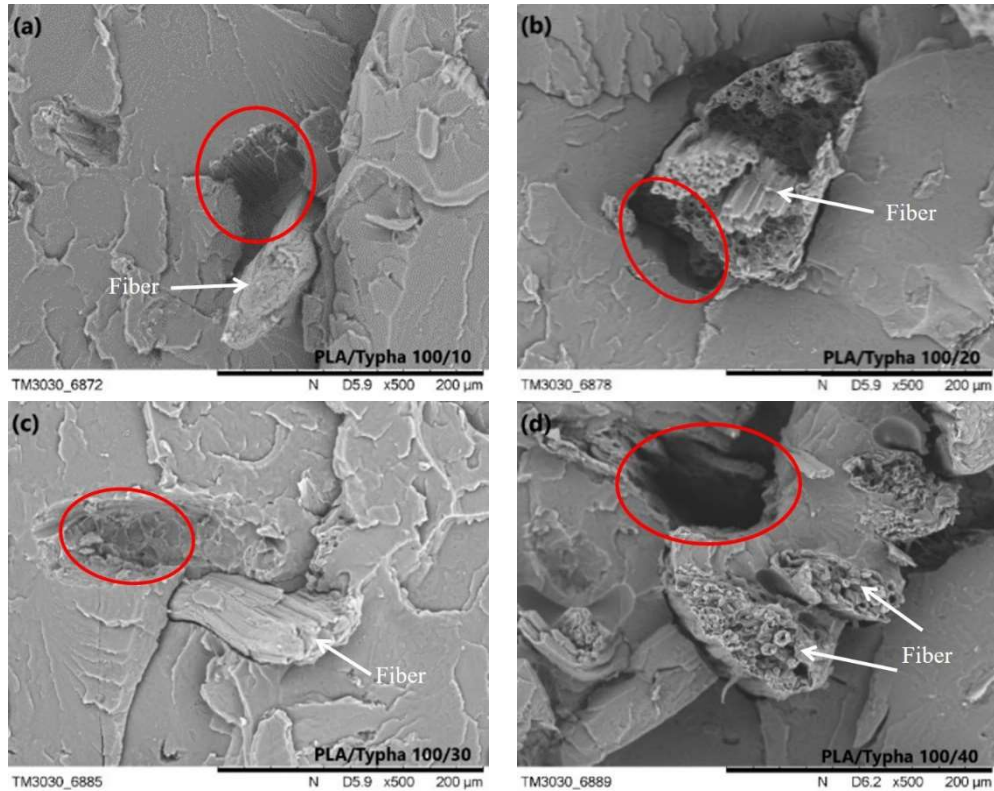


Figure 2 Morphology of PLA/Typha composites at ratio of (a) 100/10, (b) 100/20, (c) 100/30 and (d) 100/40

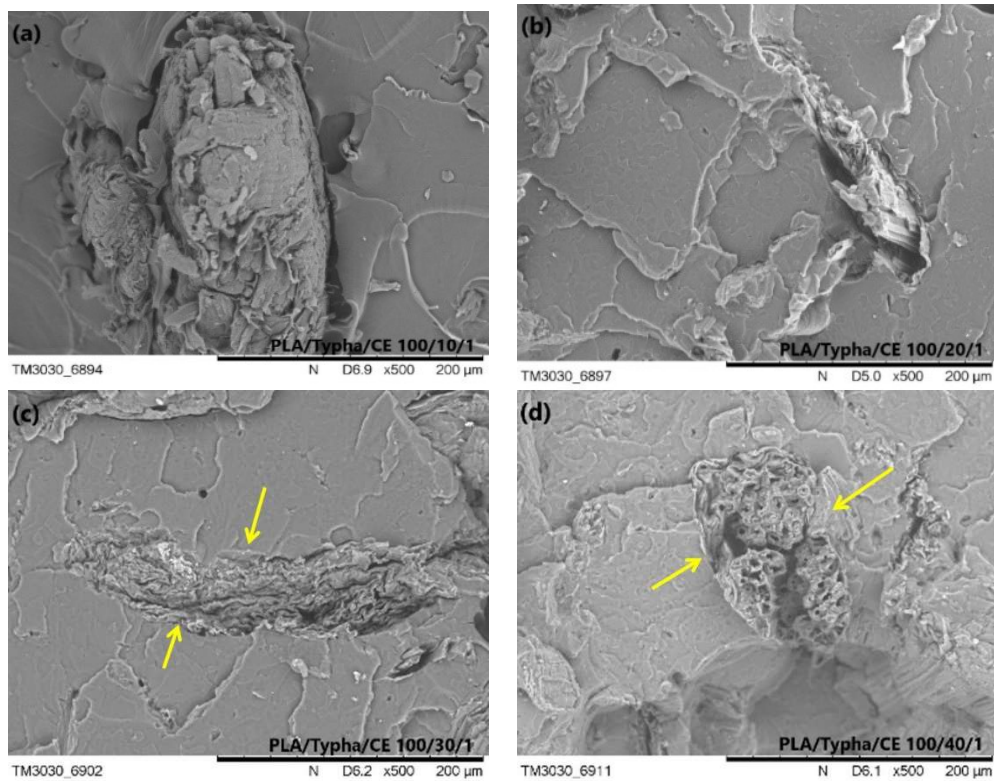


Figure 3. Morphology of PLA/Typha added reactive compatibilizer composite at ratio of (a) 100/10/1, (b) 100/20/1, (c) 100/30/1 and (d) 100/40/1

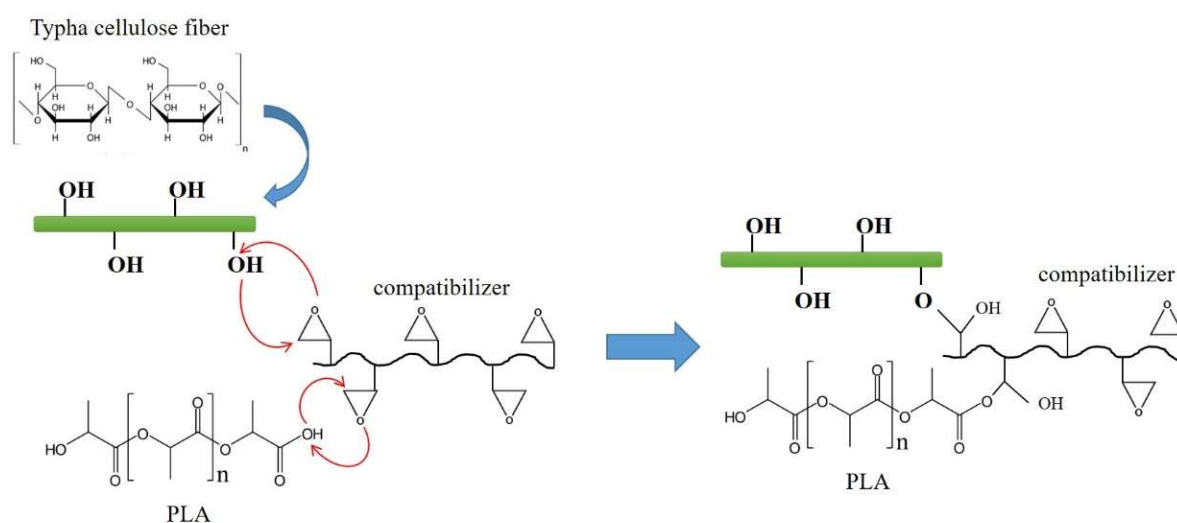
3. Melt flow index

The melt flow index (MFI) results of all samples were summarized in Table 1.

Table 1. Melt flow index of all samples

Formula	MFI (g/10min)	S.D. (±)
Neat PLA	3.516	0.039
PLA/Typha 100/10	3.146	0.227
PLA/Typha 100/20	3.108	0.065
PLA/Typha 100/30	1.653	0.118
PLA/Typha 100/40	0.668	0.329
PLA/Typha/CE 100/10/1	0.854	0.137
PLA/Typha/CE 100/20/1	0.529	0.009
PLA/Typha/CE 100/30/1	0.379	0.077
PLA/Typha/CE 100/40/1	0.144	0.018

The MFI value of neat PLA was 3.516 g/10 min. For PLA/Typha composites without reactive compatibilizer, the MFI values tended to be lower with the increase of fiber content. This associated with the flow disturbance by the fiber and provided obstruction to flow of the polymer melt. This result was also observed for PLA/Typha composites which added reactive compatibilizer. Additionally, PLA/Typha composites with the reactive compatibilizer addition showed the lower MFI value than that of composites without reactive compatibilizer for all ratio. These results implied the good reaction between PLA/Typha composites and reactive compatibilizer. The reactive compatibilizer (CE) consists of multifunctional epoxide which is the reactive group and provides the excellent possibility to react with both hydroxyl and carboxyl groups of PLA and hydroxyl groups on cellulose fiber (Khankrua, Pivsa-Art, Hiroyuki, & Suttiruengwong, 2014). The possible reaction was presented in the scheme 1.



Scheme 1 Possible reaction between PLA, Typha cellulose fiber and reactive compatibilizer

4. Mechanical properties

The tensile strength, Young’s modulus, elongation at break and impact strength of neat PLA and PLA/Typha composites were shown in Figure.4(a)-4(d), respectively.

From Figure 4(a), tensile strength of neat PLA was 51 MPa, approximately. For PLA/Typha without adding reactive compaibilizer, the tensile strength of composite for all ratios significantly decreased and lower than that of neat PLA. In the case of composite adding reactive compaibilizer, tensile strength of all ratio was higher than those of composite without adding reactive compaibilizer. It could be seen that PLA/Typha at ratio of 100/30 adding reactive compaibilizer exhibited the lowest tensile strength. This may be due to the higher fiber content, fiber might prefer to react between themselves and became stiff bundle in the matrix that lower strength than PLA matrix. Therefore, it possesses the lower in tensile strength. Meanwhile at ratio 100/40 the fiber also became bundle and bigger than at 30 phr, hence, it showed the higher tensile strength than PLA/Typha at 100/30. Considering Young’s modulus (as shown in the Figure 4(b)), it could be seen that Young’s modulus of composites without adding reactive compaibilizer slightly increased with increase of fiber content and they were greater than that of neat PLA (1224 MPa). Furthermore, composites adding reactive compaibilizer exhibited higher Young’s modulus than those of composites without adding reactive compaibilizer for all ratios.

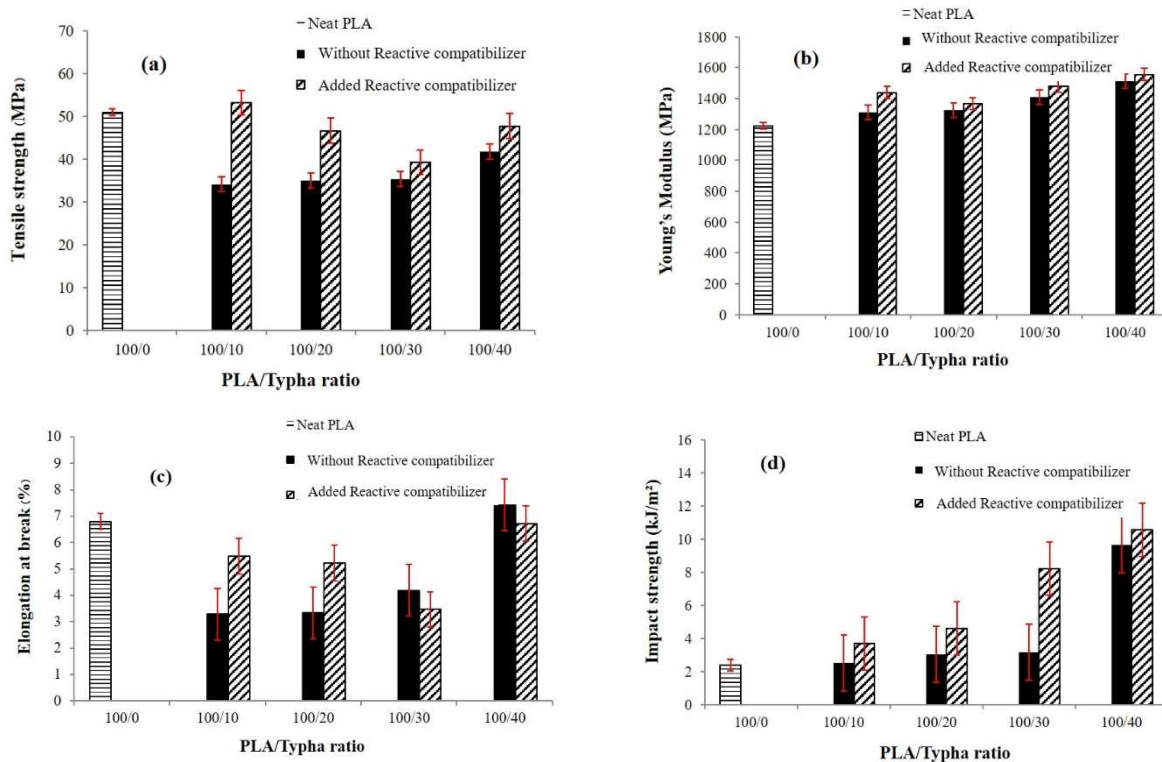


Figure 4. Mechanical properties of composites (a) Tensile strength, (b) Young’s modulus, (c) Elongation at break and (d) Impact strength

From Figure 4(c), it found that elongation at break of neat PLA was 6.8% whereas PLA/Typha added reactive compaibilizer at fiber content of 10-30 phr were considerably decreased. This result was also similar to composite adding reactive compaibilizer. However, at fiber content 40 phr, elongation at break of both composites increased and were comparable to neat PLA. Considering at fiber content of 10-20 phr, it could be seen that the elongation at break of composite which added reactive compaibilizer was almost two-folds higher than composite without reactive compaibilizer. However, after fiber content 20 phr, elongation at break of composite which added reactive

compatibilizer were lower than that of composites adding reactive compatibilizer. This could be associated with the more reaction between reactive compatibilizer and fibers. The higher fiber content, consequently, fiber might prefer to react between themselves and became bulky and stronger. Therefore, the fiber agglomeration resulted in reduction of elongation at break.

For impact strength (in Figure 4(d)), PLA exhibited low impact strength at 2.39 KJ/m². It was obviously observed that the impact strength of PLA/Typha composite was higher when compare to neat PLA. In addition, it increased with fiber content increase. This behaviour was also observed for composite which added reactive compatibilizer. Furthermore, impact strength of composites with reactive compatibilizer addition was significantly higher than those of without one. This indicated the interfacial adhesion improvement between PLA matrix and fibers by adding reactive compatibilizer. This reason was supported by SEM micrographs and MFI results.

5. Sound absorption coefficient (SAC)

The variation of the values of sound absorption coefficients at frequency from 150-5000 Hz of samples were shown in the Figure 5. PLA/Typha composite with fiber content of 40 phr with and without reactive compatibilizer were chosen to study.

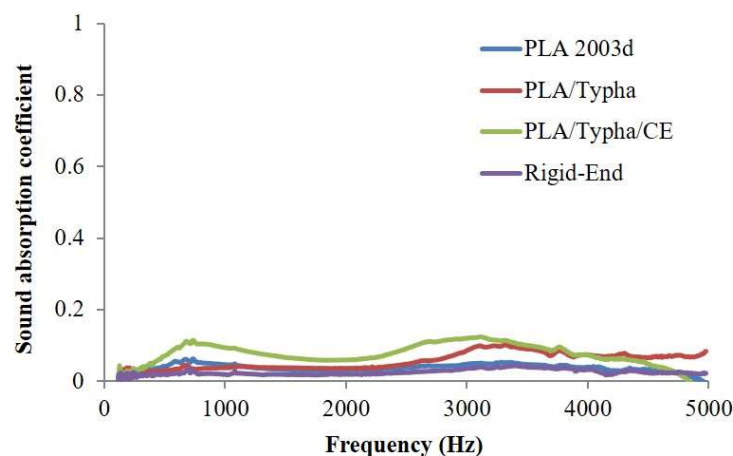


Figure 5 Sound absorption coefficient of neat PLA 2003D, PLA/Typha and PLA/Typha/CE

Generally, natural fibers have been usually mixed in material to improve the acoustic absorption properties. The effective sound absorption of the composite materials can be achieved when it consists of a more tortuous path, higher surface area, higher flow resistivity, and low porosity (Mamtaz, Fouladi, Al-Atabi, & Narayana Namasivayam, 2016). The specimens used in this study was prepared by compression molding. Dimension of specimens were 15 mm in thickness and 39.5 mm in diameter. The specimens were dense and the fibers were buried with PLA resin. The measured results could result in very low values of sound absorption coefficients in all samples, however, the results implied that the specimens exhibited the good sound reflection property.

Conclusions

The results in this work showed the successful preparation of PLA/Typha biocomposite material. The impurities in fiber were removed after treatment by alkaline solution which confirmed by FTIR analysis. The morphology of the composite which added reactive compatibilizer exhibited the good adhesion between fiber and PLA matrix, however, fiber agglomeration could also be observed. Flow properties showed that the MFI of the composites decreased with increase of fiber content. For the mechanical properties, it showed that the tensile strength, Young’s modulus and impact strength of composites which added compatibilizer were higher than those of composites

without addition of compatibilizer for all ratios. Sound Absorption test showed that the specimens could not absorb sound, but it could be a sound barrier material because of good reflection property.

Acknowledgements

The authors acknowledge the Department of Materials Engineering, Faculty of Engineering, Rajamangala University of Technology Rattanakosin, Institute of Research and Development Rajamangala University of Technology Rattanakosin for funding support. The authors are also greatly thankful to NOE Asia Pacific Co., Ltd., Thailand for sound absorption measurement.

References

- Ikada, Y., & Tsuji, H. (2000). Biodegradable polyesters for medical and ecological applications. *Macromolecular Rapid Communications*, 21(3), 117-132. doi:[https://doi.org/10.1002/\(SICI\)1521-3927\(20000201\)21:3<117::AID-MARC117>3.0.CO;2-X](https://doi.org/10.1002/(SICI)1521-3927(20000201)21:3<117::AID-MARC117>3.0.CO;2-X)
- Kabir, M. M., Wang, H., Lau, K. T., & Cardona, F. (2012). Chemical treatments on plant-based natural fibre reinforced polymer composites: An overview. *Composites Part B: Engineering*, 43(7), 2883-2892. doi:<https://doi.org/10.1016/j.compositesb.2012.04.053>
- Khankrua, R., Pivsa-Art, S., Hiroyuki, H., & Suttiruengwong, S. (2014). Effect of chain extenders on thermal and mechanical properties of poly(lactic acid) at high processing temperatures: Potential application in PLA/Polyamide 6 blend. *Polymer Degradation and Stability*, 108(0), 232-240. doi:<http://dx.doi.org/10.1016/j.polymdegradstab.2014.04.019>
- Mamtaz, H., Fouladi, M. H., Al-Atabi, M., & Narayana Namasivayam, S. (2016). Acoustic Absorption of Natural Fiber Composites. *Journal of Engineering*, 2016, 5836107. doi:10.1155/2016/5836107
- Nanthananon, P., Seadan, M., Pivsa-Art, S., Hamada, H., & Suttiruengwong, S. (2018). Facile Preparation and Characterization of Short-Fiber and Talc Reinforced Poly(Lactic Acid) Hybrid Composite with In Situ Reactive Compatibilizers. *Materials (Basel)*, 11(7). doi:10.3390/ma11071183
- Oksman, K., Skrifvars, M., & Selin, J. F. (2003). Natural fibres as reinforcement in polylactic acid (PLA) composites. *Composites Science and Technology*, 63(9), 1317-1324. doi:[https://doi.org/10.1016/S0266-3538\(03\)00103-9](https://doi.org/10.1016/S0266-3538(03)00103-9)
- Sanivada, U. K., Mármol, G., Brito, F. P., & Fangueiro, R. (2020). PLA Composites Reinforced with Flax and Jute Fibers—A Review of Recent Trends, Processing Parameters and Mechanical Properties. *Polymers*, 12(10), 2373. Retrieved from <https://www.mdpi.com/2073-4360/12/10/2373>

Investigation of Dielectric and Ferroelectric of Niobium and Lithium Co-Doped Bismuth Sodium Potassium Titanate Ceramics

Thanaporn Boonchoo¹, Chatchai Kruea-In², Phatraya Srabua³ and Wilaiwan Leenakul^{1*}

¹ Faculty of Science and Technology, Rajamangala University of Technology Phra Nakhon, Bangkok 10800, Thailand

² Faculty of Science and Technology, Chiang Mai Rajabhat University, Chiang Mai 50300, Thailand

³ Scientific and Technological Research Equipment Center (STREC), Chulalongkorn University, Bangkok 10330, Thailand

* Corresponding email: wilaiwan.l@rmutp.ac.th

Abstract

In this study was synthesized and investigated the dielectric and ferroelectric properties of Nb and Li co-doped $\text{Bi}_{0.5}(\text{Na}_{0.81}\text{K}_{0.19})_{0.5}\text{TiO}_3$ ceramics. The solid state reaction technique was used for fabrication process of this ceramic system. The temperature and dwelling time for calcinations was 850 °C and 4 h, respectively. The green pellet of the molding was sintered at 950-1025 °C for 2 h. The dielectric properties were changed depending on the level of additive contents. The dielectric constants at T_m were 5482, 3343, 2789, and 2154 for $x=0, 3, 6$ and 9 wt.% which measured at 10 kHz, respectively. The ferroelectric behaviors changed from normal ferroelectric state to ergodic relaxor ferroelectric state at $x>3$ wt% of the additive.

Keywords: dielectric, ferroelectric, calcination

Introduction

The binary lead-free of bismuth sodium titanate (BNT) and bismuth potassium titanate (BKT) ceramics are very attractive since they produce good piezoelectric properties and excellent stain properties at near morphotropic phase boundary (MPB) Kumar et al., (2012), Pham et al., (2010), Sasaki et al., (1999), Ullah et al., (2012), Kruea-In et al., (2016). The coexistence of two phase structure at MPB of $(1-x)\text{BNT}-x\text{BKT}$ was found at $x=0.16-0.20$ Sasaki et al., (1999), Ullah et al., (2012), Kruea-In et al., (2016), Elkechai et al., (1996). At around these compositions have two phase combination which phases are tetragonal and rhombohedral symmetry crystal structure Sasaki et al., (1999), Elkechai et al., (1996), Fu et al., (2012). The electrical properties of $(1-x)\text{BNT}-x\text{BKT}$ ceramics have a chance promoting as a lead-free electrical material to use in electronic device part which is potentially for replacing lead based materials. Recently, the modified BNKT by doping some rare earth and metal oxides such as Er_2O_3 Fu et al., (2012), Nd_2O_3 Yang et al., (2009), and NiO Kruea-In et al., (2015) is improved physical and electrical properties of BNKT ceramics. However, the modified of BNKT ceramics by co-doped of Nb and Li additive has not been presented so far. These motivated us to investigate the effects of small additions of $\text{Nb}_2\text{O}_5\text{-Li}_2\text{CO}_3$ in composites of $\text{Bi}_{0.5}(\text{Na}_{0.81}\text{K}_{0.19})_{0.5}\text{TiO}_3\text{-}x(\text{Nb}_2\text{O}_5\text{-Li}_2\text{CO}_3)$ ceramics in properties of dielectric and ferroelectric properties.

Experiment

The simple conventional route method for synthesized was used to fabricate the powders of $\text{Bi}_{0.5}(\text{Na}_{0.81}\text{K}_{0.19})_{0.5}\text{TiO}_3$. The high purity grade materials of Bi_2O_3 , Na_2CO_3 , K_2CO_3 , and TiO_2 were used as raw materials. Each start materials were weighed following the stoichiometry chemical formula. The weighed powders were mixed by a planetary ball milled with ethanol liquid medium and partially stabilized zirconia as a grinding medium for 24 h. The slurry after mixed was dried and

sieved. The obtained powders were calcined at 850 °C for 4 h at room atmosphere and in a covered alumina crucible. The powders from calcination process were then added with Nb₂O₅ and Li₂CO₃. The Bi_{0.5}(Na_{0.81}K_{0.19})_{0.5}TiO₃-x(Nb₂O₅-Li₂CO₃) with x=0, 3, 6 and 9 wt.% were weighed and then mixed. After drying, the obtained powders were added by 3 wt.% of a polyvinyl alcohol binder (PVA) as binder adhesive combination. The resulting powders were cold isostatically pressed for the 10 mm in diameter of pellets. After that, the green pellets were sintered at 900-1050 °C for 2 h in order to optimize sintering temperature for each composition. The obtained samples were grinded to 1 mm of thickness. Then, the both sides of the sample were painted with silver conducting layer. The dielectric properties such as dielectric constant and the loss tangent at room temperature and a wide range of high temperature were measured using an Agilent 4284A LCR meter. The ferroelectric properties were determined by a ferroelectric tester (Radiant Technologies Inc.)

Results and discussion

The frequency dependent dielectric constant and dielectric loss value at room temperature were shown in Fig. 1. All modified samples show lower dielectric constant than pure BNKT ceramic. Dielectric constant values at 1 kHz were 1541, 1088, 1135, and 1002 for x=0, 3, 6 and 9 wt.%. However, dielectric loss values were close to each condition. The dielectric loss at 1 kHz is approximately 0.04. It should be noted that all samples show dielectric loss lower than 0.07 for frequency in the range 10³-10⁶ Hz at room temperature.

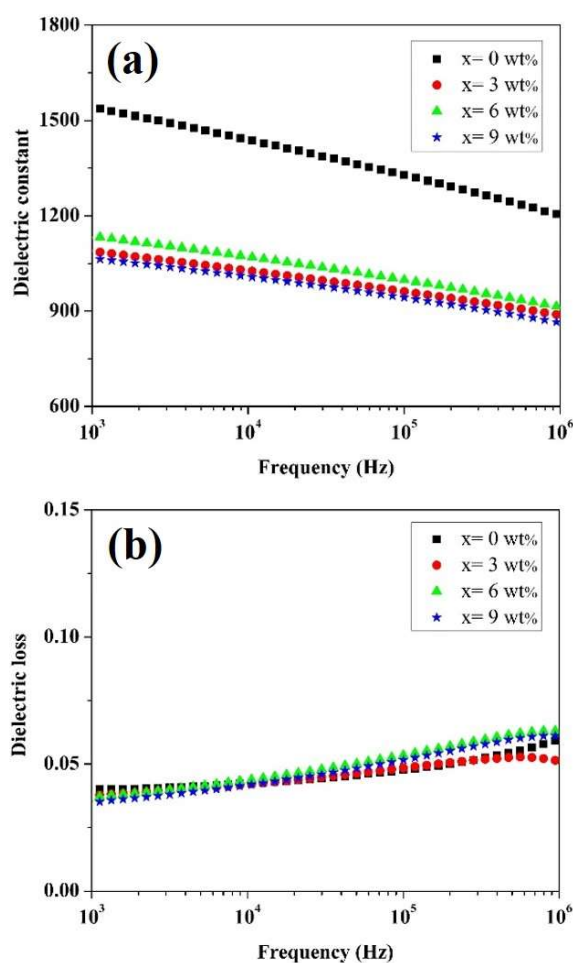


Figure 1 Frequency dependence dielectric constant (a) and dielectric loss (b) at frequency of 10³-10⁶ Hz and room temperature

Fig. 2 shows temperature dependence dielectric constant and dielectric loss of $\text{Bi}_{0.5}(\text{Na}_{0.81}\text{K}_{0.19})_{0.5}\text{TiO}_3-x(\text{Nb}_2\text{O}_5-\text{Li}_2\text{CO}_3)$ ceramics at the various frequency. The two phase transitions were observed in the unmodified sample. The first transition was around 110 °C at 10 kHz. The phase is a changing from a ferroelectric phase to anti-ferroelectric phase at this temperature. The temperature of this first transition is called the depolarized temperature (T_d). The second transition was around 320 °C at 10 kHz. This second transition, the phase is changing from anti-ferroelectric phase to paraelectric phase. The temperature of this second transition is called the maximum temperature (T_m) which were shown maximum dielectric constant Fu et al., (2012). For the modified sample, the two phase transition were merged together. The T_d could not observe in 3, 6, and 9 wt.% of doped samples. Moreover, the dielectric constant at T_m was decreased with increasing the doping contents. The dielectric constants at T_m were 5482, 3343, 2789, and 2154 for $x=0, 3, 6$ and 9 wt.%, respectively. The decreasing of the dielectric constant of modified BNKT ceramic was previously reported when the modified content higher than a limitation of diffusion. It may occur by the increasing defect in ceramics or the inhomogeneous in ceramics Fu et al., (2012).

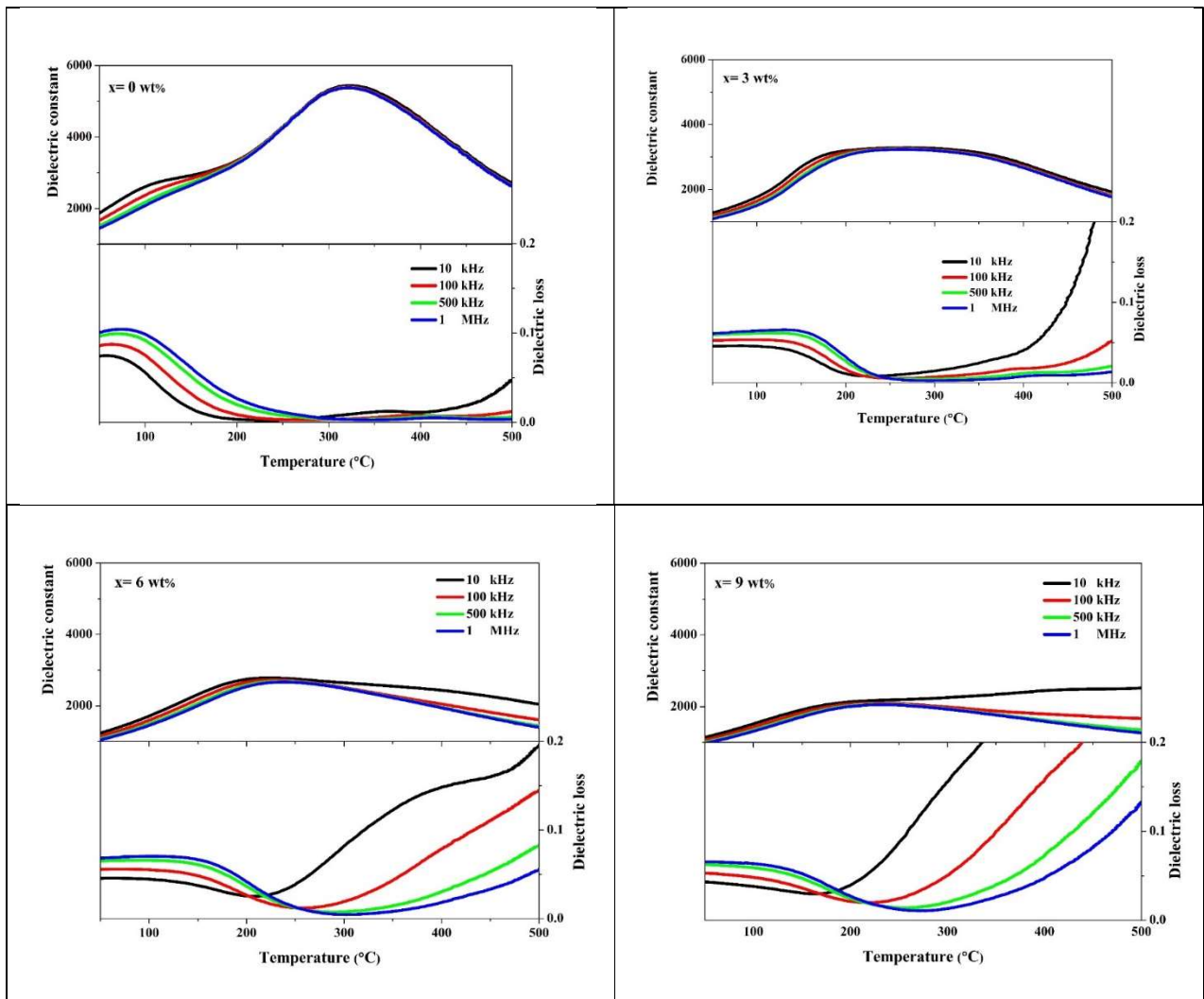


Figure 2 Dielectric constant and dielectric loss of $\text{Bi}_{0.5}(\text{Na}_{0.81}\text{K}_{0.19})_{0.5}\text{TiO}_3-x(\text{Nb}_2\text{O}_5-\text{Li}_2\text{CO}_3)$ ceramics with various temperature and frequency

The ferroelectric properties as a determination by the polarization versus electric field plots were shown in Fig. 3. The normal ferroelectric shape was presented at $x=0$ and $x=3$ wt.%. For $x > 3$

wt.%, the hysteresis loops show an ergodic relaxor properties which were low remanent polarization (P_r) and coercive field (E_c). The ergodic relaxor behavior of this modified ceramics may contribute by wide diffuse transition and frequency dispersion Pisitpipathsin et al., (2015). It should be noted that this modified content is mainly affected to phase transition from normal ferroelectric to ergodic relaxor ferroelectric of BNKT ceramics.

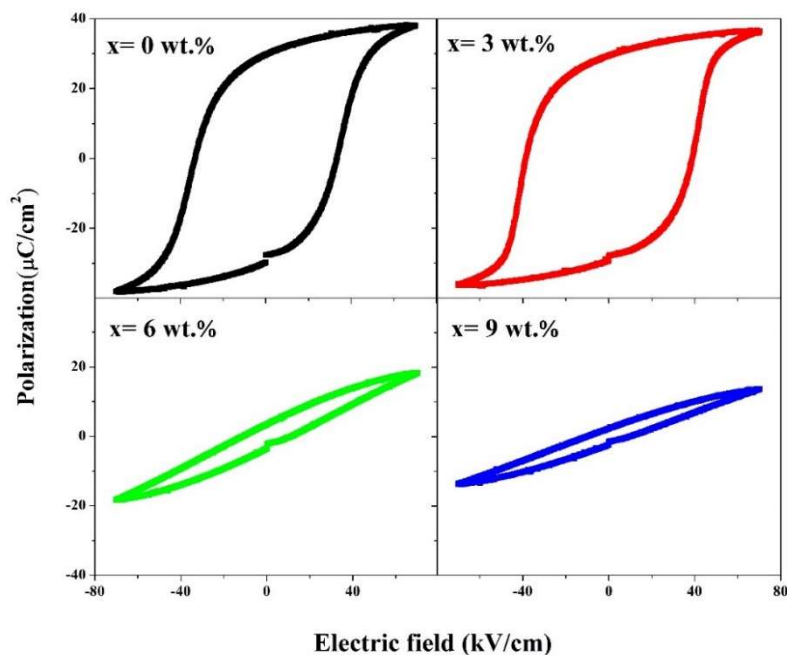


Figure 3 Polarization versus electric field (P-E) loop $\text{Bi}_{0.5}(\text{Na}_{0.81}\text{K}_{0.19})_{0.5}\text{TiO}_3-x(\text{Nb}_2\text{O}_5\text{-Li}_2\text{CO}_3)$ ceramics

Conclusion

The modified $\text{Bi}_{0.5}(\text{Na}_{0.81}\text{K}_{0.19})_{0.5}\text{TiO}_3-x(\text{Nb}_2\text{O}_5\text{-Li}_2\text{CO}_3)$ were synthesized by solid state reaction technique. The influence of additives on dielectric constant, dielectric loss at room temperature and high temperature up to 500 °C were studied. Therefore, The ferroelectric properties of $\text{Bi}_{0.5}(\text{Na}_{0.81}\text{K}_{0.19})_{0.5}\text{TiO}_3-x(\text{Nb}_2\text{O}_5\text{-Li}_2\text{CO}_3)$ ceramics at room temperature were investigated. For this study, the co-doped is significantly on dielectric and ferroelectric behaviors. The dielectric constant decreased with adding a higher amount of $\text{Nb}_2\text{O}_5\text{-Li}_2\text{CO}_3$ contents. In addition, the co-doped has the effect to ferroelectric properties which it changed from normal ferroelectric to ergodic relaxor ferroelectric.

Acknowledgements

Chiang Mai Rajabhat University supported financial this study as well as the National Research Council of Thailand (NRCT) and Rajamangala University of Technology Phra Nakorn. The author also would like to thanks, Faculty of Science and Technology Chiang Mai Rajabhat University, Faculty of Science and Technology Rajamangala University of Technology Phra Nakorn for supporting facilities.

Reference

- Elkechai, O., Manier, M., & Mercurio, J. P. (1996). $\text{Na}_{0.5}\text{Bi}_{0.5}\text{TiO}_3\text{-K}_{0.5}\text{Bi}_{0.5}\text{TiO}_3$ (NBT-KBT) system: a structural and electrical study. *Phys. Status. Solidi. A*, 152, 499-506.
- Fu, P., Xu, Z., Zhang, H., Chu, R., Li, W., and Zhao, M. (2012). Structure and electrical properties of Er_2O_3 doped $0.82\text{Bi}_{0.5}\text{Na}_{0.5}\text{TiO}_3\text{-}0.18\text{Bi}_{0.5}\text{K}_{0.5}\text{TiO}_3$ lead-free piezoelectric ceramics. *Mater. Design.*, 40, 373-377.

- Kruea-In, C., Inthong, S., and Leenakul, W. (2017). Effects of NiO nanoparticles on physics and mechanical properties of BNKT lead-free ceramics. *Appl. Mech. Mater.*, 866, 282-286.
- Kruea-In, C., Puanpia, P., Takhan, O., & Inthong S. (2016). Phase formation, microstructures, and mechanical properties of lead-free BNKT ferroelectric ceramics doped with BZZ. *Key. Eng. Mater.*, 675, 589-592.
- Kumar, K., & Kumar, B. (2012). Effect of Nb-doping on dielectric, ferroelectric and conduction behavior of lead free $\text{Bi}_{0.5}(\text{Na}_{0.5}\text{K}_{0.5})_{0.5}\text{TiO}_3$ ceramic. *Ceram. Int.* 38, 1157-1165.
- Pisitpipathsin, N., Kantha, P., Pengpat, K., Promsawut, M., and Pojprapai, S. (2015). Effect of KNbO_3 on physical and electrical properties of lead-free BaTiO_3 ceramics. *Ceram. Int.*, 41, 3639-3646.
- Pham, K., Hussain, A., Ahn, C. W., Kim, I. W., Jeong, S. J., Lee, J.S. (2010). Giant strain in Nb-doped $\text{Bi}_{0.5}(\text{Na}_{0.82}\text{K}_{0.18})_{0.5}\text{TiO}_3$ lead-free electromechanical ceramics. *Mater. Lett.* 64, 2219-2222.
- Sasaki, A., Chiba, T., Maniya, Y., & Otsuki, E. (1999). Dielectric and piezoelectric properties of $(\text{Bi}_{0.5}\text{Na}_{0.5})\text{TiO}_3$ - $(\text{Bi}_{0.5}\text{K}_{0.5})\text{TiO}_3$ relaxor ferroelectric ceramics. *Jpn. J. Appl. Phys.* 38, 5564-5567.
- Ullah, A., Ahn, C. W., Lee, S. Y., Kim, J. S., & Kim, I. W. (2012). Structure, ferroelectric properties, and electric field-induced large strain in lead-free $\text{Bi}_{0.5}(\text{Na,K})_{0.5}\text{TiO}_3$ - $(\text{Bi}_{0.5}\text{La}_{0.5})\text{AlO}_3$ piezoelectric ceramics. *Ceram. Inter.* 38, S363-S368.
- Yang, Z. P., Hou, Y. T., Liu, B., & Wei, L. L. (2009). Structure and electrical properties of Nd_2O_3 doped $0.82\text{Bi}_{0.5}\text{Na}_{0.5}\text{TiO}_3$ - $0.18\text{Bi}_{0.5}\text{K}_{0.5}\text{TiO}_3$ ceramics. *Ceram. Int.*, 35, 1423-1427.

Copper(II) Oxide/Reduced Graphene Composite Electrodes for Supercapacitors Performance

Santi Rattanaveeranon^{1*}, Knavoot Jiamwattanapong², Eugene Kilayco³
& Rungsan Ruamnikhom¹

¹*Applied Physics Material Laboratory (APM Lab.), Physics Program, Faculty of Liberal Arts, Rajamangala University of Technology Rattanakosin (RMUTR), Nakhonpathom 73170, Thailand*
²*Department of General Education, Faculty of Liberal Arts, Rajamangala University of Technology Rattanakosin (RMUTR), Nakhonpathom 73170, Thailand*

³*Environmental Science, Faculty of Science and Technology, Rajamangala University of Technology Rattanakosin (RMUTR), Nakhonpathom 73170, Thailand*

* Corresponding email: santi.r@rmutr.ac.th

Abstract

High capacitance property of a capacitor is of great interest from both scientific and industrial points of view. In this research, we reported a method for increasing the capacitance of reduced graphene oxide (rGO) by depositing copper (II) oxide (CuO) on the rGO surface. The rGO was prepared by reducing graphene oxide (GO) with hydrazine as the reducing agent. By mixing GO with copper salts in a chemical reaction, CuO/rGO composites were created. The specific surface area of the samples was determined using Brunauer Emmett Teller (BET) analysis with the nitrogen adsorption method. The physical and chemical properties of the composites were investigated using scanning electron microscopy (SEM), atomic force microscope (AFM), and X-ray diffractometry. The I-V curve and capacitance were measured with a Potentiostat/Galvanostat. The results show that CuO can enhance the capacitance of rGO. The CuO/rGO composites exhibit high chemical stability and capacitance up to $165.42 \text{ F}\cdot\text{g}^{-1}$, which is higher than rGO ($113.15 \text{ F}\cdot\text{g}^{-1}$) and annealed graphite ($53.12 \text{ F}\cdot\text{g}^{-1}$). The mechanisms of capacitance enhancement based on both pseudocapacitor and double layer capacitance are reported and discussed.

Keywords: Capacitance, Copper Oxide Nanoparticle, Reduced Graphene Oxide

Introduction

The electrochemical capacitor, also known as a supercapacitor, has a high power density, a long life, and excellent safety properties. It has been widely used in various fields, including memory backup, electric vehicles, power quality management, battery improvement and renewable energy applications [Novoselov et al. 2005]. A variety of materials such as porous carbon, transition metal oxides, and conducting polymers have been investigated for improving the performance of supercapacitor [Kim et al. 2011]. Although these materials perform worse than composite materials [Wang et al. 2016], they can improve capacitance through two mechanisms: electrical double-layer and pseudocapacitive characteristics. The first requires materials with large surface area to store charges using an electrostatic principle and the second requires materials that can provide electrochemical reaction [Georgakilas et al. 2012]. A hybrid electrochemical capacitor is a capacitor that takes advantage of both characteristics. Researchers show that the composite materials containing both characteristics allow them to achieve higher capacitance and energy density compared to the use of single material.

Graphene is a single layer of carbon atoms that are sp^2 -bonded having a hexagonal lattice [Novoselov et al. 2005] and has been investigated considerably for several years due to its significant potential for both fundamental studies and technological applications [Wang et al. 2016].

Theoretically, the specific surface area of graphene was calculated to be $2600 \text{ m}^2 \cdot \text{g}^{-1}$ [Wang et al. 2012; Huang et al. 2012]. The high surface area may help to improve the electrochemical double-layer characteristics. For example, high reduced graphene oxide (HRGO), which has the specific surface area of $468.6 \text{ m}^2 \cdot \text{g}^{-1}$, provides the capacitance of $128 \text{ F} \cdot \text{g}^{-1}$ at a current density of $1 \text{ A} \cdot \text{g}^{-1}$, while rGO provides only $41 \text{ F} \cdot \text{g}^{-1}$ [Wang et al. 2016]. Additionally, when the electrochemical property of rGO was studied in three different electrolytes (1.0 M NaNO_3 , 1.0 M H_3PO_4 , and 1.0 M KOH), it was discovered that rGO could improve the surface area from $13.8 \text{ F} \cdot \text{g}^{-1}$ to $62.4 \text{ F} \cdot \text{g}^{-1}$ in 1.0 M NaNO_3 , from $24.5 \text{ F} \cdot \text{g}^{-1}$ to $101 \text{ F} \cdot \text{g}^{-1}$ in 1.0 M H_3PO_4 , and from $52.4 \text{ F} \cdot \text{g}^{-1}$ to $160 \text{ F} \cdot \text{g}^{-1}$ in 1.0 M KOH , respectively [Galal et al. 2018]. CuO nanoparticles are electrochemically active species that can provide pseudocapacitive characteristics. As a result, these two can be combined for the fabrication of a hybrid capacitor that can use both faradaic and non-faradaic processes for charge storage and improved electrochemical properties.

In this research, we synthesized a CuO/rGO composite by growing CuO nanoparticles on graphene oxide and then chemically reducing them to form the CuO/rGO composite. The composites were coated on a stainless steel electrode for electrochemical measurement.

Materials and methods

Synthesis of graphene oxide

Graphene oxide was synthesized using Hummers' method [Hummers et al. 1958]. In brief, 3g graphite powder (20 μm size, 99.99% purity from Lianyungang Jinli Carbon) was heated in an oven at $300 \text{ }^\circ\text{C}$ for 2 hours to remove impurities. The annealed graphites were then mixed with concentrated sulfuric acid, sodium nitrate and potassium permanganate under controlled temperature to obtain grey suspension. Following that, 3 ml of 30% H_2O_2 was slowly added to the beaker while being stirred to obtain a yellow-brown suspension. The suspension was stirred at room temperature for 30 minutes before being rinsed with deionized water until the pH was neutral. Finally, the GO was ready for rGO and CuO/rGO composite fabrication. To make reduced graphene oxide, 36 mg of graphene oxide was mixed with hydrazine monohydrate solution (NH_2NH_2) at a rate of 3 mg/ml (GO : NH_2NH_2) in a 500 ml round-bottom flask and stirred at 80°C for 12 hours using the reflux method. The solution and rGO precipitate were then washed away with water through vacuum filtration until the waste water pH was neutral. Finally, the rGO precipitate was dissolved with 50 ml of distilled water.

Synthesis of copper (II) oxide on reduced graphene oxide hybrid nanoparticle materials

GO was dispersed in deionized water to form a 30 ml of $0.2 \text{ mg} \cdot \text{ml}^{-1}$ GO dispersion. It was then sonicated for 30 minutes. Then 0.2 M of CuCl_2 was added into the GO dispersion. Following that, 30 ml of NaOH 0.1 M was gently dropped into the solution while stirring to achieve a pH of 10, and 1 ml of hydrazine solution was added. After 20 minutes of ultrasonication, it was allowed to react for 2 hours at $80 \text{ }^\circ\text{C}$. Finally, using centrifugation at 5,000 rpm for 20 min, the black precipitate was rinsed several times with deionized water. To obtain copper oxide formation, the final precipitation was annealed at $300 \text{ }^\circ\text{C}$ for 2 hours in the tube furnace under atmospheric air.

Spectroscopic measurements

Before each characterization, GO, rGO and CuO/rGO composites were dropped on glass-slide substrates and dried on the hotplate. The morphology of materials was investigated a transmission electron microscope (TEM, JEOL 1200) and a field emission scanning microscope (FESEM, Hitachi, s-4700). The structural property was studied using X-ray diffraction (XRD, Bruker D8 Advance diffractometer with Cu K (radiation)) at a slow scan rate of 0.021 degree/s .

Electrochemical measurements

The measurements were conducted in a two-electrode system using 2 mol·L⁻¹ KOH aqueous solutions. The electrochemical performance of the prepared materials was evaluated using cyclic voltammetry (CV), and galvanostatic charge/discharge (GCD) measurements on a Versastat4 workstation. The loading amounts of GO, rGO, and CuO/rGO composites (weight of active material) were mixed with 0.5 mg/ml of polyaniline (PANI) binder, determined by the weight difference of approximately 3.3 mg between the electrodes before and after testing [Li et al. 2011].

Results and Discussion

Morphology of copper (II) oxide on reduced graphene oxide

CuO/rGO composite was dropped on silicon wafer and dried at 80 °C for 2 hours in a N₂ tube furnace. Fig.1(a) shows a TEM image of CuO nanoparticles with a particle size smaller than 100 nm. Fig.1(b) shows a SEM image of CuO/rGO composites with an average CuO nanoparticle size of 66.32 ± 14.83 nm, as seen in Fig.1(d). The CuO nanoparticles were grown uniformly on rGO. Fig.1(c) shows an AFM image of exfoliated rGO dispersion in DI-water after coating on a silicon wafer surface. The AFM results revealed rGO sheets at the nanometer scale. The minimum layer thickness of rGO sheets was 1.2 nm, with approximately 4 layers (the average gap between two flat surfaces was 0.34 nm), indicating that the rGO sheet was characterized by few monolayers of graphene sheet in each particle, as well as completeness of the graphene plane after chemical reaction preparation [Bhavana et al. 2017].

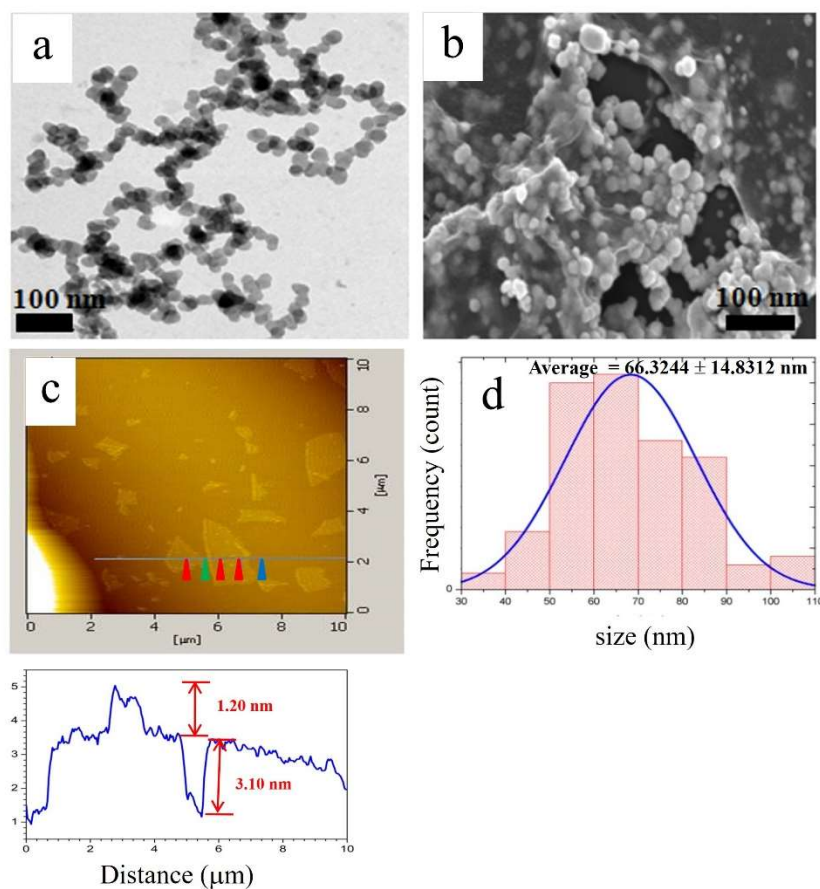


Figure 1 (a) TEM image of CuO nanoparticles, (b) TEM image of CuO/rGO composite, (c) AFM images of rGO, and (d) size distribution of CuO nanoparticles on rGO

Fig.2(a) shows the XRD patterns of the CuO/rGO composite after annealing at 300 °C for 2 h, the (Cu/Cu₂O)/rGO composite before annealing, and the rGO. Bragg’s reflections for CuO nanoparticles were observed in XRD patterns at 2theta values of 32.52°, 35.46°, 38.73°, and 48.80°, indicating the monoclinic planes (JCPDS No. 45-0397) [110], [002], [111] and [-202], respectively [Kollu et al. 2014]. Fig.2(b) shows the XRD pattern of copper (I) oxide nanoparticles at room temperature. Copper (I) oxide was observed in the XRD pattern at 2theta values of 36.41° and 61.34° corresponding to the [111] and [220] planes of cubic structure (JCPDS No.05-0667), respectively [Lakhera et al. 2017]. There were also three peaks, 43.64°, 50.80°, and 74.42°, which correspond to the [111], [200], and [220] planes, respectively. These peaks support the face centered cubic (FCC) structure of the copper element (JCPDS No. 04-0836) [Theivasanthi et al. 2010]. Fig.2(c) shows the XRD pattern of rGO occurring as a main peak at 2theta at approximately 25 degrees.

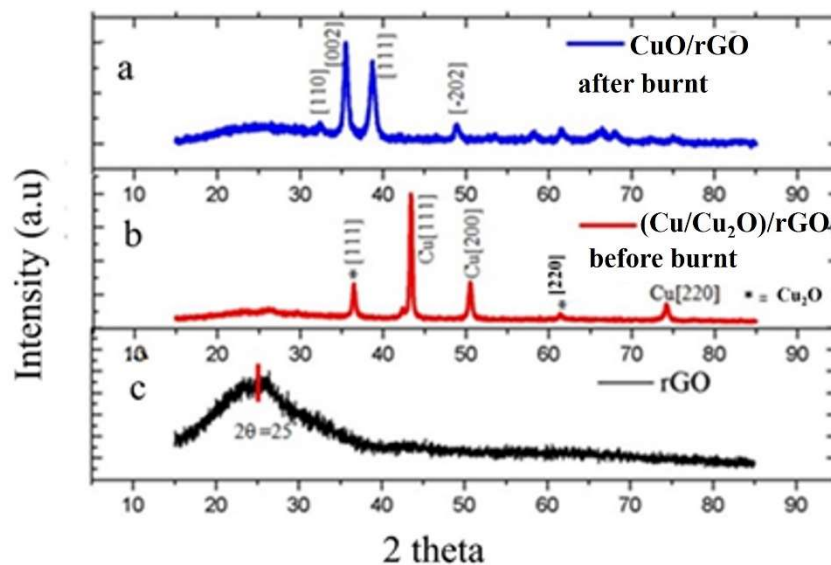


Figure 2 XRD diffractograms of (a) CuO/rGO composite, (b) (Cu/Cu₂O)/rGO and (c) rGO

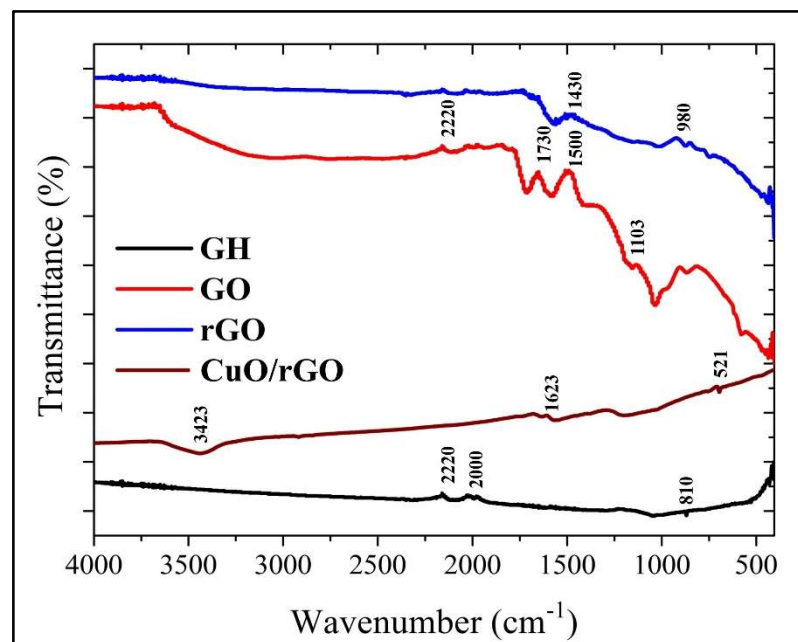


Figure 3 FT-IR spectra of the as-prepared GH, GO, rGO, and CuO/rGO composites

Fig.3 shows the FT-IR spectra of annealed raw graphite (GH), GO, rGO, and CuO/rGO composites. The broad absorptions at about 3432 and 1623 cm^{-1} refer to the hydroxyl groups. The absorption band at 1053 cm^{-1} indicates the stretching vibration of C-O. The C=O vibration band at 1724 cm^{-1} (for rGO/CuO NPs) is further debilitated after hydrothermal reaction due to the transition of GO to rGO. In addition, the strong absorption band at 521 cm^{-1} is attributed to the vibration of the Cu-O bond [Liu et al. 2013]. The specific surface area, total pore volume, and average pore size of the carbon-based materials are shown in Table 1. Copper (II) oxide can be grown on the rGO surface helping the specific surface area of the composite improved.

Table 1 Comparison of specific surface area, total pore volume, and average pore size of the carbon-based materials.

Sample	Specific surface area (m^2/g)	Total pore volume (cc/g)	Average pore size (nm)
Raw graphite	4.50	0.086	76.60
Annealed raw graphite	117.26	0.128	4.37
rGO	625.89	0.956	6.11
CuO/rGO	649.30	0.679	4.18

Note: Annealed raw graphite was obtained after thermal treatment of raw graphite at 300 $^{\circ}\text{C}$ for 2 h.

Electrochemical ELDC applications

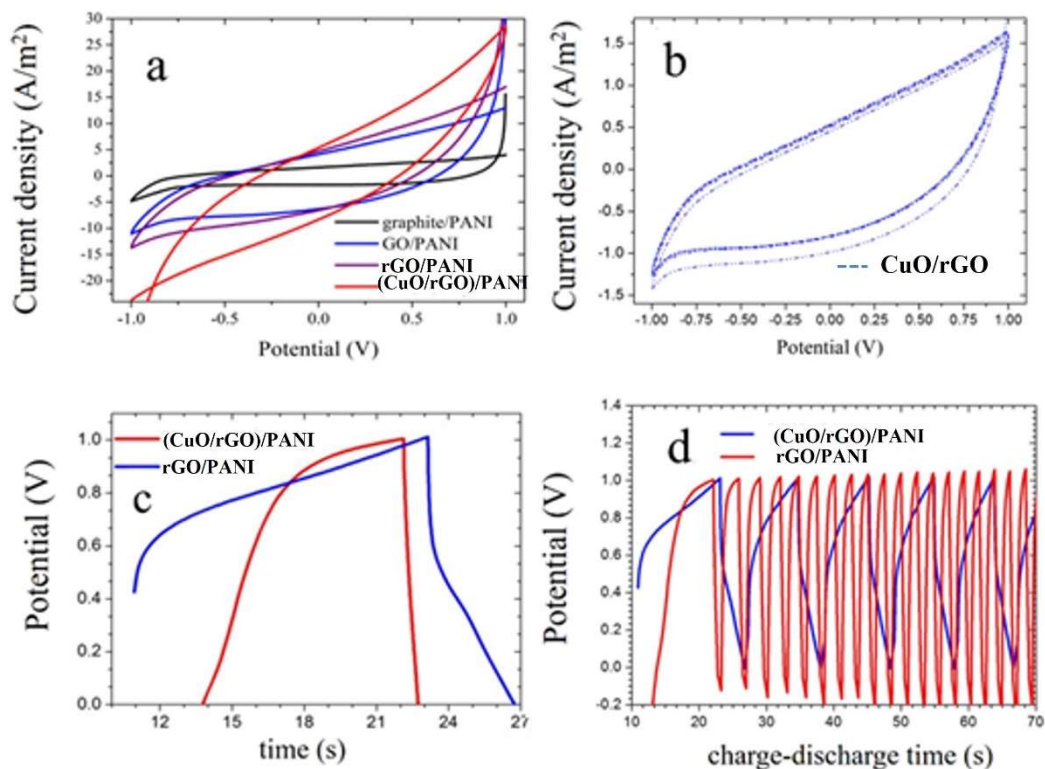


Figure 4 (a) CV curve of graphite, (b) GO, rGO and CuO/rGO nanocomposites with fixed scan rates at 50 mV/s in 2 M of KOH b CV curve of CuO/rGO composites as run scanned 5 cycles at 50 mV/sin 2 M of KOH, (c) Galvanostatic charge-discharge curves of rGO (1 cycle), and (d) CuO/rGO composite at 100 cycles

The samples of annealed raw graphite, GO, rGO and CuO/rGO composite were coated in 98 % stainless steel pure which the thickness of 1 mm and packed on a two-electrode cell configuration of an electric double capacitor. Fig.4(a)-(d) show the electrochemical characterization of the capacitors. According to the calculation, the CuO/rGO composites offer high chemical stability and capacitance of $165.42 \text{ F}\cdot\text{g}^{-1}$, which is higher than rGO ($113.15 \text{ F}\cdot\text{g}^{-1}$) and annealed graphite ($53.12 \text{ F}\cdot\text{g}^{-1}$).

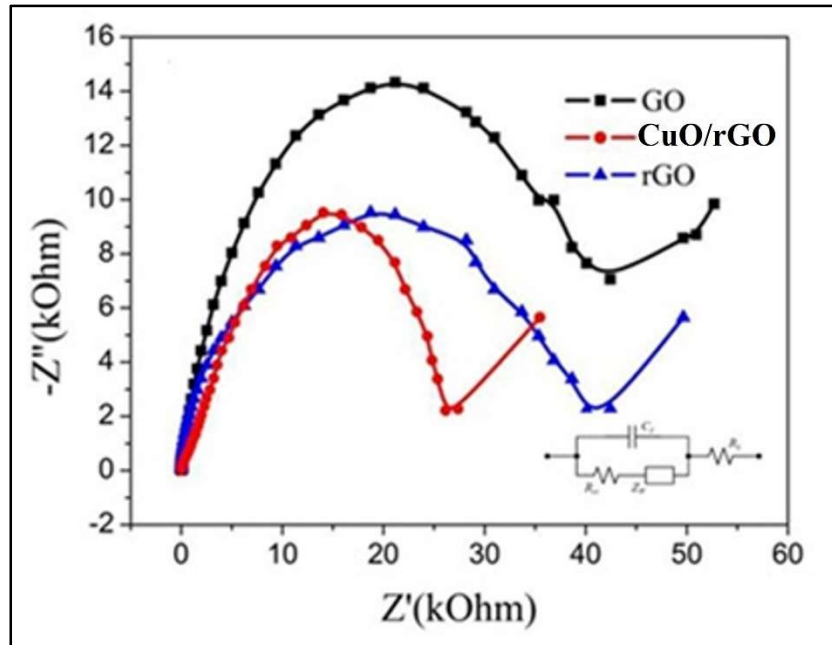


Figure 5 Nyquist plots of different composites electrodes: GO, rGO, and CuO/rGO composites

Fig.5 shows the results from the electrochemical impedance spectroscopy (EIS) of GO, rGO, and CuO/rGO composites in 2 M KOH aqueous electrolyte. The EIS was appeared with a frequency range of 0.1 Hz-10 kHz and a DC bias of 5 V. The straight line in the low-frequency range, which is called the Warburg resistance, is caused by the frequency dependence of ion diffusion/transport from the electrolyte to the electrode surfaces [Huang et al. 2018]. The curve shape in high frequency region corresponds to the charge transfer limiting process and the double-layer capacitance in parallel with the charge transfer resistance (R_{ct}) of which contact interface is between the electrode and electrolyte solution [Pajkossy et al. 2018]. In addition, the CuO/rGO composite exhibits a higher electrical conductivity than the rGO and GO materials.

Conclusion

In conclusion, the study demonstrates that the addition of CuO nanoparticles into rGO can improve the capacitance of an electrochemical capacitor. The capacitance-enhanced mechanism may be directly attributed to the synergistic effects of CuO nanoparticles and rGO. CuO nanoparticles can be used to improve the pseudocapacitive property of rGO-supercapacitors. CuO nanoparticles help to increase the surface area of rGO, which is important for the capacitor’s pseudocapacitive properties, and rGO contributes high electrical conductivity and electrochemical double-layer capacitance.

Acknowledgments

This study was financially supported by Rajamangala University of Technology Rattanakosin (RMUTR), with KMUTT providing the Potentiostat/Galvanostat instrumentation.

References

- Bhavana G, Niranjana K, Kalpataru P, Vigneshwaran, K, Shailesh J, & Fisher, VI. (2017). Role of oxygen functional groups in reduced graphene oxide for lubrication. *Scientific Reports*, 7(1): 1-14.
- Dubal DP, Chodankar NR, Gund GS, Holze R, Lokhande C D, & Gomez RP. (2015). Asymmetric Supercapacitors based on Hybrid CuO@Reduced Graphene Oxide@Sponge versus Reduced Graphene Oxide@Sponge Electrodes. *Energy Technology*, 3(2), 168-176.
- Georgakilas V, Otyepka M, Bourlinos AB, Chandra V, Kim N, Kemp C K. (2012). *Functionalization of graphene: covalent and non-covalent approaches, derivatives and applications*. *Chemical Reviews* 112:6156-214.
- Galal A, Hassan HK, Jacob T, Atta NF (2018). Enhancing the specific capacitance of SrRuO₃ and reduced graphene oxide in NaNO₃, H₃PO₄ and KOH electrolytes. *Electrochimica Acta*, 260: 738-747.
- Huang J. (2018). Diffusion impedance of electroactive materials, electrolytic solutions and porous electrodes. Warburg impedance and beyond. *Electrochimica Acta*, 281,170-188.
- Huang X, Qi X, Boey F, Zhang H. (2012). *Graphene-based composites*. *Chemical Society Reviews* 41:666-686.
- Kim K, Choi JY, Kim T, Cho S H, & Chung HJ. (2011). A role for graphene in silicon-based semiconductor devices. *Nature*, 479,338-344.
- Kollu P, (2014). Green synthesis of CuO nanoparticles using phyllanthus amarus Leaf extract and their antibacterial activity against multidrug resistance bacteria. *International Journal of Engineering Research & Technology (IJERT)*, 3,639-641.
- Lakhera SK, Venkataramana R, Watts A, Anpo M, Neppolian B. (2017). Facile synthesis of Fe₂O₃/Cu₂O nanocomposite and its visible light photocatalytic activity for the degradation of cationic dyes. *Research on Chemical Intermediates*, 43(9), 5091-5102.
- Liu Y, Ying Y, Mao Y, Gu L, Wang Y, Peng X. (2013). CuO nanosheets/rGO hybrid lamellar films with enhanced capacitance. *Nanoscale*, 5, 9134-9140.
- Novoselov KS, Geim AK, Morosov SV, Jiang D, Katsnelson MI, Grigorieva IV, Dubonos SV, Firsov AA. (2005). Electric field effect in atomically thin carbon films. *Nature*, 306, 666-669.
- Pajkossy T, Jurczakowski R. (2017). Electrochemical impedance spectroscopy in interfacial studies. *Current Opinion in Electrochemistry*, 1(1), 53-58.
- Theivasanthi T. Alagar M. (2010). *X-Ray diffraction studies of copper nanopowder*. General Physics Retrieved from <http://www.arxiv.org/abs/1003.6068>.
- Wang C, Zhou J, Du F. (2016). Synthesis of Highly Reduced Graphene Oxide for Supercapacitor. *Journal of Nanomaterials*, 2016:1-7.
- Wang H, Lin J, Shen ZX. (2016). Polyaniline (PANI) based electrode materials for energy storage and conversion. *Journal of Science: Advanced Materials and Devices*, 1, 225-255.



RMUTCON

Session 5:

**Tourism Cultural and
Creative Technology**

The Creation of Rong Ngeng Rhythms on Drum Set

Sittichok Kabilapat*

*Western Music Department, Faculty of Fine and Applied Arts Songkhla Rajabhat University, 160
Kanchanavanich Road, Khao Rup Chang Subdistrict, Mueang Songkhla District, Songkhla
Province, 90000, Thailand.*

** Corresponding email: aoddrum1@gmail.com*

Abstract

In Southern Thailand, Rong Ngeng music in Pattani province is an art form that blends Western and Eastern performance cultures. Therefore, the instruments in the Rong Ngeng music are formed by a combination of Western and Eastern music instruments. One of the important instruments that determine the rhythm of Rong Ngeng's music and dance is the Large Ramana. This creative study aims to arrange the Ramanna rhythmic pattern of Rong Ngeng music into the notation for drum set and to incorporate this piece into drum set and percussion course's curriculum. The composer will present the rhythmic pattern of the Ramana, which is the main rhythmic instrument in the Rong Ngeng music to use for playing on the drum set. By bringing the notes in the part of the Ramana in the Yoget rhythm of the song Laguduva that use 4/4 time and the tempo is 120, then, rearrange it into a Latin rhythm (Samba) on drum set. It is the creation and arrangement of folk music rhythms to develop more into contemporary music. This is the preservation, continuation of wisdom and the dissemination of arts and culture of southern folk music to the international.

As a result, the composer incorporates this creative contemporary composition within his instruction as well as the drum set and percussion course. He uses this song as a starting point for discussions about multiculturalism with his students, discussing about contemporary music and culture. Furthermore, the composer uses this creative art work to inspire his students to create their own works of art.

Keywords: Creativity, Rong Ngeng rhythm, Drum set

Introduction

In the South of Thailand is a folk music that deserves to be preserved. Inherited and created for the continuation one of the folk music is Rong Ngeng in Pattani. Rong Ngeng is an art form that combines western and eastern performance cultures. Therefore, the instruments in the Rong Ngeng ensemble are formed from the combination of western and eastern instruments (Prapas Kwanpradab, 2003: 25) The instruments used are violin, small tambourine, gong, cymbal, krub and large tambourine which in the past was not recorded, used the characteristics of the cultural inheritance of the villagers in the form of folk games and performances that reflect the way of life well-being and culture or is something that creates love and unity of the people. Rong Ngeng music has been inherited and come together until it becomes unique and varies. According to local characteristics, often as a musical activity, entertainment, dance, until becoming a folk performing arts and Thai dance. Which is consistent with Rong Ngeng music that has an important characteristic that shows the integration between cultures (Tassaneeya Witsaphan, 2007:35) until it becomes something that should be cherished, inherited, created to remain with Thailand forever.

The ensemble has an important instrument, namely the tambourine, which is an instrument that indicates and determines the slow-fast, style and mood of other instruments in that song by telling the rhythm of the music and the band's dramatic performances. Rong Ngeng drum “rabana” comes from the Malay language called “rabana”, shaped like a flat drum. Rabana stretched with leather only on one side. It is a rhythmic accompaniment to Tan Yong, Rong Ngeng music. Traditionally, tambourine

drums are used to direct the sounds of Spanish, Italian and Indian folk songs. The drum face is made of goat skin. To set up a tambourine skin take a stick and pull the rope firmly then check the sound in order of tone. Setting the tone relative to the universal note but using observation from the different sounds of the two drums, with the smaller one that will have a higher sound than the big one. When the show is finished, the rope must be loosened.

This creative study aimed to arrange the rhythmic patterns of Rong Ngeng music as the notes for the drum set and used this work to assemble a drum kit and percussion. The composer will present the rhythm of the tambourine, which is the main rhythmic instrument in the Rong Ngeng ensemble for playing the drum set by bringing the notes in the tambourine part of the drum which is played in the yoghurt rhythm in Laguduvo song. There is a rhythm that is fast and fun, coupled with the dance and the weight rocking back and forth in the 1st and 2nd rhythms (Atiphon Anukul, 2007:24).

Creating a Yoket Rhythm in Laguduvo by rearranged Latin rhythm (Samba), which is a rhythm adapted from Brazilian folk music that takes 4/4 times and has a rhythm of 120. It is the creation and arrangement of folk music rhythms to develop into contemporary music which is conservation inherit wisdom and disseminating the arts and culture of southern folk music to the international.

As a result, the composer incorporates this creative contemporary element into his teaching as well as drum set and percussion courses. He used the song as a starting point for discussions about multiculturalism with his students by discussing about contemporary music and culture. Composers also use this creative work of art to inspire students to create their own art.

The researcher studied the hitting technique and the sound of a large tambourine drum of the yoghurt rhythm in the Laguduvo song to get the desired sound and combine with the transcription of the notes into the drum set as follows:

There are 4 sounds of a large tambourine, as detailed below:

- 1). The sound of the tambourine, using the fingertips of all 4 fingers to hit the edge of the tambourine
- 2). The sound of the tambourine by using half of the palm to hit the inside of the tambourine's face.
- 3). Pah sound, use the palm to hit obliquely in a flickering style on the edge of the tambourine.



Figure 1 A large tambourine drum

Characteristics of a large leaf drum made of flat round wood, pierced through both sides and a one-sided drum. The drum skin is made of goat skin to stretch the skin of the drum, rattan or rope is used to add tension, or to soften the drum, a wedge is used at the end of the drum and hammered to make it tight and taut as required and affects the sound of the tambourine drum. Let's borrow photos from the website to use before taking photos by ourselves again.



Figure 2 The researcher demonstrates the beating of a large-leaf tambourine.

The big drums, the placement of the hands and the placement of the fingers are very important, which affects the sound of all three sounds and obtains a quality sound.



Figure 3 The researcher and the violinist
Researcher: Mr. Sittichok Kabilpat
Violinist: Assistant Professor Wichai Meesri



Figure 4 Notation for large drums of the yoga rhythm in the Laguduwo on music staff.

From studying the notes of the large tambourine, it is the main rhythm used in the *Laguduwo*. The author recorded a note and set the tone and the placement of the hands to get the desired sound as follows. Set in the 1st measure, using the left hand to hit at the same time in the 1st stroke to get a sound which determines the note to be on the 4th line and the sound of the hand, use the palm diagonally to flick the edge of the tambourine, which sets the note to be in the 3rd measure.



Figure 5 Notation, ball, trick and insertion of a large drum in the rhythm of the yoghurt of the Laguduwo song on the music staff.

In addition to the main rhythm of the large tambourines, the part that gives a new dimension and doesn't make it a repetition of the yoghurt rhythm have a ball hit effects and interpolation in songs by playing at the end of each part of the song. There is a technique of using fingers and palms as shown in figure 4 to get the desired sound.



Figure 6 Notation for large drums of the main yoga rhythm and the ball in the Laguduwo song by create a Latin rhythm (Samba) on music staff.

The author has a creative idea by bringing the main rhythm notes and the delivery of the yo-ket rhythm from the double trumpet notes to the Latin rhythm (Samba) by splitting the notes to the instruments of the drum set, namely snare drums, ride cymbals and high tom, in part A and adding a variety of sound in part B by splitting the notes to the ride cymbals, tom 1 and front toms to add a variety of sounds and fun emotions more aggressive to Latin rhythm (Samba).

ลาชฎาว

Composer by Sittichok Kabilapat

$\text{♩} = 96$

Violin

Piano

Bass Guitar

Drums

Am Am Am E7

5 **A**

Vln.

Pno.

Bass

Dr.

Am Bm^(b5) E Am Am Bm^(b5) E Am

9

Vln.

Pno.

Bass

Dr.

Am Am Bm^(b5) Dm Dm E7 Am



2

13



Vln. Am Am Bm(b9) Dm Dm E7 Am

Pno.

Bass

Dr.

17

B



Vln. Am fma7 Am Dm E7 Am

Pno.

Bass

Dr. **B**

21



Vln. Am fma7 Am Dm E7 Am

Pno.

Bass

Dr.

3



25

Vln. 1. 2.

Pno. Am Am

Bass

Dr. 1. 2.

29

Vln. C

Pno. D E Amaj7

Bass

Dr. C

33

Vln. Amaj7 Amaj7 Amaj7 Amaj7

Pno. Amaj7 Amaj7 Amaj7 Amaj7

Bass 4

Dr. 4

Detailed description: This is a musical score for a band consisting of Violin (Vln.), Piano (Pno.), Bass, and Drums (Dr.). The score is divided into three systems of measures. The first system covers measures 25 to 28. Measure 25 has two first endings (1. and 2.) with a repeat sign. Chords Am and Am are indicated below the piano staff. The second system covers measures 29 to 32. Measure 29 has a first ending with a 'C' box above it. Chords D, E, and Amaj7 are indicated below the piano staff. The third system covers measures 33 to 36. Measures 33-36 have a consistent Amaj7 chord indicated below the piano staff. The drum part features a consistent pattern of eighth notes in measures 25-28 and 33-36, with a '4' above the staff in measures 35 and 36, likely indicating a four-measure phrase or a specific drum pattern.

4

37

Vln. *A⁷maj⁷ A⁷maj⁷ A⁷maj⁷ A⁷maj⁷*

Pno. */ / / /*

Bass */ / / / 8*

Dr. */ / / / 8*

41

Vln. *A/C# Bm G#^o E D E A A/C# Bm G#^o E D E*

Pno. */ / / / / / / / / /*

Bass */ / / / / / / / / /*

Dr. */ / / /*

45

Vln. *A*

Pno. */ / / /*

Bass */ / / /*

Dr. */ / / /*



Figure 7 Notation (Score) created in Latin rhythm (Samba) on music staff.

The author performed the score of this music in a re-created Latin rhythm (Samba).

Conclusion and recommendations

Guidelines and methods of thinking about arranging Southern folk rhythms to be in a universal format and can be applied in various fields, such as arranging various rhythms of songs, composing songs until recording notes in a universal format for the study of music.

Yoga rhythm arrangement to the large tambourine in the Laguduvo song on the drum set in Latin rhythm (Samba) can be used as an exercise in teaching drum kit. In addition, it can also be applied to create a variety to play with international music in various forms in order to mix with the aura of Southern folk music in that song, as well as to be able to use it as a concept in composing. Contemporary style songs in order to spread the culture of folk music to the world.

References

- Anukul, A. (2007). *Song of the Asleemala group of songs*. Master of Arts Thesis Music Major, Mahidol University.
- Khamma, A. (2018). Na Thap Prabkai rhythm for drum set. *Rangsit Music Journal Rangsit University*, 13(2).
- Khwanpradub, P. (2003). *Rong Ngeng Music: A Case Study of the Faculty of Khaday Verdeng*. Faculty of Fine and Applied Arts, Rajabhat Institute Songkhla.
- Performing Arts, Intangible Cultural Heritage February 7, 2022, Retrieved from <http://ich.culture.go.th/index.php/th/ich/performing-arts>.
- Riley, J. (1994). *The Art of Drumming*. Publication: Manhattan Music.
- Walker, M. (2009). *World Jazz Drumming*. Master of Arts Thesis Music Major: Boston, Berklee.
- Wisaphan, T. (2007). *Folk dancing in Pattani Province*, Bangkok: Chulalongkorn University Press.

The Creation of the Song Power of Love: Orchestral Arrangements

Suttirak Iadpum*, Atipon Anukool

*Western Music Department, Faculty of Fine and Applied Arts Songkhla Rajabhat University, 160
Kanchanavanich Road, Khao Rup Chang Subdistrict, Mueang Songkhla District, Songkhla
Province, 90000, Thailand.*

** Corresponding email: oviolin1@yahoo.com*

Abstract

This study's objective was to compose the song Power of Love and arrange it into an orchestra style. The song Power of Love was written by the composer in September of 2021. The composer was inspired by the song “Song of the Violin” written by Asst. Prof. Prapad Kwanpradub was nominated and received "Best Song of Pangea in Classic genre" at the InterContinental Music Awards in 2021, Los Angeles, California, America.

The composer was impressed with the beauty of this song. He then, appropriate the melody from the song “Song of the Violin” to write the lyrics for the song Power of Love, the purpose is to perform this song to Asst. Prof. Prapad Kwanpradub as a gift for his retirement ceremony.

The song's lyrics were written by the composer and rearranged the song into orchestra style. The introduction use 3/4 (simple triple meter), this part uses Tertian Harmony and Quartal Harmony to support the main melody. The oboe and flute play the main melody along the vocal part. The highlight in the performance is using breaking chords style (Arpeggios). For every part of the song, the percussion would enhance tone colors to the orchestra as appropriate. In addition, Thai folk, and Western Classical musical styles are used in the work.

As a result, the composer incorporates this song within his instruction as well as the orchestration, large classical ensemble, conducting, and composition course. He uses this song as a starting point for discussions about Thai culture with his students, discussing music, language, and other aspects of Eastern and Western culture. Furthermore, the composer uses the song to inspire his students to create their own works of art. The composer and his collaborators have performed this Power of Love song at the retirement ceremony at Songkhla Rajabhat University.

Keywords: Creativity, Power of Love, Orchestral Arrangement

Introduction

Orchestral compositions play the important role in many types of music such as symphony, narrative music, opera, etc. Composing music for an orchestra is an arts work that requires a lot of study because there are many types of music instruments using in the orchestra. The composers must study the instrumentation, musical instrument restrictions, in order to lay out the proper orientation of the composition. In addition, the composer must have knowledge of arranging, which is a course of music theory. (Suttajit, 2011: 87)

In order to arrange a harmonious composition, the arranger must know the melody and understand the mood of the song, what the composer wants to convey or express in any aspect. So, the arranger will be able to pass on the meaning of the song. The main melody, If the arranger composes the main melody of the song, he will understand the mood of the song, what it wants to convey. In case of the arranger is not the one who compose the song, he must find the meaning of the song and understand the mood of the song. The melody inserted in the song is a short melody created by the arranger to insert the main melody, making the melody beautiful according to the creativity of the arranger. (Leesomboonpon, 2010: 72)

Most of the composers in the 20th century always have their own idea to compose and arrange the contemporary music that allow their creatives ideas development, which is a unique approach of each composer. (Nimanrattantkul, 2008:111).

Power of Love is a contemporary vocal song in the ternary form (three-part form). The composer appropriates the melody from the song “*Song of the Violin*” written by Assistant Professor Prapad Kwanpradub. This song was nominated and received "Best Song of Pangea in Classic genre" at the InterContinental Music Awards in 2021, Los Angeles, California, America.

Asst. Prof. Prapad Kwanpradub is a professor in the Western Music Department, Faculty of Fine Arts, Songkhla Rajabhat University. He was the originator of violin teaching in the university level in southern Thailand. He is a famous violin teacher and have taught numerous students in southern Thailand. He retired on September 1, 2021, and on that day was the day when his students would hold a retirement ceremony for him. The composer was one of his students. The composer was impressed with the beauty of his original song “*Song of the Violin*”. He then, appropriate the melody from the song “*Song of the Violin*” to write the lyrics for the song Power of Love, the purpose is to perform this song to Asst. Prof. Prapad Kwanpradub as a gift for his retirement ceremony.

Objectives

The following are the three key objectives in composing the songs:

1. To compose the song Power of Love in a vocal style influenced by the song “*Song of the Violin*” written by Asst. Prof. Prapad Kwanpradub
2. To arrange and perform the song Power of Love as an Orchestra stye for the retirement ceremony at Songkhla Rajabhat University.
3. To incorporate this piece into the orchestration, large classical ensemble, conducting, and composition course.

Clarifying Creative Cognition.

Creative Methodology

The composer divided the composing process into two major parts when creating this song: The process of writing lyrics and arranging them for an orchestra is described in detail below.

1. Composing a lyric of the song.
 - 1.1 Determine the scope of the song's content based on the love, bond, and respect of students towards the teacher which is Asst. Prof. Prapad Kwanpradub.
 - 1.2 To produce the lyrics, the author must use Thai words that describe virtue, meritoriousness, and great contributions of Asst. Prof. Prapad Kwanpradub.
 - 1.3 In order to feature the lyric and the melody borrow form the original song "*Song of the Violin*", the composer must construct the lyrics utilizing Thai vocabulary that appropriate with the melody of the song.
 - 1.4 The song features a D major scale with the syncopated rhythm of Thai pop music, as well as diatonic Western harmonies.

2. The Arrangement

The composers used the ideas of Tomaro and Wilson (Tomaro, M & Wilson J., 2009: 282-283) and Anukool (Anukool, 2011:90-96) to apply for the arrangement process:

- 2.1 Determine the arrangement's scope based on the type of ensemble. The instruments used are classified as an orchestra, which includes the string, woodwind, brass, harp, celesta, piano, and percussion sections.
- 2.2 To achieve multiculturalism, the composition incorporates Thai and Western Classical musical idioms.
- 2.3 The composer uses a Ternary Form to combine contemporary and classical music in this song's arrangement (three-part form).

Basic Data Creation: Descriptive music study of contemporary music and classical music theoretical concepts in music composition; Techniques for playing a musical instrument, string, woodwind, brass, harp, celesta, piano, and percussion sections in the form of an orchestra.

Creative Tools: To create this song, the composer experimented with sounds and chords on a piano and guitar. The music score was also written using a computer and notation software.

Creative Process: A study of song information in order to create descriptive music by listening to a variety of songs, observing, analyzing, and composing the songs.

Creative Style: This is a song with lyrics in a creative style (vocal music style). It has also been arranged for orchestra in both contemporary and classical styles.

Creative Techniques: The main melody and lyrics are designed to be simple and easy to remember for the listener. The goal is to perform this song to Asst. Prof. Prapad Kwanpradub as a gift for his retirement ceremony. The composer rearranged the song into an orchestra. The introduction use 3/4 (simple triple meter), this part uses Tertian Harmony and Quartal Harmony to support the main melody. The oboe and flute play the main melody along the vocal part. The highlight in the performance is using breaking chords style (Arpeggios). For every part of the song, the percussion would enhance tone colors to the orchestra as appropriate. In addition, Thai folk, and Western Classical musical styles are used in the work.

The Lyric of the song *Power of Love*.

In order to feature the lyric and the melody borrow form the original song “*Song of the Violin*”, the composer must construct the lyrics utilizing Thai vocabulary that appropriate with the melody of the song:

ด้วยแรงแห่งรัก ในเสียงดนตรีสร้างสรรค์ ด้วยความผูกพันรักมั่นในความเป็นครู
ด้วยศรัทธาก็รู้ว่าครูผู้สร้างยิ่งใหญ่ ด้วยความหวังใยของครูไม่มีวันจาง
จึงมีวันนี้ วันที่เรามากกราบครู อยากบอกให้รู้รักครูผู้คอยเติมฝัน
จากในวันนั้น ที่ครูชี้ทางให้เรา บรรเลง ชัดเกล้า พวกเราจึงมีวันนี้
*ด้วยแรงแห่งรัก ครูคือผู้สร้างยิ่งใหญ่ ต่อฝันให้ศิษย์ก้าวไกล หัวใจครูช่างงามล้ำ
ด้วยแรงศรัทธาที่ครูนั้นคอยสร้างคน บ่มเพาะด้วยความอดทน ผลิผลของครูยิ่งใหญ่
และในวันนี้ วันที่ครูได้ชื่นชม สิ่งที่สั่งสม ศิษย์ดีอยู่ทั่วเขตคาม
เหล่าศิษย์จึงขอสืบสาน รักษาความดีงาม ร่วมใจประสาน เพื่อครูประภาสของเรา

The song's lyrics combine Thai words intend to describe virtue, meritoriousness, and great contributions of Asst. Prof. Prapad Kwanpradub. The purpose is to perform this song as a gift for his retirement ceremony.

The Composition

The song *Power of Love* was written by the composer in September of 2021. The composer was inspired by the song “*Song of the Violin*” written by Asst. Prof. Prapad Kwanpradub. *Song of the Violin* was a solo violin song, it's not a vocal song. This song was nominated and received “Best Song of Pangea in Classic genre” at the InterContinental Music Awards in 2021, Los Angeles, California, America. The composer, then, rearranged the song to be the song *Power of Love* in D major scale in 4/4 time and the tempo is 75. The main melody uses a D major scale in the Ternary form (three-part form). The lyrics of the song are combined Thai words intend to describe virtue, meritoriousness, and great contributions of Asst. Prof. Prapad Kwanpradub.

In the first period (Bars 1-10) consists of 4 sub phrases. It is a relationship between the melody of rhythm from sub phrases that creating a similar rhythm to make it easier to remember. In the second period (Bars 11-20) consists of 2 large phrases. It is a relationship between the melody in the Contrasting period. The first period uses a similar form to the second period. The ending part (coda) takes the main melody from the end of the first period to end the song. Overall, the pitch used to compose this song, the lowest note is on A3 and the highest note is on E5. In creating the main melody of this song each period of the song focuses mainly on the use of anacrusis.

The Arrangement

The composer reworked the song into an orchestral arrangement. The concept is based on the love, bond, and respect of students towards the teacher which is Asst. Prof. Prapad Kwanpradub. The instruments used are classified as an orchestra, which includes the string, woodwind, brass, harp, celesta, piano, and percussion sections. To achieve multiculturalism, the composition incorporates Thai and Western Classical musical idioms. The composer uses a Ternary Form to combine contemporary and classical music in this song's arrangement (three-part form).



The image shows a musical score for the introduction of the song "Power of Love". The score is written for a full orchestra and includes the following parts: Celesta, Violin I, Violin II, Viola, Cello, Contrabass, Chords, Flute I, Oboe I, Clarinet I, Horn, Harp, Violin I, Violin II, Viola, Violoncello, and Contrabasso. The score is in 3/4 time and features a variety of dynamics and articulations. The Celesta part is the most prominent, playing a melodic motif. The string parts provide harmonic support. The score is divided into two systems, with the second system starting at measure 19. The Chords part shows a sequence of chords: Em7, A7, D, D7, G#7, F#m7, Em7, and A/C#.

Figure 2 The introduction part of *Power of Love* song

The introduction consists of a motif of the main melody, which is used to create a new melody by using the celesta, an ancient keyboard instrument to play this part. Along with the use of triad

chords and quartal harmony to create a simple, calm, and feeling of respect Asst. Prof. Prapad Kwanpradub on his retirement.

Once finished at the end of the introduction part, it leads to the main melody in part A, which is solo by the oboe and flute alternating with string group, woodwind, and harp.



This musical score shows the main melody of part a'. The instruments listed on the left are: Hsa. LI I, Hsa. III I, Cel, Tpta U, Tpta U, Vln I, Vln II, Vla, Vcl, Ch, and Chords. The score includes dynamic markings such as *mf* and *mp*. The chord progression at the bottom is: D, A⁷, E⁷, A⁷, D, D⁷, G⁷.

Figure 3 The main melody of *part a'*

The main melody in part a' the strings played the main melody with the brass section to support both the accompaniment and counter-melody. The string instruments play the main melody using Third in string writing theory along with the double octave lower technique, while the celesta is played in the form of an arpeggio chord.



This musical score shows the Chorus part (part B). The instruments listed on the left are: Fl. LI I, Ob. LI I, Cl. LI I, Bsn., Hrn. 2, Hrn. 1, Tpta LI I, Tpta LI I, Tpta LI I, Tpta LI I, Tpta LI I, Tpta LI I, Harp, Vln I, Vln II, Vla, Vcl, Ch, and Chords. The score includes dynamic markings such as *f*, *mf*, and *mp*. The chord progression at the bottom is: E⁷, A⁷, D, A⁷, D⁷, G⁷, F⁷.

Figure 4 The Chorus *part (part B)*

The chorus part (part B) featured a solo performed by a French horn and trumpet to show greatness. In this part, the string instrument plays an ostinato arrangement technique to create the effect of upper harmony. In addition, the woodwind line has the characteristics of scale running, giving it a feeling of liveliness.



Figure 5 The Ending part (part a’)

Part a' is the ending part. The highlight is in bringing the original melody come to play in a higher melody in the octave using the technique of third in string writing theory, played by high string. In this part, harp, accompanied by an arpeggio style with a eight note trippet join with a sixteen note of viola. This principle makes this part of the song feel like it's moving forward smoothly.

Result

The Power of Love song is a vocal song arranged for orchestra in a contemporary music style. This composition was inspired by the song “Song of the Violin” written by Asst. Prof. Prapad Kwanpradub was nominated and received "Best Song of Pangea in Classic genre" at the InterContinental Music Awards in 2021, Los Angeles, California, America.

The composer was impressed with the beauty of this song. He then, appropriate the melody from the song “Song of the Violin” to write the lyrics for the song Power of Love, the purpose is to perform this song to Asst. Prof. Prapad Kwanpradub as a gift for his retirement ceremony. The song's lyrics were written by the composer, and they combined Thai words intend to describe virtue, meritoriousness, and great contributions of Asst. Prof. Prapad Kwanpradub.

The composer rearranged the song into an orchestral arrangement. The instruments used are classified as an orchestra, which includes the string, woodwind, brass, harp, celesta, piano, and percussion sections. To achieve multiculturalism, the composition incorporates Thai and Western Classical musical idioms. The composer uses a Ternary Form to combine contemporary and classical music in this song's arrangement (three-part form). The introduction use 3/4 (simple triple meter), this part uses Tertian Harmony and Quartal Harmony to support the main melody. The oboe and flute play the main melody along the vocal part. The highlight in the performance is using breaking chords style (Arpeggios). For every part of the song, the percussion would enhance tone colors to the orchestra as appropriate. In addition, Thai folk, and Western Classical musical styles are used in the work.

Integration and Innovation in Creative Work

The composer incorporates the Power of Love song into his teaching in the orchestration, large classical ensemble, conducting, and composition course. He uses this song as a springboard for

discussions about multiculturalism with his students, discussing music, language, and other facets of Eastern and Western culture. Additionally, the composer uses the song to motivate his students to create original works of art. The composer and his collaborators have performed this Power of Love song at the retirement ceremony at Songkhla Rajabhat University.

Moreover, the composer believes that this song will continue to serve as a body of knowledge in the fields of academic music and music education.

Discussions and Suggestion

The song "*Power of Love*" was written in September of 2021. This work of arts was inspired by the song "*Song of the Violin*" composed by Asst. Prof. Prapad Kwanpradub in 2018. *Song of the Violin* is the song for violin solo. This song was nominated and received "Best Song of Pangea in Classic genre" at the InterContinental Music Awards in 2021, Los Angeles, California, America.

The composer was impressed with the beauty of this song. He then, appropriate the melody from the song "Song of the Violin" to write the lyrics for the song Power of Love, the purpose is to perform this song to Asst. Prof. Prapad Kwanpradub as a gift for his retirement ceremony.

The song's lyrics were written by the composer and rearranged the song into orchestra style. The introduction use 3/4 (simple triple meter), this part uses Tertian Harmony and Quartal Harmony to support the main melody. The oboe and flute play the main melody along the vocal part. The highlight in the performance is using breaking chords style (Arpeggios). For every part of the song, the percussion would enhance tone colors to the orchestra as appropriate. In addition, Thai folk, and Western Classical musical styles are used in the work.

As a result, the composer incorporates this song within his instruction as well as the orchestration, large classical ensemble, conducting, and composition course. He uses this song as a starting point for discussions about Thai culture with his students, discussing music, language, and other aspects of Eastern and Western culture. Furthermore, the composer uses the song to inspire his students to create their own works of art. The composer and his collaborators have performed this Power of Love song at the retirement ceremony at Songkhla Rajabhat University.

Suggestion

1. This composition, "*Power of Love*", is a vocal song and is rearranged into an orchestra consisting of string, woodwind, brass, harp, celesta, piano, and percussion sections. To make it more interesting, it can be arranged into a difference bands, such as string quartet, jazz, etc.
2. In terms of the qualifications of the musicians, they must be proficient at musical instruments because the composer uses various techniques to enable all musicians to show their talents outstandingly.

References

- Anukool, A. T. (2010). *Arranging for Chamber Orchestra*. Faculty of Fine Arts, Songkhla Rajabhat University.
- Leesomboonpon, P. (2010). *The principle of basic composition*. Rajburee: Muban Chombueng Rajabhat University, Rajburee
- Nimanrattantkul, S. J. (2008). *Principles of composing*. Nonthaburi: Nimman Rattanakul.
- Suttajit, N. R. (2011) *Musicalism, appreciation for western music*. Bangkok: Chulalongkorn University Press.
- Tomaro, M & Wilson J. (2009). *Instrumental jazz arranging a comprehensive andpractical guide*. Australia: Hal Leonard.

The Creation of *Power of Love*: A Cappella Arrangements

Suttirak Iadpum*, Sahaphat Aksornteang

*Western Music Department, Faculty of Fine Arts Songkhla Rajabhat University, 160
Kanchanavanich Road, Khao Rup Chang Subdistrict, Mueang Songkhla District, Songkhla
Province, 90000, Thailand.*

* Corresponding email: oviolin1@yahoo.com

Abstract

The purpose of this study was to analyze *Power of Love* and arranged into a four parts chorus. *Power of Love* was inspired by *Song of the Violin* the original music by Asst. Prof. Prapad Kwanpradub. This piece was nominated and received "Best Song of Pangea in Classic genre" at the InterContinental Music Awards in 2021, Los Angeles, California, USA.

The composer divided the composing process into 2 major parts. There is the process of writing lyrics and arranging for an acapella. The song's lyrics were written by the composer. The lyrics contain words that relay the teacher's grace and the love that everyone has given their teacher. The composer has rearranged the song into a cappella style, Thai folk, and Western Classical musical styles are used in the work. The song begins with one voice with the band. It is followed by a 4-part a cappella arranging style.

As a result, the composer incorporates this song in his classrooms such as in the chorus, small ensemble, and music theory course. He uses this song as a valuable teaching and learning tool. The students learn about Thai cultures, language, and the element of Eastern and Western music through this song. The composer hopes that this song can motivate his students to create their own works of art. Furthermore, the results of this study would be a good option for students to reap the academic benefits of music education.

Keywords: Music Creation, Power of Love, A cappella Arrangement

Introduction

Singing is comparable to the sound of the earliest human musical instruments that are present at birth (Apel & Daniel, 1960). Humans use their voices to express their emotions. Since first cry of the beginning of life to the imitation of different speech or vocals according to language and culture, vocal can be used convey emotional stories. The singer's must have an emotional connection to the song. Therefore, an audience will have the emotional reaction to the song. There are also many differences depending on the context of society and culture.

The choir in Thailand is also influenced by western nations. The adoption of the choral culture into Thailand passed by missionary. They were evident in religious schools since the reign of King Narai (Manit Chumsai, 1955; Wichathalumpak Laowanich, 2013). Later the choir received a lot of promotion and support in Christian schools such as Wattana Wittaya Academy, St. Gabriel School, Assumption School, Bangkok Christian College, Mater Dei College, St. Francis Xavier School, etc. (Kamala Chitchang, 1998; Piyanart Bunnag et al., 2005)

A cappella comes from an Italian word that describing a song sung without an instrument. It is a type of music related to worship. In short, a cappella refers to sing in which a group of people, and sings without any instrument, mostly performed by a group of singers.

Song of the Violin was the original music by Asst. Prof. Prapad Kwanpradub. This piece was nominated and received "Best Song of Pangea in Classic genre" at the InterContinental Music Awards in 2021, Los Angeles, California, USA.

Asst. Prof. Prapad Kwanpradub is a professor in the Western Music Department, Faculty of Fine Arts, Songkhla Rajabhat University. He was the very first violin teacher in the university level in southern Thailand. He is a famous violin teacher and have taught numerous students in southern Thailand. He retired on September 1, 2021, and his students have a retirement ceremony for him. The composer was one of his students. The composer was impressed with the beauty of his original *Song of the Violin*. He then, borrowed the melody from *Song of the Violin* to write the lyrics for *Power of Love*. The purpose is to perform this song to Asst. Prof. Prapad Kwanpradub as a gift for his retirement ceremony.

Objectives

The following are the three key objectives in arranging the songs:

1. To compose *Power of Love* in a vocal style.
2. To arrange and perform *Power of Love* in 4-part a cappella style.
3. To incorporate this piece into the chorus, small ensemble, and music theory course.

Creative Methodology

The process of writing lyrics and arranging for an acappella were used to create this piece of music as described in detail below.

1. Composing a lyric of the song.
 - 1.1 Determine the scope of the song's content based on the love, bond, and respect of students towards the teacher.
 - 1.2 In order to feature the lyric and the melody, the composer uses Thai words that describe virtue, meritoriousness, and great contributions of his teacher.
 - 1.3 The song written in D major scale with the syncopated rhythm of Thai pop music
2. The arrangement

The composer used the ideas of Tomaro and Wilson (Tomaro, M & Wilson J., 2009: 282-283) and Atipon Anukool (Anukool, 2011:90-96) to apply for the arrangement process:

 - 2.1 A cappella includes soprano, alto, tenor, and bass sections.
 - 2.2 The composer uses ternary form to combine contemporary and classical music in this song's arrangement (three-part form).

Basic Data Creation: Descriptive music study of contemporary music and classical music theoretical concepts in a cappella composition; Techniques for four parts singing, soprano, alto, tenor, and bass.

Creative Tools: To arrange this song, the composer experimented with sounds and chords on a piano and guitar. The music score was also written using a computer and notation software.

Creative Style: This is a song with lyrics in a vocal music style. It has also been arranged for a cappella in both contemporary and classical styles.

Creative Techniques: The main melody and lyrics are designed to be simple and easy to remember. The composer rearranged the song into a cappella. Techniques for arranging this song are 1) nisons 2) 4-part Writing 3) A cappella Arranging 4) Canon 5) Contrapuntal. The structure of the song is A-B-A (Ternary Form) the melody is in the D major scale and using time signature 4/4.

The Lyric of *Power of Love*.

In order to feature the lyric and the melody borrowed from the original *Song of the Violin*, the composer must construct the lyrics utilizing Thai vocabulary that appropriate to the melody of the song:

With the power of love in creating music with a strong commitment to being a teacher.

We know that he is the great teacher. With his concern to students will never fade.

Therefore, today is the day that we come to pay respect to him.

“We want to tell you that we love you.... our teacher who inspires our dream.”

From that day, he leaded us the way, refined our life until today.

*With the power of love.... He was a great builder.

Continue the dream for us to move on.

A beauty of his heart overflows with the faith that he keeps building us.

He cultivated with patience for great of his student’s success.

And on this day, the day he proud of all good student are all over country.

We will be preserving goodness, join together for our teacher Praphat.

The song's lyric combine Thai words describes virtue, meritoriousness, and great contributions of Asst. Prof. Prapad Kwanpradub.

The Composition

Song of the Violin was the original music by Asst. Prof. Prapad Kwanpradub. This piece was nominated and received "Best Song of Pangea in Classic genre" at the InterContinental Music Awards in 2021, Los Angeles, California, USA. The composer, then, rearranged *Power of Love* in D major scale in 4/4 time and the tempo is 75. The main melody uses a D major scale in ternary form.

Power of Love



Musical score for "Power of Love" in G major (one sharp) and 3/4 time. The tempo is marked $\text{♩} = 75$. The score consists of seven staves of music. The first staff includes a key signature change to G major and a time signature change to 3/4. It features two measures of whole rests, labeled with box A (measures 1-8) and box B (measures 9-15). A repeat sign is placed above the second measure of the 3/4 section. The second staff begins at measure 18. The third staff begins at measure 21. The fourth staff begins at measure 24 and includes a triplet of eighth notes labeled with box C. The fifth staff begins at measure 27 and includes a triplet of eighth notes. The sixth staff begins at measure 30 and includes a triplet of eighth notes. The seventh staff begins at measure 33 and includes a triplet of eighth notes labeled with box D.

uses a similar form to the second period. The ending part (coda) takes the main melody to end the song. Overall, the pitch used to compose this song, the lowest note is on A3 and the highest note is on E5. In creating the main melody of this song each period of the song focuses mainly on the use of anacrusis.

The Arrangement


The composer reworked the song into a cappella arrangement. The concept is based on the love, bond, and respect of students towards the teacher. The voices used are classified as an acapella, which includes soprano, alto, tenor, and bass parts. The composer uses a ternary form to combine contemporary and classical music in this song's arrangement (three-part form).



The image displays a musical score for four voices: Soprano, Alto, Tenor, and Bass. The score is in 4/4 time with a tempo of J = 68. The key signature has one sharp (F#). The first system (measures 2-7) is labeled 'A' and contains the following chords: D, D(sus4), and A7. A red box highlights the Soprano and Alto parts, which are labeled 'Unisons'. A green box highlights the Tenor and Bass parts, which are labeled 'Background'. The second system (measures 4-7) contains the following chords: A7, D, D7, C(maj7), and F#m7. The Soprano and Alto parts continue with the melody, while the Tenor and Bass parts provide accompaniment.

Figure 2 The arrangement of part A (measure 2-7)

This verse begins with the unisons sung in the soprano and alto part. In the tenor and bass parts used as a background act as an accompaniment line by singing the word “hoo”. This part is starting with the 5th octave in the tenor and bass tones in the second measure. Then, uses the four harmonics (4-Part writing) in measure 5-8, with the use of singing hoo, alternating with lyrics up from 2 lines to 4 lines until the end of the part.



The image shows a musical score for measures 8-14. It consists of four staves: soprano, alto, tenor, and bass. Measure 8 is marked with a '2' in the top left corner. Annotations include:

- Melody A:** A box labeled 'Melody A' points to a triplet of notes in the soprano staff of measure 9.
- Melody B:** A box labeled 'Melody B' points to a triplet of notes in the alto staff of measure 9.
- 4-Part writing:** A box labeled '4-Part writing' points to a red-bordered box encompassing measures 10-14 across all four staves.

Chord symbols are present above the staves: Em⁷, A⁷, D, D^(sus4), A⁷, D, Am⁷, D⁷, and Cmaj⁷.

Figure 3 The arrangement of part A (measure 8-14)

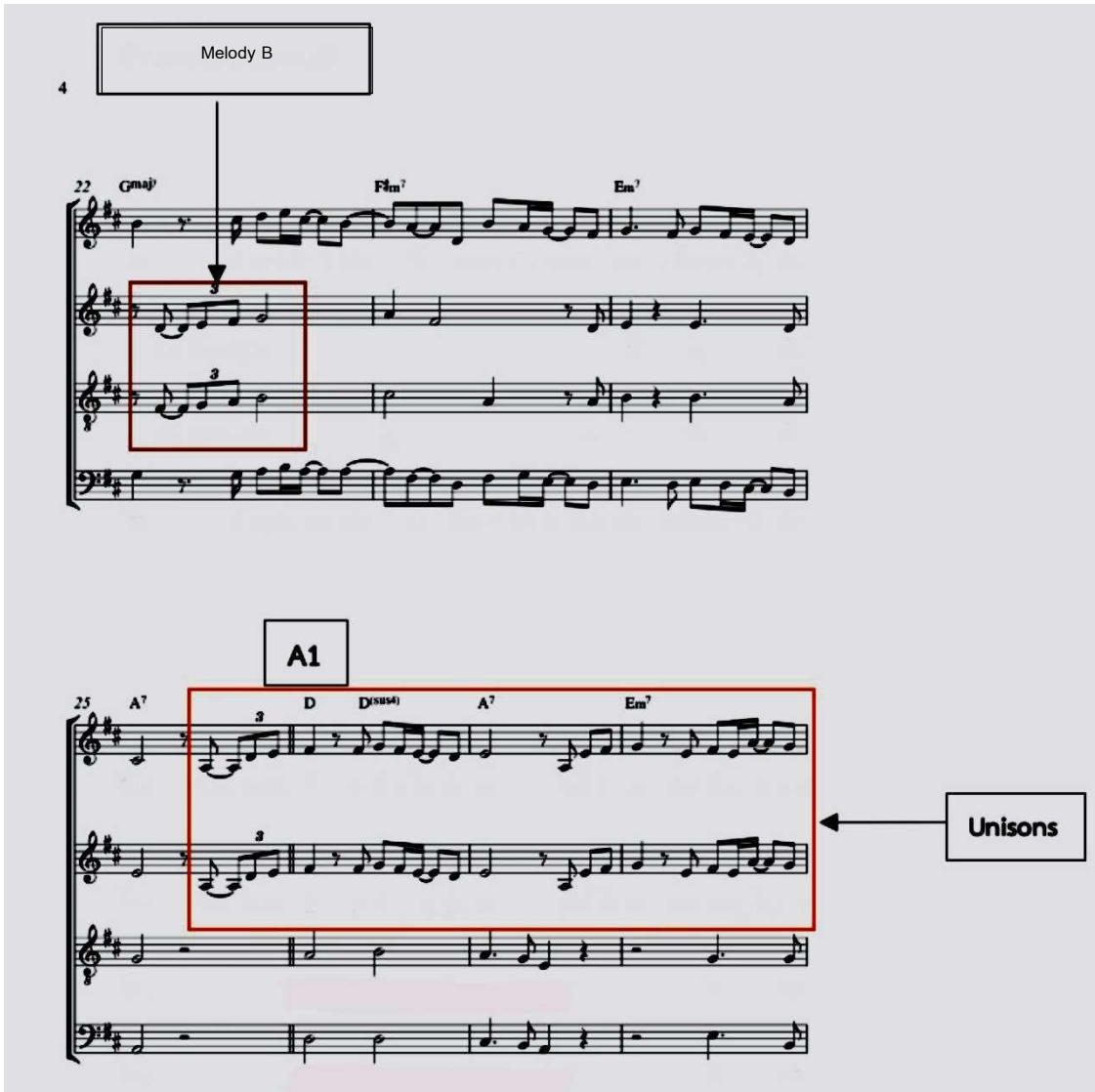
In the next part, measure 10 uses a multi-textured arrangement (Contrapuntal) with the alignment (Counterpoint) in 2 lines, which the main melody (designated as melody A) is the soprano and bass line. There are 3 pairs of choruses for the harmonious line. (Defined as melody B) is an alto and tenor chorus, octave 6 and octave 3 are imitations of singing (Canon) is the main melody sung before and harmonious melodies sang along the next part in measure 12-17 uses a four-part (4-part writing).



The image displays a musical score for a four-part arrangement. The score is divided into two sections: Part A (measures 15-17) and Part B (measures 18-21). Part A is highlighted with a red box and labeled '4-Part writing'. Part B is divided into two sub-sections, each labeled 'Melody A' and highlighted with a blue box. The score includes chord symbols (F#m7, Em7, A7, D, Am7, D7, (F#m)7) and a measure number '3' at the end of the first section. The notation includes treble and bass clefs, and various musical symbols such as notes, rests, and accidentals.

Figure 4 The arrangement of part A (measures 15-17) part B (measures 18-21)

This section begins in measure 18 with four-way harmonization. Measures 19-21 uses the alto and tenor lines to sing the word “hoo”. The notes in the chords alternating with singing a request to increase density.



The image displays a musical score for a piece in D major. It is divided into two sections. The first section, labeled 'Melody B', covers measures 22 to 25. Measure 22 is specifically highlighted with a red box and an arrow pointing to it from a box labeled 'Melody B'. The second section, labeled 'A1', covers measures 26 to 28. This section is also highlighted with a red box, and an arrow points to it from a box labeled 'Unisons'. The score includes four staves: two treble clefs (soprano and alto) and two bass clefs (tenor and bass). Chord symbols are provided above the staves: Gmaj7, Fm7, Em7, A7, D, D(sus4), A7, and Em7. Measure numbers 22, 25, and 26 are indicated at the start of their respective staves.

Figure 5 The arrangement of part A (measures 22-25) part A1 (measures 26-28)

The next part, Section B, measures 21-25, uses an arrangement using a variety of textures (Contrapuntal) and harmonious lines (Counterpoint), which the main melody (designated as melody A) are soprano and bass lines. There are 3 pairs of choruses for the harmonious line (designated as melody B). The 3rd part is an imitation of singing (Canon).

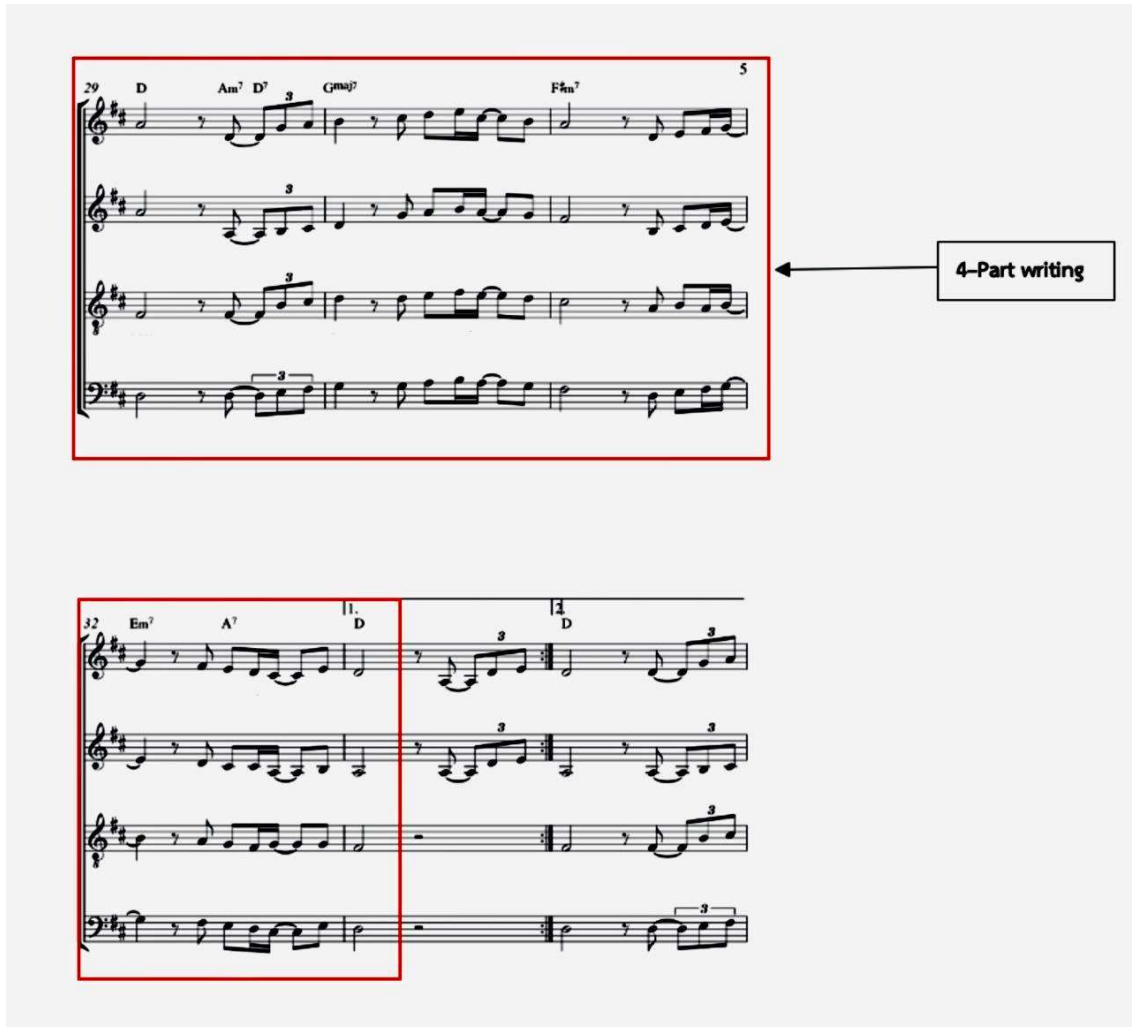


Figure 6 The arrangement of part A1 (measures 29-33)

This verse begins with the Unisons sung in the soprano and alto sections. In the tenor and bass line used as a background act as an accompaniment line. It similar to the A part by using the singing word “hoo” starting with the 5th octave in the tenor and bass tones in measure 26, then use four-part alignment (4-Part writing) in measures 29-33 to the end.

Result

The composer divided the composing process into 2 major parts. There is the process of writing lyrics and arranging for an acapella. The song's lyrics were written by the composer. The lyrics contain words that relay the teacher's grace and the love that everyone has given their teacher. The composer has rearranged the song into a cappella style, Thai folk, and Western Classical musical styles are used in the work.

The composer rearranged the song into an a cappella arrangement. The voices used are classified as a cappella, which includes the soprano, alto, tenor, and bass sections. The song begins with one voice with the band. It is followed by a 4-part a cappella arranging style with a syncopated

and diatonic Western harmony. The composer uses a ternary form to combine contemporary in this song's arrangement. Techniques for arranging this song are 1) Unisons 2) 4-part Writing 3) A cappella Arranging 4) Canon 5) Contrapuntal. The structure of the song is A-B-A (ternary form) the melody is in the D major scale and using time signature 4/4.

Discussions and Suggestion

Song of the Violin was the original music by Asst. Prof. Prapad Kwanpradub. This piece was nominated and received "Best Song of Pangea in Classic genre" at the InterContinental Music Awards in 2021, Los Angeles, California, USA.

The composer borrowed the melody from *Song of the Violin* to write the lyrics for *Power of Love*. The purpose is to perform this song to Asst. Prof. Prapad Kwanpradub as a gift for his retirement ceremony.

As a result, the composer incorporates this song in his classrooms such as in the chorus, small ensemble, and music theory course. He uses this song as a valuable teaching and learning tool. The students learn about Thai cultures, language, and the element of Eastern and Western music through this song. The composer hopes that this song can motivate his students to create their own works of art. Furthermore, the results of this study would be a good option for students to reap the academic benefits of music education.

Suggestion

This composition, *Power of Love*, is a song and rearranged into a cappella. The voices consisting of soprano, alto, tenor, and bass sections. To make it more interesting, it can be arranged into a difference band, such as brass quartet, woodwind ensemble, string quintet, etc.

References

- Apel, W., & Daniel, R. T. (Eds.). (1960). Cambridge, Massachusetts: Harvard University Press.
- Chitchang, K. (1998). *Piano lessons for women in Thai society*. (Master of Arts Thesis), Mahidol University, Nakhon Pathom.
- Chumsai, M. (1955). *History of compulsory education in Thailand*. Bangkok: Division of Foreign Affairs Ministry of Education.
- Laowanich, W. (2013). *The process becoming marginalized in music subjects in basic education courses: a method for studying knowledge archaeology*. (Doctoral thesis Music Education), College of Music Mahidol University, Nakhon Pathom. Retrieved from: <https://th.natapa.org/difference-between-acappella-and-acoustic-2455>
- Piyanart B. et al. (2005). *Concept of standard and quality of education since the reign of His Majesty the King*. Chula Chom Klao until the end of the absolute monarchy era 1868-1932 Bangkok.

Disney Song Concert: The Creation Brass Ensemble Concert for Undergraduate Bachelor of Music

Weerasak Aksornteang, Theerawut Kaeomak

Western Music Program, The Faculty of Fine Arts, Songkhla Rajabhat University

Abstract

This academic article is written from music undergraduate concert of Music major, Faculty of Fine Arts, Songkhla Rajabhat University. The authors are director of this concert. The article wrote about brass ensemble concert management for undergraduate. The main purpose of this article is to provide general information and guideline to lecturer who want to create brass ensemble concert or teach about brass ensemble course in university.

This concert is part of “SKRU Music House Concert” activities. The concert was performed on March 24th, 2021. The song in concert used Disney and Pixar popular film song. Some of the songs in concert arranged by junior student. The concert has 30 minutes long and used 1 month for rehearsal. A total of 20 students were used in this concert, consisting of 4 groups of brass instruments: trumpet, trombone, euphonium, and tuba. The concert consists of 4 acts. First act is introduction of concert used Disney Castle theme song and Mickey Mouse theme song. And second act is memory of Disney song concept. Third act is brass theater concept. The author used Korean dance style idea, musical theater idea and drill design idea from display band (type of military band) to make show in this act. And last act is hard song concept. In last act used the song which complex rhythmic note, complex time signature and used higher skill to play like Star War theme song and Pirate of Caribbean theme song.

Keywords: Concert, Brass Ensemble, Disney Song

Introduction

This article shows the process, the result and the improvement guide of live performance for Brass Ensemble’s Bachelor of Music at Rajabhat Songkhla University which name is “Disney Song Concert: Brass Ensemble”. The authors of this article are the lecture of Music Program at Rajabhat Songkhla University. We teach Brass Instrument and small ensemble class. The concert is part of brass instrument and ensemble class and part of “SKRU Music House Concert” activities. The concert was performed on March 24th, 2021. The author work with student for brainstorm idea which used many ideas of life performance and analyze for student talent. This project is laboratory of music student for find the new idea of music performance on stage and make them come true on stage.

The drama technical of the play and drill design of marching band is the new idea of this concert. The performer must understand the drama technical and learn about how to walk on drill. In addition to the performer must play music and be a character and walk in the line of drill design.

The process of concert has 4 main parts include 1). Brainstorms for the new idea 2). Plan 3). Rehearsal 4). Performance on stage. this academic article will describe the processes. Selection of concepts and theories in creative work and analysis of the results that occur during rehearsal and performance.

What is brass ensemble?

Brass Ensemble mean brass instrument band. The band gathers various types of brass instruments to play together. Brass ensemble were about 20 musicians or less. It is often called different names depending on the size of the band. For example, if a band has four musicians, it is

called a brass quartet. Or if a band has five musicians, it is called a brass quintet. this concert is a combination of many different sizes of bands. The author therefore defines this band as brass ensemble to convey that brass band It consists of music instruments: trumpet, trombone, euphonium and tuba.

The creative concept

The music performance of music major in the last 3 years focus on music skill of students. Sometimes it will be noticed that the student can play on the great skill, but they don't communicate with audience. Sometimes they don't convey the mood of the song. The concert is the two ways of communication and will have interactions between musician and audience. The musician play music and convey the message to the audience. the audience received the message in music and send the mood back to the musician. The concert will fully and perfect when the musician and the audience have a same feeling. Especially live concert because the people are interacted together. A lot of the student don't understand this fact. The author therefore applied this concept to the creation of the show by emphasizing the performance style that allowed the musicians to interpret every song playing. and find a way to communicate what is interpreted or what is the need that want the audience to know. The musician may not be just sitting or standing on stage when they play. But the musician must act as an actor who ready to present the story and the character through the music. Maybe the concert must present like a musical play which have a dance to create a novelty of the music performance style for the audience in the area.

The music used in the performance must not be classical music as usual to make the audience familiar with brass ensemble. The author has the idea that “If the band that the audience is not familiar with able to play songs that are familiar to the audience and able to convey a performance that the audience understands and has an emotional connection with. It will make the audience open to the style of the show that the audience has never received and is difficult to access in the future. The musician must understand the audience trend and open mind to learn the fact that the musician must make the audience. The song which the audience know is the best choice to make new Fanclub for the band. And it will be a good starting point for building a good audience base in the future. Choosing non-classical songs and used the familiar song will be make the Fanclub and the new audience is the main idea of this concert and help the producer theme have an idea theme for concert.

Why is it a Disney song?

The music style that appears in today's Thai society is full of diversity. The main reason is due to technological advancements. That allows people to access different cultures that they are more interested. Maybe it started with a little interest. And affect behavior. A lot of social media include Google, Youtube, Facebook, Instragram, Tiktok, Netflix, Viu, etc. As a result, the pollen of culture flew along the Internet network. and bred in the souls of those interested in cultures. This phenomenon can be explained by a cultural theory known as “the cultural diffusion theory” Narongchai Pidokrajt (2012) described these cultural phenomena as

“The principle of the cultural diffusion theory is each society and culture have its own independent starting point. When humans interact with each other, they receive exchange and bring that thing to elaborate according to what they want. This allows each society and culture to receive and exchange similar or similar.

the cultural diffusion is the result form the idea of human who make the cultural for need and circle of life. Culture is both physical and visible. in the form of a building or appliances. Used the process of obtaining from outside cultures and bringing in or improving them with their own ideas. and the abstract include faith, respect, belief.”

The music style values are acceptance the new culture become the basis of the music culture that they believe. As well as the meaning of the principle of the cultural diffusion. Although Narongchai Pidokrajt did not explain current society's interest in foreign music culture that is directly in line with the theory of cultural diffusion. but it can be interpreted using the acceptance comparison in the same view as belief. Music is the culture that diffusion in the form of personal and by Internet. The internet is the new cultural way which make the music separate forever

Go back a few decades. Cinema is the greatest media influence on cultural dissemination and still influences cultural distribution today. One of the musical cultures that is spread through the media of cinema and is engraved in the hearts of young audiences is the Disney music culture.

Disney music culture was instilled in the spirit and memory of Thai children and children around the world. The memory of a Disney song is the song that was sung in the movie princess and Disney fairy tales which made into movies.

These songs are rich in cultural diversity of music that automatically communicates cultural perspectives with children. Music can be played as a cultural medium. For example, the Mulan movie that brings a lot of Chinese music culture into the song, Aladdin's film that uses the melodic minor scale to communicate the accent of Arabian culture, Princess Frog is reinterpreted and told through the jazz and blues culture of the New Orleans era, among others. Of course, the children did not know the origins of the underlying culture. But they were able to get a sense of those cultures through movies and gaining an understanding of a new style of music culture known as “Disney Style”

Disney music is something that is easily accessible to the audience and can create a show that has a theatrical performance style. Because Disney's songs have a story involved and the general audience knows those stories very well. The producer theme used Disney theme for the concert because this segment of the target audience has been through these songs. Heard these songs from various Disney movies. Choosing a Disney song to be the theme of the concert was an idea that would appeal to a large audience.

Concept of song selection and music presentation style

The song in concert used Disney and Pixar popular film song. Some of the songs in concert arranged by junior student. The concert has 30 minutes long and used 1 month for rehearsal. A total of 20 students were used in this concert.

The concert has 30 minutes long for make the audience interested in the song. It might be easy for other types of bands. But for an unfamiliar brass ensemble may be a more difficult challenge.

Concept of song selection and music presentation style. The author is based on a psychological theory called Flow by Mihaly Csikszentmihalyi. which is mentioned on the TED Talk show (Online, 2004) was used to create the format of concert. By the flow of Mihaly Csikszentmihalyi has that

“Flow can occur in a variety of activities...you will feel natural, no force, no effort. When you enter the state of Flow, where your mind is concentrated and in a state of bliss...the feeling that the moment is fleeting. you forgot yourself and felt part of something great.”

Flow theory is the idea of creating a sequence of concert and the show style for the audience to be emotionally involved throughout the show. The concert is divided into 4 act: The introduction, the memory of Disney song concept, brass theater concept, and hard song concept. which has the process of creating works through various concepts as follows:

Act 1: The introduction

The introduction of concert used the concept of the first 30 second rule. “You have 30 seconds to make a first impression, which can last up to 15 years” the song which used in the introduction is Disney Castle theme song and Mickey Mouse theme song and used the form of blocking on stage to make first impression. The author used the student pose be Disney castle for the first impression on

stage to convey audience. In the show used trombone section take bow up to act like fairy light fly as a circle on castle. And make a character of Disney character for student.



Figure 1 Poster of concert



Figure 2 The introduction of concert.

Act 2: the memory of Disney song concept

This act is brass quintet part include Trumpet 1, Trumpet 2, Euphonium, Trombone, and Tuba. the part of memory song has 4 songs include: Lets it go from Frozen, I see the light from Tangled, Arabian night from Aladdin, and You got a friend in me from Toy Story. This part shows the traditional brass performance like stand in the half of circle on the stage and play the song like usually.



Figure 3 Brass Quintet in Act 2

Act 3: brass theater concept

This part is climax of concert. It's a theater concept with have a dancing, acting and drill of marching in the show. The author wants to present a new kind of show that student never do like this. This part has 3 songs include: Under the Sea from The Little Mermaid, Be Prepared from Lion King and the incredible theme song. The kind of song is various style of show but suitable in song. This part creates on the idea of the song is fundamental premise of Musical. Allen Cohen and Steven L. Rosenhaus (2006) said, *“The essence of musical theater is the representation of human emotions onstage, and the evocation of emotions in the audience, through the union of drama and music. This union may include spectacle, and often includes dance or choreographed movement; but the unique aspect of musical theater, whether dramatic or comedic, is the heightening of emotional impact of a story or idea through music and song. We believe that there can be no great musical theater without strong emotion. Professionals in the arts know that music is one of the most powerful ways to enhance the emotional content of a story, which is why almost every film ever made, silent or talking, has had musical accompaniment.”*

What is going on if we create brass ensemble concert by the theatrical idea is the point of create of show as follow:

- Under the Sea from The Little Mermaid

This song is Latin style. But the author used idea of Boy Band from Korea cultural to present show. The musician must dance in Korean style and play music together. The purpose of this idea wants the audience jolly up like Fanclub of Boy band or laugh in the way of musician dancing. Furthermore, the song talks about the aquatic animals under the sea. The musician must act to be aquatic animals. Acting on aquatic animal character make the student be confident on stage. And encourage students to be creative when they must imagination about their character and act like aquatic animals.



Figure 4 The dance of under the sea.

- Be Prepared from Lion King

This song present on the dramatical idea. But the character is comedy character. It was intended to be the song that communicated the most dramatic content. Because the rehearsal time have limited. The selection of this song was therefore the most appropriate. The idea of this song is allowing students to find their own identity consistent with the character. But because the students have no background in drama skill. The author chooses the best character in the worst case communicate with actor and using a negative social perspective to guide the character to them. When the actor be the character will make funny situation and make the show be comedy show. The part is the funnest part of rehearsal because the author let the actors find out the personality of the characters themselves. The actors were given the opportunity to present different perspectives according to one's self and according to your own beliefs. Often the author will use the narrative process then let the actors try improvising to find the best fit.



Figure 5 Brass theater in Be prepares

- The incredible theme song.

This song have a lot of complex time signature that is quite difficult. Students who can play these songs must be proficient. And the idea of this song used drill of marching band to make the show. Drill design is the old skill of some student who been in high school marching band. This part of the process is quite complicated. But the results turned out to be very good. Drill design on this show create by the student. The process stimulates the student to be the creator and be the director of show. The character of this song is superhero theme. The student must act to be the superhero on stage when they play. It's the best challenge for the student to show this song



Figure 6 The drill design in the incredible theme song.

Act 4: the hard song concept

The last show of this concert be the hard song concept. The hard song means the song which have complex time signature and higher range of instrument. The student must use time for practice and the learn new time signature from this part of concert. The play list of this part includes Star War theme song and pirate of Caribbean theme song, but both is difficult song. In part of audience this act of concert is a final act that impress them and make them want to be more.

The Result of Concert

The process of concert includes adoption of theatrical style, song interpretation and the story of the song, including the presentation of the songs using the concept of theatrical music for the stage performance is to develop the potential of students in the program. And provide opportunities for students to present their creativity in acting. The concert is the new kind of show in university and makes the new experience for the audience. and make the audience felt familiar with brass ensemble and enjoy with the show

References

- Allen, C. & Steven, L.R. (2006). *Writing Musical Theater*. Palgrave Macmillan.
- Flow, the secret to happiness. [Online]. (2004). Retrieved from http://www.ted.com/talks/mihaly_csikszentmihalyi_on_flow/transcript?language=en
- Narongchai Pidokrajt. (2012). *Ethnomusicology*. College of Music, Mahidol University.

The Creative Song for Piano "Lagu Kayoh Sampan" a Urak-Lawoi's Song

Sanya Phaophuechphandhu

*Department of Music, Faculty of Fine Arts, Songkhla Rajabhat University, Songkhla, 90000,
Thailand*

** Corresponding email: sanya.ph@skru.ac.th*

Abstract

Urak-Lawoi music is the music of the Urak-Lawoi people. There is a type of music called 'Rong-ngeng'. Rong-ngeng music is the local music of the Urak-Lawoi who live in Koh Lanta Island, Krabi Province. It is used both for entertainment and thanks for the vow. In the case of receiving blessings as they wished. The Urak-Lawoi tend to vow with Rong-ngeng music. This Rong-ngeng has only one violinist who remembers the melody and is also the leader of the band. Mr. Mawee Thaleluek, the leader of the Rong-ngeng band. He was the only person who memorized the melody of the song through the violin. The Lagu-gayoh-sampan song is one of many songs for the Urak-Lawoi music that expresses their ethnicity in a prominent song, which "gayoh" in the vocab of this song means boating. And the song of the Urak-Lawoi people is about to disappear. Because of the lack of succession for the next generation. The researcher then brought the "Lagu-kayo-sampan" song created in piano style. To conserve the Urak-Lawoi song This creation takes the form of piano-style playing, using the C major scale, pentatonic style, use time signature of 2/4 at a speed of 80 beats per minute, to match the folk rhythm and the original. It was used to play with the left hand instead of the rebana (folk drum). There are interactions of melody and rhythm. The intervals note is used to create music. So that players are familiar with the simple and catchy melody and arrange not to play hard. To keep the music of Urak-Lawoi and approach. When Urak-Lawoi's song reaches the public. This song will continue to be one of Urak Lawoi's well-known and remaining songs.

Keywords: Urak-Lawoi, Lagu-gayoh-sampan, Rong-ngeng, Creative piano

Introduction

The Urak-Lawoi or "Chaw Lay" is a Southern Thai word meaning "sea people" (Local Fishermen). Most of them live by the sea. Its origins come from the Austronesian ethnic group. In the past, they wandered around the islands of the Andaman Sea of Southern Thailand. These ethnic groups consist of three groups: the Moken, the Moglan, and the Urak-Lawoi. After that, they established a permanent foothold along Thailand's Andaman Sea, including Phuket, Krabi, Trang and Satun.

The life of the Urak-Lawoi people has lived for a long time. make them have a ritual and its own unique culture. The Urak-Lawoi people have been influenced by many outsiders such as they were given musical instruments to use in rituals. Speaking of rituals is The Urak-Lawoi people have their religion. It is the worship of spirits and ancestors. It is a supernatural belief and using music as a communication between humans and the supernatural. To create morale, encouragement or to cure disease. by vowing to reduce the suffering. (Sanya, 2552)

The vow of the Urak-Lawoi takes place when the Urak-Lawois are sick or have dissatisfaction. So, they came to pray at the local shrine grounds and then promised that if the results were successful as he had hoped they would perform a votive ritual by bringing Rongngeng music to dance in front of the shrine. Rong-ngeng music of the Urak-Lawoi people is therefore the only type of music that communicates between human beings and beliefs.

The creation of this song is a creative song arranged as part of the ritual song of the Urak-Lawoi people's shrine. While the author was researching music in the Urak-Lawoi way many years ago. It

has been discovered that this song is included in the votive ritual. Song used for the ritual is a song that has many songs. Ritual music is music with a specific pattern. The first song is a prelude and with other songs until there is the last song that is a specific song to finish the ritual. In this section, we will talk about one of the beautiful songs that appear in the ritual. It's called “La-u kayo sampan”. It is a melodious song that is easy to remember. therefore, used to arrange the song of the piano. To be part of teaching keyboard subjects for students and interested parties and to preserve the songs of the Urak-Lawoi people as well.

The instruments used in the Rong-Neng ensemble consist of violins, rebana drums, gongs, grubs (Thai instrument) and small duo cymbals (Thai instrument). There was one male and one female singer. in which the male chorus will act as the singer only and the female singer is both a singer and a dancer of the band.

The band's instruments can be classified as instruments in the Curt and Hornbostel systems as follows:

1. The Sound family caused by the vibration of the mass itself (Idiophone)
The Urak-Lawoi musical instrument involved in the percussion genre is the “gong”.
The Urak-Lawoi musical instrument involved in the percussion (Concussion) genre is the “small duo cymbals”.
2. The family of sounds produced by the vibration of the parchment. (Membranophone)
The Urak-Lawoi musical instrument involved in the frame drum is the “Rebana drum”.
3. The family of sounds produced by string vibrations. (Chordophones)
The Urak-Lawoi instrument involved in the bowed lute is the “violin”.

“Lagu kayoh sampan” is a song that means boating. It is a song that demonstrates the use of rhythmic intervals that represent rowing, which reflects the life of the Urak-Lawoi people between people, boats, and seas. This song thus represents their daily life. The music is so beautiful that it uses the melody that is characteristic of the melody known as the pentatonic. It's a group of five melodies that run back and forth like the melody of Thai Classic music. It makes the song memorable and one of the sweetest songs of them.

Materials and methods

The author therefore created this song in the form of piano playing. At first, part of the song was used as an introduction. To create an interesting song, it is bar 1 to bar 16. In this composition, the C major scale is mainly used. To make it easier to play, those interested will be able to understand as easily as possible. And is the original of the development of the song in the future

This song has the lowest pitch range on G3, and the highest pitch on G5. Finger operation is in the system of the C Major scale.

ลาชุกาโถยะซัมปัน
เพลงรองเงิงชาอูรักลาโว้ย บ้านสิงกาอู๋ อ.เกาะสันตา จ.กระบี่

♩=80 สัญญา เผ่าพิชพันธ์



Piano

Pno.

Pno.

Pno.

Figure 1 Introduction

The form of music in the ternary form is A A B A. The main melody of the song is from bar 17 to bar 35. (Figure 2)



The figure displays a piano score for the main melody, organized into five systems. The first system, labeled '2' at the top left, begins at bar 17 and is marked with a box 'A'. The second system starts at bar 21. The third system starts at bar 25. The fourth system starts at bar 29. The fifth system, labeled '33' at the top left, begins at bar 33 and is marked with a box 'B'. Each system consists of a grand staff with a treble clef and a bass clef, with 'Pno.' written to the left of the staff. The melody is primarily in the treble clef, with some accompaniment in the bass clef. The score includes various musical notations such as notes, rests, slurs, and dynamic markings like 'p' and 'mf'.

Figure 2 Main melody.

There is a rapid upscaling called “Griss”, as shown in Figure 3. To imitate the singer's vocals similar to howling sounds, which makes the song more interesting.



Figure 3 Griss.

There is a play between the left hand and the right hand. to represent the cry between a man and a woman, Male voices are low notes. shown in section A as shown in Figure 4.



Figure 4 Male voices.

The author replaced the female vocals in part B, which is 1 octave higher than the male vocals as shown in figure 5. To show the difference between male and female vocal projects and to show that this song is sung by both men and women.

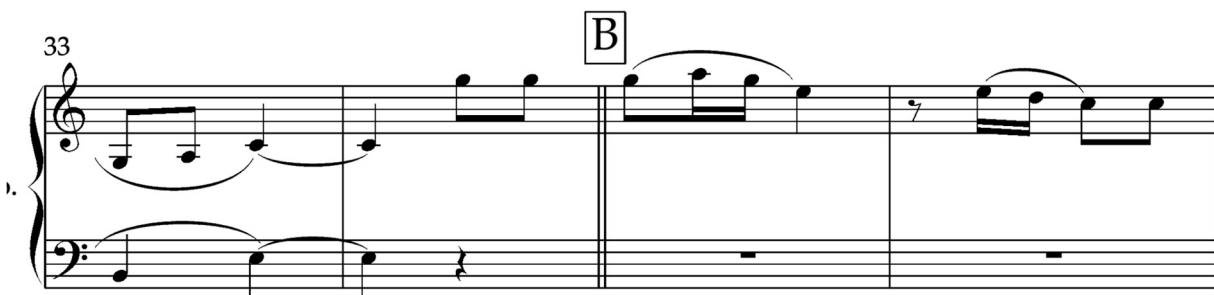


Figure 5 Female voices.

- In section C, the author wants to modify the melody. to be more interesting and imitate the waveforms of the sea with the ups and downs of the sound, as shown in figure 6



Figure 6 waveforms in section C.

The A minor chord is used in bars 61 through 63 to provide a tight group of chords to represent the sound of a large wave hitting the boat, as shown in Figure 7.

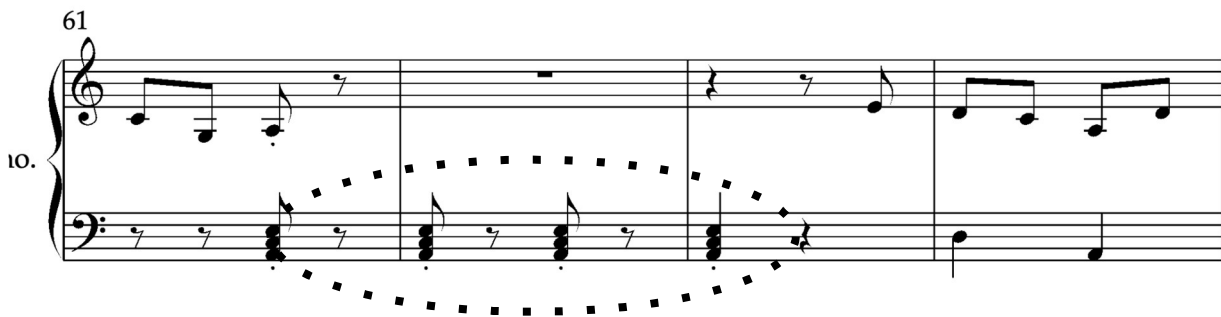


Figure 7 A minor chord

After that, In the part D, a part that is similar to part B of the song in order to return to the normal melody. which instead of returning to normal sailing in the sea. This song therefore simulates the image of the Urak-Lawoi people, Ships, and seas were integral to the creation of this song.

Conclusion

Rong-Neng music of the Urak Lawoi people is hard to find. Their music currently lacks a systematic inheritance. The instrument used primarily for the violin. and is a machine that requires high capability, highly skilled to be able to inherit music like this. The author created this song using inspiration from the Urak-Lawoi song, which was created by playing with piano instruments. Because it is an instrument that can show the best melody performance. Therefore, it was created with the C Major scale and the easiest to access. The melody used is a familiar melody like the 5 note group, known as the pentatonic scale, which is a group of notes that are often used by Thai classical music. The author created it in order to inherit the song Rong Neng of the Urak Lawoi people. And is another confirmation of the music of the Urak-Lawoi people.

References

- Phaophuechphandhu, S. (2009). *Music in the way of life's Urak-Lawoi*. Academic Conference on Ritual Music (37th: 2009: Thammasat University, Rangsit Center). Bangkok: Bangkok: Tech Promma, T. (2012). *An Analysis of Rear Admiral Veeraphan Vawklang's Musical Arrangement on Santa Lucia for Orchestra*. Bangkok: Srinakarinwirot University.
- Sokatyanurak, N. (1999). *Musical Analysis*. Bangkok: Chulalong University.

Thailand's Case: The Destination Country's Influence on Tourist Satisfaction

Thanaphon Ratchatakulpat, Walisara Yongyingpraser, Gumporn Supasettaysa, Holger Kieckbusch, Varunya kaewchueaknang and Lalida Joomsoda

Rajamangala University of Technology Phra Nakhon, 10300, Thailand

** Corresponding email: gumporn.s@rmutp.ac.th*

Abstract

Thailand's government and marketing promotion in a certain market have an effect on tourists' perceptions of the destination's image. For foreign travelers, the destination's image has become critical. Thailand needs this country approach in order to increase the country's gross domestic product. The study aims to investigate the perception of international tourists regarding Thailand's destination image and destination satisfaction. The researcher corrected the date by using the survey as the quantitative, and the total number of respondents was 570.

The study results show that the destination image is the essential factor in predicting tourists' satisfaction. The international traveler considered Bangkok to be one of the safest places to travel, and the infrastructures are well-equipped for the tourists. Other factors influencing destination satisfaction are Thai gastronomy and street foods, local people, and cultures.











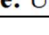
The main marketing mix that Thailand should apply should be the promotion that the Thai government should emphasize to the target group. In this case, it would be the Australian travelers. The implications of this study will give further information about a particular country's tourist sector and will explain the government's position and engagement in facilitating and supporting the country's plan. These improvements are beneficial to a thriving nation, and Thailand will serve as an example for ASEAN and other countries striving to improve their destination country image in the worldwide tourist industry.

Keywords: Destination country, Destination satisfaction, Country image

Introduction

Thailand's tourist business, notably the tourism sector, is one of the country's most important economic contributors to income and gross domestic product (GDP) (Thailand Board of Investment, 2016, 2020). In particular, the local government has been involved in the Thailand medical sector by utilizing national government agencies and policy efforts to support and develop this business in order to create revenue for the government of Thailand. The government's participation in the marketing effort was largely influenced by the TAT's success with the "Amazing Thailand" marketing and promotion campaign, which was part of the fifth Five-year tourist development plan (1997-2001). A program titled "The Thailand Extreme Makeover" was launched by the TAT in 2014-2015 in order to find a person who was interested in cosmetic plastic surgery. The purpose of this tournament is to raise awareness of Thailand as a tourism destination. (Thailand(TAT), 2015).

Table 1 International tourism expenditure in 2015 and 2016

Rank	Country	UNWTO Region	International tourism receipts 2016 \$billion	International tourism receipts 2015 \$billion
1	 China	Asia	261	250
2	 United States	North America	122	112.9
3	 Germany	Europe	81	77.5
4	 United Kingdom	Europe	64	63.3
5	 France	Europe	41	38.4
	 Russia	Europe	-	34.9
6	 Canada	North America	29	29.4
7	 South Korea	Asia	27	25.0
8	 Australia	Oceania	27	23.5
9	 Italy	Europe	25	24.9
10	 Hong Kong	Asia	24	--

Source: UNWTO Tourism Highlights, (2017)

Despite, Australia is 8th rank, and its country is geographically closet comparing to other English spoken travelers. The researcher considered to choose this target from the distance and incoming number of international travelers. Australian tourists contribute to 65,773.90 million baht, an increase of 7.92% from previous year (Department of Tourism, 2016). This data indicates that it is crucial to study this native speaker traveler that may significantly impact the Thai tourism industry.

Encourage the tourist industry to be recognized as a critical tool in addressing the country's economic problems, providing jobs for people, and boosting overall income levels. Furthermore, in accordance with government policy, marketing efforts should be made to ensure that tourism plays an important part in improving the quality of life in all regions of Thailand. The majority of the consumer experience is comprised of a series of complicated interactions between subjective responses of customers and objective characteristics of a product (Addis & Holbrook, 2001). According to tourism studies, travelers' experiences during journeys have mostly involved viewing and learning about various cultures as well as enjoying and living in varied lifestyles (Stamboulis & Skayannis, 2003). According to McIntosh and Siggs (2005), travelers' experiences are distinctive and emotive, and they have a high level of personal significance.

According to previous research, a tourist's experience has a direct impact on his or her propensity to return (Hosany & Witham, 2010; Cole & Chancellor, 2009; Hsu & Crofts, 2006; Oh et al., 2007). The majority of researchers discovered a favorable relationship between visitors' experiences and their willingness to return. In other words, travelers' intents to return to a destination impact their favorable appraisals of the experience they had previously (Um, Chon & Ro, 2006). When consumers are pleased and have a positive experience during an activity, according to Petrick, Morais, and Norman (2001), they are said to be engaged. They are more inclined to do so in the future. This was noted by Weed (2005) that sporting event attendees who appreciate their sports tourism experience will most likely return for another sporting event or similar experience in the future.

It was shown that those who had a good picture of the destination would have a positive perception of their on-site experiences, which would result in a greater degree of satisfaction and behavioral intentions to revisit the place, as reported by Lee et al. (2005). This study aims to study the perception of international travelers' perception of the destination country campaign and future intention to return to Thailand.?

Table 2 International tourism expenditure in 2015 and 2016

Country of Residence	No. of Arrivals	+/- (%)	Length of Stay (Days)	Per Capital Spending			No.	Tourism Receipts		
				Baht/Da y	+/- (%)	US\$/Day		Mil. Baht	+/- (%)	Mil. US\$
ASEAN	8,078,262	+19.31	5.60	5,106.35	+5.75	149.09		231,002.31	+25.95	6,744.59
-Brunei	17,433	+25.17	6.92	5,819.71	+1.84	169.92		702.07	+36.34	20.50
-Cambodia	544,818	-1.99	6.45	4,559.05	+7.72	133.11		16,020.84	-10.40	467.76
-Indonesia	470,820	-5.01	5.66	5,286.42	+2.74	154.35		14,087.46	-3.60	411.31
-Laos	1,230,521	+15.68	5.79	4,267.36	+9.82	124.59		30,403.81	+28.14	887.70
-Malaysia	3,470,553	+30.87	4.83	5,240.74	+3.72	153.01	2	86,254.70	+41.30	2,518.39
-Myanmar	263,422	+26.80	8.28	4,988.37	+5.81	145.65		10,880.33	+34.50	317.67
-Philippines	301,297	+1.67	7.94	4,905.93	+3.16	143.24		11,736.47	+7.18	342.67
-Singapore	1,074,755	+11.90	5.60	6,136.30	+5.79	179.16		36,932.09	+26.76	1,078.31
-Vietnam	767,643	+33.93	6.22	5,023.23	+4.91	146.66		23,984.54	+37.41	700.28
China	7,981,407	+72.31	8.14	5,982.79	+8.83	174.68	1	388,694.10	+93.71	11,348.73
Russia	877,120	-45.06	17.07	4,587.00	+0.66	133.93	3	68,678.73	-39.06	2,005.22
Australia	816,053	-2.56	13.43	6,001.49	+4.98	175.23	5	65,773.90	+7.92	1,920.41
UK	896,591	+2.91	17.29	4,294.89	+4.87	125.40	4	66,579.60	+8.93	1,943.93
Japan	1,349,388	+7.53	8.06	5,188.52	+3.82	151.49	7	56,430.67	+16.26	1,647.61
South Korea	1,359,211	+22.51	7.72	5,417.58	+2.64	158.18	6	56,847.18	+30.48	1,659.77
USA	827,110	+12.61	13.38	5,021.99	+1.34	146.63	8	55,577.00	+6.55	1,622.69
India	1,039,395	+14.67	7.64	5,849.26	+2.18	170.78	9	46,448.85	+23.98	1,356.17
France	648,382	+6.80	17.60	3,872.45	-0.03	113.06	10	44,190.48	+7.94	1,290.23

Methods

The contribution of this study indicates the respondent perception toward Thailand as country destination and the future of intention by using the quantitative method. The Yamane sample size formula was applied to the number of the study group. The total number of respondents was initially 600, but the actual data collected was 570 respondents due to the commented data on the survey. The researcher expected to have 10% missing data from the survey. The data was collected during the 2017 December at the international airport, Thailand.


The following propositions and hypotheses are put up as suggestions:

- H1: Marketing Mix has a direct effect on the destination country
- H2: Marketing Mix has a direct effect on destination satisfaction
- H3: Destination satisfaction has a direct effect on Future intention

Result

Male visitors from Australia prefer to travel to Thailand over female passengers, with 58 percent of male travelers picking Thailand as their preferred destination. When they arrived in Thailand, the majority of them were between the ages of 29 and 30. The most of them are single, with 72 percent being unmarried. They traveled to Thailand for their pleasure and vacation. The 8.6 percent of those who have been to Thailand have come more than six times. The majority of them are familiar with Thailand because of the media. They spend their time in Thailand for around 5-7 days. They remained at a hotel and a guest house, respectively. The travel arrangements that they make are made by themselves through the internet. More than 40% of them prefer to travel alone, with a budget of around \$1,001-1,500 Australian dollars on average.

Table 3 Destination country’s image

No.	Tourist Confident 	Frequency	Percent
1	Thailand situation is return to normal	297	52.1
2	Thailand country is perceived to be unstable	104	18.2
3	Thailand political stability leads to safety and security in country	135	23.7
4	Thailand is greater sensitivity to be risk and/or exposure to global media information	34	6
Total		570	100

According to around 52 percent of those who responded, it has returned to normal. In comparison, 8.2 percent of the population believed that the situation in Thailand was unstable, while 23.7 percent thought that the situation in Thailand was stable, safe, and secure. In contrast, 6 percent of respondents believed that Thailand is more sensitive to being in danger.

Table 4 Descriptive Statistics Data

No.	Statement of Independent Variables	Descriptive		Interpretation	
		Mean	S.D.	Rate	*Note
Place of Tourist Attraction					
TA1	Historical monuments are well preserved in Thailand	5.86	1.445	Very high	
TA2	Leisure and recreational facilities are available at tourist’s place in Thailand	5.49	1.217	Very high	
TA3	Information boards mentioning the history and importance of monuments/places are available at the monuments.	5.37	1.119	Very high	
TA4	Tour guides are easily available at the monuments of Thailand	5.32	1.096	Very high	
TA5	Tour guides are knowledgeable and friendly.	5.47	1.079	Very high	
Infrastructure					
IF6	ATMs and banks/money exchanges are easily available in Thailand	5.27	1.328	High	
IF7	Transport facility is good in Thailand	3.96	1.907	Moderate	Acceptable
IF8	Enough space for parking is available at the tourist place in Thailand	4.45	1.395	High	
IF9	Telecommunication facility is good in Thailand	4.35	1.334	Moderate	Acceptable
Accommodation and Food					
AF10	Hotel accommodation/place of stay is easily available in Thailand	4.77	1.326	High	
AF11	Room facility and services are excellent at the place of stay/hotel.	5.12	1.401	High	
AF12	Hotel staff is polite and courteous.	4.85	1.233	High	
AF13	Fee of accommodation is fair at Thailand	4.96	1.254	High	
AF14	Food and beverages offered at the place of stay/hotel are good taste.	4.82	1.303	High	
AF15	Food and beverages offered at the place of stay/hotel are hygienic.	5.05	1.393	High	
AF16	Food and beverages offered outside the place of stay/city’s market and restaurants are good in taste.	5.06	1.292	High	
AF17	Food and beverages offered outside the place of stay/city’s market and restaurants are hygienic.	4.21	1.794	Moderate	Acceptable
AF18	Price of food outside the place of stay is fair in Thailand	4.63	1.406	High	
Hygiene and Sanitation					
HS19	There is good sanitation and cleanliness in the streets of Thailand.	3.66	1.836	Moderate	Acceptable
HS20	There is sufficient cleanliness and hygiene at the place of stay.	4.24	1.428	Moderate	Acceptable
HS21	Water is drinkable and hygienic in Thailand.	4.08	1.557	Moderate	Acceptable
HS22	Thailand is free from mosquitoes.	3.64	1.767	Moderate	Acceptable
Promotion and Marketing					
PM23	Thailand is recognition internationally.	5.28	1.236	High	
PM24	Thailand is has been promote worldwide.	5.59	1.049	Very high	
PM25	Tourism in Thailand could promote through cooperation with the international tourism institutions	5.42	1.192	Very high	
PM26	Thailand could run promotion and marketing activities together with ASEAN countries at worldwide holiday packages	5.51	1.116	Very high	
Thailand Destination Image					
IM27	Safety problem problems are destroying the image of Thai tourism	5.58	1.124	Very agree	Preventive
IM28	Military coup in May 2014 was destroying the image of Thai tourism	4.93	1.561	Agree	Preventive
IM29	Unsolved murder of two British backpackers in September, 2014 was destroying the image of Thai tourism	5.25	1.195	Very agree	Preventive
IM30	Thailand is the great value for money destination	5.85	1.053	Very agree	Preventive
IM31	Thai tourism were welcome, friendly, amazing, happy and exciting	6.38	925	Strongly agree	Promoted
IM32	The most important factor for tourists coming to Thailand is ‘beautiful beaches’	6.47	912	Strongly agree	Promoted
IM33	The most important factor for tourists coming to Thailand is ‘variety of spas’	6.45	1.007	Strongly agree	Promoted
IM34	The most important factor for tourists coming to Thailand is ‘wellness clinics’	6.20	1.183	Strongly agree	Promoted

A negative perception of Thailand among Australian tourists comes from Thailand destination images such as Thailand safety issues and political instability. The findings indicate that they agree on these issues that impact Thailand's image as a tourist destination. The responder strongly agrees with Thailand's popularity as a tourist destination in terms of a positive aspect. Many Australian tourists who travel to Thailand rely on these essential variables.

Table 5 Multiple Regression Analysis for Destination satisfaction

Variable	Unstandardized Coefficients		Standardized Coefficients	t	Sig.
	B	Std. Error	Beta	B	Std. Error
(Constant)	1.338	.194		6.901	.000
Place of Tourist Attraction (x ¹)	.336	.041	.451	8.290	.000
Infrastructure (x ²)	-.042	.024	-.063	-1.729	.084
Accommodation and Food (x ³)	-.053	.030	-.068	-1.778	.076
Hygiene and Sanitation (x ⁴)	-.033	.018	-.059	-1.785	.075
Promotion and Marketing (x ⁵)	.147	.042	.184	3.541	.000
Thailand Destination Image (x ⁶)	.095	.037	.108	2.593	.010
R = .622		Adjust R ² = .380			
R ² = .387		SE = .59115			

a Dependent Variable: Destination Satisfaction

The beta weight as well as the statistical significance were calculated and investigated. According to the beta weights and p-values, only three of the five predictive factors were found to be statistically significant when it came to destination satisfaction. In addition, they are a site of attraction (= .336; p=.000***), a place of promotion and marketing (= .147; p=.000***), and an image of tourism (= .095; p=.010*)

The results reveal that infrastructure, cleanliness, and sanitary conditions did not significantly influence the value of destination satisfaction (-.041; p=.084, n/s; -.033; p=.075, n/s; -.041; p=.084, n/s). In a similarly, neither accommodation nor food had a statistically significant impact on destination satisfaction (p=.076, n/s).


Table 6 Regression Analysis for Destination Satisfaction and Destination Loyalty

Variable	Unstandardized Coefficients		Standardized Coefficients	t	Sig.
	B	Std. Error	Beta	B	Std. Error
(Constant)	.754	.091		8.247	.000
Destination Satisfaction	.543	.023	.706	23.763	.000
R = .706		Adjust R ² = .498			
R ² = .499		SE = .40916			

a Dependent Variable: Destination Loyalty

The predictive variable "destination satisfaction" is created from the regression analysis. This means that the variance to explain the predictors of the variables is 48.9 percent (Adjust R².498 x 100 = 48.9 percent). Adjust R² provides the ability to explain the relationship between destination satisfaction and destination loyalty. The findings reveal that the degree of destination pleasure was a significant predictor of the value of destination loyalty (r=.543; p=.000***). This means there was a correlation between Destination Satisfaction and Destination Loyalty. The satisfaction of travelers would make them come back and refer to the pleasure of being in Thailand.

Table 7 Future Intention to revisit Thailand

No.	Tourist Perception 	Frequency	Percent
1	Not likely at all	30	5
2	Unlikely	20	4
3	Likely	190	33
4	Very likely	330	58
Total		570	100

Most Australian visitors perceived a positive travel experience in the Thailand destination. They express the belief that they are likely or highly likely to return to Thailand for a holiday within the next two years, with around 94.8 percent stating that they will return. As a result, the significant majority of Australian visitors say that they will certainly and most likely recommend Thailand as a vacation destination to their friends and relatives. This would be a key strategy of the Thai government or other related institutes, Private and Public, which can apply to the following year's marketing plan.

Discussion Finding

The findings demonstrate that the location of tourist attractions, promotion, and marketing, as well as the marketing of the Thailand destination, are all positively associated to Australians' happiness with their trip. Infrastructure has no link to the number of people that travel in Australia. For Australian tourists, the quality of their accommodations and cuisine, as well as the cleanliness and hygiene of their surroundings, have no significant link with their overall happiness with their location. This is in line with the Suhartanto, Ruhadi & Triyuni (2016) and Chen, Lee, Chen & Huang (2011).

The majority of Australian visitors who travel to Bangkok believe that the city is a safe place to travel. When compared to the city's outskirts, the infrastructure is well-maintained and structured. Thailand's reputation as a tourist destination may be damaged as a result of pollution, safety concerns, and horrendous environmental conditions, among other factors. Tourists from Australia are particularly attracted to Thailand since the country's criteria and the environment in Bangkok are familiar to them. People are well-versed in Thailand due to the assistance of tourist information centers and travel experts.

As a result, Bangkok's public transit infrastructure is still inadequate and inefficient. Taxi drivers do not adhere to the rules, which include utilizing the meter and driving cautiously and safely to the destination. Pollution and a thriving environment are represented in Bangkok's brand power image and have an impact on travelers' contentment with their travel destination (Arasli & Baradarani, 2014). Bangkok offers a diverse range of attractions and activities, and the city is open at all hours of the day and night. Thai people are extremely kind and generous, and they extend the most gracious welcome. Thai cuisine, particularly street food, is distinctive, catching the attention of Australian tourists.

References

- Addis, M. & Holbrook, M. (2001). On the conceptual link between mass customization and experiential consumption: an explosion of subjectivity. *Journal of Consumer Behaviour*, 1(1), 50-66.
- Arasli, H., & Baradarani, S. (2014). European Tourist Perspective on Destination Satisfaction in Jordan's industries. *Procedia-Social and Behavioral Sciences*. 109(2014), 1416-1425.

- Chen, C.M., Lee, H.T., Chen, S.H. & Huang, T.H. (2011), “Tourist behavioural intentions relation to service quality and customer satisfaction in Kinmen National Park, Taiwan”. *Journal of Tourism Research*, 13(5), 416-432.
- Cole, S.T. & Chancellor, H.C. (2009). “Examining the festival attributes that impact visitor experience, satisfaction and re-visit intention”. *Journal of Vacation Marketing*, 15(4), 323-333.
- Department of Tourism. (2016). Retrieved from January 2018 available <http://newdot2.samartmultimedia.com/home/details/11/221/25515>
- Han, H., Hsu, L.-T. & Lee, J.-S. (2009). *Empirical investigation of the roles of attitudes toward green behaviors*. overall image, gender, and age in hotel customers’ eco- friendly decision making process, *International Journal of Hospitality Management*, 28(4), 519-28.
- Hosany, S. and Witham, M. (2010). “Dimensions of cruisers’ experiences, satisfaction, and intention to recommend”. *Journal of Travel Research*. 49(3), 351-364.
- Kandumpully, J. & Dwi Suhartanto. (2000). *Customer loyalty in the hotel industry: the role of customer satisfaction and image*.
- Lee, C.K., Lee, Y.K. & Lee, B.K. (2005). “Korea’s destination image formed by the 2002 world cup”. *Annals of Tourism Research*. 32(4). 839-858.
- Mcintosh, A.J. & Siggs, A. (2005). “An exploration of the experiential nature of boutique accommodation”. *Journal of Travel Research*. 44(1). 74-81.
- Oh, H., Fiore, A.M. & Jeoung, M. (2007). “Measuring experience economy concepts: tourism applications”. *Journal of Travel Research*. 46(2). 119-132.
- Petrick, J.F., Morais, D.D. and Norman, W.C. (2001). “An examination of the determinants of entertainment vacationers’ intentions to revisit”. *Journal of Travel Research*. 40(1). 41-48.
- Stamboulis, Y. & Skayannis, P. (2003). “Innovation strategies and technology for experience-based tourism”. *Tourism Management*. 24(1). 35-43.
- Thailand (TAT), T. T. A. of. (2015). *Thailand Extreme Makeover Season 2 unveils three finalists for the lifetime beauty transformation - TAT Newsroom*. <https://www.tatnews.org/2015/09/thailand-extreme-makeover-season-2-unveils-three-finalists-for-the-lifetime-beauty-transformation/>
- Thailand Board of Investment. (2016). *Thailand: Medical Hub Policy*. http://www.boi.go.th/upload/content/BOI-brochure_2016-medical-20160524_24249.pdf
- Thailand Board of Investment. (2020). *Thailand Medical Destination Finding Wealth in Wellness*. 30(May). <http://www.boi.go.th/upload/content/TIRMay2020.pdf>
- Um, S., Chon, K. & Ro. Y.H. (2006). “Antecedents of revisit intention”. *Annals of Tourism Research*. 33(1). 199-216.
- UNWTO Tourism Highlights, (2016) Retrieved from <http://www.e-unwto.org/doi/book/10.18111/9789284418145>
- Weed, M. (2005), “Sports tourism theory and method: concepts, issues and epistemologies”. *European Sport Management Quarterly*. 5(3). 229-242.

Arrangement of Lenang Songs for Violin Solo

Wichai Mesri*

*Western Music Department, Faculty of Fine and Applied Arts Songkhla Rajabhat University, 160
Kanchanavanich Road, Khao Rup Chang Subdistrict, Mueang Songkhla District, Songkhla
Province, 90000, Thailand.*

** Corresponding email: aviolinjazz@gmail.com*

Abstract

This creative research article is an arrangement of Lenang songs for violin solo. It is part of Rong Ngeng song research. The case study of Mr. Seng Abu aims to create and disseminate Rong Ngeng music culture. This song presented in the style of popular music including the concept of composition and analyzing the composition of music academically. Lenang is the basic song to play Rong Ngeng music. This song performed both slow and fast rhythms. The results of the study found that bringing the melody of "Lenang" to arrange for violin solo. The arrangement is in the G Major scale. The form of the song is divided into 3 parts, namely the ABA section. The composer has a concept arranging the harmony in a manner that preserves the main melody and inserting a pair of sound techniques to create a melody dimension. As well as using the technique of playing in a chord form to make the music more diverse in terms of rhythmic style, melodies are performed alternately with slow, fast and slow rhythms. The fast part uses a rhythmic arrangement technique based on I-nang rhythm which is the basic rhythm of Lenang song. The creation of the time wanted to present the method of playing Rong Ngeng songs and to disseminate Rong Ngeng music to those who are interested.

Keywords: Rong Ngeng music, Lenang Song, Violin

Introduction

Rong Ngeng music is a cultural heritage of people in the Southern Region of Thailand. There is a development in music resulting from the combination of Western music and Eastern music. This music has musical instruments representing and sampling the unique sounds of both cultures. The fusion of Rong Ngeng music has been part of the local people to this day. Consequently, Rong Ngeng music has a unique melody resulting from the combination of culturally diverse accents. There is a characteristic melody with the aura of various cultures such as yoghurt rhythm songs. Most of them will have an aura of melody and rhythm that has been influenced by Europeans. I-nang rhythm song often was a traditional Malay melodies and rhythms. The standard song that is popularly played and is known to people in the three Southern border provinces, namely Taliquipas, Lajuduwo, Mau Inang Java, Mau Inang Lama, Pujo Pisang, Prakampao, Anodi dee, Lenang and others.

Lenang song is a popular song used to play or accompanying the show. It is another Rong Ngeng song that most people are familiar with. Rong Ngeng music in the three southern border provinces is a song with a beautiful melody and rhythm styles. Thus, making the melodious song and fun at the same time and with an uncomplicated songwriting style. It is characterized by the structure of one part song but using repetitions and rhythm changes to create an interesting song. The composer is therefore interested in presenting Lenang's song in the form of violin solo only. In addition, the violin is considered of the main instrument that play in the main melody. Therefore, the composer use Lenang songs in this research to promote Rong Ngeng music and to be used for educational purpose.

Creative method

Ideas for compositions

The initial concept adopted by the composer for arranging the violin solo of “Lenang” would be in the form of keeping the main melody simple, easy to remember. Due to this creation, the composer chose to use the violin as the main instrument to perform the main melody in a single piece. The composer then intervened violin technique and the rhythmic rhythm of I-nang to create colorful in the performance. Those who are interested can bring it to play to improve their violin skills on different occasions.

LENANG SONG



Figure 1 Example of the main melody

Preliminary concepts: rhythm, melody, and song structure

In order to maintain the aura of Rong Ngeng music, the composer assigns this creative work to use ABA style. It's in the G major scale and with a very short main melody. In addition, the inspiration to bring the melody to create new music, new is like still reminiscing on the old melodies that are in memory. The composer therefore sets the tempo rate for each part of the song as follows: Section A (slow), tempo 4/4, approximately 65 bpm, 9 bars, Section B (fast), 2/4 tempo, 85 bpm, 6 bars and parts. A (slow) returns to use the tempo rate 4/4 at a speed of about 65 bpm for 12 rooms, as shown in Table 1.

Table 1 The structure of the composition of Lenang songs

Part A	Part B	Part A
Slow	Fast	Slow
Measure 1 - 9	Measure 14 - 29	Measure 30 - 41

The concept of arranging the A1 section.

Arranging the melody in the A1 verse, the composer uses the concept of keeping the original rhythm with a slow tempo. Then, makes it possible to convey the mood of melodies that are beautiful. For the chorus, the composer chooses Double stop technique. The compiler used perfect 8th and perfect 5th interval for the harmonization as shown in measures 2 - 3 and measures 8 - 9. The composer then used techniques for playing chord patterns. This is a technique that requires the bow to be dragged onto the strings simultaneously on all 3 strings to produce the desired chord sound (measures 4 – 6). For most main melodies, the composer chooses to maintain the main melody of the song by playing. Single line mainly to create awareness and build familiarity with the original melody of the song and use the reverse again according to the original structure as shown in Figure 2

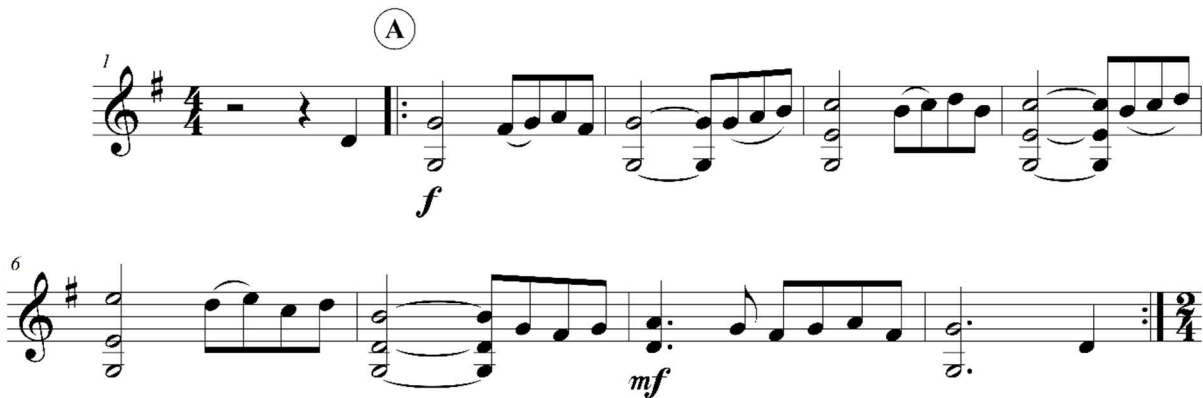


Figure 2 melody of part A

The concept of arranging welded pipes

Arrangement of welding rods, the composer uses the concept of introducing, the rhythmic technique of playing the tambourine in the I-nang rhythm with medium speed by setting the tempo rate 2/4 to create a rhythmic pattern to indicate the change in the rhythm of the song as well as creating a sense of fun. In order to become familiar with the rhythmic pattern of the changing rhythm before leading to the B-line melody, the composer chose to use the double-stop technique in the perfect 8th and perfect 5th interval to create the movement of the line. Bass on the rhythmic pattern of I-nang beats as shown in Figure 3.



Figure 3 Rhythmic welding rod

The concept of composing part B

Arranging the melody in part B, the composer still use the concept of keeping the original rhythm of the song with medium speed to show the mood of melodies and rhythms. For the chorus, the composer chooses to use the Double stop technique mainly. In order to create the conciseness of the song based on the rhythmic pattern of I-nang rhythm to compose the B-section. The composer used a more diverse octave with a wider octave for violin. Therefore, it is another important condition that must be taken into account the potential of the tool and the positioning of the finger system in the instrumentation. In addition, part B also has a rhythmic proportion that is involved. The composer

therefore chose to preserve the melody along with the octave that is suitable for playing the double stop technique throughout the song and use the reverse again according to the original structure of the song including intermittently inserting the technique of playing chord patterns as shown in Figure 4.



Figure 4 melody of part B

The concept of composing the A2 section.

Arranging the melody in the A2 verse, the composer used the idea to bring the listener back to the original rhythm with a slow tempo to bring back a melody. For the chorus, the composer chose a technique of changing the chorus of the melody to 1 octave higher. Then the composer used a technique for playing chord patterns that reversed the notes in the chords to expand the wider harmonies. By this technique, the bow must be dragged onto all 4 strings at the same time in order to produce the desired chord sound. The idea of creating chords on the violin, was to applying techniques to make it interesting. In this part, the composer also wants the violin to replace the accordion, the instrument that plays the role of chords in the minor-Rong Ngeng orchestra. The majority of the main melodies, the composers choose a single line instrumentation to bring back the perception and familiarize yourself with the original melody of the song. There are not reversing the original structure of the song but uses a method to expand the main melody at the end of the song (shown in Figure 5).

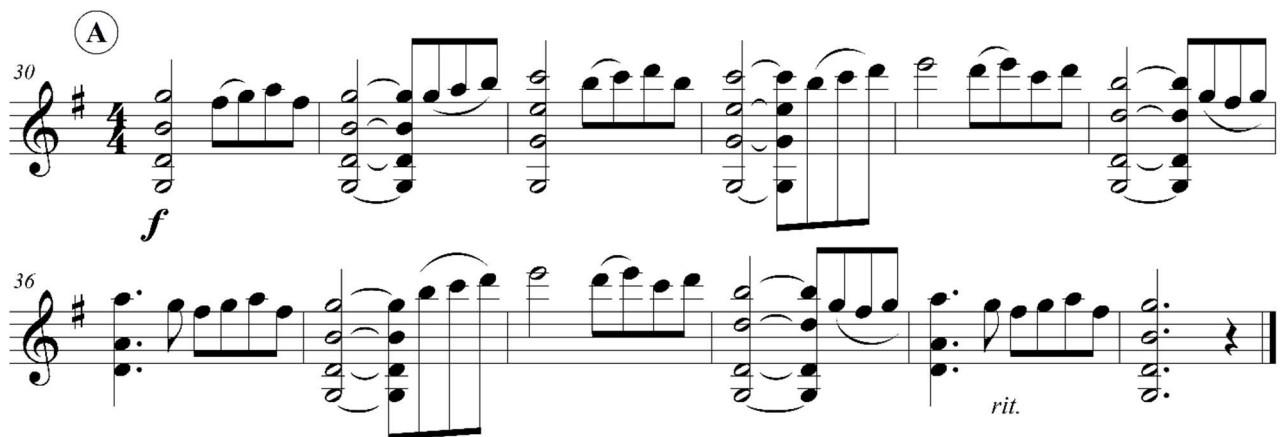


Figure 5 melody of part A

Results and discussion

This arrangement of Lenang songs for violin solos created by the composer in order to present the Southern folk song. There is the wisdom of the people in the area developed from a blend of diverse cultures until becoming a unique local music. It has an interesting playing style. The composer recognized the value of folk music that should be inherited both traditional and further development in a new way in accordance with the era with secondary melodies that use different scales of both major and minor scales. It is a huge consequence of the development of melodies based on culture to present the creative process technique. It is the concept of developing the old body of knowledge and extending it with a new method.

The composer has applied the knowledge of western music theory and applied it in the creation. The composer has chosen to use the original structure ABA. This form found in common folk songs by using G Major scale. It is a sound scale suitable for playing violins which is the only main instrument in the minor Rong Ngeng orchestra. Therefore, the determination of this scale is important to influence the use of the techniques that will follow for the A-line main composition. The composer still uses a slow tempo. The speed is about 65 bpm, which is perfect for the first part of the song. In order to bring the audience familiar with beautiful melodies. Therefore, the composer does not focus on the use of harmonious voices. This song uses the principle of harmonization where the listener wants to know the movement of the chords. However, the main melody was focused as well as using the reversal to bring the listeners mood to be enjoyable with the faster rhythm. For the connecting piece, there are 4 measures, the composer inserted the idea of the rhythmic pattern of the I-nang rhythm to create a rhythmic pattern on the violin. The lowest notes on the strings were used as the bass for the rhythmic pattern. For the main melody of part B, the composer chose to use the chorus as the main melody. The verse has a fast tempo and to create awareness of the persistence of the I-nang rhythmic pattern throughout the song, the composer therefore chose a double step that is suitable for playing along with keeping the I-nang rhythm pattern. For the last verse, the composer chose to use the chord formation method on the violin. This is a technique that requires simultaneous coloring of all 4 strings and uses a method of melody changing. The composer chose to use repetitions of the melody. In order to reinforce the nostalgic feelings of the past, this is the ending of the song instead of reversing the entire song.

The purpose of this creative work was to present Rong Ngeng folk music in a new way of interpretation. However, for those who will bring the aforementioned works to play, the composer suggests that they must listen to the original version of Lenang. In order to be familiar with the melody and rhythm of I-nang which is a unique accent that is the source of this piece.

Conclusion

This creation was one of the processes that played an important role in the development of the researcher's idea to create inspirational works with Rong Ngeng music by using the main instrument in the Rong Ngeng ensemble. The violin helps develop a new way of playing the Rong Ngeng song by applying the principles of composing to create colorful and interesting things to happen which is still on the basis of keeping the original melody which is the main intention of the editor. At the same time, this work presents no less challenges because it is the intention to choose only violin to perform. The preservation of the melody and the I-nang rhythm of the tambourine along with violin skills are required. Make sure the performer understanding the structure of the original song. This song and the choice of sound in the song is not very complicated. This work is useful to those whom who are interested.

References

- Adler, S. (2002). *The Study of Orchestration*. New York: W.W. Norton & Company.
- Dhamabutra, N. (2009). *Composition of Contemporary Music*. Bangkok: Chulalongkorn University Press.
- Nimmanrattanakul, L. (2009). *Principles of Music Composition*. Nontaburi: Nimmanrattanakul Press.
- Phancharoen, N. (2011). *Music Dictionary*. (4th ed). Bangkok: Kate Carat Press 00.0
- Sokatianuko, N. (2001). *Singularity and Analysis*. Bangkok: Chulalongkorn University Press.



RMUTCON

Session 6:

**Visual Information
Processing and
Color Vision**

Color Constancy Assessed by the Elementary Color Naming under RGB-LEDs

Phubet Chitapanya¹, Chanprapha Phuangsuwan², and Mitsuo Ikeda²

¹*Color science and Human vision, Mass Communication Technology, Rajamangala University of Technology Thanyaburi, Thailand.*

²*Color Research Center (CRC), Mass Communication Technology, Rajamangala University of Technology Thanyaburi, Thailand.*

* *Corresponding email: phubet_c@mail.rmutt.ac.th*

Abstract

Nowadays, Light-emitting diodes (LED) have become wide using lighting instead of a fluorescent lamp which has various benefits such as multi-color generation. In this experiment, 23 chromatic color chips and three achromatic chips were assessed by 100 participants inside a booth decorated like an actual living situation. The booth was lit by only RGB-LED light, which thirteen illumination conditions, including white light as D65. The other colors were red, yellow, green, cyan, blue, and magenta. Each subject judged each color chip by the elementary color-naming method, which required a percentage of chromaticness, whiteness, and blackness. Then, the observer had to assess a portion of color depending on the opponent's color theory as red, yellow, green, and blue, in which red and green cannot be observed and judged together and vice versa. Our result showed area ratio, which is color area perception under test light condition compared to area perception under D65, and color constancy had a similar agreement that cyan, yellow, and green illumination was not recommended to use in the case of poor color constancy when increasing a saturation light.

Keywords: color constancy, LED, elementary color naming

Introduction

There are three factors in human vision, the spectral power distribution of the light source, the spectral reflectance of an object, and the spectral sensitivity of human perception. Human has the ability to stably perceive the same object regardless of colored illuminations. This phenomenon is called color constancy. For example, a white object seen under white light would be perceived as white under another light.

Color constancy index or CCI was a measurement to study the performance of chromatic adaptation under a test illumination. It was ranged from 0 to 1 as poor color constancy to perfect color constancy. Typically, CCI was studied by matching and achromatic setting methodology. The tasks were based on physical color space, such as a chromaticity diagram. Also, the adjustment setting was not a natural task as we do in daily life. Another method was color naming which is a familiar step as we usually call the object's color name. Categorical color naming (Ma, R., Liao, N., Yan, P., & Shinomori, K. 2018, Troost, J. M., & De Weert, C. M. 1991) is the method that requires a participant to call the color generally based on eleven basic color naming. The color constancy could be obtained by averaged and calculated based on the centroid of the color category within the same color name. The problem was a limitation of this method. The color naming mandatory forces a participant to name a stimulus with hesitation.

Nowadays, Light-emitting diodes or LEDs is dominated the fluorescent lamp with various benefits such as less energy consumption and generating numerous color light. In the case of changing illuminant spectral power distribution, the color perception is also affected. However, there was little research about color appearance under LEDs light.

In this study, twenty-six color chips were perceived and judged by 100 participants under thirteen illumination conditions with an elementary color-naming method (Ikeda, M. 2004, Phuangsuwan, C., Ikeda, M., & Mepean, J. 2018, Pungrassamee, P., Ikeda, M., Katemake, P., & Hansuebsai, A. 2005). This naming method was absolute judgment and allowed researchers to figure out the color appearance of objects based on the perception of color space as a quantitative measurement.

Experiment

Two experiments were designed to obtain both color appearance of the color chip with and without adapted to color light. Figure 1 shows the apparatus for experiment 1. The booth was designed and decorated like an actual living condition. A grey rectangular on the table acted as a background with a color chip (6 cm square) will be placed on it. The boom was illuminated by LEDs hanging on the left ceiling of this room. The light could only be controlled by the computer connected through cable wire outside the room. Figure 2 shows the experimental booth used to obtain the stimuli's color appearance without adapting to the test light condition. The booth was extended and divided into the test room and the subject room. The test room was the same as experiment 1, except the color chip will be placed on the standing pole instead of the table. On the other hand, the subject had to move to the subject room, which was illuminated by only white reference light, D65. The participant could see the stimulus through a small hole between these rooms.



Figure 1 Apparatus for experiment 1

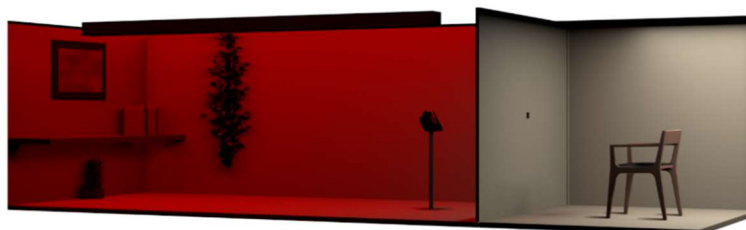


Figure 2 Apparatus for experiment 2

There were twenty-six color chips used in this experiment, as shown in Table 1. The color chips were designed based on three groups. The first was the 15 test color sample used to study and calculate the color rendering index. The second was a gamut of the printer, Konica Minolta C83HC, which we used to reproduce these stimuli. There were eight-color chips in the second group. There were three color chips: neutral, white, and black, classified as an achromatic group for the last one.

Table 1 Color chips

Chip No.	Hue (°)	Luminance (cd/m ²)	a*	b*	Type
01	16	5.39	61.49	17.93	TCS
02	21	9.08	18.84	7.22	TCS
03	33	10.25	17.6	11.39	TCS
04	45	9.18	43.02	43.74	Gamut
05	53	15.99	13.83	18.17	TCS
06	83	8.21	3.35	28.88	TCS
07	88	16.83	3.03	71.75	TCS
08	88	9.06	2.57	70.28	Gamut
09	109	9.83	-16.74	48.3	TCS
10	113	4.18	-11.86	27.61	TCS
11	133	9.61	-52.95	56.13	Gamut
12	140	8.55	-30.8	25.56	TCS
13	148	5.38	-39.93	24.79	TCS
14	179	9.33	-56.05	1.28	Gamut
15	185	8.72	-19.63	-1.8	TCS
16	220	9.9	-37.67	-31.69	Gamut
17	258	4.02	-9.09	-44.09	TCS
18	259	8.67	-5.45	-27.05	TCS
19	270	7.87	-0.12	-36.67	Gamut
20	298	8.81	16.44	-31.35	TCS
21	319	7.45	40.9	-35.81	Gamut
22	319	1.46	12.62	-10.96	TCS
23	356	8.25	60.61	-4.75	Gamut
B	337	0.75	0.59	-0.25	Achromatic
N	237	5.59	-16.2	-2.55	Achromatic
W	247	23.02	-2.11	-5.16	Achromatic

There were 13 illuminations shown in Table 2, including the white light as D65. There were six hues, red, yellow, green, cyan, blue, and magenta. The light conditions could be divided into less vivid light and vivid light. The illumination of each situation generally varied between 95 – 101 lx except B2 as a limited of LEDs (Phillips: Kinetics color cover MX power core) used in this experiment. For B2, the illumination was 80 lx.

Table 2 Illumination Conditions

Illuminations	u'	v'	Illuminant (lx)
D65	0.200	0.466	100.9
R1	0.369	0.492	97.9
R2	0.538	0.518	99.1
Y1	0.253	0.506	98.6
Y2	0.307	0.546	97.1
G1	0.138	0.520	99.4
G2	0.075	0.575	98.5
C1	0.154	0.423	100.6
C2	0.108	0.381	101.0
B1	0.170	0.326	95.2
B2	0.140	0.187	80.6
M1	0.270	0.409	98.6
M2	0.339	0.352	97.2

One hundred participants, who were students from the Rajamangala University of Technology Thanyaburi, assessed these color chips by using the elementary color-naming method. Each participant gave an amount percentage of chromaticness, whiteness, and blackness for each set. Then, another amount of the opponent's color theory was judged as red, yellow, green, and blue.

Result

The result obtained by the naming method could be transferred and plotted on a graph called a polar diagram. The result showed that the color perception area of the less vivid light group was less than the saturated group. The color constancy index could be calculated based on the distance between perception and physical shifts, as shown in Equation 1. In the equation, the ‘a’ symbol was a perception based on the distance between color naming results under D65 to test illumination. The ‘b’ symbol was a physical shift judged by experiment 2 under test illumination away from D65.

$$CCI = 1 - \frac{a}{b} \quad (1)$$

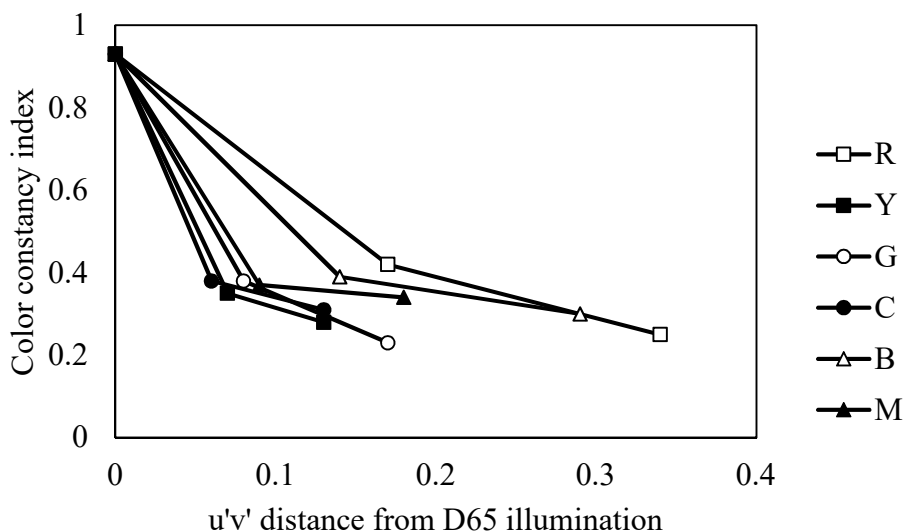


Figure 3 Color constancy index result

The result of calculating color constancy is shown in Figure 3. The graph clearly shows that the color constancy index was poor when increasing light saturation as $u'v'$ distance away from D65 on the abscissa. Especially, the color constancy index was dropped early under cyan, green, and yellow illumination. Our results suggested avoiding these lights in the case of vivid illumination requirements.

References

- Ikeda, M. (2004). Color appearance explained, predicted and confirmed by the concept of recognized visual space of illumination. *Optical Review*. 11(4), 217-225. doi:10.1007/s10043-004-0217-x
- Ma, R., Liao, N., Yan, P., & Shinomori, K. (2018). Categorical color constancy under RGB-led light sources. *Color Research & Application*. 43(5), 655-674. doi:10.1002/col.22241
- Phuangsuwan, C., Ikeda, M., & Mepean, J. (2018). Color appearance of afterimages compared to the chromatic adaptation to illumination. *Color Research & Application*. 43(3), 349-357. doi:10.1002/col.22207
- Pungrassamee, P., Ikeda, M., Katemake, P., & Hansuebsai, A. (2005). Color appearance determined by recognition of Space. *Optical Review*. 12(3), 211-218. doi:10.1007/s10043-005-0211-y
- Troost, J. M., & De Weert, C. M. (1991). Naming versus matching in color constancy. *Perception & Psychophysics*. 50(6), 591-602. doi:10.3758/bf03207545

Simultaneous Color Contrast on an Electronic Display with or without a Tissue Paper under Various Room Illuminances

Janejira Mepean^{1*}, Mitsuo Ikeda² and Chanprapha Phuangsuan²

¹*Division of Color Technology and Design, Graduate School, Faculty of Mass Communication Technology, Rajamangala University of Technology Thanyaburi, Pathum Thani 12110, Thailand*

²*Color Research Center, Rajamangala University of Technology Thanyaburi, Pathum Thani 12110, Thailand*

*Corresponding email: janejira_m@mail.rmutt.ac.th

Abstract

A well-known phenomenon to show the chromatic adaptation is the simultaneous color contrast or SCC. The subject perceives an opponent or complementary color of surrounding on the achromatic test patch placed at the center. In case of an object stimulus such as a printed paper, the color of the test patch does not appear vivid, but it appears more vivid if the stimulus is covered entirely by a tissue paper. The phenomenon is explained in a way that the tissue blurs the contour of the test patch to reduce the object recognition of the stimulus and only the color remains in the surround to give a stronger chromatic adaptation. In this paper, we investigate if the tissue paper still works for an electronic display which is a self-luminous display. Ten levels of room illumination from 3 to 1600 lx were employed. Four colors, red, yellow, green, and blue were used for surround, and one gray for central test patch. The luminance was kept constant at 46, 128, 88, 15 cd/m² for the surround and 41 cd/m² for the test patch. Subjects judged color appearance of the test patch by the elementary color naming method with and without a tissue paper. The results showed that the ratio of chromaticness of test patch to the chromaticness of surround stayed constant for all the illuminance levels without-tissue but it increased at 200 lx and beyond.

Keywords: Simultaneous color contrast, Electronic display, Room illuminance, Tissue paper

Introduction

The simultaneous color contrast or SCC is the phenomenon to show mechanism of the chromatic adaptation to the surrounding color, a gray test patch at the center under red surrounding was appeared cyan, for example. In the case of paper stimulus, the phenomenon is not strong and the central gray test patch is not vivid, but if the SCC stimulus is covered by a white tissue the SCC effect is much enhanced and the central gray test patch appears more vivid in color because the physical effect of a tissue is to blur the image and to reflect the white ceiling light toward a subject reducing the contrast of the image and desaturating color of the image on the surface of stimulus (Graham, H. C., & Brown, L. J. 1965) we can explain by the recognized visual space of illumination RVS theory (Ikeda, M. 2004) that a subject adapts to the color of illumination of a space constructed over the surrounding surface. (Phuangsuan, C., & Ikeda, M. 2017, Phuangsuan, C., Ikeda, M., & Mepean, J. 2018) So far, many studies use an electronic display for presenting stimulus because an electronic display is self-luminous which gives a stronger adaptation. However, the experiments are mostly performed in a dimly illuminated room to avoid the effect of reflections of the room illumination on the surface of display. In this paper we are interested to investigate if this tissue effect occurs in an electric display, by changing display luminance and room illuminance.

Experiment

Four surrounding colors; red, yellow, green, and blue were employed including the central gray patch. To obtain effect of room illumination, the illuminance in the room was changed at ten levels, 3, 6, 13, 25, 50, 100, 200, 400, 800, and 1600 lx on the display by using ceiling fluorescent lamp. Their xy chromaticities of stimuli under levels of illumination are shown in Figure 1 for without-tissue (a) and for with-tissue (b).

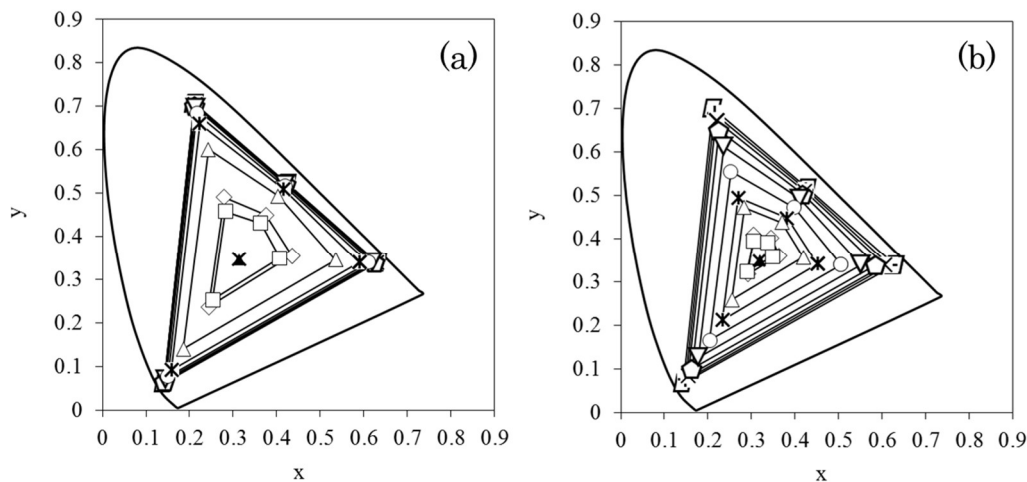


Figure 1 The surrounding colors under ten levels of illuminance without-tissue (a), with-tissue (b) (\square 3 lx, $+$ 6 lx, \times 13 lx, \diamond 25 lx, ∇ 50, \circ 100 lx, $*$ 200 lx, \triangle 400 lx, \diamond 800 lx, \square 1600 lx, \blacktriangle white point, and \times central gray patch.

A 24.1" LCD display (EIZO monitor) was used to present the SCC stimulus. The display was placed horizontally on a table and was masked with black paper which a rectangular hole in the middle. The size of the surround was 23x23 cm² and the gray patch was 3x3 cm², from the distance 50 centimeter of observation was gives 25.9° and 3.4° of visual angle, respectively. In with-tissue condition we use the one sheet of white tissue stretched flat on the frame to cover the stimulus, the size of the tissue within the frame was 13x14 cm². The haze value was 80 % and the transmittance was constant at 56 % for visible wavelength.

Ten subjects with normal color vision participated in the experiment. Subjects were asked to judge the color appearance of surround and gray patch by the elementary color naming method, namely, to estimate chromaticness, whiteness, and blackness in percentage and if there was perceived chromaticness they have to estimate the hue by unique hues, red, yellow, green, and blue in percentage also. The judgment was repeated for five times in different days.

Results and Discussion

We averaged the results of color perception of four surrounds for ten subjects and showed the result in Figure 2 and 3 open circles for the with-tissue and filled circles for the without-tissue. The abscissa shows the room illuminance and the ordinate the amount of chromaticness. Figure 2, the chromaticness of four surrounds it clearly decreased with tissue as the illuminance increased, but is quite constant for without tissue. Figure 3 shows the chromaticness of the test patches without-tissue and with-tissue. It shows a relatively constant and relatively similar value of chromaticness at all the illuminance levels, except the case of green surround, that the chromaticness slightly reduces as higher illuminance.

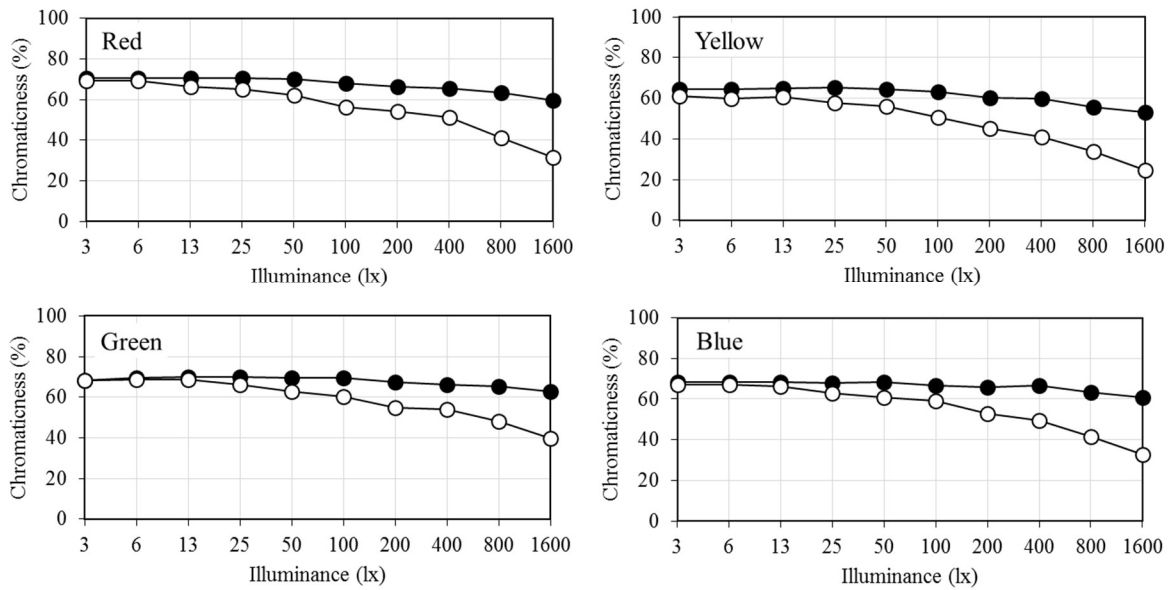


Figure 2 Amount of chromaticness of four surrounding colors with ten levels of illuminance compared between without-tissue (●) and with-tissue (○).

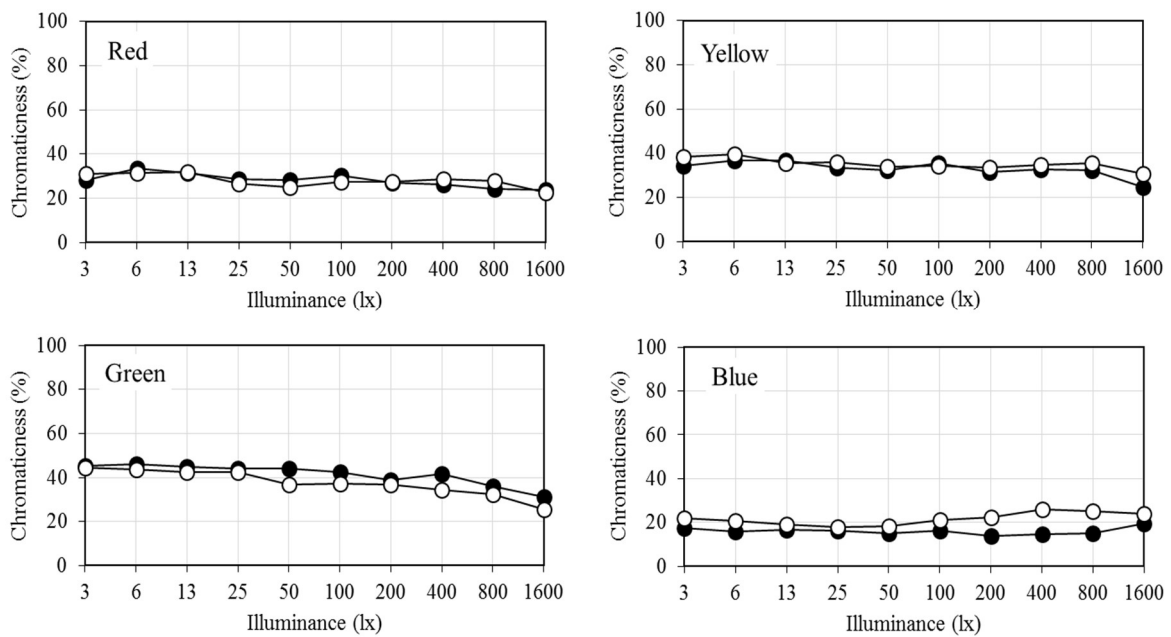


Figure 3 Amount of chromaticness of test patch in each surrounding color with ten levels of illuminance compared between without-tissue (●) and with-tissue (○).

As we are interested in the power of surround to induce color at the test patch, we took ratio of chromaticness of test patch to the chromaticness of surround as shown in Equation 1, and the results are shown in Figures 4 and 5. The abscissa shows the room illuminance and the ordinate giving the chromaticness ratio.

$$\text{Chromaticness ratio} = \frac{\text{chromaticness of test patch}}{\text{chromaticness of surround}} \quad (1)$$

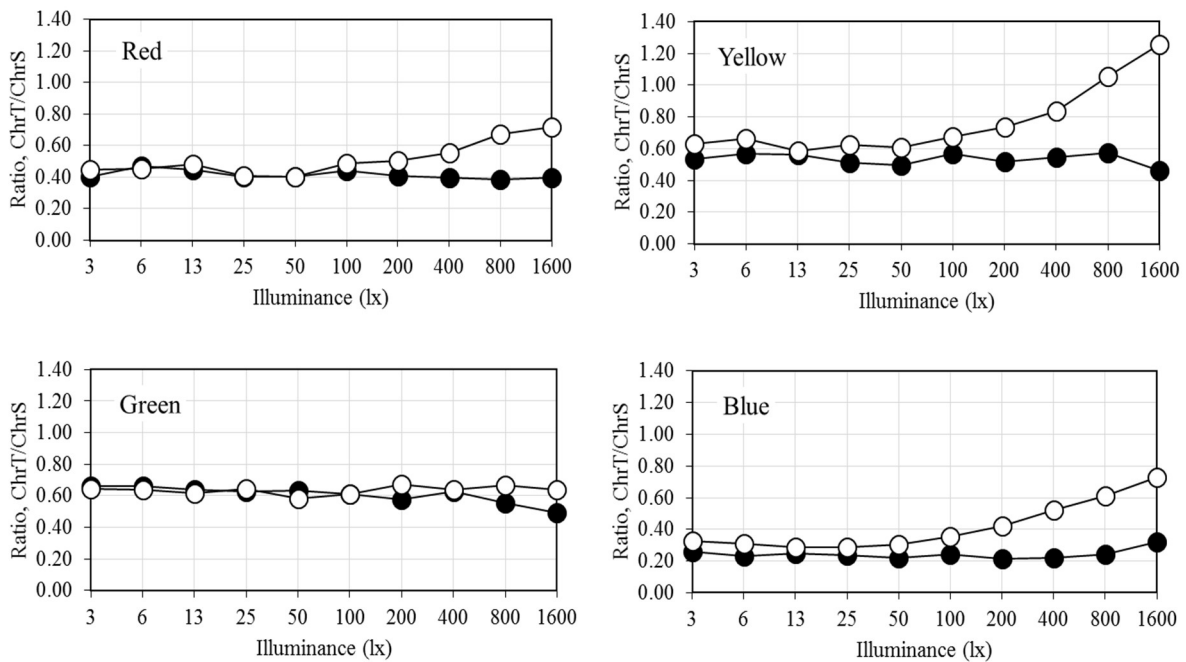


Figure 4 Chromaticness ratio of four surrounding colors with ten levels of illuminance compared between without-tissue (●) and with-tissue (○).

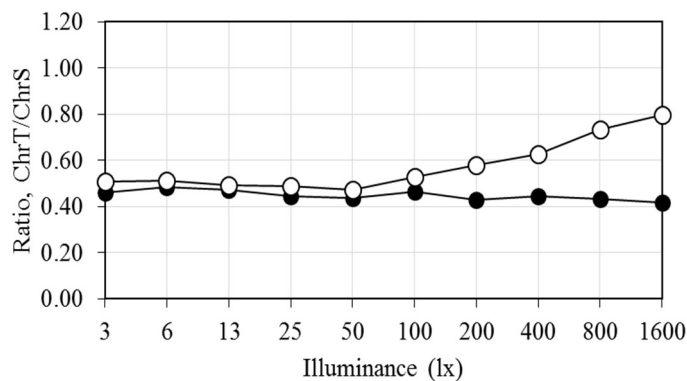


Figure 5 Averaged results from four surrounding colors compared between without-tissue (●) and with-tissue (○).

Figure 4 shows the chromaticness ratios that were obtained from Figures 2 and 3. It seems like constant under room illumination level from 3-100 lx, but increased when over 200 lx, except under green surround. Finally, their averages of all four surrounding colors are shown in Figure 5.

These results indicated that the ratio continued to increase from the illuminance 200 lx and beyond. Higher room illuminance increases the reflection of the white light from the tissue surface and the subjects seen a decreased surrounding color through the tissue paper but still perceived the appearance of simultaneous color contrast as same as without-tissue.

Acknowledgement

Janejira Mepean acknowledges Dr. Fusako Ikeda for giving her the Fusako Scholarship to study at graduate school of Rajamangala University of Technology Thanyaburi.

References

- Graham, H. C. & Brown, L. J. (1965). *Vision and visual perception: Color contrast and color appearance: Brightness constancy and color constancy*. USA: John Wiley & Sons.
- Ikeda, M. (2004). Color Appearance Explained, Predicted and Confirmed by the Concept of Recognized Visual Space of Illumination. *Optical Review*. 11(4), 217–225.
- Phuangsuwan, C. & Ikeda, M. (2017). Chromatic adaptation to illumination investigated with adapting and adapted color. *Color Research and application*. 42, 571–579.
- Phuangsuwan, C. & Ikeda, M. & Mepean, J. (2018). Color appearance of afterimages compared to the chromatic adaptation to illumination. *Color Research and Application*. 43(3), 349–357.

Individual Identify Face Detection by Principal Component Analysis (PCA)

Supannika Yongsue*, Kamron Yongsue, Onsucha Upakit,
Yuvayong Anumanrajadhon and Chirapong Yanuchit

*Brach of visual and Audio Technology, Faculty of Mass Communication Technology, Rajamangala
University of Technology Thanyaburi, Pathum Thani 12110, Thailand.*

** Corresponding email: supannika@rmutt.ac.th*

Abstract

In this research, we study individual identify Face Detection using Principal Component Analysis (PCA) for reduce the size of feature, the proposed approach can accurately detect facial features, especially the eyes, even when the images have complex backgrounds. There are three objectives of this research as follows: 1) To study three different distances, the accuracy of the face detection distance determination was tested. Conducted an experiment with a group of 30 users to detection from three different distances (1m, 1.5m, 2m). The system is used to identify people entering the system and operates on an image or person entering the system. 2) To study face detection systems using the skin color of a subject. In face detection, the two respective classes are the “face area” and the “no-face area” based on color tone values specially defined for skin area detection within the image frame. 3) To develop a face detection method which combines the Skin Color Detector and the Template Matching Method. The results of the accuracy of the PCA from the human face test found that the best distance of 1.5 meters was 90.33%. The results of the data display were found to be accurate, fast, and at a good level. The satisfaction from using the application was found to be at a good level. The results from the evaluation are compared to select the best model that is suitable for the dataset and face recognition system. This research uses 1008 images of 106 people from Digital Media Student (DMSD) datasets. The dataset is divided as a training set of 878 images and as a test set of 560 images. The best recognition result obtained from the experiment achieves with 92.80% in accuracy.

Keywords: Face Detection, Face Recognition, Principal Component Analysis (PCA), Template Matching Method

Introduction

Machine learning is about learning some properties of a data set and then testing those properties against another data set. A common practice in machine learning is to evaluate an algorithm by splitting a data set into two. We call one of those sets the training set, on which we learn some properties; we call the other set the testing set, on which we test the learned property. (Buitinck et al., 2013) improve a face recognition system using Principal Component Analysis (PCA) to extract features from the face images and reduce the dimensionality of each image and K nearest neighbors to classify data. Today’s machine learning- based AI systems excel in several complex tasks ranging from the detection of objects in images (K. He, X. Zhang, S. Ren, and J. Sun., 2016). and the understanding of natural languages (K. Cho, B. Van Merriënboer, C. Gulcehre, D. Bahdanau, F. Bougares, H. Schwenk, and Y. Bengio., 2014) to the processing of speech signals (L. Deng, G. Hinton, and B. Kingsbury, 2013). On top of that, recent AI¹ systems can even outplay professional human players in difficult strategic games such as Go (D. Silver, A. Huang, C. J. Maddison, A. Guez, L. Sifre, G. Van Den Driessche, et al., 2016) and Texas hold’em poker (M. Moravcık, M. Schmid, N. Burch, V. Lisy, D. Morrill, N. Bard, et al., 2017). The field of machine learning and artificial intelligence has progressed over the last decades.

¹The terms artificial intelligence and machine learning are used synonymously.

Face Detection is a task in images investigation which many and more applications, such as Facial Expression Analysis, Human Computer Interface, Security Systems, Face Recognitions, Man-Machine Interface, Content Base Image Retrieval (CBIR) etc. Face Detection is interesting and challenging problem. Face Detection in pattern recognition technology and computer vision technology as an important subject has high commercial value and an academic value. The main aim of face detection is to determine the location of probable faces in images (Tripathi, S., Sharma V. and Sharma S., (2011). Face detection is used to determine the size of human faces and locations in the digital images. It can detect facial features and ignores anything else, such as bodies, buildings, and trees etc. Face detection according to various approaches, are classified into four categories such as (i)- Knowledge based method, (ii)- Feature based method, (iii)- Template based method, (iv)- Machine learning method (S. A. Inalou and S. Kasaei., 2010)

Face recognition (FR) allows us to exactly identify or tag an image of a person. Day-today applications include searching for celebrities on the web and auto-tagging friends and family in images. Face recognition is a form of fine-grained classification. The famous Handbook of Face Recognition (Li et al., Springer, 2011) categorizes two modes of an FR system:

1) Face identification—Face identification involves one-to-many matches that compare a query face image against all the template images in the database to determine the identity of the query face. Another face recognition scenario involves a watchlist check by city authorities, where a query face is matched to a list of suspects (one-to-few matches).

2) Face verification—Face verification involves a one-to-one match that compares a query face image against a template face image whose identity is being claimed (Figure 1).

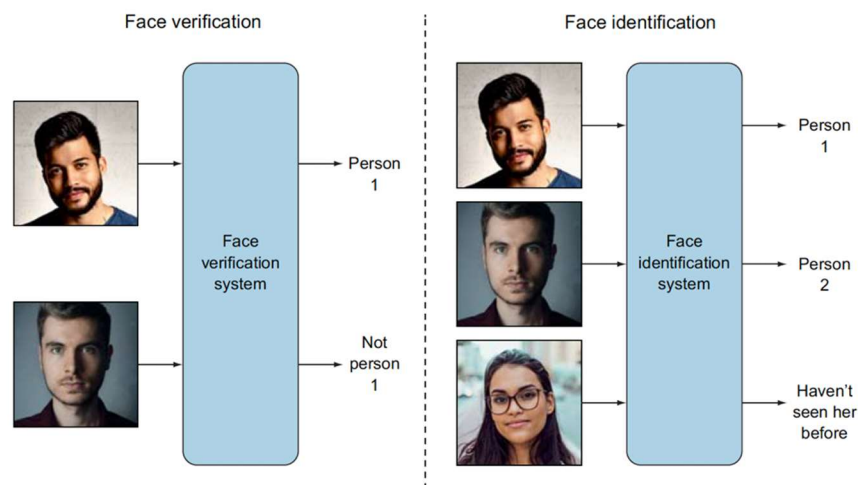


Figure 1 Example of face verification (left) and face recognition (right)
(Mohamed Elgendy ©2020 by Manning Publications)

Template Matching Method that finds the similarity between the input images and the template images (training images). Template matching method can use the correlation between input images and stored standard patterns in the whole face features, to determine the presence of a whole face features.

Edged Detector is fundamental tool in image processing and computer vision, particularly in the areas of feature detection and feature extraction, which aim at identifying points in a digital image at which the image brightness changes sharply or, more formally, has discontinuities. There is an extremely large number of edge detection operators available, each designed to be sensitive to certain types of edges. Variable involved in the selection of an edge detection operator include: Edge orientation, Noise environment, Edge structure etc. There are many ways to perform edge detection. However, the majority of different methods may be grouped into two categories: Gradient and

Laplacian. The gradient method detects the edges by looking for the maximum and minimum in the first derivative of the image. The Laplacian method searches for zero crossings in the second derivative of the image to find edges. An edge has the one-dimensional shape of a ramp and calculating the derivative of the image can highlight its location. Suppose having the following signal, with an edge shown by the jump in intensity show as figure 2 edge by jump in intensity

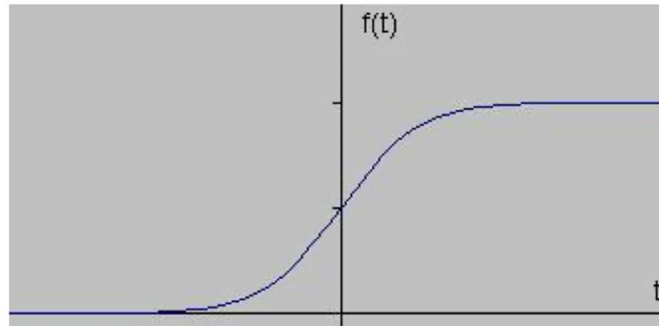


Figure 2 Edge by jump in intensity

Materials and Methods

This paper mainly the building of face recognition system by using Principal Component Analysis (PCA). PCA is a statistical approach used for reducing the number of variables in face recognition. In PCA, every image in the training set is represented as a linear combination of weighted eigenvectors called eigenfaces. A face image of $N \times N$ includes N^2 number of pixels, The result from the system detects the face of a person and creates frames around the face before sending it to face recognition.

In this paper, we have proposed a new face detection method for color images which uses a combination of the Skin Color Detection and the Template-Matching Method. Figure 3 shows the structure of the proposed method. In the first stage, we have used the skin color detector. It is used to detect the skin or non-skin regions in the images. In the skin color detector, we have used the YCbCr color space because it is widely used in the digital images. In the YCbCr, Y channel represents the luminance component of the images, and both Cb and Cr represent the chrominance component of the images. We have then distribution of human skin color modeled with a GMM (Gaussian mixture model). Then we have selected the skin regions. The result of the skin color detector (faces or non-faces) is applied to the template matching method. Finally, the template matching, we have used the trained images (eigenfaces). We can easily find the position of the eyes, nose, mouth, head etc. by the use template matching method. Therefore, we have detected the faces in this method. The block diagram of skin color detector is shown in figure 4.

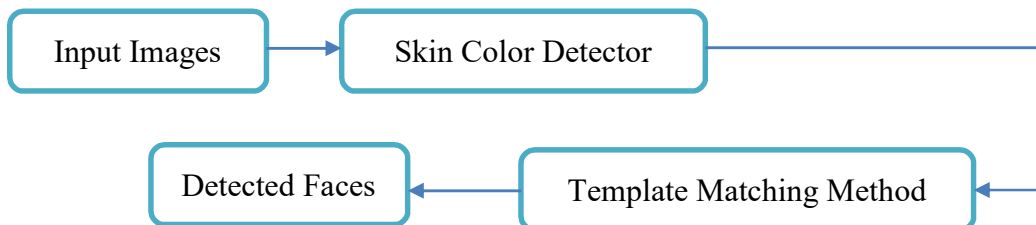


Figure 3 The structure of the proposed method

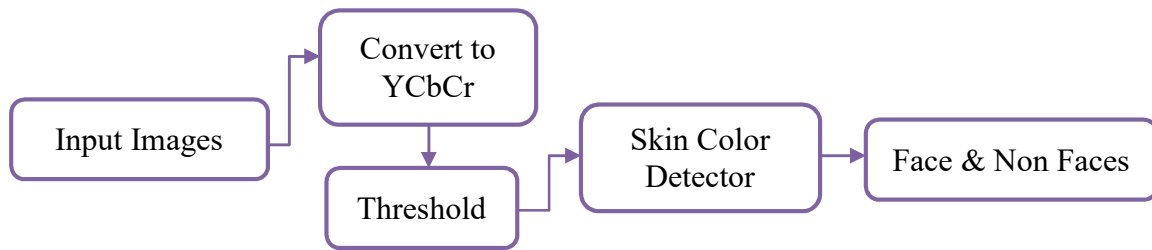


Figure 4 Block Diagram of individual identify Face Detection

The template matching is the part of the segmentation of images. In the image segmentation, there are various methods such as templated matching, edge detection, clustering, boundary detection, thresholding, texture matching. But in the proposed method, we have used only edge detection and template-matching. The sobel edge detector is used to detect the edges. The trained images are used in the template matching, so we can detect the faces and remove the non-faces. The block diagram of the template matching is shown in figure 5

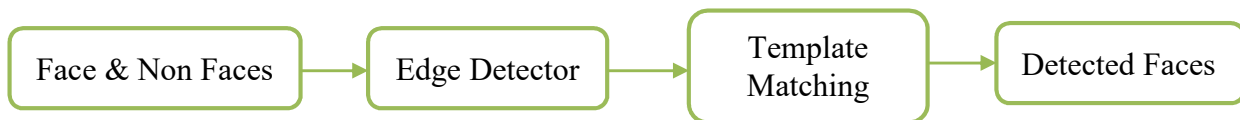


Figure 5 Block Diagram Template matching method

Experimental Result

The experiments of the face detection system are carried out on Macintosh operating system, and on a 3.1 GHz Dual-Core Intel Core i5 with 8 GB of RAM. It is implemented by python version 3. We have created the database names DMSD. This database can. We have taken 7 image of 144 persons with consist of 1008 images for our experiment. The images of each person are with different facial expression or configuration such as: without glass (normal), happy, right, left, center, bent, perk. Few examples of these images are shown (see Figure 6). These images contain multiple faces with variations in color, scale, size, expression, and position etc. In this method first we have applied the input image as shown in Figure 5 we have converted the RGB image to the gray-scale image, then we can convert the gray-scale image to the YCbCr image. So we can apply the threshold and convert the threshold image to the binary image. In this image, the value of the skin region is 1 (white), and the value of the non-skin region is 0 (black). Next we have applied the skin color detector, it can detect the next skin regions (skin pixels) and remove the non-skin pixels. We have applied the sobel edge detector and finally we have applied the template matching, and then produced the output results of the face detection. Thus, we have improved the face detection process by reducing the false positives (non faces detection).

In templated matching approach, the correlation between the reference image (template) and the target image (input) can be calculated by number of similarity measurements. Table 1, show the result of locating the face by suing ten different correlation measurements, and it demonstrate the increase in accuracy by using the OSAD against the other measurements. The accuracy of the face localization by using OSAD is 99% and that is due to the selected input image.

Table 1 Comparison between similarity measurements and OSAD on DMS dataset

Similarity Measure	Accuracy (%)
Optimized Sum of Absolute Difference (OSAD)	99%
Sum of Absolute Differences (SAD)	97%
Zero-mean Sum of Absolute Differences (ZSAD)	97%
Locally scaled Sum of Absolute Differences (LSAD)	97%
Sum of Squared Differences (SSD)	95%
Zero-mean Sum of Squared Differences (ZSSD)	95%
Locally scaled Sum of Squared Differences (LSSD)	95%
Normalized Cross Correlation (NCC)	95%
Zero-mean Normalized Cross Correlation (ZNCC)	80%
Sum of Hamming Distances (SHD)	55%

In this section a detailed experimental comparison of the above stated algorithm, we used color images obtained from DMSD which comprise of only single face. The accuracy is obtained in all the three cases by using the following equation:

$$\% \text{ Accuracy} = 100 - (\text{Rate of False Dismissal} + \text{Rate of False Detection}) \dots\dots\dots(1)$$

3.1 Results of Performance of the Proposed Method

The results of experiment show that the results of the accuracy of the PCA from the human face test found that the distance of 1.5 meters was 90.33%. Secondly, the accuracy of the PCA from the human face test found that the distance of 1 meter was 89.33%. Finally, the accuracy of the PCA from the human face test found that the distance of 2 meters was 86%.

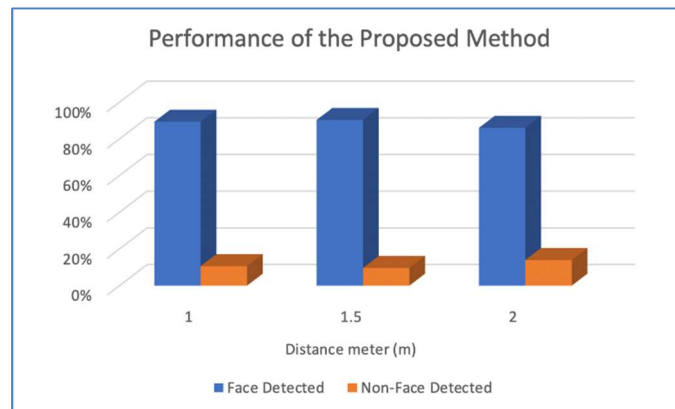


Figure 6 Performance of the Proposed Method

3.2 Result of Skin Color Based Face Detection in RGB, YCBCR and HSI Color Space

Our experiment shows very good results for proposed algorithm. The results were obtained using the previous conditional probabilities and threshold values. The false detection and false dismissal rate are show in Table 2. The low false dismissal rate shows the robustness of the algorithm. The accuracy is found to be 92.80%. Table 3 Show that the comparison of the algorithms give good results. Sample results from proposed algorithm are show in Figure 7.

Table 2 Skin Color Classification Results for Proposed Algorithm

No. of Images	False Detection Rate(%)	False Dismissal Rate(%)
560	5.25%	2.49%

Table 3 Skin Color Classification Results for Proposed Algorithm

Criterion	RGB Color Space [12]	YCbCr Color Space [12]	HSI Color Space [12]	Proposed Algorithm
Accuracy	92.69%	84.61%	73.8%	92.80%

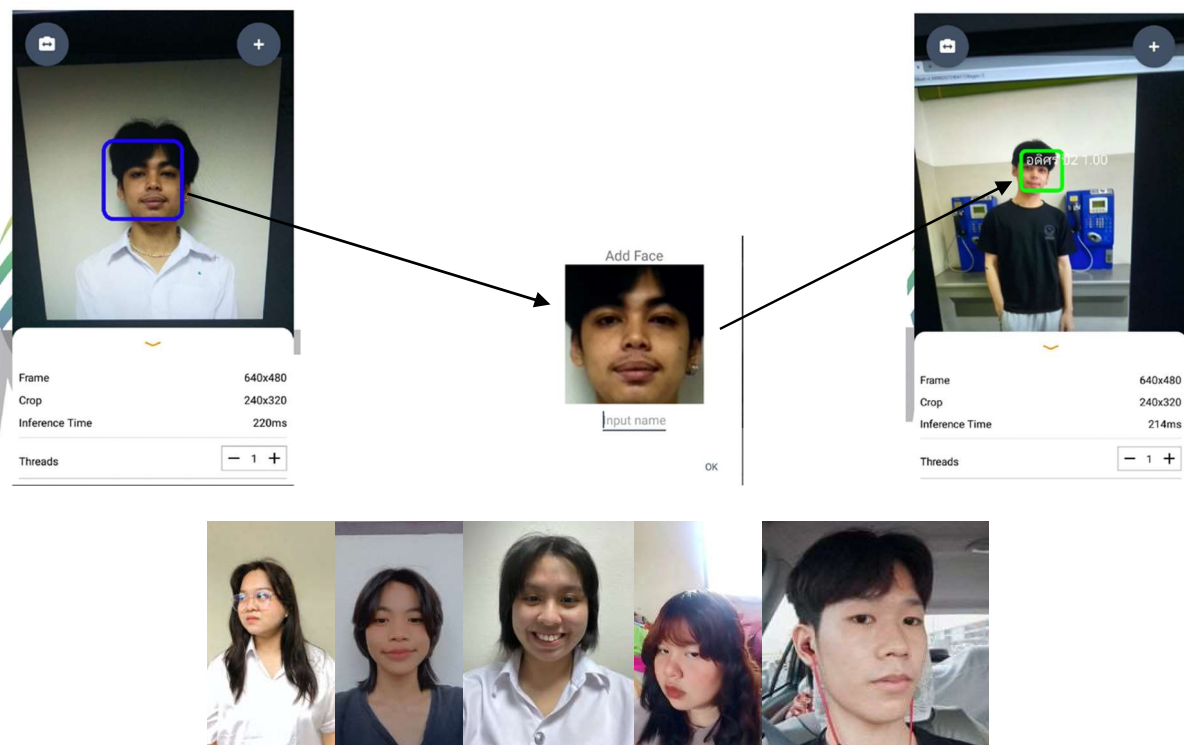


Figure 7 Sample Result of Proposed Face Detection Algorithm

3.3 Result of Face Detection using Template Matching Method

The performance of the template matching method as shown in Figure 8, In this table we have compare the Skin color detection method and the proposed method (combined the skin color detector and template matching method). This method is used to remove the non-faces and to detect the faces more accurately. Experimental results show that the performance of the proposed method is better than Skin Color Detector.

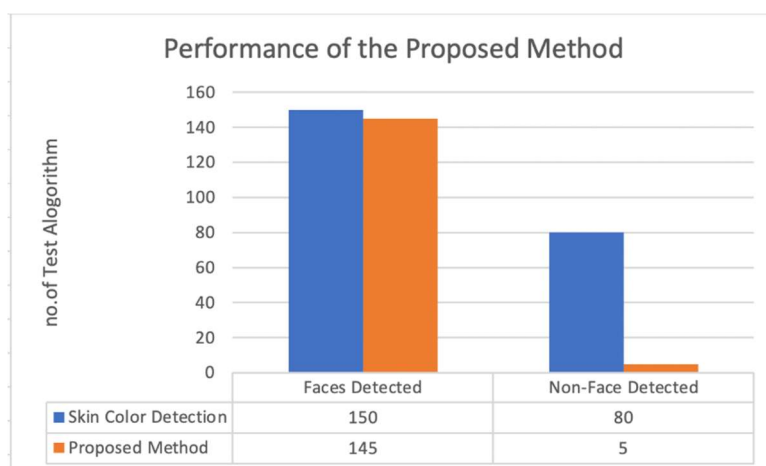


Figure 8 Performance of Face Detection using Template Matching Method

Conclusion

This paper study individual identifies Face Detection using Principal Component Analysis (PCA) for reduce the size of feature, the proposed approach can accurately detect facial features, especially the eyes, even when the images have complex backgrounds. The accuracy of the PCA from the human face test found that the best distance of 1.5 meters and the data display were found to be fast, and at a good level. The evaluation is compared to select the best model that is suitable for the dataset and face recognition system. The best recognition result obtained from the experiment achieves with 92.80% in accuracy.

Acknowledgments

Thank for Technology for Data Science ANACONDA.com (<https://www.anaconda.com>) to analyst data Retrieved from <https://blog.ragnar.co.th/blog/what-is-jupyter-notebook>. Thank for support finance and research location at Faculty of Mass Communication Technology, Rajamangala University of Technology Thanyaburi (RMUTT), Pathum Thani, Thailand. Thank blog of Sasiwut Chaiyadecha for teach in machine learning (Building the transition matrix with Python), url <https://lengyi.medium.com/transition-matrix-pd-model-1-fbc2cf04b895>.

References

- Buitinck, et al. (2013). *API design for machine learning software: experiences from the scikit-learn project*. European Conference on Machine Learning and Principles and Practices of Knowledge Discovery in Databases. Retrieved from <https://scikitlearn.org/stable/about.html#citing-scikit-learn>.
- Cho, K., Van Merriënboer, B., Gulcehre, C., Bahdanau, D., Bougares, F., Schwenk, H. and Bengio, Y. (2014). *Learning phrase representations using RNN encoder-decoder for statistical machine translation*. arXiv preprint arXiv:1406.1078.
- Deng, L., Hinton, G. and Kingsbury, B. (2013). *New types of deep neural network learning for speech recognition and related applications: An overview*. In *IEEE International Conference on Acoustics, Speech and Signal Processing (ICASSP)*, 8599–8603.
- He, K., Zhang, X., Ren, S. and Sun, J. (2016). *Deep residual learning for image recognition*. In *Proceedings of the IEEE Conference on Computer Vision and Pattern Recognition (CVPR)*, 770–778.
- Inalou, S. A. and Kasaei, S. "AdaBoost-Based Face Detection in Color Images with Low False Alarm," 2010 Second International Conference on Computer Modeling and Simulation, 2010, 107-111, doi: 10.1109/ICCMS.2010.287.

- Moravcik, M., Schmid, M., Burch, N., Lisy, V., Morrill, D., Bard, N. et al. (2017). Deepstack: Expert-level artificial intelligence in heads-up no-limit poker. *Science*, 356(6337), 508–513.
- Sasankar, P. & Kosarkar, U. (2021, Jan). *A study for Face Recognition using techniques PCA and KNN*. EasyChair The world for scientists, Preprint no. 4931. Retrieved from <https://easychair.org/publications/preprint/gS7Q>.
- Shah Zainudin, M.N., Radi H.R., Muniroh Abdullah, S. and Rosman Abd. R., et al. (2012). Face Recognition using Principle Component Analysis (PCA) and Linear Discriminant Analysis (LDA). *International Journal of Electrical & Computer Sciences IJECS-IJENS*, 12(05).
- Shih, P. and Liu, C. (2006). *Improving the Face Recognition Grand Challenge Baseline Performance using Color Configurations Across Color Spaces*, ". 2006 International Conference on Image Processing, pp. 1001-1004, doi: 10.1109/ICIP.2006.312668.
- Silver, D., Huang, A., Maddison, C. J., Guez, A., Sifre, L., Van Den Driessche, G. et al. (2016). Mastering the game of go with deep neural networks and tree search. *Nature*, 529(7587):484–489.
- Tripathi, S., Sharma V. and Sharma S. (2011). Face Detection using Combined Skin Color Detector,". *International Journal of Computer. International Journal of Computer Applications (0975 – 8887)*, 26(7).
- Zangana, H. M. (2015). A New Skin Color Based Face Detection Algorithm by Combining Three Color Model Algorithms. *IOSR Journal of Computer Engineering*, 17(3), 06-12.

Colors for Designing Advertisement Facebook Post Image of Food and Beverage Products on Facebook Fanpage

Natchaphak Meeusah*, Sirawadee Kramsuk and Juthamas Podoy

Multimedia Technology, Faculty of Mass Communication Technology, Rajamangala University of Technology Thanyaburi, Thailand

**Corresponding email: natchaphak_m@rmutt.ac.th*

Abstract

The objective of this study was to study using colors in 3 different kinds of advertising Facebook post image including pizza, burger, and bubble milk tea advertisements. There were 4 types per kind. Then quality was assessed and comments on choosing colors to create the advertising Facebook post image of food and beverage products on Facebook fanpages were compared. The methods of creating the advertising Facebook post image started from media quality assessment from 3 experts. Then comments were assessed and compared by the sample group. The sample group used from this study was 40 general persons who used Facebook in Klong 6 district from aged 15 to 40 that received from accidental sampling. The results were concluded that the quality of advertising Facebook post image of food and beverage products on 3 kinds of Facebook fanpages, designing had average score at good level with 4.64 of mean and 0.54 of standard deviation. The comparative results of comments on using colors in the advertising Facebook post image indicated that using red in pizza advertising Facebook post image had the most interest with average score at 3.83. Using red in burger advertising Facebook post image had the most interest with average score at 3.63. Using blue in bubble milk tea advertising Facebook post image had the most interest with average score at 3.52. The relevant reason was that the red and blue are warm and cool tone, respectively. These colors could properly indicate meanings of food and beverages, respectively. They could proficiently affect emotions and feelings in buying food and beverage products.

Keywords: Color, Facebook post Image, Facebook Fanpage, Food and Beverage Advertising

Introduction

Nowadays, trend of using Facebook as a social media to be a mediator in presenting the information such as living of people in general, presenting the information of the organization, or using it to connect with the main media of the unit to reduce the time for displaying the news, in which can be adapted with the communication tools of smart phone user which is supportable for using the internet as well as using other online media such as Twitter, Instagram, and YouTube etc. which work as the mediator in connecting various news. Facebook is a community of social media and useful marketing tools, low cost, high proficiency, and direct to the target group, and communicates by expanding the group to the new and old customs quickly, and efficiently. It is appeared that the organization, company, or department stores used more online market through Facebook. Especially, if it is necessary to advertise the business or products wider. Facebook fanpage is one of the online-social media which increased in numbers of members within a short period of time. The user can use to entertain or communicate or use it as a good marketing (Netrix, 2020). Moreover, the seller can run the company at any time, every location with internet connection and save the cost of labor due to the work can be proceeded by oneself, and there is no need for having the shop fronts, but product can still be sold. Therefore, the use of budget is lower as compared to the business with the shop fronts. The customer can purchase products through the Online shop as another extra optional in ordering and the buyer also can make a payment through several methods including

the service of delivering to the customer by hands. (Churwongboon, Chuvutayakorn, & Insaeng, 2017).

For Facebook Fanpage to be well recognized, a main part would be from designing of image which can indicate the identity of the brand or merchandise. Therefore, it needs to be designed interestingly and attractive to the customer. The advertisement is an important marketing which causes people to know more of products for instance, bringing the merchandise to sell, social event, or anything indicating about the identity of something. However, all mentioned represented through the image as a mediator. To design correctly and completely, there must be an important composition which is color, in this context means how to choose color to match with the products and targets (D2design, 2018).

Color is something representing about emotions and feelings with difference. The color chosen to use must need to reflect each other. Color choosing therefore needs holistic consideration of the media. We call the color which conducts this feeling that “Psychology of color”. Therefore, the brand must conform to using of the merchandise as well (Simon Bonello, 2013). Color is the external stimulus which human beings can acknowledge through eyes and causes different feelings (Graves, 1951). Psychologically, “color” affects emotions and feelings of human beings in which each tone or group of colors can conduct feelings and emotions differently. Therefore, color is very popular to be applied with various works that influence restaurant and advertisement about food, because color can stimulate the consumer to feel hungry and causes the consumer to not hungry as well. Therefore, choosing of color for designing of the advertisement is very important (Promjeen & Chaetnalao, 2019) which affects the positive attitude of the consumer and behavior of purchasing (Lichtlé, 2007; Seher, 2012).

According to the source and importance of the mentioned problems, we can see that color is very important to the feelings of those who see. If we choose a proper color in designing the image, it then can stimulate the consumer to be interested and decide to order the merchandise. The researcher focused on studying about the way of using color in designing the Facebook post Image with these following objectives, 1) to design Facebook post Image of the food and beverage products with different color background, 2) to study the quality of Facebook post Image of food and beverage products from the expert, and 3) to compare the interest of the background color of the Facebook post Image of food and beverage products from sample groups, by choosing Pizza, Hamburger, and Bubble tea as the representatives on designing food and beverage types used on Facebook post image because these products are popular amongst young adults who are the selective samples in this study with the expectation that the result will be useful for the entrepreneur who is using Facebook to advertise and publicize food and beverage products to be able to choose the background color in designing Facebook post Image of the merchandise efficiently and interestingly.

Related Works

1. Concept of Facebook post Image

Tonpo (2019), in the age of which the form of communication and motivation building using Facebook fanpage, the communication formats for presenting the identity can be summarized into 11 types as follows, self of the sender, revealing, clearness with frankness, attention, liveliness or showing the image relating to words, friendliness, notability, relaxation, argumentation, and exaggeration, respectively. Motivation building by 2 attractive points as follows, rational and emotional attractive points. If communicate by the mentioned formats, it will cause joy and following from lots of people in the society. Which correlating to Radsadondee (2020) analyzed the factors in acknowledging the foreign luxury fashion merchandise with generation Y consumer, it was found that the target group wants the product mark transmitting the interesting story which causes acknowledging of the product mark and there should be making the memory for the consumer to fascinate in the product mark.

However, to communicate with a group of consumers perfectly and interestingly, there are composition of the advertisement as follows (Tkann, 2020),

1) Font, it should be easy-to-read font, neat, and appropriate with the certain product brand to conduct the feelings to those who see, 2) Headline, should be compact, tight, and clear communication, 3) Photo, should be representing to business or brand of the merchandise, photo used should be suitable with its content, beautiful and easy to understand, and 4) Logo, should include title and logo of the brand for those who see the brand can remember.

The advertising role on Facebook fanpage which is the communication tool, each time of advertisement should consist of these following compositions,

1) Creating Awareness each time of advertisement with purpose to communicate directly or indirectly.

2) Providing information, the mentioned information might be useful for the merchandise, its price, location for distribution, promotion, company's information which might be useful for decision to buy of the target group.

3) Image Building, the advertisement can build the image for a brand due to the target group will correlate with many things which is seen in the advertisement without even realizing.

4) Reminding, which is for preventing the target group not to forget the brand when deciding to buy the certain merchandise needs to be made.

5) To persuade, the advertisement is responsible for persuading the target group to believe that the product is in good quality and better than opponent brand.

2. Concept of color

Color affects human being's emotions. According to the principle of psychology, color can be applied with various types of communication to help marketing person to create the quality brand. However, each color causes the specific emotional response from the consumer. Color affects the thought of deciding to buy of the consumer and increase the circulation such as product development, brand creating etc. Color tone can be divided into 2 tones as follows (Digitiv, 2018),

1) Warm color tone; red, orange, and yellow, will be helping to stimulate fresh and energetic feelings. These colors are a set of feelings, warm color tone is regarded as your best friend.

2) Cool color tone, cool color tone spectrum tends to cause peace and reliability. Blue and purple color, these colors can combine with creating the brand and become the remarkable or unique colors. Moreover, we can increase more of prominence to the composition of the image by trying to use warm color tone to create the unique with its compatible color which is the cool color tone.

Muangthanang, & Wongsiri (2021) studied about the influence of warm and cool color tone for designing the article poster with the characteristics of the message and image characterized by color tone such as 3 warm tone colors; red, orange, and yellow, and cool tone colors; blue, green, purple. Dual tone colors of warm and cool tone include purple and yellow. It was found that blue color influences the capability in recognizing the message and image. Moreover, it was found that image message and the position of presentation using cool tone color influences the recognition more than warm tone color in which correlated with Aiedkliang (2013) which found that choosing the background color banners and background color of the website affects seeing the banners. That is to say that the viewer could not see the banners because those colors resembled to each other. But the mentioned designing did not affect the information about the product. However, designing of the banner background color was not correlated with the background color of the website which can possibly cause the viewers annoyed and angry.

According to the study and reviewing the related research, we can see that color influences the perception and emotions of the viewer. Furthermore, the research in Thailand which studied about factors affecting the perception in communication of the brand on the advertising media in various formats and the influence of using warm and cool tone colors which can affect the viewer's emotions,

but there is no study concerning to using of color in accordance with different theories fitted with designing the image as a format of Page Post Image. Therefore, it causes the researcher to see how importance of choosing the suitable colors with food and beverage products through Facebook which is basically the main channel to communicate the individuality of brand.

Research Methodology

Population and participants

The researcher selected participants using the purposive sampling, the sample group must have seen the image of advertisement on Facebook and experienced in using Facebook at least 5 years. The 40 participants are between 15-40 years of age.

Experimental design

This research is Pre-experiment design in a format of One-Shot Case Study. The research methodology is as follows, 1) designing Facebook post Image of food and beverage products with different background colors, 2) studying the quality of Facebook post Image of the food and beverage products from the experts and 3) comparing the interest about background colors of the Facebook post Image of food and beverage products from the sample group by testing Facebook post Image within food and beverage products with 4 different background colors. In which the products, consist of Pizza, Burger, and bubble milk tea, were chosen by choosing the background colors in designing the advertisement for each type of products according to studying from the previous various product brands. However, each type of products remains common product image and composition, which is to cut off the interest of the different information.

The dependent variable is the interest of the sample group, the interested level consists of 5 levels; number 5 means strongly interested and 1 means strongly uninterested. However, the sample group will be tested by 3 products for each person, 4 colors for each product, 12 images in total.

Procedure

Before the test was started, the researcher explained the objectives of the research, procedure of testing, and how to score about interested level with sample group. The test was not restricted by time. The sample group tested by seeing Facebook post Image in each product through 24 inches computer display. Sorting was done using randomization method such as Pizza, Burger, and bubble milk tea, respectively. However, the test was initiated from seeing the same product with different background colors for 4 colors which was arranged in the order for 4 images. Then the sample group was allowed to score for each image according to 5 interested levels as beforementioned. Scoring the interested level for all 3 types of products. All testing, the sample group must score the interested level for all 12 images (4 colors x 3 products).

Results and Discussion

The results can be divided into 2 parts include 1) results of the quality evaluation of Facebook post Image of food and beverage products from experts, and 2) results of the comparison between the interest of the background colors of food and beverage products from the sample group.



Figure 1 Three types of food and beverage products with 4 colors used in testing.

1) Results of the quality evaluation of Facebook post Image of food and beverage products from 3 experts using the evaluation form of rating scale, following to Likert's Scale for 5 levels.

Table 1 Results of the quality evaluation of Facebook post Image from experts

Lists	\bar{x}	S.D.	Quality Level
Image	4.50	0.58	Good
Color used in designing	4.58	0.64	Excellent
Font	4.67	0.53	Excellent
Information position and composition	4.83	0.44	Excellent
Total	4.64	0.54	Excellent

From Table 1, Results of the quality evaluation of 12 Facebook post Images from experts and assessed by evaluating the quality using rating scale for 5 levels by checking and improving the media to be more productive. The average of the quality of Facebook post Image is 4.64 and in the score level of “excellent” which led into testing with the following sample group.

2) Results of the comparison between the interest of the background colors of food and beverage products from the sample group

The researcher analyzed the interest of the sample group upon 4 background colors, characterized following to types of products include Pizza, Burger, and bubble milk tea, respectively. The average of interest for each color can be shown as follows,

Table 2 Results of the comparison between the interest of the background colors of Pizza

Lists	\bar{x}	S.D.	Interested Level
Black Background	3.03	0.53	Intermediately interested
Green Background	3.54	0.59	Strongly interested
Brown Background	3.68	0.67	Strongly interested
Red Background	3.83	0.62	Strongly interested
Total	3.52	0.54	Strongly interested

Table 2 shows the comparison of the average interest of the background color of Pizza. It was found that the average of interest of Pizza product with red background color is 3.83. Second is brown background color, the average interest is 3.68, and the lowest average of interest of background is black, which its average of interest is 3.03.

Table 3 Results of the comparison between the interest of the background colors of Burger

Lists	\bar{x}	S.D.	Interested Level
Brown Background	3.12	0.74	Intermediately interested
Blue Background	3.30	0.69	Intermediately interested
Orange Background	3.51	0.51	Strongly interested
Red Background	3.63	0.63	Strongly interested
Total	3.39	0.64	Intermediately interested

Table 3 shows the comparison of the average interest of the background color of Burger. It was found that the average of interest of Burger product with red background color is 3.63. Second is orange background color, the average interest is 3.51, and the lowest average of interest of background is brown, which its average of interest is 3.12.

Table 4 Results of the comparison between the interest of the background colors of bubble milk tea

Lists	\bar{x}	S.D.	Interested Level
Brown Background	3.30	0.41	Intermediately interested
Green Background	3.33	0.57	Intermediately interested
Blue Background	3.52	0.67	Strongly interested
Pink Background	3.33	0.78	Intermediately interested
Total	3.37	0.60	Intermediately interested

Table 4 shows the comparison of the average interest of the background color of Bubble milk tea. It was found that the average of interest of Bubble milk tea product with blue background color is 3.53. Second is green and pink background colors, the average interest is 3.33, and the lowest average of interest of background is brown, which its average of interest is 3.30.



Figure 2 Results of the comparison between the interest of the sample group upon the background colors of food and beverage products; Pizza, Hamburger, and Bubble Milk Tea, respectively.

Conclusion

Studying the interest of the using different background colors of the sample group showed Pizza with green background color affected the interest at the most. Designing of Pizza with brown-red colors using red background is the principle of using Analogous color schemes or the matched opposite color in the color system. The Burger product with red background is the most interested, designing was done using brown color for Burger product and red color for background which Analogous color schemes or the matched opposite color in the color system was used. For the Bubble Mile Tea as a beverage product, blue as the background color is the most interested and designing of the brown Bubble Milk Tea using blue as a background color using the principle of complementary

color schemes or the matched opposite color in the color system which is correlated with Lichtlé (2007) and Seher (2012). Presentation the color image in the advertisement led into the positive attitude to the consumer and behavior of buying. Moreover, Pintassilgo et al (2019) concluded that color influenced strongly to the advertising image. Using of Complementary and Analogous color schemes affected the memory and attitude of the advertisement. The fact is complementary color schemes helps promoting the advertising image to become more unique (Chevreul, 1855). Moreover, the image of Bubble Milk Tea with blue background might originate from using blue background which the color was chosen from Analogous color schemes, and it becomes popular and motivating the positive attitude upon the advertising more than other color (Pintassilgo et al., 2019, and Wolfrom, 1992). Nevertheless, Seher (2012) found that color related to the perception and behavior of each person, in which each person responded to the color differently, Mostly, the consumer would be interested in primary colors more than bright, attractively used colors. However, the consumer has the culture of having the group of color and product category. From answering in the query from the consumer, it was found that food products with red, brown, and orange are favorite colors to be chosen, which matches the brands such as KFC and McDonalds, etc. The beverage products must choose blue color, etc.

From the results, we can see that designing the advertising image for food product, the designer should use primary colors and consider using Analogous color schemes and complementary color schemes theories. There should be aware of recognizing the famous marketing brand such as red background with Pizza, which is similar to Pizza Hut, and red background with Burger is similar to McDonalds and the beverage product should consider in using blue color in order for suitability with the culture and familiarity of the consumer.

References

- Aiedkliang, P. (2013). *Impact of consistency of website background color and banner background color, consistency of website content and banner content, banner format on banner visibility, product knowledge, and annoyance*, Chulalongkorn University. Bangkok, Thailand.
- Akkonkij, N. (2020). *Advertising for brand communications*, bangkok university Publishing.
- Chevreul, M.E., & Martel, C. (1855). *The Principles of Harmony and Contrast of Colors and Their Applications to the Arts*. London: Longman, Brown, Green, and Longmans.
- Churwongboon, T., Chuvutayakorn, P., & Insaeng, C. (2017) The Problems of Personal Income Tax Collecting: A Case of Facebook Online Market in Thailand in Year 2017. *Payap University Journal*, 15-30.
- D2 design. (2018). *banner design to be more beautiful than before with the technique of color selection*. Retrieved June 18, 2021, from <https://bit.ly/3sSHK0r>
- Digitiv. (2018). *The Complete Guide to Colors in Design: Color Meanings, Color Theory, and More* Retrieved June 18, 2021, from <https://shutr.bz/3EOaji6>
- Graves, M. (1951). *The art of color and design*. New York: McGraw –Hill.
- Lichtlé, M.C. (2007). The effect of an advertisement's colour on emotions evoked by an ad and attitude towards the ad. *International Journal of Advertising*, 26(1), 37-62.
- Muangthanang, C. & Wongsiri, W. (2021). The Influence of Warm and Cold Colours on Poster Design for Academic Articles. *Udon Thani Rajabhat University Academic Journal*, 8(1), 36-55.
- Nextrix. (2020). *Facebook Content Marketing Services: Marketing services, content creation on Facebook, taking care of Facebook Page*. Retrieved June 11, 2021, from <https://bit.ly/3mSBUIN>
- Pintassilgo, A. F. D. A. (2019). Complementary and analogous colors in mobile advertising: the impact of color on advertisement memory and attitude toward the ad (Doctoral dissertation).

- Promjeen, W., Chaetnalao, A. (2019). The use of light and color psychology. To design, develop Scene. Humanities, *Social Sciences and arts*, 12(6), 2152-2541.
- Radsadondee, J. (2020). *Factor Analysis of Fashion International Luxury Brand Perception: A Case Study Balenciaca Brand with GenerationY Consumer*, Graduate School, Silpakorn University.
- Seher, T., Arshad, M., Ellahi, S., & Shahid, M. (2012). Impact of colors on advertisement and packaging on buying behavior. *Management Science Letters*, 2(6), 2085-2096.
- Bonello, S. (2013). *The impact of colour in your logo design*. Retrieved June 11, 2021, from <https://bit.ly/3sMuwm6>
- Tkann, T. (2020). *Techniques for designing attractive website banners*. Retrieved October 26, 2021, from <https://bit.ly/3EPg6DS>
- Tonpo, K. (2019). The communication styles and motivation using in Thai popular facebook Fanpages, *Silpakorn University Journal*, 40(3), 25-27.
- Wolfrom, J. (1992). *The Magical Effects of Color*. Lafayette, California: C&T Publishing.

Features of Visually Impaired Persons’ Evacuation Behaviors Indoors During Earthquakes

Mariko Wayaku^{1*}, Eisuke Ikuta¹, Daiki Imai², Yukari Murakawa³ and
Hitoshi Watanabe²

¹Department of Housing and Environmental Design, Faculty of Human Life Science, Osaka City University, 3-3-138 Sugimoto, Sumiyoshi Ward, Osaka, 558-8585, Japan

²Research Center for Urban Health and Sports, Osaka City University, 3-3-138 Sugimoto, Sumiyoshi Ward, Osaka, 558-8585, Japan

³School of Nursing, Osaka City University, 1-5-17 Asahi-machi, Abeno Ward, Osaka, 545-0051, Japan

* Corresponding e-mail: ecoute-r51213@outlook.jp

Abstract

Following the Great East Japan Earthquake, support for persons with disabilities is regarded as a key consideration in disaster prevention. Some research has assessed the evacuation ability of persons with disabilities in regard to the use of institutions and architecture and equipment measures. However, no data have been reported regarding their behavior inside residential buildings during an earthquake. This study aims to reveal the features of visually impaired persons’ evacuation behaviors through a walking experiment. We carried out the test over 3 days in August 2021. The participants were 24 members of the teaching staff at a school for the blind in Osaka, 13 of whom were visually impaired and 11 sighted. The experiment was based on a simulated earthquake including a recreation of indoor damage. The participants walked two courses that were both 1-m wide and 5-m long, one of which contained five different obstacles every 1 m. We recorded their behavior, amount of exertion, and walking time using videos, a heart rate monitor, a wearable camera, and a stopwatch. The experimental results revealed that people with low vision can often recognize large obstacles, but have difficulty recognizing obstacles that are only partially in their field of vision, such as those under their feet or over their head. In addition, the evacuation speed of visually impaired individuals was easily affected by their agility and uniformly slow regardless of leg strength. These findings indicate that regular supplementary movements, involving searching, influence evacuation behavior.

Keywords: Visually impaired person, Earthquake, Evacuation behavior

Introduction

Since the Great East Japan Earthquake in 2011, support for older adults and individuals with disabilities are regarded as a key consideration in disaster prevention. The Japanese government has been taking measures to support such individuals through amendments to the Basic Act on Disaster Management. However, much work is still needed to assist their evacuation ability based on various disability characteristics. In addition, people with disabilities and their supporters cannot predict realistic evacuations, so specific issues in regard to obstacles to self-evacuation need to be addressed. Some research has assessed the evacuation ability of persons with disabilities in terms of the use of institutions and architecture and equipment measures. In the case of the visually impaired, blind persons confirm their location information through the sensations of hearing and wind pressure and by memorizing the number of route junctions and location of turning points while walking along walls in familiar places. In addition, because people with low vision rely on their eyesight to walk and make decisions, it is necessary to maintain the border between the floor and walls and to ensure that braille blocks are highly accessible during a disaster, even when there is no illumination

(KAMIYA et al. 2015). In addition, it has become clear that people with low vision have a dark impression of blue-based interiors and find it difficult to identify stair nosing. Also, the time required for evacuation is longer for blind people than for people with other disabilities because they must always check whether the path is correct before following it, and they find it difficult to evacuate independently, even if the plan is simple (KAMIYA et al. 2016). Differences in the speed of horizontal walking and stair descending have been reported between sighted people and those with visual impairments. Visually impaired people can maintain a higher walking speed than sighted people when descending stairs, even though the person density increases. In addition, the relation between horizontal walking speed and increasing person density depends on the visual impairment (Sørensen and Dederichs 2013). However, no data have been reported in regard to the behavior of such individuals inside residential buildings during an earthquake. Therefore, the present study aimed to reveal the features of visually impaired persons' evacuation behaviors through a walking experiment.

Experiment

Overview

We conducted experiments over 3 days with 24 teachers and staff members of the School for the Visually Impaired in Osaka, 13 of whom were visually impaired and 11 of whom were sighted, their ages were 47.4 ± 7.4 years and 40.0 ± 11.9 years (means \pm standard deviation). Of those who were visually impaired, six were blind and seven had low vision (narrowing of the visual field, central dark spot, or low vision). We designed two courses: one with obstacles (Figure 1) and the other without. Emergency vehicle sirens were played through speakers during the experiment to reproduce the tension of a disaster. Three video cameras (HDR-CX470, SONY, Japan) were set up on each course to record the participants' walking behaviors. All participants were equipped with a heart rate monitor (A370, POLAR, Finland) on their wrist and a wearable camera (HERO8 and HERO9 Black, GoPro, the U.S.) on their chest to analyze their locomotion and foot movement. The course walking time and time per meter was measured using a stopwatch. In addition, physical fitness measurements were taken, and a questionnaire survey was conducted. The physical fitness measurements included height, weight, body mass index, grip strength, leg extension muscle strength, flexibility (long body bending), the Timed Up and Go test (TUGT), and the two-step test.

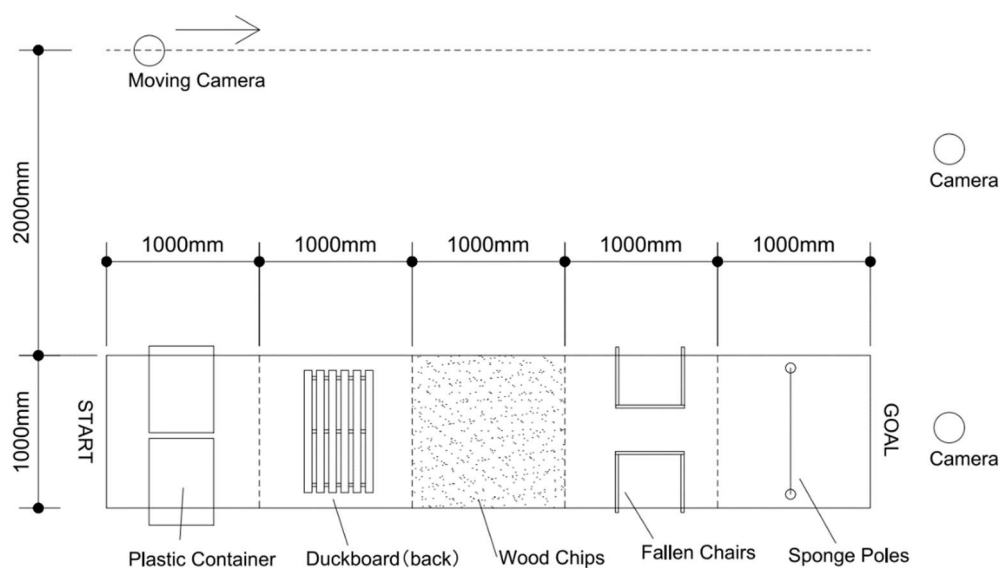


Figure 1 Course plan for the obstacle course

Experimental conditions

The walking course was 1-m wide and 5-m long, and the arrangement of obstacles was the same for all participants (Figure 2). We designated the course without obstacles as Task 1, and with obstacles as Task 2. We used a total of five types of obstacles: two plastic containers to simulate fallen furniture, a piece of slatted wood to simulate an obstacle underfoot, wood chips to simulate a piece of glass, two fallen chairs, and three sponge poles connected in the shape of a *torii* (a traditional Japanese gate) to simulate a tall obstacle (Figure 3). After resting in a seated position to stabilize the heartbeat for three minutes, the participants walked the course. Between Task 1 and Task 2, they started walking one minute after their heartbeat stabilized. The normal course was followed for Task 1, and the disaster course for Task 2. In addition, about participants on the first day, the sighted and low-vision participants walked Task 2 again while wearing an eye mask. About participants on the second and third days, the sighted and low-vision participants completed both tasks while first wearing an eye mask and then walked both courses again without an eye mask.



Figure 2 Setup of the experiment

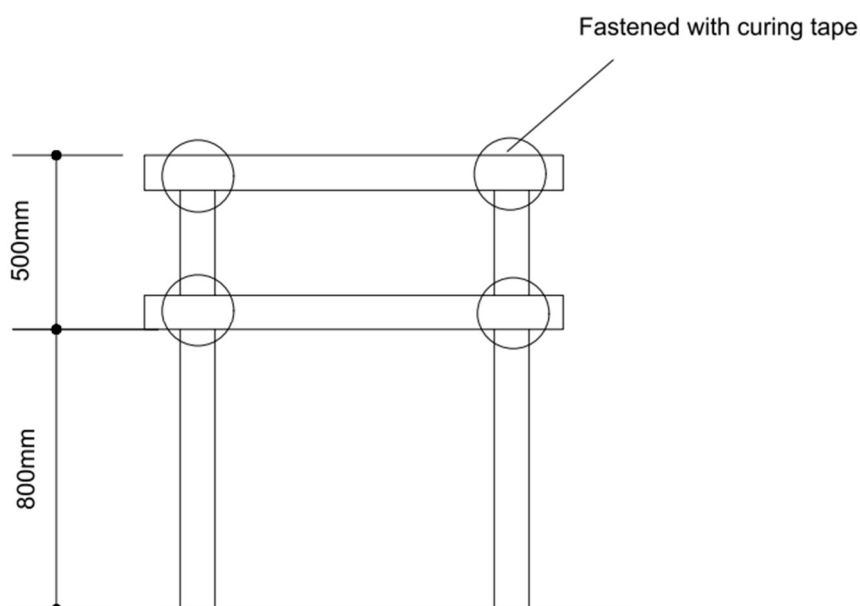
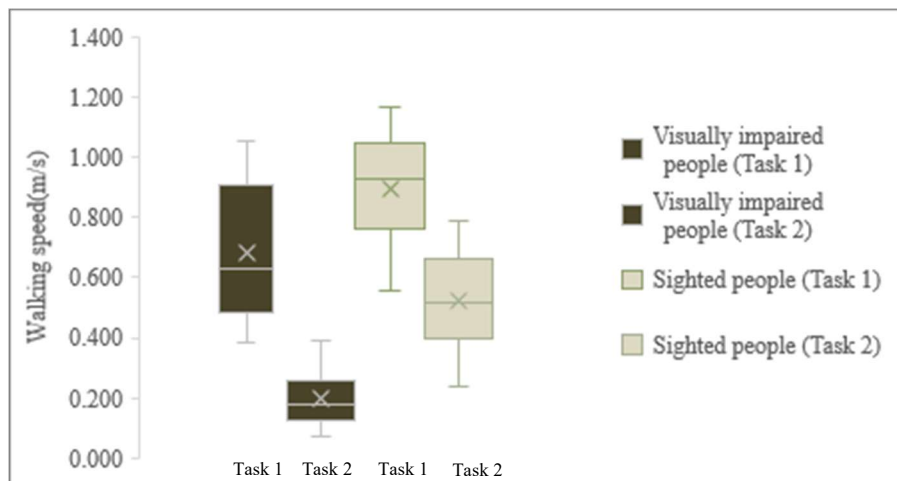


Figure 3 Schematic of the sponge poles

Results and Discussion

1. Visually impaired people and sighted people without eye mask

Figure 4 shows the results for walking speed under each condition. The average walking speeds in Task 1 were 0.685 ± 0.225 m/s for the visually impaired and 0.892 ± 0.257 m/s for the sighted, while those in Task 2 were 0.197 ± 0.088 and 0.522 ± 0.205 m/s, respectively. The speed of the visually impaired individuals tended to be slower than that of the sighted in both tasks. In addition, a comparison of walking speeds per course revealed that the average speed of sighted people during Task 2 decreased to 58.5% of that in Task 1, while that of visually impaired people decreased to 28.7%, indicating a larger decrease.



(The error bars: From the lowest, the sample minimum, the first quartile, the median, the upper third quartile, the sample maximum. ×: the average)

Figure 4 Walking speed (n=24)

Figure 5 shows the distribution of walking speeds under Task 1. The walking speed of the visually impaired was widely distributed, between 0.3 m/s and 1.1 m/s, as was that of the sighted, between 0.5 m/s and 1.2 m/s. Individual differences in normal walking speed were identified. However, as can be seen in Figure 6, which shows the distribution of walking speeds during Task 2, the visually impaired were concentrated in the range of 0.1 m/s to 0.4 m/s, while the sighted were widely distributed in the range of 0.2 m/s to 0.8 m/s, indicating a large difference in walking speed between the visually impaired and sighted in the disaster course.

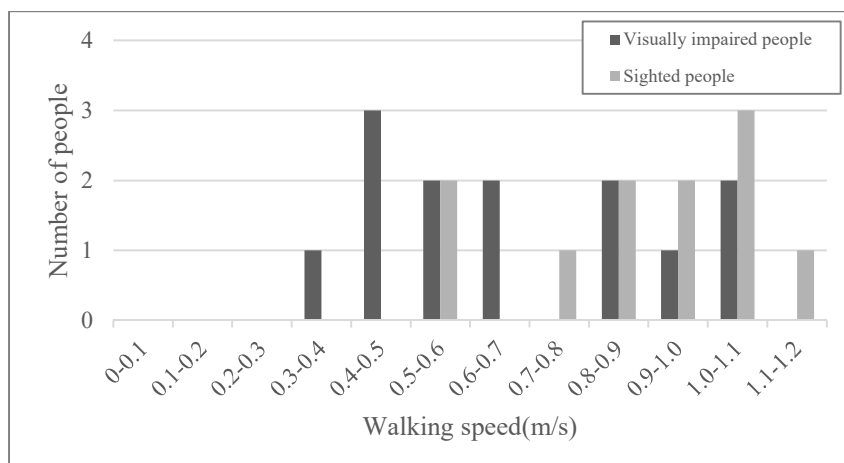


Figure 5 Distribution of walking speeds in Task 1 (n=24)



Figure 6 Distribution of walking speeds in Task 2 (n=24)

Figure 7 shows the results of one-way analysis of variance (ANOVA) and multiple comparisons in walking speed in Task 2 by disability level (blind, low vision, and sighted). Significant differences were found between groups the sighted and blind ($p < 0.05$) and the sighted and low-vision participants ($p < 0.05$).

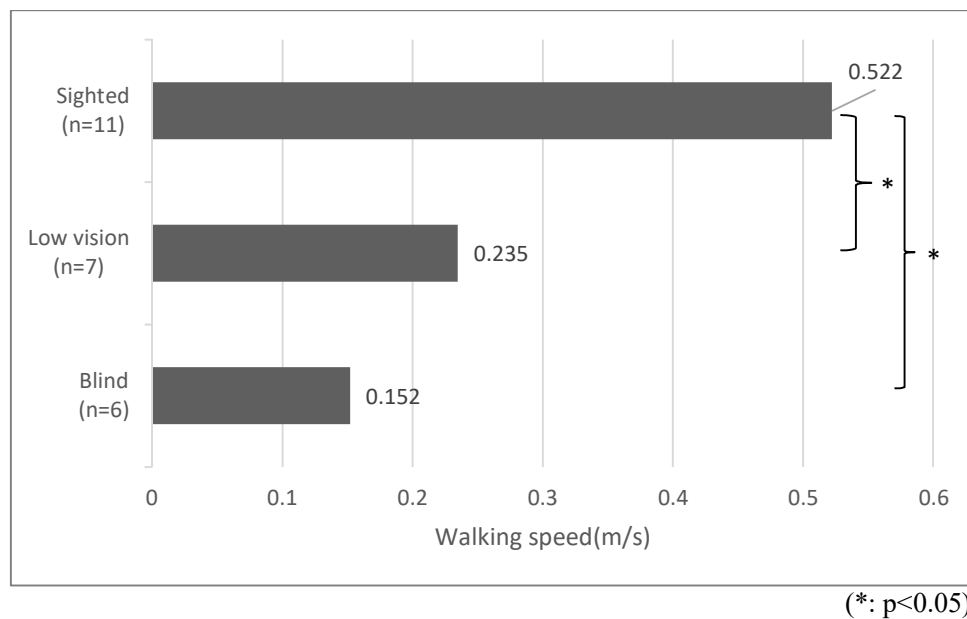


Figure 7 Walking speeds in Task 2 by disability level (blind, low vision, and sighted)

Table 1 and Figure 8 show the results of one-way ANOVA and multiple comparisons in walking speed per obstacle in Task 2 by disability level (blind, low vision, and sighted). The mean walking speed in the plastic container was 0.112 ± 0.031 m/s for the blind, 0.234 ± 0.125 m/s for the low-vision participants, and 0.425 ± 0.195 m/s for the sighted, indicating a significant difference between the blind and sighted. The average walking speed with the duckboard was 0.225 ± 0.092 m/s for the blind, 0.342 ± 0.196 m/s for the low-vision participants, and 0.794 ± 0.282 m/s for the sighted, indicating significant differences between the sighted and blind and the sighted and low-vision

participants. The average walking speed on the wood chips was 0.194 ± 0.055 m/s for the blind, 0.271 ± 0.117 m/s for the low-vision participants, and 0.685 ± 0.344 m/s for the sighted, indicating significant differences between the sighted and blind and the sighted and low-vision participants. The average walking speed with the fallen chairs was 0.146 ± 0.072 m/s for the blind, 0.234 ± 0.093 m/s for the low-vision participants, and 0.595 ± 0.181 m/s for the sighted, indicating significant differences between the sighted, blind, and low-vision participants. The average walking speed for the sponge poles was 0.162 ± 0.067 m/s for the blind, 0.192 ± 0.076 m/s for the low-vision participants, and 0.459 ± 0.173 m/s for the sighted, indicating significant differences between the sighted and blind and the sighted and low-vision participants. No significant difference in walking speed was found for the plastic containers for people with low vision compared with the sighted, so we considered that people with low vision can often recognize large obstacles, but have difficulty recognizing obstacles only partially in their field of vision, such as under their feet or above their head.

Table 1 Results of one-way analysis of variance and multiple comparisons in walking speed per obstacle by disability level

Obstacle	(I) group	(J) group	Mean difference	SE	p value	95% CI	
						Lower	Upper
Plastic container	Sighted	Total blindness	0.313**	0.081	0.003	0.103	0.523
		Low vision	0.192	0.077	0.063	-0.008	0.391
Duckboard	Sighted	Total blindness	0.569**	0.121	0	0.254	0.884
		Low vision	0.451**	0.115	0.002	0.151	0.751
Wood Chips	Sighted	Total blindness	0.491**	0.132	0.004	0.148	0.834
		Low vision	0.415*	0.126	0.01	0.088	0.741
Chair	Sighted	Total blindness	0.449**	0.075	0	0.255	0.643
		Low vision	0.361**	0.071	0	0.176	0.546
Sponge poles	Sighted	Total blindness	0.297**	0.070	0.001	0.116	0.478
		Low vision	0.267**	0.066	0.002	0.094	0.439

(SE: standard error CI: confidence intervals *: $p < 0.05$ **: $p < 0.01$)

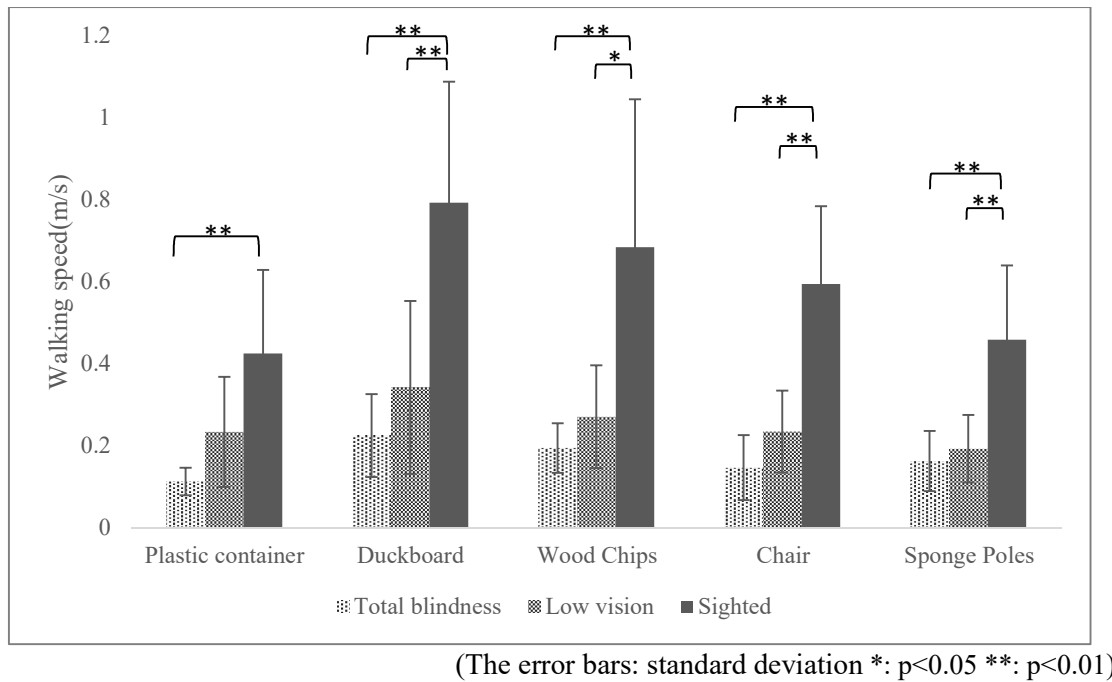


Figure 8 Walking speed per obstacle by disability level

Figure 9 shows the results of the correlation between the TUG time and walking speed in Task 2. Negative correlations were found for the visually impaired, indicating that the evacuation speed of the visually impaired is affected by their agility. In addition, we determined that individual agility among the visually impaired may also affect their search behavior during a disaster because they engage in search behavior regularly when walking in unfamiliar places. Positive correlations were found for the sighted. However, since the TUG test times are concentrated around 6 seconds, there is no significant correlation.

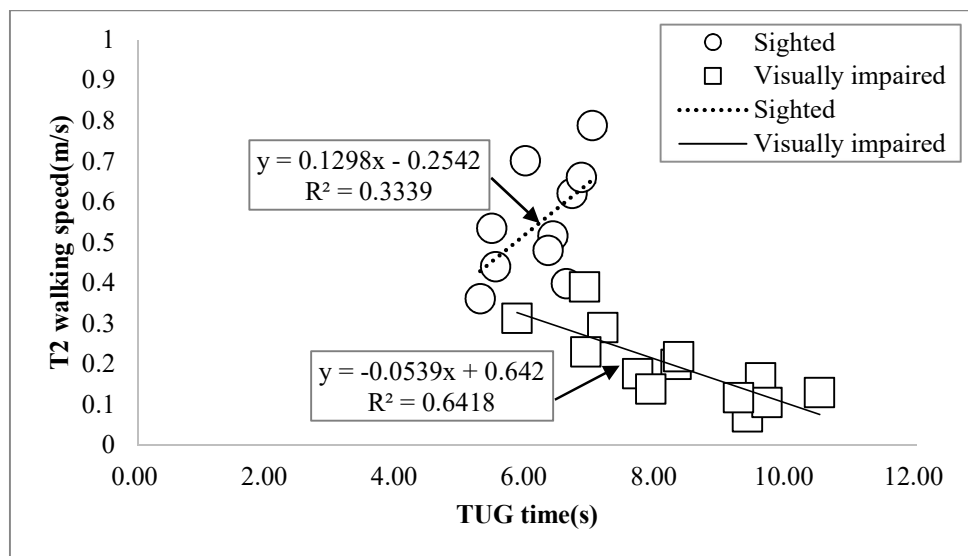


Figure 9 Correlation between the Timed Up and Go (TUG) time and walking speed in Task 2 (T2) (n=23)

※Sighted: Data for speeds of 0.300 m/s or more in Task 2 were used.

Figure 10 shows the results of the correlation between leg strength and walking speed in Task 2. A positive correlation was found in the sighted, but no correlation was found in the visually impaired. The leg strength of the sighted affected their walking speed, but the walking speed of the visually impaired during the evacuation was uniformly slow, regardless of leg strength. These findings indicate that visually impaired people reduce their evacuation speed regardless of their muscle strength because they are involved in exploratory behavior.

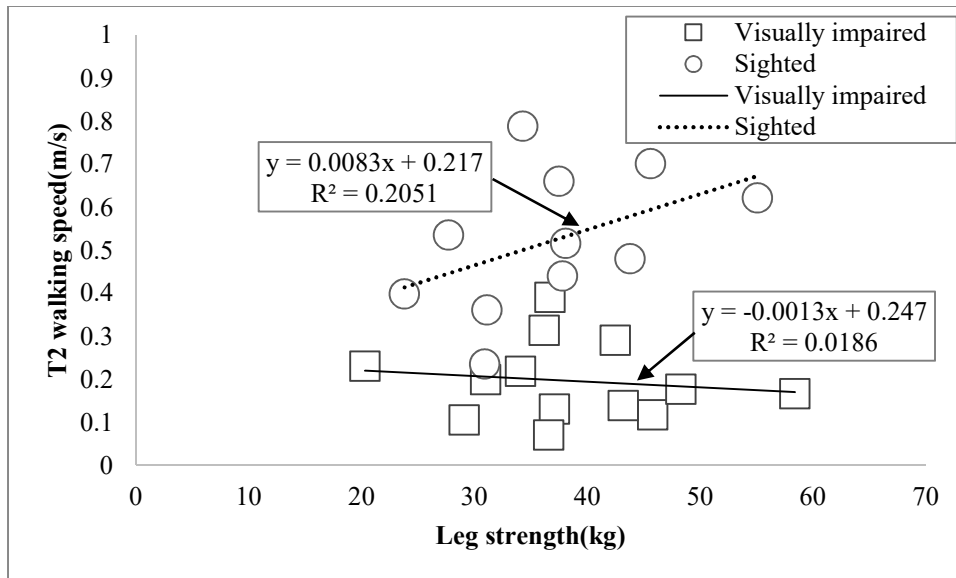


Figure 10 Correlation between leg strength and Task 2 walking speed (n=24)

2. Visually impaired people and sighted people with eye mask

Figure 11 shows the percentage increase or decrease in walking speed per obstacle based on the Task 2 average speed for visually impaired persons, sighted persons, and sighted persons with eye mask. Each group has the fastest walking speed on the duckboard. The speed was slowest on the plastic container for both the sighted without eye mask and the visually impaired, while the speed of the sighted with eye mask decreased significantly on the collapsed chair.

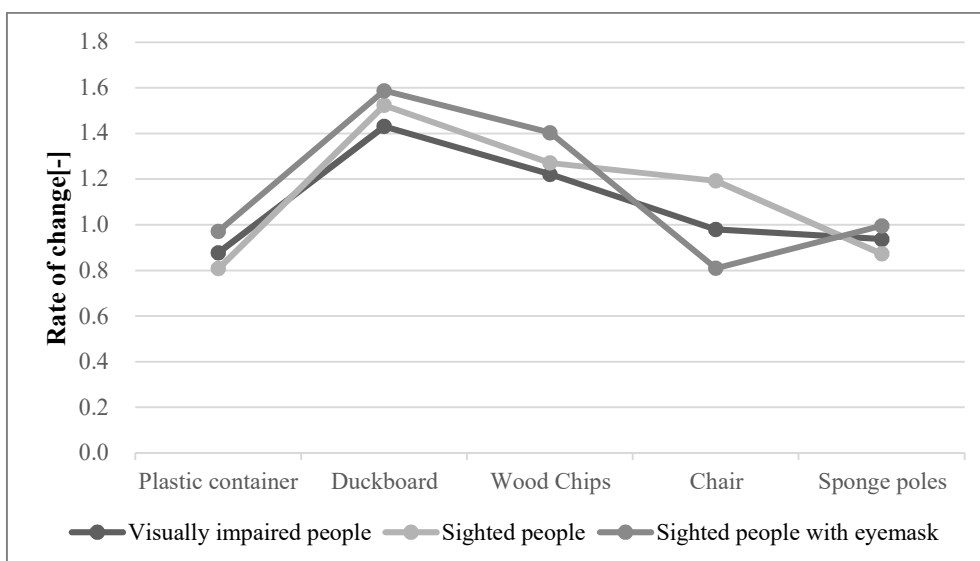


Figure 11 Percentage increase or decrease in walking speed per obstacle based on Task 2 average speed

Conclusion

In this study, we conducted a walking experiment to clarify the characteristics of evacuation behavior among visually impaired people. The results for walking speed per obstacle revealed no significant differences with plastic containers between low-vision individuals and the sighted, which suggests that people with low vision can often recognize large obstacles, but have difficulty recognizing obstacles that are only partially in their field of vision, such as those under their feet or above their head. Also, the speed was slowest on the plastic container for both the sighted without eye mask and the visually impaired, while the speed of the sighted with eye mask decreased significantly on the collapsed chair. It revealed that people rely particularly on their vision when avoiding obstacles, such as passing through narrow space between obstacles. The positive correlation found between TUG time and walking speed in Task 2 among the visually impaired suggests that their evacuation speed is easily affected by their regular agility. As for the relationship between leg extension muscle strength and walking speed in Task 2, leg strength affected the walking speed of the sighted, but the evacuation speed of the visually impaired was uniformly slow, regardless of leg strength. These findings suggest that regular supplementary movements involving searching influence evacuation behavior. In the future, we plan to analyze further the relationship between evacuation and more specific behaviors and disaster prevention awareness.

Acknowledgments

This research was funded by the Unvers Foundation. We would like to express our gratitude to all parties involved.

References

- KAMIYA, M., TSUCHIYA, S., FURUKAWA, Y. & HASEMI Y. (2015, September). [Evacuation Safety Planning Based on Behavior Abilities of Disabled: Part.1, Study of Evacuation Ability for the Physically Disabled] Shogaisya no hinan noryoku wo kouryo sita hinankeikaku ni kansuru kenkyuu sono 1 sintaisyougaisya no hinannouryoku ni kansuru zissokutyousa (in Japanese). *Architectural Institute of Japan*, 1111-1114.
- KAMIYA, M., TSUCHIYA, S., FURUKAWA, Y. & HASEMI, Y. (2016, August). [Evacuation Safety Planning with Consideration of the Evacuation Abilities of Disabled; Part 4, Field Measurement of Evacuation Behavior of Physically Disabled Pedestrians in High-Rise Building] Shogaisya no hinannouryoku wo kouryosita hinankeikaku ni kansuru kenkyuu sono 4 kousoukoukyousisetukyoyoubu ni okeru sintaisyougaisya no tandoku hinankoudou no zissoku tyousa (in Japanese). *Architectural Institute of Japan*, 247-248.
- Sørensen, J.G. & Dederichs, A.S. (2013, October). Evacuation characteristics of visually impaired people – a qualitative and quantitative study. *Fire and Materials*, 39(4), 385-395.

Color Naming of Red-Green Color Deficiencies

Miyoshi Ayama^{1*}, Minoru Ohkoba¹ and Tomoharu Ishikawa¹

¹*Utsunomiya University, 7-1-2, Yoto, Utsunomiya, 321-8585, Japan*

* *Corresponding email: miyoshi.ayama@gmail.com, miyoshi@is.utsunomiya-u.ac.jp*

Abstract

To investigate color naming property of color deficient observers (CDOs) and color normal observers (CNOs), color naming was conducted for CDOs of protan and deutan, and CNOs in experiment 1. Free color naming allowing any kind of color names and adjectives, and the color naming using 11 basic color terms (BCTs) were employed. To derive an individual internal color representation in color naming, difference scaling of color names including BCTs was carried out in experiment 2. Internal color representation here means a color space in observer's brain. Ten Munsell color chips of basic hues with high and medium chroma were employed as test stimuli. In the BCT color naming, results of CNOs were very stable showing perfect consistency and consensus in several chips in both the high and medium chroma chips. Results of CDOs for high chroma were relatively stable that both types of CDOs showed perfect consistency and consensus for Y, G, and PB, as well as YR and B in the case of protans. In contrast to that, CDOs showed large variation in medium chroma chips indicating strong chromaticness is needed for them in performing color naming similar to CNOs. By applying the data of experiment 2, internal color representation of color naming was derived, and compared with those of vision-based and recognition-based color spaces obtained in our previous study. Comparison revealed that CNOs have basically one kind of color space similar to Munsell hue circle in all situations, whereas CDOs' color space varies. Their vision-based one is C-shape, while their recognition-based one is closer to circle similar to CNOs', and their color space in color naming is in between for most observers. This suggests that CDOs integrate their vision-based and recognition-based color spaces in their brain to assign an appropriate color name to a given color stimulus.

Keywords: Congenital color deficiency, Munsell color chips, Color naming, Basic color terms, Internal color representation

Introduction

In everyday life, we see various color signals and signs in which color itself mediates information, such as red means 'stop', or yellow means 'warning', etc. Color is also used to symbolize the work of group, such as the flag color of the United Nations, UN blue represents 'peace opposite to red, for war'. Strictly speaking, these usages of color, however, hold under the assumption that all people have same color vision, and recognize the same color in their brain when they see the same object. Unfortunately, it is not true. There exists large variation in color vision originated at the front end of color vision mechanism.

The largest majority of people have 3 types of photoreceptors called S, M and L cones, each respectively sensitive to short, middle and long-wavelength regions of the visible spectrum with peak wavelengths of about 442nm, 543nm, and 570nm, respectively. We call these people CNOs (color normal observers). Second majority of people, about 4 to 8% in male and 0.2 to 0.4% in female are congenital red-green color deficiency. Percentage differs among race (Birch, 2012). They are divided into subgroups of severe and milder color vision defects called dichromat and anomalous trichromat, respectively. The former people are further divided into 2 groups with the first group that lacks L cone function (protanopia), and the second group that lacks M cone function (deutanopia). The latter people are also divided into 2 groups with the first group having normal M and anomalous M-

like cones (protanomalous), and the second group having normal L and L-like cones (deuteranomalous) (Deeb, 2006, Neitz et al.). In this study, we call them CDOs, color deficient observers. Types of CDOs and the terminology used in this study are indicated in Table 1. Other types of color vision deficiency, such as the lack of S-cone, or all types of cones, are not concerned in this study.

The reason why they are called ‘red-green color deficiency’ is because they show low discriminability in the middle to long-wavelength spectral region, i.e., green, yellow, orange, and red colors (Pitt, 1944, Wright, 1957). On the other hand, it has been known that CDOs show color naming ability comparable to those of CNOs especially for surface colors (Jameson & Hurvich, 1978, Paramai, 1996, Bonnardel, 2006, Lillo et al., 2014). In our previous studies, we have shown interesting results on this discrepancy between color discrimination and color name recognition (Ohkoba et al., 2021, Ayama et al., 2021). We conducted difference scaling experiment using color pairs and color names. In the former, observers judged perceptual difference between two colors, while in the latter, observers judged cognitive difference between two color names. Results showed that CNOs have one type of internal color representation similar to Munsell hue circle either based on visual perception or color name recognition, whereas CDOs have very different C-shape internal color representation based on visual perception, but their color representation based on color name recognition is closer to circular shape similar to those of CNOs’. Internal color representation here means a color space in observer’s brain. Then, what kind of color space do CDOs utilize when they do color naming?

Our aim is to investigate color naming property of CDOs and CNOs, and to compare the internal color space in color naming with those of vision-based and recognition-based ones obtained in our previous studies.

Table 1 Terms of color vision types used in this study

CNO/CDO	Color vision type		Functional cones		
CNO	Normal		L	M	S
CDO	Protan	Protanomalous	-	M, M-like	S
		Protanopia	-	M	S
	Deutan	Deuteranomalous	L, L-like	-	S
		Deuteranopia	L	-	S

Experiment 1: Color naming

Ten Munsell color chips of basic hues with high and medium chroma were employed as test stimuli. Table 2 indicates the labels and Munsell notations of the color chips. We used the color card consists of pair of color chips used in our previous studies, and a half portion was covered by a small gray envelope in this study. It was placed at the center of the desk which was covered by a gray cloth of about N6.5. Color chip and the surface of the table was illuminated by a fluorescent lamp of which CCT was 5000K. Horizontal illuminance at the color chip was about 560 lx. Figure 1 indicates R and PB chips of high and medium chroma.

Observer was asked to answer its color name by two color naming methods. One was a free color naming allowing any kind of color names and adjectives, and the other was a constrained color naming allowing to use only 11 basic color terms (BCTs) of “red”, “yellow”, “green”, “blue”, “orange”, “pink”, “purple”, “brown”, “white”, “gray”, and “black”. We call the latter BCT color

naming hereafter. In one session, either free or BCT color naming was conducted. Color chips were presented in a random order, each twice in a session.

Five CNOs, five protans (two protanomalous and three protanopia), and five deuteranopes participated the experiment. All of them participated our previous experiments.

Table 2 Munsell notation of the test color chips

Label	High-chroma	Medium-chroma
R	5R4/14	5R4/4
YR	5YR6.5/14	5YR6.5/4
Y	5Y8/14	5Y8/4
GY	5GY6.5/10	5GY6.5/4
G	5G4.5/10	5G4.5/4
BG	5BG4/9	5BG4/3
B	5B4/8	5B4/3
PB	5PB4/12	5PB4/4
P	5P4/11	5P4/3
PR	5PR4/12	5PR4/4

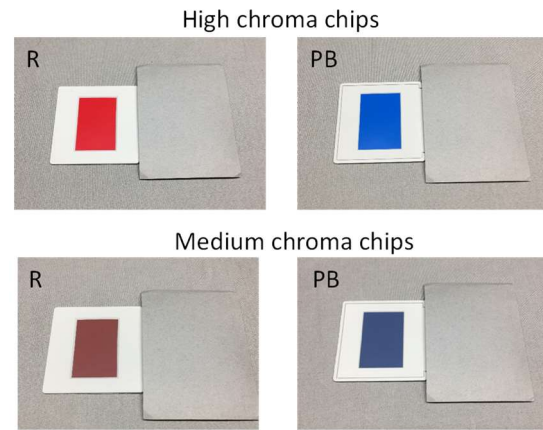


Figure 1 Examples of high and medium chroma chips

Experiment 2: Difference scaling of color names

To analyze the BCT color naming results, cognitive difference between two color names was evaluated. To compare the results with those in our previous study, “yellow-green”, “blue-green”, “blue-purple”, and “red-purple” were added to eleven BCTs. Thus 105 color name pairs, i.e., all combinations from 15 color names, were evaluated. Color name pairs were written in a random order on the answer sheet, and observer was asked to rate the cognitive distance between the two color names using a scale of 1 (very close), 2 (rather close), 3 (neither close nor far), 4 (rather far), and 5 (very far). After the observer completed the ratings of 105 color name pairs, he took about five minutes break, and then started the rating again for the same 105 color name pairs but written in the opposite order. Average of two scores were employed as the cognitive distance value of the color name pair.

Two CNOs, four protans (one protanomalous and three protanopia), and three deuteranopes participated the experiment. All of them participated the experiment 1.

Classification of color vision type

All observers were examined for their color vision using Ishihara charts, Panel D-15, and an anomaloscope. They were all male Japanese, and either university students or experimental collaborators who were introduced from the Color Universal Design Organization (CUDO). Ages of observers ranged 22 to 46. We classified color vision type based on the results of the anomaloscope. No genetic examination was done.

Results of experiment 1

Figure 2 show the results of BCT color naming of all observers. In the results of BCT color naming, consistency and consensus are often used to indicate the degree of stability of color name and corresponding color chip (Boynton & Olson, 1990). Consistency is the property that the same color name is used for the same color chip in different presentations by the same observer, and consensus is the property that the same color name is used for the same color chip by different

observers. In this study, we define the consistency rate as the number of observers who assigned the same color name to the test color chip twice and divided by 5, the total number of observers. The consensus rate is defined as the number of observers who qualified the consistency and assigned the same color name to the test color chip divided by 5. No two observers responded the same color name with qualification of consistency, the consensus rate is 0. Therefore, minimum number of the consensus rate is 0.4, i.e., 2 divided by 5.

(a) High chroma, Normals

Obs.	N18		N20		N32		N33		N34	
	1st	2nd	1st	2nd	1st	2nd	1st	2nd	1st	2nd
R	Red	Red	Red	Red	Red	Red	Red	Red	Red	Red
YR	Orange	Orange	Orange	Orange	Orange	Orange	Orange	Orange	Orange	Orange
Y	Yellow	Yellow	Yellow	Yellow	Yellow	Yellow	Yellow	Yellow	Yellow	Yellow
GY	Green	Green	Green	Green	Green	Green	Green	Green	Green	Green
G	Green	Green	Green	Green	Green	Green	Green	Green	Green	Green
BG	Green	Green	Green	Green	Green	Green	Blue	Green	Green	Green
B	Blue	Blue	Blue	Blue	Blue	Blue	Blue	Blue	Blue	Blue
PB	Blue	Blue	Blue	Blue	Blue	Blue	Blue	Blue	Blue	Blue
P	Purple	Purple	Purple	Purple	Purple	Purple	Purple	Purple	Purple	Purple
RP	Purple	Purple	Purple	Pink	Pink	Pink	Purple	Purple	Pink	Pink

(b) Medium chroma, Normals

Obs.	N18		N20		N32		N33		N34	
	1st	2nd	1st	2nd	1st	2nd	1st	2nd	1st	2nd
R	Brown	Brown	Brown	Brown	Brown	Brown	Purple	Purple	Red	Brown
YR	Orange	Orange	Orange	Orange	Orange	Orange	Pink	Pink	Orange	Orange
Y	Yellow	Yellow	Yellow	White	Yellow	Yellow	White	White	Yellow	Yellow
GY	Green	Green	Green	Green	Green	Green	Green	Green	Green	Green
G	Green	Green	Green	Green	Green	Green	Green	Green	Green	Green
BG	Green	Green	Green	Green	Green	Green	Blue	Green	Green	Green
B	Blue	Blue	Blue	Blue	Blue	Blue	Blue	Blue	Blue	Blue
PB	Blue	Blue	Blue	Blue	Blue	Blue	Blue	Blue	Blue	Blue
P	Purple	Purple	Purple	Purple	Purple	Purple	Purple	Purple	Purple	Purple
RP	Purple	Purple	Purple	Purple	Purple	Purple	Purple	Purple	Purple	Purple

(c) High chroma, Protans

Obs.	P3		P4		P11		P13		P14	
	1st	2nd	1st	2nd	1st	2nd	1st	2nd	1st	2nd
R	Brown	Brown	Brown	Brown	Red	Red	Red	Red	Red	Red
YR	Orange	Orange	Orange	Orange	Orange	Orange	Orange	Orange	Orange	Orange
Y	Yellow	Yellow	Yellow	Yellow	Yellow	Yellow	Yellow	Yellow	Yellow	Yellow
GY	Yellow	Yellow	Yellow	Yellow	Green	Yellow	Yellow	Green	Yellow	Yellow
G	Green	Green	Green	Green	Green	Green	Green	Green	Green	Green
BG	Gray	Gray	Green	Green	Gray	Green	Green	Green	Gray	Gray
B	Blue	Blue	Blue	Blue	Blue	Blue	Blue	Blue	Blue	Blue
PB	Blue	Blue	Blue	Blue	Blue	Blue	Blue	Blue	Blue	Blue
P	Blue	Blue	Blue	Blue	Blue	Blue	Pink	Purple	Blue	Blue
RP	Purple	Purple	Purple	Purple	Pink	Purple	Pink	Pink	Pink	Pink

(d) Medium chroma, Protans

Obs.	P3		P4		P11		P13		P14	
	1st	2nd	1st	2nd	1st	2nd	1st	2nd	1st	2nd
R	Brown	Gray	Green	Green	Pink	Red	Red	Red	Gray	Gray
YR	Yellow	Yellow	Orange	Orange	Orange	Orange	Green	Orange	Orange	Brown
Y	Yellow	Yellow	Yellow	Yellow	Orange	Orange	Yellow	Yellow	Yellow	Yellow
GY	Yellow	Green	Orange	Orange	Orange	Orange	Green	Orange	Yellow	Orange
G	Green	Green	Green	Green	Green	Green	Green	Brown	Green	Green
BG	Gray	Gray	Gray	Green	Gray	Green	Gray	Green	Gray	Gray
B	Gray	Blue	Green	Green	Green	Pink	Green	Gray	Gray	Gray
PB	Blue	Blue	Blue	Blue	Pink	Pink	Blue	Blue	Blue	Purple
P	Purple	Gray	Purple	Green	Blue	Blue	Pink	Pink	Pink	Pink
RP	Gray	Gray	Green	Green	Gray	Pink	Red	Pink	Gray	Gray

(e) High chroma, Deutans

Obs.	D7		D17		D18		D20		D21	
	1st	2nd	1st	2nd	1st	2nd	1st	2nd	1st	2nd
R	Orange	Red	Red	Red	Red	Red	Red	Red	Red	Red
YR	Yellow	Orange	Yellow	Yellow	Yellow	Yellow	Orange	Orange	Yellow	Yellow
Y	Yellow	Yellow	Yellow	Yellow	Yellow	Yellow	Yellow	Yellow	Yellow	Yellow
GY	Orange	Orange	Yellow	Green	Orange	Orange	Green	Green	Green	Green
G	Green	Green	Green	Green	Green	Green	Green	Green	Green	Green
BG	Green	Green	Green	Green	Purple	Green	Green	Green	Blue	Green
B	Blue	Blue	Blue	Blue	Purple	Blue	Blue	Blue	Blue	Blue
PB	Blue	Blue	Blue	Blue	Blue	Blue	Blue	Blue	Blue	Blue
P	Purple	Purple	Blue	Blue	Purple	Purple	Purple	Purple	Purple	Purple
RP	Purple	Pink	Pink	Pink	Pink	Pink	Pink	Pink	Pink	Pink

(d) Medium chroma, Deutans

Obs.	D7		D17		D18		D20		D21	
	1st	2nd	1st	2nd	1st	2nd	1st	2nd	1st	2nd
R	Green	Pink	Purple	Pink	Red	Pink	Red	Red	Red	Red
YR	White	White	Pink	Brown	Pink	Pink	Pink	Pink	Pink	Green
Y	White	White	White	Brown	Yellow	Yellow	Yellow	Yellow	Green	Green
GY	White	Brown	Brown	Brown	Pink	Orange	Green	Green	Green	Green
G	Green	Green	Green	Green	Pink	Green	Green	Green	Green	Green
BG	Green	Green	Green	Green	Red	Pink	Gray	Gray	Green	Green
B	Green	Green	Gray	Gray	Blue	Green	Green	Green	Green	Green
PB	Green	Green	Gray	Blue	Purple	Blue	Green	Green	Blue	Blue
P	Purple	Purple	Gray	Gray	Purple	Green	Purple	Green	Purple	Green
RP	Pink	Green	Purple	Pink	Red	Green	Purple	Purple	Red	Red

Figure 2 Results of BCT color naming

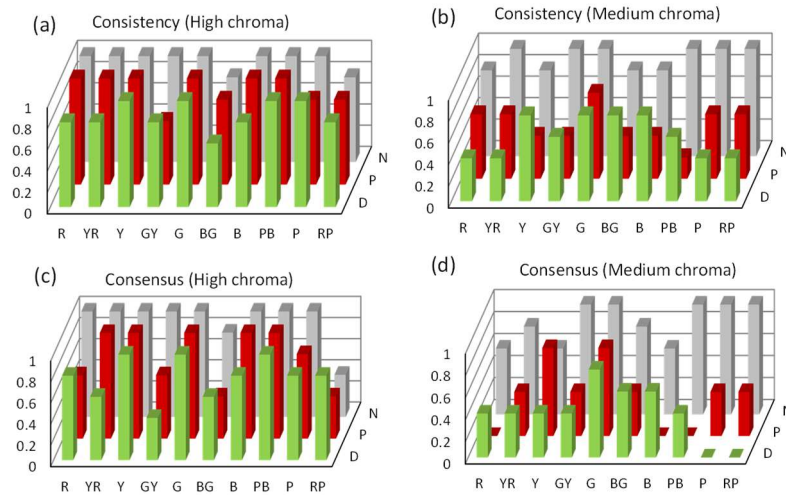


Figure 3 Consistency rate (upper) and consensus rate (lower) in the BCT color naming

Figure 3 shows the consistency rate and consensus rate for high chroma (left) and medium chroma (right) for CNOs, protans, and deutans. As shown in the figure, CNOs’ result is very stable that eight color chips in the high chroma show perfect consistency and consensus, and in the medium chroma, five chips as well. Results of CDOs for high chroma were relatively stable that both types of CDOs showed perfect consistency and consensus for Y, G, and PB, as well as YR and B in the case of protans. Color names assigned to Y, G, and PB were “green”, “yellow”, and “blue”. Also, 3 protans and 4 deutans consistently assigned “red” to R. Our results for high chroma chips showed CDOs’ color naming performance is comparable to that of CNOs as reported in previous studies cited in the Introduction. In contrast to that, CDOs’ consistency and consensus rates markedly deteriorate for medium chroma chips as shown in Fig.3 (b) and (d). Color name “green” is assigned to all color chips at least once, color names of “gray”, “white”, and “pink” appear here and there in both protan and deutan results, indicating instable performance of their color naming for medium chroma chips.

Results of experiment 2

In the experiment 2, cognitive difference between two color names was evaluated, and the difference score matrix was obtained for each of nine participants. Part of the results of observer D17 is shown in Figure 4. Scores are average values of 2 repetitions. Figure 5 (a) indicates observer D17’s color name representation derived using the difference score matrix through the MDS analysis. The iso MDS Kruskal’s non-metric multidimensional scaling method (Kruskal, 1964) was employed using the statistics software R 3.5.3. ‘S’ indicated in the lower-left is the stress value indicating the degree of discrepancy between the experimental and MDS results, and usually, less than 10 % is desirable.

D17	Red	Orange	Yellow	Yellow-green	Green	Blue-green	Blue
Red	0	1	2	2	1	4	3
Orange		0	1.5	1.5	1.5	4.5	5
Yellow			0	1	2.5	4	5
Yellow-green				0	1.5	4	4
Green					0	1	2.5
Blue-green						0	2
Blue							0

Figure 4 Part of the results of Experiment 2 for observer D17

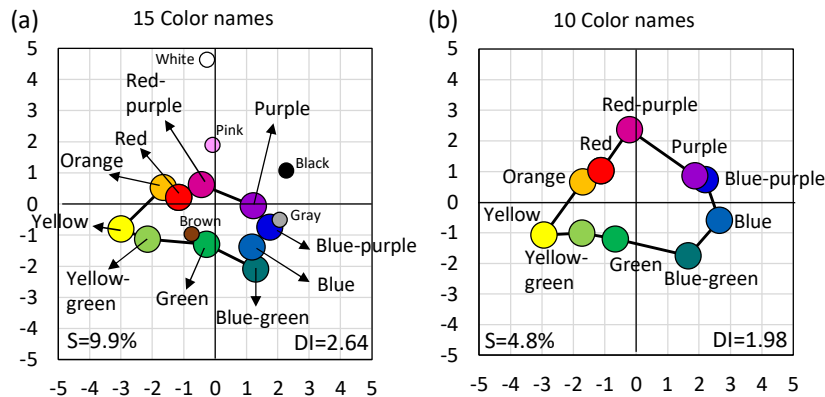


Figure 5 Color representation based on difference scaling of color names. (a) based on 15 color names in this study, (b) based on 10 color names in the previous study. Observer:D17.

We employed three dimensional space to fit the data, and the positions in the 1st vs 2nd axes plane are plotted in the graphs in Figure 5. In Figure 5 (a), 10 color names used in our previous study (Ayama et al., 2021) are indicated by large symbols and connected by a black line to compare with Figure 5 (b), which is the color name representation based on the difference scaling using 10 color names conducted in our previous study for the same observer (Ayama et al., 2021). MDS configurations of the two figures are not exactly the same mainly due to the usage of achromatic color names of “white”, “gray”, and “black” in this study.

In the MDS analysis, the shape of MDS configuration is important. In our previous study, we proposed the distortion index, DI , to indicate the degree of distortion from circle. It is defined as follows,

$$DI = \frac{\pi \cdot d_{max}^2}{4 \cdot S}$$

where S and d_{max} are the area enclosed by lines that connect the 10 color positions and the farthest distance between the color points, respectively. DI is equal to 1 when the MDS configuration is circular and increases as the MDS configuration distorts from a circular shape (Ohkoba et al., 2021). Based on the data of our 30 observers, when the DI exceeds 2, the MDS configuration starts to show partial concavity, and when it exceeds 5, the resulted shape shows clear concavity, C-shape. In neither graphs in Figure 5, DI is less than 2, and both are non-intersecting polygon shape in the order of Munsell hue circle, similar or at least closer to the results of CNOs’ indicated in Ayama et al.

Color representation based on color naming and color name differences

Color naming is the operation in which observer sees color stimulus using visual perception, and assign color name to the stimulus doing a retrieval of the most appropriate word from his/her memory, is combined. Now we have color name difference matrix for some observers. Then it is possible to apply it to individual color naming data. Figure 6 shows the procedure to estimate differences of all stimulus pairs used in the BCT color naming from individual results of color name difference. For example, in the 1st block of the session for high chroma chips, observer D17 named R “red” and GY “yellow”, while he named R “red” and GY “green” in the 2nd block of the session (See Figure 2(e)). Color name difference between “red” and “yellow” is 2, and that between “red” and “green” is 1 according to his color name difference data as shown in gray cells in Figure 4. Then average of these values, 1.5, is assigned to the difference between R vs GY. Difference values

between all pairs were calculated in the same way to fill the difference matrix, which was input to the program of MDS.

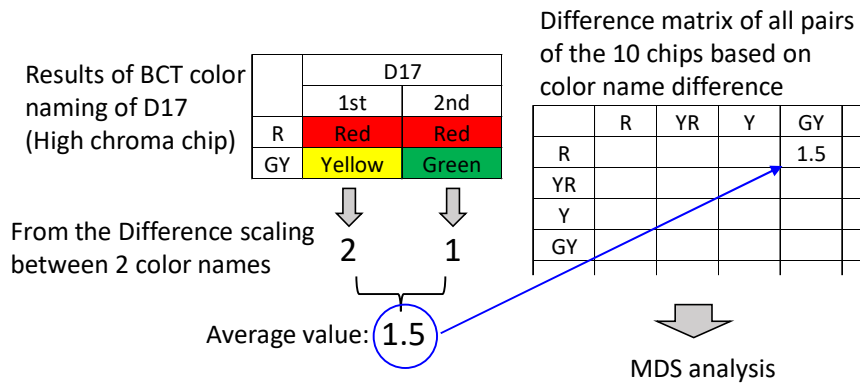


Figure 6 Procedure to estimate differences of all stimulus pairs used in the BCT color naming from individual results of color name difference

Results of high and medium chroma chips of observer D17 are shown in Figure 7(a) and (b), respectively. Result of high chroma is irregular hexagon, whereas that of medium chroma is non-simple polygon with intersecting portion.

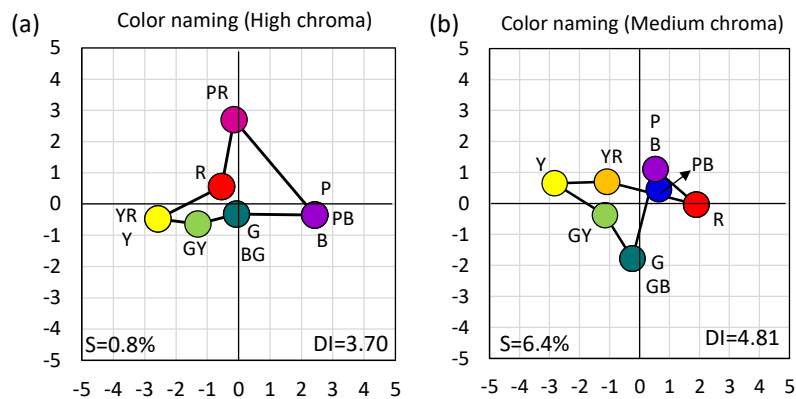


Figure 7 Color representation of color naming results based on color name difference. Observer: D17.

Comparison between color representations obtained in different procedures

For the comparison of color representations under different experimental procedure, color representations of the same observer based on perceptual color difference obtained in our previous study (Ohkoba et al., 2021) are indicated in Figure 8. In that study, pair of color chips on a card was presented and observer rated the perceptual difference using the same in this study. As shown in the figure, the MDS configurations became C-shape with *DIs* of 4.96 and 9.73 for high and medium chroma, respectively, indicating the shape is far from circle.

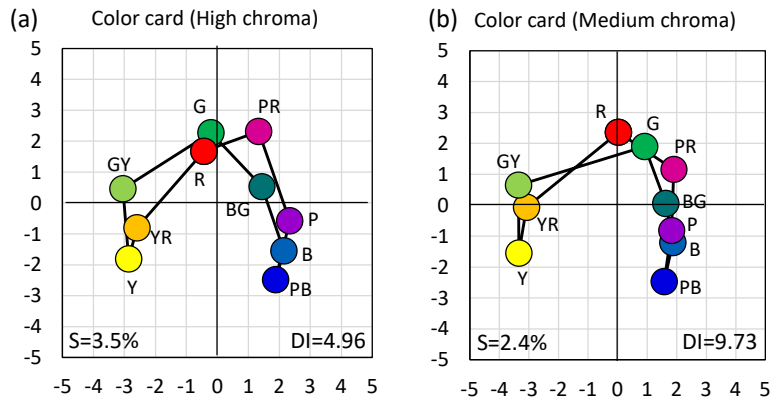


Figure 8 Color representation based on difference scaling of color cards. Observer:D17.

It is interesting to compare the relative distance between R, G, and Y in Figures 7(a) and 8(a) for high chroma chip. In Figure 7(a), R is closer to G than to Y, but the distance between R and G is about half of the distance between R and Y. In Figure 8(a), however, R is very close to G and far from Y. Distance RY is about seven times as that of RG. Same tendency is found in the results of medium chroma in Figures 7(b) and (8b). This indicates that internal color representation of the same 10 color chips for observer D17 varies depending on the derivation method. It varies whether it is derived from the difference scaling using visual perception, or it is derived from the difference of color names assigned to color chips. This variation is clearly affected by the usage of color names in the derivation of graphs in Figure 7. Color names used for R, G, and Y are “red”, “green”, and “yellow”, respectively. Distance between “red” and “green” is roughly the same as that between “red” and “yellow” in Figure 5 (a) and 5(b). This relation among color names affect the shape of MDS configuration in Figure 7, roughly in between those in Figure 5 and Figure 8.

This tendency is found in the relative distances between R, G, and B, as well as other combinations, and the *DI* value, the index to express the degree of distortion from circle, is related to this tendency. Figure 9 shows *DI* values of eight observers in different conditions. Results of high chroma and medium chroma chips are indicated in Figure 9 (a) and 9 (b), respectively. The left, middle, and right denote the results obtained in the difference scaling using pair of color chips, color naming, and difference scaling using pair of color names, respectively. It should be noted that the data of difference scaling of color names are the same in both graphs. They are based on 10 color names, e.g., in the case of observer D17, *DI* in Figure 5 (b), are plotted in Figure 9. As shown in the figure, *DI*s of CNOs are about the same low values in all conditions, except N32 shows slightly high value in color naming. The shape of their MDS configuration is more or less circular in all conditions, indicating CNOs have one type of color space in their brain whatever the derivation process is, and which is similar to the Munsell hue circle. In contrast to that, *DI* value of CDOs varies depending on the condition. For most observers, it is the highest in the difference scaling using pair of color chips and the lowest in the difference scaling using pair of color names. Exceptions are observer D18 in both (a) and (b), and observer P14 in (b). Whether the results of color naming in the middle is closer to the left or to the right depends on individuals.

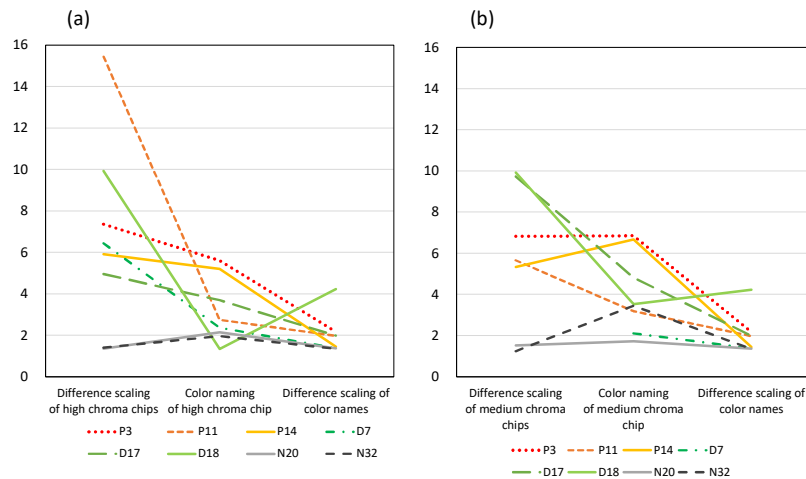


Figure 9 Comparison of Distortion Index (DI) for various color representations

Summary and conclusion

Color naming experiments and difference scaling of color names were conducted for CDOs of protan and deutan, and CNOs. Color naming results of CNOs were very stable for both high and medium chroma chips showing high consistency and consensus. Results of CDOs for high chroma chips are comparable to that of CNOs indicating their color naming ability is fairly high. However, they showed large variation in the results of medium chroma chips. This indicates that strong chromaticness is needed for CDOs to name color to object in the same way as CNOs.

Individual internal color representation was estimated for the color naming results using difference scaling data of color names, and compared with those obtained in difference scaling of color chips as well as in that using color names only. The latter two are considered to internal color representation based on visual perception and color name recognition, respectively. In other words, they correspond to vision-based and recognition-based color space. Those of CNOs do not largely vary either vision-based, recognition-based, or color naming, i.e., based on vision and recognition. On the other hand, CDOs' vision-based and recognition-based color space are generally different. Our results showed the tendency that CDOs' color space of color naming is in between their vision-based and recognition-based spaces. It is reasonable to consider that when people assign a color name to a given color chip, they integrate their vision-based and recognition-based color space in their brain. Results of this study is along with the concept.

Acknowledgement

The authors would like to thank Color Universal Design Organization to their collaboration to carry out the experiment.

References

- Ayama, M., Ohkoba, M., Ishikawa, T., Hira, S., Ohtsuka, S. (2021, August-September). Difference scaling and color naming of red-green color deficiencies. Proceedings of the AIC Conference 2021, Milan, Italy. 393-398.
- Birch, J. (2012, March). Worldwide prevalence of red-green color deficiency. *J. Opt. Soc. Am. A*, 29(3), 313-320.
- Bonnardel, V. (2006, May). Color naming and categorization in inherited color vision deficiencies. *Visual Neuroscience*, 23(3-4), 637-643.
- Boynton, R.M. & Olson, C.X. (1990). Salience of chromatic basic color terms confirmed by three measures. *Vision Res.*, 30(9), 1311-1317.

- Jameson, D., & Hurvich, L.M. (1978). Dichromatic color language: “Reds” and “Greens” don’t look alike but their colors do. *Sensory Processes*, 2, 146-155.
- Kruskal, J.B. (1964). Multidimensional scaling by optimizing goodness of fit to a nonmetric hypothesis. *Psychometrika*, 27(1), 1-27.
- Lillo, J., Moreira, H., Álvaro, L., Davies, I. (2014, August). Use of basic color terms by red–green dichromats: 1. General description. *Color Res. Appl.* 39(4), 360-371.
- Ohkoba, M., Ishikawa, T., Hira, S., Ohtsuka, S., & Ayama, M. (2021, December). Color representations of normals and congenital red–green color deficiencies: Estimation of individual results based on color vision model. *Color Res. Appl.* Early view on online. <https://onlinelibrary.wiley.com/doi/10.1002/col.22763>
- Paramei, G.V. (1996, September). Color space of normally sighted and color-deficient observer reconstructed from color naming. *Psychological Science*, 7(5), 311-317.
- Paramei, G.V. (2012). Color discrimination across four life decades assessed by the Cambridge Colour Test. *J. Opt. Soc. Am. A Opt. Image Sci. Vis.*, 29(2), A290-A297.
- Pitt F.H.G. (1944). The nature of normal trichromatic and dichromatic vision. *Proc. R. Soc. Lond A*, B132, 101-117.
- Wright, E.D. (1957). Diagnostic tests for colour vision. *Ann. R. Coll. Surg. Engl.*, 20(3), 177-191.

Dessert Appetite Aroused by A Direction of Lighting Setup

Chatchai Nuangcharoenporn^{*}, Uravis Tangkijviwat and Waiyawut Wuthiastarn

*Department of Color Technology and Design, Faculty of Mass Communication Technology,
Rajamangala University of Technology Thanyaburi, Thanyaburi, Pathumthani, THAILAND*

** Corresponding email: chatchaicnn@hotmail.com*

Abstract

Thai desserts are popular desserts in Thailand. The nature of Thai desserts shows precise and refined. Thai desserts are outstanding in taste, color, beautiful appearance and look appetite. Nowadays, the growth of business including bringing Thai desserts to sell abroad and the government sector that also encourages the consumption of more Thai desserts. Therefore, the presentation of Thai dessert media is more important. Normally, there were various factor to make photographs look interesting. In previous studies, we found that the lighting in photography is the main factor affecting the attractiveness. It's would be interesting for study using the lighting direction in dessert photography influence appetite on consumer. This study aimed to investigate a relationship between the direction of lighting and the appetite of dessert photography. In this study, Thai mung bean desserts were used as stimuli for taking a photo with different directions of lighting, consisting of a combination of four vertical elevation angles (0°, 30°, 60°, 90 degrees) and twelve horizontal side angles of food dish from 0° to 330 deg. Fifty-two participants were asked to judge their feelings on thirty-seven photographs of dessert by using an appetite scale from 1 (not looked appetizing) to 6 (looked appetizing). Expected result finding that the direction of lighting and greatly influence participants' appetizing. The results of this research can be used as a guide for the lighting set up of Thai dessert photography.

Keywords: Dessert Photography, Dessert Appetite, Lighting Setup

Introduction

Nowadays, a sharing of photography through social media, websites, and blogs becomes very popular, in particularly a food photograph [1,2]. A variety of food photographs published on cooking or restaurant website purpose to catch a customer's attention and to be appetite [3]. Many factors have an influence over customer's attention for instance an expensive ingredient, food decoration, and food composition [4]. In addition, photography techniques such as lighting setup, special effect, and camera angle are also arouse our taste sensation [5,6].

In a previous study, Kazuma et. al. [3] proposed an attractiveness prediction model for food photographs by using a machine learning system. A camera angle, an appearance of the entire food, and the appearance of the main ingredients are variables in the model. Furthermore, they also found that food photo attractiveness on customers could be affected by a lighting technique. A lighting setup not only is concerned with color temperature, but also lighting direction. Illuminants for lighting setup consist of a main light and a fill light. The main light is a primary illuminant that uses for exposing light to objects. It's located at an angle of 45° to the object. The fill light located at the opposite angle to the main light. To reduce shadows that are created from the main light and the fill light illuminance is always weaker than the key light [7]. Moreover, the direction of main light affects to direction and intensity of object's shadow. When the main light changes direction and intensity, a shadow of object could be changed. This change might affect customer's attention. This study, therefore, aimed to investigate a relationship between a lighting direction and an appetite of dessert photographs.

Methodology

Participants

Fifty-two volunteers consisted of 23 men and 29 women. Participants were age ranging from 21 to 31 years. Prior to the experiment participants were screened for color blindness using the Ishihara color test. All the participants were normal or corrected to be normal eyes vision.

Stimuli

The Thai dessert fruit-shaped mung beans, Luk-Chup were taken as a stimulus (figure 1). Intensity of illuminance levels of two lighting for the main-light and fill-light were controlled, ranging 11,000 and 5,500 lux. respectively. We controlled the position of main-light move along the side of the dish and keeping a fixed position of the camera and fill-light at 0° on horizontal side angles. Luk-Chup were served on a white dish for taking a photo with different directions of lighting, consisting of a combination of four vertical elevation angles (0°, 30°, 60° and 90° deg.) and correspond to take on twelve of horizontal angles of food dish side from 0 to 330 deg. With the step of 30 deg. (0°, 30°, 60°, 90°, 120°, 150°, 180°, 210°, 240°, 270°, 300° and 330°), respectively. With photography method, we obtained 37 dessert picture stimuli from a combination of a vertical elevation angle and a horizontal side angle.



Figure 1 Thai dessert fruit-shaped mung beans, Luk-Chup

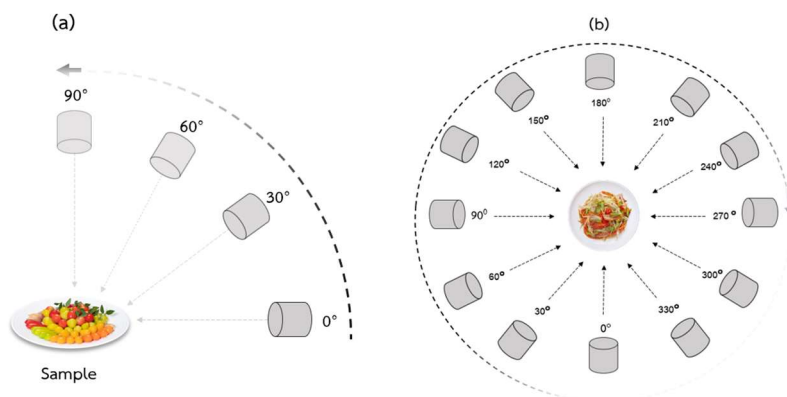


Figure 2 (a) Lighting on vertical elevation angle from 0° to 90° and (b) all position of lighting on horizontal side angles of dish from 0°, 30°, 60°, 90°, 120°, 150°, 180°, 210°, 240°, 270°, 300° and 330°

Procedure

This study was conducted on an online questionnaire. In experiment, 37 dessert photographs were order randomly presented. Each participant was asked to rate their feeling in an appetite scale for given photography. The appetite scale was ranged from 1 (extremely unappetizing) to 6 (extremely appetizing).

Result

Influences of lighting direction on horizontal side angles

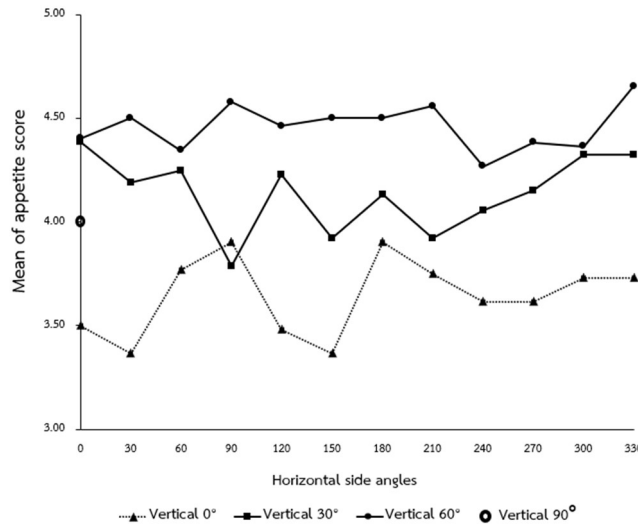


Figure 3 The difference of appetite score in each vertical elevation angles of 0°-90° classified by horizontal side angles of 0° to 330° of dessert photographs

As shown in figure 3 Data of appetite score obtained from participants were performed by means of SPSS for Window. A mean of appetite scores for dessert photography in a difference of horizontal side angles. An abscissa axis represented a horizontal side angle from 0° to 330 and vertical axis represented the mean of appetite score. In addition, vertical elevation angle 0°- 60° displayed a set of mean of appetite scores on different horizontal side angles, respectively.

Results showed that dessert photograph with vertical elevation angle 0° (▲) had the highest mean appetite score at horizontal side angles 90° ($\bar{x} = 3.90$, $SD = 1.50$) and 180° ($\bar{x} = 3.90$, $SD = 1.29$) whereas photograph with the lowest mean appetite was horizontal side angles of (90° and 150°) ($\bar{x} = 3.37$, $SD = 1.428$) and 150° ($\bar{x} = 3.37$, $SD = 1.618$). For vertical elevation angles of 30° (■), the dessert photograph with the highest mean appetite score was horizontal side angle 0° ($\bar{x} = 4.38$, $SD = 1.163$), and the lowest mean appetite on horizontal side angle of 90° ($\bar{x} = 3.79$, $SD = 1.446$) vertical elevation angle (●) 60°, the dessert photograph with the highest mean appetite score was horizontal side angle 330° ($\bar{x} = 4.65$, $SD = 1.090$). A dessert photograph with the lowest appetite score was horizontal side angle of 240° ($\bar{x} = 4.27$, $SD = 1.346$). For dessert photographs taken on the vertical angle of 90° (○) with mean ($\bar{x} = 4.0$, $SD = 1.557$). We used One-Way ANOVA analyzed to find significant the result showed that the mean appetite of dessert photographs in horizontal side angles was not a statistically significant difference at p-value 0.05.

Influences of lighting direction on vertical elevation angles

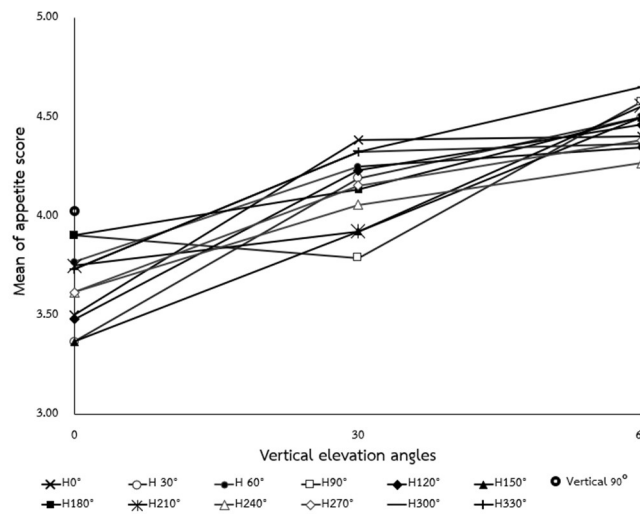


Figure 4 Comparison of mean appetite scores of food photos on vertical elevation angles

Figure 4 showed the mean appetite score of dessert photograph in each horizontal side angle from 0° to 330° classified by a vertical elevation angle 0°, 30° and 60°, where vertical axis represented the mean of appetite score and an abscissa axis represented the vertical elevation angle from 0°, 30° to 60°. For mean value of photograph with vertical elevation angles 90° was shown by an opened circle (○).

Results showed when the vertical elevation angles increase lead to the mean attractiveness of food photographs increased. For example, dessert taken under lighting at horizontal side angle 150° with vertical elevation angles 0°, 30° and 60° had mean appetite score (\bar{x} = 3.37, SD.=1.633), (\bar{x} = 3.92, SD.=1.426) and (\bar{x} = 4.50, SD.=1.276), respectively. This result occurred in all horizontal side angle except 90°, the mean appetite decreased when the vertical elevation angle increased (\bar{x} = 3.90, SD.=1.512), (\bar{x} = 3.79, SD.=1.460) and (\bar{x} = 4.58, SD.=1.194), With the mean increasing trend, vertical affects the appetite of dessert photography. Therefore, we tested with one-way ANOVA to find significance.

Table 1 One-way ANOVA of mean appetite score of dessert photograph in each horizontal side angles on vertical elevation angle of 0°, 30° and 60°

		H0	H30	H60	H90	H120	H150	H180	H210	H240	H270	H300	H330
<i>df</i>	BG:	3	3	3	3	3	3	3	3	3	3	3	3
	WG:	204	204	204	204	204	204	204	204	204	204	204	204
<i>SS</i>	BG:	28.091	35.82	10.51	19.17	27.47	33.66	10.65	19.03	11.59	16.30	13.94	24.97
	WG:	385.82	381.13	398.75	423.88	429.13	448.75	381.57	388.26	445.36	395.38	373.73	391.44
	F	4.95	6.39	1.79	3.07	4.35	5.10	1.89	3.33	1.770	2.80	2.53	4.33
	Sig.	.002*	.000**	.150	.029*	.005*	.002*	.131	.020*	.154	.041*	.058	.005*

Notes: *p<0.05, **p<0.001, H: Horizontal side angle, BG: Between Group – WG: Within Group

As shown in Table 1, the results of One-Way ANOVA of mean appetite in dessert photograph in each horizontal side angle on a vertical elevation angle of 0°, 30° and 60°. There was a statistically significant difference between vertical elevation angle and horizontal side angle with mean attractiveness score at p<0.001 (F = 38.58, p = 0.000).

It was found that the dessert photograph taken under vertical 60° of lighting could have the greatest impact on the appetite of dessert photography. The result indicated that increasing the height of vertical elevation angles of lighting tends to increase the attractiveness. This tendency was occurred in all condition. However, the mean of appetite was not significantly different at horizontal angles of 60°, 180°, 240° and 300° with p-value ($F = 1.79, p = 0.150$), ($F = 1.89, p = .131$), ($F = 1.770, p = .154$) and ($F = 2.53, p = .058$)

Discussion

Influences of lighting direction on vertical elevation angles of food dish on appetite

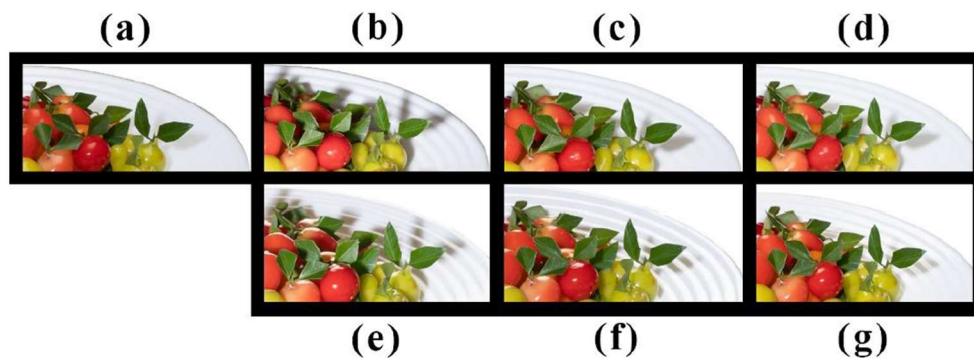


Figure 5 An example of a comparison of vertical angle food photos in shadow areas (a) V90°, (b) V0°-H0°, (c) V30°-H0°, (d) V60°-H0°, (e) V0°-H180°, (f) V30°-H180° and (g) V60°-H180°

Our finding showed that increased vertical elevation angles from 0° to 60°. This led to an increased feeling of appetite on dessert photography as well. The dessert photographs (b) Vertical 0°-Horizontal 0°, (c) Vertical 30°-Horizontal 0° compared with the (d) Vertical 60° - Horizontal 0° degrees. We found that the intensity of shadows in the dessert on the dish can be clearly reduced. The higher of a vertical elevation angle may provide a high illuminance level to convey a bright photograph. This result implied that the level of shadow intensity could reduce the feeling of appetite on customers.

Lighting horizontal side of dish not affected on attractiveness of food

Lighting direction of horizontal side angles does not affect to the appetite of dessert photography. Kazuma et al. studied of estimation of the attractiveness of food photography based on image features [3]. They suggested that a camera angle was an important factor in enhancing attractiveness. In addition, their research also was found that the type of the food including the shape and position of the appearance of main ingredient in that dish could increase the level of appetite. In this study, the dessert was used as the stimulus. It does not contain the main ingredient and no exact direction. Therefore, the changes in the type of dessert or food stimuli to other categories of foods, the horizontal side of angles might be affecting to attractiveness and appetizing on consumers. It implies that a changing type of foods would be required to understand the direction of lighting on horizontal angle change attractiveness in future experiments.

We concluded that the direction of lighting on vertical elevation angles can modulate the appetite of dessert photography. whereas horizontal angle did not statistically significant difference in appetite.

References

Cai, W., Richter, S. and McKenna, B. (2019). “Progress on technology use in tourism”. *Journal of Hospitality and Tourism Technology*, 10(4), 651-672.

- Chen, X., Ren, H., Liu, Y., Okumus, B. and Bilgihan, A. (2020). “Attention to Chinese menus with metaphorical or metonymic names: an eye movement lab experiment”. *International Journal of Hospitality Management*. 84, 102305.
- Kazuma T, Tatsumi H, Keisuke D, Yasutomo K, Takatsugu H., Ichiro I, Daisuke D, & Hiroshi, M. (2019). Estimation of the attractiveness of food photography based on image features. *IEICE TRANS. INF. & SYST.*, VOL. E102–D, NO.8 AUGUST 2019.
- Liu, I., Norman, W.C. and Pennington-Gray, L. (2013). “A flash of culinary tourism: understanding the influences of online food photography on people’s travel planning process on Flickr”. *Tourism Culture and Communication*. 13(1), 5-18.
- Martin, C.K., Nicklas, T., Gunturk, B., Correa, J.B., Allen, H.R. and Champagne, C. (2014). “Measuring food intake with digital photography”. *Journal of Human Nutrition and Dietetics*, 27, 72-81.
- Oliveira, B. and Casais, B. (2019). “The importance of user-generated photos in restaurant selection”. *Journal of Hospitality and Tourism Technology*. 10(1), 2-14, available at: <https://doi.org/10.1108/JHTT-11-2017-0130>.
- Rea MS (2000). *The IESNA lighting handbook*. 9th edn. New York: Illuminating Engineering Society of North America.

Color Name and Aroma of Thai Flowers

Chanida Saksirikosol¹, Akaradet Tongawang², Chanprapha Phuangsuwan³ and Kitirochna Rattanakasamsuk^{3*}

¹*Department of Advertising and Public Relations Technology, Faculty of Mass Communication Technology, Rajamangala University of Technology Thanyaburi, Thailand*

²*Department of Printing and Packaging Technology, Faculty of Mass Communication Technology, Rajamangala University of Technology Thanyaburi, Thailand*

³*Color Research Center, Rajamangala University of Technology Thanyaburi, Thailand*

* *Corresponding email: kitirochna@rmutt.ac.th*

Abstract

In Thailand, the essential oil is commonly used and there is a wide variety of unique aromas which obtained from the essential oil extracted from Thai flower such as Rose, Jasmine, Indian Cork, Plumeria etc. In the design of Thai aroma products, it is important to emphasize the uniqueness of the flower aroma. Color is an element that can enhance the recognition of those aroma. Therefore, this research aims to study the relationship between the color name and aroma from eight Thai flower: Rose, Jasmine, Plumeria, Cananga, Sweet Osmanthus, White Champaka, Indian Cork, and Moke. 109 subjects aged between 15-60 years old who has normal color vision are asked to smell the aroma dropped into a piece of cotton. After smelling, they must identify the color name which related to that aroma. Three color names must be selected from a set of 12 Thai basic colors which consist of red, orange, yellow, green, purple, pink, brown, blue, sky blue (*Fah*), gray, black, and white. Before each smelling, the subject's nose will be neutralized by smelling coffee beans for 5 seconds and rest for at least 5 seconds. The results show that there is a high correspondence between Thai flower aroma and yellow.

Keywords: Thai basic color, Thai flower, Aroma

Introduction

The essential oil is a natural product which can be extracted from many parts of plants such as flowers, petals, stems, seeds, etc. In Thailand, the essential oil extracted from flower such as Rose, Jasmine, Indian Cork, Plumeria, etc. is commonly used to produce Thai aroma. They are popularly used in Thai massage, traditional ceremonies to create the relaxing atmosphere. In aromatherapy, they are also used to reduce the pain and to heal the injury. Comparing between human's basic five senses: touch, sight, hearing, smell and taste, smell is not the highest sensitive sense. However, humans can discriminate between 10,000 different odors [1]. Therefore, we can perceive and discriminate each Thai flower aroma which has their own unique smell and characteristic.

For Thai aroma product design, it is important to emphasize the uniqueness of each Thai flower aroma. It is obvious that color is an element which impact customer purchasing decision [2]. Previous research has reported that there is an association between color and odor [3]. For example, there is a correspondence between the cinnamon and red color, or between the caramel and brown color. In case of Thai flower aroma, the uniqueness of smell is quite strong so that people can easily recognized their smell. There might be the correspondence between flower smell and some color such as the flower's color. For example, when people smell the Jasmine, they will refer to white which is Jasmine color. On the other hands, people will refer to red if they smell Rose. Therefore, this research aims to study the correspondence between the color name and Thai flower aroma. In this experiment, aroma of Rose, Jasmine, Plumeria, Cananga, Sweet Osmanthus, White Champaka, Indian Cork, and Moke are selected because of their distinct smell popularity.

Methodology

The subjects were 109 voluntary people which consists of 58 female, 44 male and 7 LGBT aged between 18-60 years old. All subjects had pass Ishihara test for checking their normal color vision. The stimuli were aroma of eight Thai flowers: Rose, Jasmine, Plumeria, Cananga, Sweet Osmanthus, White Champaka, Indian Cork, and Moke. Each aroma was prepared by dropping 2 drops of the aroma on a 0.5x5.0 cm perfume test paper.

The experiment started by smelling the coffee beans for 5 seconds and rest for at least 5 seconds for neutralizing subjects’ nose. Then the subjects were asked to smell the aroma on the perfume test paper. After smelling, they were asked to identify the color name which related to that aroma. Three color names must be selected from a set of twelve Thai basic colors which consists of red, orange, yellow, green, purple, pink, brown, blue, sky blue (*Fah*), gray, black, and white. This procedure was repeated until each subject have smell all aroma. The order of aroma smelling was random for each subject.



Rose
(กุหลาบ)



Jasmine
(มะลิ)



Plumeria
(ลีลาวดี)



Cananga
(กระดังงา)



Sweet Osmanthus
(หอมหมื่นลี้)



White Champaka
(จำปี)



Indian Cork
(ปีป)



Moke
(โมก)

Figure 1 Thai flowers used for aroma in this experiment

Results and Discussion

Figure 2 showed the results of selected color names from 109 subjects. The abscissa was 12 Thai basic color names [4] and the ordinate was the frequency of selected color names in three time (one color name could be selected only one time for 1 subject). The total response was 327 (109×3). First, we found that all of 12 basic color names were selected for each essential oil from Thai flowers. Second, we found that yellow color name showed highest frequency selected at 66 for White Champaka, 53 for Rose, 51 for Indian Cork, 50 for Sweet Osmanthus and 49 for Cananga, respectively. Additionally, green color name showed highest frequency selected at 64 for Moke, 57 for Plumeria and 49 for Cananga (noted; there was the same frequency selected with the yellow color name for Cananga also). White color name showed highest frequency selected at 59 for Jasmine.

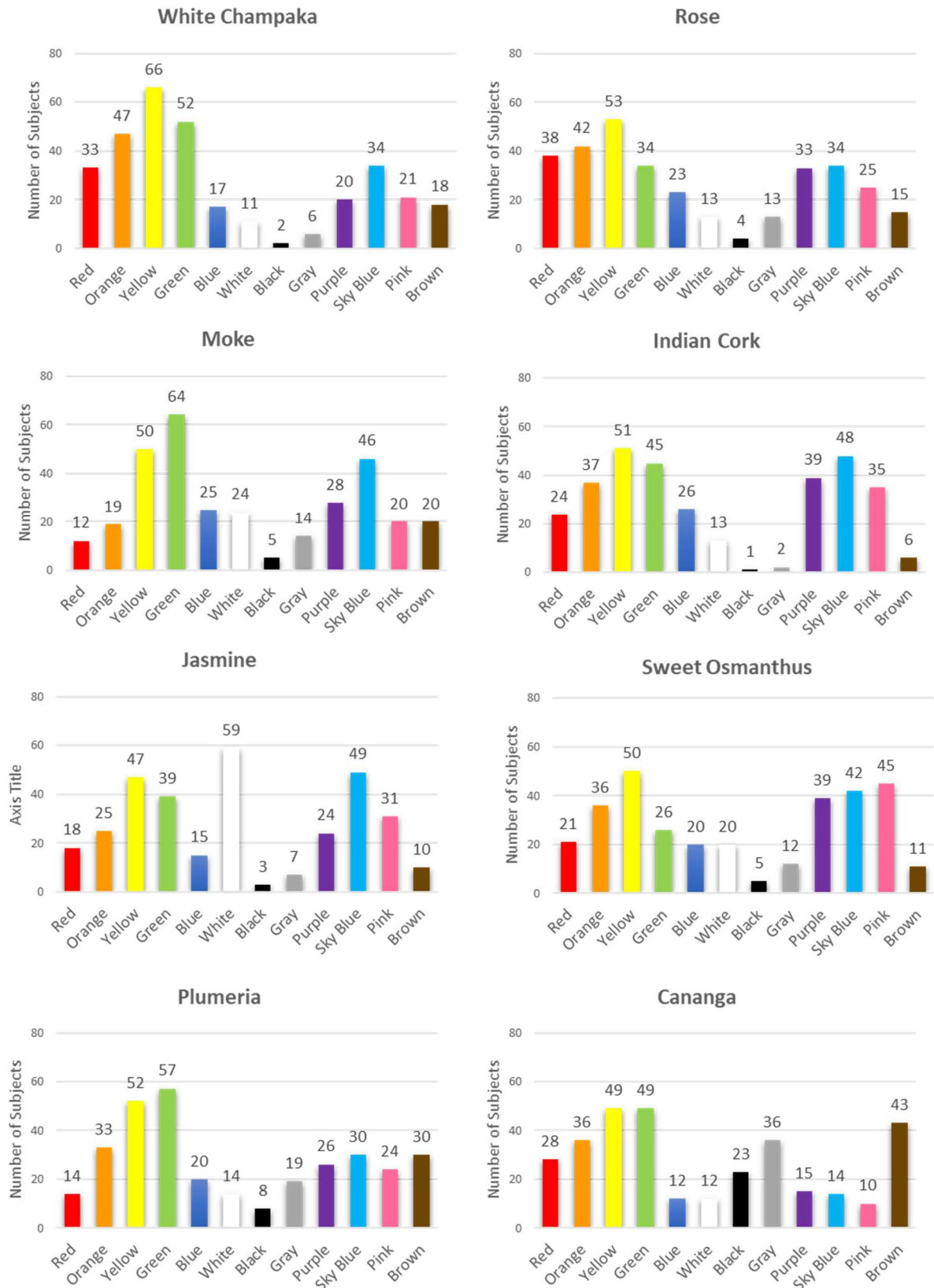


Figure 2 The selected color names of Thai flower by 109 subjects

In addition to the highest frequency, we also found that two other high-frequency colors were associated with essential oils, see in Table 1. White Champaka was yellow, green and orange, respectively. Moke was green, yellow and sky blue (Fah). Jasmine was white, sky blue (Fah) and yellow. Plumeria was green, yellow and orange. Rose was yellow, orange and red. Indian Cork was yellow, sky blue (Fah) and green. Sweet Osmanthus was yellow, pink and sky blue (Fah). Cananga was distributed in color name such as yellow, green was the same highest frequency, secondary high frequency was brown and third secondary frequency was orange and gray, respectively. The result implied that color and smell of essential oil from Thai flowers has some relationship in yellow and green.

Chanisthar et al. (2019) showed the relationship between color and smell of Thai flower aroma by asking the observers smelled aroma and selected the color that represented to that smell from the Munsell color book [5]. This method was different from the present paper at the observers smelled and thought about the color name which did not give any information about color to the subject. We supposed this present method may show the real color that represented to that smell.

Table 1 Top three rank of selected color name

Essential oil from Thai flowers	Color name		
	First rank	Second rank	Third rank
Whit Champaka	Yellow	Green	Orange
Moke	Green	Yellow	Sky blue (Fah)
Jasmine	White	Sky blue (Fah)	Yellow
Plumeria	Green	Yellow	Orange
Rose	Yellow	Orange	Red
Indian Cork	Yellow	Sky blue (Fah)	Green
Sweet Osmanthus	Yellow	Pink	Sky blue (Fah)
Cananga	Yellow	Green	Brown
			Orange
			Gray

Conclusions

Through this experiment we can say color and aroma from Thai flower had some relationship. Particularly, yellow color was somehow showed strong relationship with the smell of Thai flowers. However, the different method might give the difference of the color that related to the smell of Thai flower. The further experiment will be investigated more details about color such as hue, lightness and saturation, etc.

Acknowledgement

We would like to thank Miss Yanika Jaitieng for collecting the data in this research.

References

- Kavinna, K. (2021). *Properties of essential oil*. Retrieved from website : <https://oem.thaimedicos.com/2021/12/02/benefits-of-essential-oils/>.
- Levitan, C. A., Ren, J., Woods, A. T., Boesveldt, S., Chan, J. S., McKenzie, K. J., Dodson, M., Levin, J. A., Leong, C. X. R., & van den Bosch, J. J. F. (2014). Cross-Cultural Color-Odor Associations. *PLoS ONE*, 9(7), e101651. <https://doi.org/10.1371/journal.pone.0101651>.
- Patitanang, N., Phuangsuan, C., Kuriki, I., Tokunaga, R. and Ikeda, M. (2019). Thai basic color terms and new candidate nomination. *Proceeding of ACA2019 Nagoya*, 164-169.
- Seher, T., Arshad, M., Ellahi, S., & Shahid, M. (2012). Impact of colors on advertisement and packaging on buying behavior. *Management Science Letters*, 2(6), 2085–2096. <https://doi.org/10.5267/j.msl.2012.06.011>.



Trainaja, C., Phuangsuwan, C. and Ikeda, M. (2019). Colors to represent fragrance, *Journal of the Color Science Association of Japan*, 43(3), Supplement, 233-236.

The Effectiveness of Augmented Reality Data Access through a Smartphone

Kanok Chinda, Chanida Saksirikosol* and Ploy Srisuro

Department of Advertising and Public Relations Technology, Faculty of Mass Communication Technology, Rajamangala University of Technology Thanyaburi, Thailand

** Corresponding email: chanida_s@rmutt.ac.th*

Abstract

Augmented Reality (AR) is a technology that combines the real world with virtual reality using software and connecting devices such as a camera from a smartphone or tablet. The virtual picture will emerge on the screen of the mobile phone or display device and will immediately interact with the user. Augmented Reality technology has gained popularity and is being utilized in a wide range of applications. AR technology has been utilized in advertising to gain customer attention, especially in a period where everyone is dealing with the COVID-19 pandemic, where AR technology helps develop new experiences for consumers. Due to the high cost of AR production, the advertiser should avoid the issue of information access. As a result, the purpose of this study is to investigate the image recognition factors that influence access to AR via a smartphone by analyzing geometric shapes such as squares, triangles, circles, and Oval. The number of shapes is increased and sorted at random. The effectiveness of AR data access through a smartphone is then evaluated using 30 subjects.

The results revealed that the format of the photos used to construct the AR Marker influences the display's accuracy and sensitivity. It features an oval outside border and a design. There are also Abstract details inside. It was rated as the most accurate, with a score of 92.2 percent.

Keywords: Augmented Reality, Image Analysis, Advertising, Image Recognition, Smart Device

Introduction

Manufacturing and communication technologies are changing at a rapid pace. As a result, many businesses are progressively replacing conventional labor with computer equipment, robots, or electronic gadgets. In today's economy, more informed and competent workers are needed in manufacturing, creative labor, planning, design, and the usage of more modern or complex technologies. Augmented Reality (AR) is another technology that has been used in communication and as a tool for advertising. AR is a technology that mixes the real world with virtual reality using software and linked devices such as a mobile phone's camera and a tablet. The virtual picture will appear on the computer screen, mobile phone screen, or display device. The virtual visuals that arise will immediately interact with the user in either a 3D static image or motion.

Many stores have been impacted and forced to close their doors as a result of the COVID-19 outbreak. It also makes it hard for customers to buy or try on things on their own. The inability to test a product before purchasing it is a big issue for customers, prompting entrepreneurs to alter their trade practices. Many organizations are interested in using AR technology to mimic virtual reality items for customers to test out things, and it is frequently utilized to create a distinctive and memorable picture of products and services.

Using this technology to enhance sales and marketing is another way to increase consumer recognition and credibility in the scenario when cellphones are the 5th factor, but producing AR is rather costly. If there is an issue with obtaining diverse information via AR, the product owner may miss out on the opportunity to market their items. The goal of this research was to investigate the parameters influencing AR accessibility via smartphone-like mobile devices by developing AR Markers in square, circle, oval, and triangle shapes.

Methodology

Squares, circles, ovals, and triangles were used in the AR Marker development process to produce a face-like pattern on both the outer contour and the inner detail of the Marker. It is separated into two types: regular patterns with distinct outlines of the inner and outer frames, and abstract inner and outer frames, with a total of 16 pictures, as shown in Figure 1.

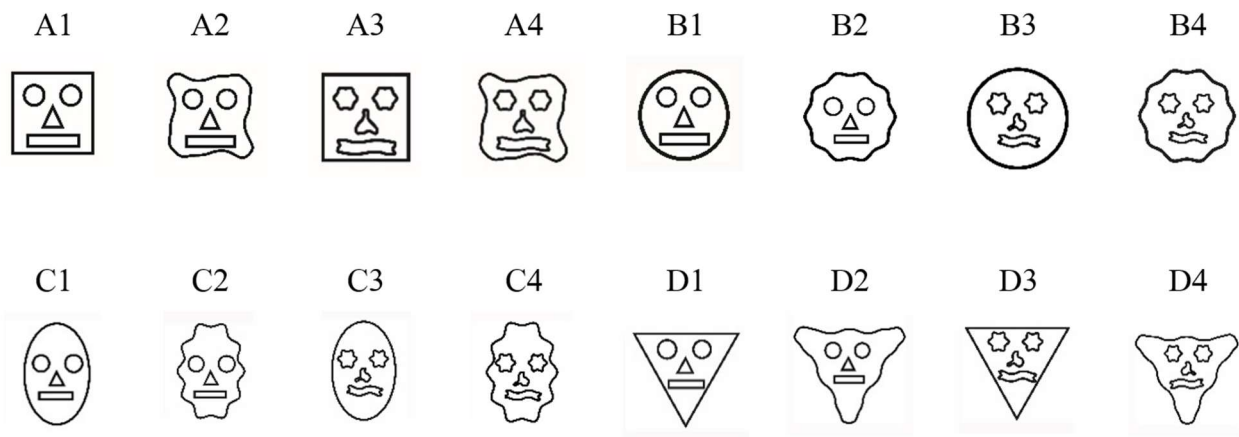


Figure 1 The 16 AR Markers

To construct a Marker Database, all 16 AR Marker images were submitted to the VIDINOTI website, which is a website used to create AR as illustrated in Figure 2. To test the functioning with a Smartphone, the V-Player application was installed.

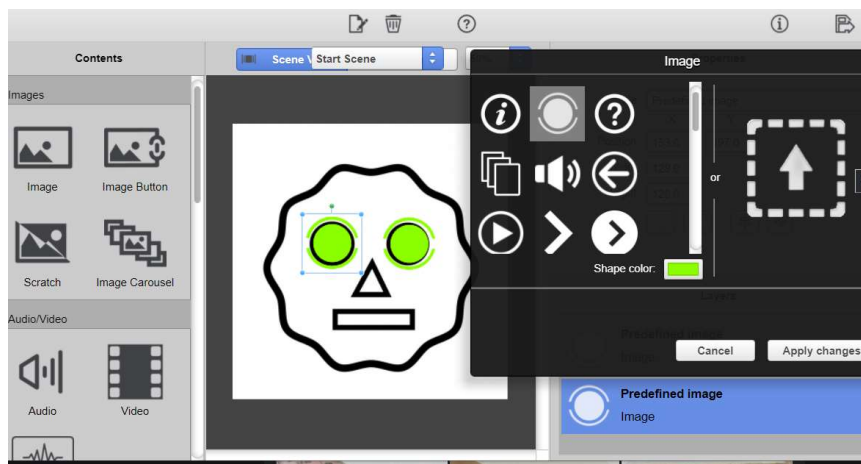


Figure 2 Creating AR Marker through VIDINOTI website

A group of 30 people were shown the AR Marker. The sample scanned the image at random, one image at a time. The light was regulated inside a room such that shadows did not obscure the Marker. The sample must be retested three times via an app on a smartphone or tablet. The sample assessed the display's accuracy. The data's presentation was timed to determine how soon the AR Marker shows.

Result

A study of the factors affecting AR accessibility through a smartphone from 16 AR Marker images discovered that the top three AR Marker patterns were able to display correctly, as shown in

Figure 3. These were image C3 (image with an oval outer border), image D2 (image with abstract triangular outer border, with arithmetic internal details) with a display accuracy of 91.1 percent, and images C1, C4 and D1 with the same evaluation score of 85.6 percent.

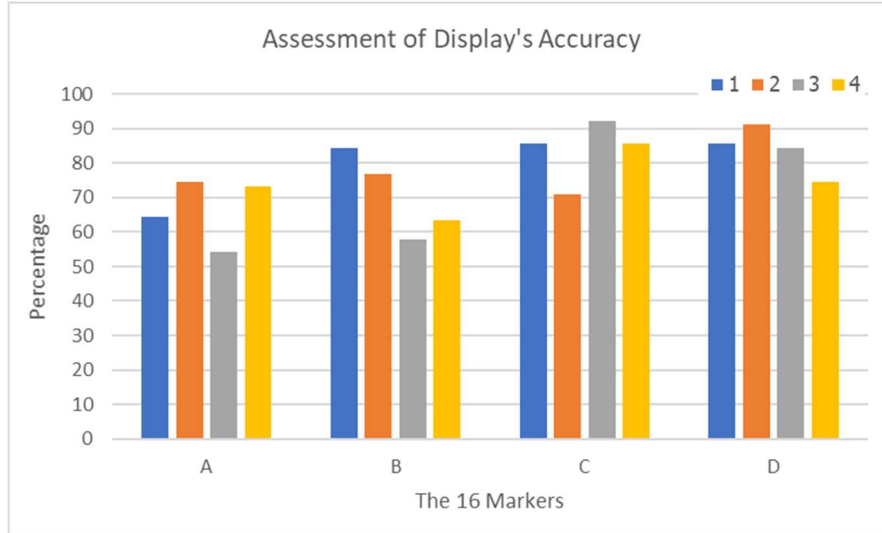


Figure 3 Assessment of Display’s Accuracy

The top three AR Marker patterns examined for the fastest rendering were image B3 with an average speed of 1.77 second, image A4 with an average display speed of 1.79 second, and image D3 with an average display speed of 1.82 second in the examination of AR Marker rendering speed. Image B2, which took the longest to produce, had an average display speed of 1.82 second equivalent to 2.35 second, as shown in **Figure 4**.

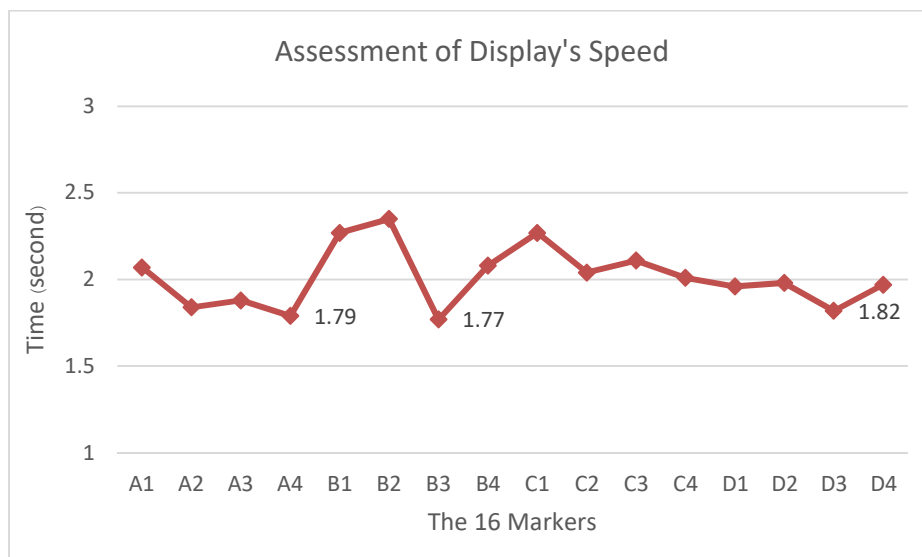


Figure 4 Assessment of Display’s Speed

Conclusion

The image that accurately displays the information and takes the least time is image D3 with the rendering speed of 1.82 seconds and the score for the accuracy of impressions was 84.4 percent,

according to a study of factors affecting the access to AR through a smartphone from 16 images of AR Marker. This study proposed an image format for creating an AR Marker that may be utilized as a reference for advertising design. The image with the outline of the outside border differs from the image with the outline of the interior detail. However, due to the tiny number of samples, it cannot be characterized as a Systematic Rule. As a result, more samples and picture formats should be investigated in the future.

References

- AR Technology with Customer’s Experience for Business Efficacy after Covid-19 (2021). Retrieved from website: <https://workpointtoday.com/augmented-reality-digital-disruption-01/>.
- Cirulisa A, Brigmanis KB (2013). 3D outdoor augmented reality for architecture and urban planning. *Procedia Computer Science*, 25, 71-79.
- Foresight Factory report (2021). retrieved from website: <https://forbusiness.snapchat.com/blog/what-consumers-want-as-they-return-to-stores-us>.
- How difference between AR and VR for Advertising (2020). Retrieved from website: <https://www.teedd360.com/how-different-ar-vr/>.
- Khaoluang, D. and Anukulwetch, A. (2018). *The Development of Virtual Reality Interactive 3D Learning Materials by Using Augmented Reality (AR) Technology for Enhance Thinking Skill’s Vocational Education Students with Different Critical Thinking levels*. Burapha University.

The Comparison of the Weather Forecast Program with Thai Sign Language and Captioning between Hearing Impaired, Deaf and Hearing

Waiyawut Wuthiastarn

*Photography and Cinematography Technology department, Faculty of Mass Communication
Technology, Rajamangala University of Technology Thanyaburi, Thanyaburi, Pathumthani, 12110
THAILAND*

** Corresponding email: waiyawut_w@rmutt.ac.th*

Abstract

The research examines how Thai sign language and captioning help the hearing impaired and the deaf understand the weather forecast program on television. This research objective was investigated the satisfaction of the contents from the weather forecast program when the hearing impaired and the deaf perceived the weather forecast program on television compared to the hearing. A Quasi-Experimental was designed for this research and selected data by Google Online. The hypothesis tested was used by One Way ANOVA. The finding showed that captioning was preferred by the hearing, the deaf but the hearing impaired unsatisfied. The hearing, the hearing impaired and the deaf were satisfied on Thai sign language and results found that the score of understanding was not different significantly between the hearing and the hearing impaired or the deaf.

Keywords: Thai sign language, captioning, hearing impaired, deaf, hearing

Introduction

Announcement of the National Broadcasting and Telecommunications Commission on Promoting the protection of the right of people with disabilities to access or recognize and take advantage of television programs B.E. 2556 (2016) establishing laws on television access for disabled and disadvantaged people. The National Broadcasting and Telecommunications Commission (NBTC) has provided TV stations with facilities by promoting the protection of disability rights to access or recognize and take advantage of television programs classified by disability as follows: Types of deaf and hearing impaired people to have facilities include: Sign Language Interpreter Service Captioning service Blind or low vision types include facilities including Audio Description. The law has been in effect since 2016, which means that if this law was applied seriously, the law was enforced. These three services must be performed in television business in proportion to the legal limits from 2016 to 2020.

Despite the announcement of the National Broadcasting and Telecommunications Commission on Promoting the protection of disability rights to access or recognize and utilize the 2016 television program, it has also been found that produced TV shows often separate facilities, causing disabled people and people with disabilities did not benefit from the assessing in television business, so this study was interested in studying the satisfaction of television programs that provide Thai sign language interpreters and captioning by conducting a study comparing the hearing impaired and the deaf to normal people. In this study, it was made to study only sign language interpreter services and captioning, which provide facilities for access television media instead of audio services. This was because the number of beneficiaries of captioning services was the largest in the number of service recipients available from people with hearing impairments. People who were deaf or deaf who can read Thai sign in addition to people with hearing impairments who benefit from captioning, they're not. It also includes old people whose hearing deteriorates, cannot hear the same sound, can use captioning reading instead of audio to gain access to TV program, and also foreigners who want to

learn Thai language can take advantage of captioning to practice Thai grammar. Sign language interpreter services have a smaller number of users because sign language was a language that communicates only to the deaf community, thus making it legal to define the proportion of services given to a smaller volume than subtitles instead of audio.

In addition, as a result of the new outbreak, Coronavirus 2019 or COVID-19 causes TV broadcasters to wear face masks in order of the center for the administration of the situation due to the outbreak of the communicable disease coronavirus 2019 (COVID-19). Defined, the phenomenon hindered the hampering of hearing impaired or the deaf viewers who often use the broadcaster's lip reading, thus making it impossible to read lips from broadcasters. The assumption of how to make providing captioning and sign language interpreters services to help hearing impaired and deaf people access the contents of the TV program. By providing captioning and sign language interpreters along with presentations on the program. This may be a way to allow deaf and the hearing impairment to access content from television media in the state of TV broadcasting under the COVID-19 pandemic.

Objective

1. To compare satisfaction with the programs that provide captioning service for hearing impaired and the deaf.
2. To compare satisfaction with the programs that provide sign language interpreters for hearing impaired and the deaf.

Methodology

The study titled " The comparison of the weather forecast program with Thai sign language and captioning between hearing impaired, deaf and hearing" surveyed satisfaction from watching TV program produced as weather forecast programs 5.30 minutes long, then let the viewer who were 97 deaf, 38 hearing impaired and 67 normal people do a satisfaction assessment of the captioning consist of the letter, font size, font color, the number of letters and the length of appearance of the letters was provided by the viewers and to perform a satisfaction assessment of sign language interpreter services, including: size of sign language interpreter frame, the position of the sign language interpreter frame, the background color of the sign language interpreter, sign language gestures, and the dress code of the sign language interpreter, assessed through a Google Form questionnaire. After that, the data was analyzed statistically by testing variance between groups with statistics. One Way ANOVA and Independent Sample T –Test was significant level at 0.05

Results

The study of comparing the quality of weather programs with Thai sign language interpreters and subtitles instead of voices between the deaf. The survey showed that there were 83 male and 119 female informants, including 202, according to Table 1.

Table 1 Gender Information

Gender	Number (persons)
male	83
female	119
Total	202

The informants in this survey have hearing levels divided into three groups, as shown in Table 2.

Table 2 Hearing Level Information

Hearing level	Number (persons)
deaf.	97
hearing impaired	38
normal people.	67
Total	202

Survey of informant groups by age level It was found that there were informants with age levels as shown in Table 3.

Table 3 Age Level Information

Age level	Number (persons)
Under 25 years old	110
25 years – 35 years	38
36 years – 45 years	30
46 years – 50 years	12
More than 50 years old	12
Total	202

A comparison of the quality of the weather list with captioning between the deaf, hearing impaired with normal people, as shown in Table 4.

Table 4 Difference Test Results, Satisfaction in Captioning Classified by Hearing Level

Hearing level	amount	average	standard deviation	F Value	df	p.
normal people.	67	3.6866	0.95233	3.183	201	0.044*
hearing Impaired	38	3.2263	0.86639			
deaf	97	3.6392	0.99651			
Total	202	3.5772	0.96922			

From Table 4 explains that people with hearing impaired were less satisfied with providing captioning than the deaf and normal. Considering the details of providing captioning for testing to know the hearing level group, there was a satisfaction in providing subtitles instead of audio. Using the Least Significant Difference (LSD) method for multiple comparisons, which resulted in the test results as shown in Table 5.

Table 5 Multiple Comparisons to Test Differences in Narration Instead of Audio Satisfaction Classified by Hearing Level group

Hearing Level	normal people		hearing impaired	deaf
	3.6866	3.2263	3.6392	
normal people	3.6866	-	0.46025* (0.019)	0.04739 (0.756)
hearing impaired	3.2263	-0.46025* (0.019)	-	-0.41286* (0.026)
deaf	3.6392	-0.04739 (0.756)	0.41286* (0.026)	-

From Table 5 explains that hearing impaired people were less satisfied with providing captioning than normal people. There was less satisfied with providing captioning than deaf people. There was different from the sign language interpreter service satisfaction survey. It was statistically not statistically significantly different from the sign language interpreter service. As shown in Table 6.

Table 6 Results of Sign Language Interpreter Satisfaction Difference Test Results Classified by hearing level

Hearing level	amount	average	standard deviation	F Value	df	p.
normal people	67	3.9701	0.90403	2.486	201	0.086
hearing impaired	38	3.5421	1.18359			
deaf	97	3.9134	0.97635			
Total	202	3.8624	1.00302			

Discussion

According to this study, sign language interpretation and captioning services can satisfy the normal people, the hearing impaired and the deaf. Instead, they found that hearing impaired people were less satisfied with captioning on average than the samples who were normal and the deaf. However, this study found that people with hearing impairments were worthy of satisfaction in providing subtitles instead of voices (3.2263) while normal were satisfied with captioning (3.6866) and the deaf were worth the satisfaction of providing captioning (3.6392). When comparing multiples to test the differences in satisfaction in providing captioning. Classified by hearing level group, hearing impaired people were less satisfied with providing captioning than normal and were less satisfied with providing captioning than deaf people at a significant level of 0.05.

It was reality because the manufacturer has not yet fully complies with the law. Because of the overlap of definitions in the law, such as news programs or material types, captioning broadcast times cannot be calculated instead of audio. Sign language interpreter and audio description too. (Sirimit

Praphanturakit, 2019, pp. 172 -173), while Waiyawut Wuthiastarn surveyed the need for closed captioning of viewers in Bangkok. It was found that closed captioning or captions were less satisfying in deaf than normal people (Waiyawut Wuthiastarn, 2019, p. 207). Research by Li, Gong and Kawabata, Yasuhiro, (2021) found that using graphics and character in TV news programs may increase the emphasis on news content. When the experiment was conducted, it was found that the color and concentration of graphics and letters were found. It can stimulate the audience's perception of the TV news. In this study, graphics and apostles were used in weather programs, which was highly likely that graphics and apostles generate interest that interfere with character in the captioning of the hearing impaired. As a result, the results of the satisfaction survey had lower scores than normal and deaf people.

References

- Gong, L. and Yasuhiro, K. (2021). “Effects of OCT color on value perception in the news context”. Retrieved from https://www.researchgate.net/publication/354760963_Effects_of_open_caption_telo_color_on_value_perception_in_the_news_context_From_the_tone_perspective.
- Praphanturakit, S. (2019). “Rethinking Genre and Proportions of Services for Sign Language, Closed Captions and Audio Description in Thai Television Enterprises”. *Journal of Journalism*, 12 (1), 124-190.
- Wuthiastarn, W. (2019). “A Survey of Closed Captions Viewing in Bangkok”. *Journal of Journalism*, 12(1), 191-214.



RMUTCON

Session 8:

**Food Innovation and
Smart Farm**

Effect of Temperature on Ascorbic Acid and Lycopene in Mixed Tomato Juice and Mandarin Juice

Wattana Wirivutthikorn^{1*} and KMS Jodie Lazuardi Haickal²

¹Department of Agro Industrial Technology, Faculty of Agricultural Technology, Rajamangala University of Technology Thanyaburi, Pathum Thani, 12130, Thailand

²Department of Food Science and Technology, Faculty of Agricultural Engineering and Technology IPB University Kampus IPB Dramaga Bogor, 16680, West Java, Indonesia

* Corresponding email: wattana@rmutt.ac.th

Abstract

The maintaining levels of major nutrients which the main compositions during manufacturing are essential criterion to manufacture qualities of mixed Thai fruit juices. The purpose of this research was to study the effects of different pasteurized temperatures on ascorbic acid and lycopene in mixed Thai mandarins and tomatoes beverage products. This research consisted in four experiments: 1) no pasteurization (control); 2) pasteurization temperature of 65°C for 30 minutes; 3) pasteurization temperature of 70°C for 15 minutes and 4) pasteurization temperature of 75°C for 1 minute. Physical properties (L^* , color as $+a^*$ and $+b^*$, sedimentation and total soluble solid) were significantly different in all experiments ($p \leq 0.05$), but except for the pH and sedimentation. Experiment 1 received the lowest values of a^* , b^* and percent of sedimentation of 4.90, 4.63 and 18.84, respectively. Chemical properties (percentage of acidity, ascorbic acid and lycopene) were evaluated. The results showed that Experiment 1 had the highest ascorbic acid and lycopene contents values of 7.11 mg/100 ml and 52.6 mg/100 ml, respectively. The study of product shelf life was done at temperature of 4°C for 15 days. It was found that the Experiment 4 had the highest ascorbic acid loss values of 4.54 mg / 100 ml, whereas the Experiment 3 gave the lowest percentage of lycopene loss values of 19.64. The chemical properties revealed that the temperature was increased higher than 65°C, but the pasteurization time was reduced. The tendency of loss of ascorbic acid was not different, otherwise lycopene degradation received higher values than control. The results obtained, the study on effects of heat on ascorbic acid and lycopene in heated and tomatoes, as heat treatment underneath various manufacturing factors would capable to the most manufacturing determinants effective for good production of beverage in the industrial scales.

Keywords: Ascorbic Acid, Lycopene, Tomato, Mandarin, Juice.

Introduction

Nowadays, health drink products play a greater role in everyday life, with most of the drinks being derived from the ingredients of plants or herbs. Few consumers may not require vegetables, but they can enjoy the benefits of the various types of Thai herbs that can be processed in the form of health drinks. At present, the product of beverage enrolls a higher part in a daily breath, with ready-to-drink fruit juices in the local mart. In Thailand, most of the beverages being modified from the mixed ingredients of Thai plants. Most consumers do not like to take vegetables due to the unpleasant odor and bitter taste of vegetables. The advantages of the various kinds of Thai crops that can be manufactured in the health drinks form in different kinds of ready-to-drink mixed Thai fruits and Thai vegetable beverages (Pinitglang and Saiprajong 2018). Tomatoes are the plant botanically of the fruits of learnt such as *Lycopersicon esculentum*. Tomatoes have popularly been revealed to be a good beginning origin of nutrient values, for example natural antioxidants comprising ascorbic acid (vitamin C) vitamins A and complexes of vitamin B, the same as

flavonoid, and the mixed lycopene carotenoid. Lycopenes have been concerned like cholesterol lowering compounds with as antioxidants. One fruit, i.e. dried tomato consists of 9 percent water, contains of 4 percent carbohydrate and less than 1 percent each of protein and fat. One hundred grams quantities, raw tomato has 14 milligrams of ascorbic acid and 449 micrograms of β -carotene. (Rathleen et al. 2000). Tomato juice is interesting more intention due to the phytochemical values of a lot of Thai vegetables. Product of tomatoes are expanding in reputation related to postulates of scientific which lycopenes, the main pigments of carotenoid related red color within tomato, has anti carcinogenic and anti inflammatory property. Different carotene as β type and other closely connected carotenoid, lycopene activity has no pro-vitamin A interaction. (Horvitz et al. 2004). Mandarins are essential for the delicious flavor of their new fruits, but relatively few data are available citrus fruits, for example oranges or lemons. Mandarins are essential chemical components, comprising of 34 μg / 100 g of vitamin A and 155 μg / 100 g of carotene as β -types. (Shaw 1991). Extraction of Juices are main methods to have sufficient water amounts, enzyme, vitamin and mineral, all necessary for well-being. The citrus manufacturing industry observes the market of all requires for products of manufacturing which has properties look alike latest products. Ready to serve citrus juice manufacturing has constituted ordinary within some ages; those beverages will form in an absence of the long-established manufacture over limited water voiding and its succeeding restoring at the point of use (Crupi and Rispoli 2002). Pasteurization has long been the standard method to extend the shelf-life of fruit vegetable juice and dairy products, as well as a means to reduce microbial load and the risk of food-borne pathogens. However, the process has limitations, which include cost effectiveness, high energy input, and reduction of product quality/sensory evaluation. Currently, the shelf-life of closed container, pasteurized milk is 8–14 days depending on the level of the heat treatment and the process itself uses a significant amount of energy (Myer et al 2016). The researcher was interested in further study of the previous research, but lacking of important information about the effects of pasteurization on fruit juice qualities. (Wirivutthikorn 2020). This will be an advantage method in preventing the loss of nutrients such as ascorbic acid, lycopene and save energy to a minimum value in order to keep the maximum nutritional values. The main factor aims of the work was to study the suitable impacts time and temperature conditions on the products as physico-chemical qualities in terms of brightness and color (L^* , $+a^*$ and $+b^*$ values), percentage of sedimentation and total soluble solid, pH, total acidity, ascorbic acid and lycopene and the shelf life of the products. The database gained from the work was a good choice to make tomatoes and mandarins as main Thai raw material for health drink manufacturing to enhance the essential nutritional qualities and good health of consumers also find a solution to the issue of utilization by product that are manufactured with additional values.

Experiment

Physico-Chemical Attributes of Mixed Beverages in Raw Materials

The first procedure in preparation process of mixed beverage (40:60 ratio of mandarins and tomatoes drink) in order that evaluate some properties of physico-chemistry (other characteristics was described in the analysis of physico-chemical products qualities procedure) such as: TSS (total soluble solids), pH, percentage of total acidity, lycopene and ascorbic acid contents were measured as numerical changes modified from Wirivutthikorn (2020).

Effect of Temperature and Pasteurization Time on Ascorbic Acid and Lycopene Contents in Mixed Mandarin Juices and Tomato Juices

The work was carried out as four experiments (three replications) by selection the best condition (mixed mandarin juices and tomato juices 40:60) from Wirivutthikorn (2020) which were: 1) no pasteurization (control); 2) pasteurization temperature at 65°C, 30 minutes; 3) pasteurization

temperature at 70°C, 15 minutes; 4) pasteurization temperature at 75°C, 1 minute. The tomatoes were washed using clean water and cut into small pieces (diameter 4-5 centimetres) and extracted them with a juice extractor, subsequently filtered through white cheesecloth in frozen stainless steel. The mandarins were thoroughly washed using clean water, halved them into small pieces (diameter 5 centimetres) and extracted them with a juice extractor using clean water in frozen stainless steel as preparation of tomatoes. The mixed juices were aerated using steam injection in stainless steel pot. After that, studying effects of temperatures and times explained in each experiment. These mixed juices were put within a 250 milliliter of colored glass bottles (sterilized type) covered with a lid immediately cool with cold water and storage temperature (4°C, 15 days) for further physico-chemical qualities analysis (Xiumin et al. 2019).

Numerical Data Analysis

Data were evaluated and marked from all experiments (three repetitions) for data analysis. This design of experimental as physical and chemical qualities were computed using a design of factorial completely randomized (CRD) 4x4. Evaluation of these differences of the mean within all treatments were computed with the method of DMRT (New multiple range test of Duncan) at $p \leq 0.05$ using SPSS software version 17 (Aydar 2019).

Analysis of Physical Appearances

The physical appearance of the products was performed as physical changes by observation with the eye. The observed values were recorded as: appearance, color, smell and taste. The results were appeared in Table 1.

Analysis of Physico-Chemical Products Qualities

The preparation process of all examples from in the solution form were poured into the beaker of 50 milliliter to analyze as (L^*) value (lightness) and color as ($+a^*$) value (redness) and ($+b^*$) value (yellowness) were performed with Minolta model CR-10 instrument as recorded values modified from as AOAC (2005). This score of sedimentation was measured using of a 200 milliliter of cylinder of scaling (pour 100 milliliter of liquid into 100 milliliter of cylinder of scaling and stand at lower temperature (4°C) (24 hours) to remark and record changes of sedimentation level as percentage marks modified from AOAC (2005).

The preparation process of all examples in the a solution form were the same as above L^* , a^* and b^* method to analyze value of pH (AOAC 2000) and percentage of total acidity were marked with meter of pH (OHAUS ST 3100 F type) and titration with sodium hydroxide (0.1 N), phenolphthalein (indicator marks) modified from Pomeranz and Meloan (1994). This total soluble solid was analyzed by addition 1-2 drops of aliquot onto the hand refractometer and marked value as ($^{\circ}$ Brix) modified from Pomeranz and Meloan (1994). The lycopene and ascorbic acid were also analyzed as numerical marks modified from AOAC (2000); Pomeranz and Meloan (1994). All of the products were kept at 4°C for 15 days to investigate chemical values and observed the transitions in the quantity of total ascorbic acid and total lycopene values (AOAC 2000; Pomeranz and Meloan 1994).

Shelf Life Investigation of Lycopene and Ascorbic Acid Amounts of Mixed Mandarins and Tomatoes Beverage Product during 15 days

All of the products that had been prepared and evaluated for the above data. It had been used to study the shelf life of them. All of these products were kept at 4°C in the controlled refrigerator cabinet for 15 days. This research focused on the clearly chemical changes of lycopene and ascorbic acid during 15 days (0,5,10 and 15) which changed over a wide range of 7-10 days (Xiumin et al. 2019).

Results and Discussion

1. Analysis Results of Preliminary of Chemical Properties. Mandarin and tomato drinks that could be prepared. These data showed which mandarin and tomato drinks gave few values of pH of 3.35 and 4.15, respectively. This percentage of total acidity (calculated values as citric acid form) and TSS (total soluble solids) in mandarin and tomato drinks were 0.84, 9.16°Brix and 0.35, 7.58°Brix, respectively. Ascorbic acid content within mandarin and tomato drinks were 8.67 and 5.42 milligram / millilitre, respectively. Lycopene content within tomato drink was 50.90 milligram /100 gram. From the chemical properties analysis, mandarin drink revealed which gave higher value of pH than tomato drink, however received higher total acidity percentage. This ascorbic acid content was similarly, since tomato comprises range of ten percent of organic acids and five to ten percent of solids, those were less than mandarin juices. In nature, acids of organic are appeared in the fruit forms of malic acid and citric acid. This essential coloring substance consists within mandarin and tomato drinks is a lycopene type, that is a dark- red crystal during the maturation of tomato. This value was higher than the mandarin juices (Hussain et al. 2019; Li et al. 2019) The analysis results were related with the latest research (Wirivutthikorn 2020).

Table 1 Main Characteristics of Mixed Mandarins and Tomatoes Beverage Product.

Experiments	Attributes			
	appearance	color	odor	taste
no pasteurization	many suspended tomato	bright red	only tomato	sweet and sour
pasteurization temperature at 65°C, 30 minutes	many suspended tomato	bright red	tomato and little mandarin	sweet and sour
pasteurization temperature at 70°C, 15 minutes	medium suspended tomato	little mixed red and orange	tomato and little mandarin	sweet and sour
pasteurization temperature at 75°C, 1 minute	few suspended tomato	little mixed red and orange	tomato and little mandarin	sweet and sour

2. Physical Appearances. From Table 1, observation all the external characteristics of the products, it was found that the tendency of different temperatures and times affected on the color of the product and the amount and dispersion of sedimentation, but did not affect on the odor and taste. This effect could be explained as a consequence of the losses of lycopene and ascorbic acid during the heating process at different temperatures and times. The using of higher pasteurization temperatures results in pale color concerned to the use of higher temperatures to accelerate the oxidation and isomerization reactions quickly (Hussain et al. 2019; Wirivutthikorn 2020).

Table 2 Analysis of Physical Properties of Mixed Mandarins and Tomatoes Beverage Product.

Experiments	Analyzed values					
	pH ^{ns}	TSS [*]	L [*]	+a ^{*ns}	+b [*]	sedimentation ^{ns} (%)
no pasteurization	3.37	7.87 ^b	35.50 ^b	4.90	4.63 ^b	18.84
pasteurization temperature at 65°C, 30 minutes	3.38	8.70 ^a	34.73 ^c	5.35	4.90 ^b	21.59
pasteurization temperature at 70°C, 15 minutes	3.38	7.37 ^c	36.13 ^a	5.50	7.33 ^a	21.49
pasteurization temperature at 75°C, 1 minute	3.38	6.40 ^d	34.83 ^c	5.75	5.20 ^b	20.94

*a,b,...means various consonants within a column reveal differences evaluated by means of DMRT. (new multiple range test of Duncan) at the 95 percent level of significance, ns = non significant.

3. Physical Characteristics. The result from Table 2 indicated a tendency for the (L*) (brightness) and color as (+a*) (redness) and (+b*) (yellowness) value and percentage of sedimentations depend upon various time ratios relation with temperature. The result concerned which whole marks were statistical differences ($p \leq 0.05$) (whereas on +a* and percentage of sedimentation value). The use of heat at high temperatures and times differences affect on the L*, +a* and +b* (Hussain et al. 2019). The brightness and yellowness did not tend to increase with increasing temperatures and times except for the redness. According to the experimental method, because at high temperature, ascorbic acid decomposes easily. These isomer forms which are within all of trans are within the mono cis type or poly cis form with interactions of oxidation. Two changes of these interactions be able to appear at the same time. Isomerization interaction during heat treatment, isomerization of carotenoids trans-cis be able to appear versus this association versus temperature and time. These changes involve process clearly results in a change in color but did not affect on the change in the aroma and taste of the products (Li et al. 2019). Naturally, the mandarin juice and tomato juice are bright yellow color (Chiang et al. 2008). There was a tendency toward redness value was increasing due to amount of high temperature (Li et al. 2019). Both tomato and mandarin have opaque fibers and suspended in the aliquot. The volume of sedimentation measurement was not significantly different ($p > 0.05$). Possible reasons were that the ratio of tomatoes to mandarins are the same in all experiments, therefore, the sediment quantity was not different (Qia et al. 2019). The pH was not statistically different. The results from the pH measurement could be seen that there was no statistical difference due to the tendency of heat, high temperatures and time differences, which did not affect on the measurement. The measured values depend on the fruit types and mixed ratios. In addition, both of the same ratios were used, resulting in no difference in measurement values. The total soluble solid from each treatment was different (Wen et al. 2019). This difference causes in the production process, the heat causes the water to evaporate, resulting in an increase in the amount of dissolved solids. The experiment with pasteurization temperature at 65°C, 30 minutes received the highest total soluble solid. One possible reason is that in addition to heat at high temperatures, time is an important factor, and this experiment used the maximum heating time, resulting in the chemical decomposition resulting in the amount of total soluble solid.

Table 3 Analysis of Chemical Properties of Mixed Mandarins and Tomatoes Beverage Product.

Experiments	Analyzed values		
	TA*	AA*	LP*
no pasteurization	0.65 ^a	7.11 ^a	52.6 ^a
pasteurization temperature at 65°C, 30 minutes	0.59 ^b	4.69 ^c	51.9 ^a
pasteurization temperature at 70°C, 15 minutes	0.54 ^c	4.99 ^c	45.1 ^b
pasteurization temperature at 75°C, 1 minute	0.52 ^d	6.65 ^b	42.7 ^c

N.B. *TSS = total soluble solid (°Brix), *TA = total acidity (%), *AA = ascorbic acid (mg/100 ml), *LP = lycopene (mg/100 ml).

*a,b,...means various consonants within a column reveal differences evaluated by means of DMRT (new multiple range test of Duncan) at the 95 percent level of significance, ns = non significant.

4. Chemical Characteristics. From Table 3, the result showed that the total soluble solid, total acidity percentage, ascorbic acid and lycopene were significantly different ($p \leq 0.05$). There was a tendency change was corresponding with the total acidity in the citric acid form that was lower with the increased times at high temperatures. Naturally, organic acids (such as citric acid and other acid) are found in a lot of food types involving sour taste fruits or juices, for example tangerine and lemon. Because of tomatoes and mandarins contain carotenoid as an important pigment (Siti Rashima et al. 2019). Moreover, tangerine is a good source of ascorbic acid, tomato juices also contain more β -carotene and lycopene than the tangerine juices, those are modified out of fruit which is yellow. Because the people consume juices of tomato and juices of tangerine and would be changed to carotenoids as vitamin A form and β carotene, comprising some acids of organic, for example high acid of malic and acid of citric acid, consequence within tastes of sour. Increasing the heating temperature results in a chemical change compared to the sample within computed ascorbic acid value quantity (Nawade et al. 2020). Furthermore, the tomato juices also contain less lycopene and β carotene than juices of mandarin, which are modified from some fruits that are yellow (Nawade et al. 2020). These results indicated that the use of various temperatures and times results in the decomposition of various levels of ascorbic acid. This reduced value concern ascorbic acid is water soluble vitamin, few stabilities, easy degradation since contacted to air and illumination, heat and some ions of metal. This L-ascorbic acid degradation throughout the period of storage involves oxygen oxidation left within headspace throughout hot loading manufacture, however these values were too great differences, feasibly because of ratios water and carrot juices (Akpolat et al. 2020). These various lycopene values decreased in the higher with decreasing in the temperature at 75°C for 1 minute. Many possible reasons are by reason of the quantity of heat spend within manufacturing step, resultant within arrangement of lycopene a high temperature isomer, because the structure of carotenoids (as natural) are within form of trans. Heat treatment as pasteurization, sterilization or radiation are changed into the form of cis that is more fluent within interaction than trans form and will absorb illumination at less ranges of an appropriate wavelength (Wirivutthikorn 2018) resultant within less marks. Besides, the degradation interaction by reason of oxidation interactions such good as ascorbic acid changes. This chemical reaction changes relates to the quantity of oxygen and lights. This ascorbic acid degradation be able to be discharged using prolonged times. It is able to be associated by trans isomer interaction (Charoenphun and Sophe 2018; Wirivutthikorn 2019).

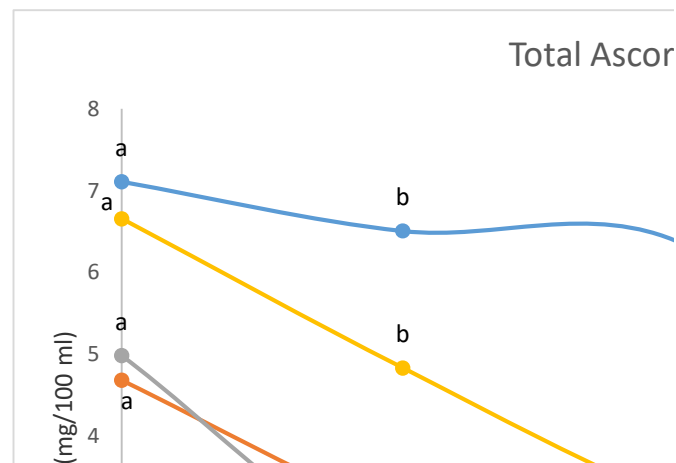


Figure 1 Relationships of Total Ascorbic Acid at Different Storage Time.

N.B. Experiment 1 means no pasteurization.

Experiment 2 means pasteurization temperature at 65°C, 30 minutes.

Experiment 3 means pasteurization temperature at 70°C, 15 minutes.

Experiment 4 means pasteurization temperature at 75°C, 1 minute.

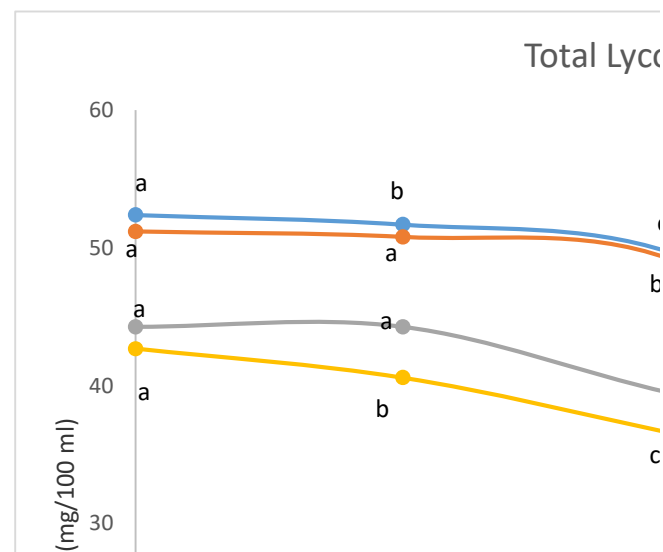


Figure 2 Relationships of Total Lycopene at Different Storage Time.

N.B. Experiment 1 means no pasteurization.

Experiment 2 means pasteurization temperature at 65°C, 30 minutes.

Experiment 3 means pasteurization temperature at 70°C, 15 minutes.

Experiment 4 means pasteurization temperature at 75°C, 1 minute.

5. Changes of Total Ascorbic Acid during 15 Days. The results indicated a tendency of total ascorbic acid relationships at different storage (Figure 1), time and period referred very fast from this result of the investigations. This result indicated that the tendencies of vitamin C to decrease in all experiments from the day 1 to the day 15. All products were stored at 4°C on the quantity of ascorbic acid for during of 15 days and measured ascorbic acid every 5 days. These products were stored at cold temperature until the day 15. The result showed that the quantity of ascorbic acid was in the range of 1.50-3.80 mg / 100 ml. The ascorbic acid amount decreased from initial value. The fact, an example of a water soluble vitamin, i.e. ascorbic acid has little stability,

can degrade certainly while exposed within the sun, some oxygen, mild heat some metal ions and storage environments. Moreover, this pasteurization or sterilization manufacture temperature destroy ascorbic acid form, resulting in quicker decomposition in the L-ascorbic acid form rather than the type of D ascorbic acid. Furthermore, by reason of the product storage period, the interaction of oxidation can react and might respond out of the rest gas of oxygen within this packaging storage the hot or cold comprising manufactures (Wirivutthikorn 2019). The ascorbic acid is the main factors of a lot of decomposition. Based on theory, the ascorbic acid is a strong reducing substance, hence it is easily oxidized in the air environment, unstable and clearly degrades when heated underneath at high temperatures. Moreover, from the information, it was found that the storage during in range of 5-15 days, the quantity of ascorbic acid rapidly decreased in overall experiments. These causes due to ascorbic acid degradation are associated with accumulated oxygen amount, flame, and storage environments (Kumar Saini and Sookeum 2018; Peng et al. 2018; Wirivutthikorn 2020).

6. Changes of Total Lycopene during 15 Days. There was a tendency toward relationships of lycopene at different storage (Figure 2) it showed that the trend changes of lycopene to decrease less than the ascorbic acid transits in all experiments from the day 1 to the day 15. On the lycopene quantity for 15 periods, this lycopene measurement (each and every 5 days) revealed which this lycopene quantity gave this trends decreased within the primary of 5 days of storage intervals. Next, it showed a tendency to reduce quick up to the day 15. For a possible reason, tomato is a bright red pigment (carotenoid as a main pigment), has a lot of lycopene content, may change into dark red products, and the lycopene quantity are found in concentrated tomato is usually lower than it. Due to the losses that occur during the lycopene manufacturing has a major number of double bonds, which can forecast that there are two transits in the manufacturing and lycopene storage into isomerization interaction (Ancos et al. 2020; Wirivutthikorn 2019; Wirivutthikorn 2020). About these isomers which are within overall trans form is within as mono-cis or poly- cis types with oxidation reaction. Overall of the chemical interactions be able to appear at the same time. Isomerizations throughout at high temperature manufacturing, carotenoids cis and tran isomerizations be able to appear versus some relationships about time cause effects within during product shelf life. There is no added interaction of cis and trans isomerizations, except for have a tendency to especially this reverse change trans interaction and the interaction which be able to increase primarily, after that oxidation reaction is degradation of lycopene out of the interaction of oxidation, that is non reversible interaction type and will be caused to degrade. Based on related theory, some little molecules section associate such as various substances i.e. methyl heptinone, acetone, aldehyde, levulinic acid and they possibly exposed glyoxal, those cause the visible color freshening. For one possible reason, lycopene are found in Thai plants as fruit and vegetable associate with protein to a complicated structure form in the food network system. Hence, the heat treatment at various temperatures and times cause the lycopene complex structure of to split. The resulting in a less stable lycopene, resulting in added sensitivity to ultraviolets, lights, heats, acids and oxygen. For the above reasons about products cause to mention unstable products during shelf life. These reactions depend on various parameters, involving physical characteristics chemical changes such as the manufacturing steps, moisture content, water activity, detection of oxygen gas conditions with some metal ions for example and iron and copper. The appearance of compounds that stimulate or restrict oxidation of chemical reaction and lipid components underneath highly strong acid and base states (Ancos et al. 2020; Obasi et al. 2017; Wirivutthikorn 2019; Wirivutthikorn 2020).

Conclusion

In conclusion, studying of different heat treatment affected on the physical and the chemical properties of blended mandarins and tomatoes juices. Experiment 3 gave the lowest percentage of lycopene loss values of 19.64. The results indicated that the formulation of beverage produced from Thai fruits and vegetables can be developed as its nutritional and antioxidant qualities can be accepted by consumers.

Acknowledgments

The researchers would like to thank the 4th grade students and officials of the Department of Agro Industrial Technology, the Faculty of Agricultural Technology Rajamangala University of Technology Thanyaburi (RMUTT), Pathum Thani, Thailand that contributed some parts in the research. The Faculty of Agricultural Technology provided support facilities and budgets on our research for this conference.

References

- Akpolat, H. et al. (2020, July). High-throughput phenotyping approach for screening major carotenoids of tomato by handheld raman spectroscopy using chemometric methods. *Sensors*, 20: 1-13.
- Ancos, B.D., Rodrigo, M.J., Moreno, C.S., Cano, M.P., & Zacarias, L. (2020, June). Effect of high-pressure processing applied as pretreatment on carotenoids, flavonoids and vitamin C in juice of the Sweet Oranges ‘Navel’ and the Red-Fleshed ‘Cara Cara’. *Food Research International*, 132, 1-9.
- AOAC. (2005). *Official method of analysis*. 18th ed. Verginia: The Association of official Analytical Chemists.
- AOAC. (2000). *Official method of analysis*. 17th ed. Verginia: The Association of official Analytical Chemists.
- Aydar, A.Y. (2019, April). Statistical methods in optimization of food materials. *European International Journal of Science and Technology*, 8(3), 33-40.
- Charoenphun, N., & Sophe, G. (2018, March). Healthy drinks from mushrooms and longan. *J. of Science and Technology*, 28(3), 480-493.
- Chiang, K.H., Tan, F.J., & Yichi, H. (2008, April). Evaluation of microbial inactivation and physicochemical properties of pressurized tomato juice during refrigerated storage. *LWT-Food Science and Technology*, 41(3), 367-375.
- Crupi, F., & Rispoli, G. Citrus juices technology. (2002). In: Dugo G. and Di Giacomo A. (eds), *The Genus Citrus*. London: Taylor & Francis.
- Horvitz, M.A., Simon, P.W., & Tanumihardjo, S.A. (2004, April). Lycopene and β -carotene are bioavailable from lycopene ‘Red’ Carrots in humans. *European Journal of Clinical Nutrition*. 58(5), 803–811.
- Hussain, A., Pu, H., & Sun, D.W. (2019, December). Measurements of lycopene contents in fruit: A review of recent developments in conventional and novel techniques. *Critical Reviews in Food Science and Nutrition*, 59(5), 758-769.
- Kumar Saini, R., & Sookeum, Y. (2018, February). Carotenoid extraction methods: A review of recent developments. *Food Chemistry*, 240(1), 90-103.
- Li, H., Zhao, C., Tian, H., Yang, Y., & Li, W. (2019, December). Liquid–liquid microextraction based on acid–base-induced deep eutectic solvents for determination of β -carotene and lycopene in fruit juices. *Food Analytical Methods*, 12, 2777-2784.
- Myer, P.R., Parker, K.R., Kanach, A.T., Zhu, T., Morgan, M.T. & Applegate, B.M. (2016, May). The effect of a novel low temperature-short time (LTST) process to extend the shelf-life of fluid milk. *Springerplus*, 5(1), 660-667.

- Nawade, B. et al. (2020, January). Analysis of apocarotenoid volatiles during the development of *Ficus carica* fruits and characterization of carotenoid cleavage dioxygenase genes. *Plant Science*, 290, 1-13.
- Obasi, B.C. , Whong, C.M.Z. , & Ameh, J.B. (2017, July). Nutritional and sensory qualities of commercially and laboratory prepared orange juice. *African Journal of Food Science*, 11(7), 189-199.
- Peng, Q.Y., Zhu, C., & Pan, S. (2018, November). Carotenoids, flavonoids and ascorbic acid in juice of orange cv. Cara Cara. *Food Chemistry*, 265(1): 39-48.
- Pinitglang, S., & Saiprajong, R. (2018, January-April). Formulation of super berry beverage containing anthocyanin extract from Thai Black Jasmine Rice based on sensory analysis. *Agricultural Sci. J*, 49(2) (Suppl.), 25-28.
- Pomeranz, Y., & Meloan, C.E. (1994). *Food Analysis: Theory and Practice*. 3rd ed. Van Nostrand Reinhold.
- Qia, Y. et al. (2019, April). Carotenoid accumulation and gene expression in fruit skins of three differently colored persimmon cultivars during fruit growth and ripening. *Scientia Horticulturae*, 248, 282-290.
- Rathleen, M.D., Rao, A.V., & Agarwal, S. (2000, October). Role of antioxidant lycopene in cancer and heart disease. *Journal of American College of Nutrition*, 19(5), 563–569.
- Shaw, P.E. (1991). Volatile compounds in foods and beverages. In: Maarse H. (ed.), New York, NY: Marcel Dekker Inc.
- Siti Rashima, R., Maizura, M., Wan Nur Hafzan, W.M., & Hazzeman, H. (2019, October). Physicochemical properties and sensory acceptability of pineapples of different varieties and stages of maturity. *Food Research*, 3(5), 491-500.
- Wen, P., Hu, T.G., Linhardt, R.J., Liao S.T., Wu, H., & Zou, Y.X. (2018, November). Mulberry: A review of bioactive compounds and advanced processing technology. *Trends Food Sci Technol*, 83, 138-158.
- Wirivutthikorn, W. (2018, September). Effect of ratio of okra gac fruit and passion fruit on color and preferences of mixed juice. *International Journal of Food Engineering*, 4(3), 212-215.
- Wirivutthikorn, W. (2019, September). Optimum ratios of okra and tangerine on production of mixed juice with lycopene supplementation. *International Journal of GEOMATE*. Special Issue on Science, Engineering & Environment, 17(61), 8-13.
- Wirivutthikorn, W. (2020, January-April). Appropriate tomato and mandarin ratios on development of blended tomato juice and mandarin juice products. *Current Research in Nutrition and Food Science*, 8(1), 340-348.
- Wirivutthikorn, W. (2020, March). Different ratios of riceberry residues and water on health drink beverage formulation. *International Journal of GEOMATE*. Special Issue on Science, Engineering & Environment, 18(67), 128-134.
- Xiumin, F. et al. (2019, January). Lycopene cyclases determine high α - β -carotene ratio and increased carotenoids in bananas ripening at high temperatures. *Food Chemistry*, 283(15), 131-140.

Study of Relative of UAV Imagery and NDVI for Maize Yield Estimation

Phoomchai Traidalanon, Kiattisak Sangpradit *

*Department of Agricultural Machinery Engineering, Faculty of Engineering, Rajamangala
University of Technology Thanyaburi, Pathum Thani, 12110, Thailand*

** Corresponding email; k.sangpradit@rmutt.ac.th*

Abstract

The objective of this research has created an aerial geographic mapping with an unmanned aerial vehicle (UAV). This study was used for analyzing the growth of maize by using Normalized Difference Vegetation Index (NDVI). The work was considered the relation between NDVI and received from analyzing the light waves Red (668 nm), Green (560 nm), NIR (842 nm) and Red Edge (717 nm), and the products yielded from a trial area of KSP Equipment Co. Ltd. The location of the study area is in Lam Sai, Wang Noi District, Phra Nakhon Sri Ayutthaya Province which is started from June to November 2021. Areas used for experiments in the size of 12,467 square meters for separating into 198 blocks of 6x10 square meters/block. Additionally, a multispectral camera is capable of detecting 5 different wavelengths (Red, Green, Blue, NIR and Red Edge). This technique is used to capture the area of experiment. The NDVI calculations were done when the age of the maize was 82 days old and the harvesting was made when the age was 107 days old.

The results found that, the usage of multi wavelength photograph could be used to calculate NDVI. Measuring the weight of the maize seed from 10 randomly chosen areas it could be found that the relation between value of NDVI and weight of the maize seed goes in the similar direction with 87% relationship and 95% level of confidence. After then statistical values were used to predict the weight of the maize seed. The results are present as the NDVI value was 50-59%, the weight of seed is found of 8.1 kilograms. The NDVI value is 60-69%, the weight of seed is found of 15.6 kilograms. The NDVI value is 70-79%, the weight of seed is found of 23.1 kilograms. The NDVI value is 80-89%, the weight of seed is found of 30.6 kilograms. Finally, if the NDVI value is 90-100%, the weight of seed is found of 38.1 kilograms which is compared to the actual weight and the error is found of $\pm 3\%$

Keywords: *aerial mapping, UAVs, NDVI, multi-wavelength photograph, maize yield estimation*

Introduction

Corn can be classified into several types according to botanical classification and classification according to planting objectives. Fodder corn is grown to cut fresh stalks to feed animals. There are two open hybrid varieties of corn: hybrid corn and pure corn (Nantaka S.). In 2020/21, global maize production for animal feed increased by 19.78 million tons, bringing total production to 1,136.31 million tons (Bangkokbiznews). For Thailand's production in 2020, the production efficiency was 726 kg/rai/cycle, or 4.7 million tons. This is not enough to meet the domestic demand for feed corn, which is 8.7 million tons (Office of Agricultural Economics). There are also issues that caused the price of maize to fall over the past season, due to the concentration of produce from September to November. Farmers cultivate in undocumented areas resulting in low quality yields. There is a need to reduce cultivation of forest encroachment and adjust the proportion of production each season by expanding the planting area during the dry season to also replace part of the second crop (Sanddy).

Smart farming brings technology to manage the cultivation system can monitor, collect data, analyze and solve planting problems in real-time, while being able to display growth data and

predict accurate yields (ARDA). Remote sensing is one of the Technology to assist in measurement and to analyze data such as photographic analysis, Normalized Difference Vegetation Index (NDVI), stem number or yield measurement (Mitr Phol). To further improve soil and increase soil fertility, an unmanned aerial vehicle (UAV) was used to create an aerial geographic mapping, with applications based on data acquisition frequency and the altitude of aerial photography from each type of aircraft. Images obtained by UAV are relatively high resolution compared to satellite images. The spatial resolution is quite limited. Users should take pictures on clearly days and this drone photography has low coverage, hotspot area just 1 -1 0 km². Spectral Resolution selection varies depending on user needs. Currently, many types are used like multispectral, hyperspectral and thermal (Paolo D.F.). Moreover, precision farming is one of the agricultural revolutions which focuses on the right management in the right place at a reasonable rate and at the right time, both in terms of the fertilizing use of pesticides sowing or tilling and irrigation to increase the yield or quality of crops and reduce the use of fertilizers and pesticides (David J.M.).

The NDVI vegetative index was measured by plant leaf Near-infrared spectroscopy (NIR) reflectance, with mature plants having a higher reflectance than incomplete plants. The work was considered the relation between NDVI and received from analyzing the light waves Red (668 nm), Green (560 nm), NIR (842 nm) and Red Edge. (717 nm). Digital photographs were used to assess the area of rice leaves for analysis of rice growth trends. It is most accurate at 12:00 a.m., when it is brightest. But there was also an error that caused the analysis to shift as more and more plants grew to the point of overlapping leaves (Napat R.). There are also many applications for NDVI and aerial photography, NDVI response and yield studies on nitrogen fertilizer application in waxy corn (Panath J.), sugarcane production evaluation (Preeyanan S. and Cheerawat N.). Multi-spectral photography is more costly than normal photography. Sometimes, plant detection and counting can also be done from High resolution RGB photos using unmanned aerial vehicles (Etienne D.), but these methods have limited efficiency. This is because plant health cannot be analyzed from colors that invisible to the naked eye.

The main objective of this study is to apply aerial imagery of unmanned aerial vehicles to generate aerial geographic mapping and to perform a Normalized Difference Vegetation Index (NDVI) for maize yield estimation.

Materials and Methods

Study area and plant material

The location of the study area is at KSP Equipment Co. Ltd., in Lam Sai, Wang Noi District, Phra Nakhon Sri Ayutthaya Province, Thailand. Cultivation of fodder corn on the aforementioned areas started from June to November 2021. The experimental area of 12,467 square meters was divided into two equal parts: plot A and plot B. Plot A is a witness. There is no soil amendment in this area. Plot B has a soil improvement, which is the location that we are interested in this study. The maize used for the test was cultivar CP303 with a fresh harvest of 105 days and a dry harvest of 115 days. This maize variety can be grown in both flat and hilly areas, provided that the soil is fertile and there is good rainfall. The average yield should be expected at 1,500-2,000 kg/rai at 25-30% humidity (CPP). For this study, planting distance of 70 x 17 centimeters, 1 plant per hole, equivalent to 13,400 plants/rai. Fertilizer period is 14, 25 and 40 days. Basically, maize fertilization was applied 2 times at 14 and 40 days of maize, but this study helped to improve the precision fertilization. Therefore, additional fertilization was applied at 25 days of maize as shown in Table 1. Watering during the corn growth phase, after the corn has germinated, is in the average amount of 50 cubic meters/rai/week.

Table 1 Fertilizers given to maize

Fertilizing while planting		1 st time		2 nd and 3 rd time
Fertilizer formula	0-0-60	18-46-0	46-0-0	46-0-0
Fertilizer amount (kg/rai)	19	14	14	18

Figure 1 shows the reference grid was placed on maize field. On the side enclosed by flagpoles is an analytical area of 1 x 1 square meters/block, and on the sides a reference grid of 3 x 3 square meters/block is drawn. Next, we analyze images from drones and NDVI by keeping a yield value of at least about 50 grid per test plot.



Figure 1 Reference grid on maize field

Data acquisition device and software

The camera drone used is the Dji Matrice 200 Series V2, a medium-sized drone (Figure 2). This drone is wind resistant, allowing for continuous shooting and can detect obstacles in all directions. If using a small drone, it can't fight the wind. Shooting can be highly error-prone. This device can be used in conjunction with the App Pix4 Dcapture to map the flight and to command automatic flight.



Figure 2 Camera drone

This study wanted to measure the NIR reflectance. Therefore, a specialized camera such as multispectral camera is needed. Figure 3 shows DJI Phantom 4 Multispectral which was used to

take an aerial picture for agriculture. It can be used to check soil conditions, fertility of plants to help analyze and increase productivity in agriculture. One set consists of 6 lenses: red edge, Near-Infrared(NIR), visible light, green, red and blue. This multispectral camera provides a resolution of 18.9 cm/pixel. It has a wide viewing angle (62.7°), which results in more distortion and sharpness decreased. Dji Terra is required for image analysis but its price is higher than other programs.



Figure 3 Multispectral camera

Additionally, a multispectral camera is able to detect 5 different wavelengths (Red, Green, Blue, NIR and Red Edge). This technique is used to capture the area of experiment. For aerial geographic mapping, we used other basic programs instead of expensive ones. Quantum GIS (QGIS) is a type of Geographic Information System data manipulation program with an easy to understand and easy to use Graphic User Interface (GUI). QGIS is developed under an open-source license that can be used without restrictions. QGIS is developed with a wide range of features, both for general purpose such as retrieving image data query table, analyzing location data (Spatial query) as well as presenting data in a map both offline and online (Geographic Information Division).

NDVI calculations

The NDVI calculations were done when the age of the maize was 82 days old and the harvesting was made when the age was 107 days old. Perform calculations by inserting formulas into the QGIS program. The reference equation is derived from the NDVI calculated as follows:

$$\text{Normalized Difference Vegetation Index (NDVI)} = \frac{\text{NIR} - \text{RED}}{\text{NIR} + \text{RED}}$$

Results and Discussion

Data acquisition

Field preparation for testing began in June 2021 for plot A and plot B. Then, maize was planted with seeds in July 2021. Three weeks after cultivation, the first aerial photographs were taken with drones. The image will not be analyzed with NDVI method because there is no noticeable growth. Two more photographs were then collected at 12 weeks after planting when fodder corn began to grow significantly, and at 14 weeks after planting when it approached harvest maturity. Thus, the maize was harvested at the age of 107 days in October 2021. NDVI calculations were used for the following last two aerial photographs. Figure 4 shows the three aerial photographs that were mapped on the Plot B using the QGIS program.

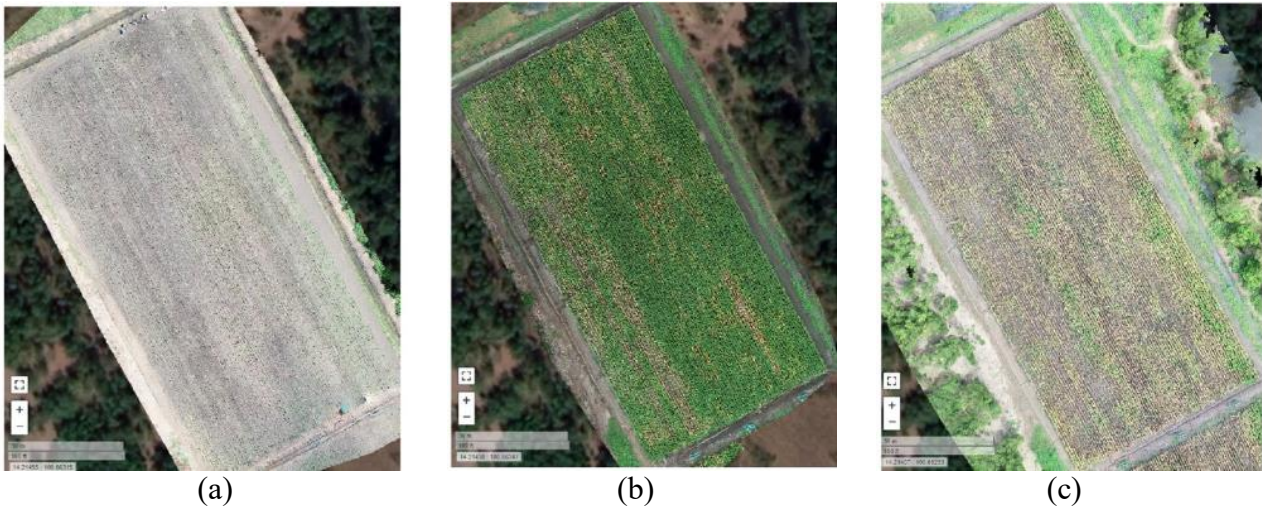


Figure 4 Drone photographs on (a) 3 weeks after planting, (b) 12 weeks after planting, and (c) 14 weeks after planting

Reference grid

A reference grid of 1 x 1 square meters/block and 3 x 3 square meters/block was tested on the QGIS program. As shown in the Figure 5, both grid reference cases were found to result in too many blocks. It is inconvenient to study each block. Therefore, the new size was resized to have a value of 6 x 10 square meters/block and a total of 99 blocks was obtained. When we consider the total area of both plot A and plot B, areas used for experiments of 12,467 square meters for separating into 198 blocks.

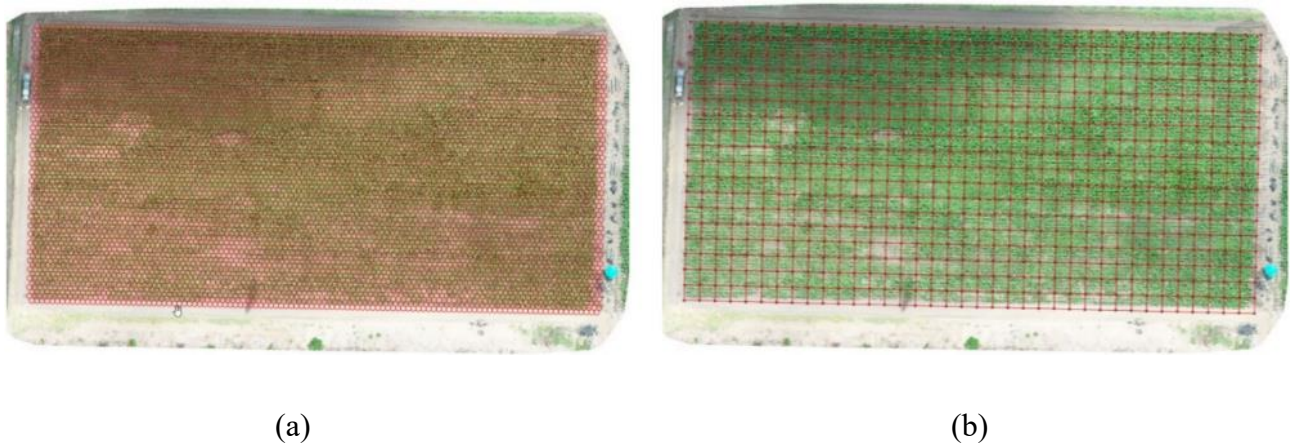


Figure 5 Reference grid of (a) 1 x 1 square meters, and (b) 3 x 3 square meters

The showed found that the use of multi wavelength photography could be used to calculate NDVI. Figure 6 shows the measurement of the maize seed weight from 10 randomly selected areas on the two plots. There are two reasons for the randomization of such areas. First, it is easier to harvesting and secondly, we want to select a percentage of canopy in the range of 50 to 100. Each block also shows additional details as shown in Figure 7; including the ID name, coordinate in Universal Transverse Mercator (UTM) system, and percentage of canopy. The UTM coordinate system is a series of sixty zones that project east and north coordinates in meters. The distance from

the central median is the east coordinate and the distance from the equator for all zones is the north coordinate (The Engineering ToolBox). Users can filter the minimum and maximum canopy level to see the values of interest which showed a blue box around the zone. It can be operated separately between plot A and plot B.

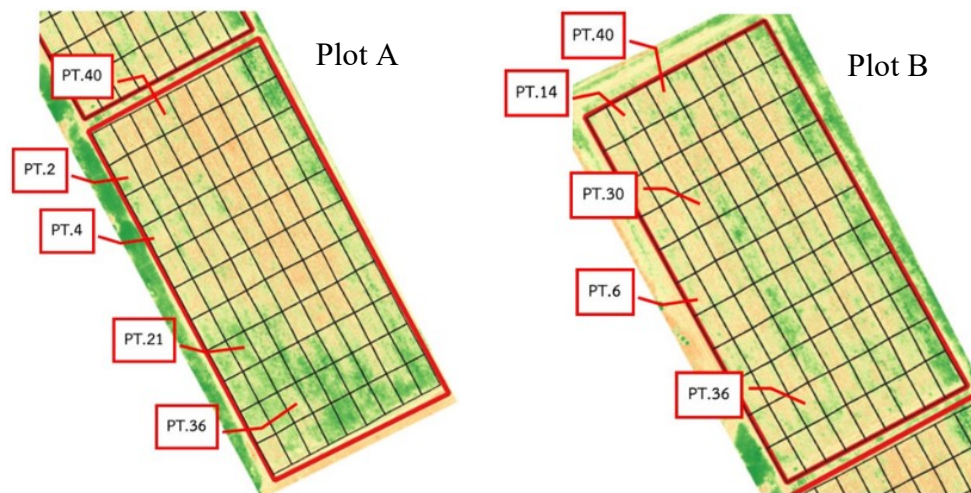


Figure 6 Randomly chosen areas on plot A and plot B



Figure 7 Information displays in each reference grid

Relative of NDVI and weight of the maize seed

On plot B, it was observed that there is a relationship between value of NDVI and weight of the maize seed from 5 randomly chosen zones. It goes in the similar direction with 87% relationship and 95% level of confidence as shown in the Figure 8. If the percentage of canopy is high, it means that the NDVI is high. It was found that the productivity was increased accordingly.

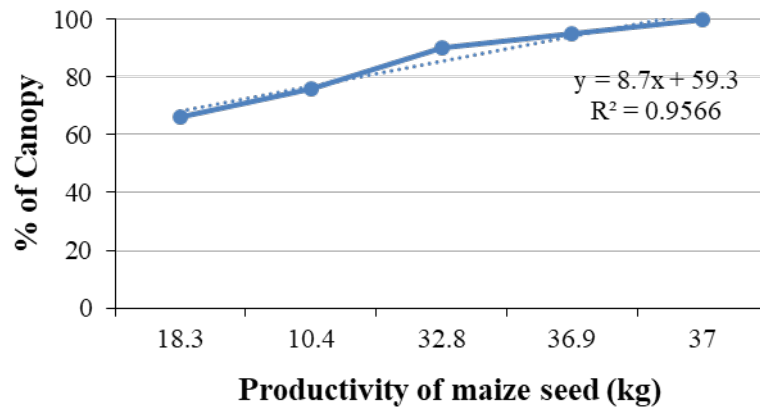


Figure 8 Relation between percentage value of canopy and weight of the maize seed

Relative of NDVI for maize yield estimation

Then, statistical values were used to predict the weight of maize seeds. Linear regression analysis is used to find the equations used to predict maize yield. According to Statistics How To, the equation of a line is $Y = a + bX$ where Y is the dependent variable, X is the independent variable, a is the y-intercept and b is the slope of the line.

$$a = \frac{(\sum y)(\sum x^2) - (\sum x)(\sum xy)}{n(\sum x^2) - (\sum x)^2}$$

$$b = \frac{n(\sum xy) - (\sum x)(\sum y)}{n(\sum x^2) - (\sum x)^2}$$

After calculating this value, the resulting linear equation is $Y = 0.75X - 36.88$ for maize yield prediction. Figure 9 shows the yield obtained from the data collection of 5 samples in plot B and calculating values from the equations obtained to predict yield for each percentage equal to the sample.

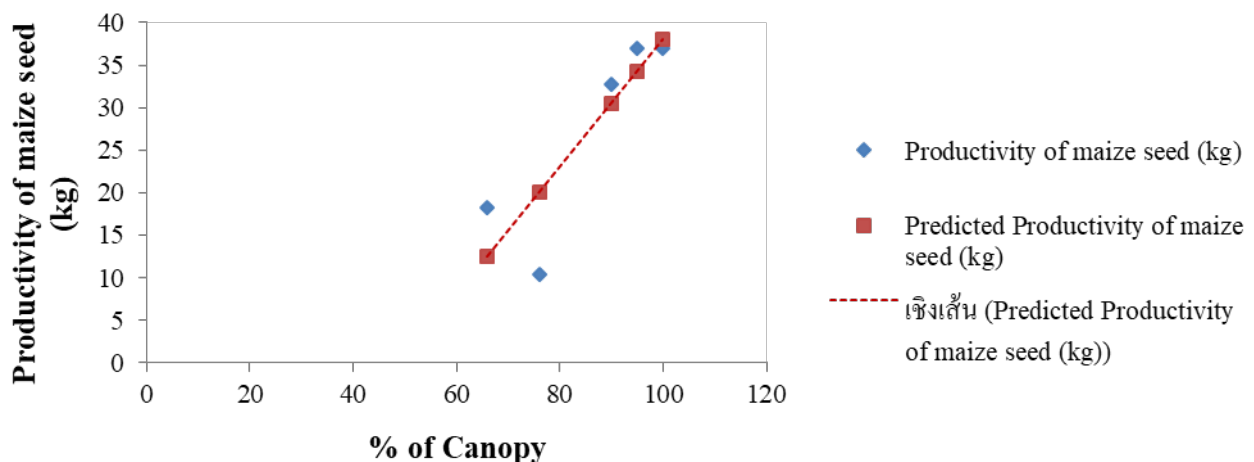


Figure 9 Relation between percentage value of canopy and productivity of the maize seed

The results obtained in table 2 are present as the NDVI value was 50-59%, the weight of seed is found of 8.1 kilograms. The NDVI value is 60-69%, the weight of seed is found of 15.6 kilograms. The NDVI value is 70-79%, the weight of seed is found of 23.1 kilograms. The NDVI value is 80-89%, the weight of seed is found of 30.6 kilograms. Finally, if the NDVI value is 90-100%, the weight of seed is found of 38.1 kilograms which is compared to the actual weight and the error is found of $\pm 3\%$.

Table 2 Value of NDVI and weight of maize seed

NDVI value	Weight of maize seed (kg)
50-59%	8.1
60-69%	15.6
70-79%	23.1
80-89%	30.6
90-100%	38.1

Conclusion

The introduction of unmanned aerial vehicles such as drones to assist in aerial photography. This helps to see the sum of all growth on the planting plot. In addition, the introduction of QGIS to help mapping and calculating the NDVI value is very useful. Because it is a program that can be used easily and for free, we can select reference grids to analyze the results as appropriate. It is also possible to display the corresponding result values at each test point with both east and north coordinates and percentage of canopy. This allows users to monitor and predict their own productivity. In addition, such analysis allows for accurate fertilizer at test points where plant fertility is a problem. This will reduce over-fertilization where the plants can grow well and can increase the total yield when all areas are equally full of growth. The test showed that the correlation of percentage completeness and yield was highly correlated with 87% relationship and 95% level of confidence. When the regression equation was found, only an error of $\pm 3\%$ in predicting yield versus yield was actually found. The values obtained from a single harvest can be inaccurate. Repeating recalculation multiple harvesting seasons is necessary to determine the accuracy of multi-wavelength image maize grain weight analysis under control parameters. In addition, the comparison with other methods in terms of accuracy or operating costs must be considered. It is important to develop techniques of yield estimation and precision fertilization in the future. The amount of fertilizer will be reduced according to the appropriateness of growth, when the corn is 25 days old.

Acknowledgments

The authors would like to thank Department of agricultural machinery engineering, Faculty of engineering, Rajamangala University of Technology Thanyaburi and KSP Equipment Co. Ltd., for cooperation and support for this research.

References

- ARDA. (2018). *Smart Farming*, Khwāmsamret læ khwām thāthāi hæng yuk samai [Smart Farming, Success and Challenges of the Ages]. Agricultural Research Development Agency (Public organization), Retrieved from https://www.arda.or.th/knowledge_detail.php?id=6.
- Bangkokbiznews. (2020). "Jurin" khø prakanphai khāophōt liang sat pīkān phalit hoksipsī ["Jurin" knocks insurance on maize for the year of production 64]. Retrieved from <https://www.bangkokbiznews.com/business/929385>.

- Cheerawat N., Khwantri S., Chanreaksa C., Jetsada P., Seree W., Supasit K. and Mahisorn W. (2019). Feasibility Study of Sugarcane Yield Prediction Using NDVI, $CI_{red\ edge}$ Indices Associated with Volume of Digital Surface Model (DSM), *Khon Kaen Agr. J.*, 47(4), 679-694.
- CPP. (2019). *Thurakit malet phan khāophōt [Corn seed business]*. Retrieved from <https://www.cpp-worldwide.com/business-type/75>.
- David J.M. and Yuxin M. (2016). Precision Farming, Land Resources Monitoring, Modeling, and Mapping with Remote Sensing, 161-178.
- Etienne D., Gaëtan D., François J., Philippe B., Alexis C., Benoit de S. and Frédéric B. (2021). Plant detection and counting from high-resolution RGB images acquired from UAVs: comparison between deep-learning and handcrafted methods with application to maize, sugar beet, and sunflower crops, bioRxiv preprint, 1-18.
- Geographic Information Division (2018). Khwāmṛū thūapai kīeokap prōkrām [General knowledge of the program]. Quantum GIS 3.2 (Bonn) Program Manual, 1-89.
- Mitr Phol. (2018). Remote Sensing, Theknōlōyī samrūat khōmūn raya klai [Remote Sensing, Remote Sensing Technology]. Retrieved from <http://www.mitrpholmodernfarm.com>.
- Nantaka S., Tipwan N. and Chalisa B. (2019). Khāophōt liang sat [Maize]. Saraburi Provincial Agriculture and Cooperatives Office, 1-111.
- Naphat R., Raksak S. and Kriengkri K. (2020). Using Digital Image for Estimation Leaf Area of Rice, *Thai Science and Technology Journal*, 28(9), 1717-1724.
- Office of Agricultural Economics. (2020). Kānkhā Thai kap tāngprathēt [Thai and foreign trade]. Retrieved from <http://impexp.oae.go.th/service/t1.php>.
- Panath J., Sununtha K., Petchporn C. and Yasushi K. (2020). NDVI response to nitrogen fertilizer application in waxy corn using UAV imagery, *Khon Kaen Agr. J.*, 48(5), 1068-1081.
- Paolo D.F., Tania L., Alice C., Chiara G., Pasquale D., Marco M., Gherardo C., Luca C. and Michele M. (2021). Multispectral Sentinel-2 and SAR Sentinel-1 Integration for Automatic Land Cover Classification, *land*, 10 (6), 611.
- Preeyanan S., Piyatida B., Waratchaya P. and Arunprapa P. (2019). Sugarcane Yield Estimate from Remotely Sensed Data in Nakhon Sawan Province, Kasetsart University, 1-35.
- Sanddy. (2017). Rūāng kao lao mai khāophōt liang sat plūk dai mai phōchai tæ thammai lon talāt? Old story new telling, maize not enough to grow, but why oversupply? Retrieved from <http://oknation.nationtv.tv/blog/ninlapunsandy/2017/07/19/entry-1>.
- Statistics How To. (2022). Linear Regression: Simple Steps, Video. Find Equation, Coefficient, Slope. Retrieved from <https://www.statisticshowto.com/probability-and-statistics/regression-analysis/find-a-linear-regression-equation/>.
- The Engineering ToolBox. (2008). UTM to Latitude and Longitude Converter. Retrieved from https://www.engineeringtoolbox.com/utm-latitude-longitude-d_1370.html.

A Smart Trap Device for Detection of Corn Armyworm in Maize Harvest

Jérôme Planchais and Kiattisak Sangpradit*

*Department of Agricultural Machinery Engineering, Faculty of Engineering, Rajamangala
University of Technology Thanyaburi, Pathum Thani, 12110, Thailand*

** Corresponding email: k.sangpradit@rmutt.ac.th*

Abstract

Maize is one of five major crops in Thailand. Maize produced approximately 4.5 million tonnes of total national yield in the 2019/20 crop year. In recent years, Thailand's domestic maize production has not been adequate to meet domestic requirements, and small quantities of grain have been imported. Moreover, some types of insects (called pests) are undesirable in agriculture as they decrease productivity as well as cause considerable financial losses. Chemical control is the most widely applied for efficiency and practicality reasons. However, all insecticides available in the market are extremely toxic and may cause health problems in humans and damage in nature life. These insecticides are also expensive and require several applications in the plantations during the year. Use of technology can reduce production losses, including the use of resources in production cost-effectively and environmentally friendly. New solutions have been attempted motivated by the evolution of a series of technologies such IoT, cloud computing, electronic traps, and advanced insect's identification techniques. Digital Agriculture is emerging as a trend offering technological artifacts to face the problems related to plantations on farms. The key objective is protecting human health and natural life. Secondary objectives are to decrease the economic cost of pest control, the possibility to monitor the trapping operation and to receive the effectiveness feedback in real-time. The smart trap with pheromone allows it to capture corn armyworm, *Mythimna separata* Walker, a pest that infests corn from 20 days of age to the pod stage. Then, the camera will give images in the box. Images captured are analysed to determine the number of pests in the smart trap. The electronic board allows us to calculate that. The purpose is to recover the data on a monitoring platform to supervise the problem in the culture. We report results on insect pests that can reach a detection accuracy ranging from 97%.

Keywords: Smart Trap, Image Processing, Electronic, Corn Armyworm, Maize

Introduction

Maize is one of the 5 largest agricultural production in Thailand. Indeed, Thailand has a lot of maize fields. Farms make up 33% of agricultural land in addition to rice, cassava, sugarcane, and rubber. In 1984/85, 12.4 million rai (nearly 2 million ha) were planted to maize, ranking second only to rice of 9.5 million ha. In 1984, Thailand exported 3.0-3.7 million tons of maize and earned nearly 10,000 million baht (US\$ 400 million), but thereafter maize area began to decline and occupied only 7.3 million rai (nearly 1.2 million ha) by 2002-03, with a production of around 4.5 million tons (Benchaphun Ekasingh).

Agriculture provides food and medical products, so this area is very important for humanity. However, some types of pests are undesirable in agriculture. They decrease productivity as well as cause considerable financial losses. Major diseases and pests identified included downy mildew, rust, rats, and stem borers, although maize is more tolerant to diseases than other up land crops (Benchaphun Ekasingh). In Figure 1, we can see a corn armyworm in photograph A and its larva in photograph B. The larva is the pest that destroys maize plantations. It is a major pest in Thailand for maize. Large amounts of leaf tissue are consumed by larger fall armyworm larvae. This results in a

ragged appearance to the leaves similar to grasshopper damage. The larvae are less impacted by pesticides, it is therefore necessary to trap and detect the adults upstream.

The chemical control is the most widely applied for efficiency and practicability reasons (Bustillo). However, all insecticides available to use in agriculture are extremely toxic. This is the cause of health problem in humans and damage in nature life. During the year, it is necessary to apply pesticides several time in the plantations. These insecticides increase the budget of farmer. A more measured use of pesticides and adapted to the importance of the problems detected in the fields would allow to reduce the costs.

New technologies are beginning to be mass-produced. The use of techniques such as Internet of Things (IoT) and image processing are emerging in agriculture to find solutions to the problems encountered (Martineau). All these new technologies provide task automation and better management of information such as the arrival of pests in a field. The smart trap is used in areas other than agriculture, for example in urban areas (Panagiotis Eliopoulos). The purpose of a smart trap in agriculture is to reduce the use of pesticides and therefore to protect human health. This also results in lower costs.

The purpose of this study is to develop a smart trap. The target is the Corn Armyworm. The function of this trap is to capture and count the number of pests in a field to monitor problems and adjust pesticide use accordingly. This paper is organized as follows. First of all, material and method describe the location and hardware and software used. Then results and discussion presents and analyses the obtained results. Finally, we conclude the paper and suggests future works.



Figure 10 The Corn Armyworm (A) and his larva (B)

Material and Method

Study area

The location of the study area is at KSP Equipment Co. Ltd., in Lam Sai, Wang Noi District, Phra Nakhon Sri Ayutthaya Province, Thailand. Cultivation of fodder corn on the aforementioned areas started from June to November 2021. Areas used for experiments in the size of 12,467 square meters, which is equally divided in two, into Plot A and Plot B. The maize used for the test was cultivar CP303 with a harvest of 105 days and 115 days for fresh harvest and dry harvest respectively. The average yield should be expected at 1,500-2,000 kg/rai at 25-30% humidity (CPP). The smart trap was installed in the middle of the field between Plot A and Plot B, so that the pheromones are the maximum range. A smart trap with a sachet of pheromone is enough to cover the whole field. The installation took place after sowing corn in the field. The pesticide was not used at the beginning of the plantation to be able to see the pest problems appear. There is no internet access at this location, which is why the system is equipped with a 4G key

Smart trap and Pheromone

The box with pheromone allows to capture pests. Then, the camera will give images in the box. Images captured are analyzed to determine the number of pests in the smart trap. The electronic board allow to calculate that. Humidity and temperature sensors can be added to get more information of environment. The purpose is to recover the data on a responsive site to supervise the problem in the culture.

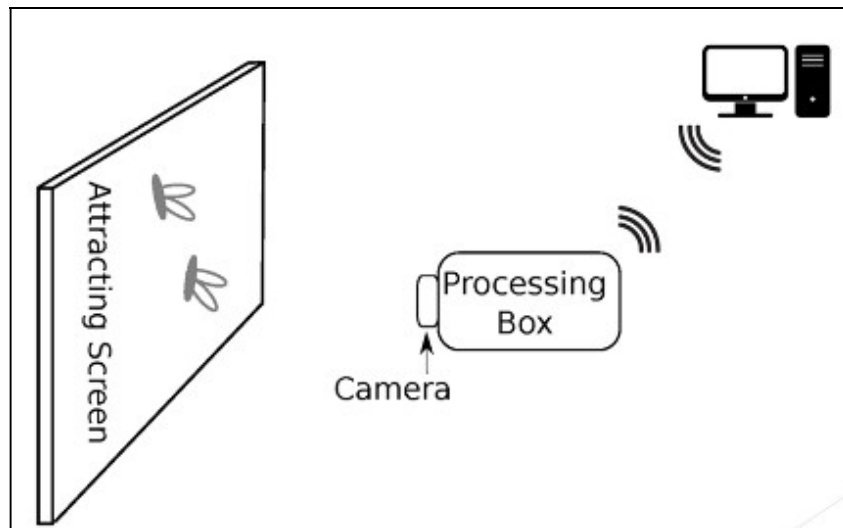


Figure 11 Illustration of Smart Trap System

A specific attractive substance must be used to attract the Corn Armyworm. The female-produced sex pheromone of *S. frugiperda* is often used to monitor populations to time insecticide application. Pheromones enable mating disruption and mass trapping.

Hardware

As shown in Figure 3, the system consists of several elements with a control part, a power part and the elements allowing screen capture and the transfer of collected information. A solar panel is used to power the various elements of the system. This allows battery life in the field. The embedded system is composed of a Raspberry Pi 4, a Pi camera, an SD card, a 4G key and optionally a GPS. The Raspberry Pi integrates an ARM Cortex-A72 processor and image acquisition and analysis software. This electronic card is connected by DCMI to a pi camera which captures images on a regular basis and stored in the SD card. The 4-BIT SPI interface allow the communication of the processor with the SD card. Subsequently, 4G key allows internet access and data transfer on Line and Grafana. The software is written in Python language and OpenCV library is used to image processing.

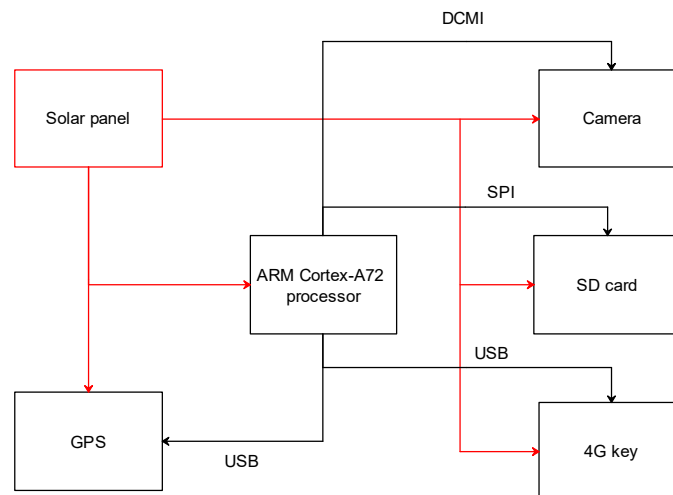


Figure 12 System diagram of smart trap

Image Processing

The camera is positioned facing the bottom of the trap to allow an overview of the pests inside, showed in Figure 4 and a color photo with 640x480 resolution is taken at a specific time during the day. The photography is on RGB (Red Green Blue) channels model.



Figure 13 Hardware setup

The images taken are then converted into the HSV (or HSL) color space. This model is based on a human perception of color. The hue is commonly called color mainly red, yellow, green, cyan, blue or magenta. We often represent the hue in a circle and give her value in degrees over 360 degrees. For example, yellow color corresponds to 120°. Saturation refers to the intensity of the color between gray (low saturation or desaturation) and pure color (high saturation). The saturation is usually expressed as a percentage or between 0 and 1. The value corresponds to the brightness of the color, between black (low value) and average saturation (maximum value). The value is usually expressed as a percentage or between 0 and 1.

The system filters with the parameters implemented to detect pests. A mask of the image is created then the shapes obtained are analyzed. The counting of the shapes corresponding to the insects is then carried out. In figure 5, we can see seven insects. Each identified insect is marked

with a white dot. The blue dot corresponds to two insects. The system differentiates them because the two are glued together. The color difference depending on the case allows feedback to know how the software managed to identify this or that pest.



Figure 14 Example of image captured with pest count

IoT

An Internet of Things IoT middleware has two main roles: 1) it stores data pushed from the smart trap software component; and 2) it provides data to the Web application component. This project send data on Line application for the test. In this project data is sent over Line and Grafana.

Results and Discussion

Efficiency

The results of the prototype trap evaluation are shown in Figure 6. We relate the system count to the manual count. The slope of the regression line indicates the association between the manual count and the system count. R^2 represents the fraction of the total variance of the system count. Manual count variation explains this variance. We can see from these results that R^2 is very high. Automatic counting is very close to manual counting.

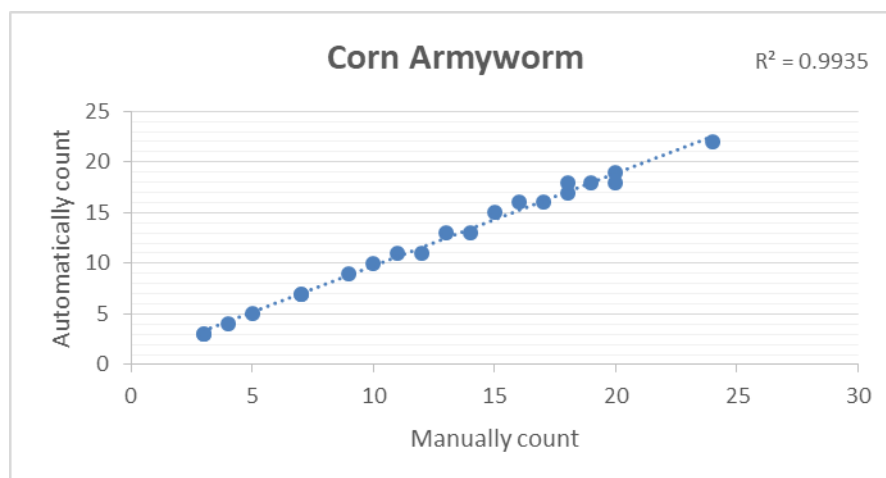


Figure 15 Accuracy of the automatic counting in comparison with actual detection

The numbers of the captures measured by the system were compared to those counted manually. This comparison allows to determine the accuracy of the developed system. The error between manual counting and counting by image processing allows to define the inaccuracy of the system. The accuracy of the system is calculated with an equation (1), which is shown as follows:

$$a = 1 - \frac{|Mc - Ma|}{Mc} \quad (1)$$

where a is the counting accuracy of the system, Mc is the number of manual counting pests, and Ma is the number of the automatically counted pests. The results are shown in Table 1.

Preliminary tests were done on a single day on site. As it is clearly presented, our smart trap is very accurate, achieving about 97% accuracy on automatic counts compared with manually counted numbers of captured insects. The accuracy of our system in detecting insect presence is also shown by the very high correlation ($R^2 > 0.99$ in all cases) between the generated signals and actual numbers of insects caught in the trap.

Table 1 The counting accuracy of the proposed smart trap.

Automatically count	Manually count	Accuracy % (a)	Mean accuracy
1	1	100.00%	
3	3	100.00%	
3	3	100.00%	
4	4	100.00%	
5	5	100.00%	
7	7	100.00%	
7	7	100.00%	
9	9	100.00%	
10	10	100.00%	
11	11	100.00%	
12	11	91.67%	
13	13	100.00%	97.48%
14	13	92.86%	
15	15	100.00%	
16	16	100.00%	
17	16	94.12%	
18	18	100.00%	
18	17	94.44%	
19	18	94.74%	
24	22	91.67%	
20	18	90.00%	
20	19	95.00%	

Effect of brightness

The brightness is modified on the original photographs to test its influence on the effectiveness of image processing. We can see, in Figure 7, the difference in processing due to brightness. On image A, the luminosity has been lowered by 50. There is a counting error compared to the original photograph. In fact, the decrease in luminosity affects the counting. Pests are less

distinguishable by analysis. The insects stuck together have more difficulty in being differentiated. The more the brightness is increased, the more the detection will have difficulty counting. On image A, the luminosity has been increased by 50. We can see that the brightness helps in the detection of insects. Pests are much sharper on photography masks. Image capture during the tests was done early in the morning. But taking an image when the brightness is greater would increase the efficiency of the system. Image capture should be done around noon to maximize brightness. This would reduce errors when counting pests.

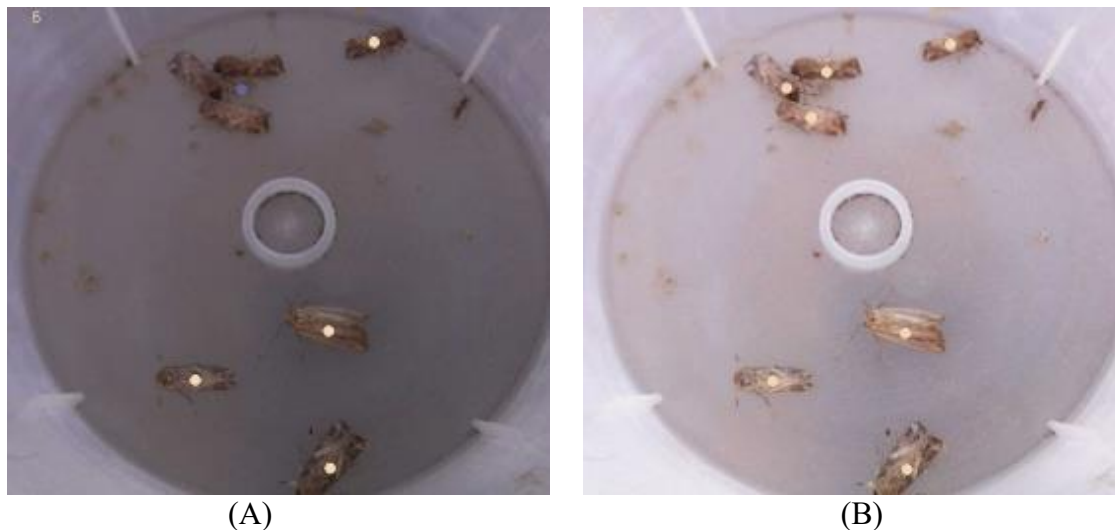


Figure 16 Brightness influence

A timer switch is used to save the energy. It engages when the light starts to appear and feeds the card for 45 minutes. The system can take pictures for image processing at this time. The system therefore works in the morning when the brightness allows a good picture to be taken. This system allows to manage the problem of light and energy.

Conclusion

Thanks to the Internet of Things, it has become possible to provide supervision in different fields of application. Agriculture is an important field where automation and data analysis can be very useful. Pests are a major problem for plantations. They decrease production and increase costs with the use of pesticides. The smart trap is a system that captures these pests using pheromones and provides valuable information to growers.

The smart trap developed in this project is completely autonomous with power supply via solar panel and on-board electronics. The cost and the size of the system are not very high. The smart trap has very good accuracy. The collected data can be visualized without having to go to the place of culture. This allows a better knowledge of pests in the field and therefore better management of pesticides. The developed smart trap has a high accuracy (>97%). But light plays a very important role in detecting pests. Image capture should be done around noon to maximize brightness.

For future developments, a GPS can be added to locate an installed smart trap. On a large field, a single smart trap is not enough to map the pest population. Indeed, pheromones only disperse in a limited area. With several smart traps equipped with a GPS and installed in a field, a map can be created to determine the areas where the problems appear. The treatment of the field with pesticides would then be adapted to the population of pests.

Acknowledgments

The authors would like to thank Department of agricultural machinery engineering, Faculty of engineering, Rajamangala University of Technology Thanyaburi and KSP Equipment Co. Ltd., for cooperation and support for this research.

References

- Andrade, R., Rodriguez, C., Oehlschlager, A. C. (2000). Optimization of a Pheromone Lure for *Spodoptera frugiperda* (Smith) in Central America. *Braz. Chem. Soc.*, 11(6), 609-613, 2000.
- Beilhe, L. B., Raymond Mahob, Y., David R. Hall, Martijn ten Hoopen, G., Babin, R., Field optimization of pheromone traps for monitoring and controlling cocoa mirids.
- Bustillo, E. a.; Villalba, A. (2004). "Manejo da Broca-do-café". Anais do Workshop Internacional do Manejo da broca-do-café. Instituto Agrônômico do Paraná - Londrina/PR [S. l.].
- Connolly, A. (2018). "Digital agriculture". *Research World Magazine*, [S. l.], v. 2018, no. 72, pp. 34-36. DOI: 10.1002/rwm3.20714.
- CPP. (2019). *Thurakit malet phan khāophōt [Corn seed business]*. Retrieved from <https://www.cpp-worldwide.com/business-type/75>.
- Damon, A. (2000). "A review of the biology and control of the coffee berry borer". [S. l.]. *Bulletin of entomological research*, vol. 90, no. 6, pp. 453-465, 2000. DOI: 10.1017/S0007485300000584.
- Eliopoulos, P., Tatlas, N. A., Rigakis, I. (2018). A “Smart” Trap Device for Detection of Crawling Insects and Other Arthropods in Urban Environments.
- Ekasingh, B. (2004). *Maize in Thailand: Production Systems, Constraints, and Research Priorities*, Chiang Mai University.
- Ekasingh, B., Gypmantasiri, P. (2004). *Maize in Thailand: Production Systems, Constraints, and Research Priorities*.
- Figueiredo, V. A. C., Mafral, S. B., Rodrigues, J. J. P. C., A Proposed IoT Smart Trap using Computer Vision for Sustainable Pest Control in Coffee Culture.
- OpenCV Team. (2000). "The OpenCV Library". Date accessed: 02/17/2020. Available at: <https://opencv.org/>.
- Preti, M., Verheggen, F., Angeli, S. (2020). Insect pest monitoring with camera-equipped traps: strengths and limitations.
- RPF. (2020). "Raspberry Pi Foundation". Date accessed: 01/25/2020. Available at: <https://www.raspberrypi.org/>.
- Rust, M.K., Su, N.Y. Managing social insects of urban importance. *Annu. Rev. Entomol.* 2012, 57, 355–375.

The Study of Melon Pulp Color on Physicochemical Properties and Antioxidant Activity of Melon Juices and Melon Powders

Siriluck Surin¹, Pimpan Pimonlat², Nantipak Chantadirokporn³, Sudarat Bunbanterng³ and Peerapong Ngamnikom^{3*}

¹*Division of Food Science and Technology Management, Faculty of Science and Technology, Rajamangala University of Technology Thanyaburi, Pathum Thani 12110, Thailand*

²*Division of Crop Production, Faculty of Agricultural Technology, Rajamangala University of Technology Thanyaburi (Rangsit Campus), Pathum Thani 12130, Thailand*

³*Division of Food Science and Technology, Faculty of Agricultural Technology, Rajamangala University of Technology Thanyaburi (Rangsit Campus), Pathum Thani 12130, Thailand*

* *Corresponding email: peerapong_n@rmutt.ac.th*

Abstract

Melon is a unique taste and flavor with specific nutritional value, especially phenolic compounds and vitamin A. In addition, it is easily spoiled with 3 – 4 days at room temperature. Therefore, it needs to be processed to several products. Generally, the melon pulp can be divided into two types which is green and orange. The aim of this research was to study the color of melon pulps affecting the physicochemical properties and antioxidants of melon juices and melon powders. The varieties of green melon were Green net and Emerald gem, and orange one were Chunchai and Madam orange. The spray drying process was used to produce powder products. The conditions were 170 °C of input temperature and 85 °C of output temperature. The drying carriers were maltodextrin and inulin. The results showed that the melon juices were pH 8.10 – 8.80 and 9 – 12 °Brix. The range of nutritional values of all melon juices showed 0.3 – 12.5 % of carbohydrate, 6.6 – 9.3 % of fiber, 0.4 – 2.8 % of ash and no detection of protein and fat. The antioxidant activity (for DPPH) and total phenolic content of green melon pulp were higher than orange one significantly. The Green net variety had the highest DPPH and total phenolic compounds at 4.64 % inhibition and 10.37 ppm GAE, respectively. For the powder samples, the yield of powder using maltodextrin had higher than inulin. The solubility of all powders was in the range of 74 – 94 %. The powders using maltodextrin showed better sensory acceptance, however the powders using inulin contained higher fiber content. The DPPH value and total phenolic content of melon powder of Green net variety was the highest which it had 10.1 – 10.5 % inhibition and 26.9 – 31.4 ppm GAE. Conclusion, the green melon pulp contained higher antioxidant activities.

Keywords: *Melon, Juice, Powder, Physicochemical properties, Antioxidant activity.*

Introduction

Melon (*Cucumis melo L.*) is a plant in the Cucurbitaceae family which is commonly grown in several part of Europe, Asia and Africa. There are many varieties and shapes of melon. They are many common names such as sweet melon, netted melon, muskmelon, cantaloupe, winter melon (Silva et al., 2020). The melon pulp is sweet, juicy and rich of nutrients. It is a source of dietary fiber, minerals, especially potassium, vitamin C. Moreover, it contains high polyphenols and carotenoids which are bioactive compounds. Melon has low fat, cholesterol and salt content (Gómez-García et al., 2020).

Processing of melon extends shelf life and also increases value of melon. There were several studies about melon processing: flesh trimmed fresh melon using chitosan as coating material (Poverenov et al., 2018), dried melon (Dias da Silva et al., 2016), using of melon powder in bakery

products (Salehi et al., 2020). In addition, seed and peel of melon were also studied for extraction of bioactive compounds and used for food or cosmetic purposes as well (Gómez-García et al., 2020; Silva et al., 2020).

The spray drying process is a suitable process for fruit powder. It involves many factors in process control which were carrier, inlet temperature, outlet temperature, hot air velocity, feed rate and food properties. The food that is feed in the chamber of spray dryer should not be too high viscosity because of the difficulty of feeding liquid food through a nozzle. The droplets will become too large which affects clump of powder particle at the wall of chamber. Then it makes low product yield. (Dams et al., 2019; Sarabandi et al., 2018; Sathyashree et al., 2018; Archaina et al., 2017; Chuacharoen, 2017; Alves et al., 2016; Khuenpet et al., 2016; Selvamuthukumar and Khanum, 2014; Phisut, 2012; Jittanit et al., 2010; Phoungchangang and Sertwasana, 2010). There were several works of fruit powders using spray drying process which was similarly with our present study such as pomegranate powder (Muzaffar et al., 2016), cantaloupe (Solval et al., 2012) and watermelon powder (Quek et al., 2007).

The stickiness, wall deposition and low yield are challenging issues in spray drying process of fruit and vegetable juice. Because they contain sugars and or organic acid compounds such as fructose, glucose, sucrose, citric acid, malic acid, tartaric acid etc. These kinds of compounds are low molecular weight with low glass transition temperature (T_g), for example 62 °C for sucrose, 5 °C for fructose. The drying temperature in the chamber is always more than 40 °C then a carrier agent (or wall material) needs to be used. The carrier agent in spray drying process is not only supporting material for the producing powder but also protect food (core material) from environment such as heat, air and light etc. The carrier agent needs to be inexpensive, food grade, readily available, and legally allowed. The basic carrier agent is carbohydrate polymers which can be separated in 3 groups: (i) starch and its derivative (such as maltodextrin, dextrin, cyclodextrin etc.), (ii) gums (such as gum arabic, alginate, gum karaya etc.), (iii) cellulose and its derivatives (such as cellulose, carboxymethylcellulose, inulin etc.). The popular carrier agent is maltodextrin with a dextrose equivalent (DE) of 10 – 20 due to less turbidity at high concentration. For gums and cellulose groups also show other functional properties like prebiotic function. The selection of carrier agent depends on the purposes of the process and the properties of final product (Shishir and Chen, 2017; Watson et al., 2017).

The main color of melon pulp is green and orange, then the aim of this work was to study the color of melon pulps affecting the physicochemical properties and antioxidants of melon juices and melon powders. So, the four varieties of melon were selected as the example of pulp color by which Green net and Emerald gem varieties were green pulp, and Chunchai and Madam orange varieties were orange pulp. The spray drying process was used to produce powder products with the condition of 170 °C input temperature and 85 °C output temperature. The maltodextrin and inulin were selected as carrier agent.

Materials and Methods

Materials

Four varieties of melon; Green net, Emerald gem, Chunchai and Mandam orange, with an average weight of 3 – 4 kg/melon were purchased from a local market (Si Mum Mueang market) in Pathumthani, Thailand. All melons were 2nd ripening stage according to their average total soluble solid content of 11 °Brix (Cantwell, 2015). They were kept in refrigerator at 4 °C and used for experiment within 14 days. Both maltodextrin (DE 10 – 12) and inulin were purchased from Krunghthepchemi Co., Ltd., Thailand. All chemicals used in this study were of reagent grade.

Melon juice preparation

The melons were cleaned with water and left them dry with air. Then they were cut into halves, deseeded and peeled. The edible part (mesocarp) was cut into small pieces and blended using food processor. Melon purees were filtrated by colander and thin white cloth respectively. Melon juices were pH in range of 8.1 – 8.8 and total soluble concentration (°brix) in range of 9 – 12. Then the juices were calculated yield and measured color. For juices of spray drying process, the juice mixture was prepared by addition of maltodextrin or inulin 30 %w/v. The solution of carrier agent was prepared by mixing with water of 1:1 ratio and heated at 60 °C until totally dissolved. The juice and carrier agent solution were mixed to obtain required concentration with heating at 60 °C. The final juice mixture concentration was 20 °brix. The samples were kept at 4 °C before spray drying process, however these samples would be used in experiment within 24 hours.

Spray drying process

Each juice mixture treatment was homogenized before spraying. The sample was heated at 50 – 60 °C with continuous stir during the spray drying process. The spray dryer (model 120 LPH, MMM group, Germany) was controlled with inlet air temperature at 170 °C, outlet air temperature at 85 °C and flow rate at 0.07 liter per minute. The powder sample came out to the sample bottle then powder was put into laminated bag and kept in darkness, cool and dry place.

Physical properties

The melon juice samples were determined pH, brix and color including calculated yield. The melon powder samples were calculated yield of spray drying process and evaluated water activity (A_w), color, bulk density, and water solubility index.

The pH was measured by pH meter (model HI98103, Hanna, USA). The brix value was measured using refractometer (model RF11, Extech, Japan). The A_w was measured using water activity meter (Aqua Lab 4TE, Meter group, Germany). The color was measure in CIE LAB system (L^* , a^* and b^*) using color meter (Color Flex EZ, Hunter Lab, USA).

For bulk density, 30 g of powder sample was put into a 100 ml measuring cylinder, then gently knock the bottom of cylinder on a table for a few times. The volume of powder could be read by scale on cylinder. The bulk density was calculated by following equation.

$$\text{Bulk density } \left(\frac{\text{g}}{\text{cm}^3} \right) = \frac{\text{Mass of melon powder in cylinder}}{\text{Volume of melon powder in cylinder}} \quad (1)$$

For water solubility index, 2.5 g of powder sample was placed in a centrifuge tube. Then distilled water 30 ml was added, shook and covered tube, and left it for 30 minutes. After that the sample tube was centrifuged at 3,000 rpm for 15 minutes. The supernatant was poured into a weighted aluminum cup (lid and cup were dehumidified and cooled to room temperature before used). The cup was dried at 105 °C in hot air oven until a stable weight was obtained weight of dried solid. The water solubility index (WSI) was calculated by the following equation.

$$\text{WSI (\%)} = \frac{\text{Weight of dried solid}}{\text{Weight of melon powder}} \times 100 \quad (2)$$

Proximate analysis

Both juice and powder samples were analyzed moisture, protein, fat, ash, fiber, and carbohydrate according to the method of AOAC (2000). The carbohydrate was calculated by subtraction of other components.

DPPH and total phenolic content

The method of DPPH assay and total phenolic content were adjusted from Randhir and Shetty (2004) and Burguieres et al. (2007). The fresh and powder samples were differently prepared before analysis. For fresh sample, the melon was cut, peeled and blended with food processor. The puree sample 2 g was mixed with 20 ml of 95 % ethanol. Sample was shaken with a shaking incubator (NB-205V, N-Biotek, Korea) which conditions were 25 °C, 2,000 rpm and 3 days. After that it was centrifuged at 4,000 rpm for 20 minutes (D-78532, Hettich, Germany). The supernatant was kept in an amber glass bottle at 4 °C before analysis. For powder sample, 1 g of powder and 10 ml of 50 % ethanol were mixed in a centrifuged tube. Then sample was prepared with the same method.

Antioxidant capacity analysis of 2,2-diphenyl-1-picrylhydrazyl by DPPH assay was analyzed by following method. Extracted sample was pipetted 100 µl and mixed with 3 ml of 60 µM DPPH, left in dark place for 10 minutes. The absorbance of sample was measured at a wavelength of 517 nm. The control sample used 100 µl of 95 % ethanol instead of extracted sample. The antioxidant capacity as a percentage of inhibition was calculated by following equation.

$$\text{Inhibition (\%)} = \frac{(\text{Absorbance of control} - \text{Absorbance of sample})}{\text{Absorbance of control}} \times 100 \quad (3)$$

The total phenolic content (TPC) was analyzed using the Folin-Ciocalteu’s reagent method. Extracted sample was pipetted 1 ml and added 1 ml of 95 % ethanol, 5 ml of distilled water and 0.5 ml of 50 %v/v of Folin-Ciocalteu phenol reagent, then mixed and left it for 5 minutes. The 5 %w/v of sodium carbonate 1 ml was added in sample solution, then left the sample in dark place for 1 hours. The absorbance of sample was measured at a wavelength of 725 nm. TPC was calculated against the standard curve of gallic acid, equation was followed below.

$$\text{TPC} = c \times \frac{V}{m} \quad (4)$$

Where TPC = total phenolic content in extracted sample (ml / g of extracted sample)
 c = gallic acid concentration obtained from the graph of the extract (mg/ml)
 V = volume of the extracted sample (ml)
 m = weight of the extracted sample (g)

Sensory evaluation

A ranking test was chosen in sensory evaluation of melon powders. The eight samples (4 varieties of melon with 2 carrier agents) were served to 30 panelists. The melon powder was reconstituted with water at 1:1 weight ratio before serving to the panelists. Then each panelist ranked all samples from the highest to lowest of overall preference.

Statistical analysis

The complete randomized design (CRD) was used in this experiment but sensory experiment used randomized complete block design (RCBD) as an experimental design. Analysis of variance (ANOVA) and Duncan’s new multiple range test (DMRT) were used for analyzing data with a 0.05 level of confidence. All experiments were performed in triplicate and data were expressed as the mean and standard deviation. The analysis was conducted using PASW statistic version 18 (IBM, Armonk, NY, USA).

Results and Discussion

Production of melon powders

Melon juice of each variety was extracted with blending and squeezing method. Melon juice yield of Green net, Emerald gem, Chunchai and Madam orange were 66.05, 57.94, 45.85 and 54.74 % respectively. All powder samples and spray drying yield were showed in Table 1. The melon juice with maltodextrin (GM, EM, CM and MM) gave higher powder yield than juice with inulin (GI, EI, CI and MI). Maltodextrin is a modified starch while inulin is a natural polysaccharide which extracted from plant such as chicory root and artichoke etc. Addition of maltodextrin or inulin could increase the total soluble solid content in juice and reduce the moisture content of the powder product. Maltodextrin is proved to be a good encapsulant that entraps low molecular weight sugars and acids therefore it facilitates spray drying and reduces the stickiness of the spray-dried product. Inulin gave lower yield and it might be due to its chemical structure. Structure of inulin contains fructose units, which has relative higher hydrogen bond when compared to maltodextrin, and it has health properties including stimulated immune system, prebiotic function, sweetener (Michalska-Ciechanowska et al., 2020).

Table 1 Powder samples and their yield.

Samples	Yield (%)
Green net-Maltodextrin (GM)	14.29 ± 0.85
Green net-Inulin (GI)	7.83 ± 0.98
Emerald gem-Maltodextrin (EM)	13.60 ± 1.12
Emerald gem-Inulin (EI)	9.89 ± 0.70
Chunchai-Maltodextrin (CM)	14.92 ± 0.95
Chunchai-Inulin (CI)	8.47 ± 0.69
Madam orange-Maltodextrin (MM)	15.29 ± 1.09
Madam orange-Inulin (MI)	8.51 ± 0.77

Physical characteristics of melon juices and powders

The juice color of melons was significantly different (Table 2). The L* value which was whiteness of sample, the juice of Green net and Madam orange were the most whiteness. For a* value, the higher positive value was more red color, and the higher negative value was more green color. The Green net and Emerald gem showed more negative a* value than the others, which it meant that juices showed more green color. For b* value, the higher positive value was more yellow color, and the higher negative value was more blue color. The b* value of Chunchai and Madam orange, which were orange pulp, were lower value than the left two melons. However, the juice of both orange pulp melon gave higher a* value which it means that they showed more red color. So that they were orange color of melon juice. In case of powder color, maltodextrin and inulin did not affect powder color. The powder from green pulp melon showed negative a* value while the powder from orange pulp melon showed positive a* value. These results correlated with their original pulp color. For L* value, all powder samples were whiteness.

Table 2 Color (L^* , a^* and b^*) of melon juices and melon powders.

Samples	L^*	a^*	b^*
<i>Juice</i>			
Green net	40.99 ± 0.40 ^a	-5.87 ± 0.80 ^c	35.36 ± 1.10 ^a
Emerald gem	38.37 ± 0.21 ^c	-8.64 ± 0.01 ^d	33.44 ± 0.02 ^b
Chunchai	33.12 ± 0.02 ^d	8.41 ± 0.05 ^a	31.10 ± 0.02 ^c
Madam orange	40.97 ± 0.00 ^b	-2.60 ± 0.02 ^b	30.53 ± 0.13 ^d
<i>Powder</i>			
GM	93.87 ± 0.01 ^b	-0.58 ± 0.00 ^c	8.38 ± 0.01 ^c
GI	92.94 ± 0.01 ^c	-0.66 ± 0.00 ^{cd}	9.28 ± 0.01 ^b
EM	93.36 ± 0.07 ^b	-0.72 ± 0.00 ^d	7.07 ± 0.04 ^d
EI	93.20 ± 0.00 ^b	-1.29 ± 0.00 ^{de}	8.41 ± 0.01 ^c
CM	94.46 ± 0.02 ^a	1.27 ± 0.00 ^b	7.92 ± 0.01 ^d
CI	92.25 ± 0.01 ^c	1.99 ± 0.00 ^b	10.86 ± 0.01 ^a
MM	92.52 ± 0.01 ^c	2.12 ± 0.00 ^a	9.75 ± 0.02 ^b
MI	92.44 ± 0.00 ^c	2.01 ± 0.00 ^a	10.13 ± 0.02 ^b

The letters showed statistical significance which were separately analyzed between juice and powder samples.

The bulk density, WSI and A_w of all powder samples were showed in Table 3. The bulk density of all powders was similar value, which it was in range of 0.52 – 0.53 g/cm³. The powder samples using maltodextrin or inulin showed significant difference of WSI and A_w . The range of value was 74 – 93 % for WSI and 0.34 – 0.57 for A_w . There was lower A_w with the powder using inulin comparing with maltodextrin. There were no value trends among melon varieties and carrier agents. By the way, the WSI of GM was the highest value while EM was the lowest value.

Table 3 Bulk density, water solubility index and water activity of melon powders.

Samples	Bulk density (g/cm ³)	WSI (%)	A_w
GM	0.53	93.7 ± 2.3 ^a	0.51 ± 0.02 ^a
GI	0.53	84.3 ± 2.4 ^b	0.34 ± 0.02 ^c
EM	0.53	74.5 ± 6.7 ^c	0.52 ± 0.03 ^a
EI	0.52	89.0 ± 7.1 ^b	0.41 ± 0.01 ^b
CM	0.53	80.4 ± 4.3 ^b	0.57 ± 0.04 ^a
CI	0.53	80.3 ± 3.9 ^b	0.37 ± 0.02 ^c
MM	0.53	75.5 ± 6.6 ^c	0.54 ± 0.02 ^a
MI	0.53	80.2 ± 5.7 ^b	0.46 ± 0.03 ^b

The letters showed statistical significance which were separately analyzed between juice and powder samples.

Chemical characteristics of melon juices and powders

According to the proximate analysis in Table 4, the results did not find protein and fat in both juice and powder samples. In case of juice samples, all juices showed moisture 80 – 90 %. Green net showed the highest ash (2.77 %) and fiber (9.26 %) content. The orange pulp melon (Chunchai and Madam orange) had lower amount of carbohydrate content than the green one (Green net and Emerald gem). This means that Chunchai and Madam orange would give less sweet taste than others. For powder samples, the moisture content of all samples was in range of 2.5 – 4.4 % due to

the spray drying process. The amount of ash, fiber and carbohydrate of powder samples were different with the juice samples because the powder contained carrier agent 30 %w/w, then it changed content ratio. The powder from Green net (GM and GI) showed the highest ash content which it was similar trends as its juice. The fiber content of powders using inulin had higher fiber content in comparison with powders using maltodextrin because the inulin also acted as soluble fiber. Normally, inulin could be used as prebiotic in fermented process or food source of microflora in our gut. The carbohydrate content showed value in range of 89 – 92 %. The increasing of carbohydrate content due to the addition of carrier agent, which they were carbohydrate-based material.

Table 4 Proximate analysis of melon juices and melon powders

Samples	Moisture (%)	Ash (%)	Fiber (%)	Carbohydrate (%)
<i>Juice</i>				
Green net	80.39 ± 9.39 ^c	2.77 ± 1.01 ^a	9.26 ± 0.66 ^a	7.56 ± 8.32 ^b
Emerald gem	79.75 ± 0.98 ^d	0.88 ± 1.96 ^d	6.6 ± 0.15 ^d	12.50 ± 1.17 ^a
Chunchai	90.55 ± 0.20 ^a	0.41 ± 0.22 ^c	8.76 ± 0.41 ^b	0.26 ± 0.28 ^d
Madam orange	89.61 ± 0.26 ^b	0.81 ± 0.422 ^b	8.30 ± 0.45 ^c	1.27 ± 0.31 ^c
<i>Powder</i>				
GM	3.64 ± 2.12 ^c	1.55 ± 38 ^{ab}	2.90 ± 0.45 ^e	91.46 ± 2.10 ^b
GI	2.69 ± 1.82 ^c	1.55 ± 0.38 ^{ab}	3.56 ± 0.15 ^d	92.18 ± 2.02 ^{cd}
EM	5.25 ± 2.40 ^a	0.55 ± 0.19 ^d	3.93 ± 0.15 ^d	90.26 ± 2.44 ^c
EI	2.51 ± 1.76 ^{de}	0.44 ± 0.19 ^e	4.66 ± 0.55 ^c	92.38 ± 2.18 ^{cd}
CM	3.41 ± 1.86 ^{cb}	1.22 ± 0.19 ^b	5.20 ± 1.15 ^b	90.17 ± 1.02 ^c
CI	5.61 ± 1.96 ^a	0.99 ± 0.33 ^c	6.20 ± 0.34 ^a	87.19 ± 2.08 ^e
MM	3.11 ± 0.23 ^{ce}	0.44 ± 0.19 ^e	2.70 ± 0.17 ^e	93.75 ± 0.54 ^a
MI	4.37 ± 2.04 ^b	0.55 ± 0.19 ^d	5.23 ± 0.20 ^b	89.84 ± 1.66 ^d

The letters showed statistical significance which were separately analyzed between juice and powder samples.

The analysis of DPPH and total phenolic content (TPC) of juice and powder samples were showed in Fig. 1 and 2, respectively. The results showed that melon juice from orange pulp had lower DPPH and TPC than green pulp as (Fig. 1A and 1B), Chunchai resulted the lowest values which were 0.56 %inhibition and 6.77 ppm GAE for DPPH and TPC respectively. Green net and Emerald gem showed the highest DPPH (4.5 – 4.6 %inhibition) but Green net had the highest TPC of 10.37 ppm GAE.

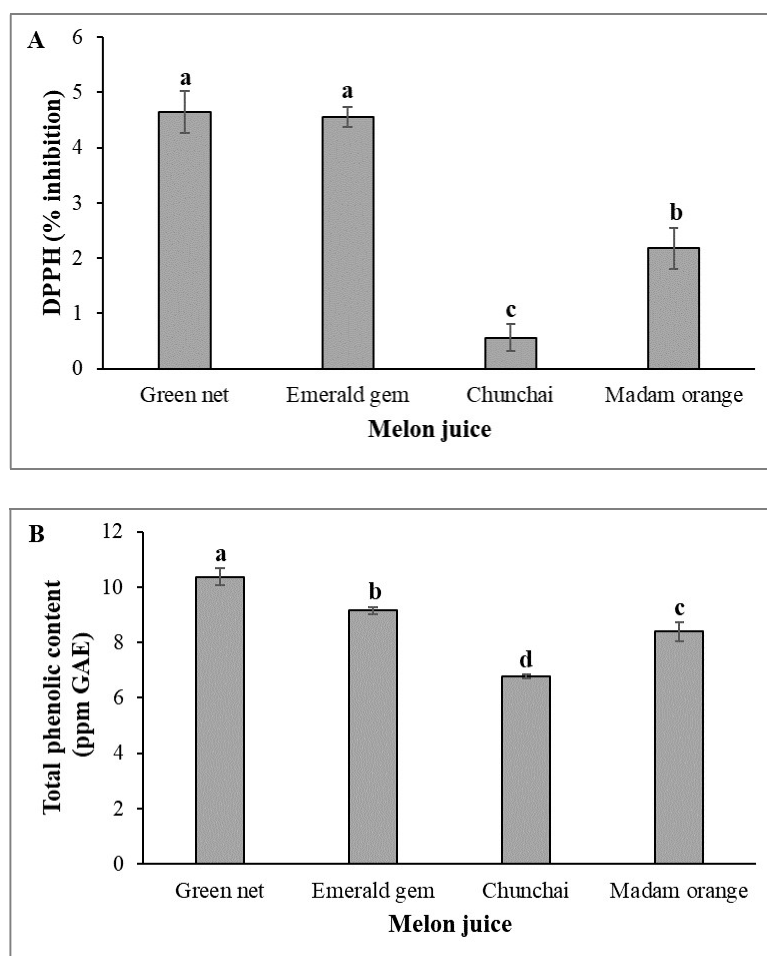
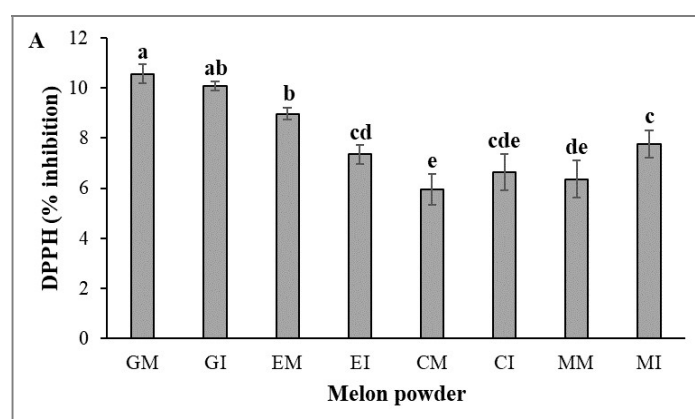


Figure 1 Antioxidant activity of melon juices; DPPH assay (A), and total phenolic content (B). Bars with different letters are significantly different at $P \leq 0.05$.

For powder samples, The DPPH and TPC of powder showed higher value than juice samples, this might be due to the higher nutrient concentration of powder in analysis. GM and GI had the highest DPPH and TPC which were correlated with its juice. GM had 10.55 % inhibition of DPPH and 26.96 ppm GAE of TPC, while GI had 10.06 % inhibition of DPPH and 31.43 ppm GAE of TPC It did not clear to find the effect of carrier agent on DPPH and TPC content in sample.



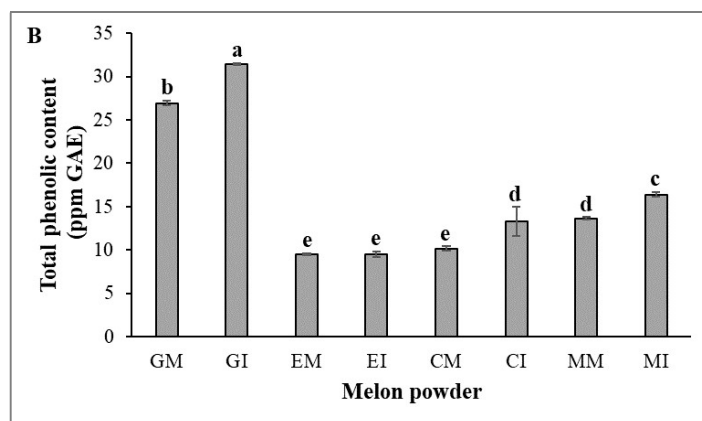


Figure 2 Antioxidant activity of melon powders; DPPH assay (A), and total phenolic content (B). Bars with different letters are significantly different at $P \leq 0.05$

Sensory evaluation of melon powders

According to the Table 5, the ranking test showed that CM was the most acceptance and EM was the least acceptance. CM gave lower amount of antioxidant capacity than others. However, the GM might be the best sample in this work because it showed very high antioxidant capacity among all samples and high acceptable preference (2nd rank). The powder using of maltodextrin gave better preference than powder using of inulin, excepted Emerald gem variety.

Table 5 Overall acceptance of melon powder from ranking test.

Samples	Order of overall acceptance
CM	1
GM	2
MM	3
CI	4
GI	5
MI	6
EI	7
EM	8

Conclusion

This experiment was interested that the melon juice from green pulp color (Green net and Emerald gem varieties) contained higher DPPH assay and TPC than melon juice from orange pulp color (Chunchai and Madam orange varieties). The maltodextrin was better supported spray drying yield in comparison with inulin, however inulin was better functional carrier agent in terms of prebiotic. The juice from Green net showed higher nutrition which was ash and fiber, and antioxidant activity than other samples. The GM could be the best sample in this experiment because it gave high antioxidant activity, high yield and high overall acceptance.

Acknowledgments

This research was supported fund by Faculty of Agricultural Technology, Rajamangala University of Technology Thanyaburi (RMUTT), Pathum Thani, Thailand. The researchers would like to thank all facility staffs of Food Science and Technology, Faculty of Agricultural Technology, RMUTT.

References

- Alves, N. N., Messaoud, G. Ben, Desobry, S., Costa, J. M. C., & Rodrigues, S. (2016). Effect of drying technique and feed flow rate on bacterial survival and physicochemical properties of a non-dairy fermented probiotic juice powder. *Journal of Food Engineering*, 189, 45–54.
- AOAC. (2000). Official method of analysis. 17th ed. *The association of official analytical chemists*, Virginia, USA.
- Archaina, D., Leiva, G., Salvatori, D., & Schebor, C. (2017). Physical and functional properties of spray-dried powders from blackcurrant juice and extracts obtained from the waste of juice processing. *Food Science and Technology International*, 24(1), 78–86.
- Burguieres, E., McCue, P., Kwon, Y.I. & Shetty, K. (2007). Effect of vitamin C and folic acid on seed vigour response and phenolic-linked antioxidant activity. *Bioresource Technology*, 98(7), 1393 – 1404.
- Cantwell, M. (2015). *Ripening melons*. UC Davis: Postharvest Technology Center.
- Chuacharoen, T. (2017). Development of Spray-Dried Lime Juice Powder with Improved Bioactive Compound Retention. *Suan Sunandha Science and Technology Journal*, 4(2), 7–12.
- Dams, S., Holasek, S., Tsiountsioura, M., Malliga, D., Meier-Allard, N., Poncza, B., Lamprecht, M. (2019). An encapsulated fruit, vegetable and berry juice powder concentrate increases plasma values of specific carotenoids and vitamins. *International Journal for Vitamin and Nutrition Research*, 91, 77–86.
- Dias da Silva, G., Barros, Z. M. P., Batista de Medeiros, R. A., Oliveira de Carvalho, C. B., Brandao, S. C. R., & Azoubel, P. M. (2016). Pretreatments for melon drying implementing ultrasound and vacuum. *LWT - Food Science and Technology*, 74, 114–119.
- Gómez-garcía, R., Campos, D. A., Aguilar, C. N., Madureira, A. R., & Pintado, M. (2020). Valorization of melon fruit (*Cucumis melo L.*) by-products: Phytochemical and Biofunctional properties with Emphasis on Recent Trends and Advances. *Trends in Food Science & Technology*, 99, 507–519.
- Jittanit, W., Niti-att, S., & Techanuntachaikul, O. (2010). Study of Spray Drying of Pineapple Juice Using Maltodextrin as an Adjunct. *Chiang Mai Journal of Science*, 37(3), 498–506.
- Khuenpet, K., Charoenjarasrerk, N., Jaijit, S., Arayapoonpong, S., & Jittanit, W. (2016). Investigation of suitable spray drying conditions for sugarcane juice powder production with an energy consumption study. *Agriculture and Natural Resources*, 50, 139–145.
- Michalska-Ciechanowska, A., Majerska, J., Brzezowska, J., Wojdyło, A., & Figiel, A. (2020). The influence of maltodextrin and inulin on the physico-chemical properties of cranberry juice powders. *Chem Engineering*, 4(2), 4010012.
- Muzaffar, K., Dinkarrao, B. V., & Kumar, P. (2016). Optimization of spray drying conditions for production of quality pomegranate juice powder. *Cogent Food & Agriculture*, 2, 1–9.
- Poverenov, E., Arnon-rips, H., Zaitsev, Y., Bar, V., Danay, O., Horev, B., & Rodov, V. (2018). Potential of chitosan from mushroom waste to enhance quality and storability of fresh-cut melons. *Food Chemistry*, 268, 233–241.
- Phisut, N. (2012). Spray drying technique of fruit juice powder: some factors influencing the properties of product. *International Food Research Journal*, 19(4), 1297–1306.
- Phoungchandang, S., & Sertwasana, A. (2010). Spray-drying of ginger juice and physicochemical properties of ginger powders. *Science Asia*, 36, 40–45.
- Quek, S. Y., Chok, N. K., & Swedlund, P. (2007). The physicochemical properties of spray-dried watermelon powders. *Chemical Engineering and Processing*, 46, 386–392.
- Randhir, R., Lin, Y.T. & Shetty, K. (2004). Stimulation of phenolics, antioxidant and antimicrobial activities in dark germinated mung bean sprouts in response to peptide and phytochemical elicitors. *Process Biochemistry*, 39(5), 637 – 646.

- Salehi, F., & Aghajanzadeh, S. (2020). Effect of dried fruits and vegetables powder on cakes quality: A review. *Trends in Food Science & Technology*, *95*, 162–172.
- Sarabandi, K., Peighambaroudost, S. H., Mahoonak, A. R. S., & Samaei, S. P. (2018). Effect of different carriers on microstructure and physical characteristics of spray dried apple juice concentrate. *Journal of Food Science and Technology*, *55*(8), 3098–3109.
- Sathyashree, H., Ramachandra, C., Nidoni, U., Mathad, P., & Naik, N. (2018). Rehydration properties of spray dried sweet orange juice. *Journal of Pharmacognosy and Phytochemistry*, *7*(3), 120–124.
- Selvamuthukumar, M., & Khanum, F. (2014). Optimization of spray drying process for developing seabuckthorn fruit juice powder using response surface methodology. *Journal of Food Science and Technology*, *51*(12), 3731–3739.
- Shishir, M. R. I., & Chen, W. (2017). Trends of spray drying: A critical review on drying of fruit and vegetable juices. *Trends in Food Science & Technology*, *65*, 49–67.
- Silva, M. A., Gonçalves, T., Alves, R. C., Oliveira, M. B. P. P., & Costa, H. S. (2020). Melon (*Cucumis melo L.*) by-products: Potential food ingredients for novel functional foods?. *Trends in Food Science & Technology*, *98*, 181–189.
- Solval, K. M., Sundararajan, S., Alfaro, L., & Sathivel, S. (2012). Development of cantaloupe (*Cucumis melo*) juice powders using spray drying technology. *LWT - Food Science and Technology*, *46*, 287–293.
- Watson, M. A., Lea, J. M., & Bett-Garber, K. L. (2017). Spray drying of pomegranate juice using maltodextrin / cyclodextrin blends as the wall material. *Food Science and Nutrition*, *5*, 820–826.

Effect of Solvent Types and Concentrations on the Bioactive Compound from Lime Peel by Low Power Ultrasound Assisted Extraction

Suriyaporn Nipornram^{1*} and Riantong Singanusong²

¹*Department of Agro-Industry, Faculty of Science and Agricultural Technology, Rajamangala University of Technology Lanna, Phitsanuloke Campus, Phitsanuloke 65000, Thailand.*

²*Department of Agro-Industry, Faculty of Agriculture, Natural Resources and Environment, Naresuan University, Phitsanulok 65000, Thailand.*

*Corresponding email: surinipo@gmail.com

Abstract

Lime peel is a rich source of polyphenols including phenolic acids and flavonoid. The ultrasound assisted extraction method has been widely applied in extraction of polyphenols from plant materials due to its ability to help in reducing extraction times and increasing extraction yields. However, there have been a few reports on the effects of solvent types and solvent concentrations on the polyphenols by the ultrasound assisted extraction. The aim of this work was therefore to investigate the effects of solvent types (methanol, ethanol and acetone) and concentrations (20, 50 and 80 % v/v) using ultrasound assisted extraction on the antioxidant activity, total phenolic content, total flavonoid content and flavanone glycosides (hesperidin and narigin) of lime peel. The results showed that the lime peel extract obtained from using 80 % acetone provided the highest antioxidant activity (IC₅₀ by DPPH radical scavenging 4.32 mg/ml), total phenolic content (1,338.18 mg of gallic acid equivalent/100 g DW), total flavonoid content (781.89 mg of quercetin/100 g DW) and flavanone glycosides (622.53 mg of hesperidin and 57.94 mg of narigin/100 g DW). Therefore, 80% acetone was regarded as a suitable solvent for extraction of polyphenols by ultrasound assisted extraction from lime peel.

Keywords: Ultrasound assisted extraction, Lime peel, Flavonoid, Hesperidin, Narigin

Introduction

The citrus consumption in the last few years is continuously increasing with an estimated global production of citrus fruits up to 50 million tons in the session 2010 – 2012 (Khan et al., 2010; United States Department of Agriculture, 2013). Consumption of lime is mostly in the form of juice, so there is a peel available which accounts for half the weight of the volume. Most peels are disposed as waste, which causes pollution to the environment. Nowadays, renewed interest in the use of plant materials as a source of naturally bioactive compounds has grown. There have been many reports on the benefits of citrus peels which contain total polyphenol contents in peels of lime, lemons, oranges and grapefruits were higher than that of the fresh (Peterson et al., 2006; Gorinstein, 2001).

Lime peel contains phenolics, flavonoids, ascorbic acid, carotenoids and reducing sugars and high antioxidant activity (Guimarães et al., 2010) which can help the body scavenge free radicals effectively. Moreover, these polyphenolic compounds have been found effective in many health-related properties, such as antioxidant, anticancer, antiviral and anti-inflammatory activities (Tripoli, 2007).

The extraction capacity and efficiency of different methods for polyphenol from citrus peels have been evaluated, such as solvent extraction, enzyme-assisted extraction and heat treatment (Benavente-García et al., 1997; Procházková et al., 2011). However, these extraction methods have low efficiency, such as long extraction time, high temperature and large volumes of organic solvent

used which can be resulted in an environmental pollution. Furthermore, polyphenols are very sensitive to light, heat and oxygen. Therefore, it is necessary to build efficient extraction method and keep the stability of polyphenols.

Ultrasound assisted extraction (UAE) has attracted more and more attention due to its higher extraction efficiency with shorter extraction time compared to traditional methods, such as solvent extraction and soxhlet extraction (Ma et al., 2008). The ultrasonic enhancement is mainly attributed to behaviors of the bubbles of cavitation upon the propagation of the acoustic waves. Collapse of bubbles can disrupt biological cell wall to facilitate the release of extractable compounds (Chemat et al., 2011). There have been many solvent types for isolation of polyphenols from citrus plants by ultrasound assisted extraction, for example methanol was used for extraction of phenolic compounds from plant materials (Zia, 2006; Londoño-Londoño et al., 2010). In addition, food grade ethanol (Khan et al., 2010) and acetone (Oboh, 2012) were used for extraction of polyphenols especially flavonoids from citrus peels. However, there have been a few reports on the effects of solvent types and solvent concentrations on the polyphenols by the ultrasound assisted extraction from lime peel.

This work aimed to study the effects of solvent types (methanol, ethanol and acetone) and concentrations (20, 50 and 80% v/v) using UAE on the antioxidant activity, total phenolic content, total flavonoid content and flavanone glycosides (hesperidin and naringin) of lime peel.

Materials and methods

Plant Materials

Lime, (*Citrus aurantifolia*) 4 months after bloom, were collected from Phitsanuloke province, Thailand. The peels were cut into a size of 1 cm² and dried in hot air oven at 60 °C for 2 h or until reaching a moisture content of 9-10%. The dried peels were grounded with a blade mixer, sieved through a 50 mesh and kept in a brown glass bottle at -20 °C until used.

Ultrasound assisted extraction (UAE)

For the UAE experiments, an ultrasonic bath was used as an ultrasound source. The bath (model 175DAE, Crest Co. Ltd., Malaysia) was a rectangular container (16.4 cm x 13.3 cm x 10.2 cm). The transducers (frequency 38.5 kHz) were annealed at the bottom. The ultrasonic power level 5 (50.93 W) was used in this study. One g of ground dried peel was added into 20 ml of solvent in a 120 ml brown glass bottle. The bottle was immersed into the ultrasonic bath which contained 1200 ml of water at 40 °C for 30 min. After extraction, the supernatant was filtered under vacuum through Whatman paper No. 4 and analyzed for the antioxidant activity, total phenolic, flavonoid, hesperidin and naringin content.

Experimental design

The factorial randomized complete block designs was used for the experimental design to determine the factor in this study with 3 replications. The effects of two factors, including the extraction solvents (methanol, ethanol and acetone) and solvent concentrations (20, 50 and 80% v/v) on the antioxidant activity (DPPH radical scavenging activity), phenolic compounds and flavonoid from citrus peels by UAE were investigated. The total of 9 different experiment combinations were analyzed.

HPLC analysis

HPLC analysis were carried out on an Agilent 1100 chromatograph using a UV detector at 280 nm and a C18 reversed-phase column (Agilent TC-C18 250 mm x 4.6 mm, 5 µm) operated at 37 °C. The mobile phase consisted of two solvents: 0.5% acetic acid (A) and 100% acetonitrile (B). The solvent gradient in volume ratios was as follows: 10–30% B over 20 min. The solvent gradient

was increased to 35% B at 25 min and it was maintained at 35% B for 5 min at 1 ml/min. The injection volume was 20 μ l (Khan et al., 2010). Analyses were performed at least three times and only mean values were reported. Quantification was carried out by using the external standard method and the final concentrations were calculated in mg/100 g DW.

Total phenolic content (TPC)

The total phenolics content was determined according to the method of Anagnostopoulou et al. (2006). The reaction mixture was consisted of 0.5 ml of the aqueous extract (1 ml extract diluted in solvent 10 ml at a ratio of 1:10), 5 ml of distilled water and 0.5 ml of the Folin–Ciocalteu’s reagent. After a period of 3 min, 1 ml of saturated sodium carbonate solution was added. The 10 ml volumetric flasks were vortexed and allowed to stand for 1 h. The absorbance was measured at 725 nm in spectrophotometer (model DR/4000U, HACH Co. Ltd., USA). The total phenolic content was expressed as mg gallic acid equivalent /100 g DW.

Determination of antioxidant activity (DPPH radical scavenging activity)

Antioxidant activities were determined according to the method of Anagnostopoulou et al. (2006). Aqueous extract 1 ml was added to 2 ml of 1 mM DPPH in methanol. A blank was prepared using the reaction solvent without sample. Absorbance at 517 nm was determined after leaving the sample and blank for 30 min at room temperature in the dark room. The inhibition of DPPH activity was calculated according to the following equation:

$$\text{Scavenging activity (\%)} = [(A_{\text{control}} - A_{\text{sample}})/A_{\text{control}}] \times 100$$

(A_{control} = absorbance without extract; A_{sample} = absorbance with extract)

IC_{50} value (mg/ml) is the concentration at which the scavenging activity was 50% from linear regression analysis.

Total flavonoid content

Total flavonoids were measured using a colorimetric assay according to the method of Ramful et al. (2010). Aqueous extract 2.5 ml was added to 150 μ l of 5% aqueous $NaNO_2$ and the mixture was vortexed. A blank was prepared using solvent without sample. After 5 min, 150 μ l of 10% aqueous $AlCl_3$ was added. One ml of 1 M $NaOH$ was added 1 min after the addition of $AlCl_3$. Solution was mixed and the absorbance was measured at 510 nm. Total flavonoids were calculated with respect to quercetin standard curve. Results were expressed in mg of quercetin equivalent /100 g DW.

Statistical analysis

Experimental results are expressed as means. All measurements were replicated three times. The data were analyzed by analysis of variance (ANOVA) and the means separated by Duncan's multiple range test.

Results and discussion

The results of the variability factors including extraction solvent types (methanol, ethanol and acetone) and solvent concentrations (20, 50 and 80% v/v) and interaction effects between the variability factors of lime peel by UAE shown significantly different ($p \leq 0.05$) on DPPH radical scavenging activity (IC_{50}), total phenolic, total flavonoid, hesperidin and naringin content. However, the interaction effect between the variability factors on the DPPH radical scavenging activity (IC_{50}) did not show significant difference ($p > 0.05$) as shown in Table 1.

The solvents used in this study were methanol, ethanol and acetone. They were different in

their polarities (Table 2) relative to polyphenol of lime peel as phenolic acid, flavonoid, flavanone glycoside (hesperidin and naringin) were polar compounds (Gattuso et al., 2007). Recent results from others reported that polyphenol and antioxidant activity from pummelo extract was significantly different on comparison with solvent type (Jayaprakasha et al., 2008) which support the results from this study.

Table 1 Analysis of variance for main and interactive effects on the antioxidant activity and polyphenols as an effect of type and concentration of extraction solvent using UAE of lime peel (means and significance of differences)

Source of variation	DPPH Radical scavenging activity (IC ₅₀)	Total phenolic content	Total flavonoid content	Hesperidin content	Naringin content
Extraction solvents (A)	xx	xx	xx	xx	xx
Solvent concentration (B)	x	xx	xx	xx	xx
Interaction A x B	ns	xx	xx	xx	xx

xx = $p \leq 0.01$; x = $p \leq 0.05$; ns = no significant.

Properties of the extracts from lime peel using UAE with three different solvent types showed that acetone gave the highest antioxidant activity (lowest DPPH IC₅₀) 4.59 mg/ml, total phenolic content 1179.60 mg gallic acid equivalent /100 g, total flavonoid content 679.11 mg quercetin equivalent/100 g, hesperidin content 365.10 mg/100 g and naringin content 33.11 mg/100 g ($p \leq 0.05$) as shown in Table 1. The different extraction efficiencies of these solvents are attributed to their differing polarities and viscosities. Although, the polarity indices of acetone, methanol and ethanol are similar but acetone has the low viscosity 0.32 cP (Hemwimol et al., 2006). When ultrasound was applied, ability to extract polyphenol by acetone was increased because acetone can be easily diffused into the plant matrix. As for the influence of liquid viscosity, acoustic cavitation occurs more easily in the liquid with low viscosity because the ultrasonic intensity applied could more easily exceed the molecular forces of the liquid. In addition, the liquid with low viscosity has low density and high diffusivity, and can easily able to diffuse into the pores of the plant materials (Chemat et al., 2011). The result was also in agreement with the others who reported that acetone was used to extract anthraquinones from *Morinda citrifolia* by ultrasonic (Hemwimol et al., 2006) and free soluble phenolic from citrus peel.

Table 2 Properties of methanol, ethanol and acetone (at 25 °C)

Type of solvents	Polarity index	Surface tension (mN/cm)	Vapor pressure (mmHg)	Viscosity (cP)
Methanol	5.1	22.6	127.05	0.60
Ethanol	5.2	23.7	59.02	1.20
Acetone	5.1	23.7	229.52	0.32
Water	9.0	72.8	23.80	0.89

Source: Hemwimol et al. (2006)

The findings are in good agreement with Khan et al. (2010) that ethanol:water ratio of 80% (v/v) were chosen as optimal for extracted hesperidin and naringin from fresh citrus peel. However, 20% (v/v) solvent concentration showed the lowest antioxidant activity (DPPH IC₅₀), total flavonoid, hesperidin and naringin content of 5.28 mg/ml, 554.33 mg quercetin equivalent/100 g, 160.99 mg/g and 17.15 mg/g, respectively ($p \leq 0.05$) because viscosity, surface tension and polarity increased due to increasing in water level as a result polyphenol difficultly diffused from the plant matrix into solvent.

Table 3 Effect of solvent types and concentrations of solvent on DPPH radical scavenging activity, total phenolic, total flavonoid and hesperidin and naringin content using UAE of lime peel (means and significance of differences)

Effect of types and concentration solvents		DPPH radical scavenging activity (IC ₅₀) mg/ml	Total phenolic content (mg/100 g)	Total flavonoid (mg/100 g)	Hesperidin content (mg/100 g)	Naringin content (mg/100 g)
Solvent types	Methanol	4.60b	855.06c	525.58c	223.02b	27.24a
	Ethanol	5.50a	927.87b	597.82b	184.67c	17.65b
	Acetone	4.59b	1179.60a	679.11a	365.10a	33.11a
Solvent concentration (%)	20	5.28a	929.69b	554.33b	160.99c	17.15c
	50	4.95ab	1084.93a	623.36a	224.95b	25.69b
	80	4.75b	947.92b	624.81a	392.84a	35.81a

a, b and c – Mean values with different letters in columns are significantly different; $p \leq 0.05$.

The extracts using methanol, ethanol and acetone at concentration of 20, 50 and 80% (v/v) by UAE contained total phenolic and total flavonoid content with the range of 644.61-1338.18 mg gallic acid equivalent/100 g and 508.38-781.00 mg quercetin equivalent/100 g, respectively. The result was also in agreement with another reported that lime peel contain total phenolic content of 811 mg/100 g (Kuljarachanan et al., 2009).

The acetone 80% extract had the highest total phenolic contents and total flavonoid content 1338.18 mg gallic acid equivalent/ 100 g and 781.89 mg quercetin equivalent/ 100 g, respectively ($p \leq 0.05$) as shown in Table 4 because it was low in viscosity (Table 2), Therefore, polyphenol can be easily released into the solvent.

Table 4 Total phenolic, total flavonoid, hesperidin and naringin content from lime peel using UAE with different solvent types and concentrations

Treatments		Total Phenolic content (mg/100g)	Total flavonoid content (mg/100g)	Hesperidin content (mg/100g)	Naringin content (mg/100g)
Solvent types	Solvent concentration (%)				
Methanol	20	868.55±17.16f	515.55±30.69ef	139.61±12.87e	10.80±4.43e
	50	1054.13±14.78c	508.38±18.03f	201.58±52.35cd	37.05±5.54b
	80	860.95±33.34f	552.82±52.83e	322.50±66.32b	32.16±9.23bc
Ethanol	20	936.68±14.99e	593.70±66.47d	128.77±37.56e	15.58±5.75de
	50	983.87±55.39d	660.05±63.49c	148.87±98.43de	17.67±9.65de
	80	644.61±66.28g	539.70±48.87ef	276.35±28.02b	23.64±8.39cd
Acetone	20	983.83±29.28d	553.77±72.08e	210.57±88.00c	24.28±16.94cd
	50	1216.80±32.27b	701.66±57.02b	321.06±38.00b	24.20±4.60cd
	80	1338.18±63.13a	781.89±43.52a	622.53±57.24a	53.39±26.38a

a, b, c, d, e, f and g – Mean values with different letters in columns are significantly different; $p \leq 0.05$.

Hesperidin and naringin were major flavonoid of citrus peel (Wang et al., 2008; Garg et al., 2001; Giannuzzo et al., 2003; Pellati et al., 2004). The extract using 80% acetone had the highest hesperidin and naringin content of 622.53 and 53.39 mg/100 g, respectively as shown in Table 4. There has been reported that citrus peel contains 100-2900 mg/100 g hesperidin (Wang et al., 2008) and 19.3-492 mg/100 g naringin (Abeysinghe et al., 2007) which in agreement with this present study.

Radical scavenging activity (IC_{50}) of nine extracts from lime peel of different solvents and concentrations were tested by DPPH method and the results are illustrated in Figure 1. Acetone and methanol at 20, 50 and 80% (v/v) extracts inhibited DPPH radicals significantly higher than that of ethanol extracts because acetone and methanol had lower viscosity than that of ethanol (Hemwimol et al., 2006). In addition, phenolic acid, flavonoid, hesperidin and naringin can be easily diffused into solvent. Therefore, the extracts are intercept the free radical chain of oxidation and donate hydrogen from the phenolic hydroxyl groups, thereby forming stable end product. The extracts isolated from citrus peels are free radical scavengers and primary antioxidants that react with DPPH radical, which may be attributed to its proton donating ability. The antioxidant activity of the citrus peel fractions was ascribed to their hydrogen donating ability (Jayaprakasha et al., 2007).

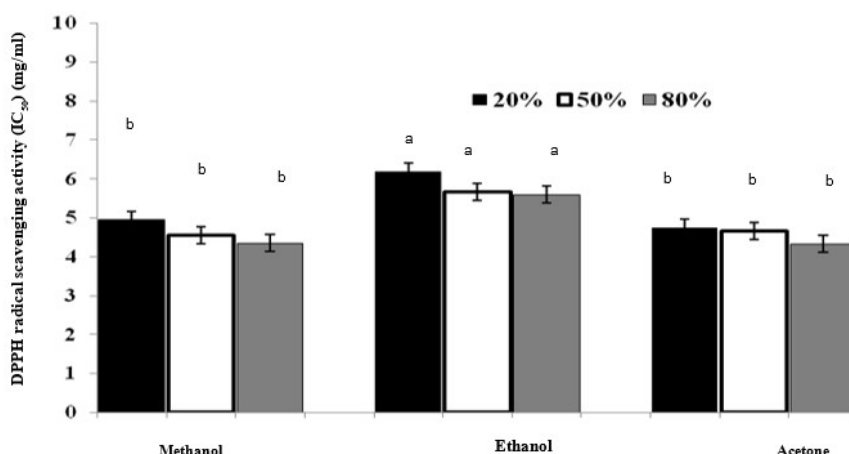


Figure 1 DPPH radical scavenging activity (IC_{50}) of lime peel extracts of different types and concentrations of solvent using UAE (a and b – Mean values with different letters above bars are significantly different; $p \leq 0.05$.)

Conclusion

This study showed that the factors in the UAE had a significant influence on the DPPH radical scavenging activity (IC_{50}), total phenolic content, total flavonoid content, hesperidin content and naringin content of lime peel were solvent type and solvent concentration. The interaction of factors, acetone at 80% (v/v) was regarded as a suitable solvent for extraction of lime peel as it had the highest antioxidant activity (DPPH IC_{50} 4.32 mg/ml), total phenolic content (1,338.18 mg of gallic acid equivalent/100 g DW), total flavonoid content (781.89 mg of quercetin/100 g DW) and flavanone glycosides (622.53 mg of hesperidin and 53.39 mg of naringin/100 g DW).

References

- Abeysinghe, D. C., Li, X., Sun, C., Zhang, W., Zhou, C., & Chen, K. (2007). Bioactive compounds and antioxidant capacities in different edible tissues of citrus fruit of four species. *Food chemistry*, 104(4), 1338-1344.
- Anagnostopoulou, M. A., Kefalas, P., Papageorgiou, V. P., Assimopoulou, A. N., & Boskou, D. (2006). Radical scavenging activity of various extracts and fractions of sweet orange peel (*Citrus sinensis*). *Food chemistry*, 94(1), 19-25.
- Benavente-García, O., Castillo, J., Marin, F. R., Ortuño, A., & Del Río, J. A. (1997). Uses and properties of citrus flavonoids. *Journal of agricultural and food chemistry*, 45(12), 4505-4515.
- Chemat, F., & Khan, M. K. (2011). Applications of ultrasound in food technology: processing, preservation and extraction. *Ultrasonics sonochemistry*, 18(4), 813-835.
- Garg, A., Garg, S., Zaneveld, L. J. D., & Singla, A. K. (2001). Chemistry and pharmacology of the citrus bioflavonoid hesperidin. *Phytotherapy research*, 15(8), 655-669.
- Gattuso, G., Barreca, D., Gargiulli, C., Leuzzi, U., & Caristi, C. (2007). Flavonoid composition of citrus juices. *Molecules*, 12(8), 1641-1673.
- Giannuzzo, A. N., Boggetti, H. J., Nazareno, M. A., & Mishima, H. T. (2003). Supercritical fluid extraction of naringin from the peel of *Citrus paradisi*. *Phytochemical Analysis*, 14(4), 221-223.
- Gorinstein, S., Martín-Belloso, O., Park, Y. S., Haruenkit, R., Lojek, A., Číž, M., Caspi, A., Libman, I. & Trakhtenberg, S. (2001). Comparison of some biochemical characteristics of different citrus fruits. *Food chemistry*, 74(3), 309-315.

- Guimarães, R., Barros, L., Barreira, J. C., Sousa, M. J., Carvalho, A. M., & Ferreira, I. C. (2010). Targeting excessive free radicals with peels and juices of citrus fruits: grapefruit, lemon, lime and orange. *Food and Chemical Toxicology*, 48(1), 99-106.
- Hemwimol, S., Pavasant, P., & Shotipruk, A. (2006). Ultrasound-assisted extraction of anthraquinones from roots of *Morinda citrifolia*. *Ultrasonics Sonochemistry*, 13(6), 543-548.
- Jayaprakasha, G. K., Girenavar, B., & Patil, B. S. (2008). Antioxidant capacity of pummelo and navel oranges: Extraction efficiency of solvents in sequence. *LWT-Food Science and Technology*, 41(3), 376-384.
- Khan, M. K., Abert-Vian, M., Fabiano-Tixier, A. S., Dangles, O., & Chemat, F. (2010). Ultrasound-assisted extraction of polyphenols (flavanone glycosides) from orange (*Citrus sinensis* L.) peel. *Food chemistry*, 119(2), 851-858.
- Kuljarachanan, T., Devahastin, S., & Chiewchan, N. (2009). Evolution of antioxidant compounds in lime residues during drying. *Food Chemistry*, 113(4), 944-949.
- Londoño-Londoño, J., de Lima, V. R., Lara, O., Gil, A., Pasa, T. B. C., Arango, G. J., & Pineda, J. R. R. (2010). Clean recovery of antioxidant flavonoids from citrus peel: Optimizing an aqueous ultrasound-assisted extraction method. *Food Chemistry*, 119(1), 81-87.
- Ma, Y., Ye, X., Hao, Y., Xu, G., Xu, G., & Liu, D. (2008). Ultrasound-assisted extraction of hesperidin from Penggan (*Citrus reticulata*) peel. *Ultrasonics Sonochemistry*, 15(3), 227-232.
- Oboh, G., & Ademosun, A. O. (2012). Characterization of the antioxidant properties of phenolic extracts from some citrus peels. *Journal of food science and technology*, 49(6), 729-736.
- Pellati, F., Benvenuti, S., & Melegari, M. (2004). High-performance liquid chromatography methods for the analysis of adrenergic amines and flavanones in *Citrus aurantium* L. var. amara. *Phytochemical Analysis: An International Journal of Plant Chemical and Biochemical Techniques*, 15(4), 220-225.
- Peterson, J. J., Beecher, G. R., Bhagwat, S. A., Dwyer, J. T., Gebhardt, S. E., Haytowitz, D. B., & Holden, J. M. (2006). Flavanones in grapefruit, lemons, and limes: A compilation and review of the data from the analytical literature. *Journal of food composition and analysis*, 19, S74-S80.
- Procházková, D., Boušová, I., & Wilhelmová, N. (2011). Antioxidant and prooxidant properties of flavonoids. *Fitoterapia*, 82(4), 513-523.
- Ramful, D., Baborun, T., Bourdon, E., Tarnus, E., & Aruoma, O. I. (2010). Bioactive phenolics and antioxidant propensity of flavedo extracts of Mauritian citrus fruits: Potential prophylactic ingredients for functional foods application. *Toxicology*, 278(1), 75-87.
- Tripoli, E., La Guardia, M., Giammanco, S., Di Majo, D., & Giammanco, M. (2007). Citrus flavonoids: Molecular structure, biological activity and nutritional properties: A review. *Food chemistry*, 104(2), 466-479.
- United States Department of Agriculture/Foreign Agricultural Service. (2013). Citrus: World markets and trade, Retrieved from <http://usda.mannlib.cornell.edu/MannUsda/viewDocumentInfo.do?documentID=1774>.
- Wang, Y. C., Chuang, Y. C., & Hsu, H. W. (2008). The flavonoid, carotenoid and pectin content in peels of citrus cultivated in Taiwan. *Food chemistry*, 106(1), 277-284.
- Zia-ur-Rehman. (2006). Citrus peel extract-A natural source of antioxidant. *Food Chemistry*, 99(3), 450-454.

Parameter Study for Scratch Detection in The Poultry Industry

Jullachak Chunluan, Nattida Juewong and Kiattisak Sangpradit*

Rajamangala University of Technology Thanyaburi, Pathum Thani, 12110, Thailand

** Corresponding email: k.sangpradit@rmutt.ac.th*

Abstract

The poultry industry is an important production process that has made chickens Thailand's main export product. Many families raise chickens and send them to the slaughterhouse for this processing. Both frozen and chilled chicken are available sold in a variety of meat products: whole chicken, bone-in legs, drum, breast, or wings. According to the statistics of Thailand's important export products to the world in recent years, chicken has turned out to be the number one export product. The volume reaches up to 80 percent compared to other types of livestock, which are worth about 100 billion baht/year. Most of them are processed chicken products, over 75% of all chicken products exported. At a time when the industry is experiencing strong growth, production has to be fast and of high quality to respond to the demand perfectly. Sorting the quality of chicken in order to sell high-quality products takes time and skilled workers. The application of technology will help to solve these problems. Image processing is the process of having computers calculate and process images to obtain the information that interests us both qualitatively and quantitatively. Preliminary parameter testing allows the optimal setting for the chicken scratch detection test to be selected: brightness, minimum-maximum pixel detection, and shooting distance. This study tested the parameters of an image with dimensions of 2268 x 4032 pixels. The image was taken in a dimly lit slaughterhouse and at a dissection speed of 120 animals per minute. According to this study, when the brightness is increased by 25 within the range of -150 to 150, it can detect more accurately. The test gives false results when the minimum pixel value is 50 pixels. In addition, the shooting distance has little effect on the scratch detection from the picture where the whole chicken can be clearly seen.

Keywords: *Poultry industry, Slaughterhouse, Image processing, Scratch, Detection*

Introduction

Chickens are classified in order Galliformes, it is a bird that weighs quite heavily and feeds on the ground (Leonard M.L.). At dusk, each chicken returns to roost in its own unique position. Some chickens can sleep on the ground, but most of them sleep on trees or shrubs (Johnson R.A.). There has been a long history of chicken raising in Thailand which was originally raised local chickens. Until about 30 years ago, the technology of producing various kinds of animals has progressed a lot, especially chicken breeds and rearing. Modern chicken production technology has been accepted in Thailand for over 20 years and a breeding system has been developed as an industrial system. Breeding in the industrial system is divided into two types: broilers and layers (Manop M.). The broilers in the slaughterhouse are sold in whole chicken or trimmed to separate the main parts such as bone-in legs, drum, breast or wings. Some parts will be adapted according to the needs of customers such as yakitori products. When the chicken meat is packaged, the refrigerated product will be stored in a temperature-controlled room not exceeding 2 degrees Celsius. Frozen products will freeze the product temperature below - 18 degrees Celsius and then bring it to the cold room (Demeyer D.).

The poultry industry is an important production process that has made chickens Thailand's main export product. Many families raise chickens and send them to the slaughterhouse for this

processing. According to the statistics of Thailand's important export products to the world in recent years, chicken has turned out to be the top export product. The volume reaches up to 80 percent compared to other types of livestock, which are worth around 100 billion baht/year. Most of them are processed chicken products, with over 75% of all chicken products exported (Office of the Permanent Secretary Ministry of Commerce). Broiler production is expected to increase by 2-3 percent in 2021, gradual recovery from a decrease in 2020. The outbreak of COVID-19 has reduced the consumption of chicken meat in the country, offsetting a slight increase in exports of chickens in 2020. At a time when the industry is experiencing strong growth, production has to be fast and of high quality to respond to the demand perfectly. Sorting the quality of chicken in order to sell high-quality products takes time and skilled workers. The application of technology will help to solve these problems.

Image processing is the process of having computers calculate and process images to obtain the information that interests us both qualitatively and quantitatively. There are several important steps involved, such as optimizing the image quality, eliminating image noise, splitting the object of interest out of the image to bring the object image to quantitative analysis. We can then analyze these quantitative data and create a system to be useful in other fields such as medicine, technology, agriculture, industry (Sillovely). Digital image processing can help improve images to be more user-friendly. Management, storing and sending images and automatic image analysis also helps build computer vision (Riyamongkol P.). There are many applications of image processing in the food industry (Davies E. R. and Tie F.) and in agriculture, for example, the process of separating the size and species of processed squid (Thammachot N.), evisceration system of chicken (Chen Y., 2018 and 2020), estimation of Barqi breed sheep weight (Chintan B.), egg weight (Duangkamol D.) and also poultry weight (Lotufoa R.A.), identification and classification of poultry eggs (Jeremy L.) detection of defects on chicken meat (M. Barni) or inspection of poultry carcasses (Yoon S.C. and Yang C.C., 2005 and 2010).

The main objective of this study is to test three preliminary parameters: brightness, minimum-maximum pixel detection, and shooting distance. Then, these parameters perform for scratch detection in the poultry industry.

Materials and Methods

Study area

The location of the study area is at KVS Fresh Products Company Limited, in Hua Dong, Kao Liao District, Nakhon Sawan, Thailand. A slaughterhouse trades in the livestock market which consists of poultry and swine farms by receiving products from the farm to separate the customers. Chickens come from many farms. Transport can shuffle all chickens in each house on a farm, but it does not mix between farms. In order to trace the information that the chickens from which farm have problems. A farm has from 20,000 to 200,000 chickens, with about 3-10 chicken houses per farm. The transport of chickens is carried by trucks, where one truck can carry a maximum of chickens from 2 houses. The distance between the farm and the slaughterhouse is around 40-400 kilometers. If the journey is long, there will be a stop for give the rice and water to the chickens. It should not be parked in the sun for a long time and should be sprayed with water at the stop. This long-distance transport is one of the problems that can cause chickens to scuffle each other during travel and cause scratch on the meat which can't sell at a good price. For this study, the chicken was photographed on the hanger in the slaughterhouse for scratch detection. The handrail speed is 120 animals per minute.

Device setting and software

The device set in the slaughterhouse consisted of the smartphone, phone tripod, and background cardboard (Figure 1). The main camera on a smartphone was used to take a photo for

this study. The provided phone stand stabilizes smartphone photography and thus obtains a test image that is in the same shooting position. It is recommended to use a standard-sized tripod as high as possible because the chickens transported in the slaughterhouse are suspended on high rails. The background cardboard was used to reduce interference from other objects. This image segmentation is one of the steps in image processing. This cardboard was blue with 60 x 60 cm² size and 3 mm thick. Once we have the original image, we transfer the file to the computer for image enhancement and image processing. The specification of the main camera on a smartphone and laptop are shown in table 1 and Table 2, respectively.



Figure 17 Device setting at KVS Fresh Products Company Limited

Table 2 Specification of the main camera on a smartphone

Category	Specification
Single	12 MP, f/1.7, 26mm (wide), 1/2.55", 1.4µm, Dual Pixel PDAF, OIS
Features	LED flash, auto-HDR, panorama
Video	4K@30fps, 1080p@30fps (gyro-EIS), 1080p@60fps, 720p@240fps, HDR, stereo sound rec., OIS

Table 3 Specification of notebook computer

Category	Specification
Processor	Intel Core i7
Operating System	Windows 10
RAM	16.00 GB
Storage	Dual: SSD + HDD hybrid storage
Graphics	NVIDIA GeForce

The software used for study parameters is Adobe Photoshop and LabVIEW. We want to study the parameters that affect image processing. Therefore, the test images were controlled to have the same characteristics. Pictures were edited and removed background with the Lasso tool or Quick Selection tool at Toolbar by using Adobe Photoshop. Uninterested objects were deleted and filled with blue color. In addition, images were adjusted for each parameter. Then, the LabVIEW program is used to process the image. LabVIEW is a system-design platform and development environment for a visual programming language from National Instruments (NI). The NI software is built to improve engineering productivity and help tackle engineering challenges.

Parameter testing

Preliminary parameter testing allows the optimal setting for the chicken scratch detection test to be selected: brightness, minimum-maximum pixel detection, and shooting distance. This study tested the parameters of an image with dimensions of 2268 x 4032 pixels. The image was taken in a dimly lit slaughterhouse and at a dissection speed of 120 animals per minute. Brightness parameter testing was initiated by adjusting the brightness of 5 images for testing in brightness levels 25 and 50. In the Adobe Photoshop program, values can range from -150 to +150 for brightness. Parameter of minimum-maximum pixel detection was directly tested in the LabVIEW program on the front panel that is the user interface for the Virtual Instrument (VI). Finally, testing the parameters in terms of shooting distance, we enlarged the chicken on the image to make it smaller and larger to simulate shooting at different distances between the camera and the chicken.

Results and Discussion

Data acquisition

During the shooting process, the images weren't clear at the speed of this work, 120 animals per minute. We tried to take better pictures with self-timer mode that takes 3 photos after a delay. The chicken samples were graded by quality level by experts working in quality assurance. In reality, chicken appears 1-2 marks, 3-5 marks, and more than 5 marks from level A to C respectively. The standards were calibrated with the number of objects by using a technique developed in LabVIEW: 0-19 marks, 20-29 marks, and more than 30 marks from level A to C respectively. Figure 2 shows the display on the front panel, that detects scratches on the chicken, which is an interesting object within the image or that's a dark object. The default threshold value is 128, but in this case, it will be replaced with the value of 135 for better data acquisition. A minimum object size of 150 pixels and maximum object size of 3000 pixels were set as the basis for this test. Scratches, which are considered dark objects in this image processing, are framed in red. Then the number of objects is counted as a quality classification. There is a Boolean to be represented by a green switch in the A level button.

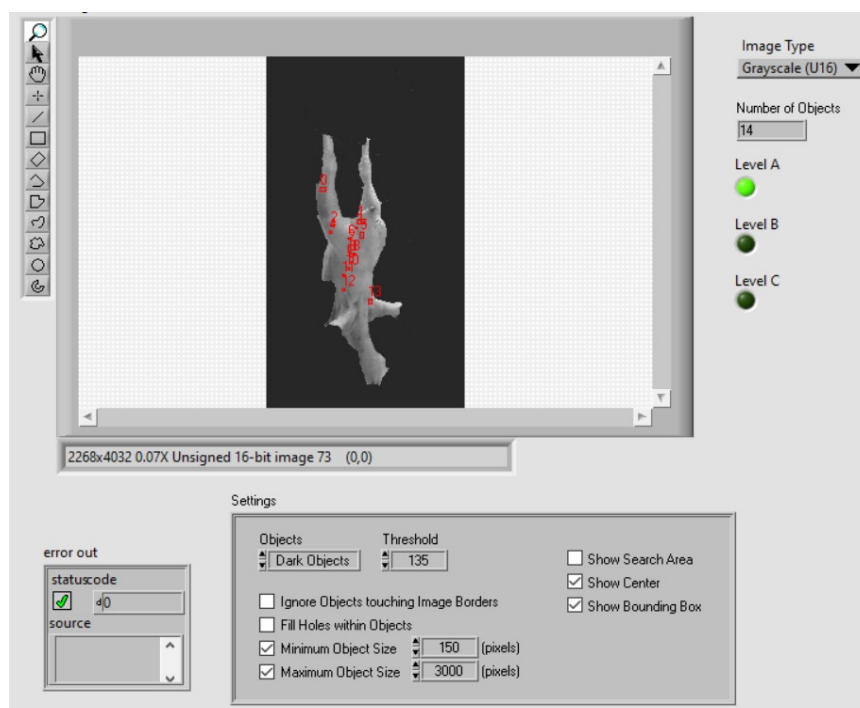


Figure 18 Program results display on the front pane

Effect of brightness

As shown in Figure 3, the number of objects present on 5 samples of a picture that change in number is shown when the brightness is increased at 25 and 50. The "operator" column indicates what quality score the operator gave for a chicken. The "developed technique" column is the score assigned by the image processing of this same chicken. By changing these numbers, there will also be a change in the quality level in the developed system (Table 3). Sample No. 1 is the one that has no problem with basic scratches detection. When the brightness is increased to 25, there is no change in the number of scratches. As for images samples No. 2 and 3, there was a shadow problem before. Enough to increase the light to 25 of the brightness can solve the detection problem, because it provides a level of quality that meets the operators. In addition, samples No. 4 and 5 had problems with some parts of the chicken as a bright object and an unspecified program error respectively. We found that adjusting the brightness can help to solve these problems because it still shows results that don't match the expert working. According to this study, when the brightness is increased by 25, it can detect more accurately. But at level 50, too much data were lost to the point that the system was not properly tested.

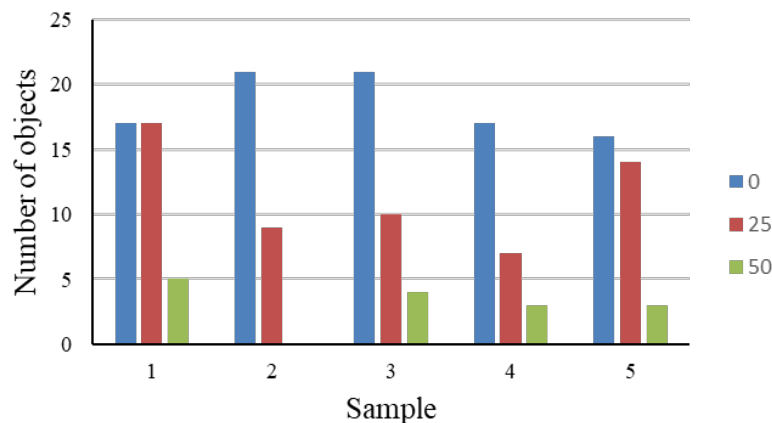


Figure 19 Number of objects detected on 5 samples when brightness level changes

Table 4 Results of algorithm analysis and comparison with operator depending on brightness

Sample	Brightness	Operator	Developed techniques
1	0	A	A
	25	A	A
	50	A	A
2	0	A	B
	25	A	A
	50	A	A
3	0	A	B
	25	A	A
	50	A	A
4	0	B	A
	25	B	A
	50	B	A
5	0	B	A
	25	B	A
	50	B	A

Effect of minimum-maximum pixel detection

The test gives false results when the minimum pixel value is 50 pixels (Table 4). When the minimum is 150 and 200 pixels, the number of objects is very close. Increasing the maximum value did not change the quality level of the chicken, but the number of objects is constantly changing. It was found that when the maximum was increased to 2500 and 3000 pixels, the results were consistent in all cases. As a result, it was found that the basic settings, minimum object size of 150 pixels and maximum object size of 3000 pixels, provide relatively accurate image processing.

Table 5 Results of algorithm analysis and comparison with operator depending on minimum-maximum pixel detection

Pixel minimum	Pixel maximum	Number of objects	Operator	Developed techniques
50	500	18	A	A
100	500	11	A	A
150	500	8	A	A
200	500	8	A	A
50	1000	21	A	B
100	1000	14	A	A
150	1000	11	A	A
200	1000	10	A	A
50	1500	22	A	B
100	1500	15	A	A
150	1500	12	A	A
200	1500	11	A	A
50	2000	23	A	B
100	2000	16	A	A
150	2000	13	A	A
200	2000	12	A	A
50	2500	24	A	B
100	2500	17	A	A
150	2500	14	A	A
200	2500	13	A	A
50	3000	24	A	B
100	3000	17	A	A
150	3000	14	A	A
200	3000	13	A	A

Effect of shooting distance

The original image before editing is 2268 x 4032 pixels and the length of the chicken is 2880 pixels (Figure 4). The size of the prototype image was scaled down to be smaller to further increase the shooting distance and scaled to a larger size when simulating close-up photography. The stages tested ranged from 2480, 2680, 2880, 3080, 3280, 3480 to 3680 pixels, relative to the size of the chicken. The number of objects changes when the chicken pixel size changes, where the number of minimum-maximum pixel detection of this system is fixed (Figure 4). In addition, the shooting distance has little effect on the scratch detection from the picture where the whole chicken can be clearly seen.

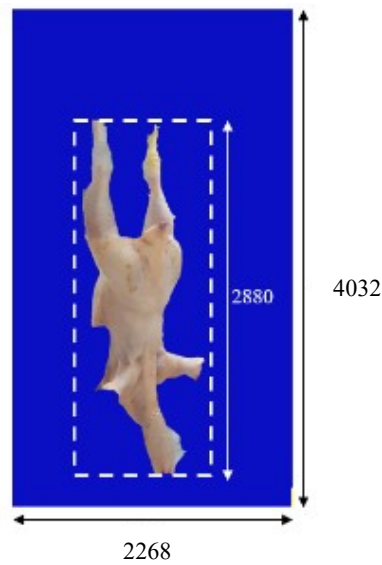


Figure 20 Dimension of the original image

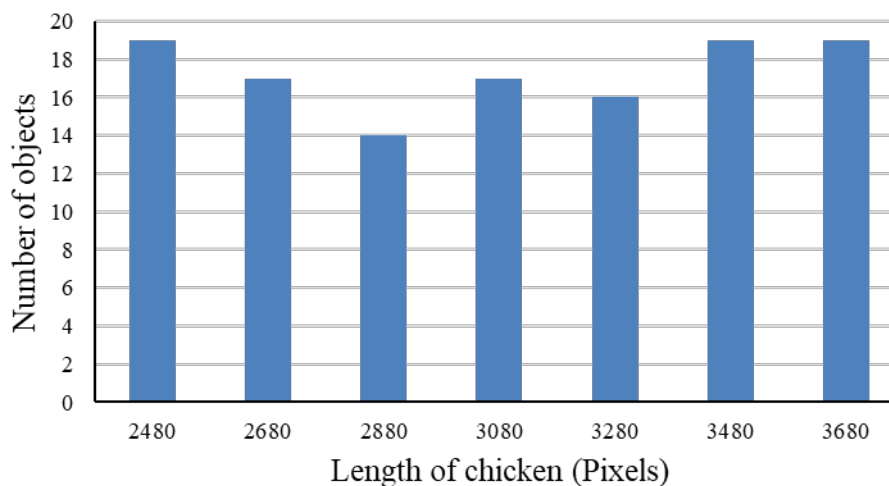


Figure 21 Number of objects detected when the size of chicken changes

Conclusion

Testing the parameters that affect image processing gives us a better understanding of the detection system. In order to, an algorithm created is been able to respond to a variety of data and detect accurately. From this test, it was found that increasing the amount of brightness while taking the photo will improve the detection of scratches on the chicken. This eliminates the shadowing problem that causes dark object detection errors in the LabVIEW program. Minimum-maximum pixel detection and shooting distance are related. Because of the smaller chicken when the shooting distance is longer, the size of the dark object detected is as well smaller. So, there have fewer pixels. There are some points that we are not interested in studying due to the dark object size that fits the threshold of the maximum value. Likewise, when the chicken is larger, the small spots on the meat that we do not want to detect can reach the minimum threshold. But this problem did not affect the quality level of the chickens because the number of objects is all within the same detection range. This test, allows the researcher to choose the most effective parameter to create a scratch detection algorithm on chickens in the slaughterhouse.

Acknowledgments

The authors would like to thank the department of agricultural engineering, faculty of engineering, Rajamangala University of Technology Thanyaburi, and KVS Fresh Products Company Limited, for cooperation and support for this research.

References

- Barni, M., Cappellini, V., Mecocci, A. (1997). Color based detection of defects on chicken meat, *Image and Vision Computing*, 15, 549-556.
- Chen, Y. and Wang, S.C. (2018). Poultry carcass visceral contour recognition method using image processing. *Journal of Applied Poultry Research*, 27(3), 316-324.
- Chintan, B., Hassanien, A.E., Nirav, A.S. and Jaydeep, T. (2018) Barqi breed Sheep Weight Estimation based on Neural Network with Regression, ResearchGate.
- Dangphonthong, D., Pinate, W. (2016). Analysis of weight egg using image processing, *Proceedings of Academics World 17th International Conference*, Tokyo, Japan.
- Davies, E.R. and Royal, H. (2013). *Machine vision in the food industry*, Robotics and Automation in the Food Industry, University of London, UK, 75-110.
- Demeyer, D., Toldrá, F. and Leroy, F. (2014). Fermentation, *Encyclopedia of Meat Sciences* (Second Edition). Vol. 1, pp. 467-474.
- Jeremy, L., Thomas, K. and Daniel, E. (2019). Identification and Classification of Poultry Eggs: A Case Study Utilizing Computer Vision and Machine Learning, *Computer Science*.
- Johnson, R.A. (1963). Habitat preference and behavior of breeding jungle fowl in central western Thailand, *Wilson Bull.*, 75(3), 270-272.
- Leonard, M.L. and Horn, A.G. (1995). Crowing in relation to status in roosters, *Anim. Behav.* 49(5), 1283-1290.
- Manop, M. (1999) Kānlīang sat [Animal husbandry] Faculty of Veterinary Medicine Chulalongkorn University <http://pioneer.netserv.chula.ac.th/~vsuntare/docum/rued42.htm>.
- Office of the Permanent Secretary Ministry of Commerce (2021). The main export products of Thailand according to the structure of exports products.
- Ponnarong, P. (2020). Poultry and Products Annual, Thailand, Global Agricultural Information Network, United States Department of Agriculture.
- Riyamongkol, P. (2019). Digital Image Processing - Chapter1: Introduction. *Electrical and Computer Engineering*, Naresuan University, 1-44.
- Silllovely, (2013) Theknōlōyī kām pramūan phon phāp [Image processing]. *Advanced technology*, Retrieved from <https://silllovely.wordpress.com>.
- Thammachot, N. (2016). Development of an Image Processing System for Splendid Squid Sizing and Specie Classification, Prince of Songkla University, 1-161.
- Tie, F. (2011). The Applications of Vision Technology in Food Processing. *Advanced Materials Research*, Vols. 183-185, pp. 1327-1331.
- Yang, C.C., Chao, K., Chen, Y.R. (2005). Development of multispectral image processing algorithms for identification of wholesome, septicemic, and inflammatory process chickens, *Journal of Food Engineering*, 69(2), 225-234.
- Yang, C.C., Chao, K., Kim, M.S., Chan, D.E. (2010). Machine vision system for on-line wholesomeness inspection of poultry carcasses, *Poultry Science*, 89(6), 1252-1264.
- Yoon, S.C., Park, B., Windham, W.R. and Lawrence, K.C. (2011). Line-scan hyperspectral imaging system for real-time inspection of poultry carcasses with fecal material and ingesta, *Computers and Electronics in Agriculture*, 79(2), 159-168.

Influence of Germination Time on Some Properties of Soybean and Black Sesame

Naruemon Mongkontanawat* & Witit Lertnimitmongkol

Department of Food Innovation and Business, Faculty of Agro-Industrial Technology, Rajamangala University of Technology Tawan-ok Chanthaburi Campus, Chanthaburi, 131 Moo10, Phuang, Khoa Kitchakut district, Chanthaburi, 22210, Thailand

**Corresponding email: naruemon_mo@rmutto.ac.th*

Abstract

In order to increase bioactive compound of cereal by germination process as previously reported, so, the objective of this study was to determine the germination time on γ -aminobutyric acid (GABA) content, germination percentage and length of radicles of two kind of cereals including soybean and black sesame. Experimental design used was completely block design (CRD). Three germination times 0, 12 and 24 hours were studied under germination condition at room temperature for 24 hours in soybean and black sesame. Results revealed that significantly ($p < 0.05$) highest GABA content of soybean and black sesame was found when the incubation time was at 24 hours with the values 67.11 ± 1.78 and 22.84 ± 0.82 mg/100g, respectively. For germination percentage and length of radicles, 24 hours of incubation time was also exhibited significantly ($p < 0.05$) highest with the levels 91.00 ± 2.50 and $61.00 \pm 1.41\%$; 0.35 ± 0.02 and 0.02 ± 0.05 mm., respectively. The moisture content of soybean was indicated higher than black sesame. The value of moisture content of soybean and black sesame were 4.50 ± 0.21 , 4.50 ± 0.25 and $4.44 \pm 0.16\%$; 2.49 ± 0.20 , 2.55 ± 0.22 and $2.57 \pm 0.27\%$ for 0, 12 and 24 h, respectively. This finding demonstrated that GABA content of soybean and black sesame could be improved by 24 h germination. Then, the chosen conditions of two kind of cereals were selected to produce the instant healthy beverage in the further process.

Keywords: germination, soybean, γ -aminobutyric acid, black sesame

Introduction

Nowadays, cereals are containing high protein quality and different phytochemicals which possess for many biological functions, such as antioxidant, antitumor effects and antidiabetic (Lau et al., 2012). Especially, soybean and sesame are the health grains which popular consuming in Thailand. Also, soybean (*Glycine max* L.) is famous food legumes in China, Korea, Japan and Thailand.

Soybean proteins are high quality proteins, rich in lysine, and their amino acid profile resemble that of cereal proteins (Castrorubio et al., 2006). This bean has been received considerable in disease prevention, especially in relation to osteoporosis, heart disease and cancer (Messina & Messina, 2000).

Sesame (*Sesamum indica* L.) belongs to the Pedaliaceae family, which is grown in tropical area including Asia, Africa and America (Basso et al., 2021). The seeds contain many compound that have antioxidant activity such as sesamin, sesamol, sesamolol and sesaminol (Rangkadilok et al., 2010).

Germination is a natural process occurred during growth period of seeds when they meet the minimum condition for growth and development (Sangronis et al., 2006). In germination process, cereal seeds softening the kernel structure after germination in the texture. Recent studies showed that germination can further enhance the nutrition and medicinal value of edible seeds (Gan et al.,

2017). Because, there are many hydrolytic enzymes activated, which may produce minor nutrients such as γ -aminobutyric acid (GABA), simple sugars, peptides and vitamins (Moongngarm & Saetung, 2010).

γ -Aminobutyric acid (GABA) is a four carbon nonprotein amino acid that is produced by decarboxylation of L-glutamic acid that catalyzed by glutamate decarboxylase enzyme (Chua et al., 2019). GABA provides many beneficial effects for health including decreasing blood pressure, a potential treatment for neurological and sleep disorders, diuretic effect, tranquilizer effect, anticancer and others (Oh and Oh, 2004; Chung et al., 2009).

In soybean, the germination process induced a substantial increase in saponin content, oestrogenic compounds and phytosterol. Lipase and α -galactosidase activities increased while lipoxygenase activities reduced after a germination. So, the substantial odour and flavor scores of germinated soybean were improved (Bau et al., 2000). Moreover, germination process increased bioactive compound in soybean including isoflavones, genistein, daidzein, total aglycone (Huang et al., 2014).

In sesame, the germination process reduced in fat content whereas linolenic acid, P, Na, sesamol and α -tocopherol were increased (Hahm et al., 2009). Additionally, Vongsudin et al. (2011) reported that protein content, GABA and vitamin B1 of germinated cereals (Thai rice, maize, soybean and sesame) were increased, while lipid, fiber, carbohydrate and phytic acid content were decreased.

Since, there are many research from soybean and black sesame as mention above have been reported. However, there was no information reported to studied optimal germination time on GABA content produced yellow soybean and black sesame. Therefore, the aim of this investigated was to assess the effect of germination time on GABA content. Also, germination percentage, length of radicles and moisture content were monitored.

Materials and methods

Material

Soybean (*Glycine max* L.) and black sesame (*Sesamum indica* L.) (Taitip brand) were purchased from a local store in the district of Kao Kitchakut, Chanthaburi province and then transported to the laboratory.

Germination preparation

Germinated soybean and black sesame were prepared according to modified methods described by Mongkontanawat et al (2018). Briefly, the samples were soaked in tap water at the ratio of seeds and water (1:10) at 40 °C for 6 hours in the tray. Then, the water was drained and incubated at room temperature for 24 hours. The germination was stopped by drying using a hot air oven (Binder, Germany), at 55 °C for 4.5 hours. Then, the obtained germinated soybean and black sesame were stored at room temperature (37 °C) for 1 week stored and then their properties were evaluated. Experimental design used was completely block design (CRD) for properties determination.

Properties determination

GABA content was sent to analyze by the Institute of Food Research and Product Development (IFRPD) at Kasetsart University in Bangkok, Thailand. A sample of 2.5 g was added to 18 ml of distilled water and 2 ml of 3% sulfosalicylic acid, respectively. Then, the mixture was stirred for 30 minutes and centrifuged. The supernatant (0.1 ml) was mixed with 0.1 ml of NaHCO₃ and 0.40 ml of debsyl-C and these solutions were mixed together. The solution was placed in water bath at 70°C for 10 minutes. The obtained solution was then mixed with 0.25 ml of ethanol and 0.25 ml of 0.025 M KH₂PO₂. The γ -aminobutyric acid (GABA) was evaluated using a high performance

liquid chromatography (HPLC) (HPLC-UV detector:agilent, 1,200 serie; column:supercosil LC-DABS, 15 cm x 4.6 cm,3 um; flow rate 1 ml/min; mobile phase: gradient 80 % CH₃COONa pH 6.80, acetonitrile inject volume 5 ul; column temperature 40 °C, detector: uv 465 nm and standard GABA ≥ 99 %) (Tadashi et al., 1998). Germination percentage was calculated by using 400 seeds. Length of radicles (mm) of germinated soybean and black sesame were measured by using vernia caliper. The moister content was evaluated by using Moisture analyzer (Sartorius MA 45, Germany).

Statistical analysis

All experiments were performed in triplicate using different lots of germinated soybean and black sesame. Analysis of variance (ANOVA) ($p \leq 0.05$) were conducted the data. Significant difference among means within each experiment were separated by Duncan's multiple range test (DMRT) at a significance level of $\alpha = 0.05$ by using computer software (Helge, 2009).

Results and Discussion

From three germination time 0, 12, 24 hours were observbed in germination process at 37 °C for 24 hours of soybean and black sesame. Results revealed that significantly ($p < 0.05$) highest GABA of soybean and black sesame was found when germinated at 24 hour. The value of GABA content of soybean was 13.50 ± 0.21 , 62.58 ± 1.05 and 67.11 ± 1.78 mg/100g of dry weight and black sesame was 11.40 ± 0.04 , 19.01 ± 0.32 and 22.84 ± 0.82 mg/100g of dry weight, respectively for 0,12 and 24 hours germination as presents in Figure 1. So, the optimal germination time on GABA content produced soybean and black sesame were 24 h germination. However, the germination time was carried out until 24 hours, which was not enough to investigate the effect on GABA level. The incubation time should be conducted a little longer in order to ensure the exact effects of time on germination process on GABA level. In contrast, best on this investigation, the GABA content of soybean was exhibited higher than those black sesame. Our result was agreement with Tiansawang et al. (2016), who founded GABA content also significantly high in germinated soybean, followed by germinated black bean and soaked sesame, respectively. Moreover, Tiansawang et al. (2014) also exhibited that significantly highest the amount of GABA of mung bean found also in 24 h germination. Additionally, our results in line with Liu et al. (2011), who reported that the germinated sesame increased GABA content and phenolic compound whereas sesamin content decreased. In addition, Mostafa et al. (1987) also reported that the germination of soybean increased non-protein amino acid and decreased reducing sugar.

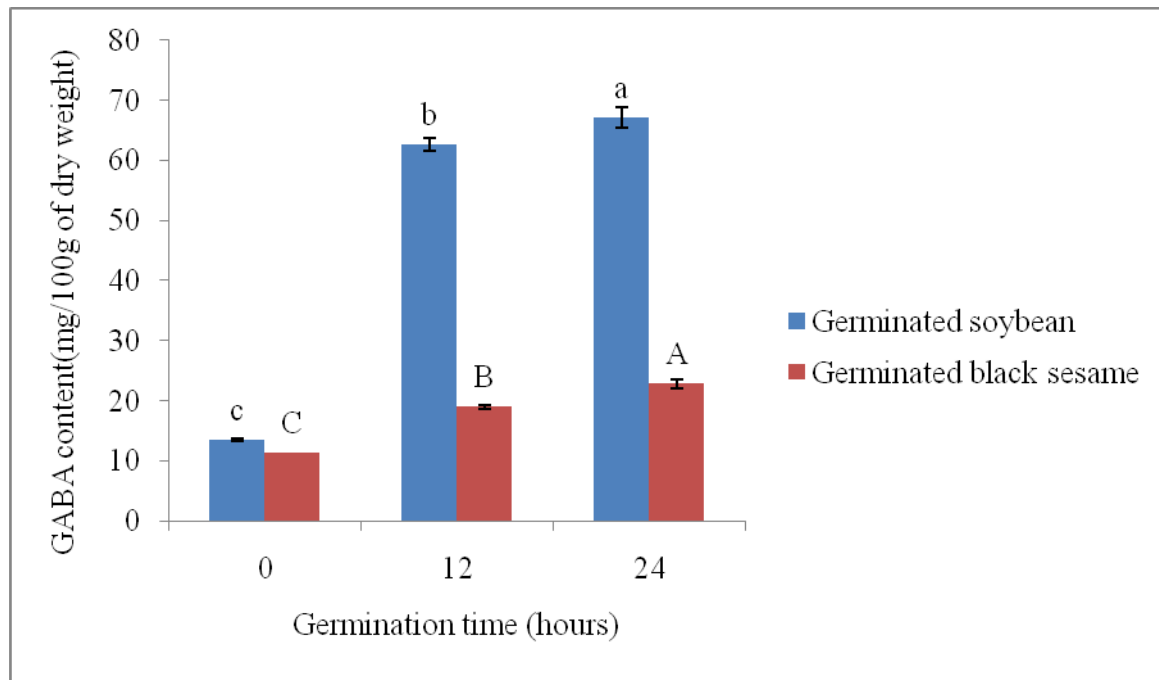


Figure 1 Effect of germination time on GABA content of germinated soybean and black sesame. Data reported are the mean±SD of triplicate determination.

For the germination percentage, the germinated soybean and black sesame were occurred when their germinated at 24 h. The value of % germination of soybean and black sesame were 91±2.5 and 61±1.41 % as shows in Figure 2. This could be due to the differences type of cultivars, old of seeds and other different, therefore, the germination percentage was different.

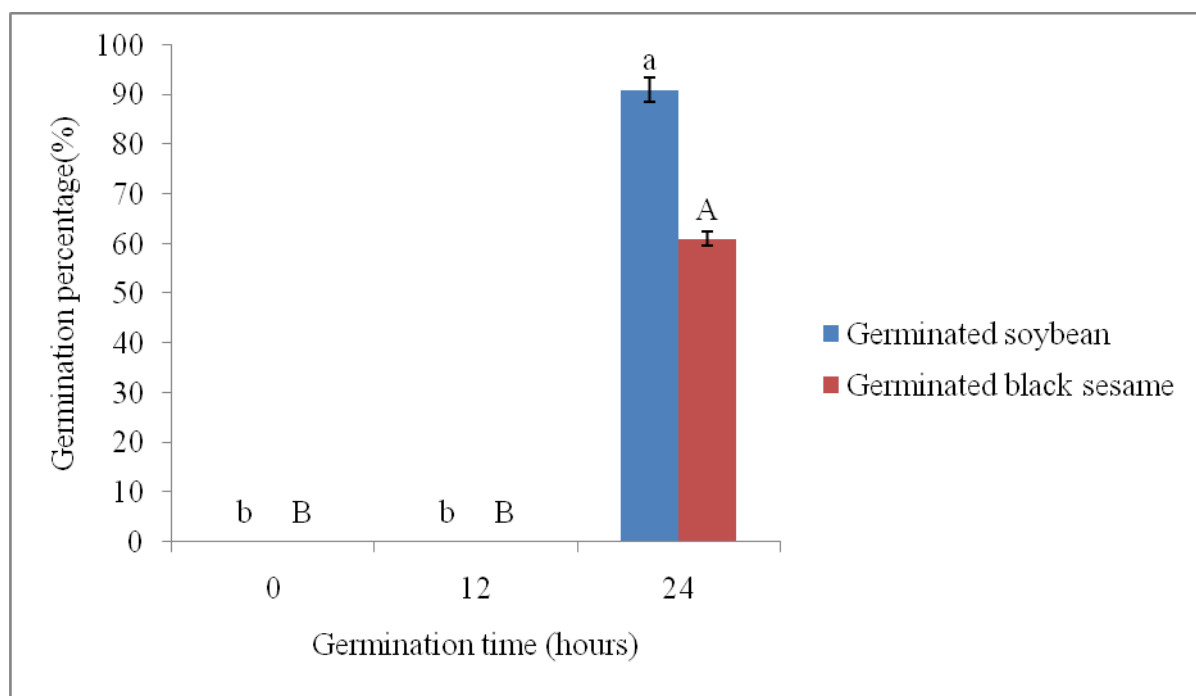


Figure 2 Effect of germination time on germination percentage of germinated soybean and black sesame. Data reported are the mean±SD of triplicate determination.

Figure 3 showed the length of radicles of soybean and black sesame. Result demonstrated that the length of radicles of soybean founded longer than those black sesame in their germinated at 24 h germination. The value of length of radicles of soybean and black sesame were 0.35 ± 0.02 mm and 0.02 ± 0.01 mm, respectively. This could be the size of soybean seed was bigger than black sesame and differ in mineral substance. The content of mineral of soybean could be higher than that of sesame. Therefore, the length of radicles of soybean was longer than those black sesame (Paucar-Menacho et al., 2010).

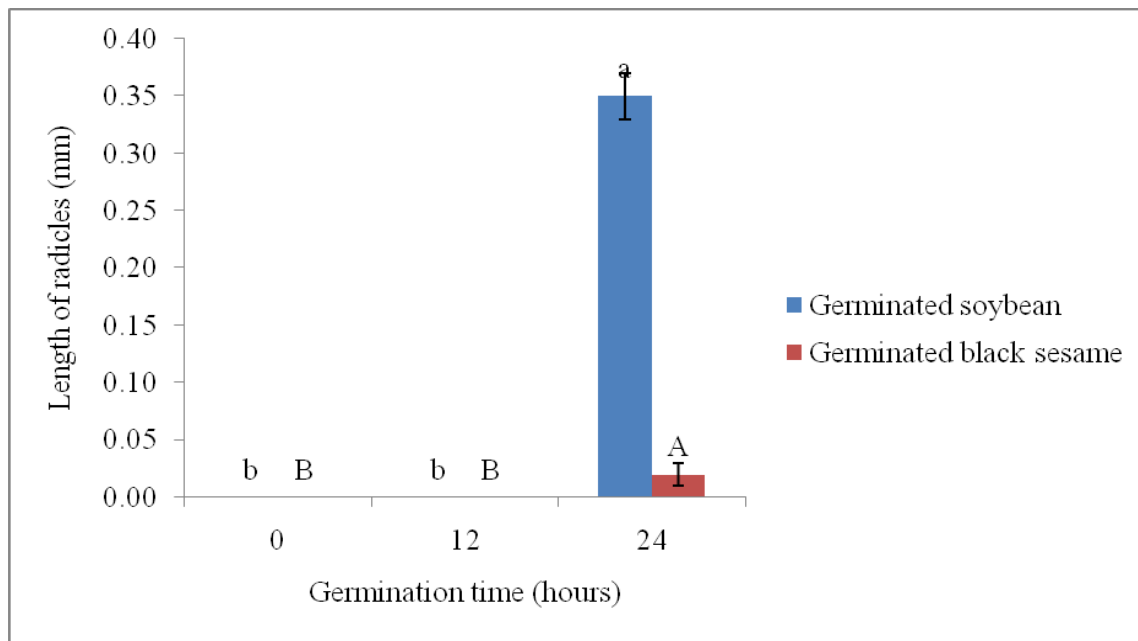


Figure 3 Effect of germination time on length of radicles of germinated soybean and black sesame. Data reported are the mean \pm SD of triplicate determination.

After the grain were germinated and dried, then the moisture content of samples were determined as represents in Figure 4. The dry basis of moisture content of soybean was 4.50 ± 0.21 , 4.50 ± 0.25 and 4.44 ± 0.16 % for 0, 12 and 24 h, respectively. For black sesame, the moisture content was 2.49 ± 0.20 , 2.55 ± 0.22 and 2.57 ± 0.27 % for 0, 12 and 24 h, respectively. This could be the structure and size of soybean and black sesame are difference, so, after the seeds were dried by hot air oven, the moisture transport from the interior of the solid to the surface, the vaporization of liquid at the surface and the transport of the vapor into gas phase, so, the moisture content is differ (Seyed et al., 1999).

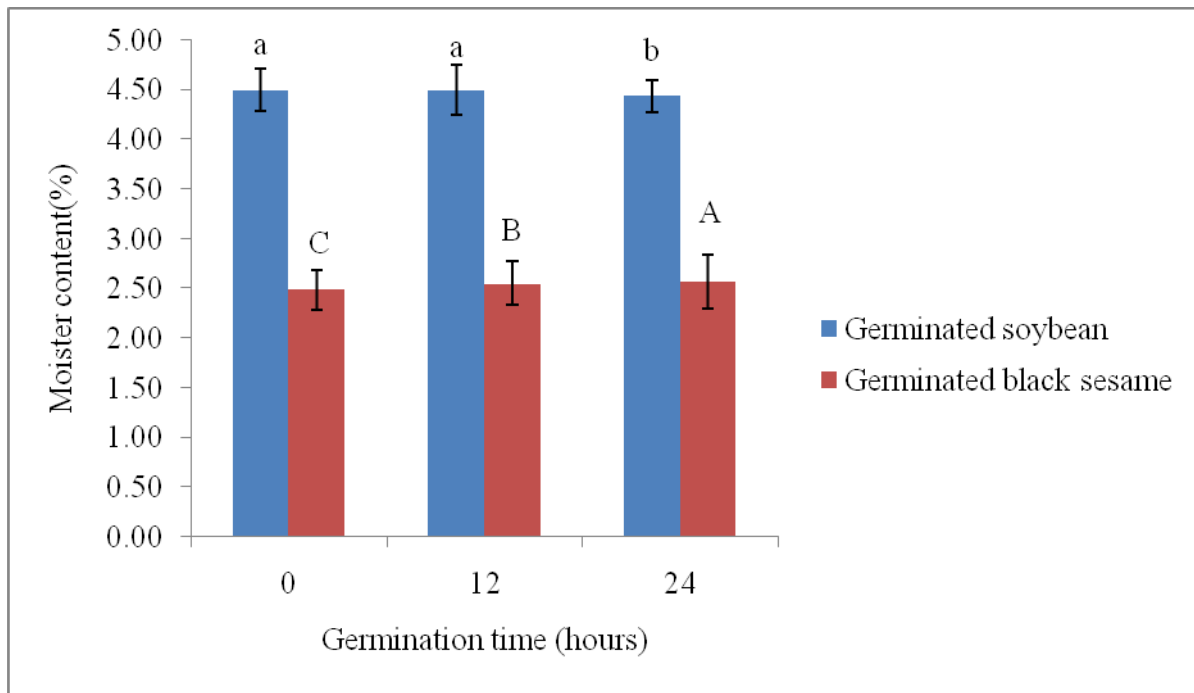


Figure 4 Effect of germination time on moisture content of germinated soybean and black sesame. Data reported are the mean±SD of triplicate determination.

Conclusion

In summary, the 24 hours germination increased the GABA content in soybean and black sesame. The GABA content of soybean showed higher than black sesame. These results suggested that the germinated soybean and black sesame are better raw materials than non-germinated seeds for gaining health beneficial substances and could be served as an alternative healthy food source for vegetarians and milk allergic consumers in the future. However, this study should be done for longer germination time in order to investigate the real effect of germination duration. In addition, others bioactive compound could be monitored such as phenolic compound, antioxidant activity, tannin content, phytic acid contents, cytotoxicity to cancer cell line and normal cell line before further application.

Acknowledgments

This research was financially supported by Rajamangala University of Technology Tawan-ok. The authors gratefully acknowledge the technical assistance of Sonsri Toikham and Dr. La-ongdao Wongekalak.

References

- Basso, A. C. D., Machado, P.M. R., Chaves, J. O., Parreiras, P. M. & Menezes, C. C. (2021). Interference of germination on the nutritional composition and antioxidant capacity of black sesame (*Sesamum indicum* L.). *British Food Journal*, 123(11), 3436-3447.
- Bau, H.M., Villaume, C. & Mejean, L. (2000). Effect of soybean (*Glycine max*) germination on biologically active components, nutritional value of seeds, and biological characteristics in rats. *Food/Nahrung*, 44(1), 2-6.
- Castro Rubio, A., Garcia, M., & Marina, M. (2006). Rapid separation of soybean and cereal (wheat, corn, and rice) proteins in complex mixtures: Application to the selective determination of the

- soybean protein content in commercial cereal-based products. *Analytica Chimica Acta*, 558(1-2), 28-34.
- Chua, J.Y., Koh, M.K.P. & Liu, S.Q. (2019). 2-Gamma-aminobutyric acid: A bioactive compound in foods. *Spouted Grains*, 25-54.
- Chung, H. J., Jang, S. H., Cho, H. Y., & Lim, S. T. (2009). Effects of steeping and anaerobic treatment on GABA (γ -aminobutyric acid) content in germinated waxy hull-less barley. *LWT-Food Science and Technology*, 42(10), 1712-1716.
- Gan, R.Y., Lui, W.Y., Wu, K., Chan, C.L., Dai, S.H., Sui, Z.Q. & Corke, H. (2017). Bioactive compounds and bioactivities of germinated edible seeds and sprouts: An updated review. *Trends in Food Science & Technology*, 59, 1-14.
- Hahm, T.S., Park, S.J. & Lo, Y.M. (2009). Effects of germination on chemical composition and functional properties of sesame (*Sesamum indicum* L.) seeds. *Bioresource Technology*, 100(4), 1643-1647.
- Helge, T.S. (2009). *Statistical Analysis of Designed Experiments*. Third Edition, Springer New York Dordrecht Heidelberg, London.
- Huang, X., Cai, W. & Xu, B. (2014). Review: Kinetic changes of nutrients and antioxidant capacities of germinated soybean (*Glycine max* L.) and mung bean (*Vigna radiate* L.) with germination time. *Food chemistry*, 143, 268-276.
- Lau, T.C., Chan, M.W., Tan, H.P. & Kwek, C.L. (2012). Functional food: a growing trend among the health conscious. *Asian Social Science*, 9(1), 198-208.
- Liu, B., Guo, X., Zhu, K. & Liu, Y. (2011). Nutritional evaluation and antioxidant activity of sesame sprouts. *Food chemistry*, 129, 799-803.
- Messina, M. & Messina, V. (2000). Soyfoods, soybean isoflavones, and bone health: A brief overview. *Journal of Renal Nutrition*, 10(2), 63-68.
- Mongkontanawat, N., Wongekalak, L., Nonmuang, W., & Thumrongchote, D. (2018). Yoghurt production from germinated native black rice (Maepayatong Dum Rice). *International Journal of Agricultural Technology*, 14, 543-558.
- Moongngarm, A., & Saetung, N. (2010). Comparison of chemical compositions and bioactive compounds of germinated rough rice and brown rice. *Food Chemistry*, 122(3), 782-788.
- Mostafa, M.M., Rahma, E.H. & Rady, A.H. (1987). Chemical and nutritional changes in soybean during germination. *Food Chemistry*, 23(4), 257-275.
- Oh, C. H., & Oh, S. H. (2004). Effect of germinated brown rice extracts with enhanced levels of GABA on cancer cell proliferation and apoptosis. *Journal of Medicinal Food*, 7(1), 19-23.
- Paucar-Menacho, L.M., Berhow, M.A., Mandarino, J.M.G., Chang, Y.K. & de Mejia, E.G. (2010). Effect of time and temperature on bioactive compounds in germinated Brazilian soybean cultivar BRS 258. *Food Research International*, 43, 1856-1865.
- Rangkadilok, N., Pholphana, N., Mahidol, C., Wongyai, W., Saengsooksree, K., Nookabkaew, S., & Satayavivad, J. (2010). Variation of sesamin, sesamol and tocopherols in sesame (*Sesamum indicum* L.) seeds and oil products in Thailand. *Food Chemistry*, 122(3), 724-730.
- Sangronis, E., Rodriguez, M., Cava, R. & Torres, A. (2006). Protein quality of germinated Phaseolus Vulgaris. *European Food Research and Technology*, 222, 144-148.
- Seyed, J.Y., Moreira, R.G. & Yamseangsung, R. (1999). Superheated steam impingement drying of tortilla chip. *Drying Technology*, 17, 191-213.
- Tadashi, A., Yoshiatsu, K., Wen Bin, Y. & Toshihiko, K. (1998). High performance liquid chromatographic determination of β -alanine, β -aminoisobutyric acid and γ -aminobutyric acid in tissue extracts and urine of normal and caminooxy acetate-treated rats. *Journal of Chromatography B* 712: 43-49.

- Tiansawang, K., Luangpituksa, P., Varayanond, W. & Hansawasdi, C. (2014). GABA (gamma-aminobutyric acid) production of mung bean (*Phaseolus aureus*) during germination and the cooking effect. *Suranaree Journal of Science and Technology*, 21(4), 307-313.
- Tiansawang, K., Luangpituksa, P., Varayanond, W. & Hansawasdi, C. (2016). GABA (γ -aminobutyric acid) production, antioxidant activity in some germinated dietary seeds and the effect of cooking on their GABA content. *Food Science and Technology*, 36(2), 313-321.
- Vongsudin, W., Laohakunjit, N. and Kerdchoechuen, O. (2011). Phytochemical change and antioxidant activities of germinated cereals. *Agricultural Science Journal*, 42(2), 113-116.

A Comparative Study of the Quality of Dietary Fiber from Defatted Rice Bran Extracted using Different Methods

Piyatida Deeam and Pilairuk Intipunya*

Department of food science and technology Faculty of Agro-Industry, 155 Muang Chiang Mai, Chiang Mai University, Chiang Mai 50100, Thailand

**Corresponding author: pilairuk.intipunya@cmu.ac.th*

Abstract

The purpose of this study was to investigate properties of dietary fiber extracted by alcoholic, alkali and enzymatic extraction from defatted rice bran, which is an industrial by-product from rice bran oil processing. Chemical and physical properties of the extracted dietary fibers from defatted rice bran were compared. The extraction solutions or enzymes were ethanol, sodium hydroxide and amyloglucosidase. The extraction parameters were concentration of the solutions or enzymes and extraction time. After alcoholic, alkali and enzymatic extraction, crude fiber, total dietary fiber, total phenolic, water holding capacity and oil holding capacity were determined. The alcoholic extraction was found to be a simple process but showed the lowest properties compared to the other two methods. Phenolic content of the extracted dietary fiber by enzymatic method was the highest ($p \leq 0.05$). Crude fiber content, total dietary fiber content, water holding capacity and oil holding capacity of the extracted dietary fiber by alkali extraction were the highest ($p \leq 0.05$).

Keywords: Dietary fiber, Defatted rice bran, Chemical property, Physical property

Introduction

All over the world, rice bran is produced more than 63 million each year (Webber, Hettiarachchy, Webber, & Sivarooban, 2014). Rice bran is mostly used as raw material in rice bran oil extraction to decrease rice mill's waste and produce high value product which is rice bran oil. Defatted rice bran is the by-product from rice bran oil processing after the oil is extracted out. Full fat rice bran and defatted rice bran have different main components. Full fat rice bran contains lipid and active phytochemicals such as gamma-oryzanol, vitamin, phenolic acid, flavonoid and tocopherols (Zhuang et al., 2019), whereas the main nutrients in defatted rice bran are protein, carbohydrate, lignin and phytic acid (Henderson et al., 2012; Zhuang, Yin, Han, & Zhang, 2019). The defatted rice bran is mostly used as animal feed. However, it is seen that defatted rice bran has good potential in being transformed into a higher value product since it contains nutritious dietary fiber.

Dietary fibers are non-starch polysaccharides that are components of plant cell wall (Mudgil & Barak, 2013). Structures and compositions of dietary fibers vary according to species of grain, vegetable and fruit (Mongeau and Brooks, 2016). Dietary fiber is one of the important nutrients for human health. Adequate consumption of fiber has been linked to diverse health benefits (Alba et al., 2018). It is found to benefit human's digestive system (Gagneten et al., 2021; Ibrahim et al., 2021; Karp, Wyrwicz, Kurek, & Agnieszka, 2017; Ma et al., 2021; Yan, Hu, Yang, & Wei, 2018). The other benefits include a decrease in total cholesterol which leads to decreasing cardiovascular risk (Zheng et al., 2019; Zhou et al., 2020). Physical properties, such as water holding capacity and oil holding capacity, can indicate a benefit of fiber for food texture improvement or increasing shelf life. The antioxidant capacity and phenolic compound of dietary fiber has been largely underestimated because chemical hydrolysis release phenolic compound from many steps of extraction. However, phenolic compounds that contain in dietary fiber survive in the gastrointestinal

tract for a long time (Vitaglione, Napolitano, & Fogliano, 2008) and provide health benefits through the antioxidant activity (George, Andersson, Andersson, & Afaf, 2020) which is related to the protection against gastric cancer (Bender et al., 2019).

Extraction is process that separated one or more of components in raw material. There are many methods for extraction that can separate components by different soluble properties (Berk, 2018). There are 2 common methods for fiber extraction, chemical extraction and enzymatic extraction. Both methods have the same purpose of removing oil, protein and starch from fiber. Chemical extraction can be done using various extraction solutions, such as alcohol which is used to extract fiber from corn silk (Kulapichitr, Nitithamyong, & Kosulwat, 2015), pomelo's albedo (Naowakul, 2016), orange (*Citrus Reticulate Blanco*), pomace (Sansawat, 2008) and pineapple core (Prakongpan, Nitithamyong, & and Luangpituksa, 2002); alkali such as sodium hydroxide used in extraction of fiber from pineapple core (Prakongpan et al., 2002) and Silverskin coffee (Narita & Kuniyo Inouye, 2012); sodium carbonate for extraction of fiber from defatted rice bran (Rinsri, 2012); potassium hydroxide for extraction of fiber from rice hull (Tanarungrangsee, Laohankunjit, & Kerdchoechuen, 2014). Extraction method can affect fiber's properties (Ng, Tan, Lai, Long, & Mirhosseini (2010), Alba et al. (2018). Enzymatic extraction involves fiber extraction by various enzymes, such as amylase, protease and cellulase (Weerakul, Sodchit, & Singganusong, 2015, Qi, Jiang, Chen, & Sui, 2011, Thannoun & Younis, 2013, Zheng et al., 2019 and Zhou et al., 2020). After extraction, fiber may be treated further to improve its properties, for example, by extrusion and micronization (Huang & Ma, 2016; Yang, Wu, Cao, Wang, & Zhang, 2021; Zhu, Du, & Xu, 2015).

Since the properties of dietary fiber can be influenced by the extraction method, this paper was aim to determine chemical and physical properties of extracted dietary fiber using different methods in order to select suitable method for fiber extraction from defatted rice bran. Extraction methods included in this study are alcoholic, alkali and enzymatic extraction.

Materials and Methods

Analysis of chemical composition of defatted rice bran

Defatted rice bran was obtained from the rice bran oil processing plant (Surin Rice Bran Oil Co, Ltd.) and kept in laminated plastic bags at -20°C. Crude fiber (FOSS-Fiber analyzer) and total dietary fiber were determined according to AOAC procedures (AOAC, 2000). Phenolic compound was extracted by ethanol for 24 h and then phenolic content was determined by Folin-Ciocalteu method (Luca, 2016).

Extraction procedure

Extract fiber from defatted rice bran by alcoholic extraction (AlcE)

Defatted rice bran was extracted for fiber using the method of Naowakul (2016) and Kulapichitr et al. (2015) with modification. The defatted rice bran sample was extracted twice with ethanol at ratio of 1 g sample: 2 ml solution with continuous agitation. The extraction parameters were concentrations of the solutions and extraction time (75%, 85% and 95% and 8, 16 and 24 h, respectively). Then, ethanol was removed by filtration through a Whatman no. 4 filter paper. The ethanol insoluble solid fraction was collected and dried in a hot air oven at 65°C for 24 h. The extracted fiber from defatted rice bran was ground and kept in sealed aluminum foil bags at room temperature.

Fiber extraction from defatted rice bran by alkali extraction (AlkE)

Defatted rice bran was subjected to fiber extraction by modifying the method of Tanarungrangsee et al. (2014). The defatted rice bran sample was extracted with sodium hydroxide solution at ratio of 1 g sample: 10 ml solution, and maintained for 1-3 h with continuous agitation,

then heated up to 90°C in a water bath. The extraction parameters were concentrations of the solutions and extraction time (1.25%, 2.50% and 5.00% and 1, 2 and 3 h, respectively). Then, the extract was cooled and water was added to the extract at 1:5 (w/w) ratio. The sample was allowed to precipitate for 20 min. This process was repeated 6 times. Then the extract was washed and dried in a hot air oven at 65°C for 24 h. The extracted fiber was ground and kept in sealed aluminum foil bags at room temperature.

Fiber extraction from defatted rice bran by enzymatic extraction (EnzE)

Fiber extraction using enzyme was carried out using the method of Weerakul et al. (2015) and Qi et al. (2011) with modification. The defatted rice bran sample was mixed with a phosphate buffer at pH 6.0 at ratio of 1:10 to dissolve the bran. Then alpha-amylase was added and incubated at 90°C for 30 min followed by cooling. Then, pH was adjusted to 8.0±0.1 by 0.275 N sodium hydroxide and protease was added, followed by incubation at 60°C for 30 min. After extracted by enzyme alpha-amylase and protease, the sample was extracted by amyloglucosidase (260 U/ml). Concentration and extraction time were varied at 0.025%, 0.050% and 0.100% and 30, 60 and 90 min (Weerakul et al., 2015). After extraction, the sample was filtered and washed by ethanol, then dried in a hot air oven at 65°C for 24 h. The extracted fiber was ground and kept in sealed aluminum foil bags at room temperature.

Analysis of dietary fiber's properties

Chemical Properties

Crude fiber (CF) (FOSS-Fiber analyzer) and total dietary fiber (TDF) were determined according to AOAC procedures (AOAC, 2000). Total phenolic content (TPC) of the sample was extracted by ethanol for 24 hour. Then, phenolic content was determined by Folin-Ciocalteu method (Luca, 2016).

Physical Properties

Water holding capacity

Water holding capacity (WHC) was measured by method of Zhang et al. (2017). Briefly, 0.5 g of the sample was vigorously mixed with 5 ml of water, followed by incubation at 25°C for 24 h. The extracted sample was centrifuged at 4000g for 10 min. Initial dry weight of sample was recorded as W_1 , the treated weight of fiber residue was recorded as W_2 . The WHC was then calculated as follows (equation 1)

$$\text{WHC (g/g)} = (W_2 - W_1) / W_1 \quad (\text{equation 1})$$

Oil holding capacity

Oil holding capacity (OHC) was measured by method of Zhang et al. (2017) with appropriate modification. Briefly, 0.5 g of the sample (M_1) was vigorously mixed with 5 ml of soybean oil, incubated at 25°C for 24 h, and centrifuged at 4000g for 10 min. The oil supernatant was then discarded and the weight of residue was recorded as M_2 . The OHC was calculated as follows (equation 2)

$$\text{OHC (g/g)} = (M_2 - M_1) / M_1 \quad (\text{equation 2})$$

Experimental Design and Statistical analysis

The experiment was conducted using a complete randomized design with triplication. The mean values of data from chemical analysis, physical analysis and *In vitro* study were analyzed for

significant difference at $p=0.05$ using general linear model and Duncan’s Multiple Range Test. Statistical analysis were performed using SPSS program version 17.0.

Results and Discussion

Chemical composition of defatted rice bran

Crude fiber (CF), total dietary fiber (TDF) and total phenolic content (TPC) of the defatted rice bran in dry basis were 10.45%, 24.97% and 1.838 mgGAE/g, respectively (**Table1**). The defatted rice bran had higher crude fiber content as compared to that reported by Zhuang et al. (2019) and Wang, Suo, Wit, Boom, and Schutyser (2016) (7.90–8.69% and 8.2–10.5%, respectively). Similar results of TDF were reported by Jue, Martin & Remko (2016) and Huang & Lai (2016), in which the TDF contents were found to be 31.7% and 24.45–24.75%, respectively.

Table 1 Chemical properties of defatted rice bran

Chemical properties	CF (%)	TDF (%)	TPC (mgGAE/g)
Defatted rice bran	10.45 ± 0.19	24.97 ± 0.87	1.838 ± 0.048

The values are expressed as means ± standard deviations (SD) of triplicate measurements.

Chemical properties of extracted fibers using different extraction methods

Crude fiber content

Crude fiber (CF) contents of the extracts obtained from different methods are shown in Table 2, 3 and 4. Extraction time slightly affected the CF content in AlcE and AlkE methods whereas it had no significant effect in EnzE method ($p>0.05$). Concentration of alcohol and alkali tended to increase the CF content of the extracted fiber ($p \leq 0.05$), whereas increasing enzyme concentration did not significantly affect the CF content ($p>0.05$). It is shown that the alkali extraction (AlkE) yielded the highest CF content ($p \leq 0.05$) as compared to the other method. This was because alkali solution was capable of removing other components from defatted rice bran better than other methods. The alkali solution removes not only lipid, protein and carbohydrate, but also removes soluble fiber and some of hemicellulose (Wongsiridetchai, 2017; Julmanlik & Kongruang, 2019; Liu, Zhang, Yi, Quan, & Lin, 2021). From statistical analysis of the results, it was seen that increasing in concentration of sodium hydroxide solution resulted in an increased CF contents ($p \leq 0.05$). Enzyme extraction method (EnzE) was able to extract crude fiber better than the alcoholic extraction (AlcE) ($p \leq 0.05$). The reason why EnzE gave lower CF content than AlkE because EnzE extracts includes soluble and insoluble fibers, and the soluble fibers are eliminated during CF analysis, yielding lower result. The CF content from AlcE was the lowest ($p \leq 0.05$). This was because ethanol solution has less ability to eliminate other components from the defatted rice bran as compared to the other methods. CF contents of the AlcE extracts were in the range of 10.63–12.75%, which is similar to that of defatted rice bran before extraction. Crude fiber mostly include cellulose and lignin contents (Requena et al., 2019), not including all of the dietary fiber content in it. Therefore, many researches prefer to analyze the fiber in terms of TDF because it includes all types of dietary fibers (Kulapichitr et al., 2015; Prakongpan et al., 2002; Tanarungrangsee et al., 2014; Zheng et al., 2019; Zhu et al., 2018). The best extraction method and condition to obtain the highest CF content in this study were AlkE using 2.50% NaOH for 2 h, giving the CF content of $54.27 \pm 0.44\%$.

Table 2 Chemical properties of extracted dietary fiber from alcoholic extraction (AlcE).

Concentration	Time (h)	CF (%)	TDF (%)	TPC (mgGAE/g)
75% EtOH	8	11.61 ± 1.37 ^a	34.94 ± 1.09 ^{ns}	0.042 ± 0.006 ^d
	16	11.40 ± 0.77 ^a	34.51 ± 4.30 ^{ns}	0.045 ± 0.000 ^d
	24	10.84 ± 0.66 ^{ab}	34.72 ± 1.46 ^{ns}	0.100 ± 0.009 ^c
85% EtOH	8	12.40 ± 0.71 ^a	35.61 ± 4.24 ^{ns}	0.043 ± 0.003 ^d
	16	10.64 ± 0.79 ^{ab}	35.74 ± 2.56 ^{ns}	0.045 ± 0.001 ^d
	24	12.43 ± 1.08 ^a	34.18 ± 1.77 ^{ns}	0.023 ± 0.001 ^d
95% EtOH	8	12.23 ± 0.31 ^a	35.26 ± 1.83 ^{ns}	0.234 ± 0.030 ^a
	16	12.16 ± 0.21 ^a	33.95 ± 1.15 ^{ns}	0.159 ± 0.022 ^b
	24	12.75 ± 0.62 ^a	34.41 ± 0.65 ^{ns}	0.166 ± 0.025 ^b

The values are expressed as means ± standard deviations (SD) of triplicate measurements. Values in the same column with different superscripts are significantly different (Duncan, $p \leq 0.05$).

Table 3 Chemical properties of extracted dietary fiber from alkali extraction (AlkE).

Concentration	Time (h)	CF (%)	TDF (%)	TPC (mgGAE/g)
1.25% NaOH	1	36.65 ± 1.83 ^e	67.58 ± 0.15 ^b	0.114 ± 0.015 ^{ns}
	2	34.89 ± 0.89 ^e	60.13 ± 0.02 ^f	0.137 ± 0.035 ^{ns}
	3	39.78 ± 1.18 ^d	64.58 ± 0.08 ^{de}	0.091 ± 0.112 ^{ns}
2.50% NaOH	1	43.31 ± 0.89 ^c	67.71 ± 0.13 ^b	0.078 ± 0.006 ^{ns}
	2	54.27 ± 0.44 ^a	71.93 ± 0.02 ^a	0.075 ± 0.061 ^{ns}
	3	50.57 ± 2.84 ^b	70.17 ± 0.42 ^a	0.078 ± 0.012 ^{ns}
5.00% NaOH	1	48.40 ± 1.09 ^b	65.12 ± 0.33 ^d	0.098 ± 0.052 ^{ns}
	2	47.45 ± 0.40 ^b	66.09 ± 0.34 ^c	0.082 ± 0.006 ^{ns}
	3	47.77 ± 0.95 ^b	63.42 ± 0.12 ^e	0.070 ± 0.024 ^{ns}

The values are expressed as means ± standard deviations (SD) of triplicate measurements. Values in the same column with different superscripts are significantly different (Duncan, $p \leq 0.05$).

Table 4 Chemical properties of extracted dietary fiber from enzymatic extraction (EnzE).

Concentration	Time (h)	CF (%)	TDF (%)	TPC (mgGAE/g)
0.025%	0.5	18.28 ± 3.11 ^{ns}	46.07 ± 6.37 ^{bc}	1.715 ± 0.088 ^{ab}
Enz.Amylo- glucosidase	1.0	19.90 ± 3.00 ^{ns}	47.10 ± 6.69 ^{bc}	1.433 ± 0.373 ^b
	1.5	19.65 ± 2.15 ^{ns}	48.46 ± 0.92 ^{bc}	1.956 ± 0.065 ^a
	0.05%	0.5	16.01 ± 0.93 ^{ns}	48.97 ± 2.36 ^{bc}
Enz.Amylo- glucosidase	1.0	16.44 ± 1.67 ^{ns}	51.22 ± 1.88 ^b	1.514 ± 0.156 ^{ab}
	1.5	17.30 ± 2.01 ^{ns}	51.32 ± 1.17 ^b	1.808 ± 0.154 ^{ab}
	0.10%	0.5	16.65 ± 0.77 ^{ns}	51.53 ± 3.86 ^b
Enz.Amylo- glucosidase	1.0	16.79 ± 0.98 ^{ns}	53.61 ± 2.52 ^c	1.794 ± 0.174 ^{ab}
	1.5	18.26 ± 2.16 ^{ns}	60.82 ± 0.67 ^a	1.649 ± 0.216 ^{ab}

The values are expressed as means as ± standard deviations (SD) of triplicate measurements. Values in the same column with different superscripts are significantly different (Duncan, $p \leq 0.05$).

Total dietary fiber

Total dietary fiber (TDF) was not significantly affected by solution concentration and extraction time when use AlcE method ($p > 0.05$), whereas the solution concentration and extraction time significantly affected the TDF content when extracted using AlkE and Enz methods. TDF content of the extracted fiber from AlkE method was the highest ($p \leq 0.05$), followed that from EnzE and AlcE methods ($p \leq 0.05$), respectively (Table 2, 3 and 4). Different extraction procedures influence the extracted dietary fiber content (Kulapichitr et al., 2015). Different extracting solutions have different abilities to remove unwanted components or non-dietary fibers and break down the structure of strong cell wall that is rich in dietary fiber (Berk, 2018). AlkE gave the highest TDF content because alkali can break down the structure of cell wall. It promotes the cracks of surface structure that makes it possible to remove unwanted parts such as proteins and starches (Zhou et al., 2020). The alkali does not only get rid of unwanted parts, but also eliminate the soluble dietary fiber and some types of hemicellulose (Julmanlik & Kongruang, 2019; Requena et al., 2019). Therefore, the main constituents in AlkE method are cellulose and lignin. The TDF content of the extract from AlkE is shown in Table 3 (ranges from 63.4–71.93%). AlkE method using 2.5% sodium hydroxide gave the highest TDF ($p \leq 0.5$). This result is similar to that reported by Kulapichitr et al. (2015) and Tanarungrangsee et al. (2014), in which TDF of 50.8–76.9% and 61.09% were found, respectively. The TDF content from EnzE method (ranges from 42.07–60.82%) was lower than that from AlkE method ($p \leq 0.05$), as shown in Table 4. Enzymatic extraction is very specific extraction method (Karimi, Azizi, Xu, Sahari, & Hamidi, 2018) because each enzyme has a different function, for example alpha-amylase eliminates starches, protease hydrolyses proteins and amyloglucosidase eliminates sugars and starches. From Table 4, it is shown that increasing the concentration of enzyme and extraction time resulted in an increased TDF ($p \leq 0.05$). The research of Zhu et al. (2018), Zheng et al. (2019) and Lina et al. (2019) reported TDF content of 79.22%, 64.88% and 70.03%, respectively, after extracted by enzymatic method. These are higher than the results found in defatted rice bran extract. The TDF content in this study was found to be highest at $71.93 \pm 0.02\%$ when extracted using 2.50% NaOH for 2 h.

Phenolic content

Table 2, 3 and 4 shows the total phenolic content (TPC) of the extracted dietary fiber using AlkE, EnzE and AlcE methods, respectively. Concentration of extracting solution and extraction time significantly affected the TPC of the fiber when extracted using AlcE and EnzE methods ($p \leq 0.05$), whereas they did not significantly affect the TPC when using AlkE method ($p > 0.05$). The EnzE method gave fiber with the highest TPC ($p \leq 0.05$). The TPC of the extract from EnzE method was several times higher than that found in other extraction methods. The results range from 1.433–1.956 mgGAE/g. The extracted fiber content obtained from EnzE using 0.025% amyloglucosidase for 1.5 h was the highest ($p \leq 0.05$). The reason for finding the highest TPC in EnzE method is because the enzymes has less ability to release phenolic compounds from the structure of cell wall than alkali and alcohol solutions. Amyloglucosidase can break down a specific bond like glycosidic bond and peptide bond to eliminate monosaccharides, starches and proteins. Lignocellulose are structures of plant cell wall consist of cellulose, hemicellulose and lignin. Moreover, phenolic compounds are also present in the polymeric form in plants, for example lignin is the polymer of monolignol. The other enzymes such as cellulase, hemicellulase and pectinase can break down the cell wall matrix. Hence, enzymes play a significant role in releasing the insoluble-bound phenolic compounds (Shahidi & Yeo, 2016). The TPC of fiber found in this study is higher than that reported by Zhu, Du & Xu (2015) (0.306 – 0.346 mg/g in qingke extract). AlkE gave lower TPC than that from the EnzE. Insoluble-bound of phenolic compounds can be released from cell wall matrix by alkaline solution by hydrolyzing ether and ester bonds (Estrada, Uribe, & Saldívar, 2014; Shahidi & Yeo, 2016). Meng et al. (2019) reported TPC content of 0.041 – 0.094

mg/g in the extract using alkali method which is similar to the result in this study. AlcE was also found to give low TPC as alkali extraction. At 95% ethanol, the TPC was the highest amongst the AlcE method. Ethanol can dissolve phenolic compound and remove it from the fiber (Baenas et al., 2020). Not only alcohol can remove phenolic compound from the fiber, it may also extract unwanted parts and lignin in which TPC is present. Additionally, extraction time of AlcE method was longer than other methods, which may allow more phenolic compounds being released from the fiber and washed out with the extracting solution.

Physical properties of extracted fibers using different extraction methods

Water and oil holding capacities

Water holding capacity (WHC) of the extracted dietary fiber from AlkE was the highest ($p \leq 0.05$). Increasing the concentration of sodium hydroxide solution significantly increased the WHC of the extracted fiber, as shown in Table 5, 6 and 7. The high WHC of dietary fiber may be influenced by many factors such as fiber composition and structure changes after extraction. The structure changes, such as breaking the intermolecular bond of cell wall that showing more hydrophobic functional groups on the surface (Meng et al., 2019; Yan et al., 2018; Yang, Wu, Song, Yang, & Kan, 2019); increased surface area and porosity (Bender et al., 2019), showing greater exposure of binding sites (Liu et al., 2021) can favor WHC. The WHC from AlkE was the highest ($p \leq 0.05$) because the alkali can break the hydrogen bonds of plant cell wall, creating hydrated hydroxide and carboxyl groups bonds allowing higher water holding capacity (Meng et al., 2019). Dietary fiber from AlkE can combine with water and form hydrogen bonds or dipole interaction within the porous structure (Liu et al., 2021). Since the fiber extracted by AlkE had the highest CF content (Table 3) which is insoluble fiber that has a loose and porous structure (Alba et al., 2018) (Liu, Zhang, Yi, Quan, & Lin, 2021), hence the WHC of the fiber from AlkE were greater than that from the other methods. The WHC from AlcE was 3.14 – 7.86 g/g, which is similar to the WHC of extracted fiber from cactus ricket which is reported to be at 4.8–4.9 g/g (Rouhou, Abdelmoumen, Thomas, & Attia, 2018). In this study, EnzE fiber extract had the WHC of 4.30–4.70 g/g, which is closed to the enzyme extracted fiber from defatted rice bran (4.89 g/g) reported by Hamid & Luan (2000) and from foxtail millet bran (3.24 g/g) reported by Zhu et al. (2018).

Table 5. Physical properties of extracted dietary fiber from alcoholic extraction (AlcE).

Concentration	Time (h)	WHC (g/g)	OHC (g/g)
75% EtOH	8	7.86 ± 0.05 ^a	2.82 ± 0.03 ^e
	16	5.01 ± 0.07 ^g	2.74 ± 0.07 ^f
	24	5.11 ± 0.14 ^e	2.50 ± 0.14 ⁱ
85% EtOH	8	4.82 ± 0.05 ^h	3.25 ± 0.07 ^b
	16	5.02 ± 0.01 ^f	2.68 ± 0.05 ^g
	24	5.27 ± 0.01 ^d	3.01 ± 0.07 ^c
95% EtOH	8	5.76 ± 0.03 ^b	3.43 ± 0.04 ^a
	16	5.42 ± 0.02 ^c	2.66 ± 0.21 ^h
	24	3.14 ± 0.03 ⁱ	2.98 ± 0.03 ^d

The values are expressed as means ± standard deviations (SD) of triplicate measurements.

Values in the same column with different superscripts are significantly different (Duncan, $p \leq 0.05$).

Table 6 Physical properties of extracted dietary fiber from alkali extraction (AlkE).

Concentration	Time (h)	WHC (g/g)	OHC (g/g)
1.25% NaOH	1	9.03 ± 0.05 ^c	4.31 ± 0.47 ^{cd}
	2	8.90 ± 0.18 ^c	3.56 ± 0.30 ^d
	3	9.00 ± 0.12 ^c	4.25 ± 0.73 ^{cd}
2.50% NaOH	1	10.67 ± 0.48 ^b	4.72 ± 0.13 ^{abc}
	2	11.01 ± 0.67 ^b	5.55 ± 0.58 ^a
	3	11.19 ± 0.29 ^b	5.08 ± 0.03 ^{ab}
5.00% NaOH	1	12.72 ± 0.51 ^a	4.72 ± 0.11 ^{abc}
	2	13.44 ± 0.17 ^a	5.26 ± 0.08 ^a
	3	13.54 ± 0.59 ^a	5.06 ± 0.08 ^{ab}

The values are expressed as means ± standard deviations (SD) of triplicate measurements. Values in the same column with different superscripts are significantly different (Duncan, $p \leq 0.05$).

Table 7 Physical properties of extracted dietary fiber from enzymatic extraction (EnzE).

Concentration	Time (h)	WHC (g/g)	OHC (g/g)
0.025%	0.5	4.43 ± 0.10 ^{bc}	3.02 ± 0.05 ^b
Enz.Amylo-glucosidase	1.0	4.69 ± 0.09 ^a	3.43 ± 0.10 ^a
	1.5	4.46 ± 0.12 ^{bc}	3.43 ± 0.13 ^a
0.05%	0.5	4.49 ± 0.08 ^{bc}	3.02 ± 0.02 ^b
	1.0	4.54 ± 0.05 ^b	3.14 ± 0.11 ^b
Enz.Amylo-glucosidase	1.5	4.30 ± 0.08 ^c	3.34 ± 0.06 ^a
	0.1%	0.5	4.70 ± 0.16 ^a
Enz.Amylo-glucosidase	1.0	4.37 ± 0.15 ^{bc}	3.43 ± 0.14 ^a
	1.5	4.39 ± 0.06 ^{bc}	3.41 ± 0.08 ^a

The Values are expressed as means ± standard deviations (SD) of triplicate measurements. Values in the same column with different superscripts are significantly different (Duncan, $p \leq 0.05$).

Oil holding capacity (OHC) of the fibers extracted from the defatted rice bran was affected in the same way as WHC when using different extraction methods. The studies of Meng et al. (2019) and Rouhou, Abdelmoumen, Thomas, & Attia (2018) reported the same responses of WHC and OHC when different extraction methods were used. The extracted dietary fiber has ability to hold oil because the lipophilic function group is exposed after extraction (Rouhou et al., 2018). In this research, OHC of AlkE extracted fiber was the highest (3.56–5.55 g/g) ($p \leq 0.05$). AlcE and EnzE extracted fibers had similar values (2.50 – 3.43 g/g and 3.02 – 3.43 g/g, respectively). Meng et al. (2019) also found that the OHC of dietary fiber extracted by alcohol was lower than that of dietary fiber extracted by alkali solution with enzyme.

Conclusions

The various properties of extracted dietary fiber from ethanol extraction, sodium hydroxide solution and amyloglucosidase enzymes were studied. Extraction method significantly influenced the chemical and physical properties of dietary fiber extracted from defatted rice bran. The dietary fiber extracted using ethanol exhibited the lowest chemical and physical properties in this study. Enzymatic extraction showed higher phenolic contents than the other method, while dietary fiber

extracted using alkaline solution contained higher crude fiber content, total dietary fiber content, water holding capacity and oil holding capacity than the other method. From the results of this study, it can be recommended that extraction method should be selected according to a specific application purpose to the fiber. Enzymatic method may be used to obtain high phenolic fiber. Alkali method may be best used when water holding and oil holding capacities are desirable. Never the less, alcoholic extraction can still be used when enzymes are not available or not cost effective, or alkali is concerned in terms of environment and consumer acceptance issues.

References

- Alba, K., MacNauantan, W., Laws, A. P., Foster, T. J., Compbell, G. M., & Kpntogiorgos, V. (2018). Fractionation and characterization of dietary fiber from blackcurrant pomace. *Journal of food hydrocolloids*, 81(2018), 398-408.
- AOAC. (2000). *Official methods of analysis of AOAC international*. 17th ed. Verginia, USA, Association of Official Analysis Chemists.
- Baenas, N., Nuñez-Gómez, V., Navarro-González, I., Sánchez-Martínez, L., García-Alonso, J., Periago, M. J., & González-Barrio. R. (2020). Raspberry dietary fibre: Chemical properties, functional evaluation and prebiotic in vitro effect. *LWT - Food Science and Technology*, 134(2020).
- Bender, A. B., Goulart, F. R., Silva, L. P. D., & Penna, N. G. (2019). Micronization and extrusion processing on the physicochemical properties of dietary fiber. *Ciência Rural*, 49(7).
- Berk, Z. (2018). *Food Process Engineering and Technology* (third ed.).
- Estrada, A. B. B., Uribe, A. G. J., & Saldívar, S.O. S. (2014). Bound phenolics in foods, a review. *Food Chemistry*, 152(1).
- Gagneten, M., Archaina, D. A., Salas, M. P., Leiva, G. E., Salvatori, D. M., & Carolina, S. (2021). Gluten-free cookies added with fibre and bioactive compounds from blackcurrant residue. *International Journal of Food Science & Technology* 56(4).
- George, N., Andersson, A. M., Andersson, R., & Afaf, K. E.. (2020). Lignin is the main determinant of total dietary fiber differences between date fruit (*Phoenix dactylifera* L.) varieties. *NFS Journal*, 21.
- Henderson, A. J., Ollila, C. A., Kumar, A., Borresen, E. C., Raina, K., Agarwal, R., & Elizabeth P. R. (2012). Chemopreventive Properties of Dietary Rice Bran: Current Status and Future Prospects. *Advances in Nutrition*, 3(5), 643-653.
- Hua, M., Lu, J., Qu, D., Liu, C., Zhang, L., Li, S., & Sun, Y. (2019). Structure, physicochemical properties and adsorption function of insoluble dietary fiber from ginseng residue: A potential functional ingredient. *Food Chemistry*, 286(15), 522-529.
- Huang, Y. L., & Ma, Y. S. (2016). The effect of extrusion processing on the physiochemical properties of extruded orange pomace. *Food Chemistry*, 192(2016), 363-369.
- Huang, Y. P., & Lai, H. M. (2016). Bioactive compounds and antioxidative activity of colored rice bran. *Food Drug Anal*, 24(3), 564-574.
- Julmanlik, T., & Kongruang, S. (2019). Functional Properties and Applications of Egg White Protein Hydrolysates. *Journal of Food Technology Siam University*, 14(1), 69-87.
- Karimi, R., Azizi, M. H., Xu, Q., Sahari, M. A., & Hamidi, Z. (2018). Enzymatic removal of starch and protein during the extraction of dietary fiber from barley bran. *Journal of Cereal Science*, 83(September 2018), 259-265.
- Karp, S., Wyrwisz, J., Kurek, M. A., & Agnieszka, W. (2017). Combined use of cocoa dietary fibre and steviol glycosides in low-calorie muffins production. *International Journal of Food Science & Technology*, 52(4).

- Kulapichitr, F., Nitithamyong, A., & Kosulwat, S. (2015). Extraction of dietary fiber from corn silk (*Zea mays*) and its application in food products. *KMUTT Research and Development Journal*, 38(1), 19-34.
- Lina, Y., Wangb, H., Raoc, W., Cuia, Y., Daiad, Z., & Shen, Q. (2019). Structural characteristics of dietary fiber (*Vigna radiata L. hull*) and its inhibitory effect on phospholipid digestion as an additive in fish floss. *Food Control*, 98, 74-81.
- Liu, H., Zeng, X., Huang, J., Yuan, X., Wang, Q., & Ma, L. (2021). Dietary fiber extracted from pomelo fruitlets promotes intestinal functions, both in vitro and in vivo. *Carbohydrate Polymers*, 252.
- Liu, Y., Zhang, H., Yi, C., Quan, K., & Lin, B. (2021). Chemical composition, structure, physicochemical and functional properties of rice bran dietary fiber modified by cellulase treatment. *Food Chemistry*, 342.
- Ma, S., Wang, Z., Liu, N., Zhou, P., Bao, Q., & Xiaoxi Wang. (2021). Effect of wheat bran dietary fibre on the rheological properties of dough during fermentation and Chinese steamed bread quality. *International Journal of Food Science & Technology*, 56(4).
- Mao, T., Huang, F., Zhu, X., Wei, D., & Chen, L. (2021). Effects of dietary fiber on glycemic control and insulin sensitivity in patients with type 2 diabetes: A systematic review and meta-analysis. *Journal of Functional Foods*, 82.
- Meng, X., Liu, F., Xiao, Y., Cao, J., Wang, M., & Duan, X. (2019). Alterations in physicochemical and functional properties of buckwheat straw insoluble dietary fiber by alkaline hydrogen peroxide treatment. *Food Chemistry*, 3(30).
- Mongeau, R. & Brooks, S. P. J. (2016). Dietary fiber: Properties and sources. In *Encyclopedia of food sciences and nutrition* (Vol. 3, pp. 1813-1822). Ottawa, QC, Canada: 3W Banting Research Centre.
- Mudgil, D., & Barak, S. (2013). Composition, Properties and health benefits of indigestible carbohydrate polymers as dietary fiber. *International journal of biological macromolecules*, 61(2013), 1-6.
- Narita, Y., & Kuniyo, I. (2012). High antioxidant activity of coffee silverskin extracts obtained by the treatment of coffee silverskin with subcritical water. *Food Chemistry*, 135(3), 943-949.
- Naowakul, B. (2016). *Production of dietary fiber from Pomelo's albedo with reduced bitterness and Its utilization in dairy Ice cream*. (Master of science). Chiang Mai University, Chiang Mai, Thailand.
- Ng, S. P., Tan, C. P., Lai, O. M., Long, K., & Mirhosseini, H. (2010). Extraction and characterization of dietary fiber from coconut residue. *Journal of Food, Agriculture & Environment* 8(2), 172-177.
- Velasco, P. M. D. R., López, R. I. I., Silva, P. A., Clemente, B. L., Mateos, R., Espinosa, R. H., & Maria de los Angeles Vivar-Vera. (2014). Antioxidant and functional properties of a high dietary fibre powder from carambola (*Averrhoa carambola L.*) pomace. *International Journal of Food Science & Technology*, 49(9).
- Prakongpan, T., Nitithamyong, A., & Luangpituksa, P. (2002). extraction and application of dietary fiber and cellulose from pine apple cores. *Food and Chemical Toxicology*.
- Qi, B., Jiang, L., Chen, Y. L., & Sui, X. (2011). Extracted dietary fiber from the soy pods by chemistry-enzymatic methods. *Proceeding Engineering*, 15(2011), 4862-4873.
- Requena, M. C., García, S. E., Tovar, Y. A. S., Cura, Y. M., González, M. L. C., Reyes, F. C., & Herrera, R. R. (2019). *Dietary fiber: Properties, Recovery, and Application* In Charis M. Galanakis (Ed.), (pp. 1-25).
- Rinsri, P. (2012). *Extraction and application of Beta-glucan from De-oiled rice bran in instant powder drink for elders*. (Master of Science). Chiang Mai University, Chiang Mai, Thailand.

- Rouhou, M. C., Abdelmoumen, S., Thomas, S., & Attia, H. (2018). Use of green chemistry methods in the extraction of dietary fibers from cactus rackets (*Opuntia ficus indica*): Structural and microstructural studies. *International Journal of Biological Macromolecules*, 116.
- Sansawat, T. (2008). *Production of dietary fiber powder from orange (Citrus reticulata Blanco) pomace*. (Master of science). Chiang Mai University, Chiang Mai, Thailand.
- Shahidi, F., & Yeo, J. D. (2016). Insoluble-Bound Phenolics in Food. *Molecules*, 21(9).
- Tanarungrangsee, K., Laohankunjit, N., & Kerdchoechuen, O. (2014). Extraction of dietary fiber from rice hull. *Agricultural Sci. J.*, 45(2), 1-4.
- Thannoun, A. M., & Younis, K. W. (2013). Extraction and evaluation of total dietary fibers from some vegetables. *Mesopotamia J. of Agric*, 41(4).
- Vitaglione, P., Napolitano, A., & Fogliano, V. (2008). Cereal dietary fiber: a natural functional ingredient to deliver phenolic compounds into the gut. *Food Science and Technology*, 19(2008), 451-463.
- Wang, J., Suo, G., Wit, M. D., Boom, R. M., & Schutyser, M. A. I. (2016). Dietary fibre enrichment from defatted rice bran by dry fractionation. *Food Process Engineering*, 186(2016), 50-57.
- Webber, A., Hettiarachchy, N. S., Webber, D., & Sivarooban, T. (2014). Heat-Stabilized Defatted Rice Bran (HDRB) as an Alternative Growth Medium for *Saccharomyces cerevisiae*. *Journal of Food and Nutrition*, 1(103), 1-6.
- Weerakul, K., Sodchit, C., & Singganusong, R. (2015). Extraction and utilization of dietary fiber from banana peels. *SDU Research Journal*, 8(3), 61-80.
- Wongsiridetchai. C. (2017). *Prebiotic properties of oligosaccharide produced from the spent coffee grounds b mannanase from Bacillus sp.* (Master of science). Thammasat University, Thailand
- Yan, J., Hu, J., Yang, R., & Wei, Z. (2018). A new nanofibrillated and hydrophobic grafted dietary fibre derived from bamboo leaves: enhanced physicochemical properties and real adsorption capacity of oil. *International Journal of Food Science & Technology* 53(10).
- Yang, B., Wu, Q., Song, X., Yang, Q., & Kan, J. (2019). Physicochemical properties and bioactive function of Japanese grape (*Hovenia dulcis*) pomace insoluble dietary fibre modified by ball milling and complex enzyme treatment. *International Journal of Food Science & Technology*, 54(7).
- Yang, M., Wu, L., Cao, C., Wang, S., & Zhang, D. (2021). Extrusion improved the physical and chemical properties of dietary fibre from bamboo shoot by-products. 56(2).
- Zhang, D., Wang, L., Tan, B., & Zhang, W. (2020). Dietary fibre extracted from different types of whole grains and beans: a comparative study. *International Journal of Food Science & Technology*, 55(5).
- Zhang, W., Zeng, G., Pan, Y., Chen, W., Huang, W., & Chen, H. (2017). Properties of soluble dietary fiber-polysaccharide from papaya peel obtained through alkaline or ultrasound-assisted alkaline extraction. *Carbohydrate Polymers*, 172(15 September 2017), 102-112.
- Zheng, Y., Wang, Q., Huang, J., Fang, D., Zhuang, W., Luo, X., & Hui, C. (2019). Hypoglycemia effect of dietary fibers from bamboo shoot shell: An in vitro and in vivo study. *Food and Chemical Toxicology*.
- Zhou, D., Liu, J., Liu, S., Liu, X., Tang, X., & Xueze L. (2020). Characterisation of alkaline and enzymatic modified insoluble dietary fibre from *Undaria pinnatifida*. *International Journal of Food Science & Technology*, 55(12).
- Zhu, F., Du, B., & Xu, B. (2015). Superfine grinding improves functional properties and antioxidant capacities of bran dietary fibre from Qingke (hull-less barley) grown in Qinghai-Tibet Plateau, China. *Journal of Cereal Science*, 65, 43-47.
- Zhu, Y., Chu, J., Lu, Z., Lv, F., Bie, X., Zhang, C., & Zhao, H. (2018). Physicochemical and functional properties of dietary fiber from foxtail millet (*Setaria italic*) bran. *Journal of Cereal Science*, 79(2018), 456-461.

Zhuang, X., Yin, T., Han, W., & Zhang, X. (2019). *Nutritional ingredients and active compositions of defatted rice bran*. In (pp. 247-270). Academy of state administration of grain, Beijing, China.

Physicochemical Quality of Gotu Kola Juice Treated by Non-Thermal Plasma

Nunnapus Bumrungrpanichthaworn and Pilairuk Intipunya *

Department of Food Science and Technology, Faculty of Agro-Industry, 155 Muang Chiang Mai,
Chiang Mai University, Chiang Mai 50100, Thailand

* Corresponding email: pilairuk.intipunya@cmu.ac.th

Abstract

Gotu kola (*Centella Asiatica*) is a medicinal plant with vital health compounds and has antioxidant properties. The leaves are eaten as salad vegetables and used for juicing. Most of the previous researches studied the effects of heat treatment and some on non-thermal technologies such as HHP and microwaves on quality of Gotu kola. Application of plasma technology in food is still limited. Therefore, this study was aimed to determine the change in quality of Gotu kola juice during plasma processing. The juice was extracted and treated with plasma at control conditions (15 kV constant power, and treatment time of 30 minutes). The plasma gas was varied by mixing argon gas (15 L/min) and air (at flow rates of 0, 5 and 10 L/min). Heat treatment at 72°C for 15 s was carried out for comparison. Some important quality factors such as phenolic compounds, antioxidant activity and physical properties were investigated. Free radicals obtained from the plasma process were also analyzed. It was found that antioxidant activity was significantly reduced but total phenolic content was slightly increased after plasma treatment as compared to untreated sample. Plasma treated juice samples contained higher total phenolic contents as compared to heat treated samples. Total phenolic compound contents of plasma treated juice were in the range of 127.32±2.83 to 149.62±0.86 ugGAE/ml, whereas the percentage inhibition of DPPH were between 13.64±0.41 to 22.12±0.43%. Amongst all plasma treatments, using argon gas alone gave better juice quality after treatment. It was also revealed that plasma production by air and argon gas produced OH, N⁺, NO₂ and NO₃ free radicals. These radicals were able to continuously react to form other free radicals which may affect both the amount of phenolic compounds and the potency of antioxidants. The results of the experiment showed that the optimum conditions for use with Gotu kola juice were plasma-generated conditions using 15 L/min of argon gas only for 10 min.

Keywords: Gotu kola juice, Antioxidant activities, Plasma technology

Introduction

Gotu kola is a medicinal plant with medicinal properties. It is commonly known as Pennywort and Gotu kola in America. Its scientific name is *Centella asiatica*. Gotu kola is often used as an herbal remedy where all parts of the plant including the leaves, stems, and roots are edible. The leaves and stems are eaten as salad vegetables in Southeast Asia (Hashim, 2011a; Hashim et al., 2011) and are commonly processed into a beverage in Thailand. Numerous studies have shown that Gotu kola contains bioactive compounds and has medicinal value. It has antimicrobial, antifungal, antidiabetic, and antioxidant activity. This is due to the production of various bioactive secondary active ingredients (Polash, Saha, Hossain, & Sarker, 2017). The anti-inflammatory activity of Gotu kola on gastrointestinal disorders has also being studied. Asthma and wound healing were mainly attributed to the terpenoid and flavonoid groups in the leaves (Belwal et al., 2019). Gotu Kola is full of phytonutrients, including tannin, flavonoid, saponin, phenol, and glycoside, which are found in leaves rather than stems (Polash et al., 2017). In addition, Gotu kola contains a triterpenoid glycoside, which consists of asiaticoside, asiatic acid, Madecassoside, and madecassic acid, as shown in Figure 1.

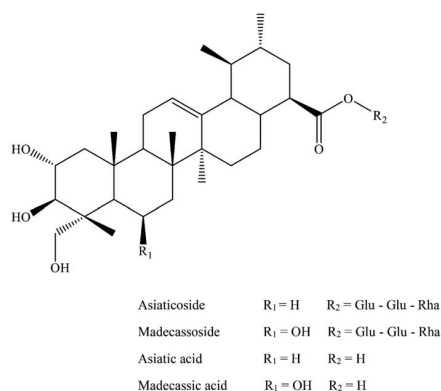


Figure 1 Structure chemical of Triterpenoid of Gotu kola

Plasma technology is divided into two groups that are fusion plasma (high-temperature plasma) and gas discharge (low-temperature plasma or cold plasma). Low-temperature plasma is a type of novel non-thermal technology, which generates exciting gas with a strong electric field. This state is under atmospheric temperature (Hou et al., 2019). Plasma is a substance that is not in a solid, liquid or gas state, but is in the fourth state called the plasma state of matter. For cold plasma, the discharge will be glow discharge in which the temperature is not higher than room temperature. Plasma operation is to use a discharging medium, which can be a gas or liquid of various types, until the formation of particles or radicals is in a plasma state. The chemical reactions are oxidizing and reducing. The type of gas to generate plasma affects the reactive species in the chamber. Plasma with nitrogen gas or air is released in a chamber solution, which can create the reactive species that are known as ROS (reactive oxygen species) and RNS (reactive nitrogen species). During plasma treatment, ROS species may be formed as H₂O₂, O₃, O₂⁻, O₂⁻², singlet oxygen (¹O₂), and atomic oxygen. RNS species are excited nitrogen (N₂), atom nitrogen (N), and nitric oxide (NO) (Ali, Cheng, & Sun, 2020). These plasma-derived radicals are produced by the decomposition of water, gas separation, and potential chain reactions. In the gas phase, ROS and RNS radicals are formed, such as the H₂O₂ radical reaction (Zhao, Ojha, Burgess, Sun, & Tiwari, 2020). The gaseous air containing N and O is suitable for atmospheric plasma formation (Dantas et al., 2021). It can therefore be used in combination with argon gas. Argon is a carrier gas, which can be used to create plasma. Nitrogen in the air and gas-water interactions produce RNS species (Zhao et al., 2020). These plasma particles have the main part in the reaction, which has an effect on destroying pathogens on the surface and encouraging the creation of new cells (Arjunan, 2011).

In Thailand, fresh Gotu kola juice is commonly consumed as vegetable or healthy vegetable drink. The heat treatment can cause color change and precipitation of insoluble solid in the Gotu kola juice which is undesirable for consumers. Nutritional value of the heat sensitive substances is also reduced. Most of the phenolic compounds in fruits and vegetables are destroyed during traditional heating processes (Zhao, Zhang, & Zhang, 2017). Therefore, non-thermal processing methods such as HPP and Ohmic have been applied. Many researchers report that HPP processing can maintain total phenolic content and antioxidant activity in fruit and vegetable products more efficiently than pasteurization (Zhao et al., 2017). There are some reports on effects of plasma on quality of orange, apple, acerola, and tomato juices. However, the effect of plasma on the quality of Gotu kola juice was not found. This study was conducted in order to investigate the effect of cold processing by plasma on quality of Gotu kola juice and to assess its potential for fruit and vegetable juice processing. Comparison to traditional thermal method was also carried out to see if plasma technology can be one of alternative techniques.

Materials and Methods

Plants material

Fresh Gotu kola (*Centella asiatica*) was procured from the local market (Muang Mai market, Chiang Mai, Thailand). The sample was kept at 4°C prior to preparation and treatments.

Preparation of Gotu kola juice

Fresh Gotu kola leaves were separated and washed in 200 ppm chlorine water to eliminate microorganisms, followed by washing in clean water 3 times to eliminate residual chlorine in the sample. Gotu kola juice was extracted using Gotu kola leaves to water ratio of 1:8. A juice extractor (EM-Ice Power, Thailand) was used for blending at speed level 1 (used the lowest speed of the blender to avoid heat generation during blending) for 1 min and the juice was separated using a hydraulic press machine (Sakaya automate Co., Ltd, Thailand). The extracted juice samples were then subjected to initial quality analysis and treatment with plasma technology and thermal method.

Plasma treatment of Gotu kola juice

The generated plasma is produced by argon gas with purities above 99.9% (Lanna Industrial Gases Co., LTD, Chiang Mai, Thailand). The plasma treatment system composes of a single electrode that is broken down underwater. A solution plasma unit was used to generate plasma which is released out of the capillary tube of 50 cm long with 10 pinholes of 1 mm in diameter. The juice samples were treated using different plasma gas combinations. Argon was used as main plasma gas at a flow rate of 15 L/min and mixed with oxygen gas at flow rates of 0 (P1), 5 (P2), and 10 (P3) L/min for plasma generation. A constant power of 600 Watts was applied for plasma generation. Gotu kola juice (2 liters) was treated for 30 min at each plasma gas combination. Temperature of the sample was monitored during plasma treatment to study the effect of plasma on temperature change and to ensure that the sample is kept under room temperature to avoid thermal acceleration of quality degradation.

Thermal treatment of Gotu kola juice

Extracted juice (500 mL) was heated until the temperature reached 72°C and kept at 72°C for 15 s (condition of high temperature short time pasteurization). Cooling was done immediately using ice water. The sample was immediately analyzed after the treatment.

Determination of DPPH inhibition

The control and treated juice samples were subjected to 2,2-diphenyl-1-picrylhydrazyl (DPPH) analysis following the method described by Chana et al. (2014). The juice sample (0.1mL) was blended with 2.9 ml DPPH solution and held for 30 min in darkness at room temperature. Absorbance was measured at 517 nm wavelength, using a spectrophotometer (Genesys 10S UV-Vis, Thermo Electron, USA). The inhibition of DPPH was calculated in percentage (%Inhibition) according to equation (1):

$$\text{Inhibition \%} = [(A_{\text{control}} - A_{\text{sample}})/A_{\text{control}}] \times 100 \quad (1);$$

where the absorbance of control is A_{control} (containing DPPH solution and 95% ethanol) and the absorbance of the extracts/reference is A_{sample} . Blank contains 95% ethanol for set zero.

Determination of total phenolic content

Total phenolic content was analyzed according to the method described by Ahmad et al. (2015) with some modification. Folin reagent was used to react with the phenolic compounds in the sample and gallic acid was used as a reference. Folin reagent was prepared with Folin-Ciocalteu

reagent (10%) and prepared sodium carbonate (Na_2CO_3) in concentrate as 7.5% before use. Folin reagent (0.5 ml) was mixed with 1.0 ml of sample and left for 8 min at room temperature. After that 4.0 ml of sodium carbonate was added and allowed to react for 2 h in darkness. Absorbance was measured using a spectrophotometer (Genesys 10S UV-Vis, Thermo Electron, USA) at 765 nm wavelength. Standard curve was analyzed using gallic acid. The total content of phenolic was calculated in terms of gallic acid equivalent (ug GAE /ml) by comparing to the standard curve.

Colorimetric Analysis

Color (L^* value, a^* value, and b^* values) of the samples was measured using a colour meter (CIELAB model, Hunterlab ColorQuest XE, Japan). The instrument was calibrated with the standard white and black ceramic plates. Colorimetric variables measured (L^* value, a^* value and b^* values) was used to calculate color changes (ΔE^*_{ab}) according to equation (2):

$$\Delta E^*_{ab} = \sqrt{(\Delta L^*)^2 + (\Delta a^*)^2 + (\Delta b^*)^2} \quad (2);$$

where the color differences (ΔL^{*2} , Δa^{*2} , and Δb^{*2}) were calculated by comparing the color values of the control (untreated juice) and treated plasma juice. The ΔE^*_{ab} presents the quality of color change after the plasma processing. Every parameter was determined in triplicate.

Viscosity measurement

Viscosity of the juice sample was measured using a viscometer (LVDV-II+, Brookfield Engineering Laboratories, Inc., Germany) equipped with a small sample cell, spindle number 28 and operated at rotation speed of 200 rpm. Measurement was done in triplicate.

Plasma gas disintegration analysis (OES spectra and nitrate and nitrite contents)

Plasma gas disintegration analysis was conducted using an optical emission spectra technique (OES technique) to measure the light scattering and the results are shown in the form of signal peaks for N-radical, argon and others. Nitrogen gas disintegration analysis was done using strip test (Waterwork, Rock Hill, USA) that allowed the observation of color change from white to pink. The level of pink color showed the amount of nitrogen gas disintegration in form of nitrates and nitrites.

Experimental design and statically analysis

The experiment was carried out using a complete randomized design with two replications. Data collected from the experiment was analyzed using SPSS ver. 17.0. One-way ANOVA and Duncan's multiple range tests were used to analyze the difference between means.

Results and Discussion

Effects plasma on temperature of Gotu kola juice

Gotu kola extracted juice was stored at 10°C prior to the experiment. Monitoring temperature during plasma treatment is useful for observing quality changes if it is due to thermal induction or plasma discharging. Figure 1 shows a slight temperature increase during plasma treatments at P1 and P2 from a starting temperature of 10°C to maximum of 16.5°C, whereas temperature of the juice in P1 starts at 16°C due to a delay in operation but reached the same maximum temperature as the other treatments. Hence, the temperature rise in all experiment was not more than 6.5°C, and it was still in chilled range and nearly 10°C below room temperature (25°C). Therefore, it is assumed that plasma treatment should not be major cause of thermal degradation of juice quality. The slight

increase in temperature during low-temperature plasma treatment may due to the creation of partially ionized plasma. It is characterized by an almost unbalanced state (Dantas et al., 2021; Kuloba et al., 2014) such as negative and positive ions, free electrons, or free radicals (Zhao et al., 2020). The free electrons obtained from the plasma source are higher than the temperature of the cation. Also, the temperature of the ions is often greater than the temperature of the neutral particles (Kuloba et al., 2014). This may be the reason for the increase in temperature of Gotu kola juice during the plasma treatment. In addition, plasma contains reactive oxygen species (ROS) and reactive nitrogen species (RNS) radicals which can have multiple chain reactions with water molecules. This type of reaction of free radicals and ions can increase the temperature of the Gotu kola juice during plasma processing.

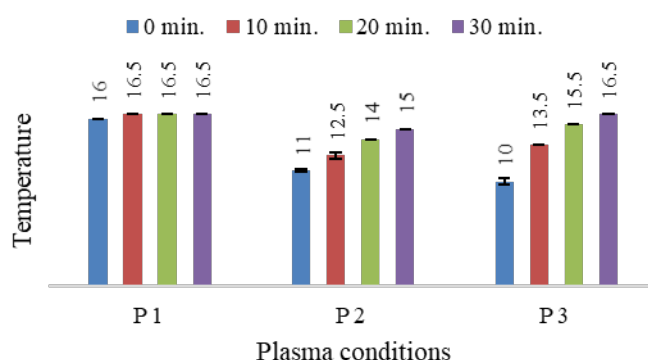


Figure 2 The changing of temperature during plasma generation in different plasma treatments on Gotu kola juice

Effects of thermal and plasma treatments on DPPH and total phenolic compound of Gotu kola juice

DPPH radical inhibition of Gotu kola juice before plasma treatment was $13.34 \pm 3.10\%$. After plasma treatment for 30 min, the DPPH radical inhibition ranged from 12.17 ± 0.06 to $22.12 \pm 0.43\%$, as shown in Table 1. The highest inhibition values were expressed in the juice after plasma treatment at P1, with the values of $22.12 \pm 0.43\%$ ($p \leq 0.05$) after plasma treatment for 10 min. Treatments at P2 and P3 resulted in increasing DPPH radical inhibitions, but the values were still lower as compared to that of the samples treated at P1. Thermal processed Gotu kola juice had DPPH radical inhibition of $13.64 \pm 0.41\%$, which was slightly higher than that of the control sample ($p > 0.05$). The increase of the percentage inhibition of DPPH of the samples treated by plasma and thermal method were compared to the control sample. It can be seen the inhibition of DPPH radical in heat treated sample did not change much as compared to the control sample, whereas plasma treatment tended to increase the inhibition of DPPH radicals as compared to those of the control and thermal treated samples. The resulting inhibition may be the result of plasma-derived reactive species. In addition, the quantitative assay of phenolic compounds is another method that can help explaining the antioxidant effect of Gotu kola juice. Because some of the metabolites of Gotu kola are phenolic compounds, they can contribute to the DPPH radical inhibition. From the analysis of total phenolic compound (TPC) content, it was found that the extracted Gotu kola had the TPC contents ranged from 127.32 ± 0.80 to $149.62 \pm 0.86 \mu\text{gGAE/ml}$. As shown in Table 1, the sample treated with plasma from argon gas at the flow rate of 15 L/min (P1) had the highest phenolic compound content ($149.62 \pm 0.86 \mu\text{gGAE/ml}$) after 20 min of plasma treatment. Thermal treatment resulted in the lowest TPC content, which was reduced from the original content in the control sample. This clearly shows thermal degradation of TPC in the Gotu kola juice. On the other hands,

plasma treatment could preserve the TPC content in the juice since it did not involve much temperature change in the processing. Treatment with argon gas alone (P1) seems to keep the TPC content closed to that of the control sample ($p > 0.05$). Plasma treatment with other gas condition slightly changed the TPC content in the juice sample but without significant differences ($p > 0.05$) when compared to the control and other plasma treated samples, except for 10 min treatments at P2.

Table 1 The antioxidants of Gotu kola juice in different plasma treatments

Treatment	DPPH (% of inhibition)	Total phenolic compound (ugGAE/ml)
Fresh Gotu kola juice	13.34 ± 3.10 ^{cd}	149.25 ± 0.46 ^a
Heated at 72°C, 15 s	13.64 ± 0.41 ^{cd}	127.32 ± 0.80 ^d
Plasma conditions		
Ar+Air: 15+0 L/min		
10 min.	22.12 ± 0.43 ^a	147.99 ± 2.47 ^{ab}
20 min.	21.73 ± 0.06 ^b	149.62 ± 0.86 ^a
30 min.	21.02 ± 1.10 ^b	149.22 ± 2.93 ^a
Ar+Air: 15+5 L/min		
10 min.	15.82 ± 0.37 ^c	142.28 ± 2.86 ^c
20 min.	15.36 ± 0.25 ^c	145.36 ± 0.25 ^{abc}
30 min.	14.93 ± 0.25 ^c	147.52 ± 1.38 ^{ab}
Ar+Air: 15+10 L/min		
10 min.	14.61 ± 0.12 ^{cd}	144.24 ± 2.07 ^{bc}
20 min.	14.19 ± 0.12 ^{cd}	145.00 ± 2.53 ^{abc}
30 min.	12.17 ± 0.06 ^d	147.89 ± 5.41 ^{ab}

The results are expressed as mean ± standard error. The values presented with different superscripts are statistically different at $p \leq 0.05$.

The DPPH antioxidant analysis was the H-atom test of antioxidants against DPPH free radicals, in the other words, its ability to donate electrons as hydrogen atoms. In this reaction, the unpaired valence electrons from the nitrogen atoms in the DPPH radicals are reduced by separating the hydrogen atoms from the antioxidant molecules. This test method shows the quantitative effect of antioxidants in the solution used to reduce the initial concentration of DPPH radicals. The report of Parcheta et al. (2021) states that the structural changes of phenolic compounds result from groups giving or accepting electrons at different locations of the phenolic ring. This reaction promotes the antioxidant activity of those compounds. The essential substances of Gotu kola are full of phytochemicals and its main group is triterpenoid (Sabaragamuwa, Perera, & Fedrizzi, 2018). Gotu kola is a plant with aromatic compounds (Yousaf et al., 2020). Other previously research was recorded that the phenolic compounds contributed to the antioxidant activity of Gotu kola (Ramli et al., 2020). The result of DPPH capacity and total phenolic content in thermal processing showed that heat can affect the content of phenolic compounds. In contrast, plasma processing showed an increase in total phenolic content after 10 min treatment. This could mean that the essential components of this juice can detach and bring the rise of radicals from the plasma. The type of radicals from plasma can receive the transportation of H-atom from bioactive components of Gotu kola juice. Therefore, the essential components in Gotu kola juice are free radicals scavenging.

However, the DPPH capacity of Gotu kola juice after plasma treatment for 30 min was reduced. This maybe because of radicals from the plasma reacted with the essential component in the juice. The free radicals from plasma generation in the juice includes O_3^- , H_2O_2 , HO_2 , NO^- , and NO_3^- . These radicals can receive the H-atom from essential components of Gotu kola. The result

showed that the total phenolic content was decreased during the early stage of plasma treatment (i.e. 10 min treatment). This could be because plasma treatment produced unstable and reactive radicals in the early stage, resulting in reactions with phenolic compounds present in the juice. These compounds have the ability to eliminate free radicals and reacting with ROS radicals. The cause of decreasing total phenolic content could also be that the formation of ROS and ozone during plasma by destroying the aromatic ring in the compound's structure because these compounds are most susceptible to ozone attack (Dantas et al., 2021; Ali et al., 2020). Another possible mechanism may be due to the oxidative degradation of phenolic compounds due to dissolved oxygen (Zhao et al., 2017). Increasing in this compound after 30 min of plasma treatment may be as the result of plasma-derived reactive species ruptures the plant cell membranes and release the phenolic compounds. Additionally, plasma can break covalent bonds and cell membranes, resulting in bioactive compounds (Hou et al., 2019) such as hydroxyl groups in aromatic rings of phenolic compounds to be released. From the structure of Gotu kola contains with aromatic compounds and OH groups (Parcheta et al., 2021; Yousaf et al., 2020), which plasma interactions may occur with these elements. The antioxidant properties are related to the compound's chemical structure, for example the number of hydroxyl groups and their joint location in the aromatic ring (Parcheta et al., 2021).

Effect of Thermal and Plasma treatment of physical properties of Gotu kola juice

Color is one of the freshness indicators of fruit and vegetable juices. Color parameters of the juice samples are shown in Table 2.

Table 2 Color and viscosity of Gotu kola juice

Treatment	L*	a*	b*	ΔE^*_{ab}	Viscosity (cP)
Fresh Gotu kola juice	33.59±0.05 ^a	0.24±0.02 ^c	55.02±0.12 ^a	-	1.09±0.00 ^{ns}
Heat treatment (72°C/15 s)	32.76±0.02 ^b	0.44±0.02 ^b	53.85±0.15 ^b	1.46±0.17 ^g	1.15±0.00 ^{ns}
Argon + Air: 15+0 L/min:					
10 min.	31.93±0.02 ^c	0.65±0.05 ^a	52.68±0.19 ^c	2.92±0.22 ^f	1.09±0.00 ^{ns}
20 min.	30.71±0.03 ^d	0.44±0.01 ^b	50.82±0.12 ^d	5.09±0.14 ^d	1.09±0.00 ^{ns}
30 min.	30.73±0.01 ^d	0.29±0.03 ^c	50.92±0.04 ^d	5.00±0.03 ^d	1.09±0.00 ^{ns}
Argon + Air: 15+5 L/min					
10 min.	30.65±0.04 ^e	0.65±0.05 ^a	52.68±0.19 ^c	3.80±0.21 ^e	1.09±0.00 ^{ns}
20 min.	30.54±0.01 ^f	-0.04±0.04 ^d	50.48±0.13 ^e	5.55±0.04 ^{bc}	1.09±0.00 ^{ns}
30 min.	30.38±0.03 ^g	-	50.25±0.07 ^e	5.74±0.07 ^c	1.09±0.00 ^{ns}
		0.07±0.05 ^{de}			
Argon + Air: 15+10 L/min					
10 min.	30.58±0.02 ^f	0.65±0.05 ^a	52.68±0.19 ^c	3.86±0.18 ^e	1.09±0.00 ^{ns}
20 min.	30.04±0.05 ^h	-0.24±0.02 ^f	49.75±0.10 ^f	6.41±0.12 ^a	1.09±0.00 ^{ns}
30 min.	30.57±0.02 ^f	-0.13±0.05 ^e	50.52±0.14 ^e	5.48±0.13 ^c	1.09±0.00 ^{ns}

The results are expressed as mean ± standard deviation. The values presented with different superscripts are statistically different at $p < 0.05$.

All juice samples were significantly darkened as shown by decreasing in the L* values after thermal and plasma treatments ($p \leq 0.05$). Plasma treatment caused the color of juice sample to be

darker than the heat treated sample. This may be due to longer exposure time to plasma and light during the experiment, which possibly caused degradation of chlorophyll compounds. The reactive species from plasma causes oxidation and isomerization of pigment by ROS attacking the structure, breaking down the double-bond of porphyrin macrocyclic of chlorophyll (Sun & Li, 2017). Additionally, the reactive species of plasma can break down carotenoid pigment causing color change (Sruthi et al., 2022). Amongst all plasma treated samples, treatment using argon gas alone for 10 min produced the juice with the least color change ($p \leq 0.05$). The L^* value significantly decreased with increasing treatment time ($p \leq 0.05$) in all plasma gas condition. When comparing the color difference values (ΔE^*), heat treatment gave the least change in color, whereas plasma treatment caused significant color changes after 10 min of treatment for all gas conditions ($p \leq 0.05$). When the ΔE is in the range of 1.5-3.0, people can perceive slight color changes. The color changes can be detected or observed when ΔE is in the range of 3.0-6.0, whereas the color changes are highly perceptible to the human eye when the ΔE is in the range of 6.0-12 (Hou et al., 2019; Lei et al., 2018). From the results, therefore, thermal treatment can better preserve the color of the Gotu kola juice. Plasma treatment can preserve the color when treated at shorter time period (i.e. ≤ 10 min). Viscosity of the juice was not significantly changed by any process ($p > 0.05$). This was because there was no aggregation, flocculation or precipitation of solid particles in the juice during treatments.

Table 3 Nitrate and nitrite concentrations in Gotu kola juice

Conditions of plasma	Nitrate (NO ₃ ⁻) (ppm)	Nitrite (NO ₂ ⁻) (ppm)
Fresh Gotu kola juice	0.50±0.00 ^{ns}	0.15±0.00 ^{ns}
Heat treatment (72°C/15 s)	0.50±0.00 ^{ns}	0.15±0.00 ^{ns}
After plasma 120 minutes		
Argon + Air :		
15+0 L/min		
10 min.	0.50±0.00 ^{ns}	0.15±0.00 ^{ns}
20 min.	0.50±0.00 ^{ns}	0.15±0.00 ^{ns}
30 min.	0.50±0.00 ^{ns}	0.15±0.00 ^{ns}
15+5 L/min		
10 min.	0.50±0.00 ^{ns}	0.15±0.00 ^{ns}
20 min.	0.50±0.00 ^{ns}	0.15±0.00 ^{ns}
30 min.	0.50±0.00 ^{ns}	1.00±0.00 ^{ns}
15+10 L/min		
10 min.	0.50 ^{ns}	0.30 ^{ns}
20 min.	0.50 ^{ns}	0.30 ^{ns}
30 min.	0.50 ^{ns}	1.00 ^{ns}

The results are expressed as mean ± standard deviation from replicate measurement. The values represented with different superscripts are statistically different at $p < 0.05$.

Concentration of nitrate and nitrite radicals of Gotu kola juice

Concentrations of nitrate (NO₃⁻) and nitrite (NO₂⁻) radicals in Gotu kola juice were analyzed using test strips. The nitrate and nitrite concentrations are shown in Table 3. After plasma treatment using argon gas at the flow rate of 15 L/min, the concentrations of NO₃⁻ and NO₂⁻ were present in the Gotu kola juice at 0.5 ppm and 0.15 ppm, respectively. When 5 L/min and 10 L/min of air were added to the plasma gas, both radicals were present at higher concentrations. The concentration of NO₂⁻ increased to 1 ppm after 30 min plasma treatment when 5 L/min of air was mixed to argon

gas. When air flow rate was increased to 10 L/min, the concentration of NO_2^- was increased to 0.3 ppm at 10 min treatment time and 1 ppm at 30 min treatment time. Increasing contents of nitrates and nitrites in Gotu kola juice may not be good for human health since nitrites can react with amines and amides in stomach that lead to synthesis of N-nitroso, causing the risk of cancer (Rezaei et al., 2014). However, the concentrations of nitrates and nitrite found in this study were very low than the FDA regulation (<500 ppm for nitrates and <200 ppm for nitrites) (Ching, 2016). Therefore, the plasma treatment is very safe for food processing.

OES emission spectra during plasma treatment of Gotu kola juice

Optical emission spectroscopy was used to analyze the free radical from source of plasma. This method is an optical emission spectroscopy that detect at the point of light source or the position of plasma generation for detection of free radicals produced by discharge. The probe of the OES was immersed in the Gotu kola juice at the point where the light bulb of the solution plasma was measured while the plasma was being generated. The results are shown in Figure 3.

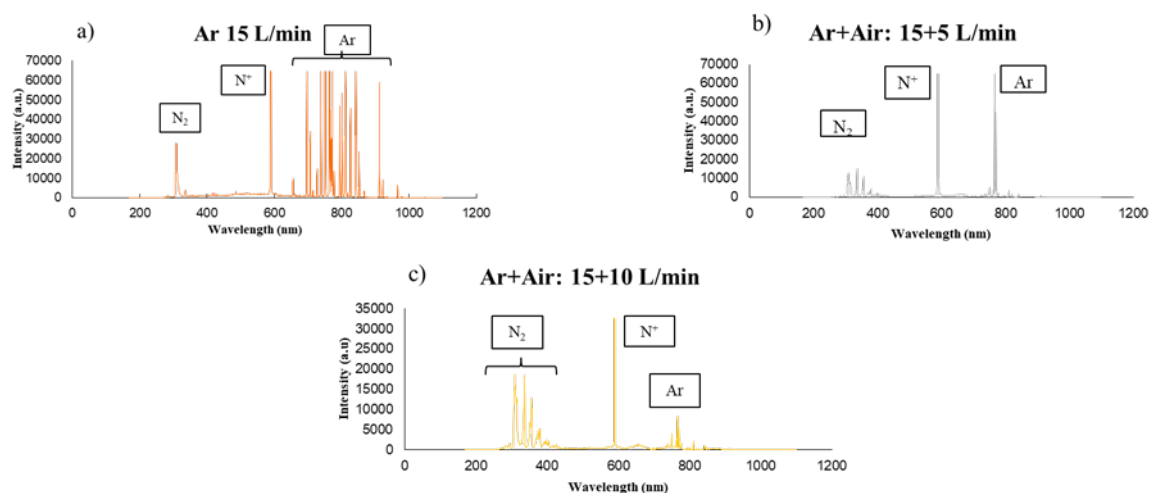


Figure 3 Optical emission spectra of the solution plasma of argon gas flow rate at 15 L/min with 3 conditions of air flow rate a) Air flow rate 0 L/min (P1) b) Air flow rate 5 L/min (P2) and c) Air flow rate 10 L/min (P3)

These radicals were generated when plasma was supplied which were likely to cause changes in the quality of Gotu kola juice. The radicals make an impact by doing a chain reaction with other surrounding radicals to cause more free radicals of other types or may react directly with the bioactive compounds of Gotu kola juice. Therefore, it is important to know how the different conditions affect different results. In this study, measurements by OES showed that argon gas only (P1, Figure 3 (a)) produced 3 plasma peaks at the wavelength of 300, 600, and 700-900 nm. N_2 radicals appeared at the wavelength of 300 nm with radical intensity of about 30,000 au. At the wavelength of 600 nm, N^+ radicals appeared with the intensity of approximately 65,000 au. The multiple peaks at the wavelength around 700-900 nm range showed the Ar radical content of approximately 65,000 au. Plasma treatment at P2 and P3 resulted in different intensities of the radicals. In P2 (Figure 3 (b)), N^+ and Ar radicals were present at intensity approximately 65,000 au, whereas the intensity of N_2 radicals were found to be lower than 20,000 au. When more air was added to the plasma gas (P3, Figure 3 (c)), the intensity of N_2 radicals was around 20,000 au, whereas that of the N^+ and Ar radicals were about 32,500 au and 10,000 au, respectively. The study by Pacheco et al. (2008) describes each wavelength as follows: at the wavelength range of 300-400

nm, NII, O, He, OI and OII are present. At wavelength of 670 nm, NI radicals are present. At wavelength of 700 nm, O radicals are present. At wavelength of 750 nm, OII and NI are presents. In addition, had been reported that the UV emission of plasma contains UVA contains N₂ which was shown at 315-400 nm, OH shown at 280-315 nm, and NO shown at 100-280 nm (Boonyawan, 2018).

The results of this study indicate that plasma-derived reactive species affect the quality of the Gotu kola juice. This is related to other studies that plasma produces oxidative effects on antioxidant polyunsaturated compounds (Fernandes, Santos, & Rodrigues, 2019). Research by (Fernandes et al., 2019) reported that N₂ glow plasma was able to generate oxidative species of antioxidants. The concentration of the RNS type was lower than that of the ROS type, which could induce longer antioxidant oxidation. Another study's results reported that glow plasma N₂ did not affect pomegranate juice on the antioxidant composition.

Conclusion

The study of plasma treatment of Gotu kola juice revealed that plasma could increase the capacity of antioxidants as compared to thermal treatment. Plasma treatment using argon gas at the flow rate of 15 L/min showed better results in terms of antioxidant capacity, total phenolic content and color. Plasma treatment time of 10 min could be selected to preserve the color of fresh Gotu kola juice. However, further study on effects of plasma on enzymatic activity and microbial activity should be conducted for food safety reason. More experiment on plasma on other chemical properties should be done also to obtain overall picture of how plasma can contribute to processing of food while maintaining maximum quality profile. Furthermore, interactions of food components with radicals of OH[•], NO, N, ROO[•], NO₂⁻, and NO₃⁻ produced in solution plasma should be investigated in detail to optimize desirable reactions and to avoid undesirable deteriorative interactions in foods. The choice of gas type, power, and plasma gas flow rate should also be considered.

Reference

- Ahmad, T., Kamruzzaman, M., Ashrafuzzaman, M., Ahmad, A., Lisa, L. A., & Paul, D. K. (2015). In vitro Antimicrobial Activity of different extracts of Gotu Kola and Water Spinach against pathogenic Bacterial Strains. *Current Research in Microbiology and Biotechnology*, 3(4), 663-669.
- Ali, M., Cheng, J. H., & Sun, D. W. (2020). Effects of dielectric barrier discharge cold plasma treatments on degradation of anilazine fungicide and quality of tomato (*Lycopersicon esculentum* Mill) juice. *International Journal of Food Science & Technology*, 56(1), 69-75.
- Almeida, F. D. L., Cavalcante, R. S., Cullen, P. J., Frias, J. M., Bourke, P., Fernandes, F. A. N., & Rodrigues, S. (2015). Effects of atmospheric cold plasma and ozone on prebiotic orange juice. *Innovative Food Science & Emerging Technologies*, 32, 127-135.
- Arjunan, K. P. (2011). *Plasma Produced Reactive Oxygen and Nitrogen Species in Angiogenesis*. (Doctor of Philosophy). Drexel, (pp. 23-30).
- Belwal, T., Andola, H. C., Atanassova, M. S., Joshi, B., Suyal, R., Thakur, S., Bisht, A., Jantwal, A., Bhatt, A. D., & Rawal, R. S. (2019). Gotu Kola (*Centella asiatica*). In A. S. S. Seyed Mohammad Nabavi (Ed.), *Nonvitamin and Nonmineral Nutritional Supplements* (pp. 265-275): Charlotte Cackle.
- Bylka, W., Znajdek-Awizen, P., Studzinska-Sroka, E., Danczak-Pazdrowska, A., & Brzezinska, M. (2014). *Centella asiatica* in dermatology: an overview. *Phytotherapy Research*, 28(8), 1117-1124.

- Boonyawan, T. (2018). Physics of Plasma. 2nd Edn. Science CMU Printing Service, Chiang Mai, 315 pp.
- Chana, N., & Chaikaew1, J. (2018). DNA damage protection activities of different solvents from *Scoparia dulcis* leaf and stem extracts. *Khon Kaen Agriculture Journal*, 46(2), 397-408.
- Chandrika, U. G. & Kumarab, P. A. A. S. (2015). Gotu Kola (*Centella asiatica*): Nutritional Properties and Plausible Health Benefits. *Advances in Food and Nutrition Research*, 76, 125-157.
- Ching, K.C. (2016). Health implications of nitrates and nitrites. *Current Topics in Toxicology*, 12, 85-91.
- Dantas, A. M., Batista, J. D. F., dos Santos Lima, M., Fernandes, F. A. N., Rodrigues, S., Magnani, M., & Borges, G. d. S. C. (2021). Effect of cold plasma on açai pulp: Enzymatic activity, color and bioaccessibility of phenolic compounds. *LWT-Food Science and Technology*, 149.
- Dasan, B. G., & Boyaci, I. H. (2017). Effect of Cold Atmospheric Plasma on Inactivation of *Escherichia coli* and Physicochemical Properties of Apple, Orange, Tomato Juices, and Sour Cherry Nectar. *Food and Bioprocess Technology*, 11(2), 334-343.
- Fernandes, F. A. N., Santos, V. O., & Rodrigues, S. (2019). Effects of glow plasma technology on some bioactive compounds of acerola juice. *Food Research International*, 115, 16-22.
- Gray, N. E., Alcazar Magana, A., Lak, P., Wright, K. M., Quinn, J., Stevens, J. F., Maier, C. S., & Soumyanath, A. (2018). *Centella asiatica* - Phytochemistry and mechanisms of neuroprotection and cognitive enhancement. *Phytochemistry Review*, 17(1), 161-194.
- Hashim, P. (2011a). *Centella asiatica* in food and beverage applications and its potential antioxidant and neuroprotective effect. *International Food Research Journal* 18(4), 1215-1222.
- Hashim, P. (2011b). MiniReview: *Centella asiatica* in food and beverage applications and its potential antioxidant and neuroprotective effect. *International Food Research Journal*, 18(4), 1215-1222.
- Hashim, P., Sidek, H., Helan, M. H., Sabery, A., Palanisamy, U. D., & Ilham, M. (2011). Triterpene composition and bioactivities of *Centella asiatica*. *Molecules*, 16(2), 1310-1322.
- Hou, Y., Wang, R., Gan, Z., Shao, T., Zhang, X., He, M., & Sun, A. (2019). Effect of cold plasma on blueberry juice quality. *Food Chemistry*, 290, 79-86.
- Ibraheem, N. A., Hasan, M. M., Khan, R. Z., & Mishra, P. K. (2012). Understanding Color Models: A Review. *ARPJ Journal of Science and Technology*, 2(3), 265-275.
- Kuloba, P. W., Gumbe, L. O., Okoth, M. W., Obanda, M., & Ng'ang'a, F. M. (2014). An investigation into low-temperature nitrogen plasma environment effect on the content of polyphenols during withering in made Kenyan tea. *International Journal of Food Science & Technology*, 49(4), 1020-1026.
- Kumar, S. N. K., Suresh, M. Kumar, S. A., & Kalaiselvi, P. (2014). Bioactive compounds, radical scavenging, antioxidant properties and FTIR spectroscopy study of *Morinda citrifolia* fruit extracts. *International Journal of Current Microbiology and Applied Sciences*, 3(2), 28-42.
- Lei, J., Li, B., Zhang, N., Yan, R., Guan, W., Brennan, C. S. Gao, H. Y. & Peng, B. (2018). Effects of UV-C treatment on browning and the expression of polyphenol oxidase (PPO) genes in different tissues of *Agaricus bisporus* during cold storage. *Postharvest Biology and Technology*, 139, 99-105.
- Manok, S., & Limcharoen, P. (2015). Investigating Antioxidant Activity by DPPH, ABTS and FRAP Assay and Total Phenolic Compounds of Herbal Extracts in Ya-Hom Thpphachit. *Advance Science*, 15(1). 106-117.
- Ng, Z. X., Samsuri, S. N., & Yong, P. H. (2020). The antioxidant index and chemometric analysis of tannin, flavonoid, and total phenolic extracted from medicinal plant foods with the solvents of different polarities. *Journal of Food Processing and Preservation*, 44(9).

- Pacheco, M., Pacheco, J., Moreno, H., Mercado, A., Valdivia, R., & Santana, A. (2008). OES analysis in a nonthermal plasma used for toxic gas removal: Rotational and excitation temperature estimation. *Laser Physics*, 18(3), 303-307.
- Pankaj, S. K., Wan, Z., Colonna, W., & Keener, K. M. (2017). Effect of high voltage atmospheric cold plasma on white grape juice quality. *Journal of Science, Food and Agriculture*, 97(12), 4016-4021.
- Parcheta, M., Swislocka, R., Orzechowska, S., Akimowicz, M., Choinska, R., & Lewandowski, W. (2021). Recent Developments in Effective Antioxidants: The Structure and Antioxidant Properties. *Materials (Basel)*, 14(8).
- Perinban, S., Orsat, V., & Raghavan, V. (2019). Nonthermal Plasma-Liquid Interactions in Food Processing: A Review. *Comprehensive Review of Food Science and Food Safety*, 18(6), 1985-2008.
- Polash, S. A., Saha, T., Hossain, M. S., & Sarker, S. R. (2017). Phytochemical contents, antioxidant and antibacterial activity of the ethanolic extracts of *Centella asiatica*(L.) Urb.leaf and stem. *Jahangirnagar University Journal of Biological Science*, 6(1), 51-57.
- Rahman, M., Hossain, S., Rahaman, A., Fatima, N., Nahar, T., Uddin, B., & Basunia, M. A. (2013). Antioxidant Activity of *Centella asiatica* (Linn.) Urban: Impact of Extraction Solvent Polarity. *Journal of Pharmacognosy and Phytochemistry*, 1(6), 27-32.
- Rajurkar, N. S., & Hande, S. M. (2011). Estimation of Phytochemical Content and Antioxidant Activity of Some Selected Traditional Indian Medicinal Plants. *Indian Journal of Pharmaceutical Sciences*, 146-151.
- Ramli, S., Xian, W. J., & Mutalib, N. A. A. (2020). A Review: Antibacterial activities, antioxidant properties and toxicity profile of *Centella asiatica*. *EDUCATUM JSMT*, 7(1). 39-47.
- Rezaei, M., Fani, A., Moini, A. L., Mirzajani, P., Malekirad, A. A., & Rafiei, M. (2014). Determining Nitrate and Nitrite Content in Beverages, Fruits, Vegetables, and Stews Marketed in Arak, Iran. *Int Sch Res Notices*, 2014, 1-5.
- Sabaragamuwa, R., Perera, C. O., & Fedrizzi, B. (2018). *Centella asiatica* (Gotu kola) as a neuroprotectant and its potential role in healthy ageing. *Trends in Food Science & Technology*, 79, 88-97.
- Seevaratnam, V., Banumathi, P., Premalatha, M. R., Sundaram, S. P. & Arunugam, T. (2012). Functional properties of *Centella asiatica* (L.): A. *International Journal of Pharmacy and Pharmaceutical Sciences*, 4(5), 8-14.
- Sruthi, N. U., Josna, K., Pandiselvam, R., Kothakota, A., Gavahian, M., & Mousavi Khaneghah, A. (2022). Impacts of cold plasma treatment on physicochemical, functional, bioactive, textural, and sensory attributes of food: A comprehensive review. *Food Chem*, 368, 1-15.
- Sun, Y., & Li, W. (2017). Effects the mechanism of micro-vacuum storage on broccoli chlorophyll degradation and builds prediction model of chlorophyll content based on the color parameter changes. *Scientia Horticulturae*, 224, 206-214.
- Triana, D. R., & Faiza, M. (2015). Antioxidant and α -Glucosidase Inhibitory Compounds of *Centella Asiatica*. *Procedia Chemistry*, 17, 147-152.
- Yousaf, S., Hanif, M. A., Rehman, R., Azeem, M. W., & Racoti, A. (2020). Indian Pennywort. In *Medicinal Plants of South Asia* (pp. 423-437): Elsevier.
- Zhao, G., Zhang, R., & Zhang, M. (2017). Effects of high hydrostatic pressure processing and subsequent storage on phenolic contents and antioxidant activity in fruit and vegetable products. *International Journal of Food Science & Technology*, 52(1), 3-12.
- Zhao, Y. M., Ojha, S., Burgess, C. M., Sun, D. W., & Tiwari, B. K. (2020). Inactivation efficacy of plasma activated water: influence of plasma treatment time, exposure time and bacterial species. *International Journal of Food Science & Technology*, 56(2), 721-732.

List of 11th RMUTIC 2020 Reviews

Asst. Prof. Dr. Alexander	HOULJENKO	North Carolina State University, USA
Prof. Dr. Yoko	MIZOKAMI	Chiba University, Japan
Prof. Dr. Ken	SAGAWA	National Institute of Advanced Industrial Science and Technology, Japan
Assoc. Prof. Dr. Hideki	SAKAI	Osaka City University, Japan
Assoc. Prof. Dr. Panjai	CHULAPAN	Chulalongkorn University, Thailand
Prof. Dr. Duangjai	THEWTHONG	Independent Scholar, Thailand
Asst. Prof. Dr. Chantiga	CHOOCHOTTIROS	Kasetsart University, Thailand
Asst. Prof. Dr. Piyawanee	JARIYASAKOOLROJ	Kasetsart University, Thailand
Asst. Prof. Dr. Amornrat	LERTWORASIRIKUL	Kasetsart University, Thailand
Asst. Prof. Dr. Pawalai	TANCHANPONG	Kasetsart University, Thailand
Asst. Prof. Dr. Nophawan	PARADEE	King Mongkut's University of Technology Thonburi, Thailand
Asst. Prof. Dr. Anyarat	WATTHANAPHANIT	Mahidol University, Thailand
Asst. Prof. Dr. Varongsiri	KEMSAWASD	Mahidol University, Thailand
Dr. Preecha	KHANTIKOMOL	Rajamangala University of Technology Isan, Thailand
Assoc. Prof. Dr. Narongsak	THAMMACHOT	Rajamangala University of Technology Isan, Thailand
Assoc. Prof. Dr. Bundit	KRITTACOM	Rajamangala University of Technology Isan, Thailand
Asst. Prof. Dr. Plengpin	PIANPUMEPONG	Rajamangala University of Technology Isan, Thailand
Dr. Jantana	SUNTUDPROM	Rajamangala University of Technology Isan, Thailand
Dr. Piyamart	JANNOK	Rajamangala University of Technology Isan, Thailand
Asst. Prof. Dr. Subongkoj	TOPAIBOUL	Rajamangala University of Technology Lanna, Thailand
Dr. Chatchawal	SRIPAKDEE	Rajamangala University of Technology Phra Nakhon, Thailand
Dr. Prakorb	CHARTPUK	Rajamangala University of Technology Phra Nakhon, Thailand
Assist. Prof. Dr. Kodchasorn	HUSSARO	Rajamangala University of Technology Rattanakosin, Thailand
Dr. Nichanach	KATEMUKDA	Rajamangala University of Technology Rattanakosin, Thailand
Dr. Sirilak	PRASERTKULSAK	Rajamangala University of Technology Suvarnabhumi, Thailand

Assoc. Prof. Dr. Danupon	KUMPANYA	Rajamangala University of Technology Suvarnabhumi, Thailand
Sub Lt. Dr. Niyawadee	SRISUWAN	Rajamangala University of Technology Suvarnabhumi, Thailand
Asst. Prof. Dr. Thongchai	ARUNCHAI	Rajamangala University of Technology Suvarnabhumi, Thailand
Asst. Prof. Dr. Paiboon	KIATSOOKKANATORN	Rajamangala University of Technology Suvarnabhumi, Thailand
Asst. Prof. Dr. Mongkol	KAEWBUMRUNG	Rajamangala University of Technology Suvarnabhumi, Thailand
Asst. Prof. Dr. Wanich	NILNONT	Rajamangala University of Technology Suvarnabhumi, Thailand
Dr. Tharanee	NAWATNATEE	Rajamangala University of Technology Suvarnabhumi, Thailand
Asst. Prof. Dr. Thanaphum	PONGSA-NGIAM	Rajamangala University of Technology Suvarnabhumi, Thailand
Asst. Prof. Dr. Wijitra	LIAOTRAKOON	Rajamangala University of Technology Suvarnabhumi, Thailand
Asst. Prof. Pongpon	NILAPHRUEK	Rajamangala University of Technology Thanyaburi, Thailand
Dr. Mathuros	PANMUANG	Rajamangala University of Technology Thanyaburi, Thailand
Asst. Prof. Dr. Piyanan	PANNIM VIPAHASNA	Rajamangala University of Technology Thanyaburi, Thailand
Dr. Myo Min	AUNG	Rajamangala University of Technology Thanyaburi, Thailand
Asst. Prof. Jaturapith	KROHKAEW	Rajamangala University of Technology Thanyaburi, Thailand
Dr. Umawasee	SRIBOONLUE	Rajamangala University of Technology Thanyaburi, Thailand
Asst. Prof. Dr. Kanokporn	CHAIPRASIT	Rajamangala University of Technology Thanyaburi, Thailand
Asst. Prof. Dr. Surachat	CHANTARACHIT	Rajamangala University of Technology Thanyaburi, Thailand
Dr. Watchara	DAMJUTI	Rajamangala University of Technology Thanyaburi, Thailand
Dr. Natnaree	SIRIWAN	Rajamangala University of Technology Thanyaburi, Thailand
Asst. Prof. Dr. Chatchai	WEERANITISAKUL	Rajamangala University of Technology Thanyaburi, Thailand
Dr. Nanjaporn	ROUNGPAISAN	Rajamangala University of Technology Thanyaburi, Thailand
Dr. Therakanya	SRIPHO	Rajamangala University of Technology Thanyaburi, Thailand
Asst. Prof. Dr. Porramain	PORJAI	Rajamangala University of Technology Thanyaburi, Thailand
Asst. Prof. Dr. Thanawan	SITTITHAI	Rajamangala University of Technology Thanyaburi, Thailand



The 11th Rajamangala University of Technology International Conference
“RMUT Driving toward Innovation, Economy and Green Technology for
Sustainable Development”

Asst. Prof. Dr. Kitirochna	RATTANAKASAMSUK	Rajamangala University of Technology Thanyaburi, Thailand
Assoc. Prof. Dr. Janprapa	POUNGSUWAN	Rajamangala University of Technology Thanyaburi, Thailand
Ms. Chanida	SAKSIRIKOSOL	Rajamangala University of Technology Thanyaburi, Thailand
Asst. Prof. Dr. Natwipa	SINSUWAN	Rajamangala University of Technology Thanyaburi, Thailand
Ms. Natchaphak	MEEUSAH	Rajamangala University of Technology Thanyaburi, Thailand
Asst. Prof. Dr. Uravis	TANGKITVIWAT	Rajamangala University of Technology Thanyaburi, Thailand
Asst. Prof. Jaturapith	KROHKAEW	Rajamangala University of Technology Thanyaburi, Thailand
Dr. Pichate	KUNAKORNVONG	Rajamangala University of Technology Thanyaburi, Thailand
Asst. Prof. Dr. Pitaya	POOMPUANG	Rajamangala University of Technology Thanyaburi, Thailand
Assoc. Prof. Dr. Warinthon	POONSRI	Rajamangala University of Technology Thanyaburi, Thailand
Asst. Prof. Dr. Sarinya	SANGKASANYA	Rajamangala University of Technology Thanyaburi, Thailand
Dr. Siriluck	SURIN	Rajamangala University of Technology Thanyaburi, Thailand
Dr. Auncha	TUNGKASTHAN	Rajamangala University of Technology Thanyaburi, Thailand
Dr. Utthapon	ISSARA	Rajamangala University of Technology Thanyaburi, Thailand
Asst. Prof. Dr. Intira	LICHANPORN	Rajamangala University of Technology Thanyaburi, Thailand
Assoc. Prof. Dr. Wiboon	TRAKULHUN	Rangsit University, Thailand
Dr. Ektinai	JANSRI	Srinakharinwirot University, Thailand



OUR PARTNERS



DAE SUNG G-3

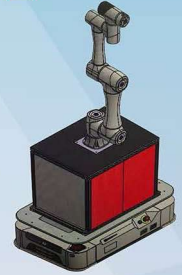


Manufacturer and Distributor

- Pneumatic/Hydraulics Training System
- CIM : Computer Integrated Manufacturing
- Electrical/Electronic Automation System
- Electronic & Telecommunication Technology
- Measuring Instrument
- CNC Training & Simulation Software
- Robot & Intelligent Training System
- Mechatronics Automation Training System
- Training Program & Teaching Aid
- Smart Logistics Technologies System
- AI & IoT Technologies System
- Basic & Advanced Smart Electric Vehicle



Electric Vehicle Integrated System



Cobot+AGV

AUTO DIDACTIC CO.,LTD.
 บริษัท ออโต ไดดักติก จำกัด
 111 Soi Sukhumvit 62/1, Sukhumvit Rd.,
 Prakanongtai, Prakanong, Bangkok 10260
 Tel. : +662-311-2717(Auto Line)
 Fax : +662-332-9372
 E-mail : ad@autodidactic.co.th
 www.autodidactic.co.th

KINETICS CORPORATION LTD.

Materials Research and Testing Instruments

CONTACT 1

E mat@kinetics.co.th
 T 02 515 8940

CONTACT 2

E teerapat@kinetics.co.th
 T 085 352 7505

Thermal Analysis Instruments

TGA, DSC, Dilatometer

Thermal Conductivity Testers

Heat Flow Meter, Laser Flash Analyzer

Low-temperature Materials Characterization System (-271.55 °C up to 126.85 °C)

Hall Effect Measurement System

Thermoelectric Generator Tester

Thin Film Measurement System

Thermal Conductivity
 Electric Resistivity
 Magnetic Properties
 Thin Film Thickness
 Sheet Resistivity
 Optical Profilometers

Imaging Analysis

SEM, EDS, AFM, RAMAN, AFM-RAMAN / AFM-IR

Packaging Testing Instruments

WVTR, OTR, GTR, Overall Migration Tester

Tribological Tester

Nano-indentor / Nano-Tensile Tester

Real-time Polarimeter

X-Ray Diffractometer (XRD)

Sample preparation

Cross-section Polisher
 Electrospinning Machine
 3D Ball Mill
 3D Printer
 3D Scanner

and more ...





***“RMUT Driving toward Innovation,
Economy and Green Technology
for Sustainable Development”***



IRD RMUTT



RMUTT

**Institute of Research and Development
Rajamangala University of Technology Thanyaburi**

39 Moo. 1 Rangsit-Nakornnayok rd. Klong 6, Pathumthani 12110. Thailand

<http://www.rmutcon.org/th/>